Regio- & Stereoselective Carbotrifluoromethylthiolation and Carboboration of Alkynes through Organomagnesium Intermediates

Prachi Shah *M.Sc.*

promotor dr hab. Wojciech Chaładaj

Warsaw 2025

The doctoral thesis was conducted with the support of grant,

NARODOWE CENTRUM NAUKI

Control of regio- and stereoselectivity of hydro- and carbofluoromethylation by hydro- or carbometalation sequence and CM functionalization

NCN OPUS 2019/35/B/ST4/00599

Acknowledgements

I would like to extend my deepest gratitude to my supervisor, Dr. Wojciech Chaładaj, whose constant support, guidance, patience, and approachable nature have been invaluable throughout my PhD journey. I am truly grateful to him for giving me the opportunity to work under his mentorship and within his team. His continuous motivation has been a driving force, pushing me forward during challenging times. His readiness to answer all my curious questions and doubts has greatly shaped my learning. Without his mentorship, I would not have experienced such a transformative phase in my life.

I would also like to thank all my current and former team members at IOC PAS, especially Bartek Bisek and Maciej Dajek, for their constant support and fruitful discussions while troubleshooting experimental challenges. I am equally grateful to former post-doctoral researcher Dr. Fatima Lucio, whose guidance during the initial stages of my PhD helped me build a strong foundation.

My sincere thanks go to the Polish National Science Centre for providing financial support for this research. I am also thankful to Ms. Maja Morawiak for performing the X-ray studies, and to Dr. Wojciech Schilf and Ms. Marta Bugaj for their assistance with NMR-related queries.

I would like to acknowledge the administrative staff, Ms. Nina Kubiak, Dr. Aleksandra Butkiewicz, and Ms. Izabela Stasiewicz, for their constant help with administrative and translation matters. I also wish to thank the cleaning staff of the institute and the hotel, whose contribution in handling the non-scientific aspects of daily life has been deeply appreciated.

My heartfelt thanks go to the friends I met along this journey, Gana, Vishali, Minu, Diksha, Ahmad, Kitti, Kasia Gorczyca, and Joanna Jaszczewska-Adamczak for their encouragement and companionship. I would also like to thank my previous mentors, Dr. Kiron Jathar (R.D. National College), Dr. Jyoti Patwardhan and Dr. Manish Hathe (Ruia College), Dr. Ashwini Sawant, and Mr. Sunil Saroj (Cipla) for shaping my early scientific career. A special thanks goes to Dr. Vijay Gupta, who consistently motivated me during my low phases and helped me resolve both technical and personal challenges.

I am deeply grateful to my relatives and cousins for supporting my parents during my stay in Poland. Without their presence, it would have been very difficult to make the tough decision of leaving India for my doctoral studies.

Lastly, I dedicate this thesis to my parents, my unwavering pillars of strength who have always believed in me and given me the courage to pursue my career. I am profoundly thankful to Ankur for encouraging me to apply for a PhD abroad and for being by my side throughout this journey. I am forever indebted to my grandmother and to my sister Urmi, whose love and faith in me have been a source of endless strength and inspiration.

Contents

List of publications related to the topic of dissertation

1) Shah, P.; Chaładaj, W. α-Selective *Syn*-Carbotrifluoromethylthiolation of Alkynes. *Org. Lett.* **2025,** *27* (10), 2498-2503. Has been highlighted in *Synfacts* **2025**; 21(06), 585.

2) Shah, P. ‡; Dajek, M. ‡; Klimczak, U.; Chaładaj, W. *syn*-Selective α-Boration-Arylation of Alkynes: Concise Access to Configurationally Defined Tetrasubstituted Alkenes. *J. Org. Chem.* (under *review*)

List of conference presentations related to the topic of dissertation

1) 20th Warsaw Seminar of PhD Students in Chemistry- ChemSession, 24, Warsaw, June 2024, poster

2) 28th International symposium: Synthesis in organic chemistry, Cambridge, July 2025, poster presentation

Streszczenie

W niniejszej rozprawie opisałam wyniki dwóch projektów badawczych dotyczących regio- i stereoselektywnej karbofunkcjonalizacji wewnętrznych alkinów przy użyciu odczynników Grignarda w sekwencyjnych protokołach prowadzonych w systemie ‘one-pot’. W pierwszym z nich na drodze syn-selektywnego karbomagnezowania, a następnie trifluorometylotiolowania pośrednich związków winylomagnezowych, otrzymałam alkeny z grupą SCF_3 w pozycji α, jako pojedyncze izomery. Transformacja ta jest godna uwagi, ze względu na brak doniesień literaturowych połączenia α- i syn- selektywności w tego typu reakcjach, oraz na potencjalne znaczenie biologiczne produktów związane z właściwościami grupy SCF_3. Metoda okazała się skuteczna dla szerokiej biblioteki substratów, a jej znaczenie wykazane poprzez dalsze przekształcanie otrzymanych związków. Badania mechanistyczne i analiza konfiguracyjna, w tym rentgenowska analiza strukturalna i 1D-NOESY, rzuciły światło na przebieg całego procesu.

Nieudane próby wprowadzenia grupy boronowej do sterycznie zatłoczonych związków winylomagnezowych (poprzez substytucję produktu pośredniego uzyskanego w reakcji karbomagnezowania wewnętrznego alkinu) doprowadziły do opracowania nowej metody karboborowania alkinów. Ta sekwencja α-selektywnego syn-arylomagnezowania połączona z borylowaniem za pomocą BpinH (pinakoloboranu) doprowadziła do otrzymania wysoce podstawionych alkenów z grupą Bpin, charakteryzujących się wysoką czystością izomeryczną i zdolnych do dalszych przekształceń w kierunku czteropodstawionych alkenów o ściśle określonej konfiguracji. Ponadto możliwość transformacji uzyskanych alkenylowych boranów dodatkowo potwierdza ich potencjalne szerokie zastosowanie w syntezie i tym samym wartość opracowanej metody. Optymalizacja i obliczenia kwantowo-chemiczne odegrały kluczową rolę w wyjaśnieniu napotkanych trudności w etapie borylowania.

Ponadto zweryfikowałam koncepcję projektu skupionego na katalizowanej miedzią addycji Michaela związków Grignarda do enonów z następczym trifluorometylotiolowaniem. Opracowana difunkcjonalizacja prowadzi do powstania α-podstawionych ketonów z grupą SCF_3, co dotychczas było odnotowane w literaturze jeden raz, gdzie podano przykład ograniczony do początkowej addycji grupy etylowej. Wstępne wyniki stanowią solidną podstawę dla przyszłych badań mających na celu opracowanie metody o szerszym zastosowaniu.

Abstract

In this dissertation, I have described results of two research projects emphasizing regio- and stereoselective carbofunctionalizations of internal alkynes using Grignard reagents in sequential one-pot protocols. The first involves carbomagnesiation followed by trifluoromethylthiolation of vinyl-magnesium intermediates, affording α-SCF_3 alkenes as single isomers with exclusive *syn*-selectivity. This transformation is noteworthy, as no prior literature demonstrates a combination of α- and *syn*-selectivity, and it is biologically relevant due to the properties of the SCF_3 group. The method proved successful across wide range of substrates and was further extended through diverse derivatizations of the products. Mechanistic and configurational studies, including single-crystal X-ray diffraction and 1D-NOESY, substantiated the findings.

Preliminary difficulties with borylation of sterically hindered vinylmagnesium species (resulting from carbomagnesiation of internal alkynes) led to the development of a new protocol for carboboration of alkynes. This sequence of α-selective *syn*-arylmagnesiation merged with borylation with BpinH efficiently delivers highly substituted alkenyl boronates with unprecedented regioselectivity, which can be converted into configurationally defined tetrasubstituted alkenes. Moreover, other post-functionalizations of these alkenyl boronates further demonstrate the broad applicability and synthetic value of the method. Optimization and DFT played a crucial in elucidating the borylation step.

Additionally, I have validated a proof of concept for project focused on Cu-catalyzed Michael addition with subsequent trifluorometylthiolation proceeding with *anti*-selectivity. This vicinal difunctionalization produces α-SCF_3 ketones, a transformation rarely explored using enones as substrates. Until now, only one example has been reported, however limited to initial addition of ethyl group to the Michael accepting partner. This preliminary finding constitutes a strong foundation for future research aimed at the development of more broadly applicable method.

List of abbreviations used

Ac- acetyl group
acac- acetylacetonate
Anis- anisyl group
Anth- anthracenyl
Ad- adamantyl
APCI- atmospheric pressure chemical ionization
BINAP- 2,2′-bis(diphenylphosphino)-1,1′-binaphthyl
^{s}Bu- *sec*-butyl
^{t}Bu- *tert*-butyl
Bn/Benz- benzyl
Boc- *tert*-butyloxycarbonyl
BBN- 9-borabicyclo[3.3.1]nonane
bpy/bipy- 2,2' -bipyridine
BP- byproduct
Cy/CyHex – cyclohexyl
CyPr- cyclopropyl; **CyBut**- cyclobutyl; **CyPen** – cyclopentyl
CPME- cyclopentyl methyl ether
cod- cycloocta-1,5-diene
CzIPN- 2,4,5,6-tetrakis(carbazol-9-yl)isophthalonitrile
CAAC- cyclic(alkyl)(amino)carbene
CAN- ceric ammonium nitrate
DFT- density functional theory
Dip- 2,6-diisopropylphenyl
dppe- bis(diphenyl phosphino ethane)
dppbz- 1,2-bis(diphenylphosphino)benzene
dppf- 1,1′-bis(diphenylphosphino)ferrocene
dmbpy- 4,4′-dimethyl-2,2′-bipyridine
dppb- 1,4-bis(diphenylphosphino)butane
dalphos – diamino-phosphine ligand
dppy- diphenyl-2-pyridylphosphine
DMAP- 4-dimethylaminopyridine
dme/DME- 1,2-dimethoxyethane
DCM- dichloromethane
DMF- dimethylformamide
DCE – dichloroethane
DMSO- dimethyl sulfoxide
DMA/DMAc- N, N-dimethyl acetamide
dr- diastereomeric ratio
D*i*BAlH - diisobutylaluminium hydride

ee: enantiomeric excess
EWG- electron withdrawing group
EI – electron impact ionization
ESI – electron spray ionization
FWHM- full width at half maximum
FG- functional group
GC – gas chromatrography
HR- higher resolution
HFIP- Hexafluoroisopropanol
HMPA- hexamethylphosphoramide
HDDA- hexadehydro-diels–alder
Hal- halogen
ICl- Iodine monochloride
ICy- 1,3-dicyclohexylimidazol-2-ylidene
IMes- 1,3-bis(2,4,6-trimethylphenyl)imidazol-2-ylidene; In **SIMes**- **S-** saturated
IPr- 1,3-bis(2,6-diisopropylphenyl)imidazol-2-ylidene
***i*Pr** – *iso*propyl; ***i*Bu** – *iso*butyl
LDA- lithium diisopropylamide
MS- molecular sieves
MOM- methoxymethyl
MeCN- acetonitrile
MTBE- methyl tert-butyl ether
MAO – methyl aluminoxane
MR- Markovnikov
mpd- bis(2,4 dimethylpentane-2,4-glycol
mCPBA- *meta*-chloroperoxybenzoic acid
MS- mass spectrometry
NOE/NOESY- nuclear overhauser effect spectroscopy.
NMR- nuclear magnetic resonance spectroscopy
NIS- N-iodosuccinimide
nep- neopentyl glycol
NHC- N-Heterocyclic carbene
NQ- naphthoquinone
***n*Pr**- n-propyl; ***n*Bu**- n-butyl; ***n*Pent**- n-pentyl; ***n*Hex**- n-hexyl; ***n*Hept**- n-heptyl; ***n*Oct**- n-octyl ;
***n*Non**- n-nonyl; ***n*Dec**- n-decyl
Nap – naphthyl
Nf- nonafluorobutanesulfonyl (also called nonaflyl)
NMP - N-Methyl-2-pyrrolidone
PFK- perfluoro kerosene
P- product
PDFA- phosphonium difluoroacetate
POL- porous organic ligand

pai- pinanediol
Phth- phthalimide
PMDTA- N,N,N′,N″,N″-pentamethyldiethylenetriamine
Piv – pivaloyl
phen- 1,10-phenanthroline
rr/ regio – regioisomeric ratio
R_f- fluoroalkyl group
SKA- silyl ketene acetal
SKI- silyl ketene imine
SDS- sodium-1-dodecanesulfonate
SET- single electron transfer
TMS- trimethyl silyl; **TES**- triethyl silyl; **TBS**- tributyl silyl
TBDPS- *tert*-butyl diphenyl silyl
TIPS- tri-isopropyl silyl
TBDMS- *tert*-butyldimethylsilyl
THP- tetrahydropyranyl
Trt- trityl (also called triphenylmethyl)
Tf- trifluoromethanesulfonyl (also called triflyl)
TFA- trifluoroacetic acid
THF- tetrahydrofuran
TPP- tetraphenyl porphyrin
Ts- tosyl group
TMS- trimethyl silyl; **TES**- triethyl silyl; **TBS**- tributyl silyl
tbbpy- 4,4′-di-*tert*-butyl-2,2′-bipyridine
TBHP- *tert*-butyl hydroperoxide
THT- tetrahydrothiophene
TBAF- tetrabutylammonium fluoride
TLC- thin layer chromatography
TS- transition state
TMEDA – tetramethylethylenediamine
TOF- time of flight
tol- tolyl group
un-Dec- undecyl
Xphos- 2-dicyclohexylphosphino-2′,4′,6′-triisopropylbiphenyl

1. Literature review

1.1 Carbometallation of alkynes

Carbometallation across alkynes, concurrently generates new C–C σ-bond and a C–M σ-bond (often referred as organometallic species), which result in higher alkene derivatives typically in one step.[1] The first instance of carbometallation was disclosed by Zeigler and Bahr with alkenes (**1**) and potassium salts of dimethylphenyl methane (**Scheme 1.1**).[2] Since then, numerous advances have been made in this field, driven by the reaction's ability to control regiochemistry and stereochemistry, often enabling the synthesis of molecules with high geometric purity, depending on the substrate, metal, and reaction conditions.[3] Several types of metals can participate, most commonly (Li, Mg, Zn, Cu, Al, B, Sn) etc. each conferring characteristic reactivity and selectivity profiles. These metals can take part in addition reactions either through direct (uncatalyzed) or with the transition metal catalyzed pathways (eg. Zr, Fe, Co, Pd, Ni, Cu) which often enhance reaction efficiency and selectivity. Depending on conditions, carbometallation reactions can occur either through intramolecular or intermolecular routes, and may proceed *via* either *syn*- or *anti*-addition pathways (see **Scheme 1.2**).[4] The precise outcome depends strongly on the type of metal used, the structure of the substrate (especially whether it contains directing groups or heteroatoms), and the specific organometallating reagent employed. The resulting metal vinyl compounds typically react with electrophiles like H_2O, I_2, etc. (without isolation) to provide functionalized alkenes. In this review, the products obtained after quenching of the carbometallated compounds are shown unless otherwise specified. The examples below highlight carbometallation reactions conducted with stoichiometric organometallic reagents and majorly cover reactions with unactivated alkynes, unless explicitly specified.

Reaction by Zeigler and Bahr (1927)

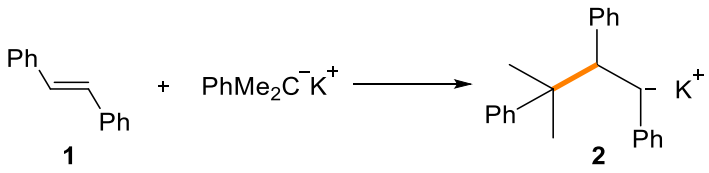

Scheme 1.1: Example of first carbometallation in alkenes

Addition pathways

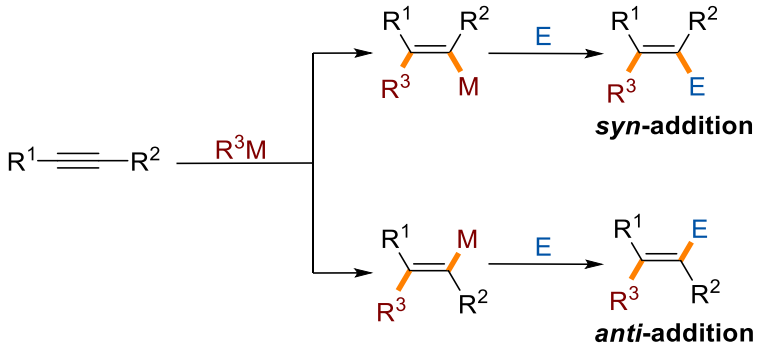

Scheme 1.2: General addition pathways for carbometallations

1.1.1 Carbolithiation

Carbolithiation employs the addition of organolithium reagents across alkynes, giving rise to tri- or tetrasubstituted alkenes.[5] However, challenges arise when alkynes at the terminal or propargylic positions are prone to deprotonation rather than carbolithiation, vinyllithium intermediates can isomerize (compromising stereocontrol), and unactivated alkynes often yield poor regioselectivity.

1.1.1.1 Uncatalyzed reactions

The Tamooka group addressed the above-mentioned issues by utilizing unsymmetrical dialkynes bearing tertiary alcohols (**3**), protected at both ends by triisopropylsilane (TIPS) and *tert*-butyldiphenylsilyl (TBDPS), to perform *anti*-selective alkyl lithiation (*n*-BuLi + TMEDA), affording *E*-configured allyl alcohols (**4**) in excellent yields (**Scheme 1.3**).[6] The authors report that TBDPS group enhances electrophilicity at the alkyne's β-position via hyperconjugation, directing the carbolithiation selectively. (*Z*)-Tamoxifen, a breast cancer therapeutic, was also prepared via ethyllithiation of diphenylacetylene[7,8].

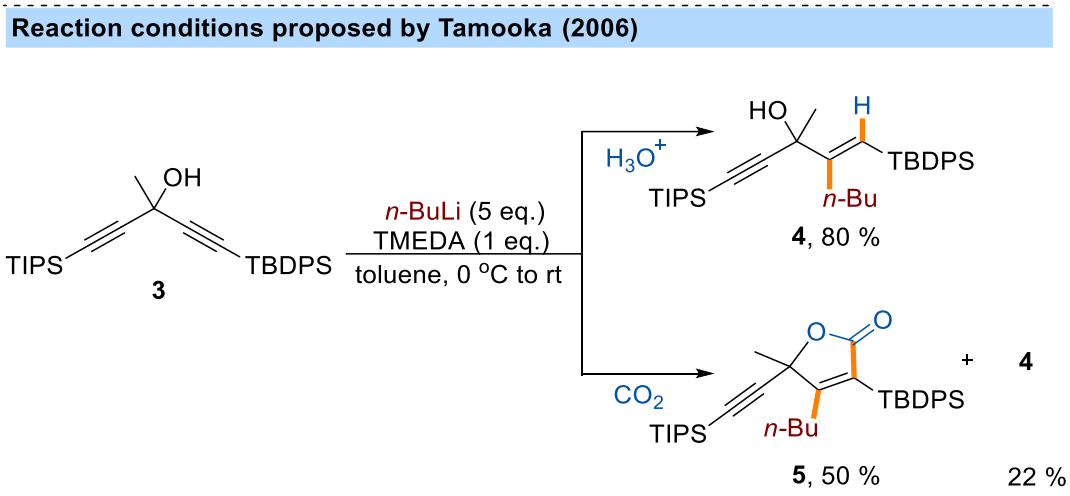

Scheme 1.3: Direct alkyllithiation of alkynol derivatives

Aryllithiation is less common than alkyllithiation because of its sluggish reactivity at low temperatures and the competing side reactions with *n*-butyl halides formed during *in situ* aryllithium preparation.

1.1.1.2 Catalyzed reactions

Hosomi and co-workers showed that Fe(III) salts (e.g., $Fe(acac)_3$) promote selective butyllithiation of homopropargyl ethers and amines (**6**), yielding *E*-alkenes in good yields, particularly with aliphatic substrates.[9] Shirakawa replaced $Fe(acac)_3$ with $FeCl_3$, adding TMEDA and phosphine ligands for butyllithiation of unactivated aryl–alkyl alkynes (**Scheme 1.4**).[10] Though regio- and stereoselectivity were modest, the method still afforded alkenes by *syn*-addition predominantly in good yields. Zinc was sometimes added to suppress *E*/*Z* isomerization when different alkyne and organolithium substituents were used. Adding a copper catalyst, facilitated aryllithiation under

similar conditions. The same group in 2005 applied analogous conditions for arylmagnesiation of unactivated alkynes (see section **1.1.9**).[11]

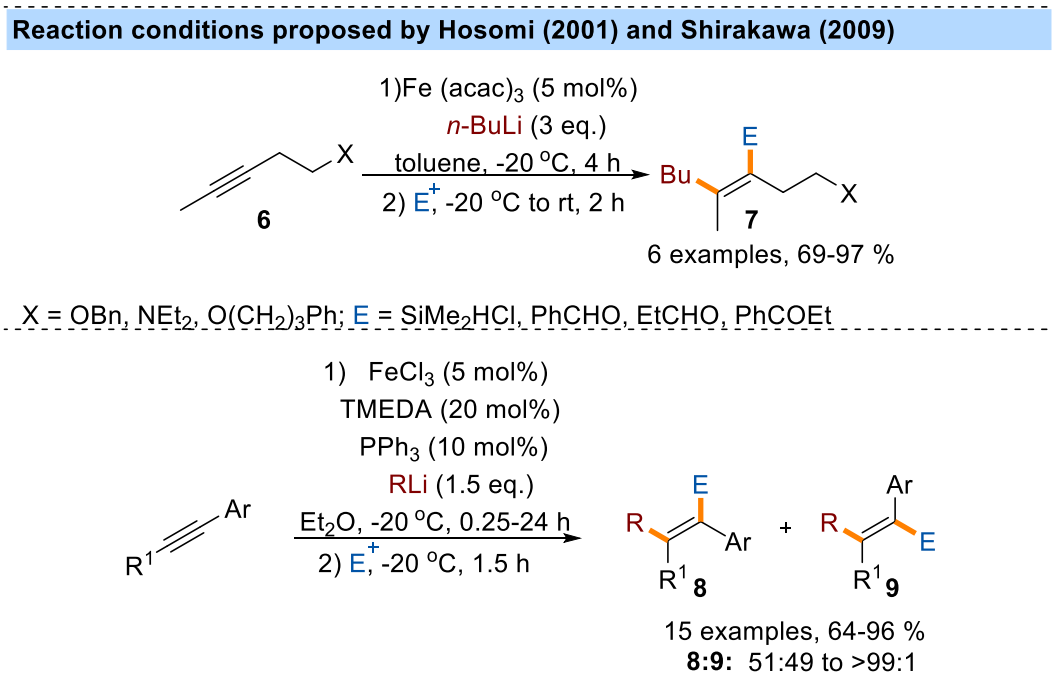

Scheme 1.4: Iron catalyzed carbolithiations

1.1.2 Carboberyllation

Experimental organoberyllium additions to alkynes remain unreported, largely because of beryllium's severe toxicity and its association with chronic beryllium disease.[12] However, thanks to the metal's significant covalent bonding character, that Dutton[13] and co-workers explored 1,1- and 1,2-carboberyllation of alkynes using organoberyllium reagents in a 2017 computational study. They found that both reaction pathways are energetically feasible with activation barriers as low as ~100 kJ mol^{-1} and that dialkyl beryllium compounds demand higher activation energies compared to diaryl counterparts. Importantly, terminal and internal alkynes should undergo aryl beryllation, and diphenylberyllium ($BePh_2$) in particular, should add to diphenylacetylene under reflux conditions within a few hours.

1.1.3 Carboindation and carbogallation of alkynes

Group 13 trihalides such as those of indium and gallium have a balance of moderate lewis acidity and high π-electron affinity due to their larger ionic radius thus allowing effective compatibility with functional groups. As a result, they enable carbometallations using mild carbon-nucleophiles (e.g., organosilicon reagents) and have the possibility to undergo chemoselective reactions.[14] Most documented carbometallations proceed via *syn*-addition across the alkyne. However, a pivotal series of reports by Nishimoto and co-workers pioneered predominantly *anti*-selective protocols.

1.1.3.1 *Syn*-carbometallation of alkynes

Carbogallation and carboindation of alkynes generally proceed through the uncatalyzed addition of organogallium or organoindium species (R–Ga/In, most often allyl), generated from metallic gallium or indium or their trihalides (MCl_3, M = Ga or In), across the C≡C bond. In some cases (e.g., terminal alkynes), this process is facilitated by activation of the alkyne with a second reagent, leading to the formation of geminal bis-metalated products. A broad range of nucleophiles can be introduced in this way, but the underlying mechanistic feature remains the same, that is the *in situ* generated organogallium or organoindium intermediates undergo *syn*-addition to the alkyne, producing vinyl–Ga or vinyl–In compounds that are subsequently quenched (by protodegallation or electrophiles) to afford functionalized alkenes or dienes (**Scheme 1.5**).

Mechanistic aspect

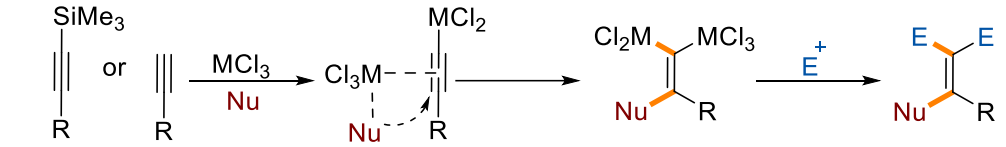

M = Ga, In; Nu = allyl bromides/iodides/silanes, silyl enol ethers, arenes, etc.

Scheme 1.5: *Syn*-selective carbogallation and carboindation of alkynes

Representative examples:

Yamaguchi and co-workers reported the first *syn*- selective alkynylgallation of alkynes by reacting silylated aliphatic alkynes with $GaCl_3$ in the presence of pyridine.[15] Shortly after, they and others developed allylgallation protocols, employing allyl silanes, allyl bromides, or homoallyl alkoxides as precursors to allylgallium reagents, to efficiently deliver 1,4-dienes.[16–19] Yamaguchi extended carbogallation chemistry to the ethenylation of silyl enol ethers using terminal silylated alkynes to efficiently synthesize α-vinyl ketones.[20,21] Similar transformations were achieved with silyl enol ethers derived from thioesters,[22] α-substituted β-keto esters,[23] and malonates. Reactions are generally rapid under stoichiometric conditions at room temperature,[20] while catalytic protocols at elevated temperatures with added base allow smooth protodegallation and suppress decomposition.[24] Other work demonstrated that phenoxy- and arylgallium reagents could also participate, with arenes undergoing regio- and stereoselective additions to alkynes under $GaCl_3$ activation.[25–28]

Butsugan demonstrated *syn*-selective allylindation of propargyl alcohols with allyl bromides, yielding both Markovnikov and *anti*-Markovnikov products depending on steric and electronic factors.[29,30] Subsequent work extended the methodology to propargylic alcohols and ethers, alkynoic acids, and internal alkynes bearing hydroxyl groups, with regioselectivity influenced by chelation and solvent choice.[31] Ranu and Yamamoto developed milder THF-based protocols for terminal alkynes and alkynols, while TMS acetylenes or internal alkynes often gave mixtures of stereoisomers.[32,33] Yamamoto further applied this strategy to benzylindation, observing *trans*-selectivity for aromatic/conjugated alkynes and non-stereoselective addition for aliphatic ones.[34]

1.1.3.2 *Anti*-carbometallation of alkynes

Nishimoto pioneered *anti*-selective allylindation using Lewis acids and allyl silanes,[35] achieving high regio- and stereoselectivity for terminal alkynes (**Scheme 1.6**).

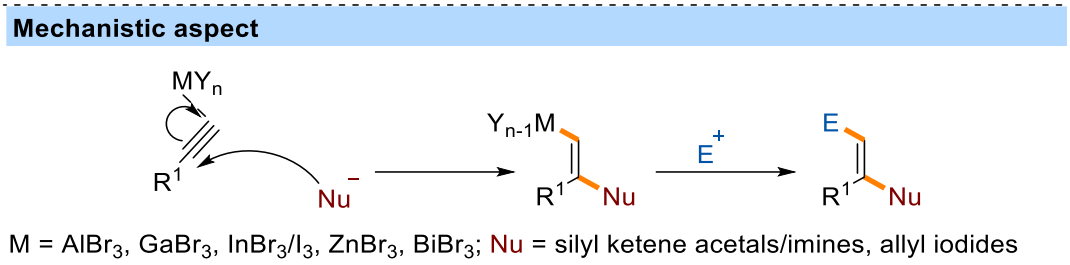

Scheme 1.6: *Anti*-selective carbometallation of alkynes

Lewis acid catalyzed ($AlBr_3$,[36] $GaBr_3$,[37] $ZnBr_2$,[38] $InBr_3/InI_3$,[39,40] $BiBr_3$[41]) reactions with alkynes employ silyl ketene acetals (SKAs) as nucleophiles. $AlBr_3$ failed to react as its strong co-ordination with oxygen of SKA inactivated it, while In, Ga, Zn, and Bi delivered β-alkenyl esters in high yields.The reactivity order with SKA was InI_3 > $GaBr_3$ > $BiBr_3$ > $ZnBr_2$, attributed to indium's superior LUMO–π interaction. X-ray studies confirmed both mono- and dialkenylgallium species, which on iodine trapping gave a single alkenyl iodide product. In contrast, $ZnBr_2$ only formed bis-alkenyl zinc intermediates. Electron-withdrawing groups enhanced yields in carbogallations, while electron-donating groups performed well in carbozincations. Without any substituents on the SKA, $GaBr_3$ and InI_3 gave no product, whereas $ZnBr_2$ maintained a decent 50% yield. Using InI_3, other nucleophiles like silyl ketene imines (SKIs), silyl cyanides, and alkynyl/allyl stannanes also underwent efficient carboindations. Although $AlBr_3$ was ineffective with SKAs, it outperformed InI_3 in SKI mediated reactions leading to cyanides in good yields. Mechanistic studies showed no transmetallation when using any Lewis acids except $BiBr_3$, which yielded α-dibromobismuthino ester (a reversible resting state). Applying the carbogallation strategy enabled the total synthesis of the terpenoid nodosol.

1.1.4 Carboalumination

Carboaluminations have clearly advanced particularly in the field of methylaluminations replacing the less reactive methylcuprations resulting in methyl substituted alkenes commonly found in terpenoid frameworks.[42]

Direct carboaluminations using organoaluminium reagents (Me_3Al or Et_3Al) does not proceed at ambient temperatures and at elevated temperatures result in the formation of alkynylaluminium (**10**) in case of terminal alkynes while commonly lead to mixtures of regioisomers (**11** and **12**) with internal alkynes (**Scheme 1.7**).[43]

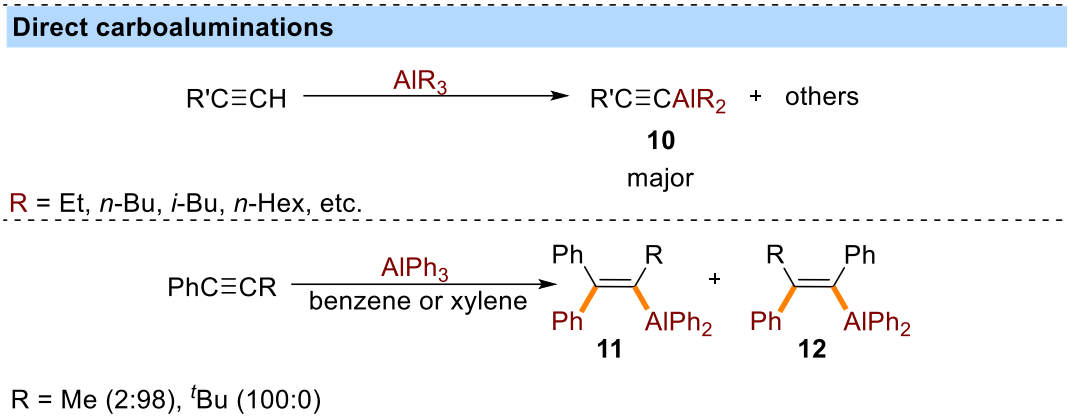

Scheme 1.7: Direct carboalumination of alkynes

1.1.4.1 Catalyzed reactions

The use of catalysts (Zr, Ti, Sc) are necessary to direct the reactions towards controlled addition. These reactions are typically *syn*-selective, although the stereochemical outcomes can vary depending upon the nature and the position of the substituents on the alkyne.

Alkylalumination of alkynes:

Negishi reported a *syn*-selective Ti-mediated methylalumination of unactivated alkynes using $AlMe_3$.[44] Terminal alkynes yielded the desired alkenes (albeit in low yield ≤30%), while internal alkynes led to allenes. Diphenylacetylenes were efficiently converted, though analogous Zr-catalyzed reactions were sluggish (**Scheme 1.8**). Zirconocene dichloride (Cp_2ZrCl_2) enabled regio- and stereoselective methylalumination of both terminal and symmetrical internal alkynes, where methylation occurs at the α-position and no deprotonation was observed in case of terminal alkynes (**Scheme 1.9A**).[45] However, using bulkier organoalanes reduced both yield and regioselectivity, likely due to competing β-elimination and hydrozirconation pathways. Experiments with Me_2AlCl-Cl_2ZrCp_2 and $AlMe_3$-$Cl(Me)ZrCp_2$ in carbometallations showed no (Me-Cl) exchange, which strongly supported that the reaction is Zr-catalyzed carboalumination and not vice versa (**Scheme 1.9B**).[42] To enhance regioselectivity when using higher alane derivatives (initially ~60:40), Wipf found that adding a stoichiometric amount of water slightly improved the reaction rate and regioselectivity (~70:30) allowing the reaction to occur at low temperatures.[46] Later, Inoue replaced Cp_2ZrCl_2 with the tetraphenylporphyrin-zirconium complex $(TPP)ZrCl_2$, improving regioselectivity further to ~88:12 for ethylalumination.[46]

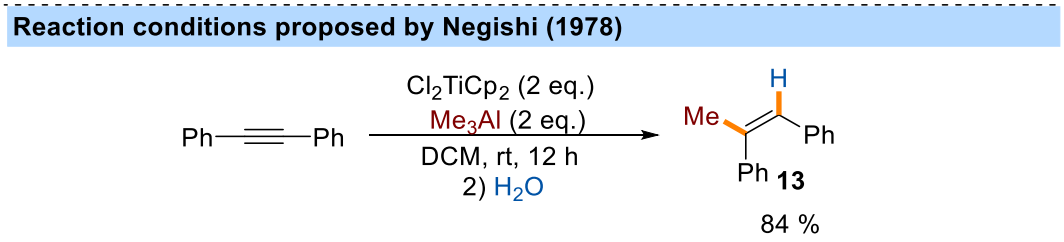

Scheme 1.8: Ti catalyzed carboalumination

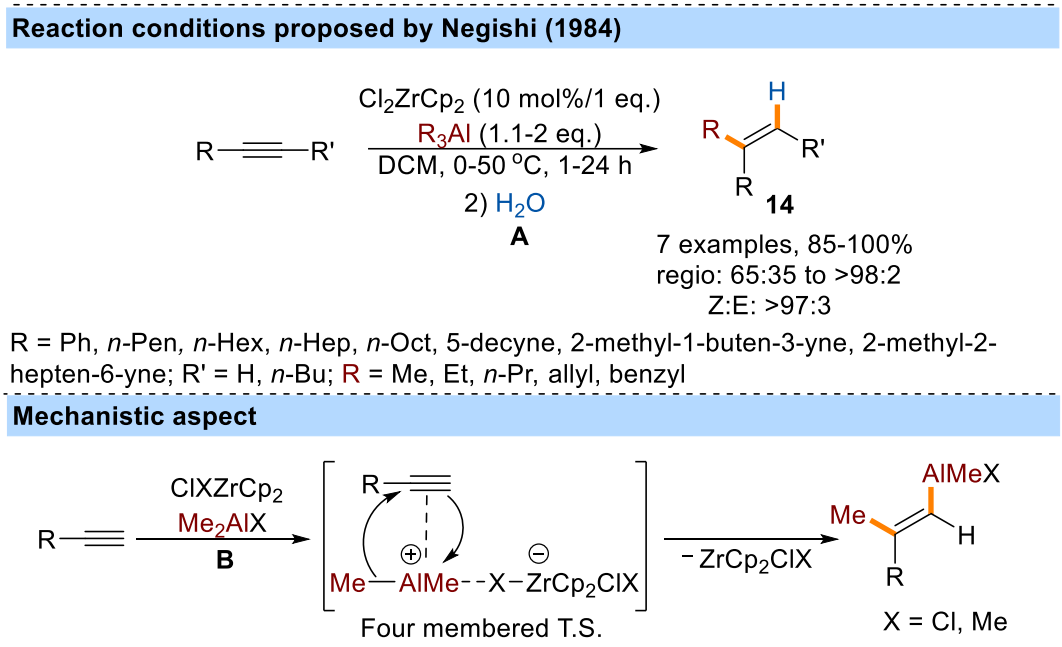

Scheme 1.9A and B: Zr-catalyzed methylalumination and its mechanism

A novel *syn*-selective catalytic method for methylalumination of alkynyl ethers was developed using cationic scandium complexes $(C_5Me_4R)Sc(CH_2C_6H_4NMe_2\text{-}o)_2$ (R = Me, $SiMe_3$) (**15a** and **15b**) (**Scheme 1.10**).[47] These catalysts outperform analogous zirconium systems in both yield and regioselectivity, adding the methyl group distal to the alkynyl ether (**16**). In contrast, TMS-substituted alkynes undergo *anti*-addition, placing Me adjacent to the ether (**17**).

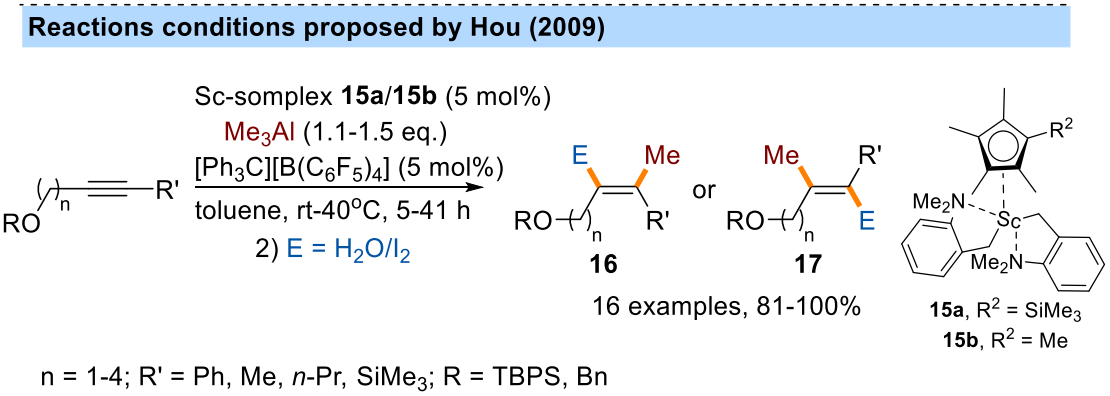

Scheme 1.10: Sc-catalyzed methylaluminations

Mechanistically, the reaction begins with alkyl-ligand exchange between the bis(alkyl) scandium complex, $[Ph_3C][B(C_6F_5)_4]$, and Me_3Al. The Sc catalyst then coordinates to the alkyne, promoting *syn* insertion to form a vinyl-scandium intermediate (**18**). Subsequent transmetallation with aluminium yields a *syn*-alkenyl alane (**19**) (**Scheme 1.11**). However, when TMS-alkynes are used, this intermediate undergoes rapid isomerization to the more stable *anti*-alkenyl alane (**20**).

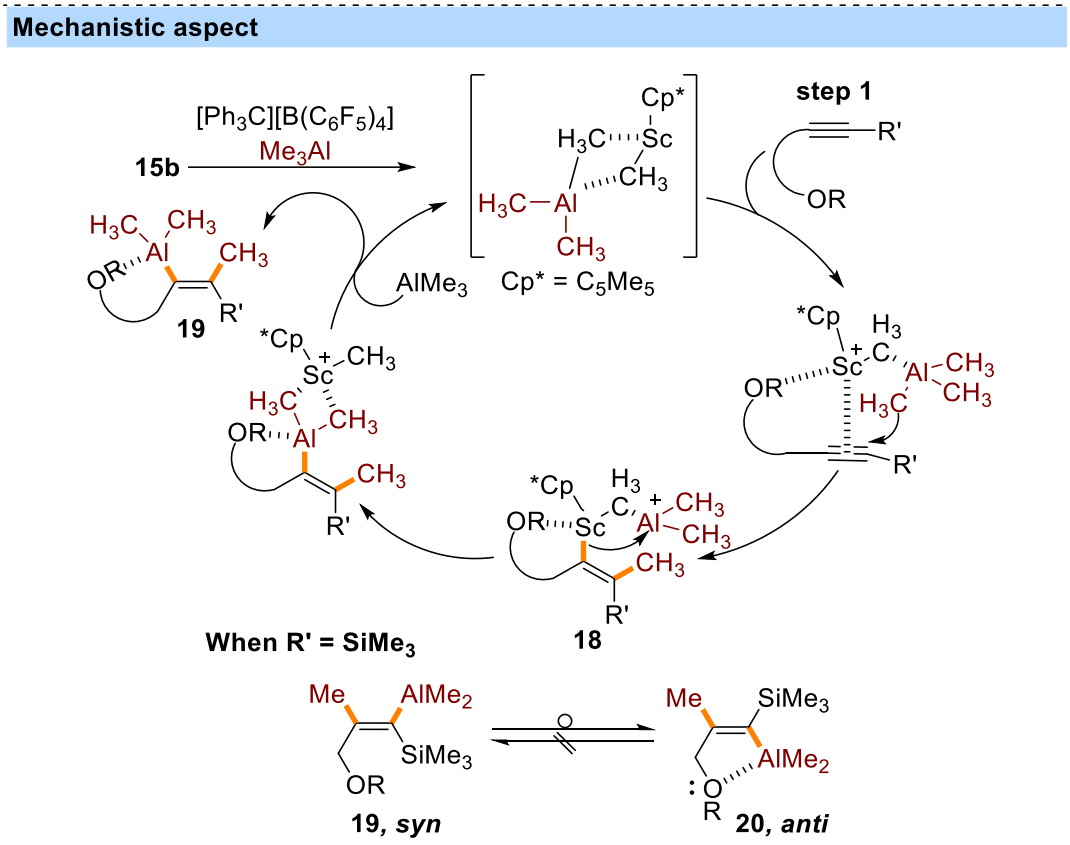

Scheme 1.11: Mechanism of Sc-catalyzed methylalumination

In 1984, Oshima employed a Hex_2Mg/Et_3Al reagent, analogous to Cp_2ZrCl_2/Me_3Al system to effect carbometallation of trimethylsilyl alkynes with higher organoalanes (**Scheme 1.12**).[48] This approach delivered products with moderate stereocontrol and in good yields, (≈ 80 % ethylated, 20 % hexylated). Intriguingly, when the TMS-alkyne featured a conjugated double bond, the addition proceeded predominantly via *anti* pathway with excellent stereoselectivity (>95:5). That same year, Miller reported a Cp_2TiCl_2-catalyzed, *syn*-selective ethyl alumination of TMS-alkynes, which he successfully applied in the synthesis of Z-tamoxifen.[49]

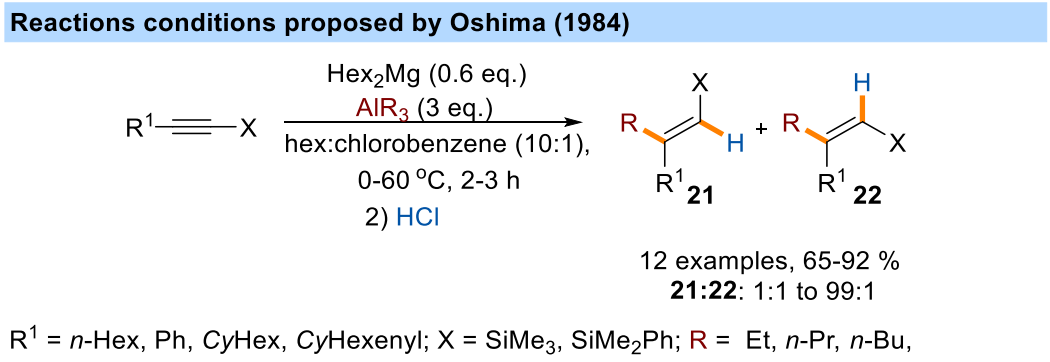

Scheme 1.12: Alkylaluminations using Hex_2Mg/Et_3Al system

Allyl and benzylalumination:

Negishi extended the Zr-promoted carboalumination protocol for *syn* selective allyl and benzylaluminations of alkynes (**Scheme 1.13**).[50] Terminal and internal alkynes when treated with allyldiisobutylalane proceeded with lower regioselectivity (α:β = 75:25) but higher stereoselectivity on iodinolysis (>98%). Benzylaluminations of terminal alkynes using tribenzylaluminum (Bn_3Al) at elevated temperature (60 °C) proceeded in good yield, albeit with moderate regioselectivity (α:β = 70:30). In contrast, analogous arylaluminations using triphenylaluminum (Ph_3Al) did not occur under the same conditions. However, Eisch demonstrated that heating internal alkynes such as diphenylacetylenes or aryl-alkyl alkynes above 100 °C with Ph_3Al efficiently yields arylaluminated products in absence of a catalyst.[51] These reactions proceed with high regioselectivity: in unsymmetrical internal alkynes, the phenyl group selectively adds to the β-position (98:2). Mechanistically, it follows a *syn*-addition pathway via a four-membered cyclic transition state.

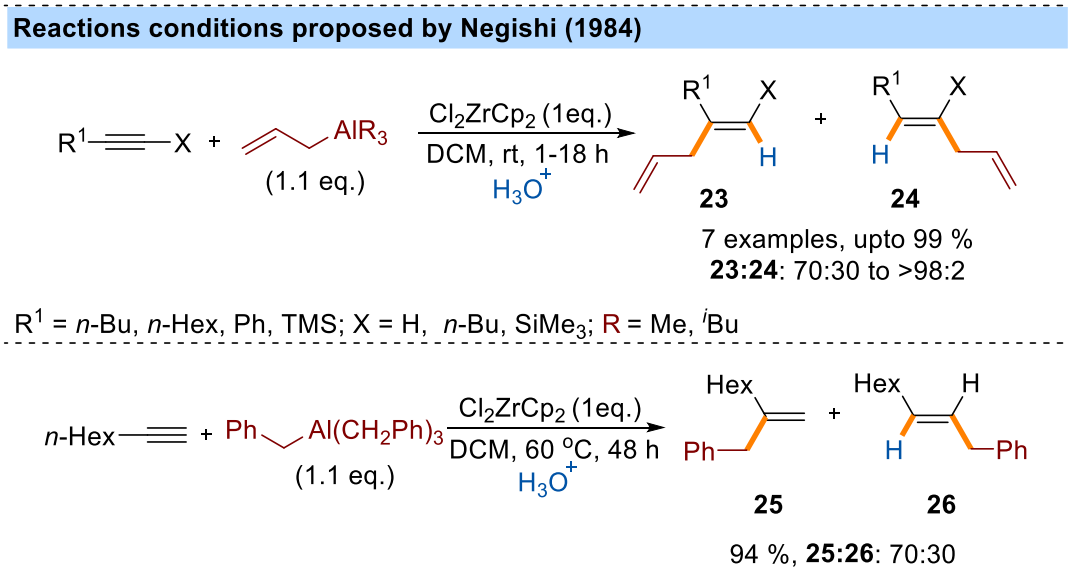

Scheme 1.13: Zr-catalyzed allyl & benzylalumination of alkynes

Expanding research in carboaluminations, Negishi reported that *syn*-selective methyl alumination of terminal and Si/Ge-substituted homopropargyl alcohols (using catalytic $ZrCp_2Cl_2$) can isomerize to *anti*-isomers (**28**) upon refluxing for 72 h (**Scheme 1.14**).[52] Longer carbon chains gave *syn*/*anti* mixtures (4:6 to 6:4), while TMS-substituted alkynols yielded predominantly *anti*-products (~88 : 12). The observed selectivity reversal supports a chelation-controlled mechanism via a cyclic aluminacycle intermediate (**27**).

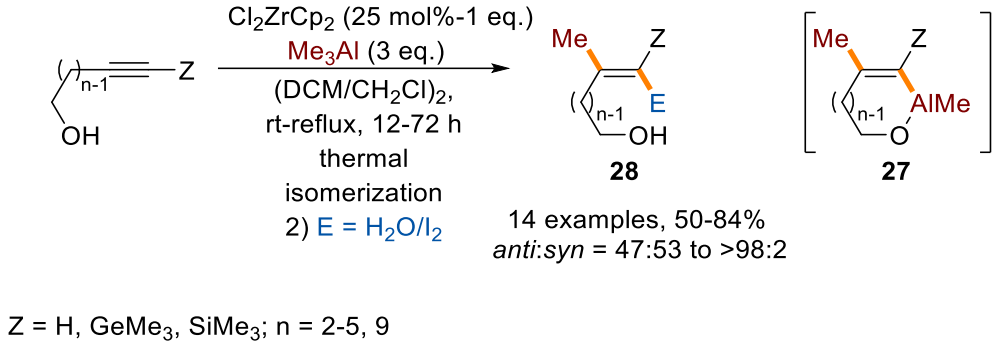

Scheme 1.14: Zr-catalyzed methylalumination of alkynes

1.1.5 Carbozirconation

Carbozirconations require the use of activation by polarization, the use of bimetallic catalysts or formation of small-ring zirconacycles to undergo carbometallation reactions.[53]

Allylzirconation:

Keisuke developed a method for *syn*-selective allylzirconation of terminal alkynes (aromatic and aliphatic) by generating allylzirconium reagents *in situ* from allenes, activated by modified methylaluminoxane (MAO) (**Scheme 1.15A**).[54] Unlike typical γ-allylations, the current α-allylations give 1,4-dienes (**29** & **30**) with excellent yield and regioselectivity for aromatic alkynes. For aliphatic alkynes, regioselectivity varies: primary alkyl substituents yield mixtures of isomers, while branched substituents produce a single product. He also applied the method to 1-iodo alkynes,[55] yielding enynes in outstanding efficiency (**Scheme 1.15B**). Isotope-labeling indicated formation of an alkylidene carbenoid (**31** or **32**), which in aromatic substrates triggers a 1,2-aryl shift. With aliphatic alkynes, the pathway diverges: either via allyl migration (since alkyl migration is slow) or through *β*-allylation followed by *β*-elimination, leading to the required products (**Scheme 1.16**).

Reaction conditions by Keisuke (1997 & 1999)

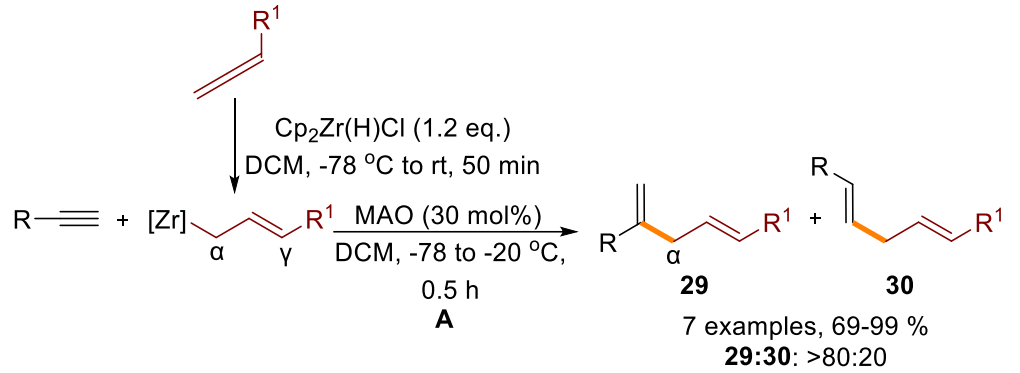

R = *n*-Pen, *n*-Oct-CH(CH_2)Ph, *m*-ClPh, *m*-OMePh, 2-Nap; R^1 = $(CH_2)_2OSi^tBuPh_2$, Ph, *Cy*Hex, *n*-Hep

R^1 = TBDPSO$(CH_2)_2$, *n*-Hep, *Cy*Hex, etc.; R = *m*, *p*-OMePh, *n*-Bu, $PhCH_2CH(CH_3)_2$, etc.

Scheme 1.15A and B: Allylzirconation of alkynes

Mechanistic aspect

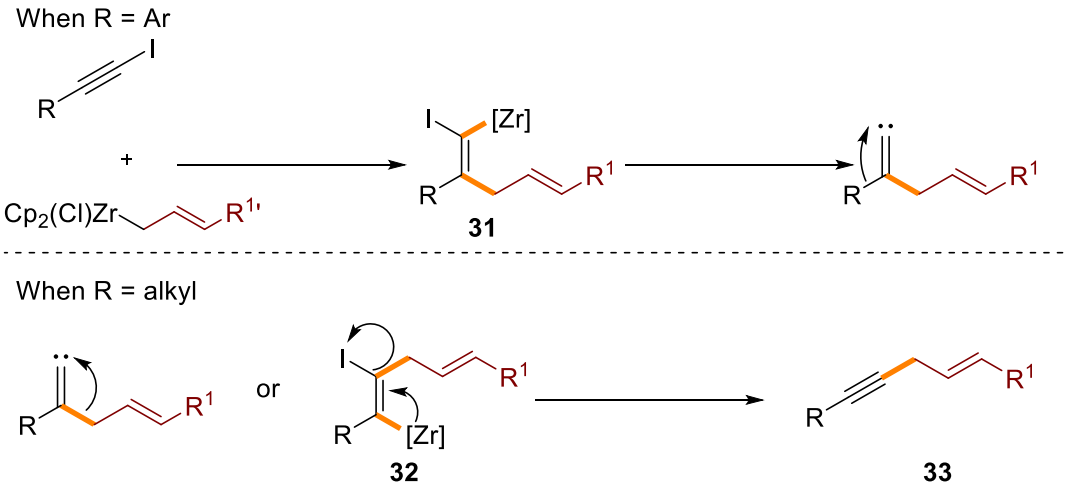

Scheme 1.16: Mechanism for allylzirconation of iodo-activated alkynes

Allylzirconation via formation of zirconacyclopentenes:

Takahashi reported *syn*-selective allylzirconation of alkynes using *in situ* generated Cp_2ZrBu_2 (from Cp_2ZrCl_2 and *n*-BuLi), Me_3P and allyl ethers proceeding with γ-selective allylation (**Scheme 1.17A**).[56] Internal silyl-substituted alkynes gave high regioselectivity, whereas aryl-alkyl and terminal alkynes yielded regioisomeric mixtures. The current mechanism deviates from conventional 4- or 6- membered transition states: it proceeds via a 5-membered zirconacyclopentene intermediate (cyclometallation, two interconverting forms, **37a** and **37b**, *vide infra*), with **37b** reverting to **37a** via β-β' C–C bond cleavage. Subsequent β-elimination of the alkoxy (OR) group furnishes the allylzirconation product (**34**) (**Scheme 1.18**). He also showed that using Cp_2ZrEt_2 (from Cp_2ZrCl_2 and EtMgBr) without phosphines improved yields for alkyl-substituted alkynes (**Scheme 1.17B**). The method was later extended to allyl chlorides (via *trans*-selectivity), allyl esters, and acetals. Notably, substituting allyl ethers with homoallylic bromides triggered γ-elimination, yielding alkenyl cyclopropanes instead (**36**).

Reaction conditions proposed by Takahashi (1995)

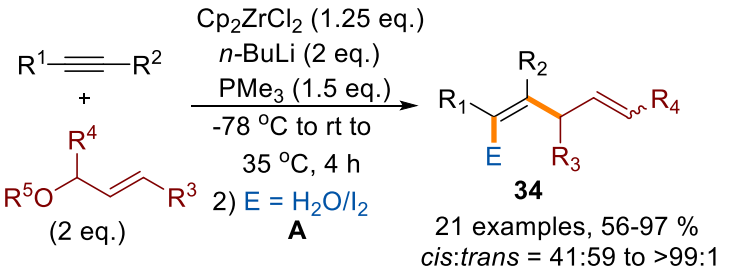

R^1 = $SiMe_3$, Ph, *n*-Pr, *n*-Hex; R_2 = *n*-Pr, *n*-Hex, H, Ph; R_3 = H, *n*-Pr; R_4 = H, *n*-Pent, OR where R = Et; R^5 = Et, Ph, allyl, Bn

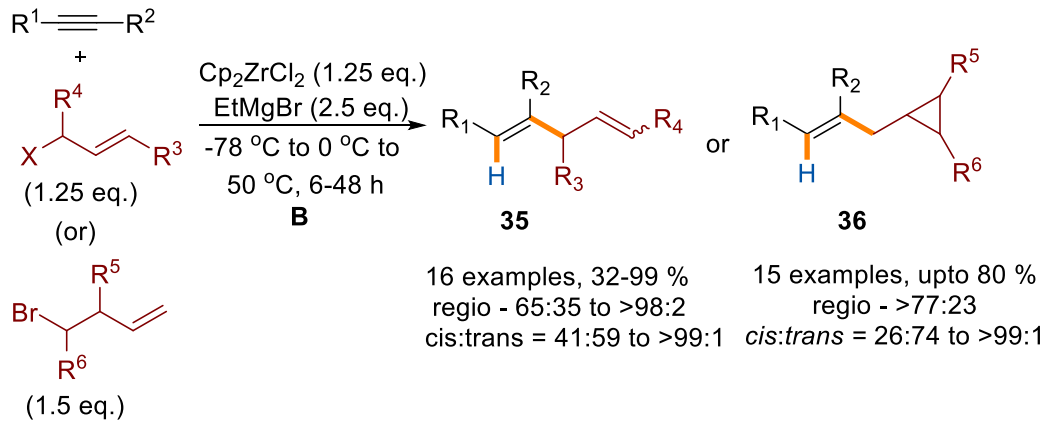

X = OR (where R = $OSiMe_3$, Ph, Bn), Cl, Br; R^1 = $SiMe_3$, Ph, Et, *n*-Pr, *n*-Bu, *n*-Hex; R_2 = Ph, H, Me, Et, *n*-Pr, *n*-Bu, *n*-Hex; R_3 = H; R_4 = H, Me, *n*-Pent, OR where R = Et; R^5 = H, Et, R^6 = H, Me

Scheme 1.17A and B: Allylzirconation through zirconacyclopentenes

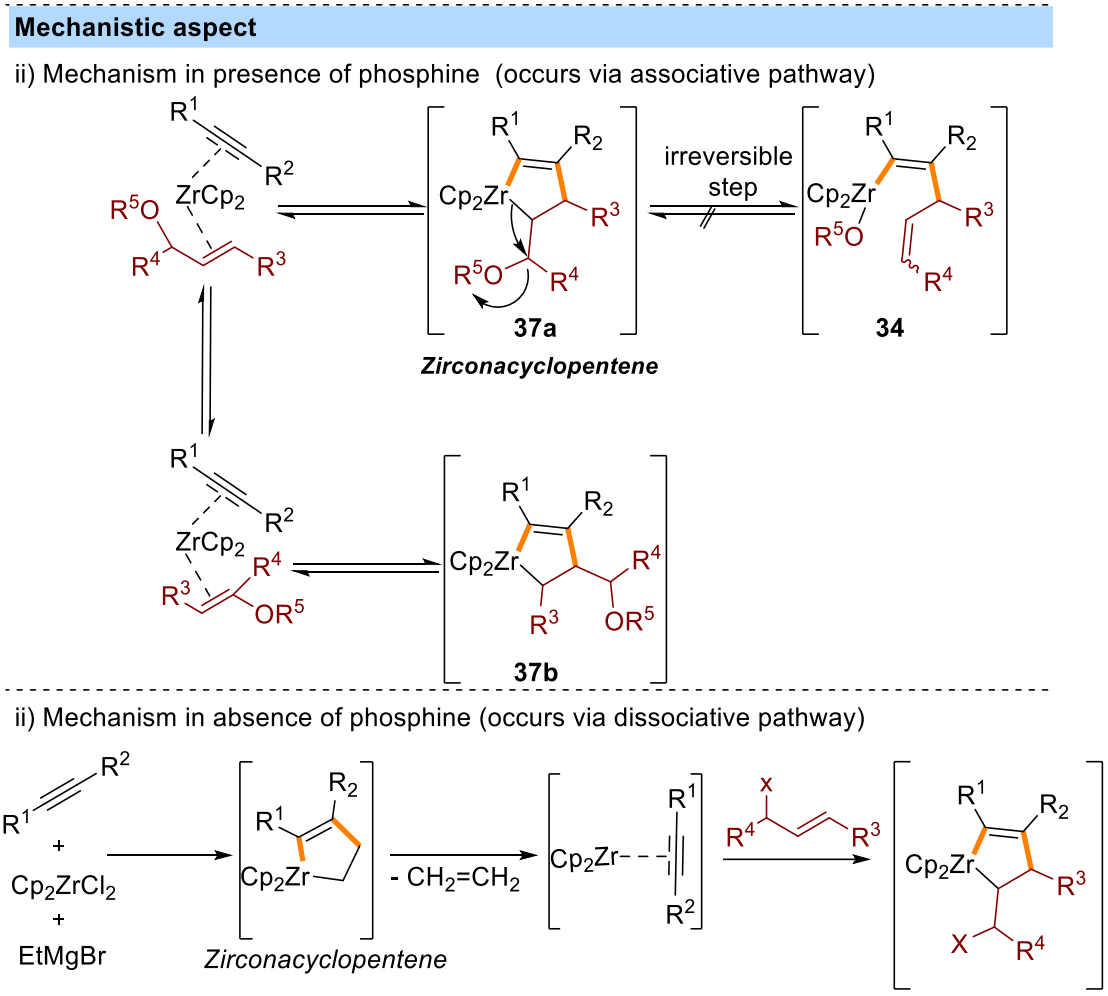

Scheme 1.18: Mechanism of allylzirconation via zirconacyclopentenes

Formation of the zirconacyclopentene intermediate is analogous to an alkyne-bound zirconocene complex, where the ethylene unit is selectively replaced by various unsaturated partners like allyl,[57] alkenyl,[57–59] alkynyl[60] variants and other functional groups.[61] For instance, Cp_2ZrEt_2 (Takahashi reagent) reacts with an alkyne to yield a zirconacyclopentene, which upon trapping with a chloroformate undergoes zircono-esterification.[62] Nishihara further adapted Takahashi's protocol using silyl-substituted allyl ethers with silylated alkynes, enabling efficient synthesis of vinyl silanes.[63]

Compared to alkylalumination, which is restricted by the nature of its alkyl groups, alkylzirconation delivers a much broader scope when applied to alkynes. Using Schwartz's reagent (Cp_2ZrHCl) to generate alkylzirconium intermediates from alkenes, this method[64] efficiently carbozirconates both terminal and internal alkynes with high regio- and stereoselectivity typically yielding the less hindered vinylzirconium isomer. However, unsymmetrical alkynes result in products with diminished selectivity.

1.1.6 Carbostannylation

Organotin reagents, while uniquely reactive, are less favored due to their toxicity and the challenge of eliminating tin residues during purification.[65] Most modern carbostannylations employ palladium or nickel catalysts to achieve *syn* additions, whereas earlier radical methods (AIBN-mediated) and lanthanum-hydride (La-H) catalysis proceed via *anti*-addition pathways, offering complementary selectivity.

1.1.6.1 Radical allylstannylation

Hosomi established an *anti*-allylstannation of alkynes using AIBN, demonstrating that electron-deficient allylstannanes significantly outperformed unsubstituted ones (**Scheme 1.20A**).[66] Terminal alkynes, both alkyl- and aryl-substituted underwent selective β-stannylation. Alkynols were also reactive, though secondary alkynols tend to form lactones unless the alcohol was protected. Internal alkynes were restricted to the electron-deficient ones (with esters via α-stannylation) yielding regioisomeric mixtures. Mechanistically, AIBN-generated stannyl radicals add to the alkyne to form vinyl radicals, which then react with allylstannane, regenerating the stannyl radical and propagating the catalytic cycle (**Scheme 1.19**).

Konno expanded allylstannations to fluoroalkylated aryl acetylenes using more electrophilic allylstannanes (ester/cyanide substituted) (**Scheme 1.20B**).[67] Remarkably, the reaction proceeded under air and reflux without AIBN. Only β-electron-withdrawing substituted allyl stannanes were effective, and reactivity declined with longer fluorinated chains. In every case, stannylation occurred α-to the fluoroalkyl group (**41**), yielding a single regio- and stereoisomer, and the resultant alkenylstannanes underwent Kosugi–Migita Stille cross-coupling to form tetrasubstituted alkenes.

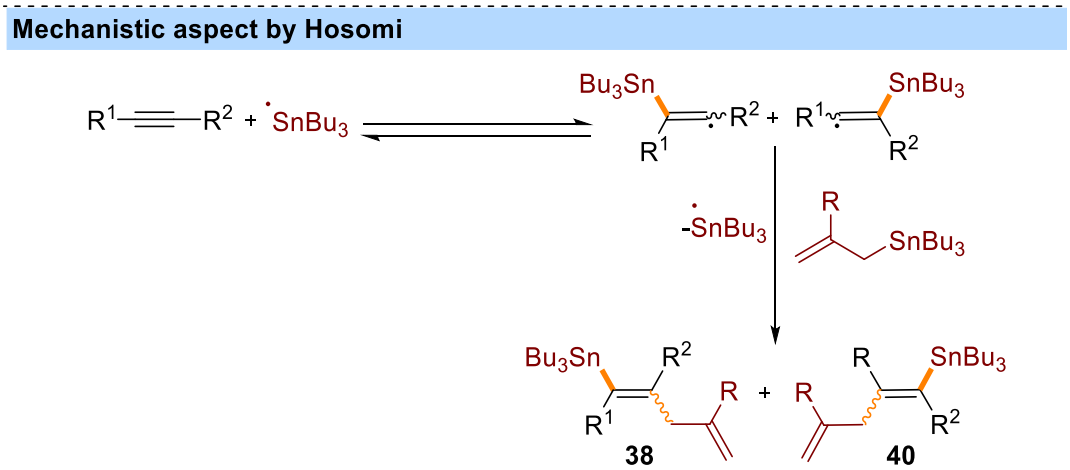

Scheme 1.19: Mechanism of radical allylstannylation

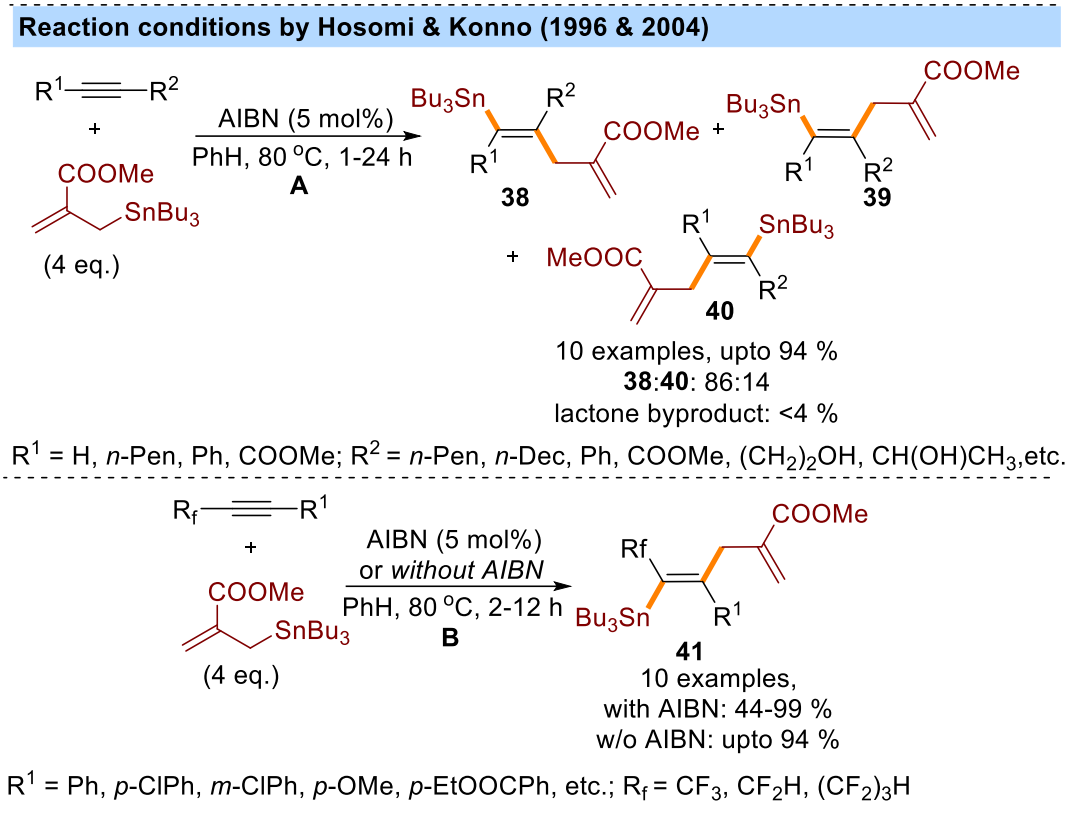

Scheme 1.20: Radical allylstannylation

1.1.6.2 Reaction of TMS-enol ethers and phenols

Yamaguchi employed tinchlorides ($SnCl_4$) for carbostannylation of terminal alkynes and silyl enol ethers (proceeding via reaction of alkynylstannanes (**44**) & α-stannyl ketones (**45**) followed by a double bond shift) (**Scheme 1.21 & 1.22**).[68] Both cyclic and acyclic silyl enol ethers selectively add to the internal carbon of the alkyne yielding *E*-isomers of the resulting enones (**42** or **43**) in good yields. However, internal alkynes did not take part in the reaction. He also demonstrated the first alkenylation of phenols to exo-alkenes (**46**) using this method.[69] By contrast, silyl acetylenes undergo stannylation adjacent to the silyl group to deliver *E*-alkenes (**47**) (**Scheme 1.23**).

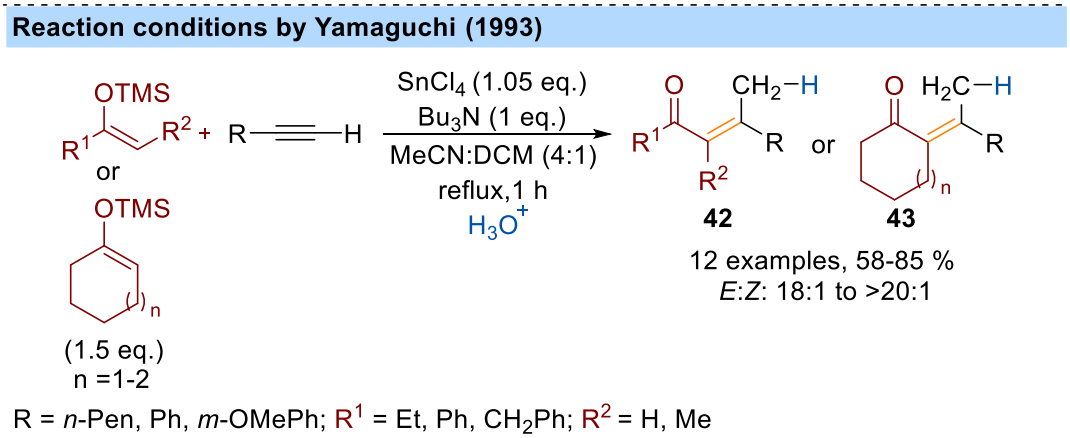

Scheme 1.21: Carbostannylation of alkynes with TMS-enol ethers

Mechanistic aspect

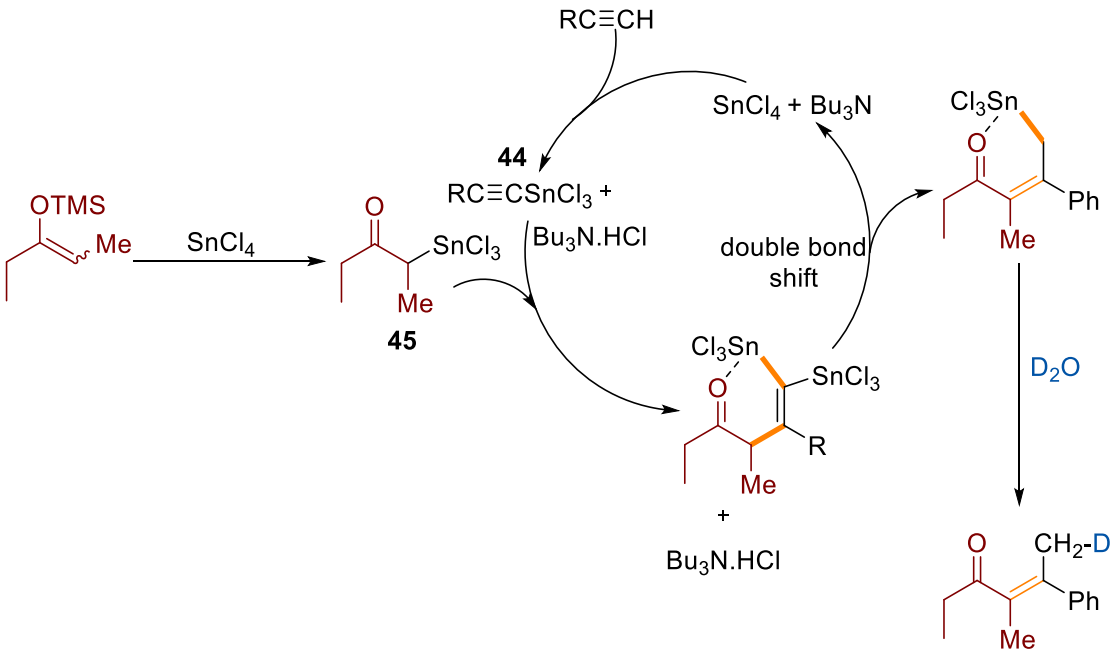

Scheme 1.22: Mechanism of carbostannylation using TMS-enol ethers

Reaction conditions by Yamaguchi (1995)

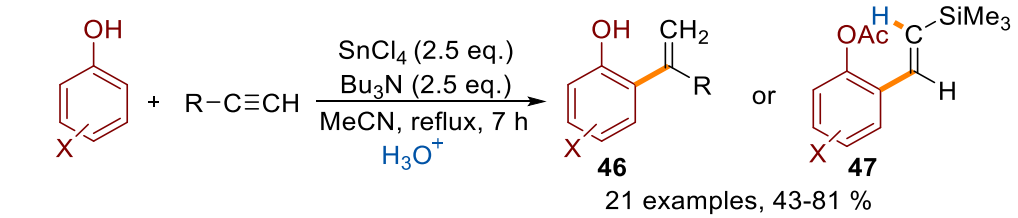

21 examples, 43-81 %

X = H, *o*, *m*, *p*-Me, *m*, *p*-OMe, *m*-Me_2N, *p*-Ph, *p*-CO_2Et *p*-^{t}Bu; R = H, *n*-Pent, $Ph(CH_2)_2$, Ph, *m*-OMePh, TMS etc.

Scheme 1.23: 1st example of direct vinylation of phenols

1.1.6.3 Catalyzed reactions

Uncatalyzed carbostannylations predominantly proceed via radical mechanisms, which often lead to mixtures of regioisomers and thus lack selectivity. This significant drawback underscores the necessity for metal-catalyzed versions (eg. Pd, Ni, La, etc.), which offers relatively superior control over both regio- and stereochemistry.

Lewis-acid mediated carbostannylations:

Yamamoto described lewis acid ($ZrCl_4$ or $EtAlCl_2$) catalyzed allylstannylation of unactivated terminal alkynes in 1999 (**Scheme 1.24**).[70] The mechanism diverges based on the alkyne type: aryl acetylenes coordinate with $ZrCl_4$ to form a zwitterionic intermediate (**50**), prompting the allylstannane to attack the opposite carbon (*anti*), producing a vinylzirconium ate complex that,

after Bu_3Sn^+ elimination and transmetallation, yields the vinylstannylated product (**48**). In contrast, alkyl-substituted alkynes form an η^2-zirconium complex (**51**), which undergoes allylation and intramolecular rearrangement (*syn*) to vinylzirconium, then transmetallates with tin (**Scheme 1.25**). The stereochemistry was unambiguously confirmed by NOE experiments. Notably, he also demonstrated that $EtAlCl_2$ can catalyze the same transformation under catalytic conditions.

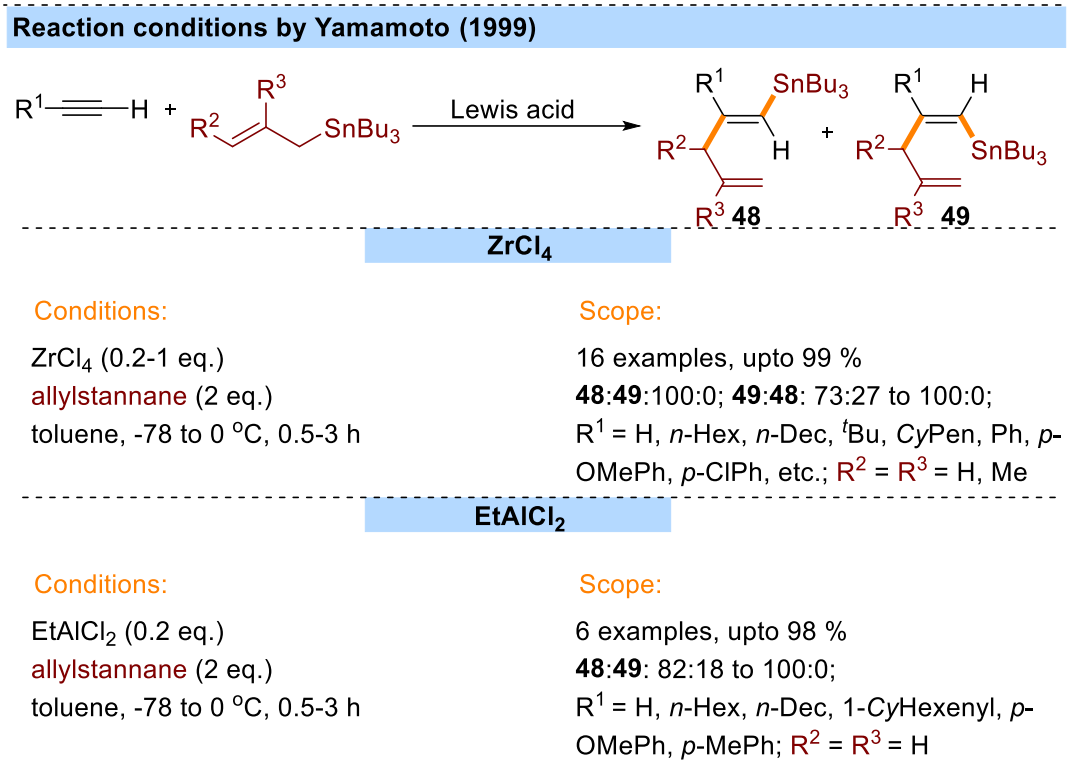

Scheme 1.24: Lewis acid catalyzed allylstannylation

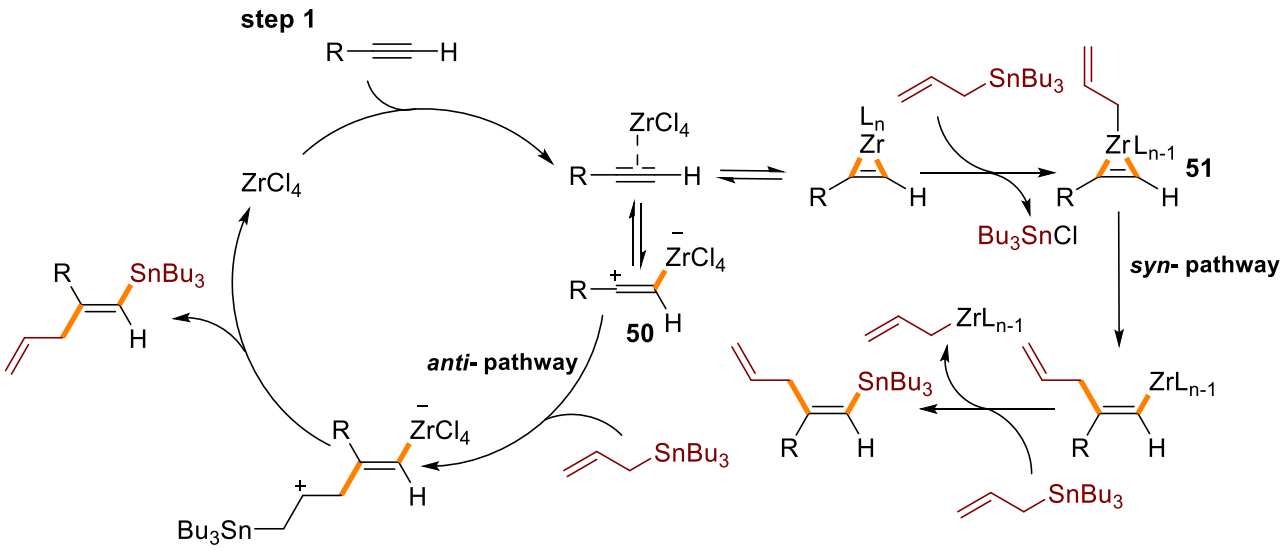

Scheme 1.25: Mechanism of Lewis acid catalyzed allylstannylatio

Palladium catalyzed alkynylstannylations:

Shirakawa utilized imino-phosphine palladium complex for *syn*-alkynylstannylation of alkynes generating enynes (**53** & **54**) efficiently (**Scheme 1.26**).[71,72] Unactivated terminal alkynes underwent preferential β-stannylation, while ester-activated terminal and internal alkynes reversed regioselectivity, albeit with minor amounts of the alternate isomers.

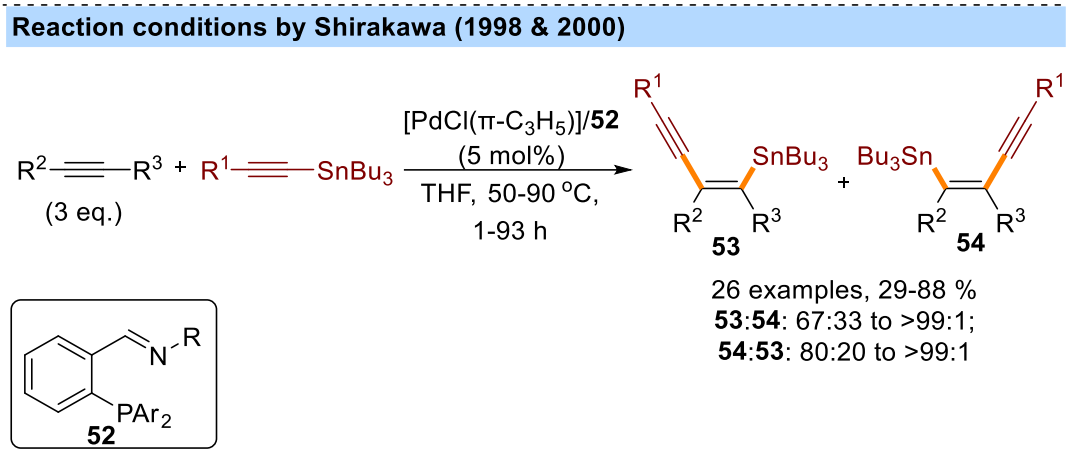

R^1 = *n*-Bu, Ph; R^2 = H, Ph, CH_2OMe, $AcHNCH_2$, Ac, CO_2Et, etc.; R^3 = H, Me; Ar = Ph; R = $(CH_2)_2Ph$, *Cy*Hex, Ph

Scheme 1.26: Pd-catalyzed alkynylstannylation

Nickel catalyzed carbostannylations:

Shirakawa advanced carbostannylations by developing Ni-catalyzed *syn*-selective protocols applicable to allyl, acyl, and alkynyl stannanes on internal alkynes, with acylstannation representing the first example of its kind (**Scheme 1.27**).[73,74] This approach smoothly transformed internal alkynes with high regioselectivity, although unsymmetrical substrates occasionally gave minor regio- and *anti*-isomers,[75] while alkynyl stannanes also stannylated unactivated terminal alkynes but failed on ester-activated or internal ones. Later, they investigated arylstannations via Pd-catalyzed *syn*-selective decarbonylative stannylation procedure using propargyl furoates and benzoylstannanes.[76] Notably, no nondecarbonylative acylstannated byproducts were obtained. In contrast using Ni-catalysts proved completely ineffective.

Lanthanum hydride (La-H) catalyzed alkynylstannylations:

Marks in 2012 presented an *anti*-selective La-H catalyzed alkynylstannylation on terminal alkynes using 2-pyridyl stannanes yielding *E*-enynes (**60**) that can be isomerized to *Z*-isomers (**62**) at high temperature (**Scheme 1.28**).[77] Sterically hindered *tert*-butyl acetylenes and disubstituted aliphatic alkynes were unreactive and other heteroaryl stannanes (furans and thiophenes) led to dimers. Mechanistically, the reaction begins with thermodynamically favoured alkynyl lanthanation (**63**) (via H_2 elimination), which triggers σ-bond metathesis of the 2-pyridyl stannane to release the active alkynylstannane species (**64**) and pyridine. This then undergoes *anti*-addition to the alkynyl–

lanthanum complex, and final protonolysis by a second alkyne equivalent yields the desired product (**Scheme 1.29**).

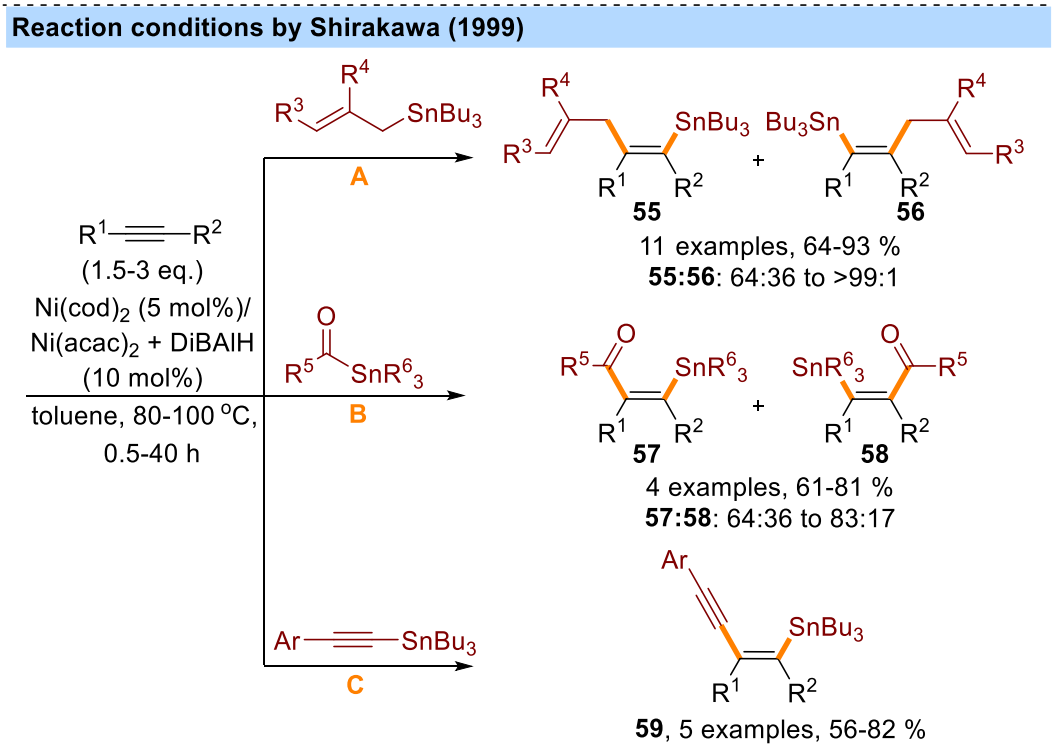

A: R^3 = R^4 = H, Me; R^1 = H, Me, *n*-Pr, *n*-Bu, *n*-Hex, TMS; R^2 = H, *n*-Pr, Ph, CO_2Et, BuC≡C
B: R^5 = Ph, $(CH_2)_5N$; R^6 = Me, *n*-Bu; R^1 = Me, *n*-Pr; R^2 = *n*-Pr, Ph
C: Ar = Ph, *o*, *p*-CF_3Ph, *p*-OMePh; R^1 = *n*-Hex, *Cy*hexenyl; R^2 = H

Scheme 1.27: Ni-catalyzed carbostannylation

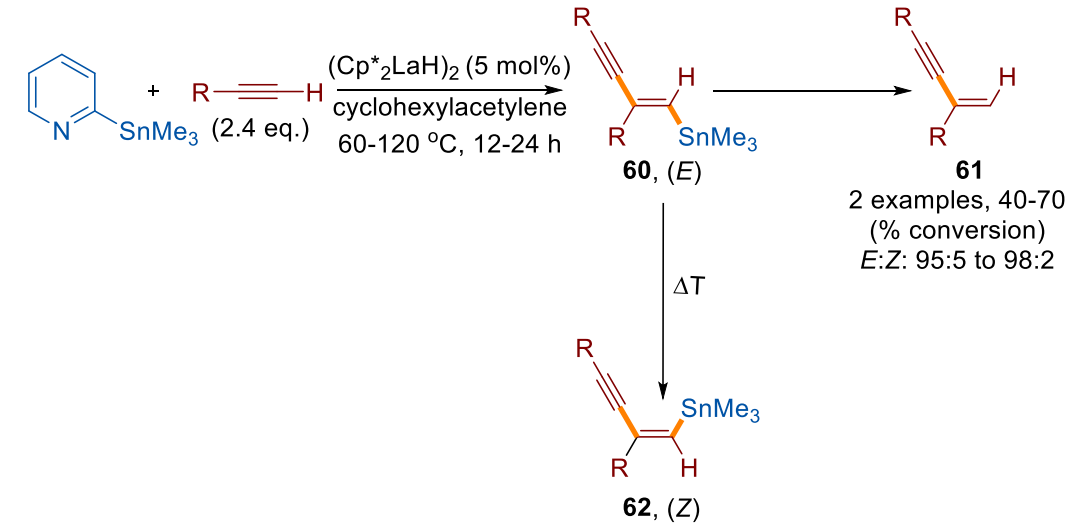

R = *n*-Bu, *Cy*Hex

Scheme 1.28: La-H catalyzed alkynylstannylation

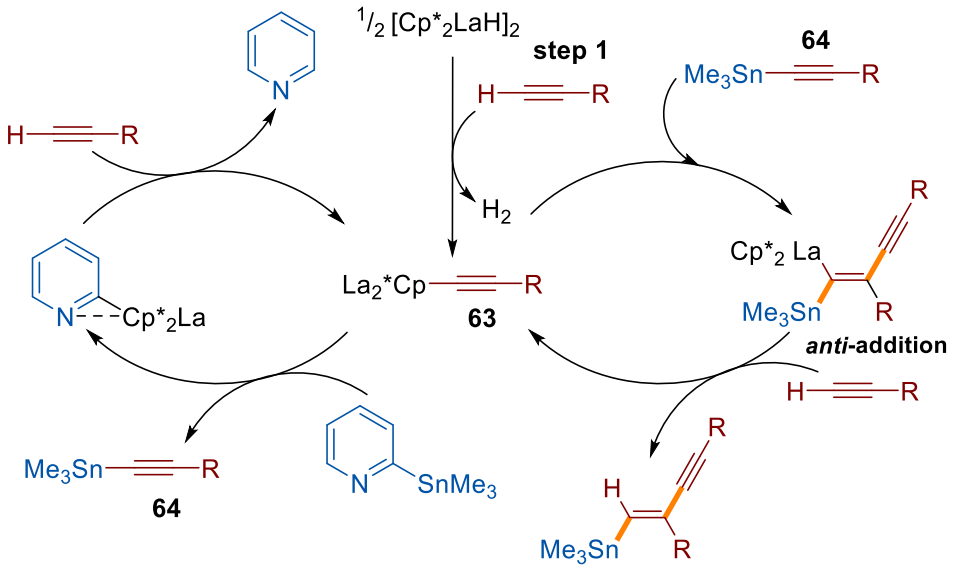

Scheme 1.29: Mechanism of La-H catalyzed alkynylstannylation1.1.7 Carbocupration

In carbocupration, organocuprates such as those derived from Grignard, (RCu·MgBr$_2$), Gilman (R$_2$CuLi·LiX), or Lipshutz reagents (RCu(CN)ZnX) undergo *syn*-selective addition to alkynes, affording substituted olefins.[78] The alkynes may be either activated by adjacent heteroatoms/functional groups or remain unactivated. The regioselectivity of addition is strongly influenced by the type of solvent and the substituents adjacent to the triple bond: depending on their nature, the process can favor either linear (α-cupration) or branched (β-cupration) products.[79]

1.1.7.1 Organocupration of functionalized alkynes

Extensive studies have been reported on the carbocupration of activated alkynes, including substrates such as alkoxy-substituted alkynes,[80–82] alkynyl carbamates,[83] sulfonyl ynamides,[84] ynamines,[79] alkynyl phosphines,[85,86] phosphine oxides,[87] phosphonates/fluorinated phosphonates,[88,89] as well as alkynyl sulfides,[90–92] sulfoxides,[93,94] and sulfones.[95] A detailed discussion of these systems, however, lies beyond the scope of this review.

1.1.7.2 Reactivity of propargyl and higher derivatives of alkynes

Ma and Lu reported that propargyl alcohols (secondary & tertiary) react with copper and Grignard via α-cupration to yield linear alkenes (**Scheme 1.30**),[96] while Normant presented β-cuprations in remote TMS-protected alkynes,[97] yielding branched products (**Scheme 1.31**). The method was also tolerant to substrates bearing other heteroatoms, acetal derivatives at the remote position, although minor amounts of linear products and dimers were also formed. The less stable the vinylcopper species, the greater the yield of **67**, stabilization by heteroatoms decreases in the order S > N > O > Br. They extended the organocuprate additions to alkynyl acetals/ketals which resulted in linear or branched products depending on cuprate structure, solvent, and polarization.[98] THF promoted linear, Et$_2$O favoured the branched product while the presence of bulky cuprates lose

selectivity, leading to mixtures. Controlling the temperature suppresses β-elimination observed majorly with magnesium cuprates.

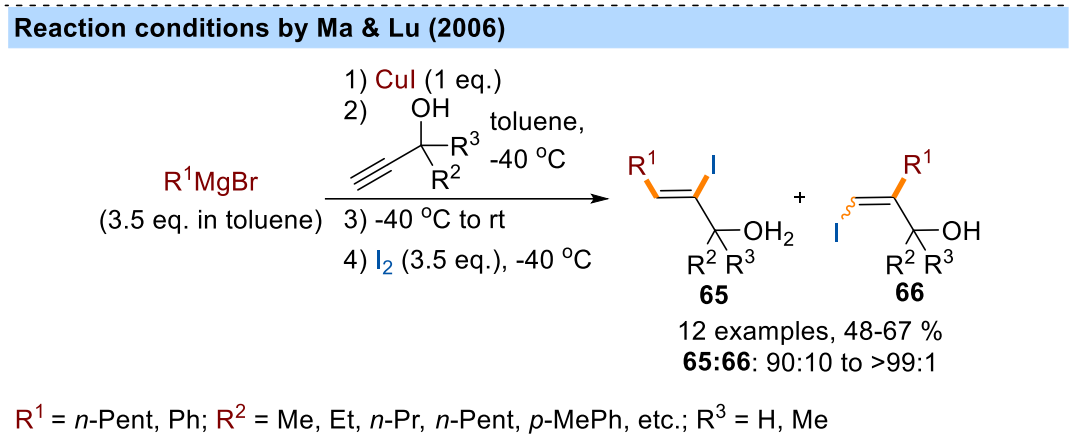

Scheme 1.30: Reaction of propargyl alcohols with magnesium cuprates

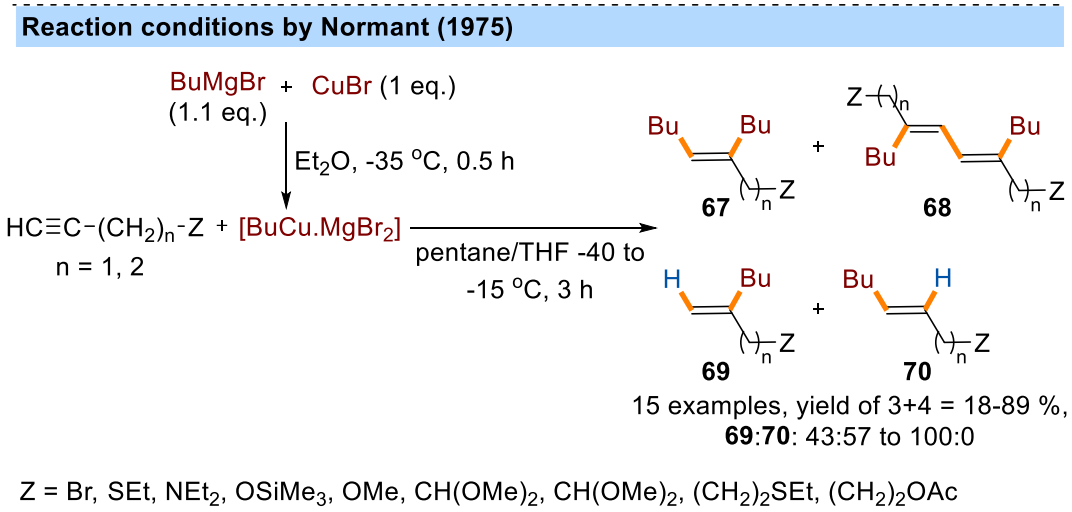

Scheme 1.31: Reaction of activated alkynes with magnesium cuprates

The addition of polyfluorocuprates to CF_3-substituted alkynes also proceeds in a *syn*-fashion, preferentially yielding the *E*-configured alkenes.[99] In contrast, Marshall showed that alkynyl epoxides react via S_N2' pathway to form allenyl alcohols (**71**) by *anti*-substitution (**Scheme 1.32**).[100]

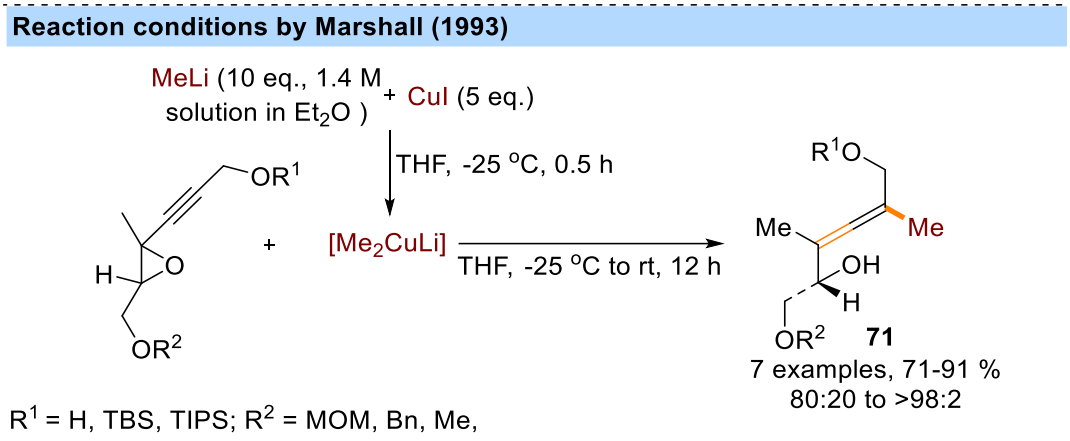

Scheme 1.32: Reaction of alkynyl epoxides with lithium cuprates

1.1.7.3 Organocupration of Unactivated alkynes

Normant and Knochel reported that lithium, magnesium and zinc derived organocuprates add to terminal and internal alkynes through *syn*-addition and β-cupration (Markovnikov), yielding branched alkenes (**Scheme 1.33**).[101–103] Reactions with internal alkynes often produce regioisomeric mixtures.[78] Primary alkyl groups transfer efficiently; however, secondary and tertiary alkyl cuprates can induce deprotonation. This side reaction may be mitigated by adding $MgBr_2$.[104]

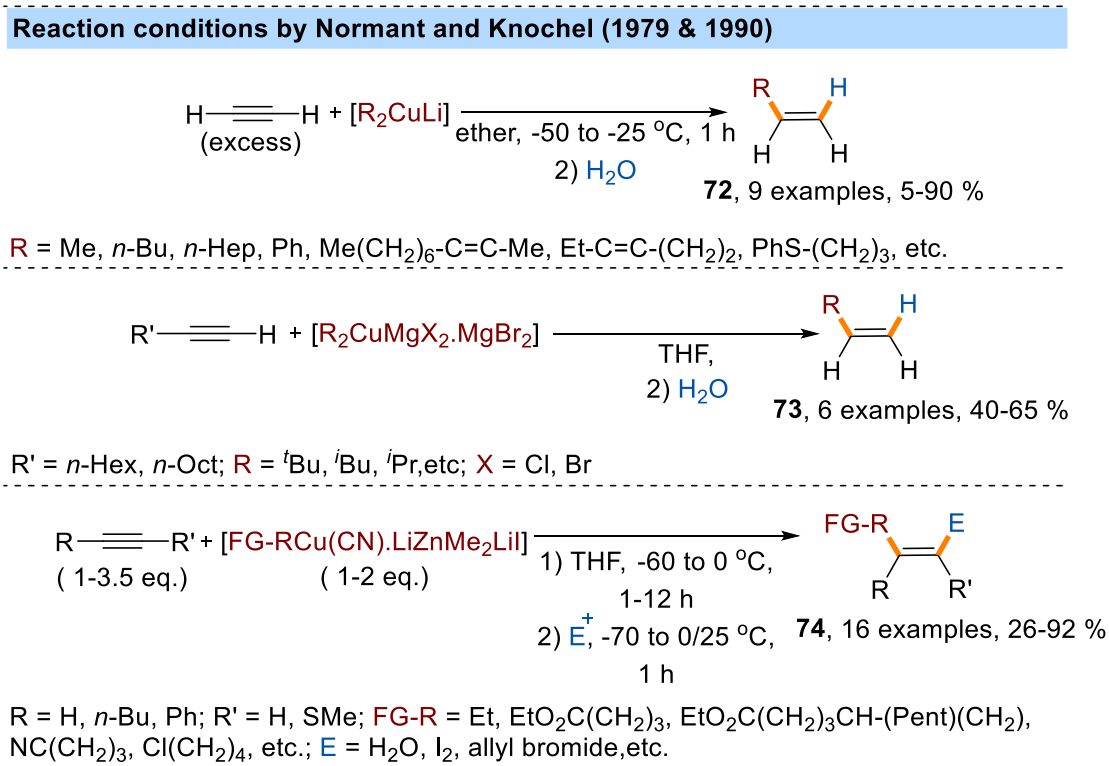

Scheme 1.33: Organocupration using Li, Mg, Zn derived organocuprates

α-Silylated cuprates and alkynes require additives (LiI or $P(OEt)_3$) to stabilize organocuprate species (**Scheme 1.34B**), while addition of LiBr, for α-silylcupration on terminal alkynes tends to induce formation of dimers.[105,106]

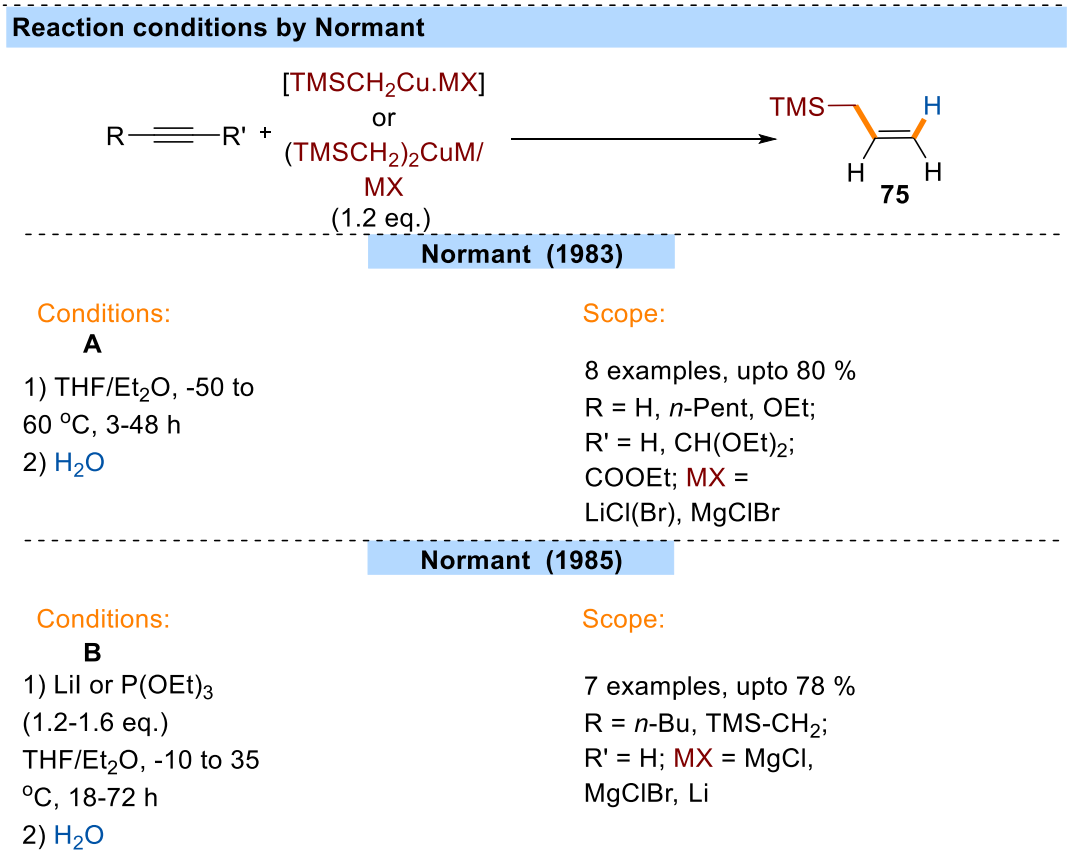

Scheme 1.34: Reactions using α-Silylated cuprates and alkynes

In contrast to terminal alkynes, Utimoto and Meijer demonstrated that trimethylsilyl and triarylsilyl substituted acetylenes undergo α-cupration, whereas monosubstituted TMS-alkynes do not participate in the reaction.[107,108]

Sterically hindered cuprates (e.g., *t*-Bu₂CuMgBr) efficiently react with protected alkynyl ketones as demonstrated by Schneider, affording alkenes in excellent yields, however, the *syn* addition often gives regioisomeric mixtures and minor *anti*-isomers.[109]

While structural characterization of organocopper clusters remains elusive, a plausible mechanism proposed by Nakamura involves initial oxidative addition to form a Cu(III) cluster, followed by reductive elimination to generate alkenyl lithium, and final transmetallation to the alkenyl copper species (**Scheme 1.35**).[110–112] These methods have enabled high stereochemical control in natural product synthesis and pheromone assembly via *syn*-selective carbocupration.[113–115] The alkenyl cuprates formed can act as versatile intermediates for various transformations.[116]

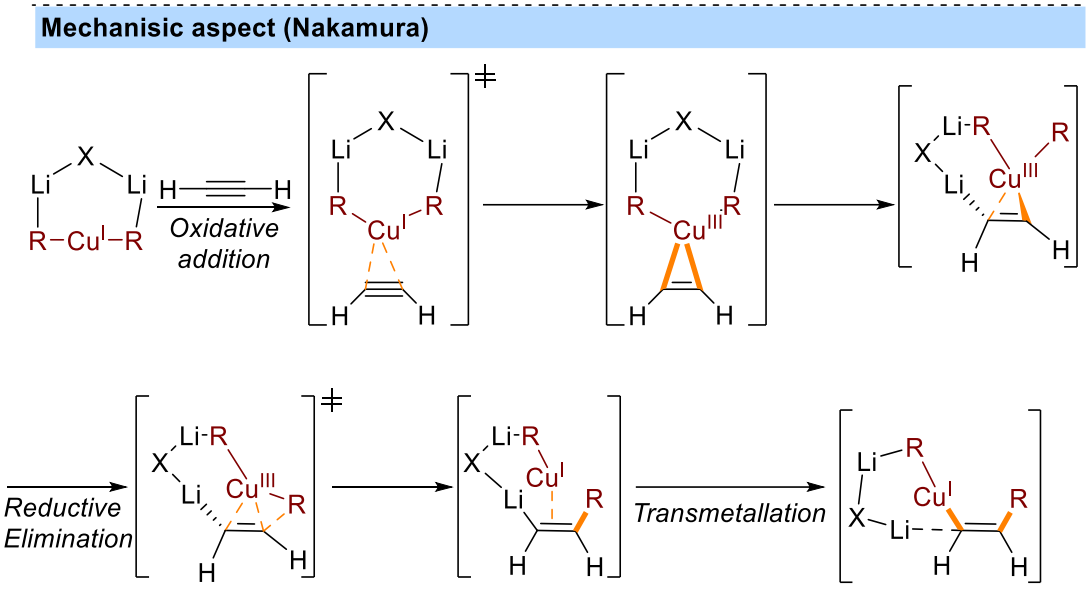

Scheme 1.35: Mechanism of organocupration of alkynes

1.1.8 Carbozincation

1.1.8.1 Uncatalyzed carbozincations

Organozinc reagents are typically unreactive towards alkynes without catalysis yet early studies revealed notable exceptions.[117] Miginiac demonstrated that under reflux in THF, sterically hindered di-*tert*-butylzinc adds to terminal aliphatic alkynes via α-zincation, giving regioselective but stereorandom *E*/*Z* mixtures (**Scheme 1.36A**).[117,118] However, addition to phenylacetylene (in Et_2O) proceeds via *anti*-carbozincation to yield a single *Z*-isomer. The selectivity successfully extended to terminal enynes to generate 1,3-dienes. Later, Knochel showed that slow addition of functionalized allylzinc bromide under sonication to propargyl and homo-propargyl alkynes achieves β-zincation, affording 1,4-dienes (**Scheme 1.36B**) in excellent yields without deprotonation; homopropargyl amines also undergo regioselective allylzincation, albeit with stereochemical mixtures (**Scheme 1.36C**).[119] In these reactions involving terminal substrates, deprotonation to form propargylic zinc intermediates precedes β-addition, often leading to 1,1-dimetallated species as observed in propargylic amines by the formation of dideuterated diene product.[120] Additionally in some cases mono and bis-addition products are also observed.[117]

1.1.8.2 Carbozincation of functionalized alkynes

Carbozincation of activated alkynes, including sulfur-,[121–124] nitrogen-,[125–130] and carbonyl-substituted systems,[131] has been extensively explored; however, a comprehensive discussion of these studies is beyond the scope of this review.

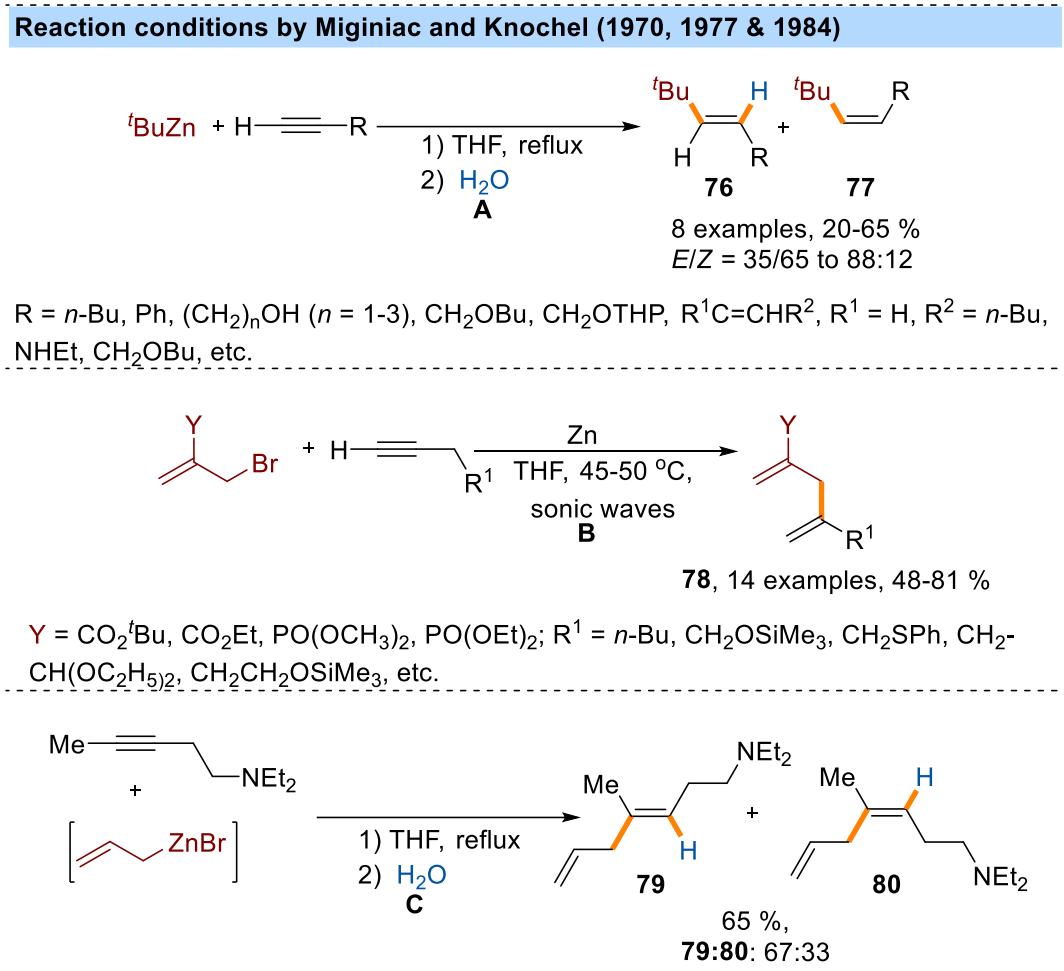

Scheme 1.36A-C: Uncatalyzed carbozincations of alkynes

1.1.8.3 Carbozincation of unfunctionalized alkynes

Catalyzed reactions

Negishi reported the first example of Zr-catalyzed alkylzincation (using Cp_2ZrCl_2) of unactivated alkynes (terminal & dialkyl alkynes) giving tri-/tetrasubstituted alkenes, via *syn*-addition (β-zincation) (**Scheme 1.37**).[132] This method was extended to allylzincation using diallyl- and dicrotylzinc derivatives.[120] When symmetric dialkyl alkynes were treated with catalytic Cp_2ZrCl_2/EtMgBr, a pathway diversion through zirconacyclopentenes (**83**) occured, which on transmetallation with Et_2Zn, gave 2-zincoethyl zinc intermediate (**84**) (**Scheme 1.38**).[133] The latter is also reported for 1-alkynyl phosphines and alkynyl amines leading to corresponding alkenes with high selectivity.[134–136] Analogous reactions using catalytic $Ti(OPr^i)_4$ proceeding via titanocyclopentenes are reported in 1-alkynyl phosphine sulfides.[137]

Reaction conditions by Negishi (1983)

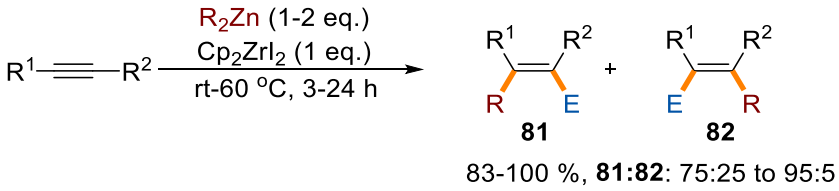

R^1 = *n*-Bu, *n*-Hex; R^2 = H, *n*-Bu,$SiMe_3$; R = Me, Et, allyl, crotyl; E = H, I

Scheme 1.37: Zr-mediated alkylzincation of alkynes

Mechanistic aspect of reaction following zirconacyclopenetene pathway

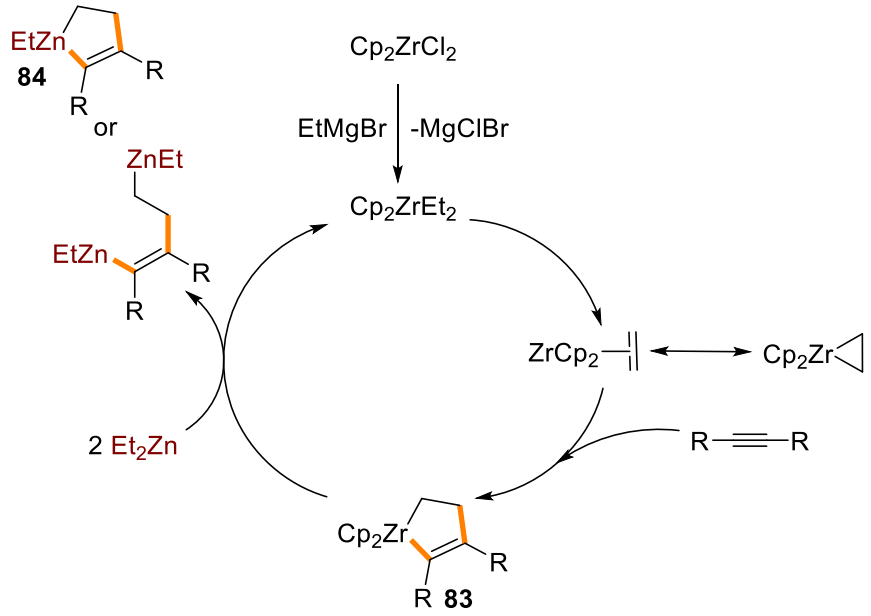

Scheme 1.38: Formation of zinconacyclopentene

Zhu introduced Fe-catalyzed vinylzincations (α-metallation) of terminal alkynes using Fe with a tridentate 1,10-phenanthrolinimine ligand (**85**), delivering dienes in excellent *syn*-selectivity (>95:5); absence of the ligand led to unselective carbozincation and polymerization.[138] The method displayed broad scope, tolerating various heteroatom-substituted substrates. Later, internal alkynes employed $FeCl_2$-bis(imino)pyridine systems (**86**) gave similarly impressive outcomes (**Scheme 1.39**).[139]

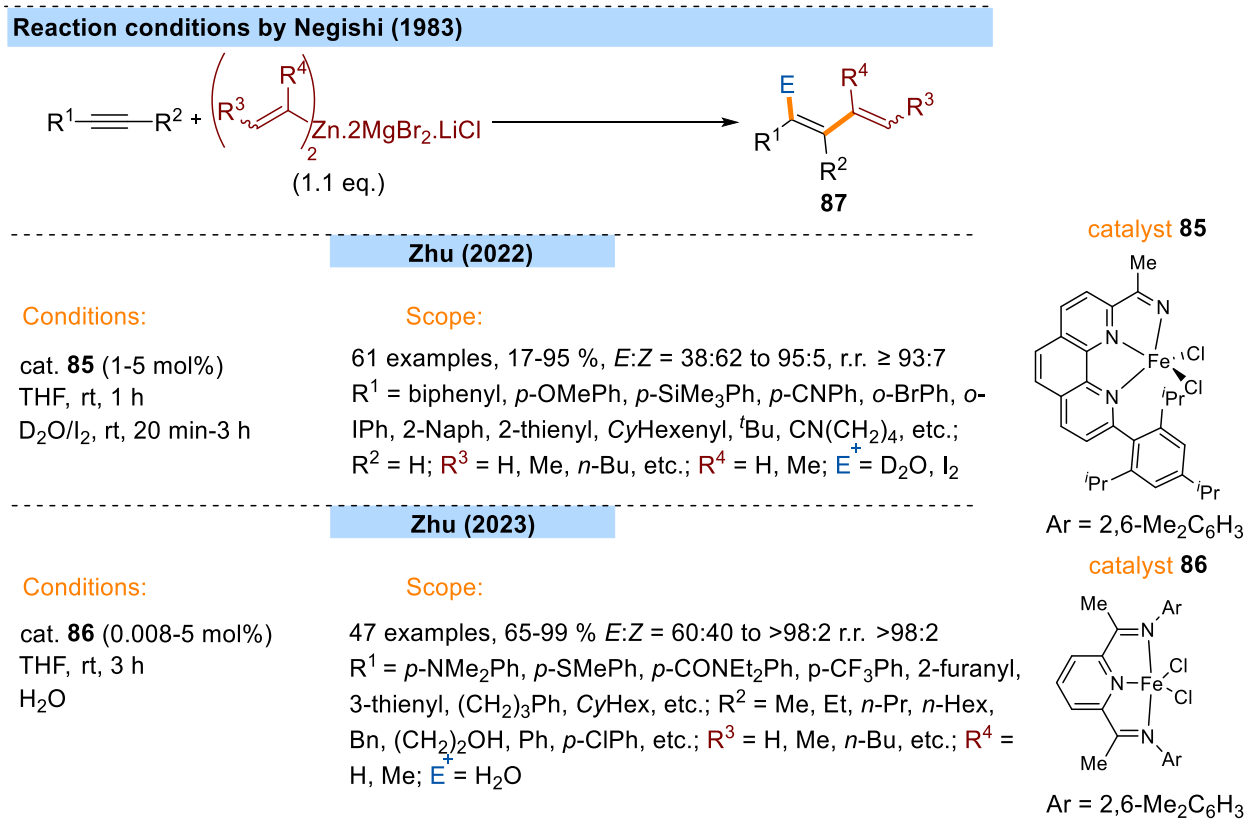

Scheme 1.39: Fe-catalyzed vinylzincation of alkynes

The Hu group pioneered a novel radical iron- catalyzed reductive coupling of aryl acetylenes with secondary and tertiary alkyl iodides, employing $FeBr_2$/ I_2/ Zn to deliver *Z*-disubstituted alkenes (*Z*:*E* = ~7:1–50:1) in good yields (**Scheme 1.41**).[140–142] The method accommodates various aryl substituents (e.g., NMe_2, CF_3, SMe, thiophenyl, halides) but shows reduced efficiency and stereoselectivity with strongly electron-deficient substrates. Mechanistically, Zn reduces Fe(II) to Fe(I), which activates the alkyl iodide to generate alkyl radicals; this adds to the alkyne, forming vinyl radical that forms the *anti*-organoiron (α-ferration) intermediate (**89**) which is transmetallated by $ZnBr_2$ to give the *anti*-carbozincated product (**Scheme 1.40**). Notably, this radical-Fe strategy was also adapted to the synthesis of Z-alkenylboronates (**90**) using $Fe(OTf)_2$ and Me_3SiI (**Scheme 1.42**).

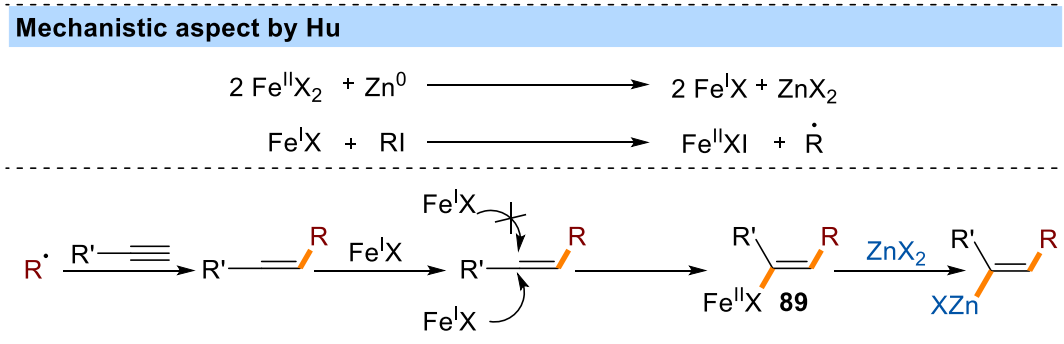

Scheme 1.40: Mechanism of *Anti*-alkylzincation of alkynes (radical route)

Reaction conditions by Hu (2015)

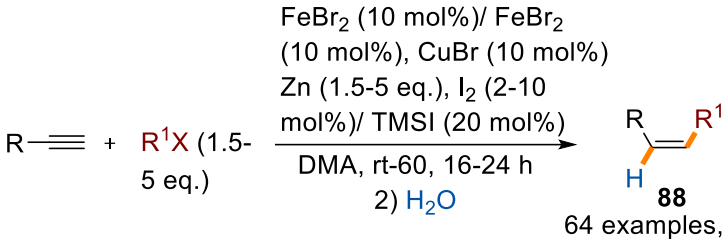

64 examples, 32-90 %
Z:*E* = 4:1 to >50:1

R = Ph, *p*-NMe_2Ph, *p*-SMePh, *p*-OMePh, ^{t}BuPh, 3-pyridyl, Ph, etc.; R^1 = *n*-Hept, *Cy*Pent, *Cy*Hex, *Cy*Hept, ^{t}Bu, 4-tetrahydro-2*H*-pyranyl, $(CH_2)_6CN$, Bn, $(CH_2)_2$OPh*p*-OMe, etc.; X = Br, I, OTs

Scheme 1.41: *Anti*-carbozincations of alkynes

Reaction conditions by Hu (2019)

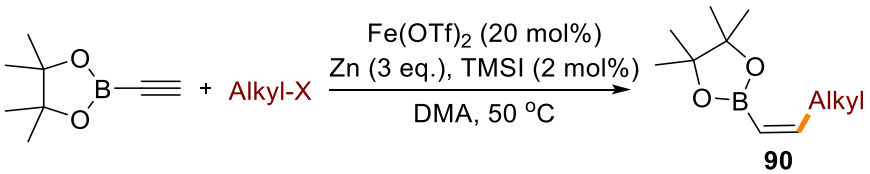

18 examples, upto 98 %
Z:*E* = 7:1 to 44:1

Alkyl = ^{t}Bu, *Cy*Hex, 4-^{t}Bu*Cy*Hex, 1-Ad, *n*-Dec, CPh_2CN, etc.; X = Br, I

Scheme 1.42: Alkylzincation of alkynyl boronates

In a series of seminal studies, Oshima and colleagues pioneered cobalt-catalyzed regio- and stereoselective carbozincation of alkynes. They first showcased $CoCl_2$-catalyzed *syn*-allylzincation of internal alkynes using allylzinc bromide, enabling the synthesis of dienes (**91**), however, homopropargyl alcohols yielded regioisomeric mixtures (**Scheme 1.43**).[144]

Reaction conditions by Oshima (2004)

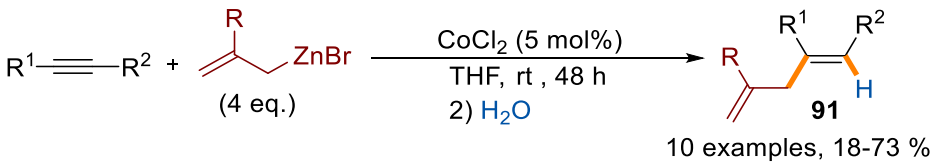

10 examples, 18-73 %

R^1 = *n*-Hex, Ph; R^2 = *n*-Pent, Ph, *p*-OMePh, *p*-ClPh, *p*-FPh, *p*-CF_3Ph, 3,5-$(CF_3)_2$Ph, CH_2CH_2OMe, R = H, Me

Scheme 1.43: Co-catalyzed allylzincation of alkynes

This work expanded to the first $CoBr_2$-catalyzed arylzincation, employing ArZnI·LiCl, which delivered α-selective addition onto unsymmetrical aryl-alkyl alkynes with excellent regio- and stereocontrol, though dialkyl and terminal alkynes gave poor yields and ~1:1 regioisomer

mixtures.[145] Corpet improved the method using $CoBr_2$(bipy) and aryl bromides, efficiently converting phenylacetylenes and sterically hindered alkynes while dialkyl substrates still led to mixtures (**Scheme 1.44**).[146]

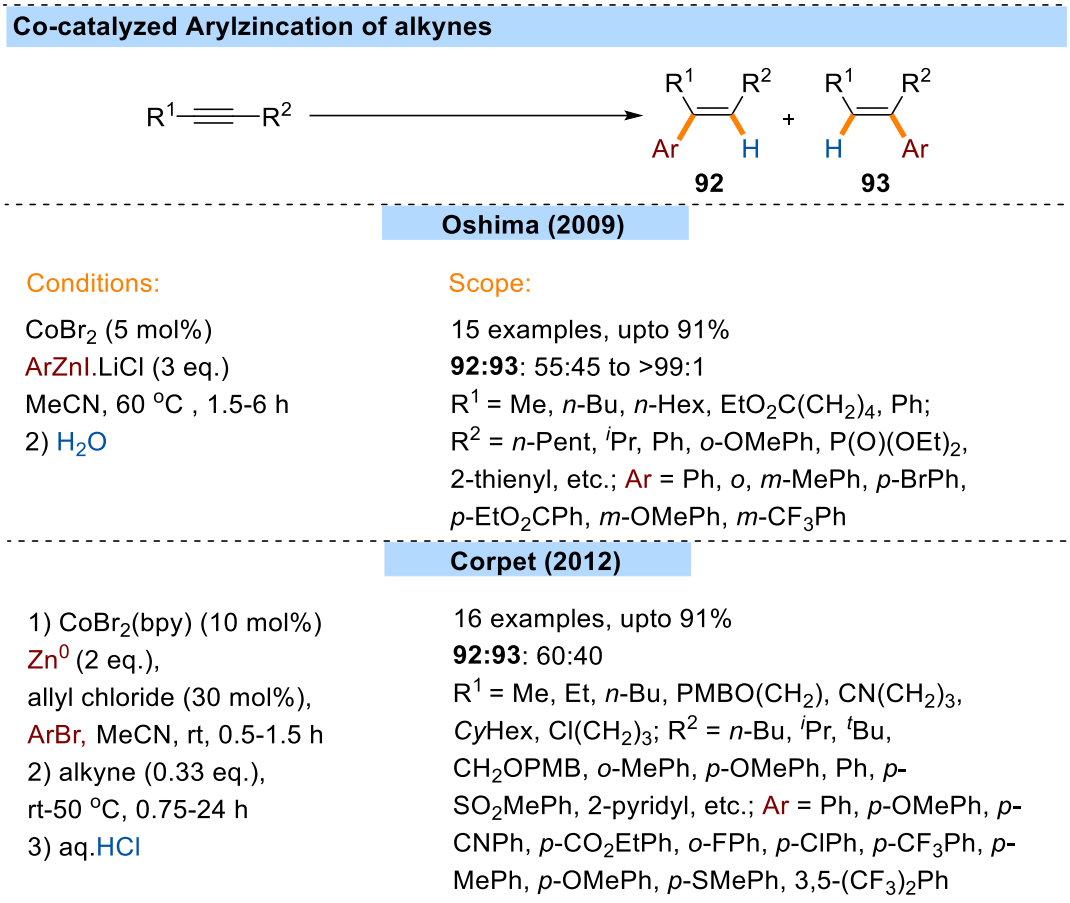

Scheme 1.44: Co-catalyzed arylzincation of alkynes

Oshima further extended the strategy to benzylzincation, achieving high regioselectivity on terminal alkynes, while unsymmetrical dialkyl substrates and electron-poor aryls remained challenging (**Scheme 1.45**).[147]

Tsuji introduced a notable Co-mediated carboxyzincation of internal alkynes, forming acrylic acid derivatives via a cobaltacycle intermediate (**95**) and subsequent ZnX_2 transmetallation (**Scheme 1.46**). Electrophilic quenching gave products in yields up to 82%, though no product was obtained with H_2O as the electrophile.[148]

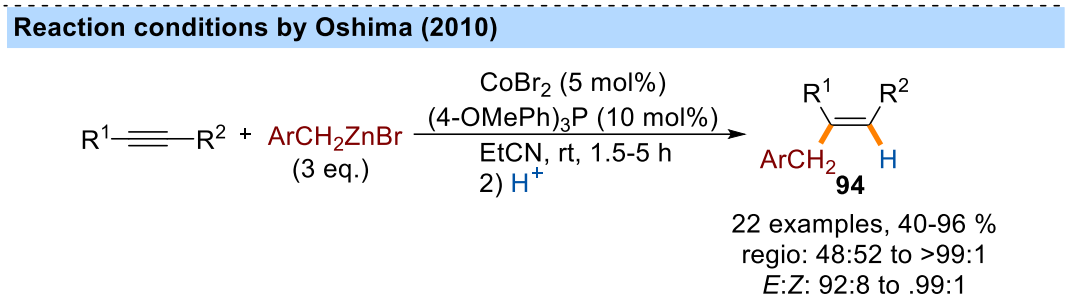

Scheme 1.45: Co-catalyzed benzylzincation of alkynes.

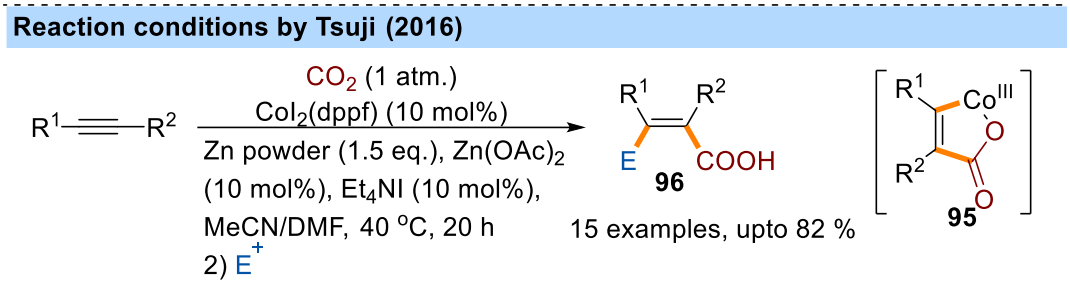

Scheme 1.46: Co-catalyzed carboxyzincation of alkynes

Knochel unveiled Ni-(II) catalyzed alkyl zincation of internal alkynes, achieving α-selective methyl and ethyl zinc additions on aryl–alkyl acetylenes with moderate efficiency (**Scheme 1.47**).[149,150] Although, increasing the alkyl chains results in regioisomeric mixtures and hydrometallated byproducts, with trimethylsilyl substituted phenyl acetylene, zinc was preferentially installed α to the TMS group (**98**).

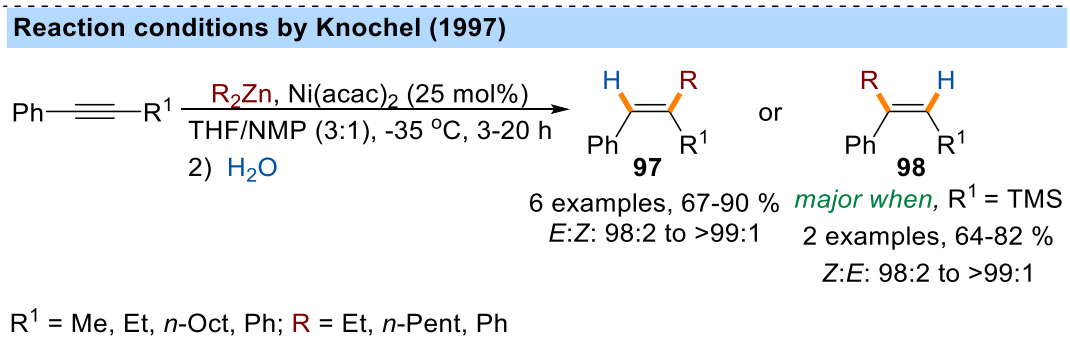

Scheme 1.47: Ni-catalyzed alkylzincation of alkynes

The method was further applied to phenylzincation, delivering tetrasubstituted alkenes with excellent stereoselectivity (**Scheme 1.48**). To reduce the excess of diphenylzinc, a mixed reagent system (Ph_2Zn + Et_2Zn, generating PhZnEt) was employed and notably, phenylbutyne underwent exclusive phenylzincation, showcasing high chemoselectivity.

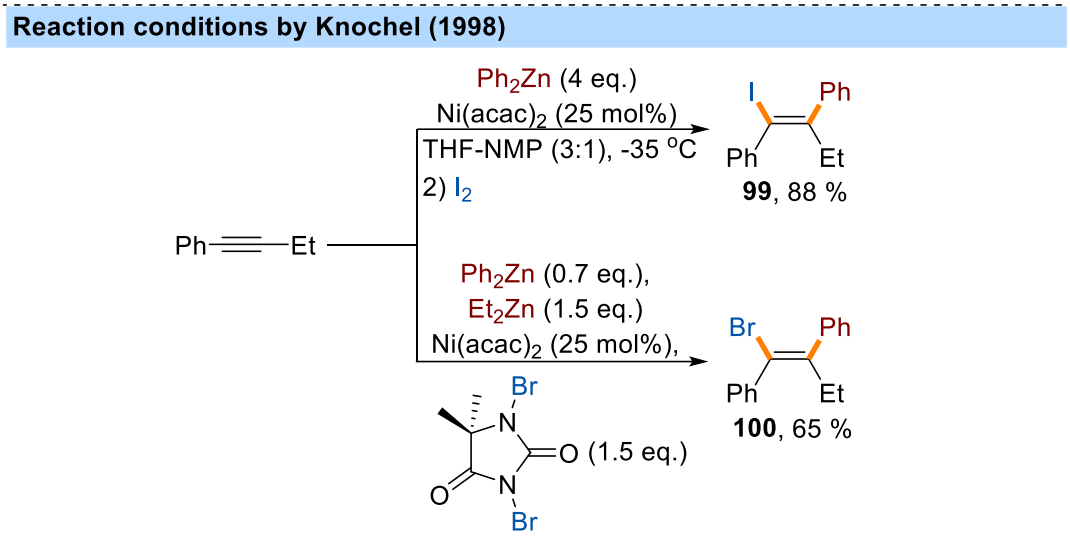

Scheme 1.48: Ni-catalyzed phenylzincation of alkynes

Hayashi described Rh-catalyzed arylzincation of unfunctionalized, symmetrical alkynes employing ArZnCl and catalytic $ZnCl_2$ (**Scheme 1.49**). The selectivity of the reaction is highly ligand specific with cycloocta-1,5 diene (cod) generating predominantly the desired alkene with small amounts of 1,4 migration byproduct (**102**) with ratio of parent product to migration byproduct ranging from (~1:1 to > 99:1).[151]

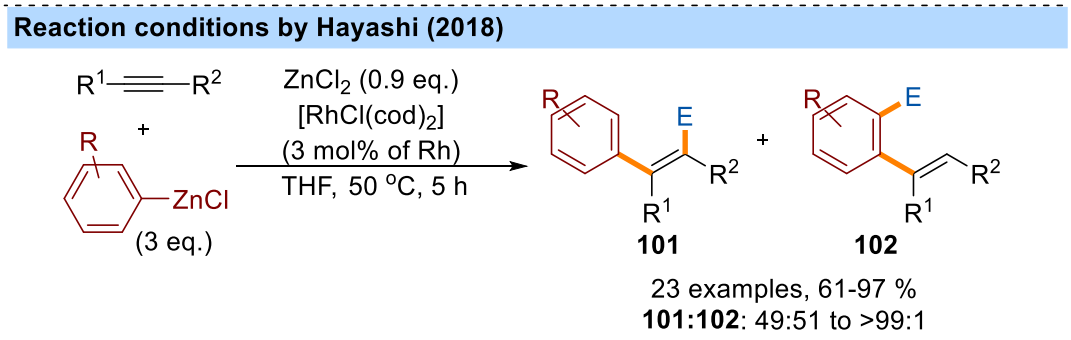

R^1 = Me, Et, *n*-Pr, *n*-Pent, *n*-Hep, ^{i}Pr, Ph; R^2 = *n*-Pr, *n*-Pent, *n*-Hep, Ph, *p*-tol, $CH_2CMe(CO_2Et)_2$, CH_2TMS; Ar = 3,5-$(OMe)_2$Ph, Ph, *p*-tol, *p*-NMe_2Ph, *m*, *p*-Me_3SiPh, *p*-FPh, *p*-CF_3Ph, *m*-OMePh, etc.; E = D_2O or I_2; E = D, I

Scheme 1.49: Rh-catalyzed arylzincation of alkynes

1.1.9 Carbomagnesiation

Carbomagnesiation of alkynes involves the addition of Grignard reagents across carbon–carbon triple bonds to form alkenylmagnesium species.[152,153] These typically add in an *anti*-fashion, resulting in controlled stereochemical patterns of the product. In contrast many transition metal-catalyzed processes, proceed via *syn* addition.[65] Such transformations can occur through intra- or intermolecular pathways,[154,155] providing rapid access to highly substituted alkenes in a single operation, thus offering broader utility in synthesis.

1.1.9.1 Intramolecular carbomagnesiation of alkynes

Intramolecular carbomagnesiation involves a system where the organomagnesium site and the alkyne are tethered within the same molecule, enabling cyclization.[156] The reaction generally occurs via addition of the *in situ* generated nucleophile within the same molecular framework, often resulting in high regio- and stereoselectivity in the product (**Scheme 1.50**). Transition metal catalysts enhance this process by increasing the electrophilicity of the alkyne, thereby accelerating the nucleophilic addition.

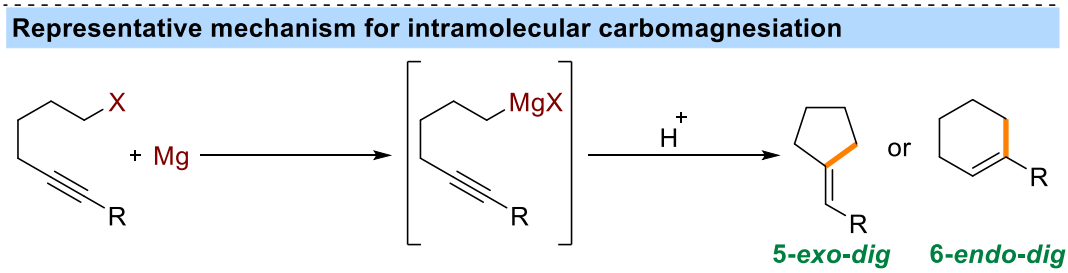

Scheme 1.50: General mechanism for intramolecular carbomagnesiation

1.1.9.1.1 Uncatalyzed reactions

Early studies on intramolecular *syn*-carbomagnesiation include Dessy's work, which employed *o*-iodophenyl-substituted tolane for the synthesis of benzylidenefluorene (**Scheme 1.51**).[157]

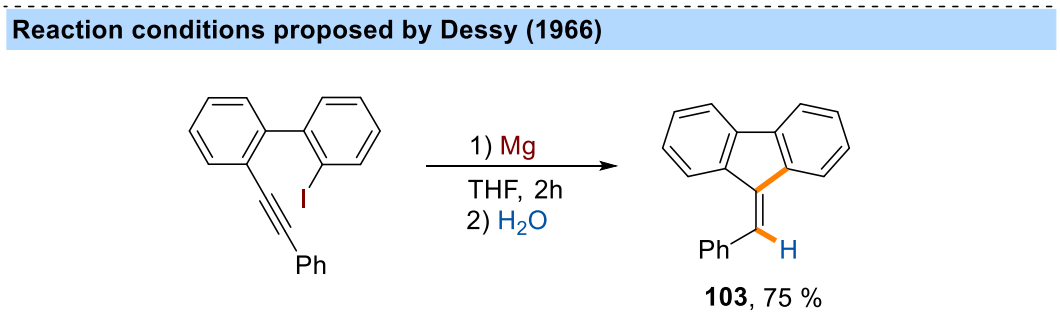

Scheme 1.51: *Syn*-carbomagnesiation of *ortho*-tethered diphenylacetylene

Richey and Rothman developed the synthesis of ethylidenecyclopentane from primary and secondary alkynyl halides by preparing the Grignard *in situ* (**Scheme 1.52**).[158] They observed a marked preference for forming five-membered rings (*5-exo-dig* cyclization) rather than six-membered rings (*6-endo-dig*). Secondary substrates yielded mixture of isomers. They attributed this selectivity to a concerted bond-forming mechanism, wherein the reactive carbon approaches along the axis of a *p*-orbital at a carbon of the triple bond, facilitating the formation of the five membered ring product. Then, Utimoto demonstrated the use of TMS-substituted primary and secondary alkynyl halides, affording exocyclic alkenes, favouring five- and six-membered rings over four membered ones (**Scheme 1.53**).[159]

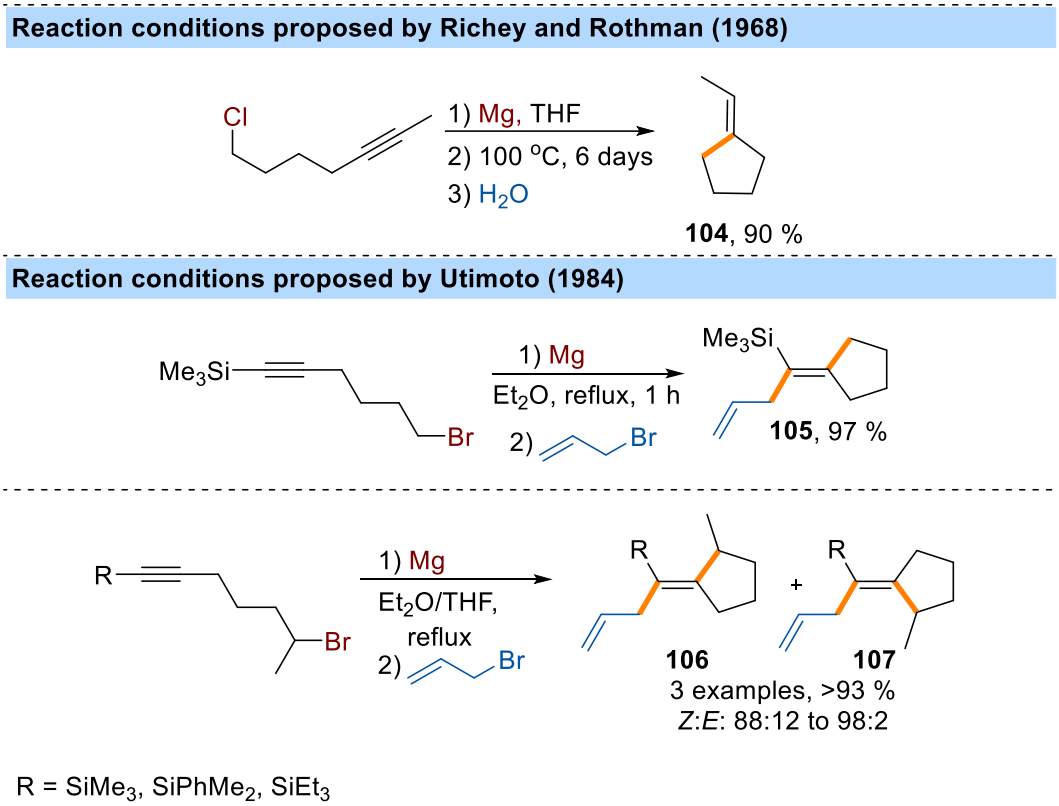

Scheme 1.52 & 1.53: Uncatalyzed carbomagnesiation of halogen-tethered alkynes

1.1.9.1.2 Catalyzed reactions

Crandall and colleagues for the first time developed a CuI-catalyzed ring-closure method with alkylmagnesium bromides and tethered internal alkynes generated from appropriate primary alkyl iodides (**Scheme 1.54**).[160] The addition of CuI substantially accelerated the reaction, underscoring the key role of transition-metal catalysis in enhancing efficiency.

Nobuaki Kambe and coworkers presented an *anti*-selective silver mediated carbomagnesiation of *δ*-haloalkylacetylenes utilizing secondary Grignard reagents proceeding via *5-exo-dig* cyclization (**Scheme 1.55**).[161] Iodides performed better than bromides while the acetal derivatives of the alkynyl halides gave a mixture of stereoisomers.

Reaction conditions proposed by Crandall (1975)

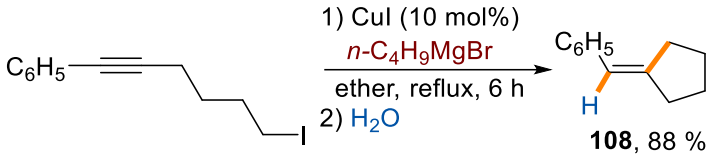

Scheme 1.54: Cu-catalyzed *anti*-carbomagnesiation of alkynes

Reaction conditions proposed by Kambe (2011)

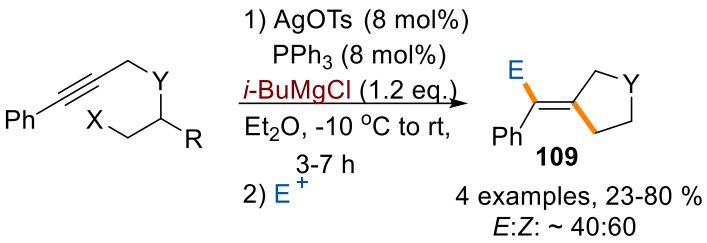

Y = CH_2, O; X = I, Br; E: H, COOH, D

Scheme 1.55: Ag-catalyzed *anti*-carbomagnesiation of alkynes

In 2012, Knochel's group developed a copper-mediated method using alkynyl(aryl)thioethers and benzothiophenes with a turbo-Grignard reagent to synthesize functionalized benzo[b]thiophenes and benzo[b]thieno[2,3-d]thiophenes.[162] While more sensitive substrates required stoichiometric amount of copper, activated propargyl derivatives reacted without any copper source. Under conventional conditions the reaction typically took 24 hours, but microwave irradiation reduced the time to just one hour. This approach was later extended to ynamides,[163] yielding functionalized indoles and azaindoles (4-, 5-, 6-, and 7-azaindoles). In 2024, Nairoukh further advanced the field by reporting a regio- and stereoselective synthesis of aza-spiro-piperidine derivatives through copper-mediated alkylmagnesiation of ynamides followed by Lewis acid-promoted cyclization.[164]

1.1.9.2 Intermolecular carbomagnesiation of alkynes

Intermolecular carbomagnesiation of alkynes is typically less reactive than the intramolecular pathways and often require elevated temperature (e.g., reflux) or the assistance of transition metal catalysts. Transition metals, particularly Ni, Cu, Fe, Ag, Zr and Cr play a crucial role by activating the alkyne π-bond and promoting the nucleophilic addition.[154] Both activated alkynes, bearing electron-withdrawing or directing groups, and unactivated alkynes, which lack such substituents, can serve as suitable substrates.

1.1.9.2.1 Uncatalyzed reactions

The initial observations in this area were reported by Ishino, Salvador, and Ichikizaki in the 1950s. Independent studies by Richey and Rein (1969) and Eisch and Merkley revealed that under reflux conditions, alkynols promote Grignard additions through hydroxyl coordination, enhancing

reactivity and stereoselectivity.[165,166] Richey and Rein demonstrated the addition of vinyl and allyl Grignard reagents yielding *trans*-dienols from propargyl and homopropargyl alcohols.

Later, A. De Silva reported the *anti*-selective addition of alkyl, homoallyl, and phenyl Grignard reagents to 1,4-difunctionalized alkynes such as alkynyl diols, monoethers, diethers, and amino alkynols/ethers predominantly yielding *E*-substituted alkenes (**Scheme 1.56**).[167] Minor amounts of allenols (**111**) were observed as side products in some cases. Alkynyl amino ethers exhibited lower reactivity compared to alcohol derivatives, and their reactions with sub-stoichiometric Grignard reagents led to increased formation of allenes (**114**). The authors proposed that the presence of an additional hydroxyl group facilitates the stabilization of the vinyl magnesium intermediate (**115**) by coordination through the Lewis basic oxygen atom (**Scheme 1.57**). This strategy was later applied by Kocienski (1994) for regio- and stereoselective (homo)allylmagnesiation in the synthesis of manoalide derivatives.[168]

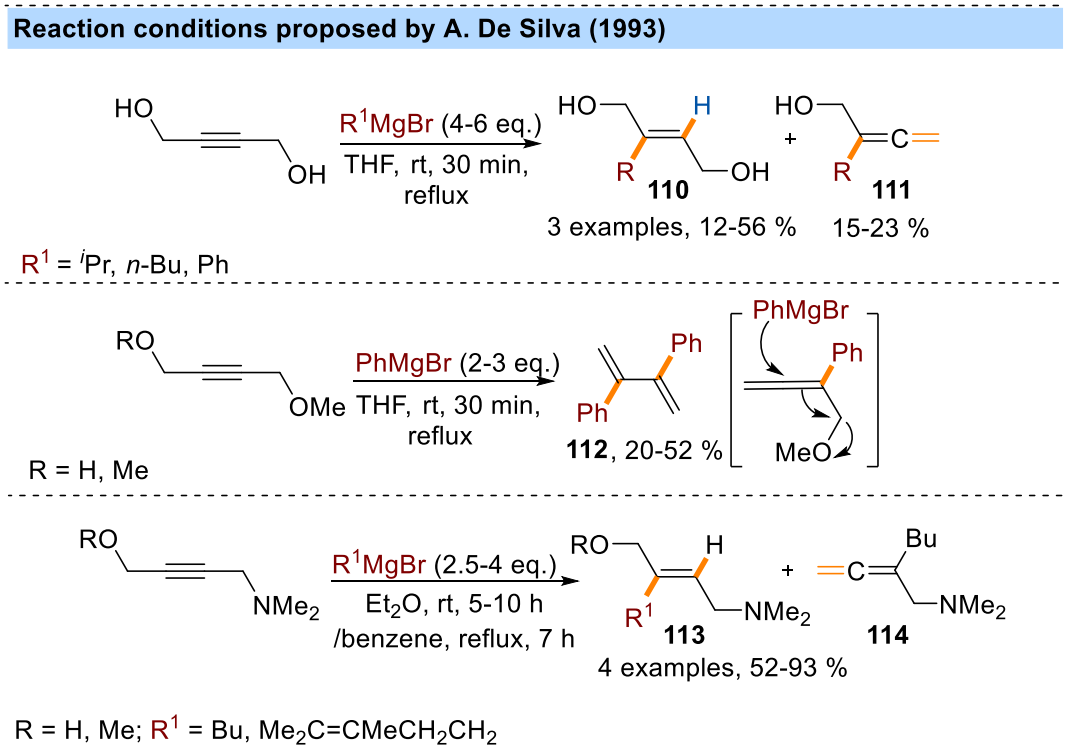

Scheme 1.56: Uncatalyzed *anti*-selective carbomagnesiations

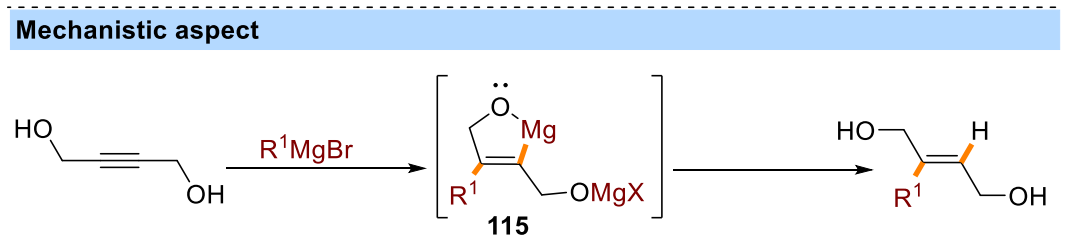

Scheme 1.57: Mechanism of *anti*-selective carbomagnesiation

A.G. Fallis later applied this strategy in 1996 and 2000 for vinyl and alkynyl magnesiation of primary propargyl alcohols using vinyl and TMS-substituted magnesium chlorides to synthesize dienes and enynes and subsequently applied it to synthesize tetrasubstituted alkenols via carbomagnesiation followed by one-pot Pd-catalyzed cross-coupling with aryl halides.[169–171] In 2005, his group further utilized propargyl alcohol derivatives from bicyclic and fused-ring ketones for vinyl magnesiation, affording trienes that underwent 6-π electrocyclic ring closure/aromatization under reflux or could be quenched with electrophiles in a one-pot process.[172]

Building on this foundation, F. Conrad Engelhardt et al. (2006) demonstrated a five-step synthesis of the anti-inflammatory prodrug rofecoxib, highlighting a key regio- and stereocontrolled arylmagnesiation of phenyl-substituted propargyl alcohols using a sacrificial reagent (MeMgCl).[173]

1.1.9.2.2 Catalyzed reactions

Reactivity of activated alkynes:

Uncatalyzed reactions with alkynes often require harsh conditions and frequently lead to unwanted side products such as allenes. These drawbacks highlight the need for transition-metal catalyzed strategies, which can offer milder conditions, improved regiocontrol, and enhanced functional group tolerance.

In light of these limitations, J. Meijer in 1974 demonstrated that copper catalysts enable *syn*-selective alkyl and aryl magnesiation of 1-alkynyl sulfides, affording *trans*-alkenyl sulfides in excellent yields.[174] A similar approach was achieved by B. Jousseaume in 1977 for magnesiation of alkynyl amines.[175]

Xie and Xian reported a *syn*-selective phenylmagnesiation of acetylenic sulfones using CuCN to yield *E*-configured vinyl sulfones (**116**) (confirmed by NOE), which were then electrophilically trapped (e.g., with allyl bromides or alkynyl iodonium salts) to afford tetrasubstituted dienes and enynes in good yields (**Scheme 1.58A**).[176] Building on this, Xie and Wang explored both phenyl- and allyl-magnesiation of acetylenic sulfones under CuCN catalysis **(Scheme 1.58B)**.[177] The resulting vinyl-sulfone Grignard intermediates were trapped with aldehydes to yield allylic alcohols (**117**) and 1,4-dienes (**118**), the latter as stereoisomeric mixtures. Mechanistic studies revealed contrasting addition modes: phenylmagnesiation followed an *anti*-addition pathway (supported by X-ray crystallography, despite lower-quality crystals), whereas allylmagnesiation proceeded via *syn*-addition as evidenced by NOESY analysis. In a subsequent study, Xie expanded on this methodology by developing a one-pot, three-component coupling of acetylenic sulfones, aryl/alkyl/allyl Grignard reagents, and α,β-unsaturated carbonyl compounds, delivering sulfonyl-substituted diallylic alcohols (**119**) regio- and stereoselectively in moderate yields (**Scheme 1.58C**).[178]

Reaction conditions proposed by Xie (2003, 2005, 2016)

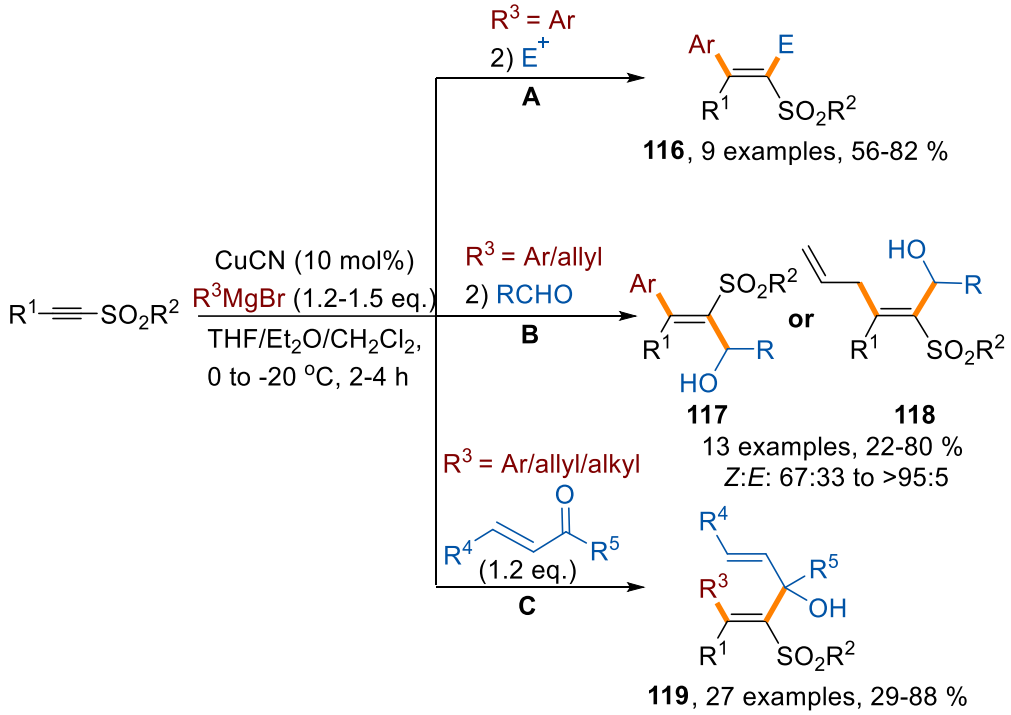

A: R^1 = Ph, *n*-Pent; R^2 = Ph, tol; R^3 = Ph, *p*-Me-Ph; E = H, allyl, alkynyl iodoniumtosylate
B: R^1 = Ph; R^2 = tol; R^3 = Ph, *p*-Me-Ph, allyl; R = *n*-Pr, Ph, *p*-ClPh, *p*-OMePh, *p*-NO_2Ph, *p*-$(CH_3)_2$NPh, PhCH=CH
C: R^1 = *n*-Bu, Ph; R^2 = tol, R^3 = Et, *n*-Bu, Bn, allyl, Ph; R^4 = Ph, *p*-ClPh, *p*-OMePh, *p*-NO_2Ph; R^5 = H, Me, Ph

Scheme 1.58: Cu-catalyzed carbomagnesiation of alkynyl sulfones

Xie developed a Cu(I)-catalyzed carbomagnesiation of acetylenic ketones with alkyl or aryl Grignard reagents, yielding tetrasubstituted allylic alcohols via subsequent addition to carbonyl moiety of the starting material (**Scheme 1.59**).[179] Reactions with non-identical groups at alkyne terminus and in Grignard reagent produced stereoisomeric mixtures.

Reaction conditions proposed by Xie (2011)

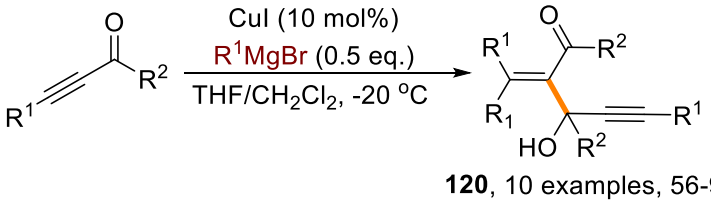

R^1 = R^1= *n*-Bu, Ph; R^2 = *n*-Pr, Ph, *p*-ClPh, *p*-OMePh, *p*-NO_2Ph, 2-furyl, 2,4-$(CH_3O)_2$Ph

Scheme 1.59: Cu-catalyzed carbomagnesiation of ynones

K. Oshima and colleagues reported copper-catalyzed carbomagnesiation of allyl-substituted ynamides, where primary Grignard reagents gave high yields, unlike secondary and aryl variants (**Scheme 1.60**).[180] The resulting intermediates (**121**) underwent Claisen-aza rearrangement to afford 4-pentenenitriles (**122**) with moderate efficiency. Although carbocupration was also explored, the copper-catalyzed carbomagnesiation provided superior results.

Reaction conditions proposed by Oshima (2007)

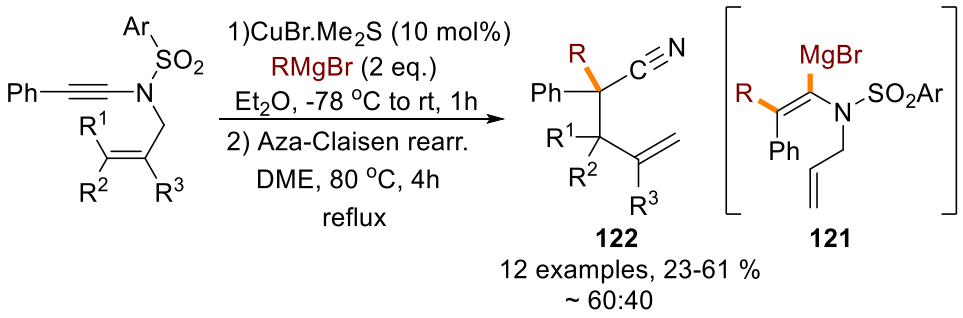

122 **121**

12 examples, 23-61 %

~ 60:40

$R^1 = R^3$ = H, Me; R^2 = H, Me, Ph; R = Et, *n*-Bu, *i*-Pr, *t*-BuCH_2, Ph; Ar = *p*-MePh, *p*-FPh,

Scheme 1.60: Cu-catalyzed carbomagnesiation of allyl-substituted ynamides

Reactivity of propargyl and higher derivatives of alkynes

In 1979, Duboudin and Jousseaume examined CuI for additions of Grignard reagents to propargyl alcohols, noting that hydroxyl groups favor *anti*-addition, while increased steric hindrance in tertiary alcohols shifts the reaction toward *syn*-addition.[181] Tertiary alcohols often yield unstable intermediates prone to decomposition into allenes. The reactivity also depended on the reagent's nature (reducing vs. non-reducing), highlighting the reaction's complexity. Negishi later applied this methodology to synthesize exocyclic alkenes from primary propargyl alcohols.[182] The Doboudin group reported a Cu-catalyzed, *anti*-selective allylmagnesiation/intramolecular *5-endo-trig* cyclization of metalated propargyl alcohols (**123**) to access cyclopentene derivatives (**Scheme 1.61**).[183] This strategy was later adopted by the Deng group for the stereocontrolled synthesis of 4-substituted 1,2-oxaborol-2(5H)-ols (**125**), which served as intermediates in Suzuki–Miyaura cross-coupling reactions (**Scheme 1.62**).[184]

In comparison, J. Ready and co-workers developed an iron-catalyzed *syn*-selective alkyl/aryl magnesiation of primary and secondary propargyl and homopropargyl alcohols, yielding predominantly *Z*-allylic and homoallylic alcohols (**Scheme 1.63**).[185] MeMgBr and EtMgBr, however, led to dimethylated and hydrogenated side products, respectively.

Reaction conditions proposed by Duboudin (1979)

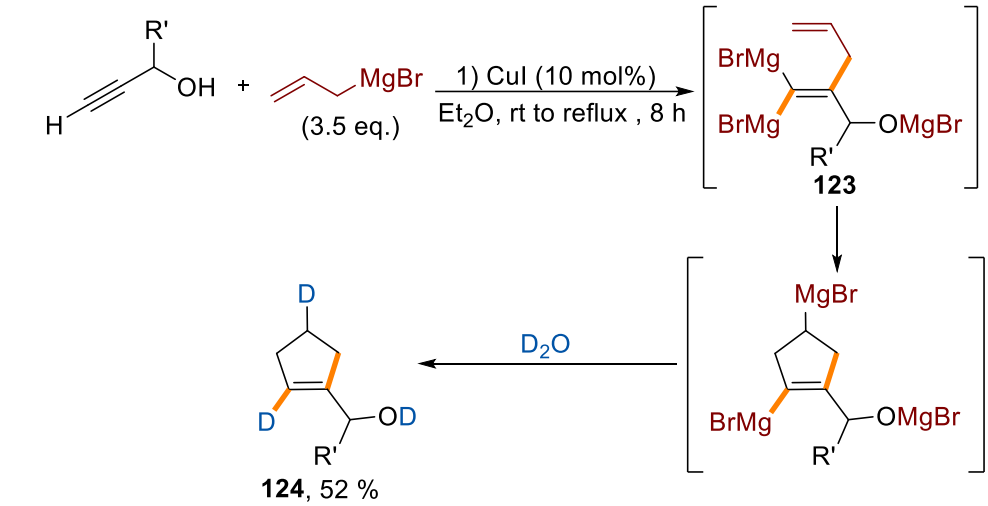

R' = H, Me

Scheme 1.61: Cu-catalyzed *anti*-carbomagnesiation-cyclization

Reaction conditions proposed by Deng (2006)

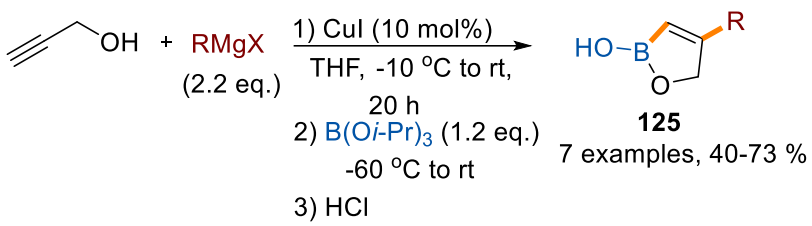

R = Et, *n*-Pr, *n*-Bu, ^{i}Pr, ^{i}Bu, Ph

Scheme 1.62: Synthesis of 4-substituted 1,2-oxaborol-2(5H)-ols using *anti*-carbomagnesiation-cyclization

Reaction conditions proposed by Ready (2006)

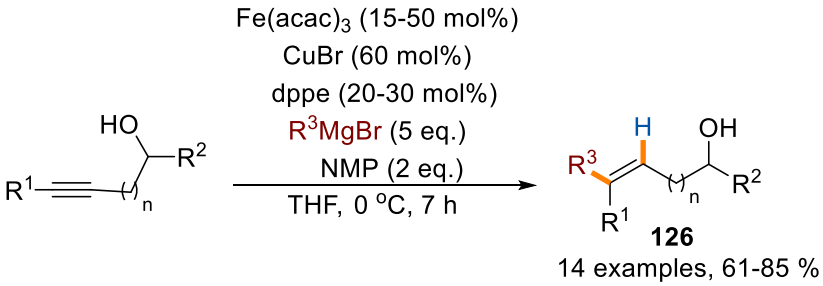

R^1 = *n*-Bu, *n*-Hex, *n*-decyl, $TBSO(CH_2)_4$, $BnO(CH_2)_3$, $Ph(CH_2)_2$, etc.;
R^2 = H, Me, *n*-Bu, $BnOCH_2$, Me_2CH; R^3 = Me, Et, Ph; n = 0-1

Scheme 1.63: Fe-catalyzed *syn*-carbomagnesiation of alkynols

K. Oshima and K. Utimoto studied *syn*-selective allylmagnesiation of methyl and alkenyl ethers of propargyl/homopropargyl alcohols using Mn salts (**Scheme 1.64**).[186] The reactions produced 1,4-dienes (**127**), allenes (**128**) (via alkoxy elimination), and stereoselective tetrasubstituted alkenes (**129**, up to 90:10 selectivity). Air exposure sometimes led to diallylation, indicating high sensitivity. Oshima expanded this to phenylmagnesiation of alkynes with coordinating groups (**Scheme 1.65A**) (e.g., ethers, amines, 2-alkynyl anilines (**130**)), though alkylmagnesiation failed in these cases.[187] However, primary Grignard reagents effectively alkylmagnesiated 2-alkynylphenols, benzyl alcohols, and alkenyl alkynols with high regio- and stereoselectivity (**Scheme 1.65B** and **1.65C**).

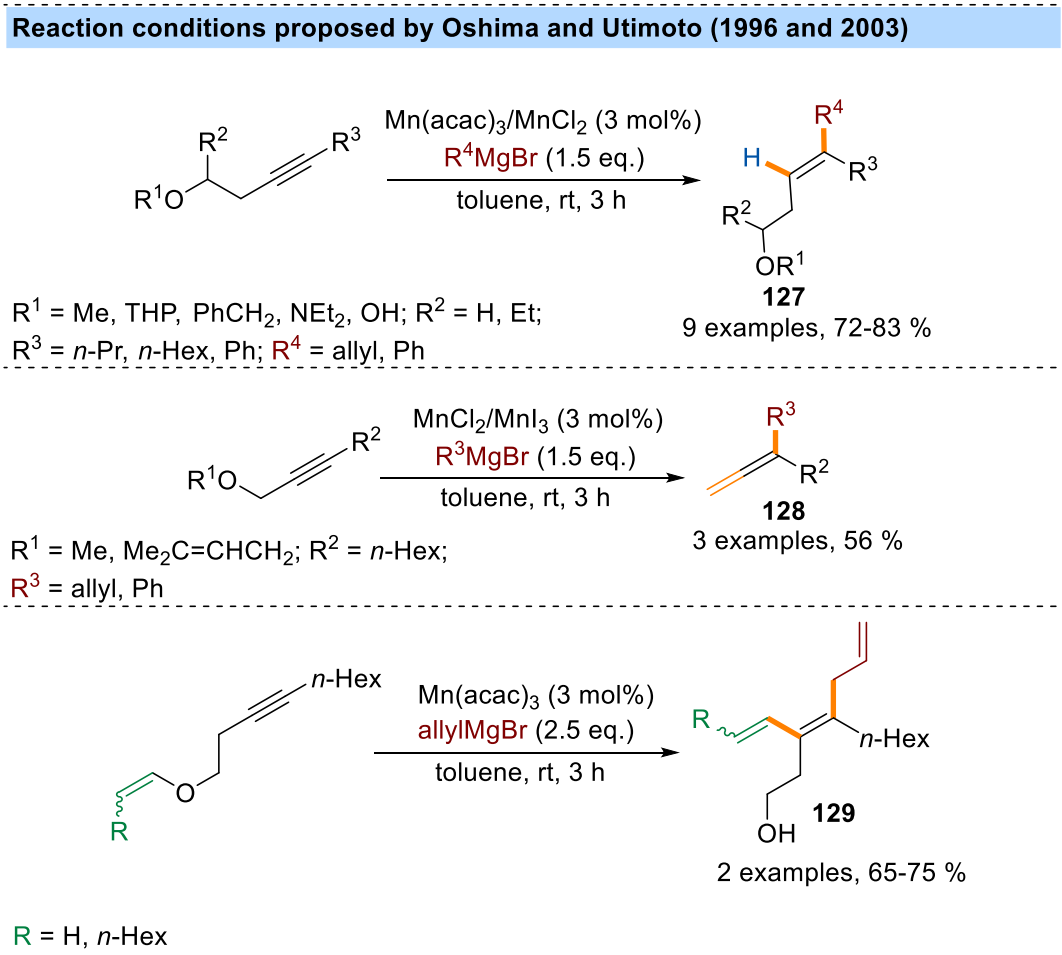

Scheme 1.64: Mn-catalyzed *syn*-carbomagnesiation of alkynol ethers

Subsequently, they developed Ni-catalyzed *syn*-selective alkenylmagnesiation of (alkynyl)arylmethanols, yielding 1,3-butadienyl-substituted benzyl alcohols (**133**) (**Scheme 1.65D**).[188] Reactivity was highly dependent on the alcohol functionality; structural variations or its absence suppressed reaction. Product distribution varied with both the alkyne and Grignard reagent structure.

Reaction conditions proposed by Oshima and Utimoto (2003 and 2007)

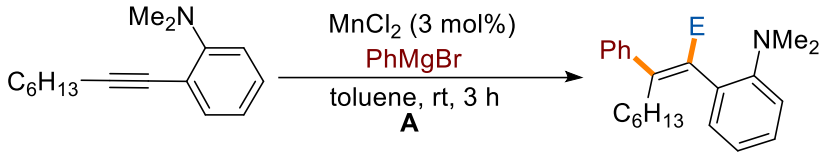

E = allyl, PhCH(OH)

130, 2 examples, 65-67 %

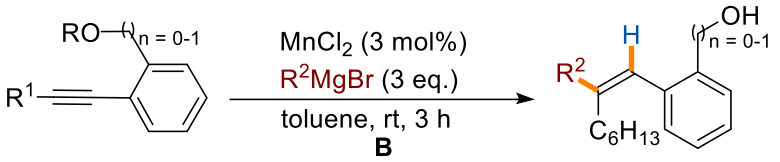

131
12 examples, 19-96 %
82:18 to 99:1

R^1 = Me, *n*-Hex, Ph; R = H, Me; R^2 = Et, *n*-Bu, ^{i}Pr, ^{i}Bu, allyl, Ph

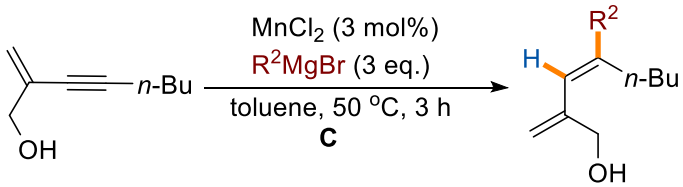

132
2 examples, 50-51 %
Z:*E* 97:3

R^2 = Et, *n*-Bu

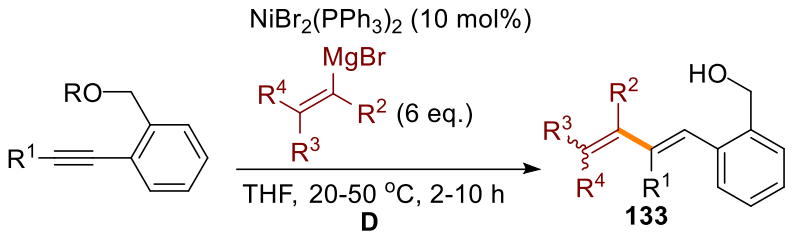

133
12 examples, <5-75 %
E:*Z*: 25:75 to >99:1

R^1 = Me, *n*-Bu, Ph; R = H, Me; R^2 = R^3 = R^4 = H, Me, Ph, $SiMe_3$

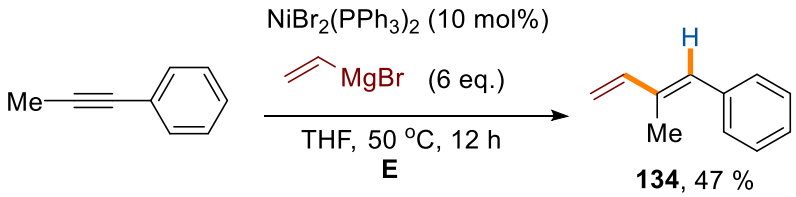

134, 47 %

Scheme 1.65: Mn and Ni-catalzyed *syn*-carbomagnesiation of alkynes

Reactivity of unactivated alkynes:

Reactions with unactivated alkynes are catalyzed using transition metals (Cu, Fe, Cr, Ag, Ni), typically proceeding via *syn*-addition pathways with the notable exception of silver-catalyzed transformations, which are predominantly *anti*-selective. These reactions involve α-metallations, leading to the placement of the carbon framework at the β-position in the case of unsymmetrical substrates.

Snider and colleagues reported Ni-catalyzed alkylmagnesiation of silylated acetylenes with methyl and ethyl Grignard reagents, yielding vinyl silanes (**135** & **136**) as regioisomeric mixtures along with minor dimeric byproducts in ethylations.[189] In 1984, this approach was extended to heteroatom-substituted silyl acetylenes.[190] Thereafter, Itami and Yoshida demonstrated that 2-pyridylsilyl-substituted alkynes undergo copper-catalyzed *syn*-arylmagnesiation with ArMgI, using the pyridylsilane as a directing group to produce tetrasubstituted olefins with high regio- and stereoselectivity (**Scheme 1.66B**).[191]

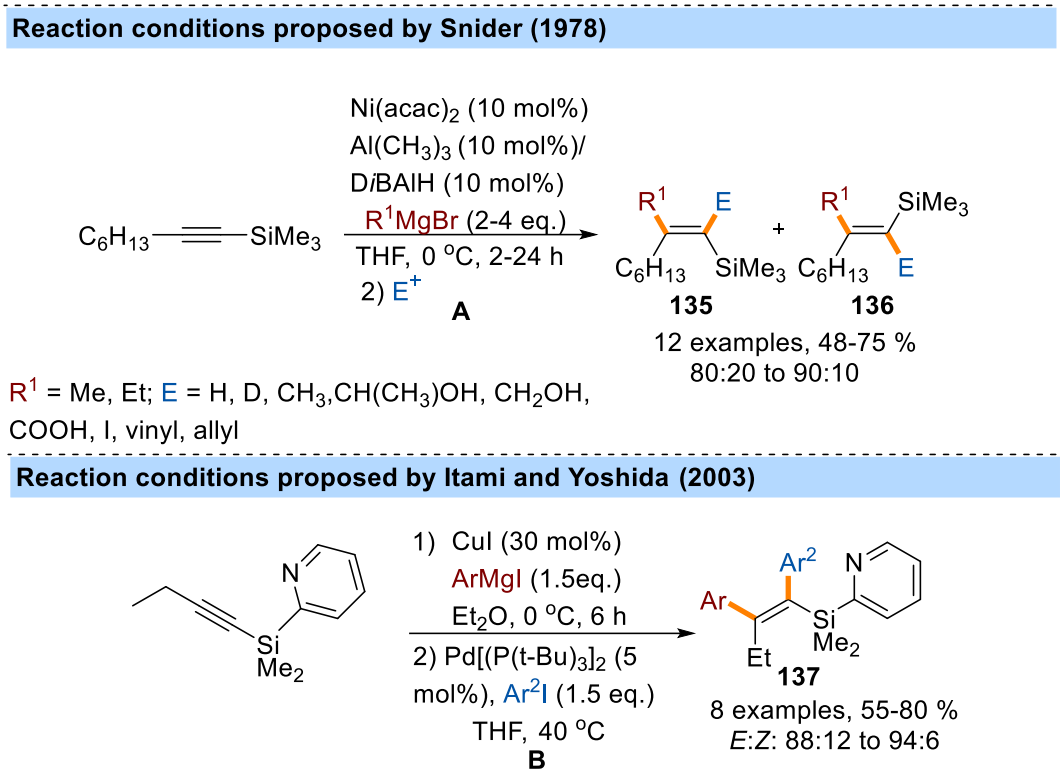

Scheme 1.66: *Syn*-carbomagnesiation of silylated alkynes

Duboudin shared the first successful Ni-catalyzed magnesiation of un-functionalized alkynes using alkyl and phenyl Grignard reagents (**Scheme 1.67**).[192] Alkyl Grignards, due to their reducing nature, led to both addition and reduction products. The reaction proceeded with *syn*-selectivity, affording alkenes as stereoisomeric mixtures in moderate yields, with reflux conditions influencing stereoselectivity. Mechanistic studies (**Scheme 1.68**) suggested that the reaction initiates from a

Ni(II) precursor, which is reduced by the Grignard reagent to Ni(0). Subsequent oxidative addition furnishes a Ni(R)MgX complex, which coordinates with the alkyne, undergoes insertion of the R–Ni fragment, and finally undergoes transmetallation with Mg to generate a vinyl magnesium species (**138**). Further hydrolysis delivers the corresponding carbomagnesiation product (**139**).

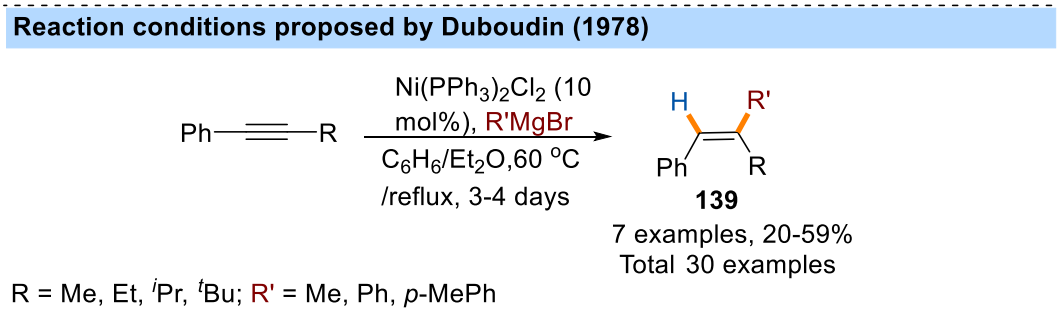

Scheme 1.67: First example of Ni-catalyzed carbomagnesiation

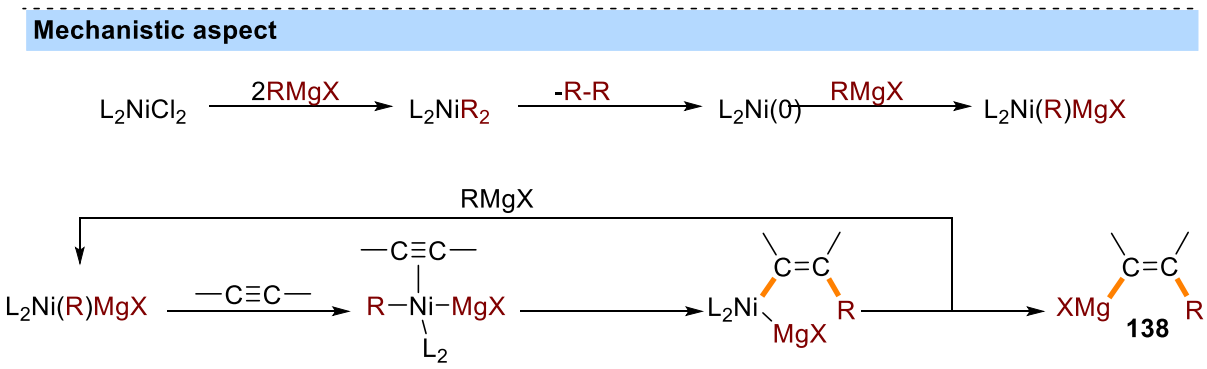

Scheme 1.68: Mechanism of Ni-catalzyed *syn*-carbomagnesiation

A mild, highly regio- and stereoselective Ni-catalyzed arylmagnesiation of diaryl and aryl-alkyl alkynes was developed by Zhao and Hor notably without the use of external ligands (**Scheme 1.69A**).[193] The *syn*-addition proceeded with exclusive formation of *E*-alkenes, delivering excellent outcomes. They extended this protocol to a three-component reaction involving arylmagnesiation followed by cross-coupling with aryl iodides, where kinetic studies identified the cross-coupling step as rate-determining (**Scheme 1.69B**).[194] A THF/toluene solvent mixture was found to enhance reaction selectivity. While unsymmetrical diaryl alkynes showed poor regioselectivity due to unselective carbomagnesiation, aryl-alkyl alkynes yielded tetrasubstituted alkenes with high selectivity (>95:5). The Yoshikai group also employed this procedure for Cu-assisted synthesis of benzophospholes from internal alkynes.[195] The generated vinyl magnesium intermediate undergoes a sequential reaction with dichloroorganophosphine followed by an intramolecular Friedel-Crafts to afford the desired products in moderate yields.

Expanding on the Xue's strategy, Xi reported a sequential arylmagnesiation and carboxylation of diaryl and aryl-alkyl alkynes, affording trisubstituted acrylic acids in good yields (**Scheme 1.69C**).[196] A plausible mechanism based on previous literature and authors observations was

proposed. Initially, the Grignard reagent reduces Ni^{II} to Ni^{0}, which coordinates with the alkyne forming a nickelate (II) complex (**144**), a further transmetalation with Grignard reagent affords another Ni(II) complex (**145**) which after reductive elimination (**146**) followed by trapping with electrophile forms the final product (**Scheme 1.70**).

Reaction conditions proposed by Zhao and Horr (2013, 2015), and Xi (2018)

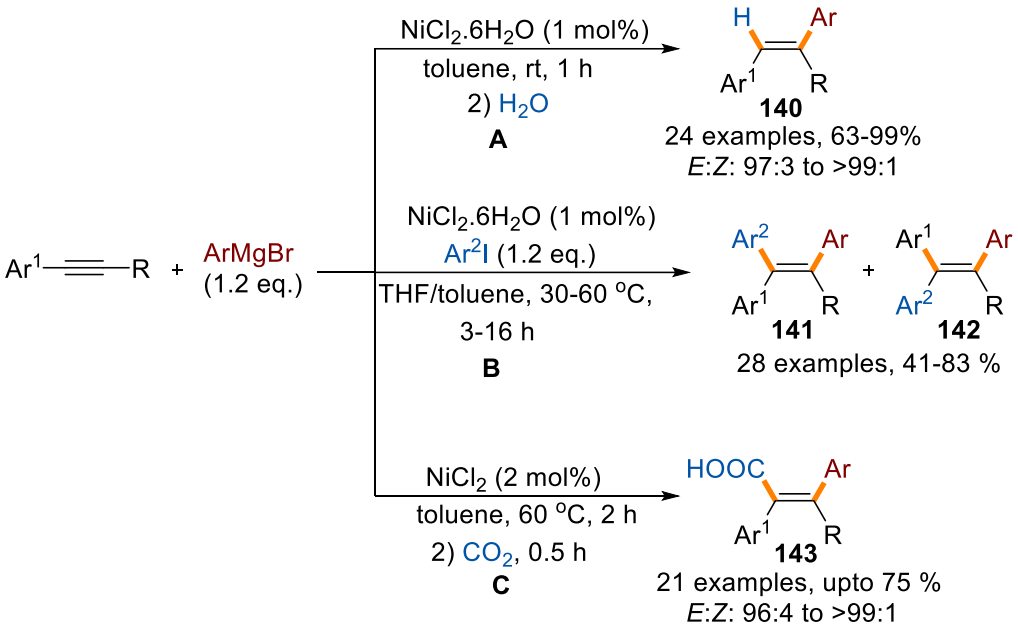

A: Ar^1 = Ph, *m*, *p*-MePh, *p*-FPh, *o*, *p*-OMePh, *p*-*n*BuPh, 1-NapPh, *p*-BiPh; R = Ar^1, *n*-Bu, $(CH_2)_3Cl$; Ar = Ph, *o*, *m*-MePh, *p*-OMePh, *p*-FPh
B: Ar^1 = Ph, *o, m*, *p*-MePh, *p*-ClPh; R = Ar^1, Et, *n*-Bu, $(CH_2)_3Cl$, $(CH_2)_3OMe$; Ar: Ph, *o, m*, *p*-MePh, *p*-FPh, *p*-OMePh, etc.; Ar^2 = Ph, *m*, *p*-MePh, *p*-FPh, *p*-OMePh, *p*-$O(CH_2)_2NMe_2Ph$, etc; diaryl: *Z*:*E*: 88:12 to 97:3; arylalkyl: 94:6 to >99:1
C: Ar^1 = Ph, *p*-MePh, *o*, *p*-OMePh, *p*-CF_3Ph, *p*-BrPh, *o*, *m*-ClPh, 1-Nap, 2-thienyl; R: Ph, Me, Et, *n*-Bu, cyclopropyl, $(CH_2)_3Cl$, $(CH_2)_2OTBS$; Ar: Ph, *p*-MePh, *o*-OMePh, *p*-F/ClPh

Scheme 1.69A-C: Ni-catalyzed arylmagnesiation of alkynes

Cheng and colleagues developed a Ni-catalyzed method for the magnesiation of internal alkynes using alkyl, aryl, allyl, and vinyl Grignard reagents with TMEDA/phosphine ligands (**Scheme 1.71**).[197] Both diaryl and aryl-alkyl alkynes were effective, yielding trisubstituted acrylic acids as the main products, though the latter also gave double insertion byproducts. In unsymmetrical diaryl alkynes, the site of carboxylation (α or β) was influenced by the electronic nature of the substituents.

Mechanistic aspect

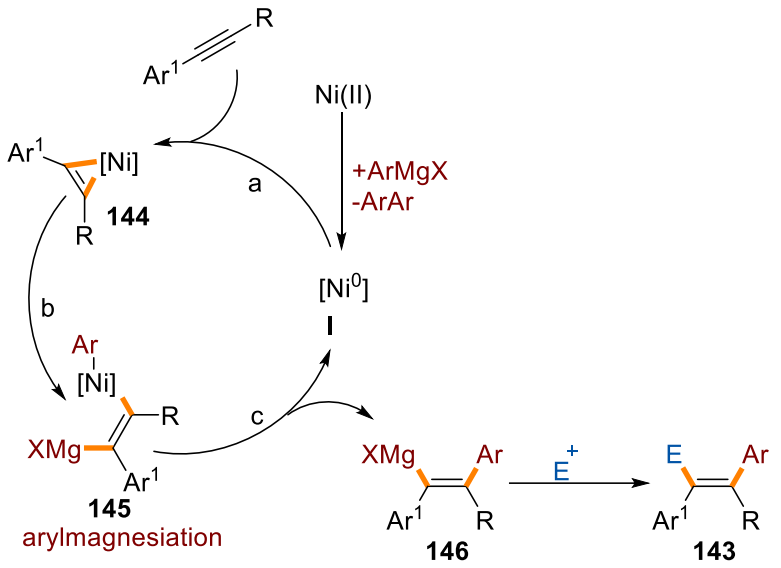

a: cycloaddition; b: transmetallation; c: reductive elimination

Scheme 1.70: Mechanistic aspect by Xi

Reaction conditions proposed by Cheng (2018)

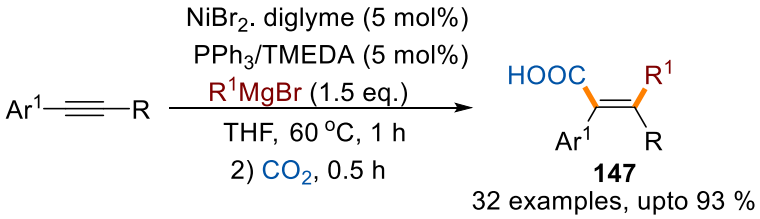

Ar^1 = Ph, *o*, *m*, *p*-MePh, p-^{t}Bu/OMePh, 1/2-Nap; R = Ar^1, *o*, *m*-OMePh, *p*-FPh, Me, Et, *n*-Bu, cyclohexyl; R^1 = Me, Et, vinyl, *p*-Me/OMe/F/^{t}BuPh, 1/2-Nap, 2-mesityl, 3,5-Me_2Ph, etc.; diaryl: α:β: 21:79 to 87:13; aryl alkyl: *E*:*Z* products & double insertion: 97:3 to 99:1

Scheme 1.71: Subsequent development in Ni-catalyzed carbomagnesiation of alkynes

Alexakis demonstrated CuBr-catalyzed *syn*-addition of alkyl magnesium reagents to acetylenes, with yields reaching a maximum of 35–40% (**Scheme 1.72A**).[198] E. Negishi (1993) introduced *syn*-selective zirconium-catalyzed ethylmagnesiation of diynes via zirconacyclopentene intermediates yielding predominantly *syn*-enynes with high efficiency (**Scheme 1.72B**), although analogous reactions on alkynes resulted in dimerization.[199] K. Oshima and coworkers, in 2003, investigated the *syn*-selective manganese-catalyzed phenylmagnesiation of selected unactivated internal alkynes, affording trisubstituted alkenes in moderate yields (**Scheme 1.72C**).[187]

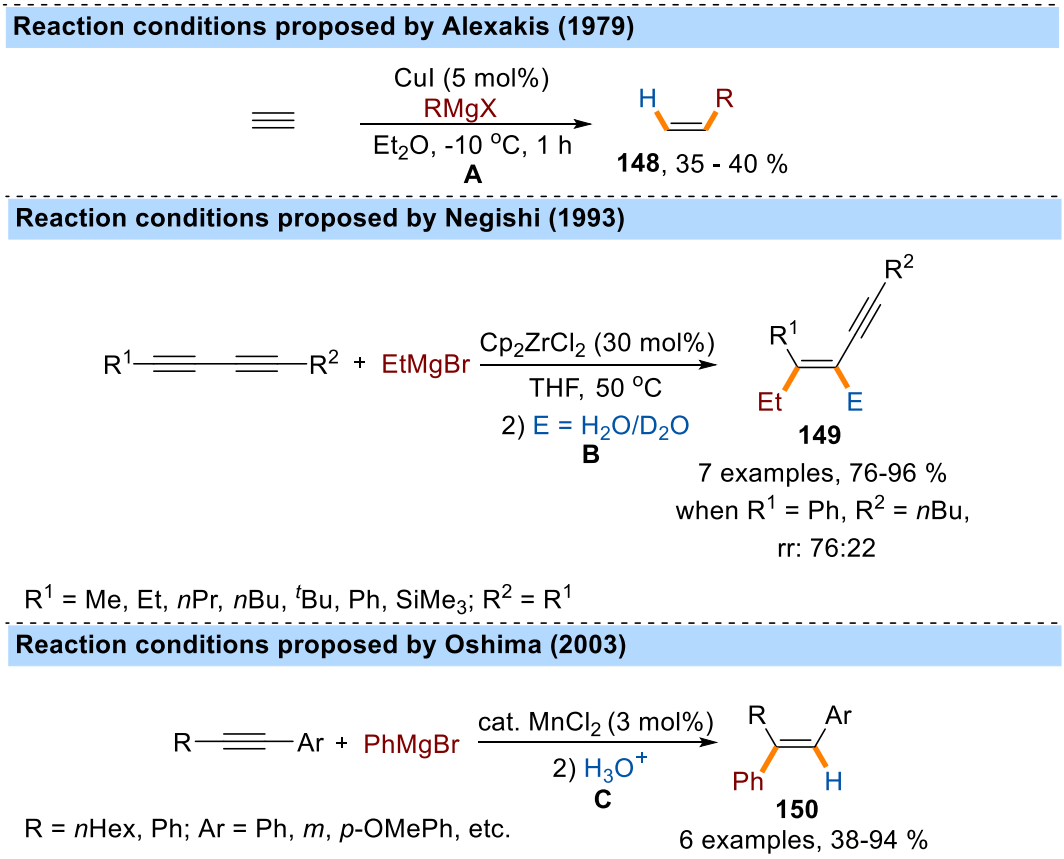

Scheme1.72: Cu, Zr and Mn-catalyzed *syn*-carbomagnesiation of alkynes

Using dual Fe/Cu catalysis in combination with phosphine ligands, Shirakawa and Hayashi achieved the *syn*-selective arylmagnesiation of alkynes to afford *E*-alkenes with excellent selectivity (>90%) and moderate efficiency (**Scheme 1.73**).[11] Guided by earlier studies, a plausible mechanism was proposed. Initially, an aryl–Fe species reacts with the alkyne to generate an alkenyl–Fe intermediate (**151**). Copper facilitates subsequent transmetalation steps, first enabling the transfer of the alkenyl group from Fe to Cu (**152**), and then from Cu to Mg (**153**) via exchange with the aryl Grignard reagent. This sequence ultimately yields the *E*-alkenyl magnesium bromide product with high stereoselectivity. Two years later, they introduced a Fe–NHC-based catalytic system that eliminated the need for both copper and phosphine ligands (**Scheme 1.74**).[200] This advancement enabled the arylmagnesiation of aryl–alkyl alkynes with a broader substrate scope, delivering predominantly *E*-alkenes in good yields, accompanied by only minor amounts of the *Z*-isomer and less than 3% of the opposite regioisomer.

Continuing their exploration of iron-catalyzed systems, Shirakawa and Hayashi developed a one-pot, *syn*-selective alkylmagnesiation of aryl–alkyl alkynes via synergistic Fe/Cu catalysis (**Scheme 1.75**).[201] This reaction relied on the *in situ* generation of primary alkyl Grignard reagents from secondary Grignard's & alkenes and required the presence of both TMEDA and phosphine ligands for optimal activity. Exclusion of any catalyst or ligand component led to significant suppression of reactivity. When the alkyl groups on the Grignard reagent and the alkyne differed, the reaction

yielded mixtures of stereoisomeric alkenes, reflecting diminished stereocontrol under these conditions.

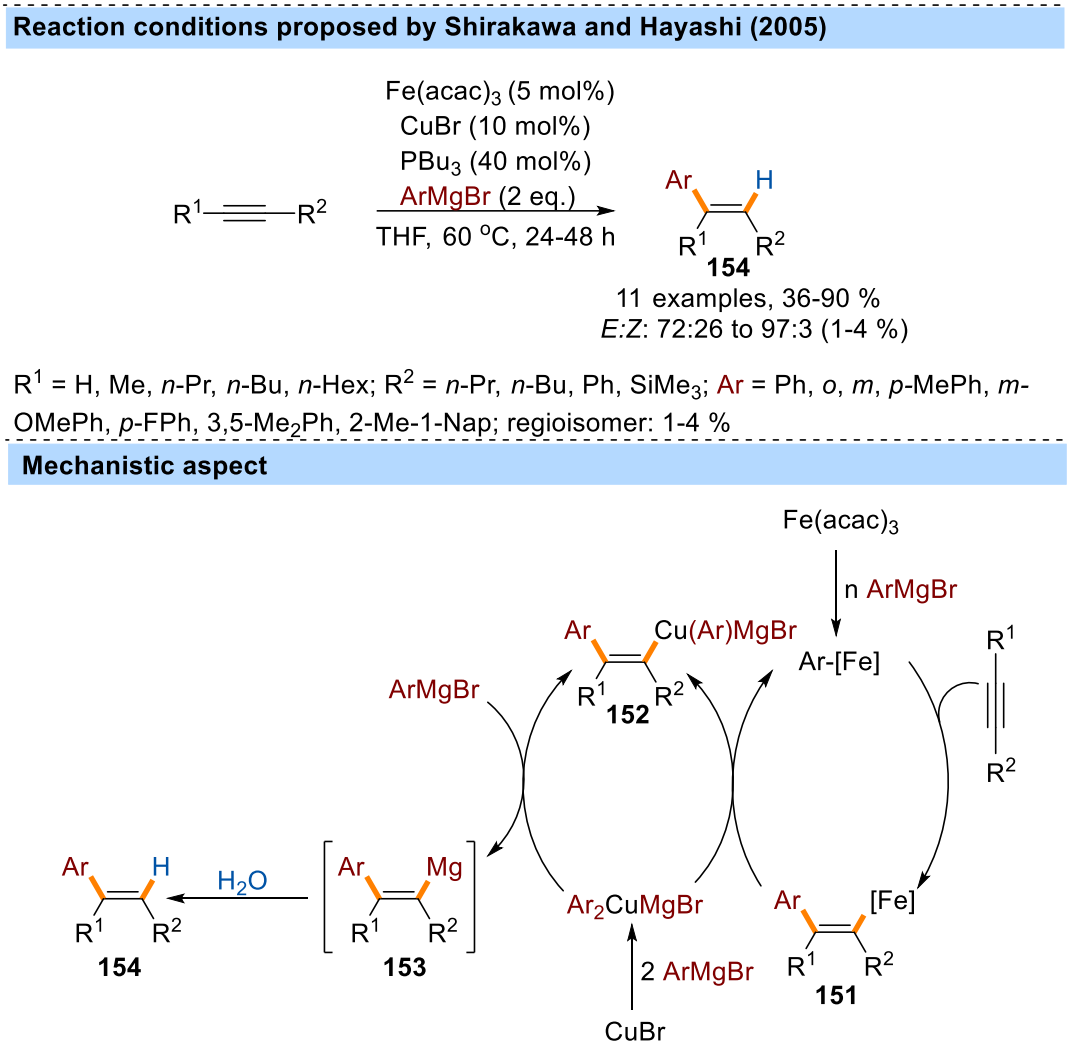

Scheme 1.73: *Syn*-arylmagnesiation of alkynes using Fe/Cu co-catalysis

Extending the scope of iron–NHC catalysis, Deng reported a distinct approach to the alkylmagnesiation of internal alkynes, achieving selective double carbometallation using an iron–NHC complex (**Scheme 1.76**).[202] This strategy enabled the formation of 1,3-dienes predominantly as *E*-isomers via *syn* addition, though minor amounts of isomeric dienes and monocarbometallation byproducts were occasionally observed. The efficiency and selectivity of the transformation were highly influenced by the steric properties of the NHC ligand. Notably, magnesiation using ethyl or phenyl Grignard reagents did not promote the double carbometallation process.

Reaction conditions proposed by Shirakawa and Hayashi (2007)

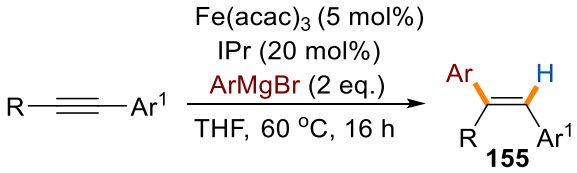

14 examples, 59-91 %
E:*Z*: 76:24 to 92:8 (1%)

R = Et, *n*-Bu, ^{i}Pr, ^{i}Bu; Ar^1 = Ph, *o*, *m*, *p*-OMePh, *p*-ClPh; Ar = *p*-MePh, *o, m, p*-OMePh, *p*-FPh, 1-Nap; regioisomer: 1%

Reaction conditions proposed by Shirakawa and Hayashi (2012)

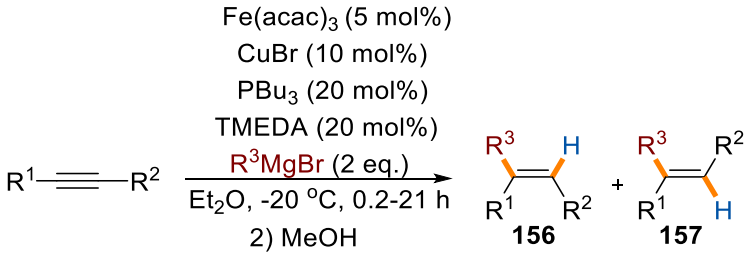

18 examples, 57-93 %
39:61 to 97:3

R^1 = Et, *n*-Bu, ^{i}Pr, ^{i}Bu, *n*-Hex; R^2 = Ph, COOEt, 2-thienyl, *o*-MePh, *p*-ClPh, *m*, *p*-OMePh, *m*, *p*-CF_3Ph; R^3 = *n*-Bu, ^{i}Bu, *n*-Hex, Me_3CCH_2, $MeO(CH_2)_4$, etc.

Scheme 1.74 & 1.75: Further variation of Shirakawa's Fe-Catalyzed carbomagnesiation Strategy

Reaction conditions proposed by Deng group (2016)

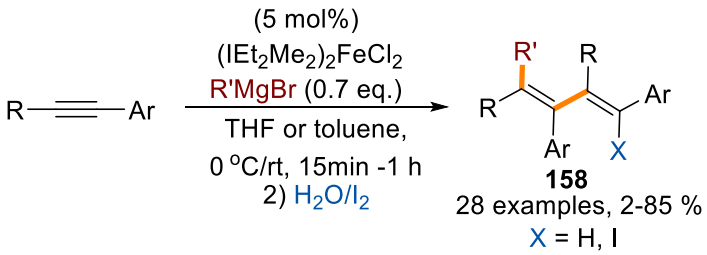

28 examples, 2-85 %
X = H, I

Ar = Ph, *o, p*-MePh, *p*-^{t}BuPh, *p*-ClPh, *p*-BrPh, 2-thienyl; R = Me, Et, *n*-Bu, Cy, ^{t}Bu, allyl, $(CH_2)_3Cl$; R' = Me, Et, CH_2(TMS), $CH_2{}^{t}Bu$

Scheme 1.76: Fe-catalyzed double carbometallation of alkynes

In a complementary approach, E. Nakamura employed conjugated diynes for Fe-catalyzed *syn*-selective phenyl magnesiation, giving access to enynes regio- and stereoselectively (except for diaryldiynes) in moderate yields (**Scheme 1.77**).[203] Interestingly, the reaction selectively involved a single triple bond of the diyne substrate. The method was compatible with MeMgBr, albeit with minor regioisomer formation, but failed with Grignard reagents bearing β-hydrogens.

Reaction conditions proposed by Nakamura (2014)

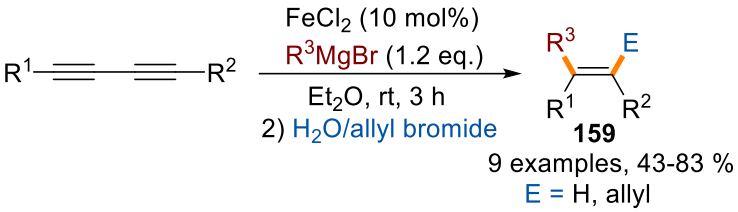

R^1 = R^2 = $SiMe_3$, *n*-Bu, Ph; R^3 = Me, Ph, mesityl, *p*-F, *p*-Me, *p*-OMePh; regisomer: 5-8%

Scheme 1.77: Fe-catalyzed carbomagnesiation of diynes

The Oshima group assessed the Cr-catalyzed phenylmagnesiation of internal alkynes using protic acid additives (**Scheme 1.78**).[204] Symmetrical aliphatic alkynes yielded trisubstituted *E*-alkenes with high stereoselectivity, while unsymmetrical aryl-alkyl alkynes produced β-arylated product along with minor amount of other regioisomer. Terminal alkynes were unreactive under these conditions.

Reaction conditions proposed by Oshima (2007)

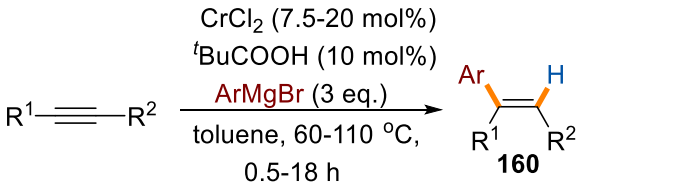

R^1 = Me, *n*-Pent, *n*-Hex, Ph; R^2 = *n*-Pent, *t*-Bu, Ph, $SiMe_3$; Ar: Ph, *o*, *m*, *p*-MePh, *m*-OMePh, *p*-ClPh

Scheme 1.78: Cr-catalyzed arylmagnesiation of alkynes

Kambe investigated the alkylmagnesiation of aryl acetylenes and aliphatic enynes using a silver catalyst, alkylmagnesium chloride, and 1,2-dibromoethane as a reoxidant (**Scheme 1.79A**).[205] Terminal alkynes yielded hydroalkylated alkenes with high *Z:E* selectivity when tertiary Grignard reagents were used, but this selectivity decreased with less hindered Grignards, reaching ~1:1 ratios with primary alkyl Grignards. For enynes, tertiary Grignard's gave mixtures of alkylated alkynes and allenes, whereas primary Grignards showed little to no reactivity. They further extended this methodology to a three-component carbomagnesiation of terminal alkynes, alkyl halides (bromides/iodides), and iso-butyl magnesium chloride (^{i}BuMgCl), wherein the alkyl group was sourced exclusively from the alkyl halide (**Scheme 1.79B**).[206] With highly branched alkyl iodides, the reaction furnished hydroalkylated alkenes with moderate *Z:E* selectivity, and no incorporation of Grignard-derived alkyl groups was observed.

Reaction conditions proposed by Kambe (2009 & 2011)

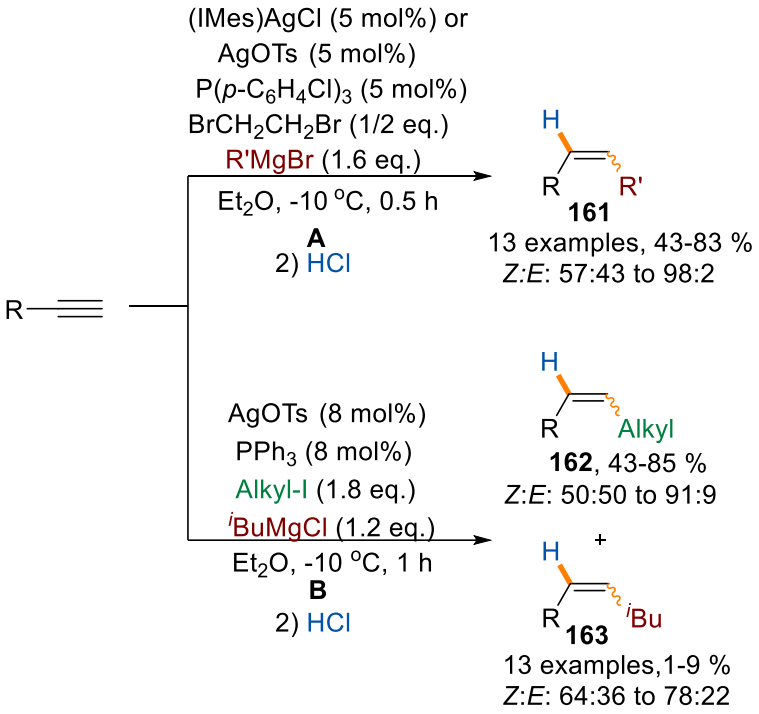

A: R = Ph, *o*, *m*, *p*-MePh, *p*-OMePh, *p*-CF_3Ph, 3-thienyl, $PhMe_2Si$
R' = *n*-Bu, *n*-Oct, ^{s}Bu, ^{t}Bu, etc.
B: R = Ph, *o*, *m*, *p*-MePh, *p*-OMePh, *p*-CF_3Ph, $PhMe_2Si$; Alkyl = *n*-Bu, ^{s}Bu, ^{t}Bu, 1-Ad, *Cy*

Scheme 1.79A and B: Ag-catalyzed alkylmagnesiation of terminal alkynes

S. Yoshida and colleagues developed a *syn*-selective carbomagnesiation method for fused, non-fused and benzoxepine-type cycloalkynes, generated *in situ* from sulfoxides (**Scheme 1.80**).[207] Using alkyl, aryl, and alkenyl Grignard reagents, they achieved the formation of 6- and 7-membered cycloalkenes in moderate to good yields. For non-fused cycloalkynes, minor diene byproducts (**165**) were also observed.

Reaction conditions proposed by Yoshida (2020)

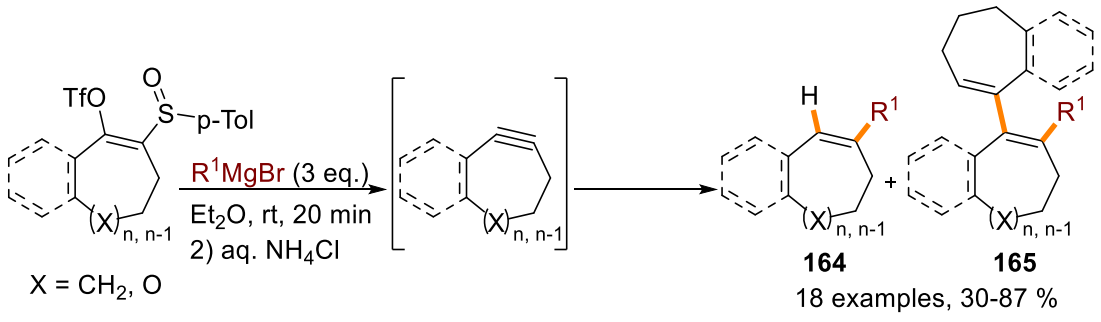

R^1 = Et, ^{i}Pr, *Cy*Pent, vinyl, Ph, *o*, *p*-OMePh, *p*-CF_3Ph, *o*-ClPh

Scheme 1.80: S*yn*-carbomagnesiation of *in situ* generated alkynes

1.1.10 Carboboration

Carboboration installs a C-C and C–B bond across an alkyne in one step, yielding versatile vinyl-boronates that enable Suzuki–Miyaura coupling, oxidations, aminations, and more.[208] After pioneering cyanoboration of alkynes, Suginome's group extended the approach to inter- and intramolecular variants. Most carboborations involve β-selective installation of boron substituent, while α-regioselective cases remain uncommon. Metal-free electrophilic or organocatalytic protocols exist, but the field is dominated by Ni, Pd, Cu, and, occasionally, Fe catalysts, delivering both *syn* and *anti*-stereoselectivity. Owing to the versatile reactivity of the vinyl-boron moiety, both electronically activated and non-activated alkynes now serve effectively as substrates. Subsequent sections outline *syn* vs. *anti*, β vs. α, intra vs. intermolecular, and metal-free vs. metal-catalyzed examples.

1.1.10.1 Intramolecular reactions

Suginome[209] studied carboborations on chloroborane tethered alkynes using Pd/Zr system (**Scheme 1.81A**). Stereoselectivity depends on the ligand: bulky phosphines (P^tBu_3, PCy_3, PAr_3) induce *anti*-addition, whereas PMe_3 gives *cis* products. This protocol accommodates a broader substrate scope, both terminal and alkyl-substituted alkynes and alkyl, aryl, or alkenyl zirconium reagents, surpassing the earlier Ni/Sn *trans*-alkynylboration protocol (**Scheme 1.81B**).[210] The resulting alkenyl chloroboranes, being moisture-sensitive, were converted into more stable pinacol derivatives.

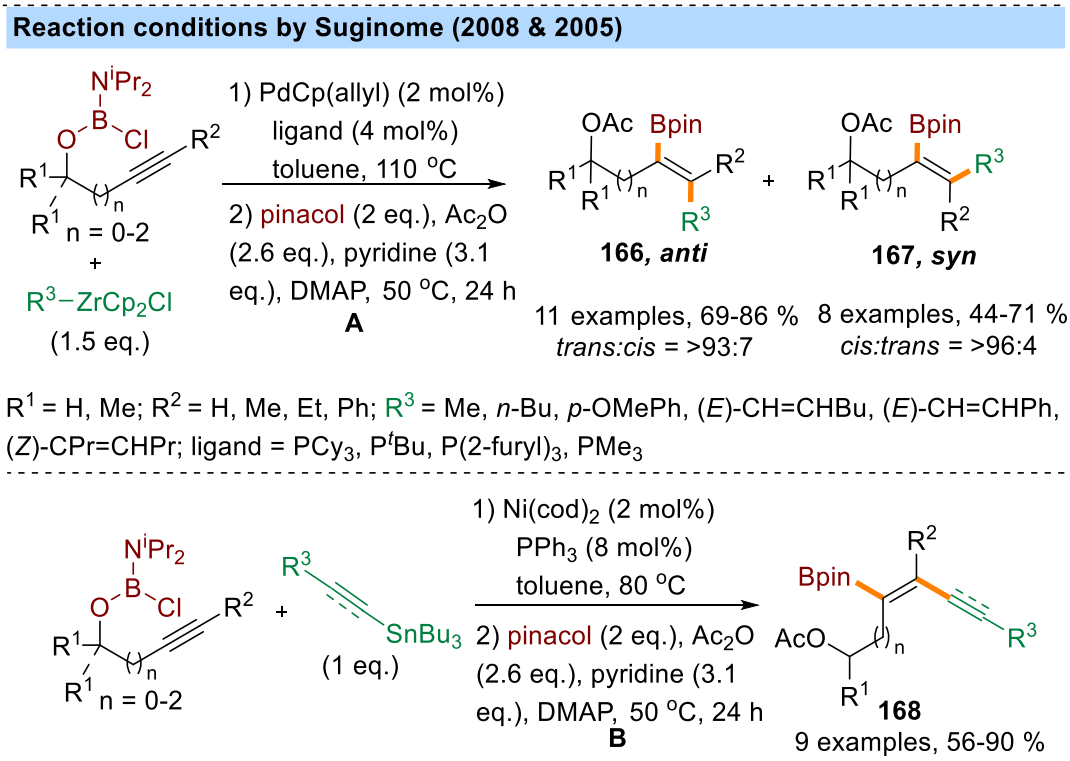

Scheme 1.81A and B: Intramolecular carboboration of chloroborane tethered alkynes

Lin[211] developed Cu-catalyzed tandem β-boration and intramolecular conjugate addition of alkynes tethered to cyclohexadienones affording bicyclic products (**170**) with excellent regio- and enantioselectivity (**Scheme 1.82**). Substitution at the quaternary center resulted in high yields and enantioselectivities. However, longer alkyl chains on the alkyne reduced both yield and enantiomeric excess. When a heteroatom was present at the distal propargylic position, the reaction halted at α-boration and product being unstable was oxidized to a ketone. Introducing a bulky group adjacent to that heteroatom restored the desired cyclization pathway. Propargyl amines, in contrast, failed to react under these conditions.

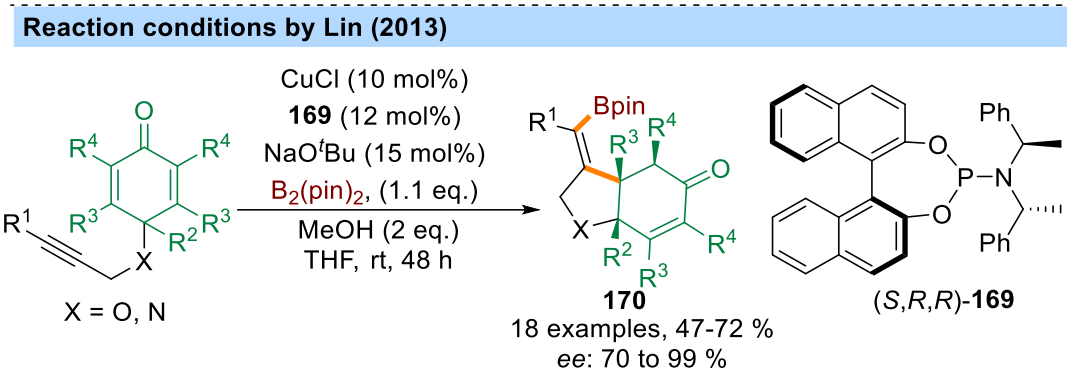

R^1 = H, Me, Et, *n*-Bu, OBn, OTrt; R^2 = Me, Et, vinyl, PhCH$_2$, *p*-BrPh, TBSO(CH$_2$)$_2$, Br(CH$_2$)$_3$, Ph, allyl, OMe; R^3 = R^4 = H, Me

Scheme 1.82: Intramolecular conjugate addition on cyclohexadienone tethered alkynes

Ito[212] developed an intramolecular Cu-mediated alkylboration of silicon-tethered alkynes using B$_2$pin$_2$ and primary alkyl bromides. Aryl, alkyl, and conjugated enynes underwent *syn*-selective alkylboration to produce alkenyl boranes with excellent regio- and stereocontrol (**Scheme 1.83**). Importantly, without the silicon tether or with an external alkyl electrophile, the reaction failed, yielding no product.

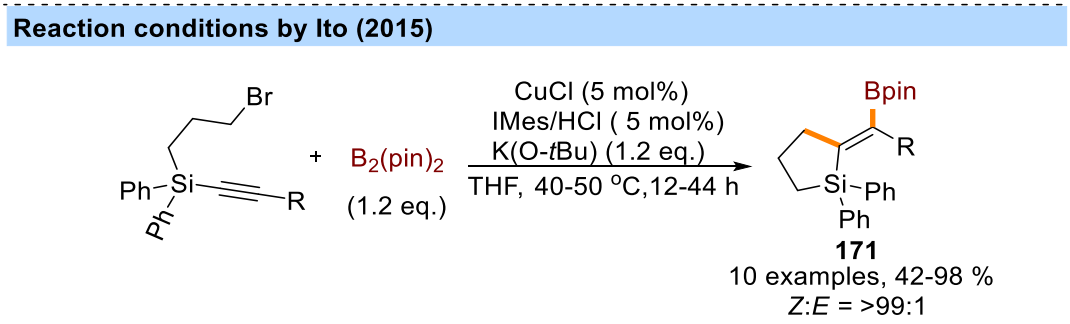

R = Bu, (CH$_2$)$_4$Ph, *Cy*Hex-CH$_2$, (CH$_2$)$_4$OTHP, Ph, *p*-OMePh, etc.

Scheme 1.83: Intramolecular alkylboration of silicon tethered alkynes

Carretero[213] reported a Cu-catalyzed intramolecular carboboration of propargyl amines bearing tethered Michael acceptors using catalytic NaO^{t}Bu and less-acidic proton source to suppress hydroboration. The *syn*-selective β-boration proceeds with high regio- and stereocontrol to furnish

pyrrolidines (**172**) in excellent yields (**Scheme 1.84**). Substituents like ^{i}Pr or aryl on the olefin and halogen, protected/free-alcohols on the alkyne are well tolerated though free alcohols cause deboration via Cu-mediated transmetallation of the boron-ate complex. Mechanistically, base promotes Cu–BPin formation, which adds across the alkyne (**173**); phosphine ligands then assist the coordination of the Michael acceptor and intramolecular migratory insertion (**174**) into the Cu–C bond under catalytic-base conditions. Final protonation liberates the product and regenerates the catalyst (**Scheme 1.85**).

Reaction conditions by Carretero (2018)

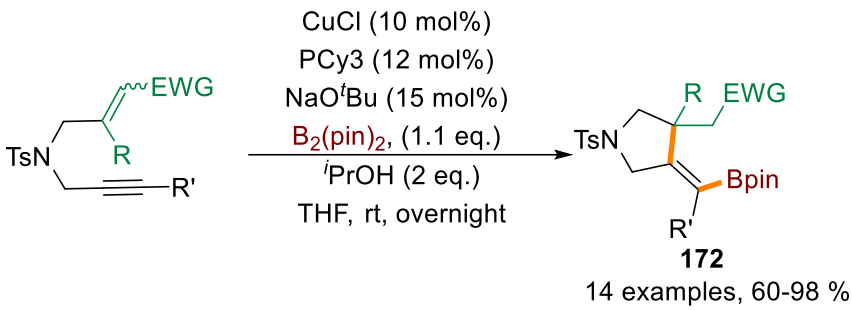

R = Me, Et, ^{i}Pr, Bn, Ph, *p*-MePh, *p*-OMePh; EWG = CO_2Me, CO_2Et, CN, CO_2CH_2-$CH{=}CH_2$, etc.; R' = $(CH_2)_2X$ where X = Ph, Cl, OTBS, OH

Scheme 1.84: Intramolecular carboboration of propargyl amines

Mechanistic aspect

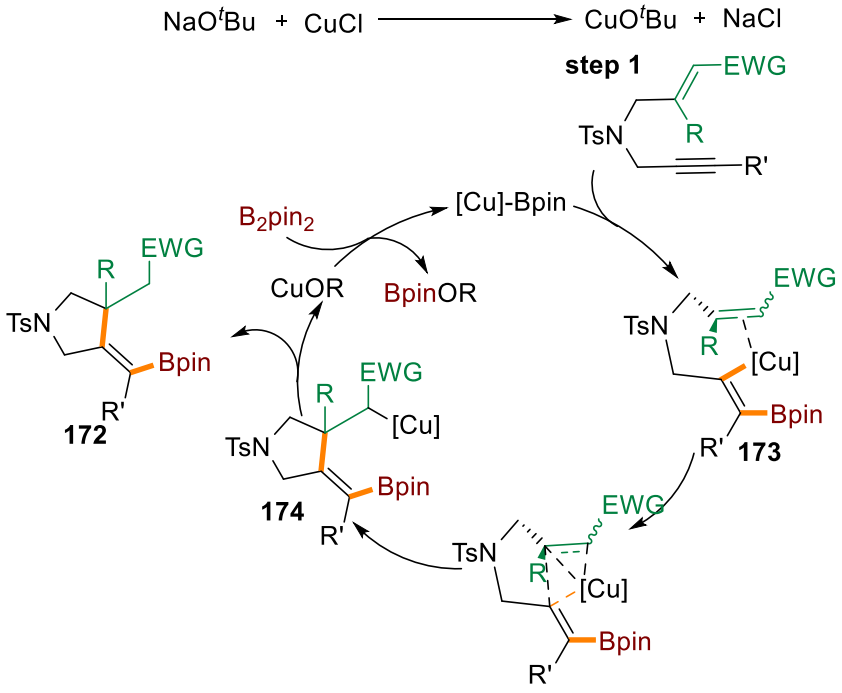

Scheme 1.85: Mechanism of Intramolecular carboboration of propargyl amines

1.1.10.2 Intermoleceular reactions

1.1.10.2.1 Uncatalyzed reactions

Bubnov[214,215] shared the first and the only instance of uncatalyzed *syn*-allylborations of acetylenes using triallylboranes (**Scheme 1.86)**. The dienyl borane products (**175**) were further transformed to 1,4 dienes (**176**).

Reaction conditions by Bubnov (1965)

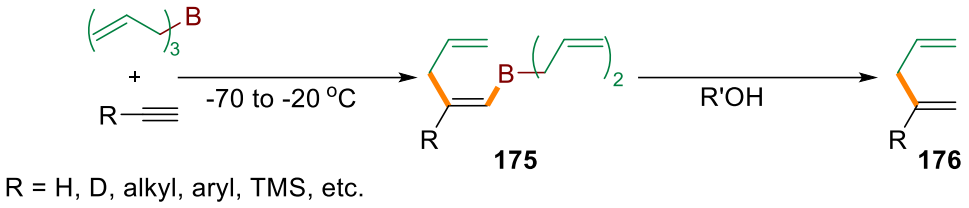

R = H, D, alkyl, aryl, TMS, etc.

Scheme 1.86: Uncatalyzed allylboration of alkynes

1.1.10.2.2 Catalyzed reactions

The reactions of unactivated alkynes are typically catalyzed via transition metals primarily using Ni, Pd or Cu (and less commonly Fe or bimetallic systems) with Cu-catalyzed carboborations standing out as a widely explored approach.

Ni- or Cu-catalyzed alkynylborations

Suginome[216] introduced a Ni-catalyzed intermolecular (silyl)alkynylboration of internal alkynes that achieved *syn*-selective addition using bulky phosphines (PCy_3,PCy_2Ph), contrasting the prior intramolecular approach (discussed above). The method showed good regio- and stereocontrol, favoring α-alkynylation in aryl-alkyl alkynes to give predominantly *cis*-isomers (**Scheme 1.87)**. Aryl- and silyl-substituted alkynyl boranes reacted efficiently, whereas alkyl variants remained unreactive. Diisopropylaminoboranes, effective in intramolecular systems, were ineffective, and slow alkyne addition was crucial to suppress oligomerization.

Reaction conditions by Suginome (2006)

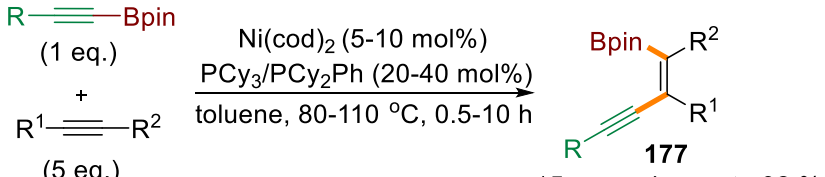

15 examples, upto 92 %
regio:80:20 to 94:6
cis:*trans*: 73:27 to 99:1

R^1 = *n*-Pr, CH_2Ph, Ph, *p*-Anis, 1-Nap, *p*-EtO_2CPh ; R^2 = Me, *n*-Pr, *n*-Bu, CH_2Ph, etc.
R = *n*-Bu, Ph, *o*-Tol, $SiMe_3$

Scheme 1.87: Intermolecular carboboration using Ni & Pd catalysts

Later, Yun[217] developed *syn*-alkynylborations of internal alkynes with precatalyst IMesCuCl and alkynyl bromides (**Scheme 1.88A)**. Both symmetrical and unsymmetrical diaryl and aryl alkyl alkynes (β-boration) were compatible, unsymmetrical diaryl substrates produced regioisomeric mixtures, while aryl–alkyl substrates delivered highly regioselective products. A secondary alkyl group bearing alkyne resulted in low yield and regioselectivity.

Fu[218] extended this approach to terminal alkynes under similar conditions (**Scheme 1.88B)**. A broad array of terminal aliphatic (both linear and cyclic), aromatic, and alkynyl-ether substrates underwent *syn* addition, preferentially yielding α-alkynylated enynes. Sterically hindered *tert*-butyl acetylene gave lower yield. Notably, in substrates containing both terminal and internal alkynes, addition occurred selectively at the terminal position.

Reaction conditions by Yun (2018)

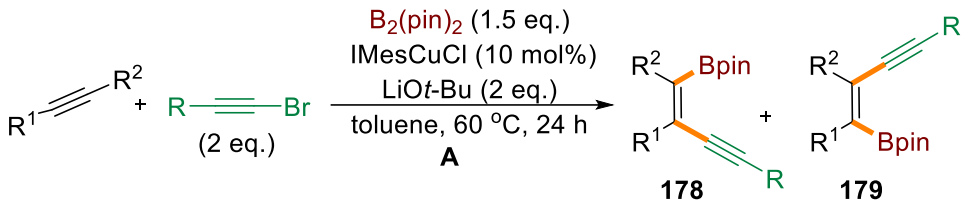

R^1 = Ph, *o*, *p*-MePh, *p*-FPh, *m*-ClPh, 3-thienyl, *p*-CNPh, etc.; R^2 = Me, Ph, *o*, *p*-MePh, *p*-FPh, *m*-ClPh, 3-thienyl, *p*-CF_3Ph, *Cy*Pent; R = TIPS, TES, TBDMS

Reaction conditions by Fu (2019)

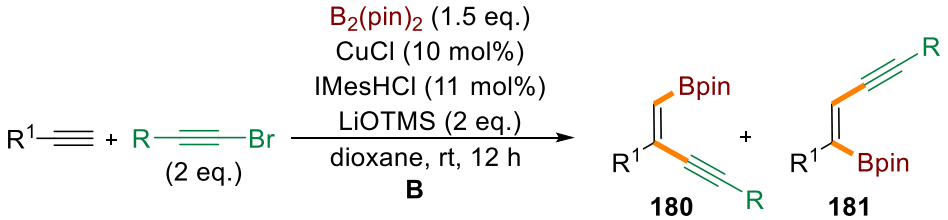

R^1 = Me, *n*-Bu, *Cy*Pr, TMS, ^{t}Bu, $(CH2)_3$OTBDMS, Ph, CH_2OBn, $(CH_2)_2$Ph, $(H_2C)_2$−C≡C^{n}Bu ; R = TIPS, TES, TMS, ^{t}Bu, Ph, etc.

Scheme 1.88A and B: *Syn*-selective alkynylborations using Cu-catalyst

Ni-catalyzed intermolecular coupling with Enones

Cheng[219] reported Ni-catalyzed three component coupling of alkynes with enones and $B_2(pin)_2$. A mixed solvent system was crucial as it suppressed reductive coupling and favored the relatively less explored, α-boration/β-alkylation of both terminal and internal alkynes. Alkynols, ethers, substituted vinyl ketones, and cyclic variants were also effective, although minor regioisomers formed with alkynols/ethers (**Scheme 1.89)**.

Mechanistically, stoichiometric studies suggested formation of a nickelacyclopentene (**182**, via cyclometallation) that undergoes protonolysis (by MeOH), followed by transmetallation and reductive elimination to yield the product (**Scheme 1.90)**. Although the authors favored this pathway, they acknowledged a possible alternative involving oxidative addition of diboron to Ni, sequential insertions of alkyne and alkene, and final protonation.

Reaction conditions by Cheng (2009)

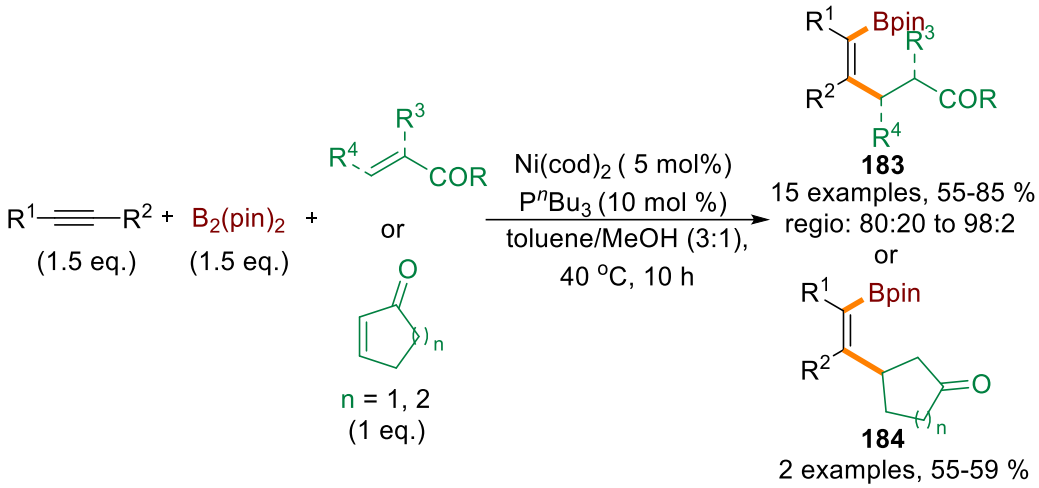

R^1 = *n*-Pr, Ph, *p*-OMePh, pyridyl; R^2 = H, Me, Et, *n*-Pr, Ph, $(CH_2)_2OH$, $(CH_2)_2OMe$;
R^3 = R^4 = Me

Scheme 1.89: α-*syn*-selective carboboration of alkynes with enones

Mechanistic aspect

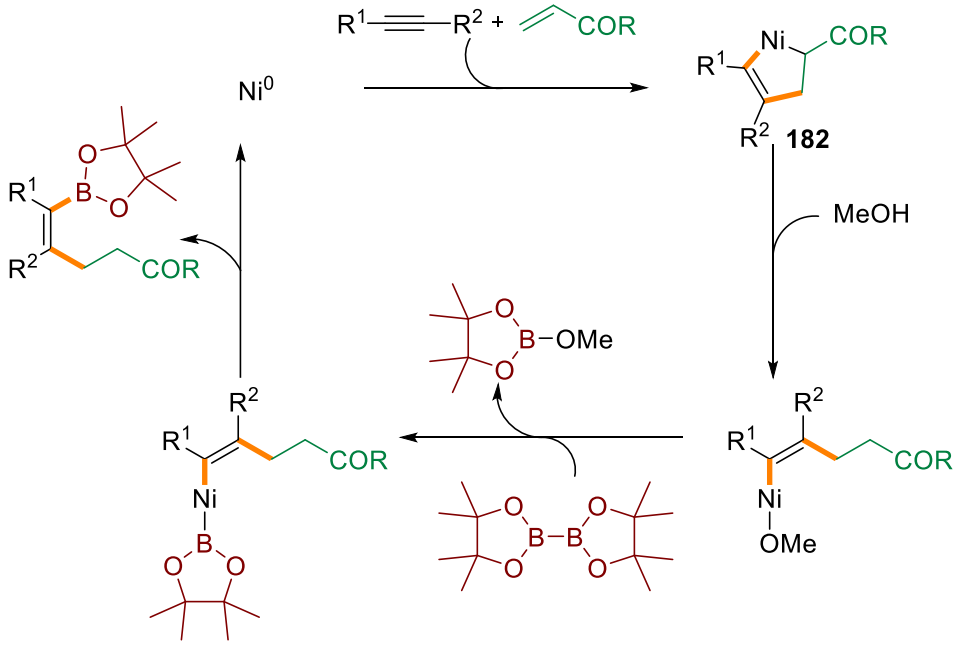

Scheme 1.90: Mechanism of carboboration of alkynes with enones

Zhu[220] developed Cu-catalyzed coupling of acetylenes using Michael acceptors and B_2pin_2. While higher derivatives of alkynes predominantly underwent hydroboration of the Michael acceptors, using excess simple acetylene enabled *syn*-addition, producing the desired Z-borylated alkenes and eliminating side reactions (**Scheme 1.91**). The protocol tolerates diverse acrylates with free hydroxy, methylsulfonyl groups, unconjugated alkynes, alkyl iodides although acrylamides were unreactive. Vinyl ketones (especially those with bulky aromatic rings) improved yields by suppressing unwanted multi-Michael additions. In addition, 1,3-dienyl ketones, acrylonitriles, vinyl sulfones, and polyethylene glycol diacrylate were also compatible with the method.

Reaction conditions by Zhu (2022)

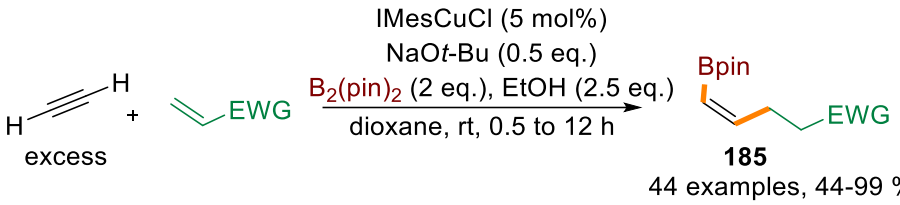

EWG = CO_2X where X = *n*-Bu, Et, Ph, $CO_2(CH_2)_2Y$ where Y = OH, I, CN, $COS(CH_2)_2Ph$, COR, where R = Et, *Cy*Hex-3-enyl, Ph, *p*-CO_2MePh, *p*-CF_3Ph, *p*-NO_2Ph, 2-furanyl, 2-thienyl, styryl, 1-Naph, 9-Anth, CN, SO_2Ph, SO_2Me, etc.

Scheme 1.91: *Syn*-selective coupling of acetylenes with Michael acceptors

Cu-catalyzed alkyl/benzyl borations

A vast majority of carboborations of alkynes occur using Cu-catalysts. Generally, a Cu–Bpin species forms *in situ* and adds across the alkyne (in a *syn* manner) to give an alkenyl–Cu intermediate, which is then trapped by an electrophile (e.g. alkyl or aryl halide) to afford the carboborated product (**Scheme 1.92**).[221]

General Mechanism for Cu-catalyzed carboborations

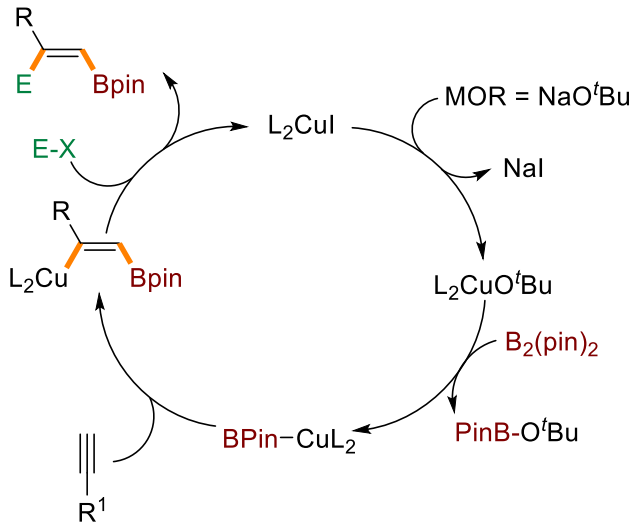

Scheme 1.92: General mechanism for Cu-catalyzed carboborations

Tortosa[221] reported CuCl-catalyzed methylboration of alkynes, proceeding via *syn* β-boration to yield trisubstituted vinylboronates as single *E*-isomers (**Scheme 1.93)**. Terminal alkynes generally gave higher yields than internal ones. The reaction also worked for secondary and tertiary propargylic ethers, but aliphatic alkynes were unreactive.

Reaction conditions by Tortosa (2012)

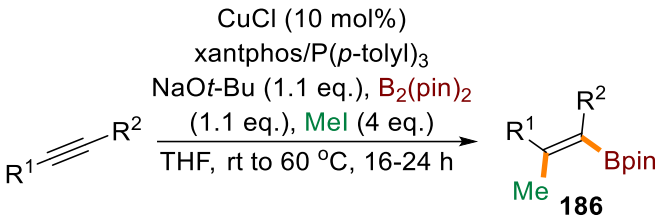

16 examples, upto 83%

R^1 = Ph, *m*, *p*-MePh, *p*-^{t}BuPh, *o*, *p*-OMePh, *p*-FPh, *p*-BrPh, 2-thienyl, 3,5-$(CF_3)_2$Ph;
R^2 = H, Me, Ph

Scheme 1.93: Cu-catalyzed methylborations

Building on this, Yoshida[222] disclosed $Cu(OAc)_2$ catalyzed *syn*-alkylborations of alkynes using alkyl/benzyl haldies (**Scheme 1.94)**. Aryl-alkyl alkynes exclusively underwent β-boration. While terminal alkynes and dialkyl participated in the reaction, the products were obtained with low to moderate regioselectivity. A range of halides, pseudohalides, and dialkyl halides proved effective in this transformation.

Reaction conditions by Yoshida (2013)

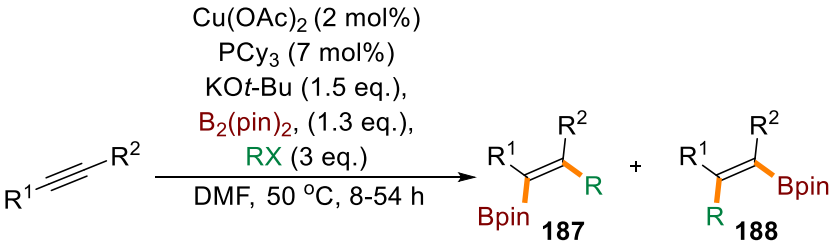

11 examples, 44-84 %
187:188: 51:49 to >99:1

R^1 = H, Me, *n*-Pr, Ph, *p*-OMePh; R^2 = *n*-Pr, *n*-Pent, *p*-OMePh, *p*-BrPh, 2-thienyl, Ph, *Cy*Pent, etc.; R = Me, *n*-Bu, *n*-Pent, 2,4,6 trimethyl benzyl, 2,4,6 triisopropyl benzyl, *p*-MeBn, *p*-OMeBn, *o*-MeBn, cinnamyl,; X = Cl, Br, OTs, $OPO(OEt)_2$

Scheme 1.94: Cu-catalyzed alkyl and benzylborations

A year later, Cazin[223] reported Cu-catalyzed methyl and benzylboration of internal alkynes that could be carried out in air (**Scheme 1.95)**. Under inert atmosphere, catalyst loading could be reduced to as low as 0.5 mol %. The reactions proceed via *syn*-addition and β-boration, delivering trisubstituted alkenylboronates with excellent yields and regio- and stereoselectivity.

Reaction conditions by Cazin (2014)

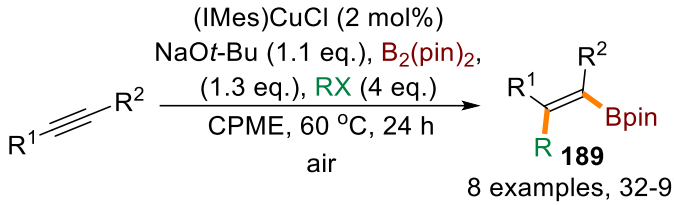

R^1 = Ph, *p*-BrPh, *p*-CO_2MePh, 2-thienyl, etc.; R^2 = Me, Et, TMS, *n*-Bu, *Cy*Hex; R = Me, Bn, *Cy*PrCH_2; X = Cl, Br, I

Scheme 1.95: Cu-catalyzed methyl and benzylborations in air

Two years later, Fu[224] demonstrated that regioselectivity of Cu-mediated alkylboration of terminal alkynes could be controlled by the ligand choice: phosphine ligands (e.g. dppbz) with $B_2(pin)_2$ yielded β-boration (*anti*-Markovnikov), while nitrogen ligands (e.g. DMAP) with $(Bpai)_2$ favored α-boration (Markovnikov), both with excellent regioselectivity (**Scheme 1.96)**. A variety of terminal aliphatic and heterocyclic alkynes including those bearing ethers, esters or amines were well tolerated, and primary alkyl and benzyl iodides participated, though secondary alkyl halides were ineffective.

Reaction conditions by Fu 2016)

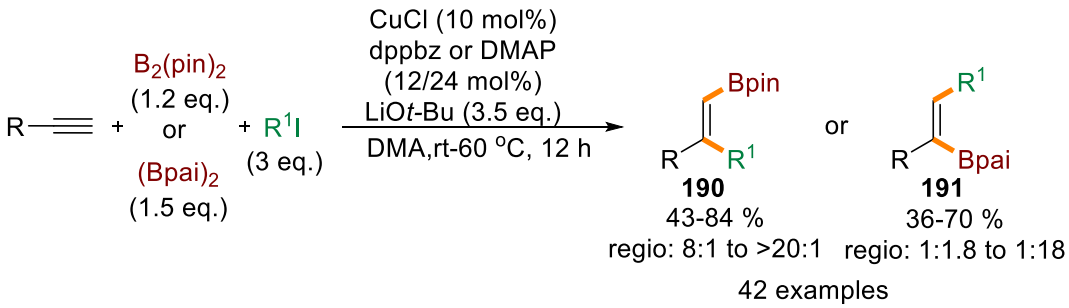

R = *n*-Pr, *n*-Bu, *n*-oct, $(CH_2)_6$S-pyridyl, $(CH_2)_6NBn_2$, *i*-Pr, ^{t}Bu, etc.;
R^1 = Me, *n*-Pr, $Ph(CH_2)_2$, $(CH_2)_4COOEt$, $(CH_2)_4CH{=}CH_2$, etc.

Scheme 1.96: Cu-catalyzed α & β-selective alkyl and benzylborations of terminal alkynes

Kanai[225] demonstrated that Cu/NHC catalyst bearing a naphthoquinone (NQ) ligand can mediate alkylboration of alkyl-substituted alkynes (**Scheme 1.97)** with minimal side reactions (boration of alkyl halide). For substrates bearing bulky alkyl substituents, heteroatoms (at propargyl position), or aryl-alkyl alkynes, the reaction proceeds via *syn*-selective β-boration/α-cupration in moderate to high regioselectivity. Terminal alkynes also react, but with only moderate selectivity. Various primary alkyl iodides are accepted although secondary derivatives did not participate in the reaction.

Reaction conditions by Kanai (2016)

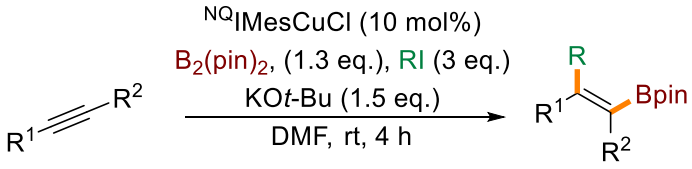

192

21 examples, upto 90 %

regio: 1.7:1 to >20:1

R^1 = Et, *n*-Pent, ^{i}Pr, $BnO(CH_2)_2$, $PivO(CH_2)_2$, $CO_2Me(CH_2)_3$, $CO_2NEt_2(CH_2)_3$, Ph, etc.;
R^2 = H, Me, Et, *n*-Bu; R = Me, Bn, $Ph(CH_2)_3$, $CO_2Et(CH_2)_3$, ^{i}Pr, etc.

Scheme 1.97: Cu-catalyzed alkyl and benzylborations

Lee[226] extended methylborations by giving access to aliphatic methyl substituted alkenyl boronates using Cu/NHC catalysis (**Scheme 1.98)**. Under mild, operationally simple conditions, this *syn*-addition/β-boration sequence delivers trisubstituted alkenyl boronates in elegant yields and >98:2 regioselectivity. Bioactive isoindolinones including isohericerin, isohericenone, and erinacerin A were synthesized using this method.

Reaction conditions by Lee (2017)

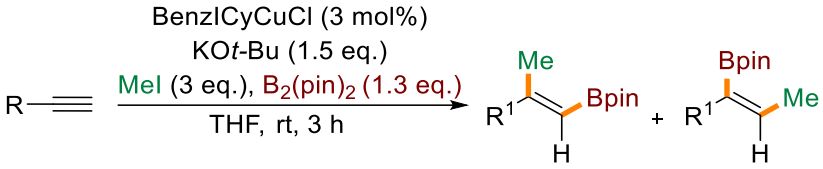

193 **194**

10 examples, 77-86 %

regio: 91:9 to >98:2

R = *n*-Bu, *n*-Hex, $(CH_2)_3Cl$, $(CH_2)_4CO_2{}^t$Bu, $(CH_2)_2$Ph, *Cy*Hex, ^{t}Bu, Ph

Scheme 1.98: Cu-catalyzed methylborations of terminal alkynes

Carretero[227] developed a Cu(I)-catalyzed *syn*-alkylboration of aryl-alkyl alkynes using a dynamic phosphine/phenanthroline ligand system, alkyl halides and B_2pin_2 to access β-borylated alkenes with high regioselectivity (**Scheme 1.99)**. The protocol shows broad scope: secondary cyclic alkyl bromides couple efficiently with electron-neutral or rich alkynes, and biologically relevant estrone, monosaccharide and gibberellic acid derivatives are well tolerated. For electron-deficient alkynes, cyclic alkyl iodides with minor condition tweaks yield better results. Likewise, propargyl ethers and primary alkyl halides bearing functional handles deliver comparably high efficiency. Mechanistically, the cycle proceeds via vinyl–Cu–B formation using trialkyl phosphines, then a ligand exchange to phenanthroline enables X-atom transfer (XAT) and radical coupling to furnish the product.

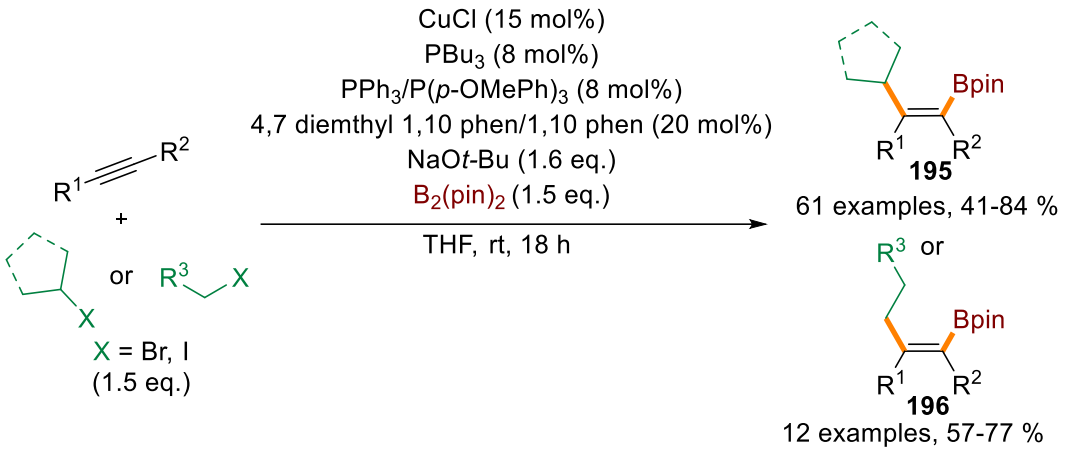

R^1 = Ph, *o*, *p*-OMePh, *p*-FPh, *p*-CO_2MePh, *p*-CNPh, *p*-CF_3Ph, 4-pyridyl, fluorenyl, 4-bipehnyl, 2-Nap, CH_2OBn, CH_2OTBS; R^2 = Me, Et, *n*-Bu, $(CH_2)_3$CONBocPh, $(CH_2)_2$Y where Y = ^{i}Pr, OTBS, OAc, Ph, CH_2OBn; Cycloalkyl = *Cy*Pen, *Cy*Hex, *Cy*Hept, oxane, oxetane, NBoc-piperidines, pyrolidines, etc.; R^3 = 1,3-dioxolane, $(CH_2)_2$Cl, CH_2-epoxide, allyl, $(CH_2)_2CO_2$Et, $(CH_2)_2$OPh, etc.

Scheme 1.99: Cu-caytalyzed *syn*-alkylborations with primary and secondary alkyl halides

Tang and Pan[228] made use of heterogeneous Cu/NHC catalysts supported on porous organic ligands to achieve highly *syn*-selective alkylboration of terminal and internal alkynes (**Scheme 1.100A)**. Homogeneous systems yielded only trace products. The method largely proceeds via β-boration across broad substrates, giving excellent yields, though regioselectivity drops slightly for aliphatic alkynes. Several primary alkyl and benzyl iodides and bromides were compatible, a notable example being the (iodomethyl)cyclopropane giving only the desired product and no ring opening product. Other cyclic and bulky borylating agents were also tolerated with similarly excellent outcomes. To simplify the catalyst system and bypass the multistep synthesis from Tang's method, Bose[229] employed low-valent copper to enable benzyl- and methylboration of terminal alkynes (**Scheme 1.100B)**. Regardless of the substitutents, both benzyl bromides and methyl iodides resulted in β-borylated olefins with high yields and outstanding regioselectivity. Additionally, conjugated enynes, heterocycles (e.g. thiophenes) and cyclic aliphatic substrates were also tolerated. In particular, benzyl bromides bearing various para-substituents on the aromatic ring were smoothly accommodated.

Reaction conditions by Tang & Bose (2024-25)

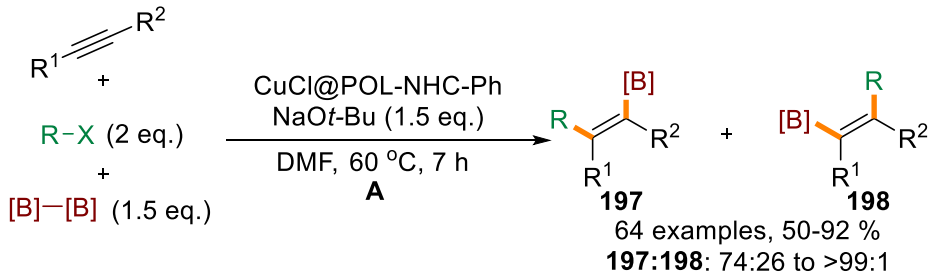

R^1 = *n*-Pr, *n*-Bu, Ph, *p*-MePh, *p*-^{t}BuPh, *p*-OMePh, *p*-BrPh, *m*-ClPh, *o*-CF_3Ph, 2-Nap, 2-thienyl, ferrocene, CH_2=CMe, CH_2OTBS, $PhNMeCH_2$, etc.; R^2 = H, Me, Et, *n*-Pr, *n*-Bu, etc.; R = Me, $(CH_2)_3$-CH_3, $(CH_2)_7$-CH_3, $EtOOC(CH_2)_3$, Bn, etc.; X = Br, I; [B] = $B_2(pin)_2$, B_2nep_2, B_2pai_2, B_2mpd_2, etc.

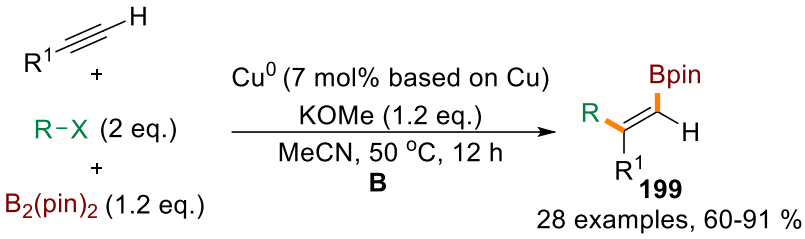

R^1 = Ph, *p*-MePh, 4-Biphenyl, *p*-OMePh, *p*-BrPh, *p*-ClPh, *p*-CF_3Ph, *p*-CNPh, 3-thienyl, *Cy*hexenyl, *Cy*Pr, *Cy*Hex, $PhO(CH_2)_2$, etc.; R = Me, Bn, 4-PhBn, 4-CF_3Bn, 4-FBn, 4-^{t}BuBn, etc.; X = Br, I

Scheme 1.100A and B: *Syn*-selective alkylborations using heterogenous and low valent copper catalysts

Fe-catalyzed alkylborations

Nakamura[230] developed an Fe(II)-catalyzed alkylboration of symmetric aliphatic alkynes with primary and secondary alkyl bromides (**Scheme 1.101**). Although the substrate scope was limited, the method afforded *syn*-selective alkenylboronates in moderate yields.

Reaction conditions by Nakamura (2015)

R = Me-$(CH_2)_9$, CN-$(CH_2)_6$, benzyl piperidine-1-carboxylate

Scheme 1.101: Fe-catalyzed *syn*-alkylborations of symmetrical alkynes

Pd/Cu catalyzed alkenyl/arylborations

Suginome[231] demonstrated Pd-catalyzed carboborations via multicomponent coupling between N,N-dimethylethylenediamine derived chloroboranes, alkenyl/arylzirconium chlorides and alkynes (**Scheme 1.102**). The reaction followed a *syn*-addition path undergoing α-alkenylation (**201**)/arylation (**202**) in terminal alkynes with high selectivity and a single example of alkenylboration in internal alkyne also followed the same route, although, alkylzirconium reagents did not participate in the reaction.

Reaction conditions by Suginome (2008)

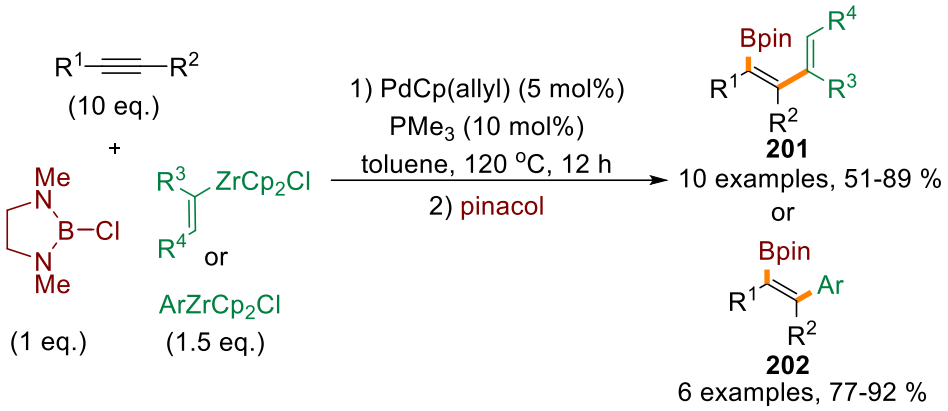

R^1 = H, Me, *n*-Pr; R^2 = *n*-Pr, *n*-Bu, ^{t}Bu, Ph; R^3 = H, *n*-Pr; R^4 = *n*-Bu, ^{t}Bu, Ph,TMS, etc.; Ar = Ph, *p*-OMePh, *p*-CF_3Ph

Scheme 1.102: Pd-catalyzed *syn*-selective borations using organozirconium reagents

Brown[232] demonstrated the first Cu-catalyzed *syn*-arylboration of alkynes using aryl iodides (**Scheme 1.103**). With enynes and unsymmetrical diaryl alkynes, the reaction produced highly substituted vinyl boronates in good yields but low regioselectivity, whereas aryl–alkyl alkynes delivered similar yields with high regioselectivity (β-boration). In contrast, terminal alkynes failed to couple, instead giving only hydroboration products.

Reaction conditions by Brown (2014)

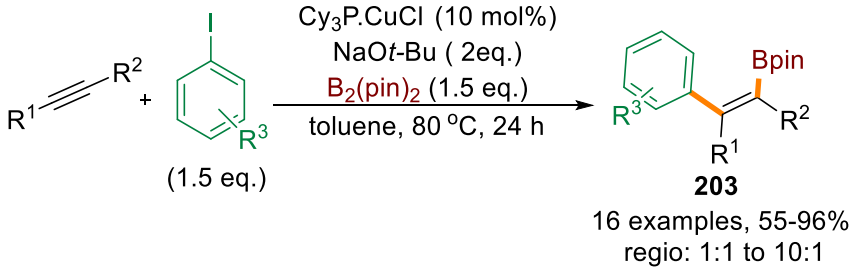

R^1 = *n*-Pr, Ph, *p*-OMePh, *p*-CF_3Ph; R^2 = Et, *n*-Pr, Ph, *o*-tolyl, MeC=CH_2, *p*-OMePh, *p*-CF_3Ph; R^3 = H, 4-OMe, 4-Me, 4-Cl, 4-CF_3, 3,5-di-Me, etc.

Scheme 1.103: Pd/Cu-catalyzed *syn*-arylborations using aryl iodides

The following year, Cazin[233] demonstrated *syn*-arylboration of (hetero)aryl–alkyl alkynes using Pd/Cu(NHC) bimetallic catalysis (**Scheme 1.104**). Diverse aryl chlorides and bromides bearing both electron-donating and withdrawing groups were accepted, and heteroaryl groups like pyridines also underwent β-boration with excellent regioselectivity.

Reaction conditions by Cazin (2015)

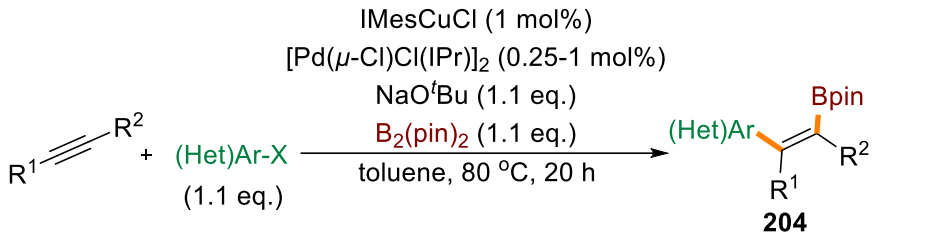

12 examples, 80-96 %
regio: 88:12 to 99:1

R^1 = Ph, pyridyl; R^2 = Et, *n*-Bu; (Het)Ar = *o*, *p*-MePh, *m*, *p*-OMePh, 2,4 di-FPh, *m*-FPh, 2/3-pyridyl, *m*-AcPh, *p*-CNPh; X = Cl, Br

Scheme 1.104: Pd/Cu-catalyzed (hetero)arylborations using (hetero)aryl chlorides and bromides

Two years later, Nakao[234] and co-workers developed a Pd/Cu-catalyzed *syn*-selective arylboration of internal alkynes, using (hetero)aryl chlorides or bromides together with $B_2(pin)_2$ (**Scheme 1.105**). Unsymmetrical diaryl alkynes yielded products with moderate efficiency and regioselectivity, while aryl–alkyl alkynes gave high yields and promising regioselectivity (proceeding via β-boration). Importantly, heteroaryl bromides (e.g. 2/3-bromothiophenes) were effective coupling partners as the corresponding chlorides failed to deliver products.

Reaction conditions by Nakao (2017)

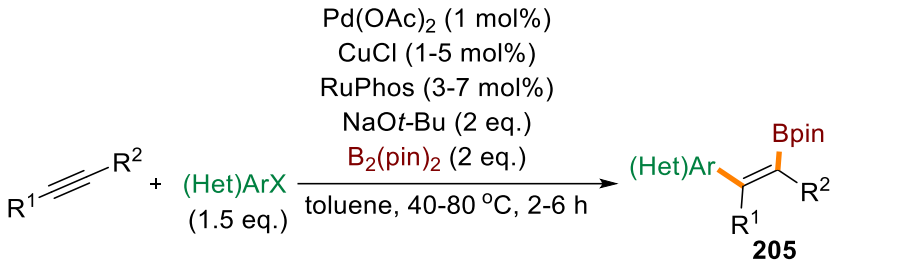

17 examples, upto 82 %
regio: 52:48 to >97:3

R^1 = Ph, *p*-MePh, *p*-FPh, *p*-OMePh; R^2 = H, Me, Et, *n*-Pr, Ph, *p*-MePh, *p*-FPh, *p*-CF_3Ph, mesityl; (Het)Ar = *p*-OMePh, *p*-AcPh, *p*-CO_2MePh, *p*-CNPh, 2-thienyl, 3-thienyl, *p*-tolyl,; X = Cl, Br

Scheme 1.105: Pd/Cu-catalyzed (hetero)arylborations using (hetero)aryl chlorides and bromides

Building on their Cu-catalyzed arylboration of internal alkynes with aryl iodides, Brown's[235] group later developed a Pd/Cu cooperative system employing Cu-pyridylidene complexes to achieve *syn*-selective heteroarylboration of internal and heteroaryl alkynes using heteroaryl bromides (**Scheme 1.106)**. This method achieves excellent *E*:*Z* selectivity (typically > 20:1) and tolerates a wide array of heterocycles including fused-ring motifs at both the heteroaryl bromide and alkyne ends.

Reaction conditions by Brown (2019)

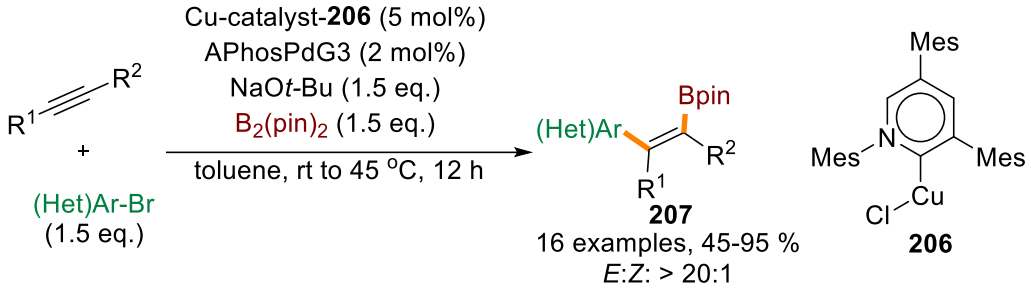

R^1 = Ph, TMS, Et, 2-thienyl, 2-methoxy 5-pyridyl, *p*-OMePh, 2-methoxy 4-pyridyl;
R^2 = Me, Et, (CH_2)NHBoc, Ph, CH_2OTBDPS, CH_2Ph; (Het)Ar = 2-methoxy 5-pyridyl, 2-methoxy 6-pyridyl, 2-methoxy 5-pyrimidyl, quinolin-3-yl, 3-furanyl, indol-6-yl, etc.

Scheme 1.106: Pd/Cu-catalyzed heteroarylborations of heteroaryl alkynes

Cu-catalyzed allylborations

Zhong[236] introduced the first Cu-catalyzed *syn*-selective allylborations on alkynes using primary/secondary allyl phosphates and $B_2(pin)_2$ **(Scheme 1.107)**. Aryl acetylenes with secondary allyl phosphates result in *E*-dienes, exhibiting γ-selectivity while alkyl derivatives lead to α/γ mixtures while primary derivatives only give γ-selective products. While terminal and cyclic allyl phosphates are tolerated, the former resulted in slightly lower yields with diaryl alkynes. Substituted allyl phosphates and shorter alkyl chains in alkynes lead to reduced yields but preserve selectivity. In the case of aryl alkyl alkynes, the selectivity of the product is governed by the steric, electronic environments and the behaviour of the alkenyl copper intermediate. Increasing the steric bulk at the γ-position of the phosphate shifts selectivity toward the α-isomer.

Mastral[237] expanded allylborations of alkynes using bimetallic catalysts (Cu/Pd) and allyl carbonates **(Scheme 1.108A)**. Both symmetrical and unsymmetrical alkynes (β-boration) including terminal ones underwent *syn*-selective addition leading to 1,4 dienes in excellent outcomes and high regioselectivity. Aliphatic terminal alkynes also reacted with the same efficiency and similar regioselectivity. A broad range of allylic carbonates (terminal/internal, primary/secondary, acyclic/cyclic) were well accommodated.

Reaction conditions by Zhong (2015)

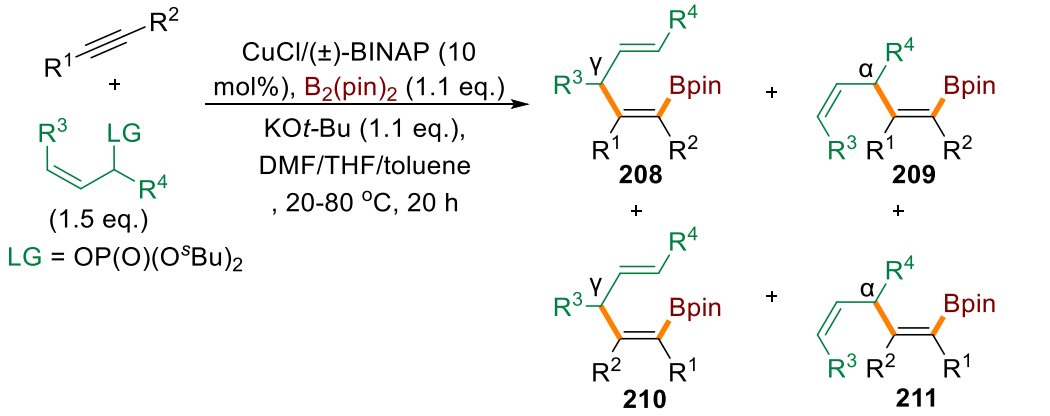

Terminal alkynes: 15 examples, 43-84 %, **208:209**: 85:15 to >99:1
Diphenyl acetylenes: 18 examples, 53-94 %, **208:209**: 37:63 to 99:1
Aryl alkyl alkynes: 9 examples, 49-93 %, **208:209:210:211**: 83:12:2:3 to 99:1:<1:<1
R^1 = Ph, *p*-OMePh, *o*, *m*, *p*-ClPh, *p*-CF_3Ph, etc.; R^2 = H, *n*-Pr, *n*-Bu, Ph; R^3 = H, Me, *n*-Bu, ^{t}Bu, Ph, $BnOCH_2$, TMS, etc.; R^4 = H, $Ph(CH_2)_2$, Et, Me, ^{t}Bu, *Cy*Hex, etc.

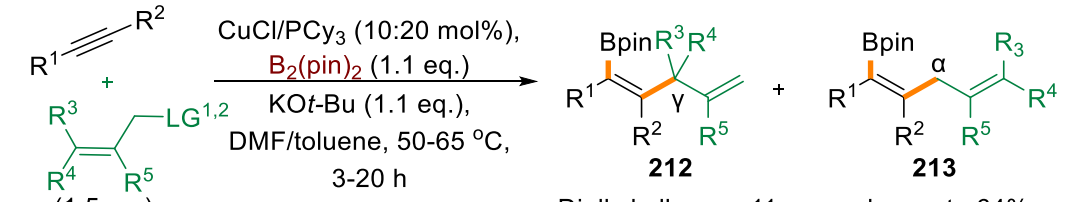

LG^1 = $OP(O)(O^iPr)_2$,
LG^2 = $OP(O)(O^sBu)_2$

Dialkyl alkynes: 11 examples, upto 64%, γ:α: 88:12 to 99:1
Diaryl & aryl-alkyl alkynes: 19 examples, 51-88%, α:γ: 79:21 to 99:1

R^1 = Et, *n*-Bu, Ph, *p*-FPh, *o, m*-ClPh, *m*, *p*-CF_3Ph; R^2 = Et, *n*-Pr, *n*-Bu, Ph, *p*-FPh, *p*-CF_3Ph, *m*-ClPh; R^3 = H, Me, *n*-Hex, ^{t}Bu, o-MePh, Ph,; R^4 = H, Me, Ph; R^5 = H, Me

Scheme 1.107: Cu-catalyzed allylborations using 1° & 2° allyl phosphates

In the successive year they reported allylborations using dihaloalkane derivatives, which resulted in dienes, convertible to dendralenes **(Scheme 1.108B)**.[238] Both terminal and internal alkynes were compatible, although the latter required slow addition of the allyl derivative to suppress the Cu-Bpin allylation. Allyl bromides bearing primary or secondary substituents reacted selectively at the substituted site to afford a single product.

Reaction conditions by Mastral (2017-18)

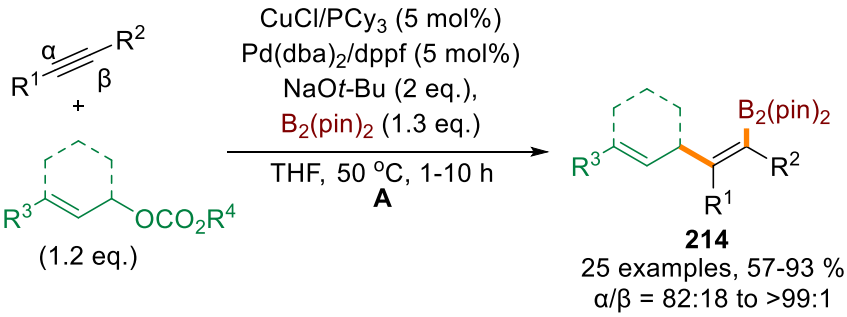

R^1 = Et, *n*-Bu, Ph, $OTBSCH_2$, $NHTsCH_2$, 3-thienyl, *Cy*Hexenyl, TMS, etc.; R^2 = H, Me, Et, Ph, R^3 = H, Me, Et, *p*-OMePh, *p*-BrPh, *p*-CO_2MePh, Ph, etc.; R^4 = Me, ^{t}Bu

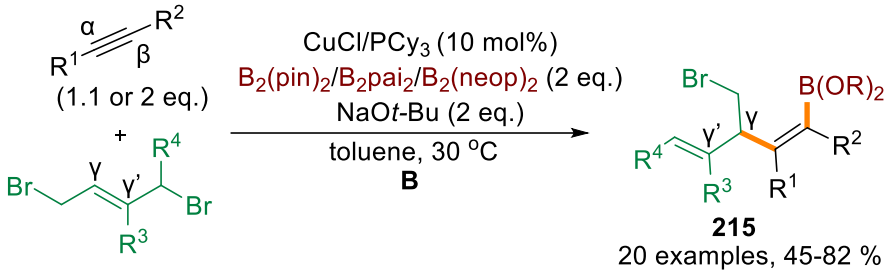

R^1 = *n*-Bu, Ph, *p*-CO_2MePh, *p*-OMePh, *p*-BrPh, *p*-ClPh, 3-thienyl, TMS, *Cy*Hexenyl, $OTBSCH_2$, etc.; R^2 = H, Me, Et; R^3 = R^4 = H, Me

Scheme 1.108A and B: Pd/Cu- catalyzed allylborations using allyl carbonates and dibromides

Engle's[239] work introduces a Cu–CAAC–catalyzed protocol for *syn*-allyl- and alkylboration of terminal alkynes using allyl phosphates or alkyl iodides and B_2pin_2, predominantly delivering α-borylated dienes (**217** or **218**) via γ-allylation (in case of allyl derivatives) with excellent regioselectivity **(Scheme 1.109)**. The method accommodates several linear and cyclic aliphatic alkynes, while NBoc-protected amines and azetidine derivatives showed modest decreases in yield and regioselectivity. γ-substituted allyl electrophiles maintained high α-selectivity via γ-allylation, although minor α-allylation (γ': α' = 93:7 to 97:3) was also observed. Alkyl iodides including ethyl, benzyl, deuterated methyl variants as well as other functionalities were well tolerated though benzyl propargyl ethers and phenyl acetylenes led to poor regioselectivity and *tert*-butyl acetylene gave <20 % yield. This method constitutes the first example of α-boration of terminal alkynes with concomitant allylation.

Reaction conditions by Engle (2022)

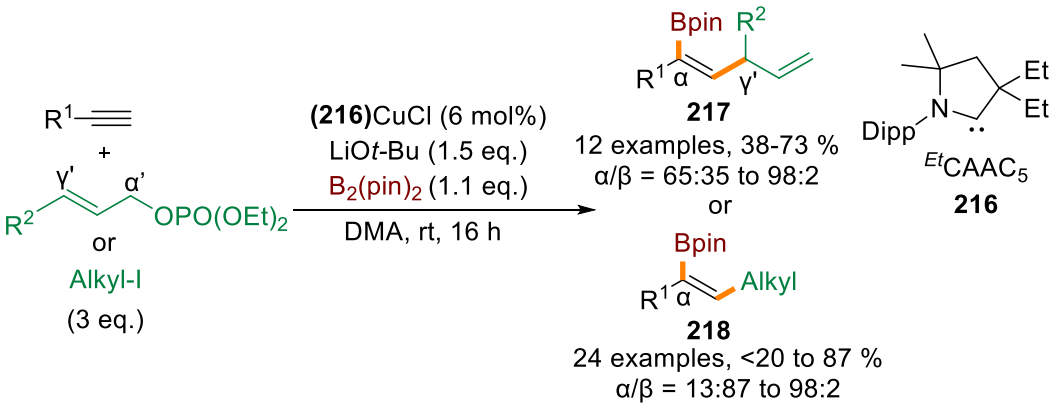

R^1 = $(CH_2)_3Ph$, $(CH_2)_5Me$, $(CH_2)_3OPh$, $(CH_2)_3CN$, $(CH_2)_4Cl$, $(CH_2)_2$-NPhth, $(CH_2)_2NHBoc$, CH_2OBn, NBoc-protected azetidine, ^{i}Pr, ^{t}Bu, Ph, Ph-$(CH_2)_3$, *Cy*Hex; R^2 = H, *n*-Pr, Ph; Alkyl = Me, Et, Bn, $Ph(CH_2)_3$, $(CH_2)_3OTBDMS$, $(CH_2)_4CO_2Et$

Scheme 1.109: Cu–CAAC–catalyzed α-selective alkyl/allylboration of terminal alkynes

Pd/Cu-catalyzed Allenylborations

Fu[240] and colleagues were the first to report Pd/Cu–NHC-catalyzed allenylboration of alkynes using propargyl carbonates or ethers with B_2pin_2 **(Scheme 1.110)**. In this *syn*-selective transformation, the boronate adds at the β-position to afford boryl-substituted ene-allenes in excellent yields. A wide range of aliphatic terminal alkynes, including functionally diverse substrates, underwent the reaction smoothly, and even skipped or conjugated enynes/diynes proved compatible. In competition experiments, a terminal alkyne reacted preferentially over a substrate bearing both internal and terminal triple bonds. Aromatic alkynes, whether terminal or internal also participated under mildly adjusted conditions. Notably, most propargyl carbonates, including bulky steroidal derivatives, performed well, although the sterically hindered phenyl propargyl carbonate retarded the reaction by stabilizing the allenyl–Pd intermediate.

Reaction conditions by Fu (2020)

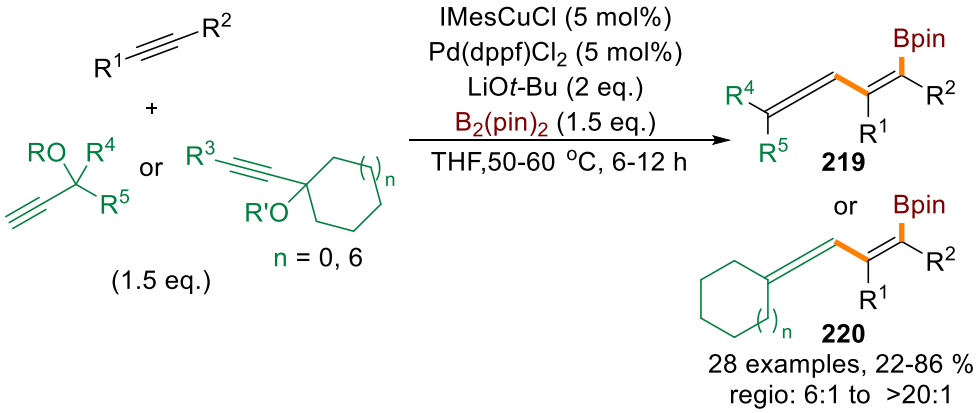

R^1 = Me, *n*-Bu, *Cy*Pr, *Cy*Hex, *Cy*Hexenyl, TMS, Ph, NBoc-protected piperidine, $(CH_2)_2OBn$, $(CH_2)_3Cl$, $(CH_2)_2Ph$, $(CH_2)_2$hexynyl; R^2 = H, Me, Ph; R^3 = H, *n*-Bu; R^4 = Me, Ph; R^5 = H, Ph; R = CO_2Me; R' = Boc

Scheme 1.110: Pd/Cu-catalyzed allenylborations

Pd-catyalyzed Fluoroalkylative borations

Zhu[241] pioneered the first Pd-catalyzed *anti*-fluoroalkylative boration of alkynes using ethyl iododifluoroacetate, delivering α-borylated alkenes with moderate efficiency **(Scheme 1.111)**. The reaction tolerated various substitutions on phenylpropyne though yields declined with *ortho*-substituents, electron-withdrawing groups, and longer or branched aliphatic chains. Notably, an estrone-derived alkyne and terminal alkynes were successfully converted; higher diboron reagents (e.g. B_2nep_2, B_2mpd_2) also proved suitable. Additionally, with enhanced catalytic loading and employing lithium iodides (LiI), bromodifluoroacetamides and ethyl bromomonofluoroacetates were transformed into desired products with decent outcomes.

Reaction conditions by Zhu (2018)

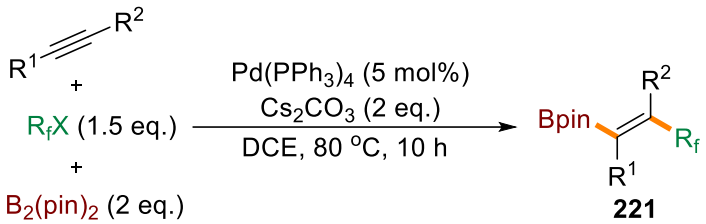

221

31 examples, upto 84 %

R^1 = *n*-Bu, Ph, *o*, *m*, *p*-MePh, *p*-^{t}BuPh, *p*-ClPh, *p*-BrPh, *p*-FPh, *p*-CF_3Ph, *p*-OMePh, *p*-OAcPh, *p*-NPhthPh, 3-thienyl; R^2 = H, Me, Et, ^{i}Pr, ^{t}Bu; R_f = CF_2CO_2Et, CF_2CONH^iPr, $CF_2CONHCy$, $CF_2CONHBn$, CF_2CONEt_2, $CHFCO_2Et$, C_4F_9, etc.; X = Br, I

Scheme 1.111: *Anti*-fluoroalkylative α-borations with halodifluoroacetates and acetamides

Chaładaj[242] and co-workers reported a Pd-catalyzed, *anti*-selective fluoroalkylative boration of alkynes using perfluorobutyl iodides and B_2pin_2 **(Scheme 1.112)**. Effective catalysis required two different ligands and a slight excess of water over base to enable transmetallation. A broad range of terminal alkynes bearing diverse electronic substituents were converted to fluoroalkyl substituted α-borylated alkenes exclusively, though *ortho*-substituted aryl substrates gave reduced yields. The method could also be extended to aryl-alkyl alkynes and other fluoroalkyl iodides with comparable efficiency.

Reaction conditions by Chaładaj (2019)

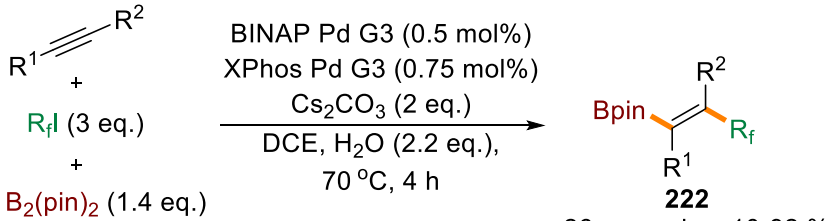

222

26 examples, 10-92 %

R^1 = Ph, *p*-^{t}BuPh, *o*, *p*-OMePh, *p*-OBnPh, *p*-FPh, *o*, *p*-BrPh, *p*-CF_3Ph, *p*-BpinPh, *Cy*Hexenyl, $(CH_2)_3Cl$, $(CH_2)_3CN$, etc.; R^2 = H, Me, Et, *n*-Bu; R_f = C_4F_9, C_6F_{13}, CF_2CO_2Et

Scheme 1.112: *Anti*-fluoroalkylative α-borations using perfluoroalkyl iodides

Zhang[243] extended Zhu's strategy by performing α-selective fluoroalkylative borations of aryl-alkyl alkynes using ethyl iododifluoroacetate, delivering (*Z*)-configured α-fluoroalkenylboronates **(Scheme 1.113)** with *Z*/*E* ratios commonly ranging between 90:10 and 98:2. The method exhibits broad functional-group compatibility (e.g. aliphatic esters, azides, phthalimides, nitro groups, thiazole rings, and secondary amines on the alkyne terminus), while terminal alkynes (aryl and aliphatic) were also effective but dialkyl alkynes remained unreactive. The procedure could be applied to bulkier fluoroalkyl iodides and fluoroalkylacetamide reagents without loss of efficiency or stereocontrol.

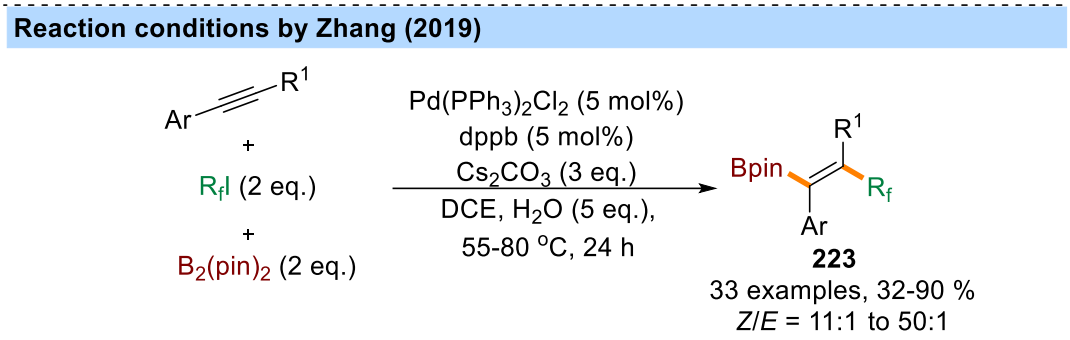

Ar = Ph, *p*-^{t}BuPh, *p*-OMePh, *p*-ClPh, *p*-CF_3Ph, *p*-TMSPh, *m*-CO_2EtPh, *m*-CHOPh, *p*-BrPh, $PhCH_2$; R^1 = H, Me, Et, *n*-Bu, Ph, $(CH_2)_nX$ where n = 3-5, X = CO_2Me, Cl, phthalimide, OH, N_3, NO_2 OTBS, $CO_2CH(Me)NHBoc$, R_f = CF_2CO_2Et, $CF_2CON(Et)_2$, CF_2CO-morpholine, C_nF_{2n+1}, n = 4, 6, etc.

Scheme 1.113: *Anti*-fluoroalkylative α-borations with halodifluoroacetates and acetamides

Mechanistically, the catalytic cycle begins with *in situ* reduction of Pd(II) to Pd(0) by B_2Pin_2 in the presence of water. The resulting Pd(0) species mediates single-electron transfer to the fluoroalkyl iodide, generating a fluoroalkyl radical that adds across the alkyne to form a vinyl radical, which is rapidly iodinated, giving a vinyl iodide via a formal *iodoperfluoroalkylation* step. This vinyl iodide then undergoes Pd-catalyzed Miyuara borylation **(Scheme 1.114)**.

Cu-catalyzed carboxylative/carbonylative borations

Hou[244] group presented *syn*-carboxyboration of alkynes with CO_2 and B_2pin_2 employing Cu/NHC catalyst **(Scheme 1.115)**. Functionalized aromatic alkynes and aryl-alkyl alkynes reacted well, giving a single regioisomer (by α-carboxylation). Phenyl acetylene also gave β-boralactone derivatives with high regioselectivity (98:2), although bulky *tert*-butyl phenyl acetylene completely suppressed product formation.

Mechanistic aspect

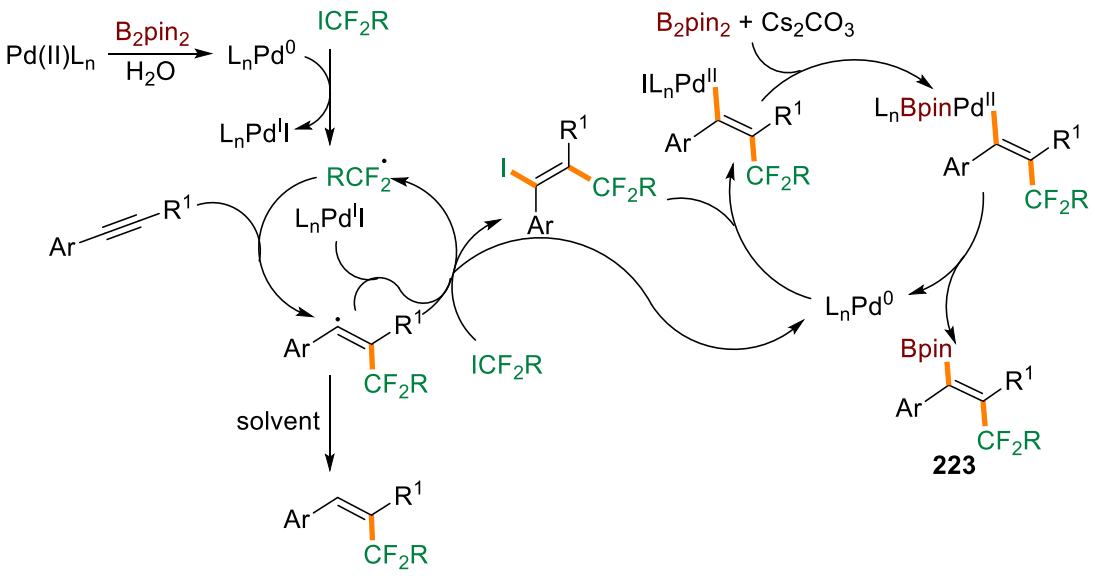

Scheme 1.114: Mechanism of *Anti*-fluoroalkylative α-borations.

Reaction conditions by Hou (2012)

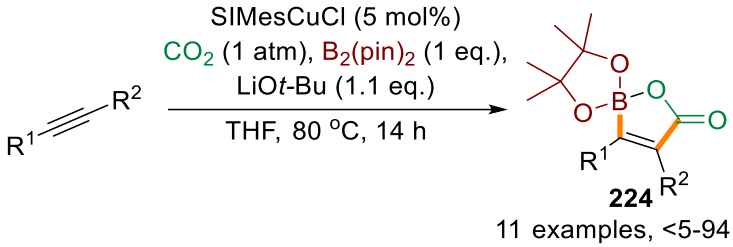

R^1 = H, Me, Et, ^{t}Bu, Ph, *p*-OMePh, *p*-MePh, *p*-tBuPh, *p*-ClPh, *p*-CO_2Et, 2-thienyl;
R^2 = Ph, *p*-MePh, *p*-OMePh, *p*-ClPh, *p*-^{t}BuPh

Scheme 1.115: Synthesis of oxaboroles by Cu-catalyzed *syn*-carboxyboration of alkynes

Mankad's[245] group developed Cu/NHC-catalyzed carbonylative carboboration of internal alkynes with alkyl iodides, CO, and B_2pin_2, giving *syn*-selective β-borylated enones (**225**), which were prone to reduction into oxaboroles (**226**) due to their limited stability **(Scheme 1.116)**. Bromoalkanes also reacted (with lower yields), while chloro derivatives were inert. Unsymmetrical alkynes gave variable regioselectivity; electron-rich alkynes performed better, while dialkyl and terminal alkynes were unreactive. Primary, secondary, and tertiary alkyl iodides could be used, though some tertiary substrates led to elimination byproducts.

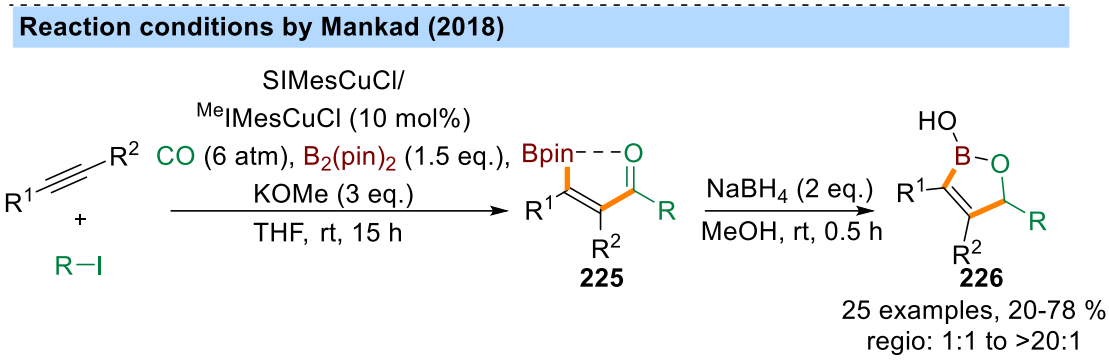

Scheme 1.116: Synthesis of oxaboroles by Cu-catalyzed *syn*-carbonylative carboboration

Mechanistically, base (KOMe), $B_2(pin)_2$, and CuCl first generate a Cu–Bpin species, which adds to the alkyne to form a β-borylated alkenyl-copper(I) intermediate. Single-electron transfer from this species to alkyl iodide produces an alkyl radical that captures CO to form an acyl radical. Radical rebound with a Cu(II) intermediate (**227**) yields a Cu(III) species (**228**), which undergoes reductive elimination to deliver the β-borylenone product **(Scheme 1.117)**.

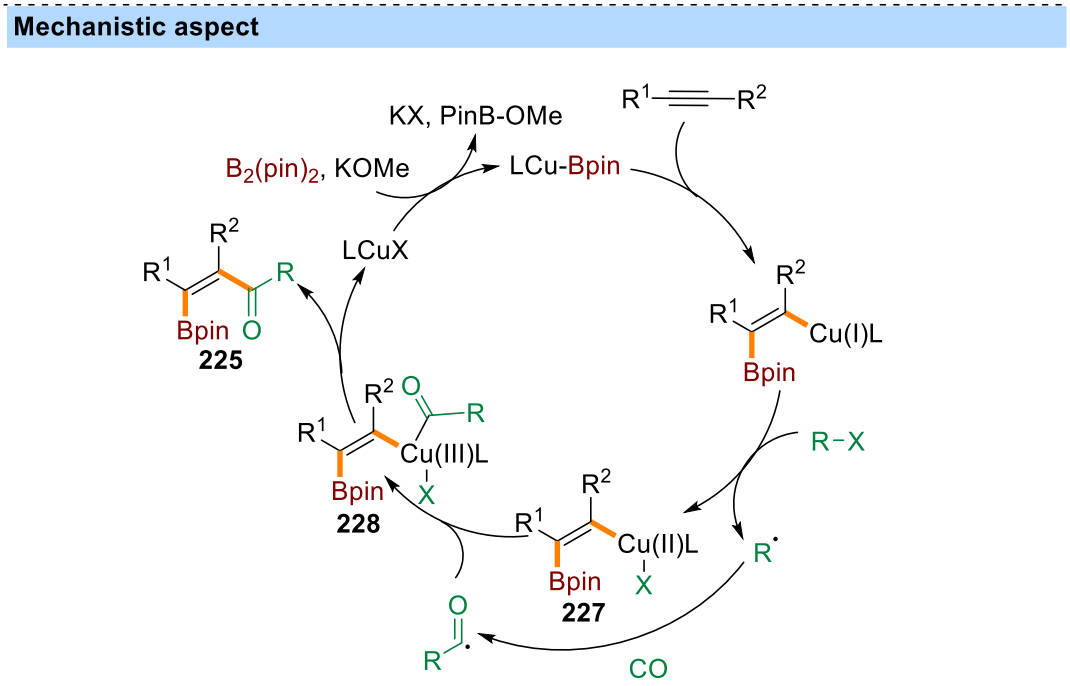

Scheme 1.117: Radical pathway of carbonylative carboboration

Having explored different carbometallation strategies, the subsequent section addresses trifluoromethylthiolation reactions.

1.2 Trifluoromethylthiolation

1.2.1 Properties of SCF_3 group

Fluorine's combination of small size and strong electronegativity gives rise to distinctive properties in fluorinated molecules, making it a key element in the design of modern organic compounds.[246] The introduction of sulfur further enhances the properties of organofluorine compounds. Notably, the trifluoromethylthio group (SCF_3), with its high lipophilicity (π_R = 1.44), strong electron-withdrawing nature (especially in the sulfoxide and sulfone derivatives),[247] metabolic stability, and bioavailability, is valuable in pharmaceutical[248–250] and agrochemical[251] applications. Several biologically[252] active compounds, such as Cafazaflur, Tiflorex, and dibenzazepine[253] derivatives, featuring this functional group are listed below **(Scheme 1.118)**.

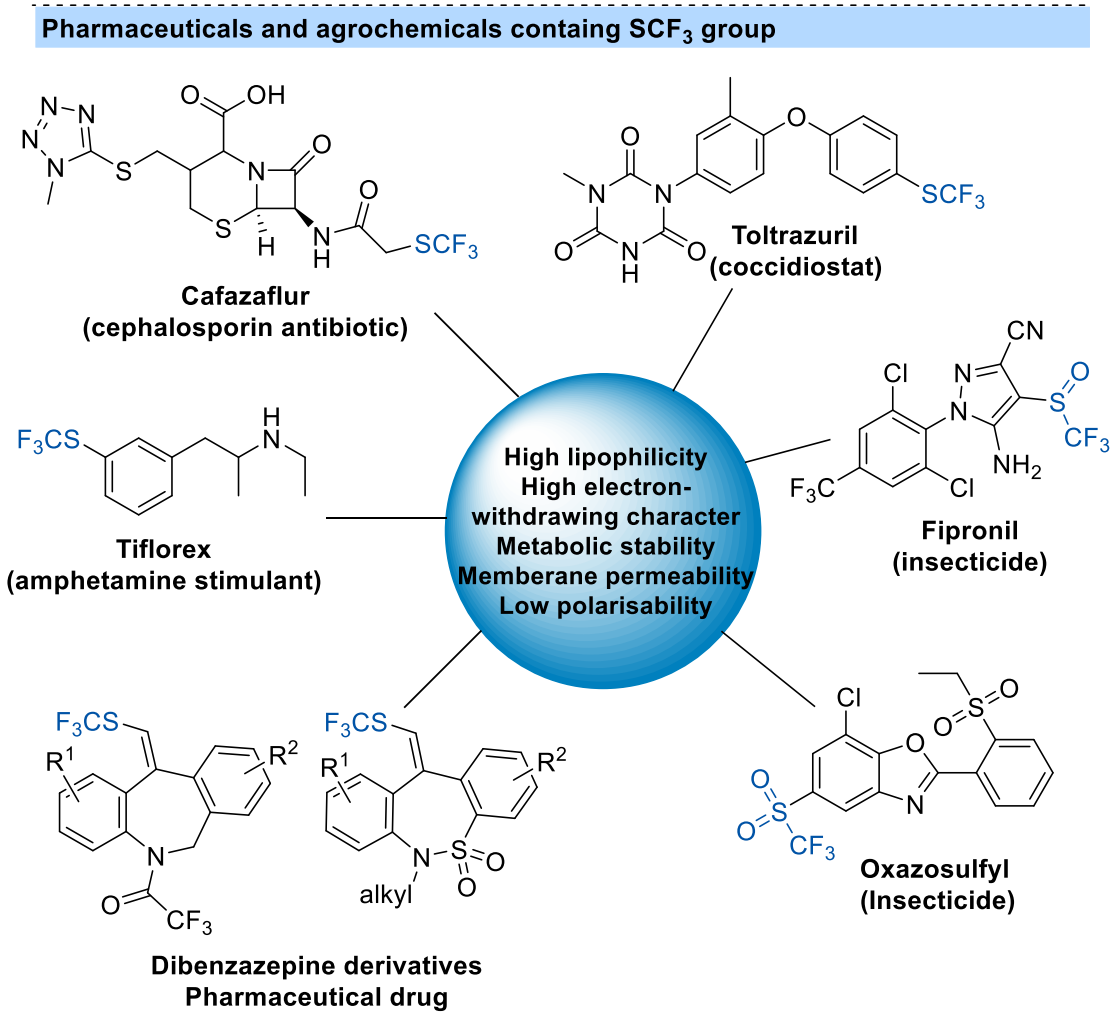

Scheme 1.118: Biologically relevant compounds containing SCF_3 group

1.2.2 Types of -SCF_3 sources

Synthetically, innumerable strategies[247,254–258] utilizing radical, electrophilic and nucleophilic sources of SCF_3 group have been developed.

Electrophilic SCF_3 donors

The first electrophilic trifluoromethylthiolating reagent, bistrifluoromethyl disulfide (CF_3SSCF_3), was developed by Haszeldine.[255] Subsequent methods included the synthesis of CF_3SCl via chlorination of CF_3SSCF_3 under UV light, and Emeleus[259] later proposed an alternative route using dry hydrogen chloride (HCl) and trifluoromethanesulfenamide (CF_3SNH_2) (**Scheme 1.119)**.

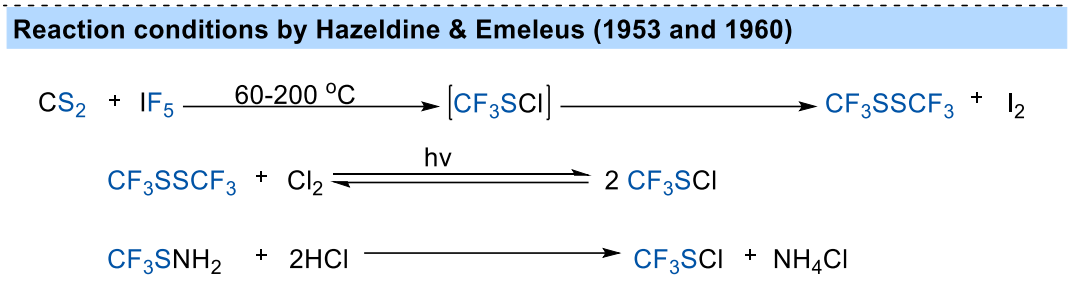

Scheme 1.119: Synthesis of CF_3SSCF_3 and CF_3SCl

Harris[260,261] demonstrated the first use of CF_3SCl in radical trifluoromethylthiolation of fluoroolefins under UV or X-ray irradiation **(Scheme 1.120)**. Notably, CF_3SCl has also shown electrophilic reactivity in the absence of irradiation,[262,263] as seen in reactions with cyclohexenes, where product stereochemistry supports the formation of an episulfonium intermediate **(Scheme 1.121)**.

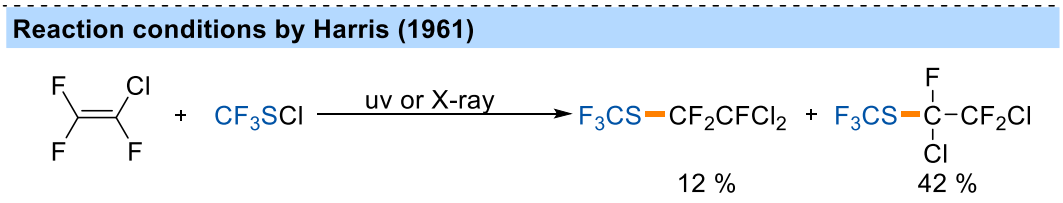

Scheme 1.120: Use of CF_3SCl as a radical SCF_3 source

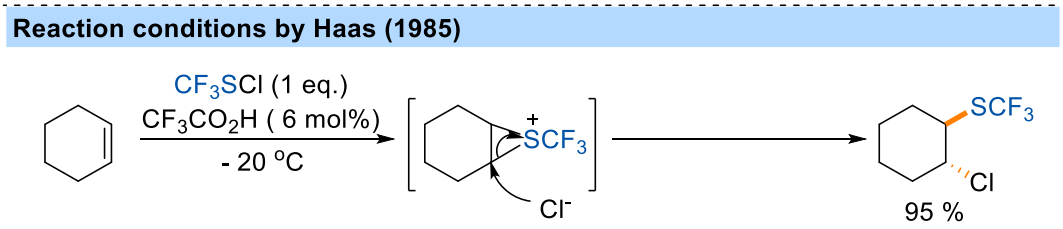

Scheme 1.121: Use of CF_3SCl as an electrophilic SCF_3 source

Novel, user-friendly electrophilic reagents have been developed to replace hazardous, gaseous CF_3SCl and volatile $(CF_3S)_2$ ones. These new reagents fall into three classes: N–SCF_3, O–SCF_3, and SO_2CF_3.[247] The N–SCF_3 reagents are derived from similar N–F systems, while O–SCF_3 reagents draw inspiration from Togni-type electrophiles. Meanwhile, SO_2CF_3 reagents (e.g., CF_3SO_2Na) initially functioned via SO_2 removal but were later found to act as electrophilic SCF_3 sources.

N-SCF_3 reagents (Scheme 1.122)

Haas[264] first attempted to prepare $(CF_3S)_3CCOCl$ using N-trifluoromethylthiosuccinimide (synthesized from silver succinimide, and CF_3SCl), but the effort was unsuccessful. Shen[265] significantly improved this synthesis by using N-bromosuccinimide and $AgSCF_3$, yielding a crystalline, air- and moisture-stable solid. This reagent has been employed intrifluoromethylthiolation of alkynes via *in situ* generation from $AgSCF_3$.[266] Separately, Munavalli[267] developed N-(trifluoromethylthio)phthalimide using potassium phthalimide and CF_3SCl to enable electrophilic trifluoromethylthiolation of enamines. Shen[265] later refined this route using N-bromophthalimide and $AgSCF_3$, while Rueping[268] introduced an alternative synthesis using N-chlorophthalimide and $CuSCF_3$ for the direct trifluoromethylthiolation of boronic acids and alkynes. These reagents have even found applications in crop protection.[269] In the following year, Wang[270] introduced the 5-NO_2 derivative of the phthalimide reagent for the aminotrifluoromethylthiolation of enones. Subsequently, Shen[271] advanced the field by synthesizing the more electrophilic N-(trifluoromethylthio)saccharin (by replacing one of the carbonyl in the N-(trifluoromethylthio)phthalimide) using N-chlorosaccharin and $AgSCF_3$. Later, Shen and colleagues removed the second carbonyl from N-(trifluoromethylthio)saccharin scaffold to greatly boost electrophilicity, yielding the potent electrophile N-trifluoromethylthio-bis(phenylsulfonyl)imide[272] (an NFSI analogue).

Billard[273] disclosed first- and second-generation trifluoromethanesulfenamides, synthesized from DAST, Ruppert–Prakash reagent, and primary amines; these reagents sometimes require Brønsted or Lewis acid activation.[274–276] Our lab successfully prepared Billard's reagents upto 10g scale.

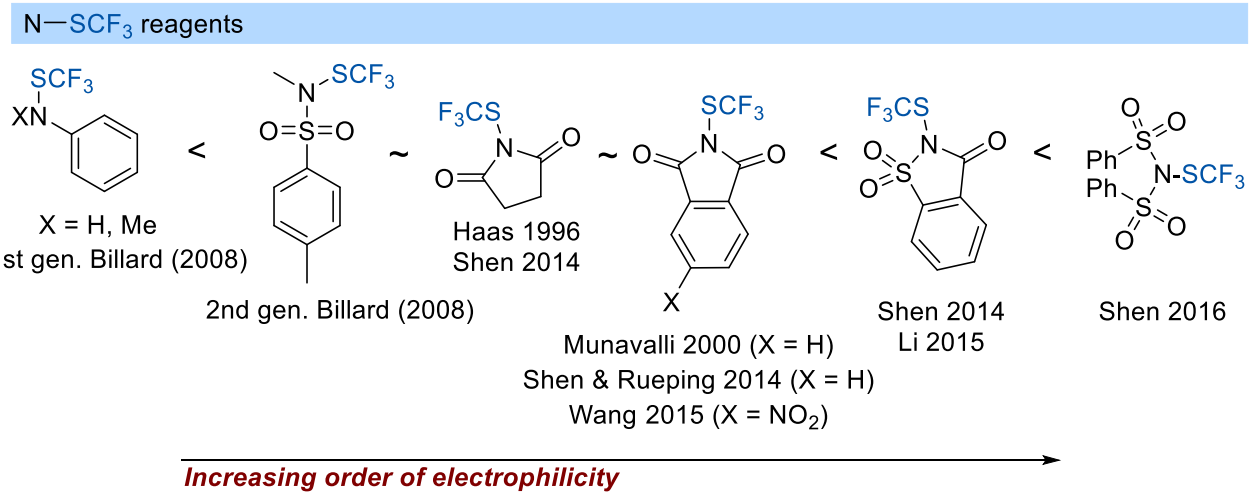

Scheme 1.122: N-type electrophilic SCF_3 reagents

O-SCF_3 reagents (Scheme 1.123)

Haas reported the synthesis of trifluoromethanesulfenyl[277] acetate (and its trifluoro[278] analogue) from CF_3SCl and sodium/silver trifluoroacetate. Despite demonstrating reactivity with cyclohexenes, electron-rich arenes, and heteroaromatics, this reagent has seen little use in subsequent literature. Motivated by Togni's reagent, Shen[279] developed a SCF_3-substituted hypervalent iodine reagent from the chloro-benziodoxole derivative and $AgSCF_3$, initially

assigning it the benziodoxole structure. Later, Buchwald[280] used the sponge X-ray method to show that it is not a hypervalent iodine compound, but rather a trifluoromethanesulfenate. Shen[281] also reported accessing the same reagent by reacting N-(trifluoromethylthio)saccharin with alcohols, and the compound showed reactivity in metal-catalyzed SCF_3-transfer.[282] The structural revision cast doubt on the role of iodine, prompting synthesis of a deiodinated analogue via a similar route. Generally, the iodine containing version performs more efficiently, though both are less electrophilic than the saccharin-derived reagent.

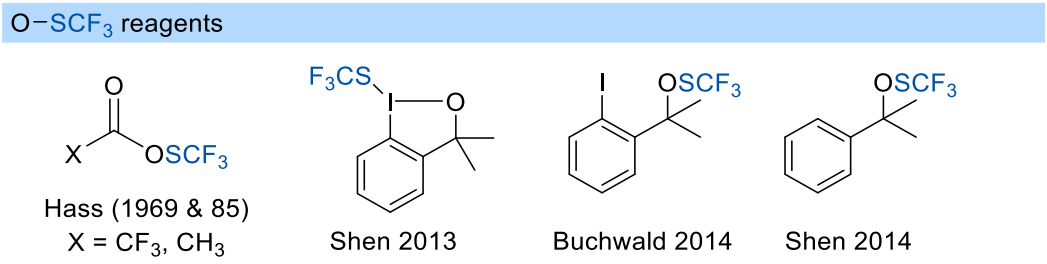

Scheme 1.123: O-type electrophilic SCF_3 reagents

SO_2CF_3 and $SOCF_3$ reagents (Scheme 1.124)

Sodium trifluoromethanesulfinate (Langloi's reagent) was initially used as a trifluoromethylating[283,284] agent by removal of SO_2 while some examples of it acting as a trifluormethanesulfonylating[285,286] agent have also been reported until Zhang[287] utilized it for direct trifluoromethylthiolation of heterocycles. Triflurormethanesulfonyl chloride (CF_3SO_2Cl) has also shown reactivity with heteroarenes[288,289] and ketones.[290] Both these reagents require the presence of a reductant. Shibata further evolved SCF_3 reagents by synthesizing trifluoromethane sulfonyl hypervalent iodonium ylide. Three years later, he developed a diazotriflone[291] derivative of this reagent. They generally require copper salts for their activation. Various nucleophiles[292–294] have been trifluoromethylthiolated using these reagents. Procter developed a sulfoxide-based SCF_3 reagent for C-H trifluoromethylthiolation of hetero(arenes).[295] It has also been employed in trifluoromethylthiolations-heterocyclizations.[296]

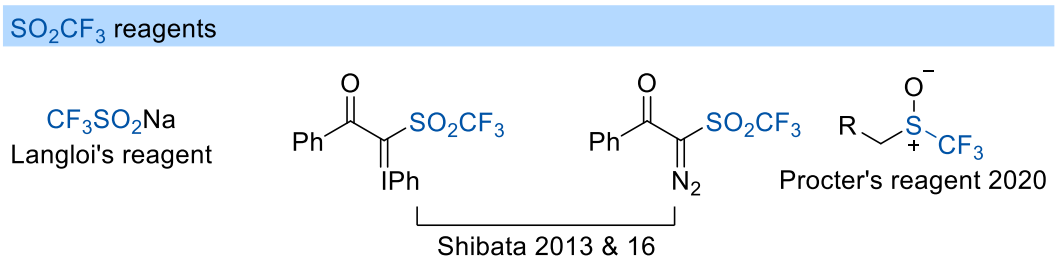

Scheme 1.124: SO_2CF_3 reagents

Nucleophilic SCF_3 donors

$Hg(SCF_3)_2$

In 1953, Hazeldine first reported bis(trifluoromethylthio)mercury, $Hg(SCF_3)_2$, synthesized from bistrifluoromethyl disulfide (CF_3SSCF_3). Later, Muetterties[297] in 1959 prepared the same reagent by reacting CS_2 with HgF_2 (at 250 °C). This mercury complex served as a precursor for nucleophilic -SCF_3 donors, yielding $CuSCF_3$ (via Cu powder) and $AgSCF_3$ (via $AgNO_3$). Despite reacting with electrophiles,[298] its application remains limited due to the high toxicity of mercury compounds.

$AgSCF_3$

To circumvent the use of toxic $Hg(SCF_3)_2$, Emeléus and MacDuff[299] (1961) developed an improved synthesis of $AgSCF_3$ via AgF and CS_2 at 140 °C in an autoclave. They also investigated its reactivity with alkyl halides. The reactivity with aryl halides[300] was limited to electron-deficient substrates due to the covalent nature of the Ag–S bond and its relatively weak nucleophilicity. Efficiency of the reaction further improved when iodide additives were employed. Although $AgSCF_3$ is a nucleophilic[301,302] reagent, it has been employed far more extensively as a radical[303–309] source.

$CuSCF_3$

After Yagupolskii's[310] 1975 synthesis of $CuSCF_3$ using $AgSCF_3$ with CuBr, alternative routes[311,312] emerged, most notably was the Weng[313]'s method, which generated an air-stable Cu(I)–SCF_3 complex by reacting copper fluoride (CuF_2), elemental sulfur (S_8), and Ruppert–Prakash reagent (Me_3SiCF_3) *in situ*, stabilized by ligands such as 2,2′-bipyridine. $CuSCF_3$ has shown high reactivity toward alcohols,[314] α-diazo esters,[315] (hetero)aryl[316]/alkenyl[317] iodides, and diaryliodonium salts.[318] Similar ammonium derived reagents are also known, though their utility in trifluoromethylthiolations remains underexplored.[319]

$Me_4N^+SCF_3^-$ & $CsSCF_3$

Tyra[320] extended Weng's procedure for the synthesis of Me_4NSCF_3 and $CsSCF_3$ using Me_4NF and CsF respectively. The nucleophilic behavior of $Me_4N^+SCF_3^-$ has been investigated using acyl,[321] alkenyl[317] and aryl[322,323] halides, as well as alkynyl(phenyl)iodoniums[324] salts.

1.2.3 Preparation of vinyl trifluoromethyl thioethers using Intermolecular approach

1.2.3.1 From pre-functionalized alkenes

Traditional approaches to trifluoromethylthiolated olefins typically rely on stereodefined, prefunctionalized alkenes (**Scheme 1.125)**. For example, vinyl boronic acids,[303,325–329] halides/pseudo halides,[330–334,251] thiocyanides,[335,336] nitro compounds and carboxylic acids can be transformed to vinyl trifluoromethyl thioethers (**229**) as demonstrated in earlier reports.[337–339]

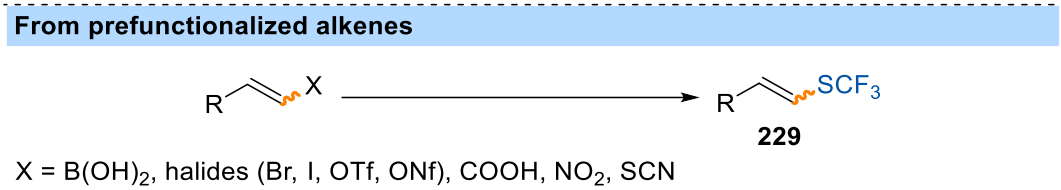

Scheme 1.125: Synthesis of vinyl trifluoromethylthio ethers from prefunctionalized olefins

1.2.3.2 From alkenes

Unfunctionalized alkenes, which offer the advantage of not requiring prior functionalization, can also serve as substrates for the direct formation of vinyl trifluoromethyl thioethers, as demonstrated in the works of Glorius and Shen (**Scheme 1.126**).[340,341]

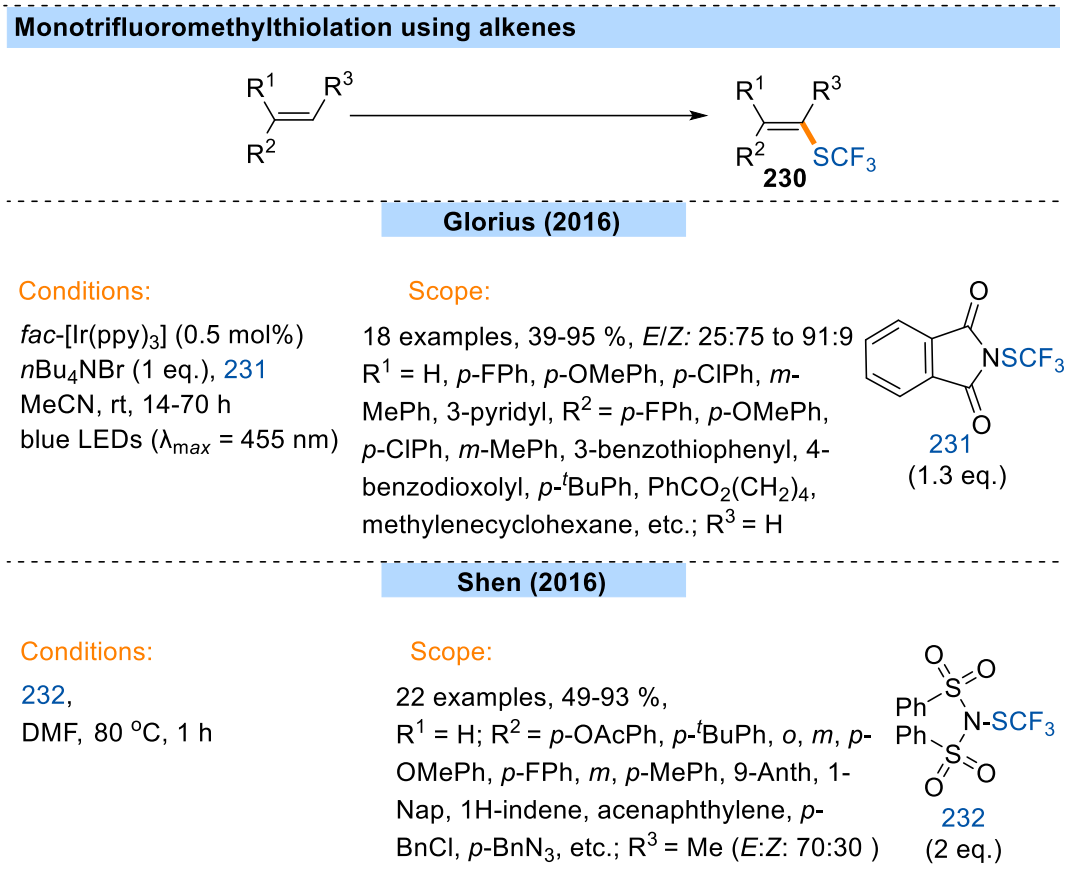

***Scheme 1.126**: Trifluoromethylthiolation of alkenes*1.2.3.3 From alkynes

Conventional methods discussed above generally require a two-step approach to synthesize vinyl trifluoromethylated compounds. In contrast, unfunctionalized alkenes and alkynes circumvent the need for prior functionalization and thus improve step economy. The known alkyne-based strategies often employ direct trifluoromethylthiolation using an SCF_3 reagent, accompanied by adjacent functionalization. This step-efficient process enables the concurrent installation of two substituents, delivering highly functionalized vinyl trifluoromethylthioethers. These transformations proceed through either radical or electrophilic pathways, providing complete regioselectivity and exclusive *anti*-selectivity.

1.2.3.3.1 Intermolecular trifluoromethylthiolation

Electrophilic approaches

Electrophilic trifluoromethylthiolation generally proceeds via attack of the alkyne on the SCF_3 donor, forming an episulfonium intermediate, followed by *anti*-addition of a nucleophile (e.g., OTf, Cl) to yield the alkenyl trifluoromethylthioether (**Scheme 1.127**). In most cases, the SCF_3 group is introduced at the β-position, as the α-carbocation is better stabilized.

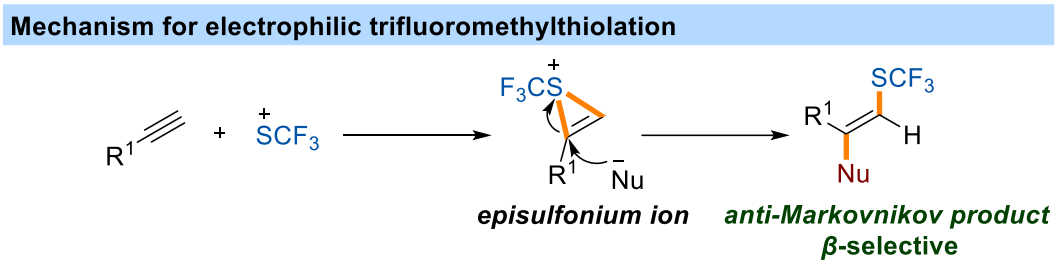

Scheme 1.127: General mechanism of electrophilic trifluoromethylthiolation

Billard[276] shared the first Lewis acid–activated electrophilic trifluoromethylthiolation of aliphatic alkynes using trifluoromethanesulfanylamides with sodium tosylate (TsONa). Although limited in scope and non-regioselective for internal alkynes, the reaction was proposed to proceed via *anti*-trifluoromethylthiolation (as in olefins), giving *E*-selective tosylated vinyl trifluoromethylthioethers (**233**) in moderate yields (**Scheme 1.128**).

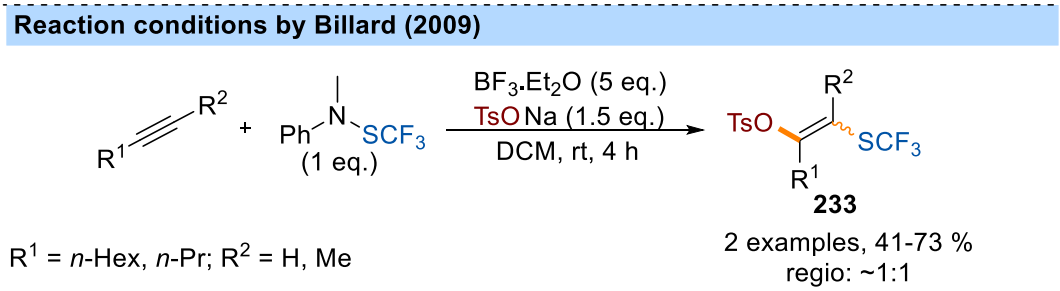

Scheme 1.128: First example of electrophilic triflruoromethylthiolation

Zhao[342] and colleagues found that selenide can activate the SCF_3 species, enabling trifluoromethylthiolation-triflation of alkynes using N-trifluoromethylthiosaccharin and triflic acid (TfOH) **(Scheme 1.129)**. Various aryl-alkyl and dialkyl alkynes underwent *anti*-addition to give β-trifluoromethylthiolated alkenes with high *E*/*Z* selectivity (>99:1) besides *tert*-butyl phenyl propyne. Aliphatic terminal and silyl-substituted alkynes also yielded products with good selectivity (>90:10), although longer reaction times (40 h) were required. Notably, phenyl propargyl tosylate formed an α-trifluoromethylthiolated enone exclusively.

Reaction conditions by Zhao (2016)

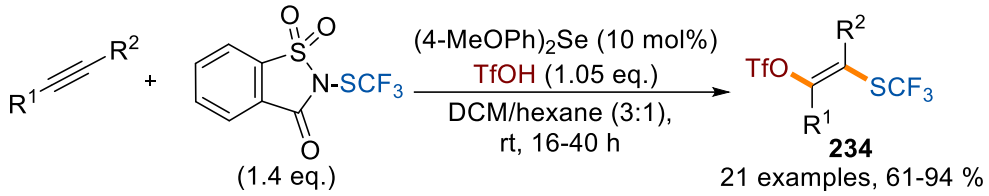

R^1 = Et, *n*-Bu, *n*-Hex, Ph, *p*-FPh, *p*-CF_3Ph, *p*-CO_2MePh, *p*-^{t}BuPh, *p*-MePh, *o*, *m*-ClPh, *Cy*Pen, TIPS, etc.; R^2 = H, Me, Et, *n*-Bu, *n*-Pen, etc.

Scheme 1.129: Diarylselenide catalyzed trifluoromethylthiolation-triflation

Zhang[343] reported the first chloro-trifluoromethylthiolation of terminal alkynes using combination of CF_3SO_2Cl with PPh_3 as a reductant **(Scheme 1.130)**. Electron-rich and halogenated substrates gave higher efficiency than electron-deficient ones, the latter improving moderately with excess reagent. *Anti*-addition afforded single isomers with Markovnikov (MR) selectivity, except propargyl ethers and amines, which yielded mainly *anti*-MR products. The MR preference was attributed to the electronically favourable conjugation of the aryl ring and the intermediary episulfonium ion, whereas in case of propargyl ethers and amines, steric hindrance of alkyl groups governed nucleophilic attack toward *anti*-MR products. Based on literature reports, that CF_3SOCl can generate CF_3SCl, the active SCF_3 donor, the authors envisioned applying this strategy without a reductant.[344] This method, being more effective, also enabled trifluoromethylthiolation of internal diphenylacetylene, affording a 70% yield.

Chloro-trifluoromethylthiolation of alkynes

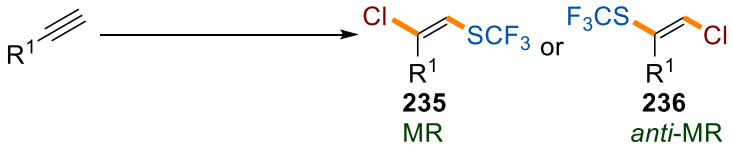

Zhang (2018)

Conditions:	Scope:	CF_3SO_2Cl (2-3 eq.)
PPh_3, DMF, 90 °C, 8 h	16 examples, <5 to 75 % With aliphatic alkynes *anti*MR:MR: >95:5; R^1 = Ph, *p*-OMePh, *p*-CF_3Ph, *p*-BrPh, *p*-NO_2Ph, *m*-OHPh, *m*-FPh, *o*-MePh, 2-thienyl, $PhOCH_2$, PhthN-CH_2,	

Zhang (2018)

Conditions:	Scope:	CF_3SOCl (3 eq.)
DMF, 90 °C, 6 h	15 examples, 52 to 91 % R^1 = *has covered similar examples as above.*	

Scheme 1.130: Chloro-trifluoromethylthiolation of terminal alkynes

Wang[345] reported a base-promoted amino-trifluoromethylthiolation of alkynoates using N-trifluoromethylthiophthalimide, installing SCF_3 at the α-position to give predominantly Z-isomers (>91:9) **(Scheme 1.131)**. The method tolerated various aryl-alkynyl esters as well as benzyl and ethyl substituents, while amides and sulfones failed to undergo the transformation.

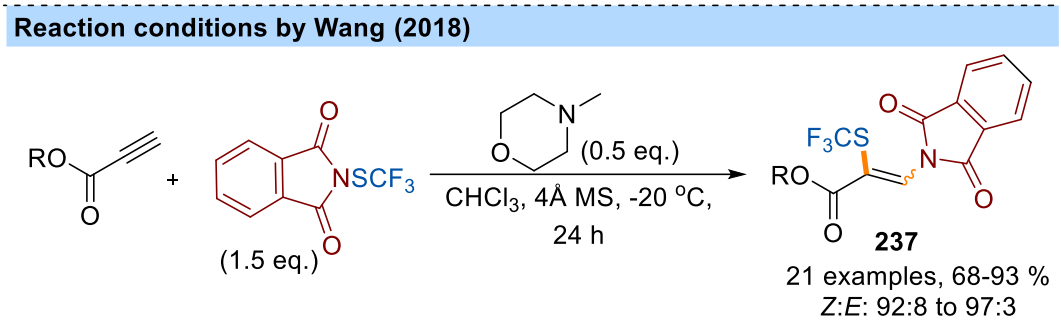

R = *p*-CF_3Ph, *o*, *m*, *p*-FPh, *o*, *m*, *p*-ClPh, *o*, *m*, *p*-BrPh, *p*-CNPh, *o, m*, *p*-MePh, *o*, *m*, *p*-OMePh, 1-Nap, Bn, Et, etc.

Scheme 1.131: Aminotrifluoromethylthiolation of alkynoates

Ellman[346] studied HFIP mediated, *anti*-carbotrifluoromethylthiolations of alkynes using the highly electrophilic N-trifluoromethylthio bis(phenylsulfonyl)imide and arenes in air **(Scheme 1.132)**. The method offered extensive scope for both alkynes (terminal and aryl-alkyl substituted) and arenes, affording β-trifluoromethylthiolated alkenes (**238**) in yields up to 87%, though no products were obtained from strongly electron-donating trimethoxybenzene or moderately electron-withdrawing bromobenzene.

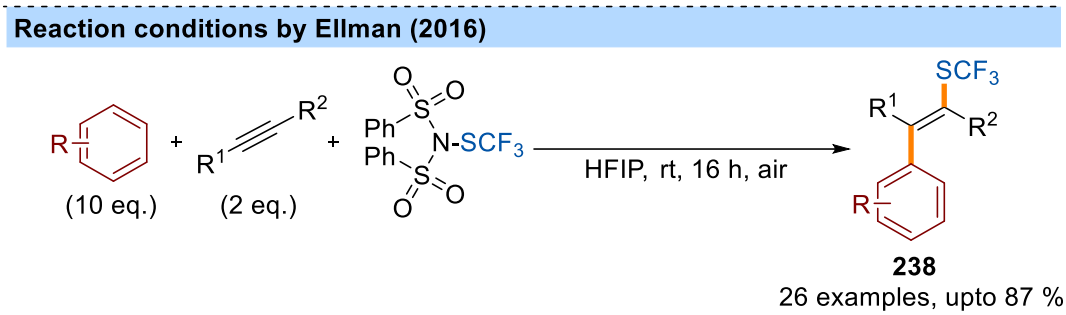

R^1 = *n*-Bu, Ph, *Cy*Pent, *Cy*Hex, methyl*Cy*Hex, $Cl(CH_2)_6$, $Ph(CH_2)_2$, $CH_3CO_2(CH_2)_4$, *p*-BrPh, *p*-CO_2MePh, *m*-OMePh, etc.; R^2 = H, Me, Et; R = H, 2,5-diOMe, 2-OMe, 2-hydroxy, 2-hydorxy-5-methyl ,2,4,6-triMe, etc.

Scheme 1.132: Carbotrifluoromethylthiolation using Friedel-Crafts strategy

Bis-trifluoromethylthiolation

While investigating Cu-catalysed alkynyl trifluoromethylthiolations, Billard's[319] group observed bistrifluoromethylthiolated alkenes from electron-deficient phenyl acetylenes and propargyl ethers/amines **(Scheme 1.133)**. Formation was promoted by 2,2′-bipyridines and suppressed by 1,

10 phenanthroline ligand, affording products in satisfactory yields. This is the first example of transition-metal catalyzed trifluoromethylthiolation of alkynes.

Reaction conditions by Billard (2016)

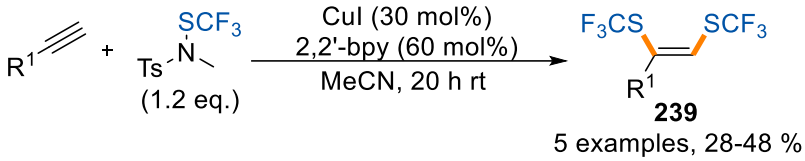

R^1 = *p*-CO_2MePh, *p*-AcPh, PhthN-CH_2, PhOCH_2, PhCO_2CH_2

Scheme 1.133: First *syn*-bis trifluoromethylthiolation of terminal alkynes

Mechanistic studies suggested activation of the SCF_3 donor by Cu(I) to form Cu(III)-SCF_3 complex, which coordinates to the alkyne, undergoes *syn*-insertion, and yields a copper–vinyl SCF_3 intermediate. β-Hydride elimination gives the alkynyl SCF_3 product (**240**), while bis-trifluoromethylthiolation (Z-selective) competes when the intermediate is stabilized by heteroatoms or electron-withdrawing groups **(Scheme 1.134)**. A secondary pathway from the alkynyl-SCF_3 product was also proposed.

Mechanistic aspect

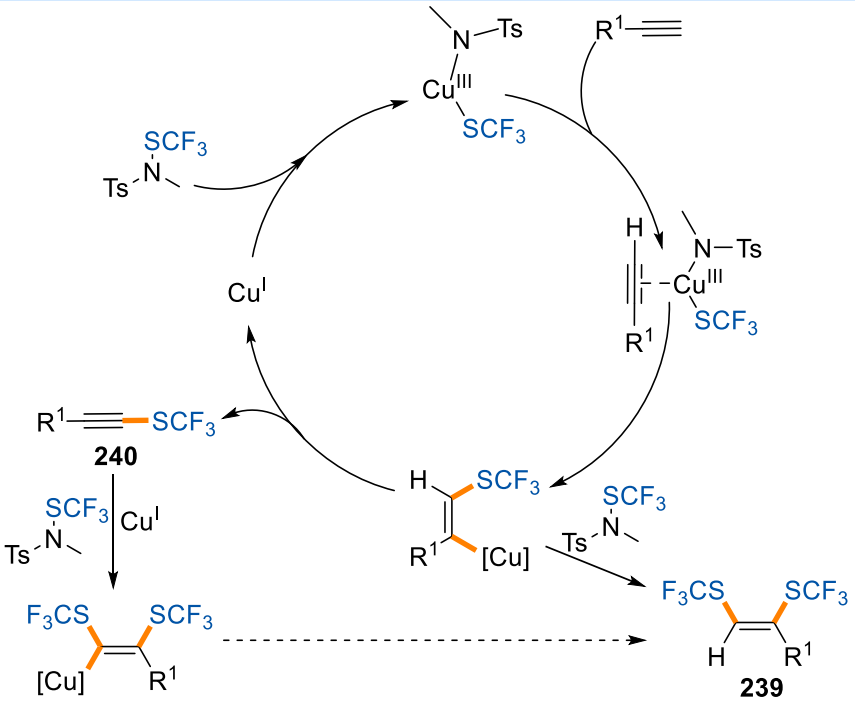

Scheme 1.134: Mechanism of Cu-catalyzed bis-trifluoromethylthiolation

In contrast to Billard's[319] method, Qing[304] achieved the first *anti*-selective bis-trifluoromethylthiolation of alkynoic acids with $AgSCF_3$ using formic acid as a co-solvent, with *trans*-configuration confirmed by X-ray analysis **(Scheme 1.135)**. Unlike Billard's protocol, which tolerated only electron-deficient alkynes, this method accommodated diverse aromatic substituents, alkyl groups, and estrone derivatives with favorable outcomes.

Reaction conditions by Qing (2017)

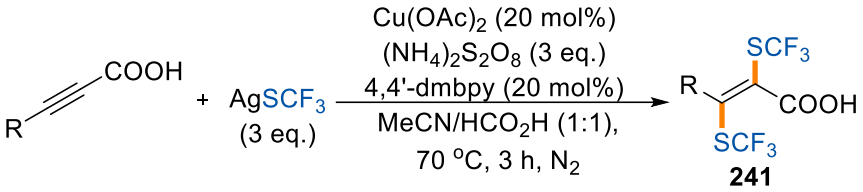

241

23 examples, 51-90 %

R^1 = Me, methylCyHex, Ph, *p*-MePh, *p*-^{t}BuPh, *p*-CHOPh, *p*-CNPh, *p*-NO_2Ph, *p*-CF_3Ph, *p*-CF_3Ph, *p*-FPh, *m*, *p*-ClPh, *o*, *p*-BrPh, 1-Nap, 3,5-diMePh, 3,4-diMePh, 3,4-diClPh, etc.

Scheme 1.135: First *anti*-bis-trifluoromethylthiolation of alkynoic acids

Radical approaches

The SCF_3 radical typically adds to alkynes in an *anti*-Markovnikov (β) fashion **(Scheme 1.136)**; in contrast, the direct formation of α-trifluoromethylthiolated alkenes is exceptionally rare. Reported strategies to access such products generally rely on a sequential radical process, wherein an initial β-addition is followed by intramolecular SCF_3 transfer to the α-position, thereby achieving the otherwise uncommon Markovnikov selectivity.

Mechanism for radical trifluoromethylthiolation

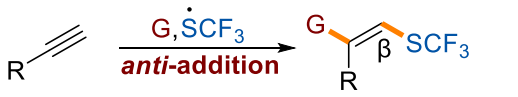

anti-Markovnikov product

β- selective

Scheme 1.136: General mechanism for radical trifluoromethylthiolation

Cao[305] presented the first hydrotrifluoromethylthiolation of terminal alkynes using $AgSCF_3$ **(Scheme 1.137)**. Control experiments revealed DMF and H_2O as the hydrogen sources. Aromatic terminal alkynes, propargyl amines, and ethers gave moderate yields of β-trifluoromethylthiolated alkenes (**242**) as *E/Z* mixtures, with exclusive *anti*-Markovnikov selectivity. Markovnikov-selective reactions produced α-SCF_3 alkenes (**243**) only from *para*-alkoxy aryl alkynes, representing the first example of α-selective trifluoromethylthiolation of terminal alkynes.

Reaction conditions by Cao (2016)

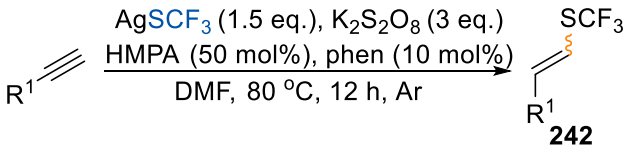

242

anti-MR selective
23 examples, 52-72 %
E:*Z*: 31:69 to 68:32

R^1 = *n*-Pent, Ph, *m*-MePh, *m*, *p*-OMePh, *p*-OEtPh, *p*-OBnPh, *p*-MeSPh, *p*-OAcPh, *p*-ClPh, *m*-$CH_3CONHPh$, *p*-NO_2Ph, *p*-$CF_3PhCO_2(CH_2)_3$, *p*-$NO_2PhCO_2(CH_2)_3$, *p*-$NO_2PhCONH$, *o*-NO_2PhOCH_2,

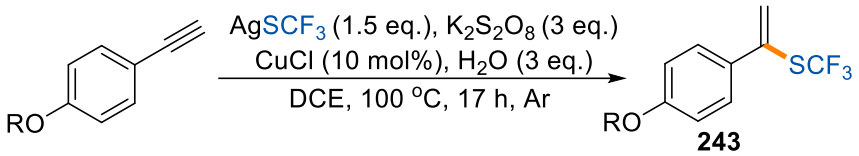

243

MR selective
8 examples, 41-81 %

R = Me, Et, Bn, *n*-Pr, *n*-Bu, *n*-Pent, ^{i}Pr, 1,3-dioxole

Scheme 1.137: Hydrotrifluoromethylthiolation of terminal alkynes

Qing[347] and coworkers developed a reductive-photocatalytic process for hydrotrifluoromethylthiolation of alkynes employing trifluoromethanesulfonic anhydride **(Scheme 1.138)**. Phase-transfer catalysts were used to improve efficiency by preventing precipitate formation. Although limited in scope, the protocol incorporated internal and alicyclic terminal alkynes and delivered stereoselectivity opposite to that reported in Cao's method (*Z*/*E* = 61:39–77:23) in satisfactory yields.

Reaction conditions by Qing (2019)

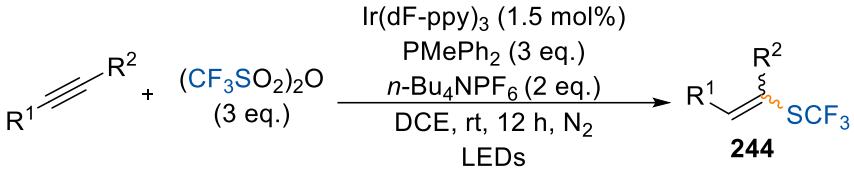

244

5 examples, 37-60 %
Z:*E*: 61:3 to 77:23

R^1 = *n*-Pent, *n*-Oct, *Cy*Hex, $Ph(CH_2)_2$, Ph; R^2 = H, Et, *n*-Bu

Scheme 1.138: Hydrotrifluoromethylthiolation using photocatalytic approach

Liang[348] introduced tandem difluoroalkylation-trifluormethylthiolation of terminal alkynes using Weng's complex and ethyl iododifluoroacetate **(Scheme 1.139)**. Screening studies revealed CsF enhances efficiency and suppresses isomerization. The reaction proved fruitful for aromatic terminal alkynes, achieving α-trifluoromethylthiolation (via *anti*-addition) with >11:1 *E*:*Z* selectivity. While less effective for aliphatic and internal alkynes, it accommodated a carbazole

unit with high selectivity (51%, *E*:*Z* = 16:1). The unique α-selectivity arises from the initial addition of CF_2CO_2Et radical followed by the transfer of SCF_3 group.

Reaction conditions by Liang (2018)

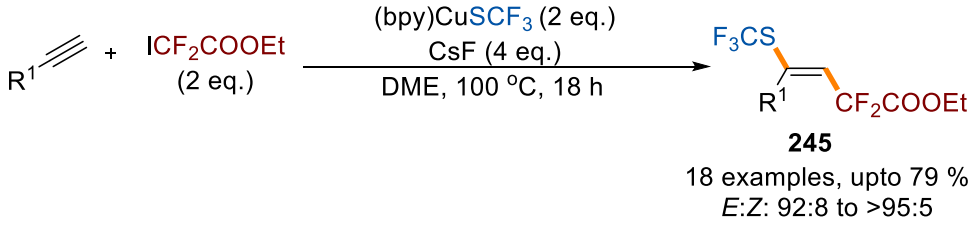

245
18 examples, upto 79 %
E:*Z*: 92:8 to >95:5

R^1 = *p*-OMePh, *p*-OBnPh, *p*-O(*n*-Pent)Ph, *p*-OAcPh, *p*-MePh, *p*-^{t}BuPh, *p*-SMePh, 4-biphenyl, 4-*n*-Pr-biphenyl, 6-OMe-2-Nap, 3,4-diOMePh, etc.

Scheme 1.139: Difluoroalkylation-trifluoromethylthiolation of terminal alkyens

Knowing that gold catalysts can add to alkynes via *anti*-additions, Xu[349] developed a photoredox–cationic gold co-catalyzed trifluoromethylthiosulfonylation **(Scheme 1.140)**. Both terminal and internal alkynes underwent α-trifuoromethylthiolation through initial addition of the SO_2Ph radical, followed by the gold assisted SCF_3 transfer, delivering the desired products in 41–77% yields. While terminal alkynes produced *E*-isomers exclusively, internal ones gave *E*:*Z* mixtures.

Reaction conditions by Xu (2018)

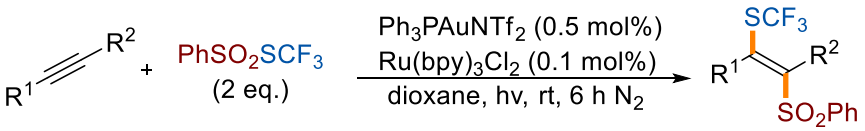

246
18 examples, 44-86 %
E:*Z*: 56:44 to 89:11

R^1 = *Cy*Pent, Ph, *p*-BrPh, *p*-FPh, *p*-CO_2MePh, *p*-OMePh, *o*, *m*, *p*-MePh, *m*-OHPh, NTs protected 3-indolyl, 3-thienyl, $CO_2MeC(Me)_2OPh$, $CO_2MeCHNHBoc(Me)Ph$, etc.; R^2 = H, Me, *n*-Bu

Scheme 1.140: Trifluoromethylthiosulfonylation of alkynes

Inspired by Billard's and Zhao's electrophilic oxytrifluoromethylthiolations[276,342] (discussed above), Qing[306] developed a Cu-catalysed radical-route for *anti*- hydroxytrifluoromethylthiolation of arylalkynones using $AgSCF_3$ **(Scheme 1.141)**. Electron-rich alkynones reacted efficiently, similar to Zhao's procedure, whereas electron-withdrawing substituents resulted in comparatively lower yields with minor 1,3 diketones byproducts obtained in both cases. Interestingly, diaryl alkynones underwent trifluoromethylthiolation-cyclization which will be discussed in the next section.

Reaction conditions by Qing (2019)

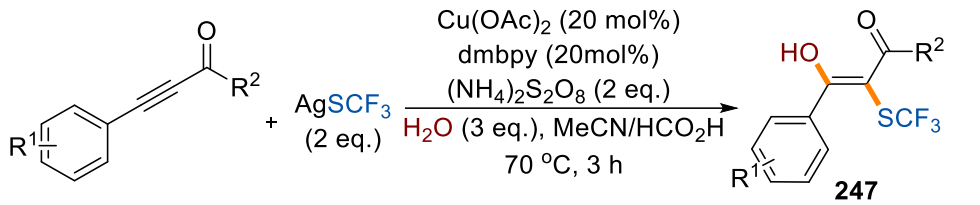

17 examples, 26-78 %

R^1 = H, 3/4-Me, 4-Et, 4-*n*-Bu, 4-OMe, 3/4-F, 2/3/4-Cl, 4-CF_3, 4-CN, 4-NO_2, 1-Nap, 2-theinyl, etc.; R^2 = Me, Et

Scheme 1.141: Hydroxytrifluoromethylthiolation of alkynones

Zhu[350] developed an SCF_3-functionalized acrylonitrile synthesis via trifluoromethylthiolation–intramolecular cyano migration **(Scheme 1.142)**. Cyanohydrin featured dialkyl alkynes with electron-withdrawing groups exhibited higher reactivity than those with electron-donating substituents. (Cyclo)alkyl and functionalized alkyl substituents at the γ-carbon were well-tolerated, giving 40–87% yields. Alkyl chain length between the cyano group and triple bond was crucial, shortening caused reduced yields, while lengthening halted reactivity. The reaction afforded *E*-isomers with high stereoselectivity but lacked regioselectivity.

Reaction conditions by Zhu (2018)

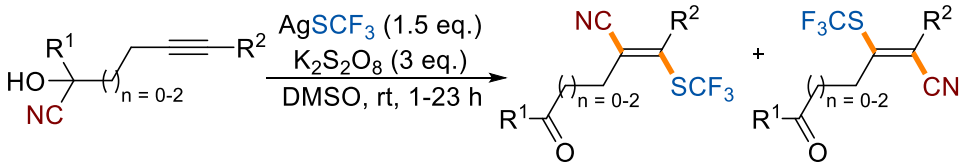

27 examples, 40-87 %

R^1 = Ph, 4-biphenyl, *p*-FPh, *o*, *p*-ClPh, *p*-BrPh, *p*-CF_3Ph, *p*-OCF_3Ph, *p*-CNPh, *p*-MePh, *p*-^{t}BuPh, *p*-OMePh, *o*, *m*-MePh, 1-Nap, 2-Nap, 2-thienyl, *Cy*Hex, Et, $PhCH_2$; R^2 = *n*-Bu, $(CH_2)_3Cl$, $(CH_2)_3CN$, $(CH_2)_4OAc$, $(CH_2)_9Me$, *Cy*Hex, etc.

Scheme 1.142: Cyano-trifluoromethylthiolation of alkynes

Zhang[351] and Wang developed an organophotocatalyzed *anti*-selective trifluoromethylthiolation-boration of alkynes using N-trifluoromethylphthalimide and B_2cat_2 **(Scheme 1.143)**. Terminal and internal alkynes gave predominantly *Z* isomers, while sterically hindered substrates like *tert*-butyl and trimethylsilyl acetylenes reacted with lower yields and moderate stereocontrol (~80:20 *Z*/*E*). Impressively, conjugated and deuterated substrates were accepted affording excellent stereoselectivity. The β-SCF_3 substituted catecholborane products were converted to stable pinacol derivatives.

Reaction conditions by Zhang and Wang (2021)

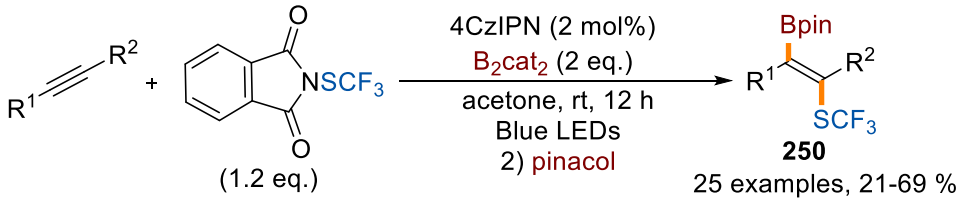

R^1 = *n*-Pent, $OTs(CH_2)_2$, *Cy*Hex, *Cy*Pr, ^{t}Bu, TMS, Ph, *m*, *p*-MePh, *p*-^{t}BuPh, *o*-ClPh, *m*-BrPh, *p*-CO_2MePh, *p*-CNPh, *p*-FPh, *p*-NHTsPh, 3-thienyl, *Cy*Hexenyl, etc.; R^2 = H, D, Me, Et, *n*-Bu, Ph,

Scheme 1.143: Trifluoromethylthiolation-boration of alkynes

Xie[352] demonstrated a multicomponent approach to access β-SCF_3-substituted 3-alkenyl quinoxalinones **(Scheme 1.144)**. Diverse substitutions on the terminal alkynes, aryl and N-terminus of the quinoxalinone were allowed, giving *E*-configured products in moderate yields. An example of aryl-alkyl alkyne being effective was also illustrated, however, diphenyl acetylene showed lack of reactivity.

Reaction conditions by Xie (2024)

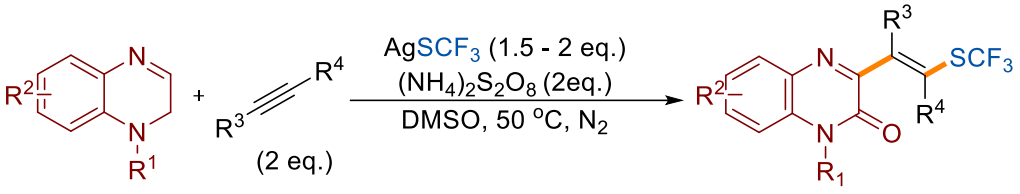

R^1 = H, Me, Et, *n*-Pent, Bn, allyl, propargyl, CH_2CO_2Et; R^2 = 6-F, 7-F, 6-Cl, 6-Br, 6-COPh, 6,7-difluoro, 6,7-dichloro; R^3 = *o*, *m*, *p*-MePh, *m*, *p*-BrPh, *p*-^{t}BuPh, *p*-FPh, *p*-OMePh, *p*-CF_3Ph, 3-thienyl, *n*-Bu, $Cl(CH_2)_3$, *Cy*Hex, $OMeCH_2$, $OH(CH_2)_5$, *Cy*Pr, *Cy*Hexenyl, $Ph(CH_2)_2$, Ph; R^4 = H, Me, Ph

Scheme 1.144: Synthesis of SCF_3-substituted 3-alkenyl quinoxalinones

1.2.4 Intramolecular trifluoromethylthiolation

These reactions proceed via addition of an SCF_3 group across an alkyne, accompanied by cyclization. When the new bond is C–C, the process is termed carbocyclization; carbon–heteroatom cyclizations are excluded here. Based on the SCF_3 source, these transformations fall into electrophilic, radical, or nucleophilic categories, discussed below.

Electrophilic strategies

Typically, the electrophilic process occurs via formation of trifluoromethylthio cation, which is attacked by the alkyne, forming an episulfonium intermediate **(Scheme 1.145)**. Subsequent

nucleophilic attack by the arene yields either bicyclic (**252**) or spirocyclic products (**253**), depending on the site of attack and type of substrate.[274,275,353,354]

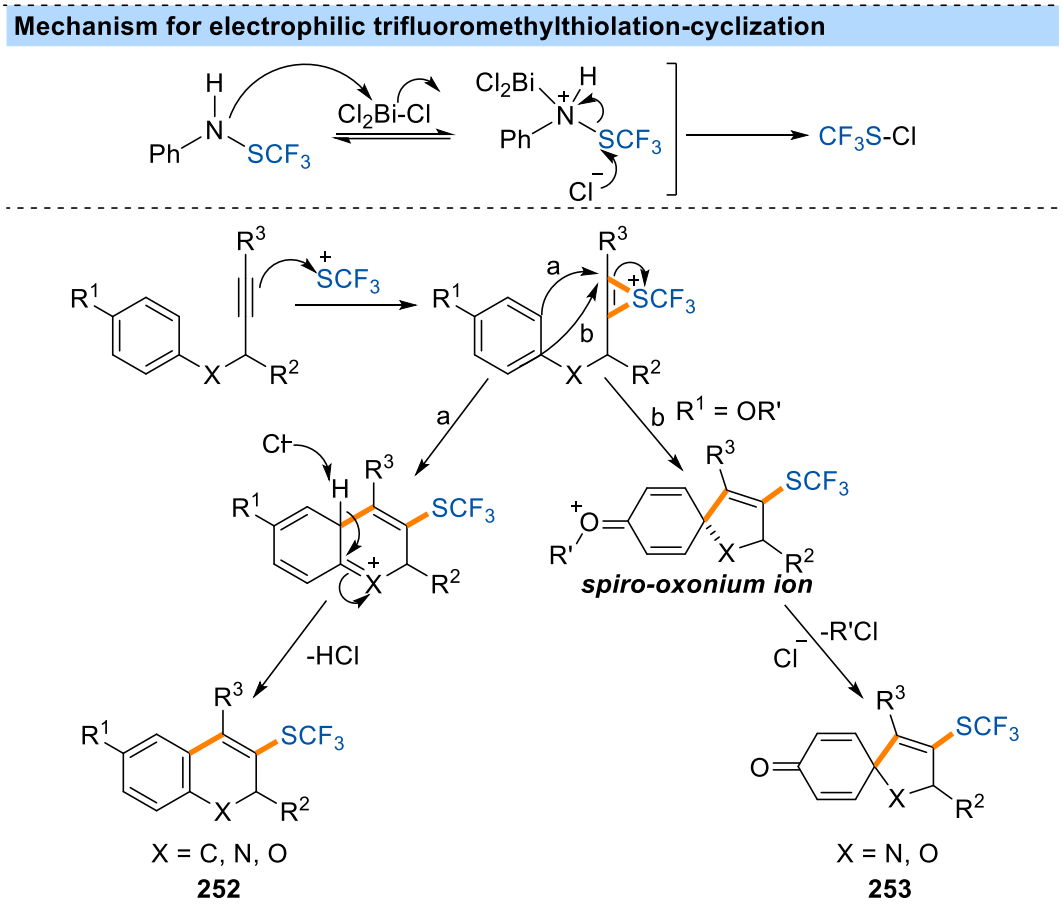

Scheme 1.145: General mechanism for electrophilic trifluoromethylthiolation-cyclization

Radical approaches

Radical processes resemble electrophilic ones, proceeding through an initial trifluoromethylthiolation followed by intramolecular cyclization **(Scheme 1.146)**. Typically, these reactions employ an SCF_3 radical source generated *in situ* using an oxidizing agent. The SCF_3 radical first adds to the alkyne to form a vinyl radical intermediate, which is followed by an intramolecular attack by aryl ring[307,355–357] or olefin[308,358–360] to yield a cyclic intermediate. Subsequent steps afford the SCF_3-functionalized cyclic product (**254**). In some cases, the initial attack proceeds by another radical (e.g. $^{\cdot}SO_2Ph$) followed by cyclization and SCF_3 radical transfer.[361] In certain cases (especially in presence of acetonitrile, acting as a solvent and hydrogen donor), the reaction pathway diverges through the formation of a spirocyclic intermediate, as observed by Qing[362] and Liu.[309] This intermediate undergoes 1,4-aryl migration, followed by further steps, to produce vinyl trifluoromethyl thioethers (**255**). Liu,[363] Reddy,[364,365] and Yang[366] further reported the formation of dearomatized spirocyclic products (**256**), particularly when *para*-alkoxy or halogen-substituted aryl rings are present. Notably, Yang also developed an electrochemical approach for generating the SCF_3 radical, offering a greener alternative to

traditional oxidative methods. Most of these transformations utilize $AgSCF_3$ as the SCF_3 donor, enabling efficient access to a wide range of 5-, 6-, and 7-membered SCF_3-containing carbocycles and heterocycles.

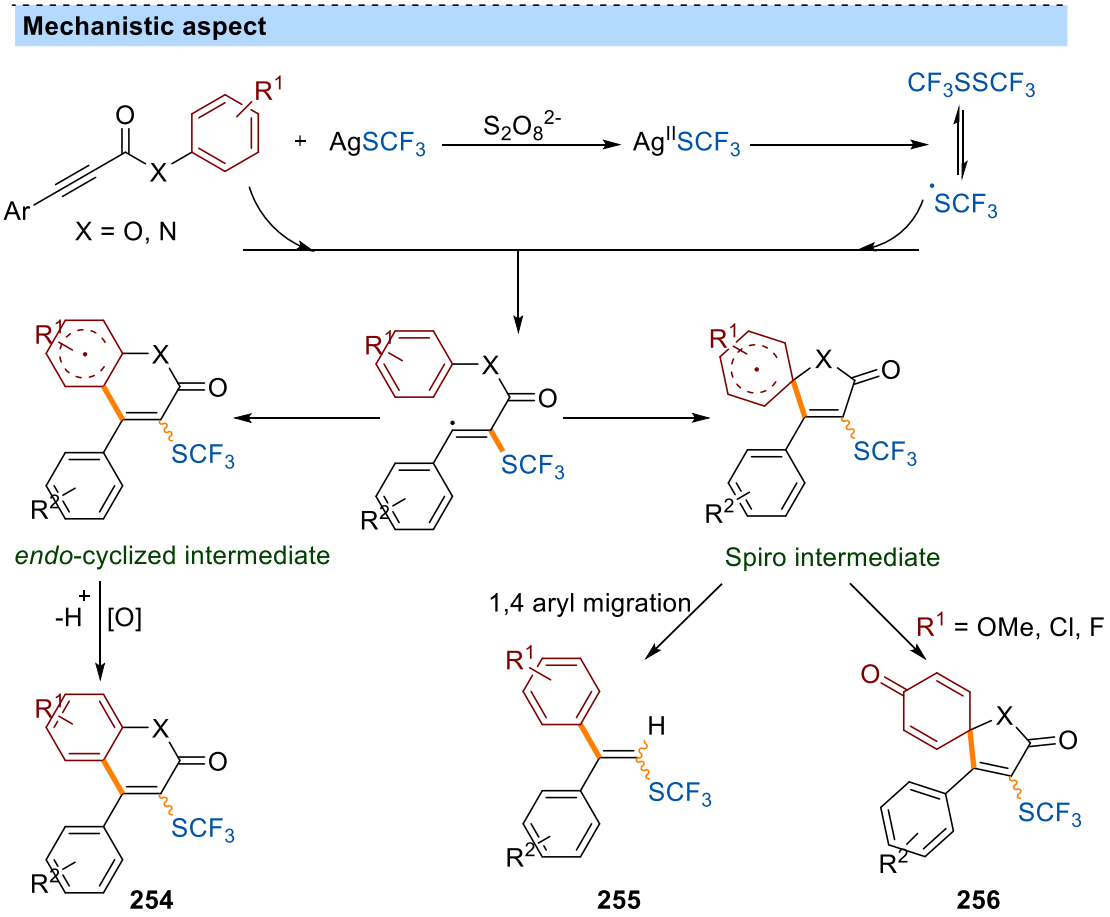

Scheme 1.146: General mechanism for radical trifluoromethylthiolation-cyclization

Nucleophilic approaches

In contrast to radical and electrophilic approaches, carbocyclization reactions utilizing a nucleophilic SCF_3 source are relatively uncommon. Notably, Lee and co-workers reported the only example of reactions involving multiyne substrates that proceed through the generation of an SCF_3 anion following a hexadehydro-Diels–Alder (HDDA)[301] reaction proceeding via an organosilver intermediate. In a subsequent study, the same group described related transformations initiating through an Alder–ene pathway.[302] In both cases, these strategies furnished SCF_3-substituted arenes **(Scheme 1.147)**, demonstrating a distinct nucleophilic mode of SCF_3 incorporation.

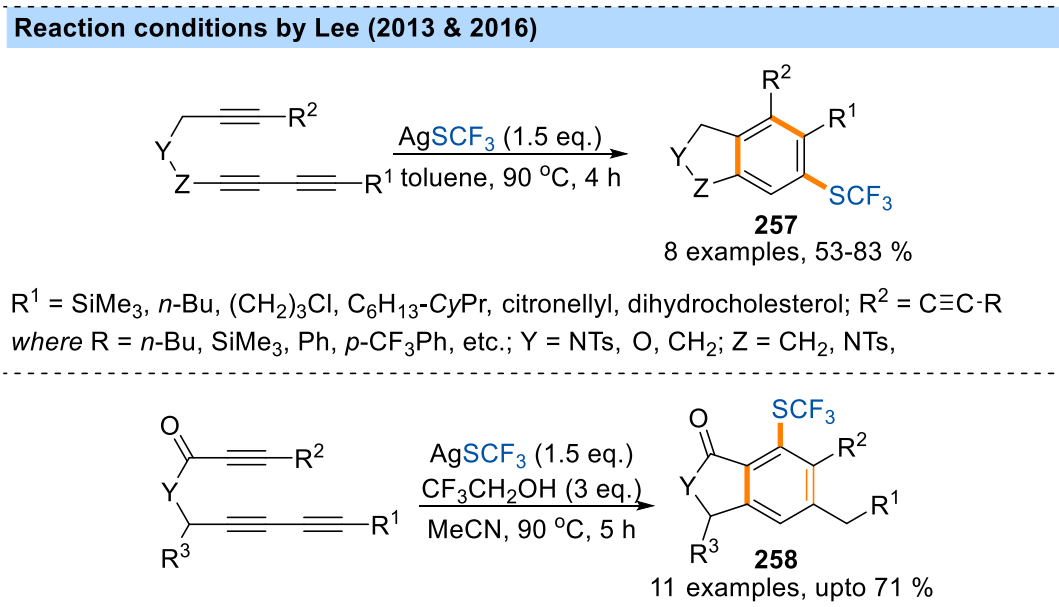

Scheme 1.147: Synthesis of arenes from multiynes via nucleophilic trifluoromethylthiolation-cyclization

Following the discussion of various carbometallation and trifluoromethylthiolation reactions, the next chapter introduces the underlying concept of this research.

2. Concept

The aim of the project was to develop selective sequential synthetic methods relying on hydro- or carbometallations of alkynes, followed by functionalizing with various (thio)perfluoroalkyl electrophiles. The organometallation step would play a decisive role in governing the regio- and stereoselectivity of the transformation, ensuring that the subsequent functionalization proceeds with retention of configuration. Importantly, the generation of vinyl-organometallated intermediates bearing a metal at the α-position would give rise to α-perfluoroalkyl(thiol)ated compounds with unique regioselectivity. Furthermore, the development of this process into a one-pot protocol will enable the sequential installation of two distinct groups, thereby affording structurally complex products in an efficient and streamlined manner. Building on the same rationale, I also envisioned testing whether a similar carbometallation-driven strategy, merged with (thio)perfluoroalkylation, could be extended to enones **(Scheme 2.1)**. In parallel, recognizing the synthetic challenges associated in accessing sterically hindered vinyl boronates, I sought to exploit sequential carbometallation followed by transmetallation with boron. Installing boron specifically at the α-position provides a powerful path to configurationally defined tetrasubstituted alkenes, which remain difficult to access by conventional approaches.

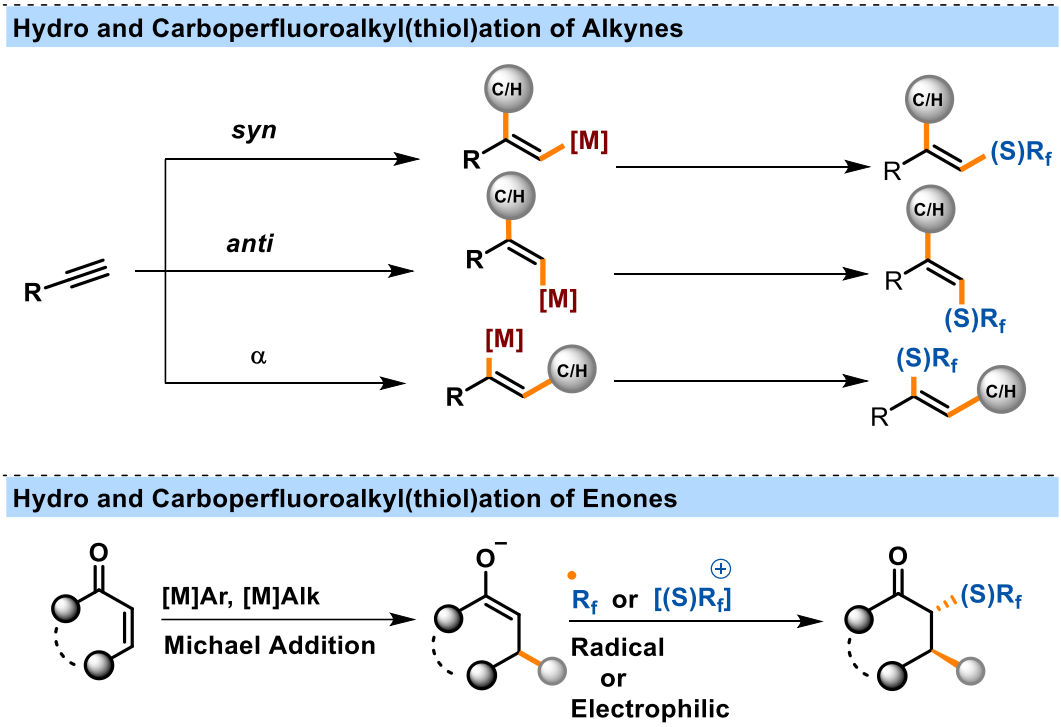

Scheme 2.1: General schematic representation of organometallation followed by perfluoroalkyl(thiol)ation

2.1 Conventional vs Current method

2.1.1 Synthesis of Perfluoroalkyl(thio)-functionalized olefins

Classical reports on the synthesis of perfluoroalkyl(thio)-substituted compounds rely on multi-step routes or prefunctionalized alkenes. While such methods generally proceed with good efficiency and retain configuration, they require prior preparation of vinyl precursors, reducing step-economy and frequently leading to stereoselectivity issues. More recently a range of methods employing additions of (thio)fluoroalkyl groups to alkynes, often with concomitant installation of another substituent emerged as a powerful tool. However, as the methods rely on radical fluoroalkylation they are typically limited to installation of fluoroalkyl substituent at β-position and feature *anti*-selectivity of difunctionalization **(Scheme 2.2)**. Similar selectivity is observed for electrophilic thiofluoroalkylation proceeding through episulfonium intermediates. In contrast, projected strategy based on initial carbometallation of alkynes would offer an opportunity to control regio- and stereoselectivity, and in the consequence would provide access to α-substituted products with *syn*-selectivity.

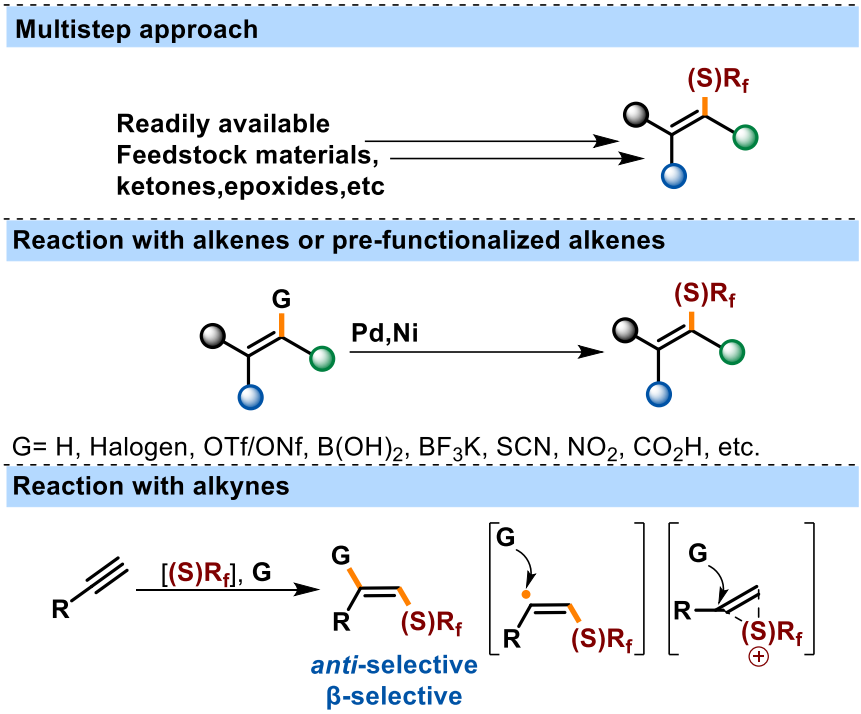

Scheme 2.2: Traditional methods for synthesis of vinyl trifluoromethyl thio ethers

2.1.2 Synthesis of Perfluoroalkyl(thio)-substituted ketones

Traditional approaches for the synthesis of (thio)fluoroalkyl-substituted ketones typically rely on direct (thio)fluoroalylation of ketones or their enolates. However, the presence of multiple enolizable centers can lead to regioselectivity issues, resulting in mixtures of products that require separation. Depending on the ketones, bis-trifluoromethylthiolation can also occur. In addition, these methods generally allow the introduction of only a single substituent at the end of the process. By contrast, enones offer a more controlled platform when combined with organometallation strategy, enabling complete selectivity and allowing rapid complexity generation in a single step **(Scheme 2.3)**.

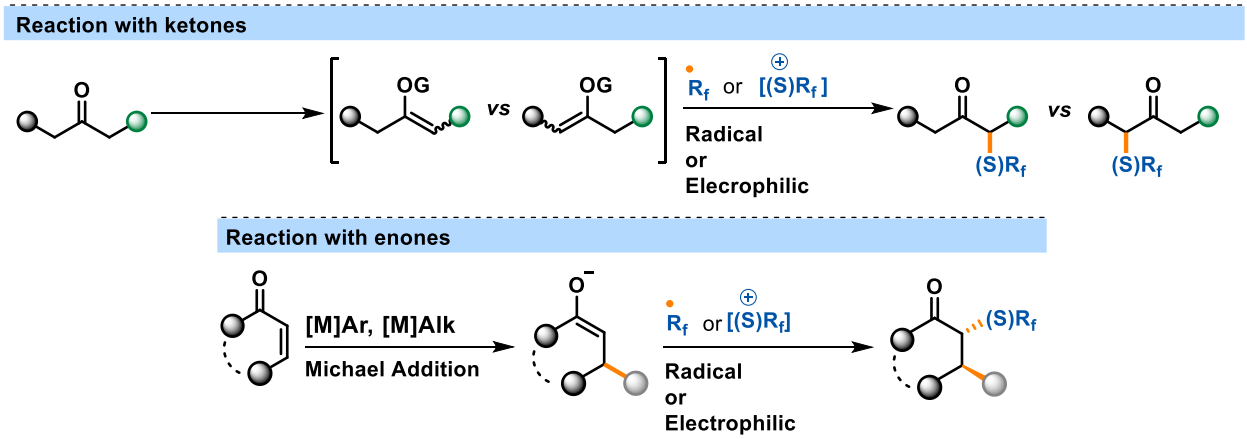

Scheme 2.3: Conventional vs current method for synthesis of α-SCF_3 ketones

Recognizing the existing gaps in literature, the next section outlines the preliminary investigations undertaken as part of this research.

3. Own research

3.1 Preliminary Trials

3.1.1 Introduction

The incorporation of fluorinated groups into small molecules profoundly alters their physical, chemical, and biological properties (as discussed above). This influence arises from their strong electron-withdrawing nature, high lipophilicity (e.g., Hansch hydrophobic parameter $\pi = 1.44$ for SCF_3 and 0.88 for CF_3), and improved metabolic stability. Owing to these unique characteristics, fluorinated motifs have become highly valuable in the design of biologically active compounds, finding widespread application in both medicinal and agrochemical research. Considering the significance of CF_3 and SCF_3 incorporation, my initial studies were directed toward hydrotrifluoromethyl(thiol)ation of alkynes.

3.1.2 Hydrotrifluoromethyl(thiol)ations of alkynes

My initial efforts focused on *syn*-selective hydrometallation of alkynes followed by quenching of the resulting vinyl hydrometallated intermediates with electrophilic trifluoromethylthiolating agents using a one-pot strategy. Specifically, Ni-catalyzed hydroalumination of terminal aryl alkynes with DiBAl-H was attempted, and the resulting intermediates were quenched with a variety of SCF_3 donors (Billard's 1st and 2nd generation, Munavalli's reagent). However, the only isolable product was the corresponding styrene, formed via hydrolysis of the hydroaluminated intermediate. To enhance the electrophilicity of the SCF_3 reagents, I explored their activation with Cu salts and bipyridine ligands. Under these conditions, minor amounts (<20%) of trifluoromethylthiolated products (**259** or **260**) were detected by NMR using *N*-4-dimethyl-*N*-[(trifluoromethyl)sulfanyl]benzene-1-sulfonamide (Billard's 2nd generation reagent) as the SCF_3 source. Interestingly, the regioselectivity of the reaction could be tuned: selective formation of either α- or β-SCF_3 alkenes was achieved by switching the ligand in the Ni catalyst from triphenyl phosphine (PPh_3) to 1,3-(diphenylphosphino)propane (dppp). Nevertheless, further optimization including variations in copper sources, ligands, trifluoromethylthiolating agents, reaction temperature, and time failed to improve the overall reaction efficiency.

To minimize potential loss of volatile products, I also switched to bulkier substrates such as *tert*-butyl phenyl acetylene derivatives. However, this modification likewise did not lead to improvement.

In pursuit of alternative strategies, transmetallation of the hydrometallated intermediates with OMeBpin to generate vinyl boronates, followed by trifluoromethylthiolation in the presence of fluoride additives (CsF, KF), was attempted but proved unsuccessful. Similarly, hydrostannylation

using *n*-Bu_3SnH with subsequent trifluoromethylthiolation of the isolated vinyl stannane failed to produce any product, while Cu-catalyzed trifluoromethylation of the hydrostannylated intermediates (from aryl–alkyl alkynes) using the Ruppert–Prakash or Togni reagent under an O_2 atmosphere resulted in stereoisomeric mixtures. On the other hand, an *anti*-selective approach based on hydromagnesiation of internal alkynes (using $MgBr_2$ and NaH), followed by trifluoromethylthiolation, delivered the desired product (**261**) in moderate yield (~40%). However, this method suffered from stereoselectivity issues when applied to unsymmetrical aryl–alkyl alkynes, limiting its broader applicability **(Scheme 3.1)**.

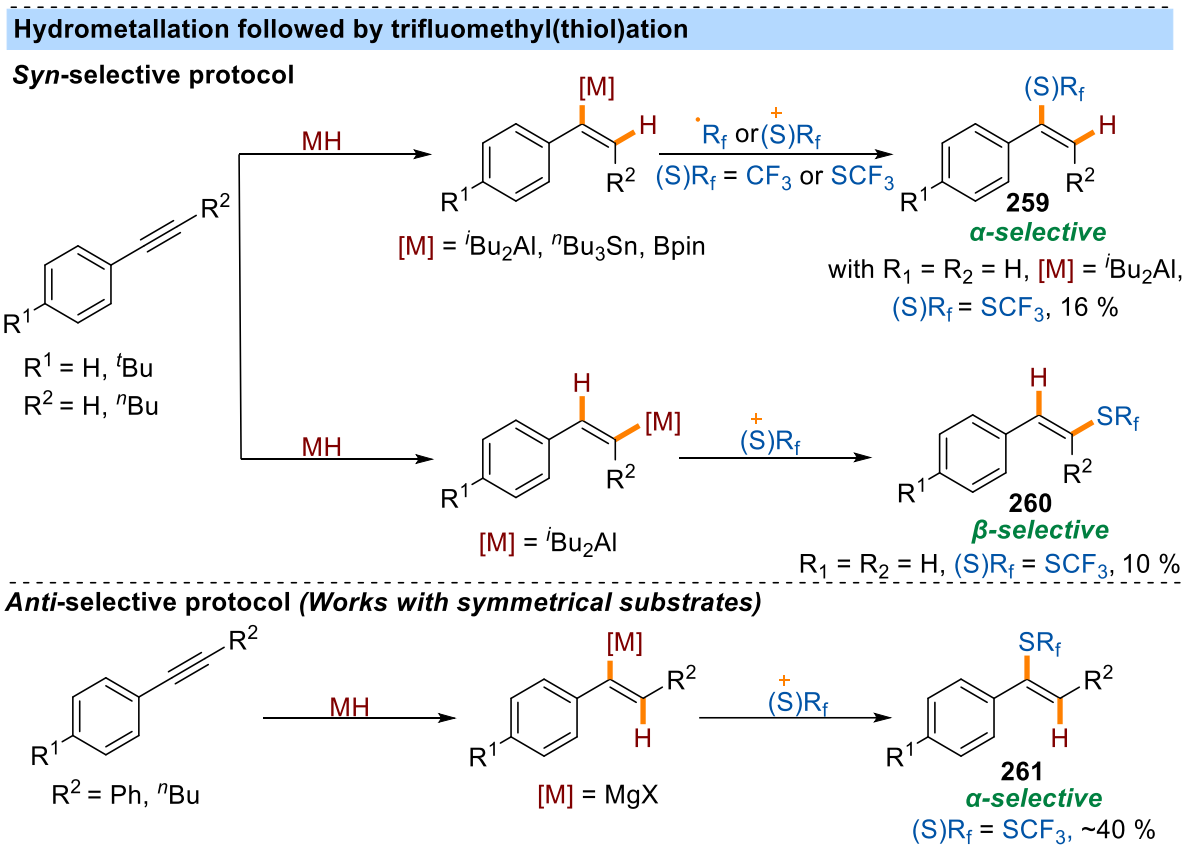

Scheme 3.1: Hydrometallation followed by trifluoromethyl(thiol)ation of alkynes

Since the hydrotrifluoromethyl(thiol)ation strategies provided only limited success, attention was next directed toward carbotrifluoromethyl(thiol)ation of alkynes as an alternative approach.

3.1.3 Carbotrifluoromethyl(thiol)ation of alkynes

Commencing with *tert*-butyl phenylacetylene as a substrate, *anti*-selective carboindation and carbobismuthation using In/BiX_3 and silyl ketene acetals were performed, and the resulting vinyl organometallic intermediates were quenched *in situ* with Ruppert–Prakash or Togni reagents in the presence of Cu(I) salts under varying conditions but there was no β-CF_3 alkene generated (**Scheme 3.2A**. Formation of the vinyl indium/bismuth intermediates was confirmed by quenching with NIS and by NMR. Trifluoromethylthiolation procedures using Cu/ligands with different SCF_3 sources at varied temperatures and times also did not yield vinyl trifluoromethylthio ethers **(262)**.

Anticipating insufficient reactivity of the vinyl indium/bismuth intermediates and considering the higher reactivity of magnesium intermediates together with the limited availability of α & *syn*-selective trifluoromethyl(thiol)ation procedures, the study shifted to carbomagnesiation. Ni-catalyzed phenylmagnesiation of 1-phenylhexyne was performed, followed by functionalization of the alkenyl magnesium intermediate with trifluoromethylating agents employing Cu sources (Scheme **3.2B** and **C**). Since direct Cu-catalyzed trifluoromethylation of magnesium intermediates was unsuccessful, further transmetallation of vinyl magnesium intermediate with $ZnCl_2$ or HBpin was carried out, and the *in situ* generated alkenyl zinc compound and boronates were subjected to trifluoromethylation. In both cases, vinyl trifluoromethyl ethers were formed, though as mixtures of stereoisomers (**263**), suggesting a plausible radical pathway.

Using an electrophilic SCF_3 source, N-trifluoromethylthiophthalimide (231) to transform the vinyl magnesium intermediate gave minor amounts of vinyl trifluoromethylthio ether, with hydrolyzed byproduct as the major component (1:3, P:BP by NMR). Subsequent reaction with CuI/bpy increased the yield of trifluoromethylthiolated product (**264**, observed by integrated signals of the SCF_3-product and hydrolyzed product of vinyl magnesium in crude mixture), establishing conditions for further optimization to improve efficiency.

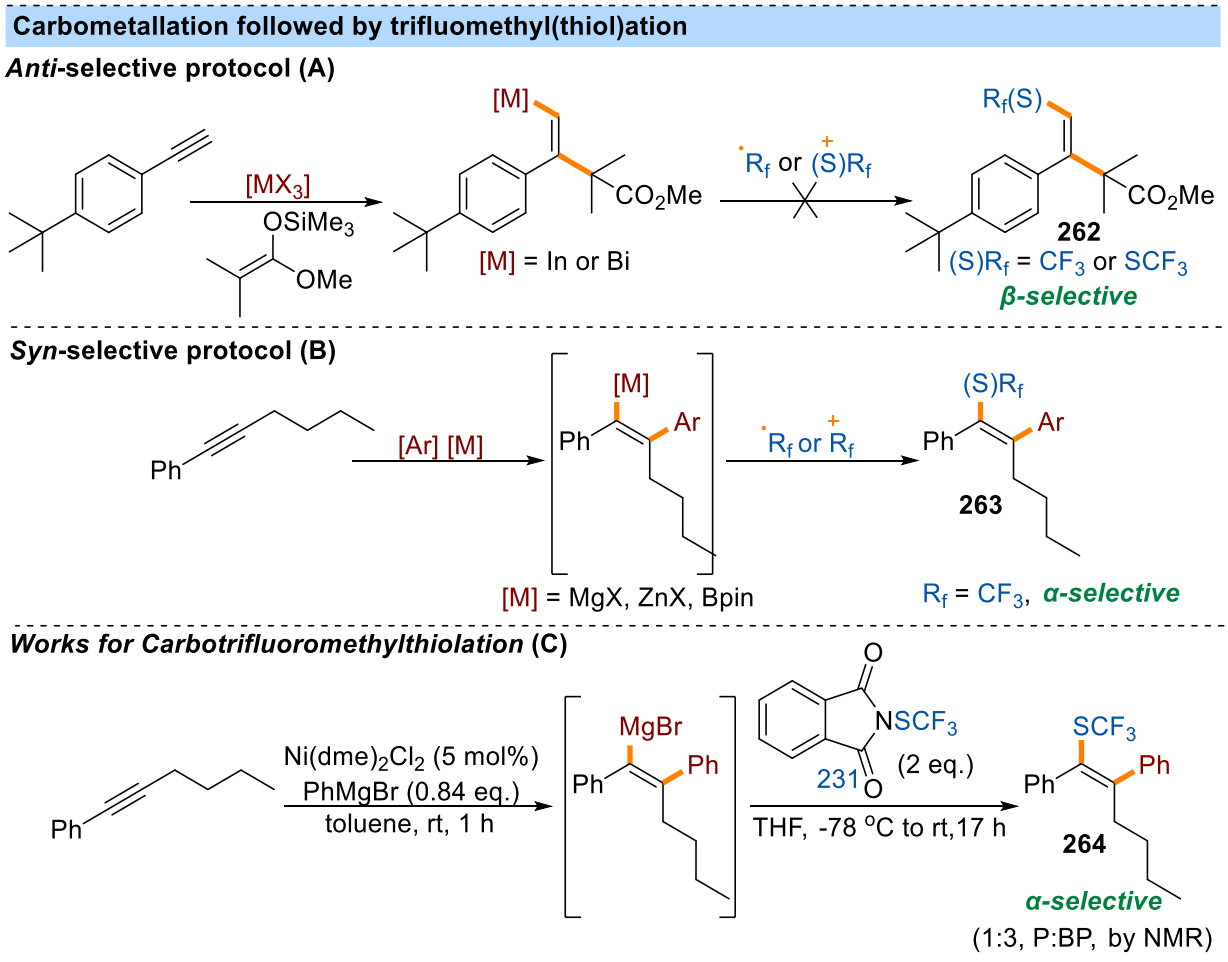

Scheme 3.2A and B: Carbometallation followed by trifluoromethyl(thiol)ation of alkynes

3.1.4 Carbotrifluoromethyl(thiol)ation of enones

Similar strategy was also tested for enones. Initially, cyclohexenone was chosen a model substrate and subjected to Cu-catalysed Michael addition with PhMgBr. The resulting Mg-enolate, silyl enol ether or enol triflate was further trifluoromethylated *in situ (***Scheme 3.3A***)*. With silyl enol ethers and Mg-enolates, reactions were attempted using different Cu(I) sources (known to activate the electrophilic CF_3 group), varying equivalents of Togni-II or Umemoto reagent at different times and temperatures. Alternatively, photocatalyzed methods (Eosin Y under visible light, 470 nm) with triflurormethanesulfonyl chloride (CF_3SO_2Cl) as the CF_3 source were tested, but no α-CF_3 ketone was obtained. With enol triflates, desulfonative transfer of CF_3 using $AgNO_3$ (varied loadings) and persulfates ($(NH_4)_2S_2O_8$ or $K_2S_2O_8$) under different conditions also gave no product (**266**). Approaches for trifluormethylthiolation using Lewis acids ($BiCl_3$, $BF_3{\cdot}Et_2O$) to activate SCF_3 sources, organocatalyst (THT), or Cu(I)/ligand systems with different trifluoromethylthiolating agents (Billard's 1st and 2nd generation, Munavalli's reagent) were also unsuccessful.

Assuming reduced reactivity or stability of the cyclic system, an open chain enone (e.g., *trans*-chalcone) was tested. It's *in situ* generated Mg-enolate afforded the α-SCF_3 ketone in 35% isolated yield using CuI and bipyridine (1:1) with N-(4-dimethylamino)phenyltrifluoromethylsulfonamide) (265) **(Scheme 3.3B)**. The identity of the product (**267**) was confirmed by NMR. With the proof of concept validated, the project was not pursued further due to time limitations. Studies on the optimization of the process and scope will be pursued by the successor.

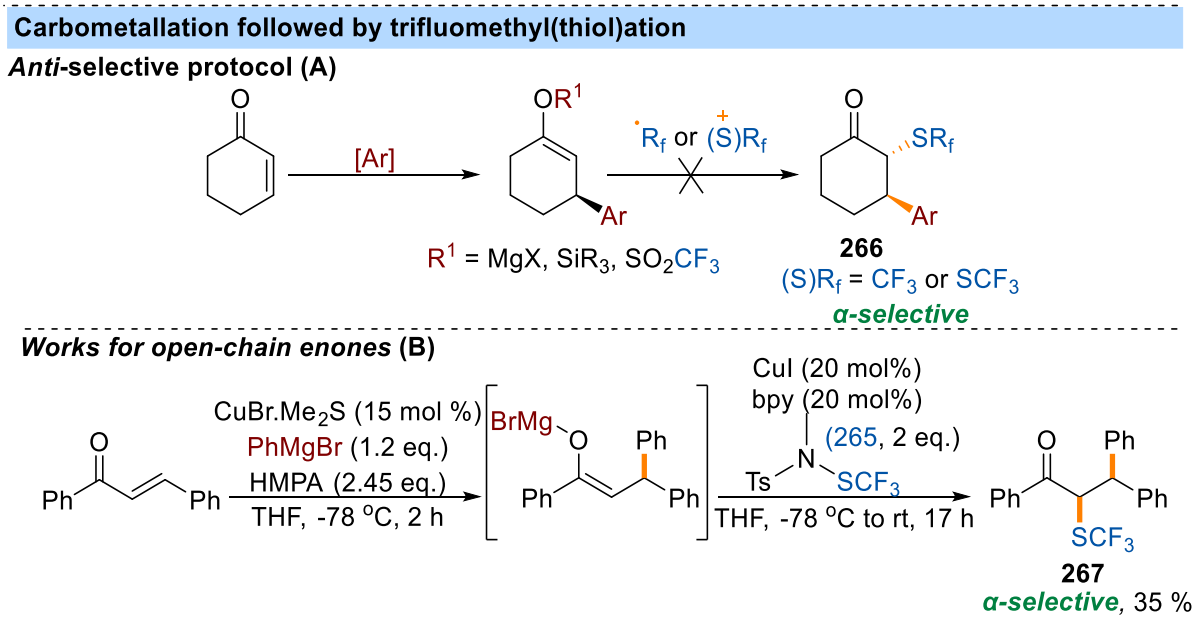

Scheme 3.3A and B: Carbometallation followed by trifluoromethyl(thiol)ation of enones

Building on the promising results obtained in the preliminary trials, further efforts were directed toward the carbotrifluoromethylthiolation of alkynes employing the carbomagnesiation strategy **(**discussed in **Scheme 3.2)**. The next section discusses the development, scope, further

transformations, configurational elucidation, mechanistic features, challenging aspects and limitations of this transformation.

3.2 α-Selective *syn*-Carbotrifluoromethylthiolation of Alkynes

3.2.1 Optimization

Optimization of carbomagnesiation of alkynes

Encouraged by preliminary results of the *syn*-selective protocol **(Scheme 3.2)**, I began to investigate the most favourable conditions for carbomagnesiation of alkynes (step 1 of the one-pot sequence). 1-Phenylhexyne was selected as a model substrate, employing phenylmagnesium bromide as the carbometallating agent. A systematic parameter screening was performed, in which a single variable was altered at a time, and the efficiency of the transformation was assessed by determining yields via gas chromatography using mesitylene as an internal standard.

At first, transition metal catalysts were screened for carbomagnesiation **(Table 3.1)**. While iron, copper and cobalt showed almost no reactivity, most of the Ni catalysts gave nearly complete conversion, affording 93% yield as the maximum (entry 1).

Table 3.1 Effect of catalyst[a]

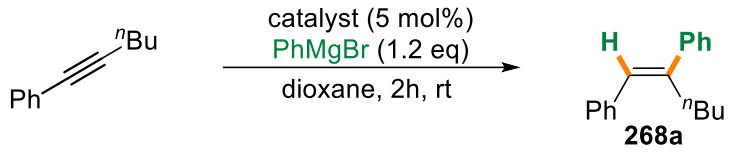

268a

Entry	NiX_2	Conversion (%)	Yield (%)
1	**$Ni(dme)Cl_2$**	**95**	**93**
2	$Ni(dme)Br_2$	95	80
3	$NiCl_2$	95	80
4	$NiBr_2$	95	80
5	$Ni(acac)_2$	100	61
6	$Ni(OTf)_2$	25	21
7	$NiCl_2.6H_20$	70	58
8	$Fe(acac)_3$	0	0
9	$Co(dme)Br_2$	14	0
10	CuI	0	0

[a]Conditions: Catalyst (5 mol%), phenylhexyne (1 mmol), PhMgBr (1.2 eq.), dioxane (4 mL), 2 h, rt; yield and conversion determined by GC using mesitylene as an internal standard.

With $Ni(dme)Cl_2$ identified as the most effective catalyst, the influence of catalyst loading was subsequently examined **(Table 3.2)**. A 5 mol% loading proved sufficient, delivering results comparable to higher loadings and affording nearly quantitative conversion (entry 2). On the contrary, lower catalyst loading resulted in diminished yields and conversions.

Table 3.2 Effect of mol% of the catalyst[a]

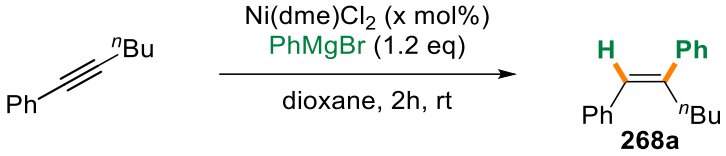

268a

Entry	Mol% of catalyst	Conversion (%)	Yield (%)
1	2mol%	85	80
2	**5 mol%**	**95**	**93**
3	10 mol%	100	93
4	15 mol%	100	94
5	20 mol%	100	94

[a]Conditions: Ni(dme)Cl_2 (x mol%), phenylhexyne (1 mmol), PhMgBr (1.2 eq.), dioxane (4 mL), 2 h, rt; yield and conversion determined by GC using mesitylene as an internal standard.

Next, the effect of the Grignard reagent stoichiometry was examined, using 5 mol% of Ni(dme)Cl_2 as the catalyst **(Table 3.3)**. Employing a slight excess of PhMgBr was necessary to achieve high yields, which compensated for homocoupling side reactions detected by GC/TLC (entry 2). The formation of biphenyl byproducts presumably originates from the initial reduction of Ni(II) to catalytically active Ni(0) species. Additionally, a dropwise addition of the reagent generally resulted in improved efficiency.

Table 3.3 Equivalents of PhMgBr[a]

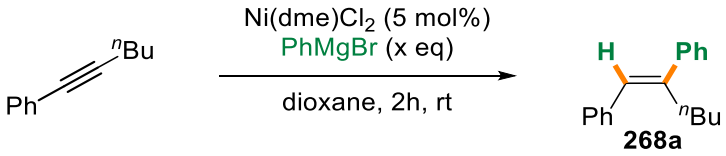

268a

Entry	Eq of PhMgBr	Conversion (%)	Yield (%)
1	1.0	100	70
2	**1.2**	**100**	**93**
3	1.4	100	92
4	1.6	100	93

[a]Conditions: Ni(dme)Cl_2 (5 mol%), phenylhexyne (1mmol), PhMgBr (y eq.), dioxane (4mL), 2 h, rt; yield and conversion determined by GC using mesitylene as an internal standard.

The influence of solvents was also examined **(Table 3.4)**, revealing that moderately polar and non-polar solvents performed much better than polar ones. While toluene afforded full conversion, yields were inferior to those obtained in dioxane (cf. entries 1 and 3). In contrast, THF gave the lowest yield amongst the three (entry 2).

Table 3.4 Effect of solvent[a]

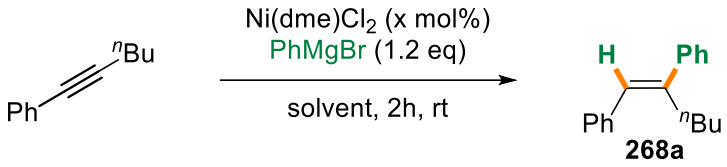

268a

Entry	Solvent	Conversion (%)	Yield (%)
1	**Dioxane**	**100**	**93**
2	THF	80	41
3	Toluene	100	62
4	MeCN	30	20
5	HMPA	18	0
6	DMPU	33	0
7	NMP	77	0

[a]Conditions : $Ni(dme)Cl_2$ (5 mol%), phenylhexyne (1 mmol), PhMgBr (1.2 eq.), Solvent (4 mL), 2 h, rt; yield and conversion determined by GC using mesitylene as an internal standard.

The reaction was monitored over a 5 h period at room temperature by quenching aliquots hourly with NH_4Cl and adding mesitylene (150 µL) and methyl *tert*- butyl ether (MTBE), followed by GC analysis. Extending the reaction did not improve efficiency, whereas 2 h was identified as the optimal reaction time with dioxane as the best solvent **(Table 3.5)**.

Table 3.5 Time of the reaction

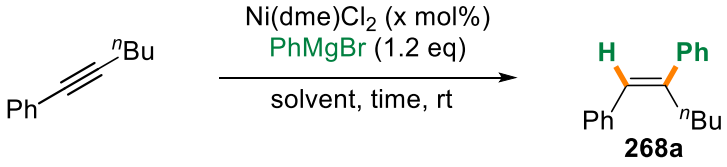

268a

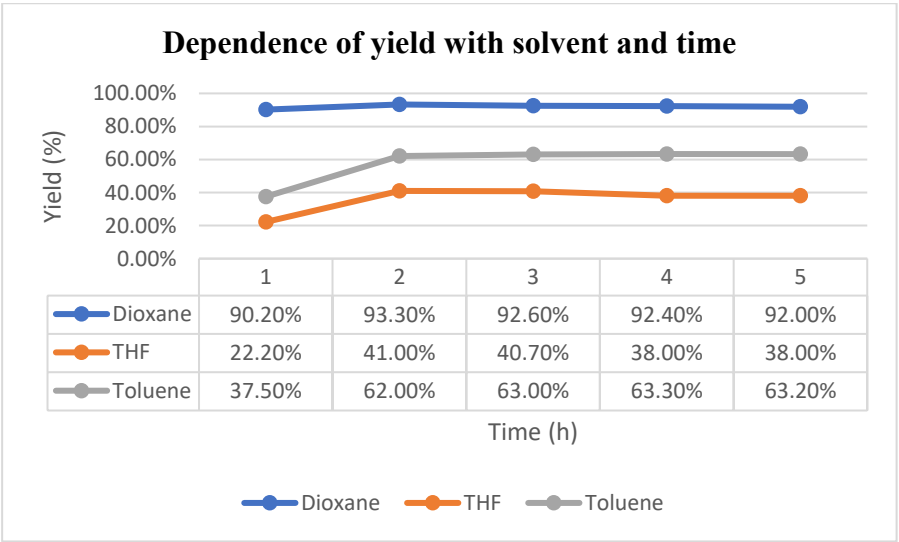

Using these conditions, [Ni(dme)Cl_2 (5 mol%), PhMgBr (1.2 eq.), dioxane, 2 h, rt] the hydrolyzed product of vinyl magnesium was obtained in 82% isolated yield, indicating that approximately 82% of vinylmagnesium bromide had formed in the reaction mixture.

In an effort to further improve the yield, various ligands were screened **(Table 3.6)**; however, the reaction performed better in their absence, giving higher yields for reaction carried out without any ligand (entry 5).

Table 3.6 Effect of ligands[a]

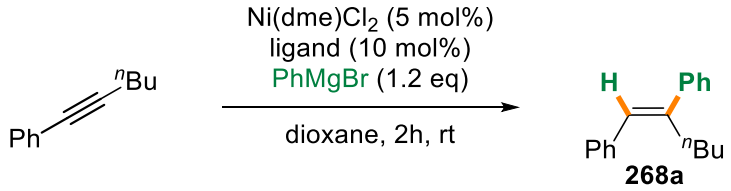

268a

Entry	Ligand	Conversion (%)	Yield (%)
1	2,2' bpy	100	75
2	1,10 phen	100	65
3	TMEDA	100	80
4	PMDTA	100	73
5	**-**	**100**	**82**

[a]Conditions: Ni(dme)Cl_2 (5 mol%), ligand (10 mol%), phenylhexyne (1 mmol), PhMgBr (1.2 eq.), dioxane (4 mL), 2 h, rt; Isolated yields reported.

Optimization for the one-pot protocol of carbotrifluoromethylthiolation

After establishing the optimal conditions for first step of the projected transformation, optimization of the one-pot carbotrifluoromethylthiolation was undertaken. Preliminary experiments indicated that the trifluoromethylthiolated alkene was formed in small amounts when Billard's 2nd generation trifluoromethanesulfenamides (**265**) was employed as the electrophilic trifluoromethylthiolating agent in the presence of Cu(I) source and bipyridine ligands.

To improve the yield of the SCF_3 product, a range of ligands were initially screened **(Table 3.7)**. Phosphorus ligands proved less effective compared to bipyridine- and phenanthroline-based systems. Notably, 4,4'-di-tert-butyl-2,2'-bipyridine and 3,4,7,8-tetramethyl-1,10-phenanthroline exhibited the best and comparable performance (entries 6 and 10), generating only minor amounts of byproducts **268a** as confirmed by GC analysis. Owing to its greater availability, 4,4'-di-tert-butyl-2,2'-bipyridine was selected for subsequent optimization studies.

Table 3.7 Effect of ligands[a]

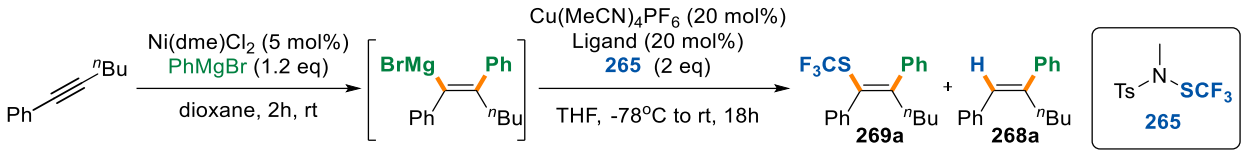

Entry	Ligand	Yield of 269a (%)	Yield of 268a (%)
1	2,2'-bipyridine	23	10
2	4,4'- dimethoxy 2,2'-bipyridine	27	11
3	4,4'-dimethyl 2,2'-bipyridine	27	10
4	5,5'-dimethyl 2,2'-bipyridine	29	9
5	6,6'-dimethyl 2,2'-bipyridine	10	11
6	**4,4'-di-tert-butyl 2,2'-bipyridine**	**42**	**10**
7	4,4′,4″-tri-tert-Butyl-2,2′:6′,2″-terpyridine	20	15
8	dipicolyl amine	15	30
9	1,10- phenanthroline	25	9
10	**3,4,7,8-tetra methyl 1,10-phenanthroline**	**45**	**13**
11	BINAP	23	17
12	Xant Phos	22	20
13	dppb	4	42
14	dppy	14	17
15	X phos	13	12
16	PMDTA	6	13

[a]Conditions: $NiCl_2$(dme) (5 mol%), phenylhexyne (0.2 mmol, 1 eq.), PhMgBr (1.2 eq.), dioxane (0.8 mL), 2 h, rt. then $Cu(MeCN)_4PF_6$ (20 mol%), Ligand (20 mol%), N-Methyl-N-[(trifluoromethyl)thio]-*p*-toluenesulfonamide **265** (2 eq.) in 0.6mL THF (0.67 M), -78°C to rt, 18 h; yield determined by GC using mesitylene as an internal standard.

The ratio of Cu source to ligand was evaluated **(Table 3.8 and 3.9)**. The reaction proceeded to approximately 50% yield with 40 mol% of both Cu and ligand (**Table 3.8** entry 4). A 1:2 Cu:ligand ratio gave improved results, with the optimal yield observed at 40 mol% loading of Cu, which was comparable to that obtained using the same copper loading and 1:3 ratio to ligand (**Table 3.8** entries 8 and 9). Further increasing the loadings of both components to stoichiometric amounts offered no additional improvement in yield (**Table 3.9** entries 5 and 6). Additionally, both $Cu(MeCN)_4PF_6$ and $CuBr{\cdot}Me_2S$ exhibited nearly equivalent activity (**Table 3.8** and **3.9** entry 8 and 4 respectively).

Table 3.8 Ratio of $Cu(MeCN)_4PF_6$ to ligand (Cu:L)[a]

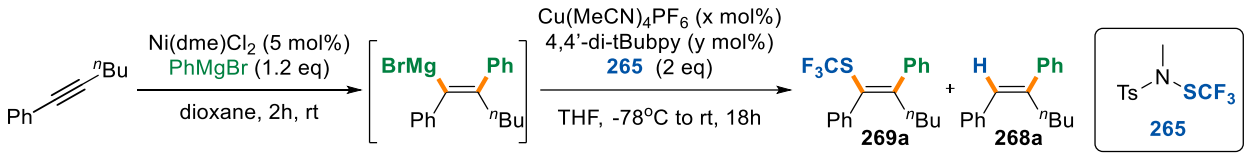

Entry	Cu (mol%): L (mol%)	Yield of 269a (%)	Yield of 268a (%)
1	5:5 (1:1)	19	8
2	10:10	22	9
3	20:20	39	9
4	40:40	48	11
5	5:10 (1:2)	26	8
6	10:20	44	7
7	20:40	56	8
8	**40:80**	**59**	**8**
9	40:120 (1:3)	64	9
10[b]	20:40 (1:2)	44	15
11[b]	40:80	58	16
12[b]	40:120 (1:3)	65	13

[a]Conditions: $NiCl_2$(dme) (5 mol%), phenylhexyne (0.2 mmol, 1eq.), PhMgBr (1.2 eq.), dioxane (0.8 mL), 2 h, rt. then $Cu(MeCN)_4PF_6$ (x mol%), 4,4'-di-tert-butyl 2,2'-bipyridine (y mol%), N-Methyl-N-[(trifluoromethyl)thio]-*p*-toluenesulfonamide **265** (2 eq.) in 0.6 mL THF (0.67 M), -78°C to rt, 18 h; yield determined by GC using mesitylene as an internal standard. [b]1,10 phenanthroline was used as a ligand in trifluoromethylthiolation step.

Table 3.9 Ratio of $CuBr.Me_2S$ to ligand (Cu:L)[a]

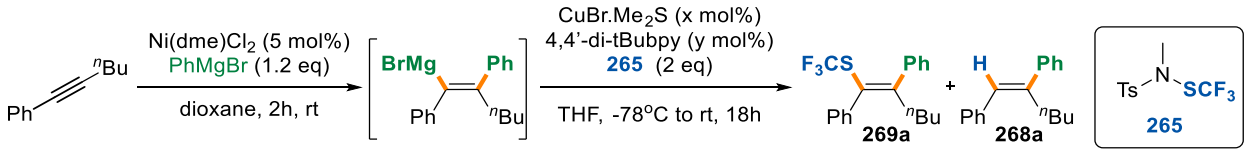

Entry	Cu (mol%) : L (mol%)	Yield of 269a (%)	Yield of 268a (%)
1	40:40 (1:1)	41	7
2	10:20 (1:2)	35	7
3	20:40	50	7
4	**40:80**	**56**	**7**
5	100:200	56	6
6[b]	100, no ligand	18	44
7[b]	20:40 (1:2)	49	30
8[b]	40:80	45	35

[a]Conditions: $NiCl_2$(dme) (5 mol%), phenylhexyne (0.2 mmol, 1eq.), PhMgBr (1.2 eq.), dioxane (0.8 mL), 2 h, rt. then $CuBr.Me_2S$ (x mol%), 4,4'-di-tert-butyl 2,2'-bipyridine (y mol%), N-Methyl-N-[(trifluoromethyl)thio]-*p*-toluenesulfonamide **265** (2 eq.) in 0.6 mL THF (0.67 M), -78°C to rt, 18 h; yield determined by GC using mesitylene as an internal standard. [b]1,10 phenanthroline was used as a ligand in trifluoromethylthiolation step.

Preliminary screening of Cu sources showed that Cu(I) salts outperformed Cu(II) salts **(Table 3.10)**. Consequently, several Cu(I) sources were evaluated. Among them, $Cu(MeCN)_4PF_6$, CuSCN, and $CuBr{\cdot}Me_2S$ gave analogous results, with $CuBr{\cdot}Me_2S$ being selected for further experiments due to its greater availability (entries 1, 3 and 6).

Table 3.10 Effect of the copper source.[a]

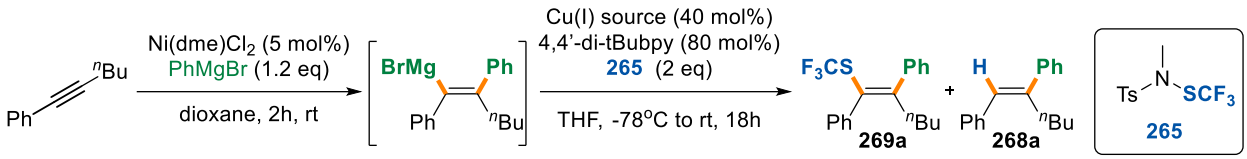

Entry	Cu(I) source	Yield of 269a (%)	Yield of 268a (%)
1	**$Cu(MeCN)_4PF_6$**	**59**	**10**
2	CuI	40	9
3	**CuSCN**	**61**	**8**
4	CuCN	54	8
5	CuCl	54	7
6	**$CuBr.Me_2S$**	**62**	**6**
7	$CuCF_3(PPh_3)_3$	33	15

[a]Conditions: $NiCl_2$(dme) (5 mol%), phenylhexyne (0.2 mmol, 1eq.), PhMgBr (1.2 eq.), dioxane (0.8 mL), 2 h, rt. then Cu(I) source (40 mol%), 4,4'-di-tert-butyl 2,2'-bipyridine (80 mol%), N-Methyl-N-[(trifluoromethyl)thio]-*p*-toluenesulfonamide **265** (2 eq.) in 0.6 mL THF (0.67 M), -78°C to rt, 18 h; yield determined by GC using mesitylene as an internal standard.

In contrast to the carbomagnesiation step, THF was found to be the optimal solvent for the trifluoromethylthiolation step (**Table 3.11**, entry 1). Moreover, increasing the amount of THF added in second step from 600 µL to 2 mL had no impact on the reaction outcome (**Table 3.12** entries 1 to 3).

Table 3.11 Effect of solvent.[a]

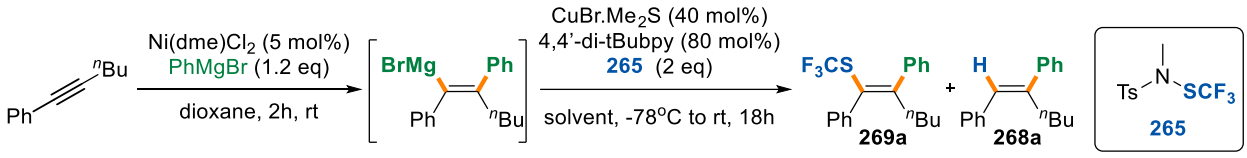

Entry	Solvent (mL)	Yield of 269a (%)	Yield of 268a (%)
1	**THF**	**59**	**5**
2	Dioxane	42	5
3	MeCN	55	7
4	Toluene	52	5
5	NMP	19	19

[a]Conditions: $NiCl_2$(dme) (5 mol%), phenylhexyne (0.2 mmol, 1eq.), PhMgBr (1.2 eq.), dioxane (0.8 mL), 2 h, rt. then $CuBr.Me_2S$ (40 mol%), 4,4'-di-tert-butyl 2,2'-bipyridine (80 mol%), N-Methyl-N-[(trifluoromethyl)thio]-*p*-toluenesulfonamide **265** (2 eq.) in 0.6 mL solvent (0.67 M), -78°C to rt, 18 h; yield determined by GC using mesitylene as an internal standard.

Table 3.12 Effect of volume of solvent.[a]

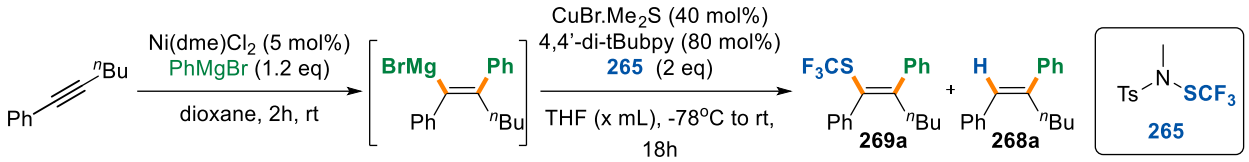

Entry	Volume of THF	Yield of 269a (%)	Yield of 268a (%)
1	**0.6**	**61**	**6**
2	1	61	7
3	2	61	10

[a]Conditions: $NiCl_2$(dme) (5 mol%), phenylhexyne (0.2 mmol, 1eq.), PhMgBr (1.2 eq.), dioxane (0.8 mL), 2 h, rt. then $CuBr.Me_2S$ (40 mol%), 4,4'-di-tert-butyl 2,2'-bipyridine (80 mol%), N-Methyl-N-[(trifluoromethyl)thio]-*p*-toluenesulfonamide **265** (2 eq.) in THF (volume), -78°C to rt, 18 h; yield determined by GC using mesitylene as an internal standard.

Performing the trifluoromethylthiolation at low temperature gave more favorable results compared to higher temperatures (**Table 3.13**, entries 1, 4 and 5). However, maintaining the reaction at –78 °C after adding the Cu source, ligand, and trifluoromethylthiolating agent resulted in low yield. This was attributed to the freezing of the solution of vinylmagnesium intermediate at this temperature, which prevented effective stirring.

Table 3.13 Effect of temperature[a]

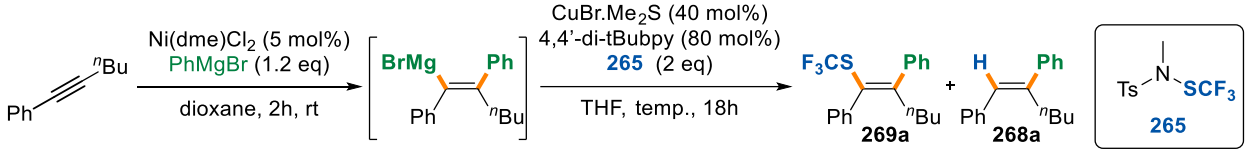

Entry	Temperature of thiolation	Yield of 269a (%)	Yield of 268a (%)
1	**-78C to rt**	**63**	**6**
2	-78C to Rt to 60°C	57	6
3	-40°C to rt	58	6
4	rt to rt	39	6
5	rt to 60°C	42	6
6	-78°C to -78°C (1h) to rt	40	8

[a]Conditions: $NiCl_2$(dme) (5 mol%), phenylhexyne (0.2 mmol, 1eq.), PhMgBr (1.2 eq.), dioxane (0.8 mL), 2 h, rt. then $CuBr.Me_2S$ (40 mol%), 4,4'-di-tert-butyl 2,2'-bipyridine (80 mol%), N-Methyl-N-[(trifluoromethyl)thio]-*p*-toluenesulfonamide **265** (2 eq.) in 0.6 mL THF, temperature, 18 h; yield determined by GC using mesitylene as an internal standard.

Using 2 equivalents of the trifluoromethylthiolating agent proved to be optimal for the reaction outcome (**Table 3.14**, entry 3). Smaller amounts of **265** resulted in decrease in yield (entries 1 and 2), while increasing the amount to 2.5 equivalents had no further effect on efficiency (entry 4).

Table 3.14 Equivalents of SCF_3-agent 265

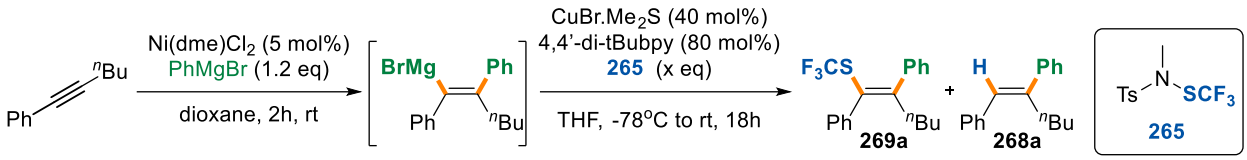

Entry	Amount of 6 (eq)	Yield of 269a (%)	Yield of 268a (%)
1	1.1	33	7
2	1.5	45	6
3	**2**	**52**	**6**
4	2.5	53	6

[a]Conditions: $NiCl_2$(dme) (5 mol%), phenylhexyne (0.2 mmol, 1eq), PhMgBr (1.2 eq.), dioxane (0.8 mL), 2 h, rt. then $CuBr.Me_2S$ (40 mol%), 4,4'-di-tert-butyl 2,2'-bipyridine (80 mol%), N-Methyl-N-[(trifluoromethyl)thio]-*p*-toluenesulfonamide 265 (x eq.) in THF (0.6 mL), -78°C to rt, 18 h; yield determined by GC using mesitylene as an internal standard.

During the screening of various previously synthesized trifluoromethylthiolating agents **(Table 3.15)**, it was observed that N-methyl-N-tosyltrifluoromethanesulfenamide (265) (Billard's[273] second-generation reagent) and N-trifluoromethylthiophthalimide (231) along with its nitro derivative (270) (Munavalli's and Wang's[247] reagents), afforded comparable results, whereas N-methyl-N-(trifluoromethylthio)aniline (271) showed no product formation.

Table 3.15 Trifluoromethylthiolating agents

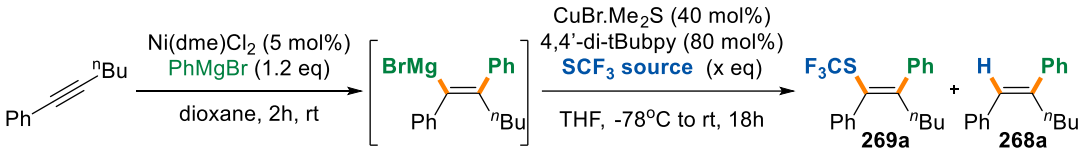

SCF_3 agents

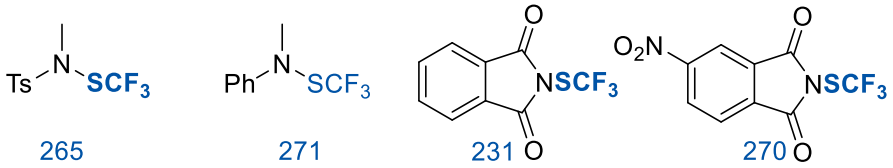

Entry	SCF_3 agent	Yield of 269a (%)	Yield of 268a (%)
1	265	52	8
2	271	0	22
3	231	49	13
4	270	47	8

[a]Conditions: $NiCl_2$(dme) (5 mol%), phenylhexyne (0.2 mmol, 1eq.), PhMgBr (1.2 eq.), dioxane (0.8 mL), 2 h, rt. then $CuBr.Me_2S$ (40 mol%), 4,4'-di-tert-butyl 2,2'-bipyridine (80 mol%), SCF_3-agent (2 eq.) in THF (0.6 mL), -78°C to rt, 18 h; yield determined by GC using mesitylene as an internal standard.

Next, the order of addition was investigated **(Table 3.16)**. Introducing the solution of the vinyl magnesium intermediate (product of step 1) dropwise into a THF solution containing Cu, ligand, and the trifluoromethylthiolating agent provided similar efficiency by GC analysis as adding Cu and ligand as solids to the vinyl magnesium intermediate, followed by the trifluoromethylthiolating agent (entry 1 and 3). Although both methods gave comparable results, the latter approach was selected for substrate scope evaluation to minimize minor losses during the transfer of the reaction mixture of the 1st step.

Table 3.16 Order of addition[a]

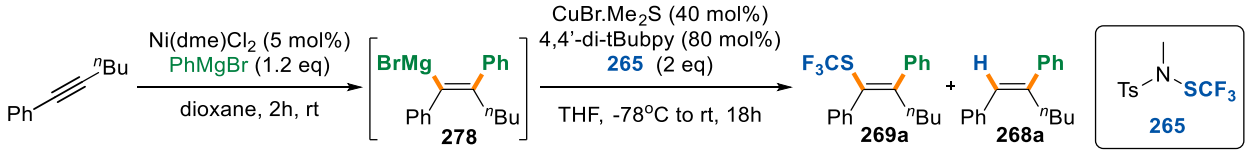

C: Vinylmagnesium species **278** (prepared by Ni-catalyzed carbomagnesiation of 1-phenylhexyne)
SCF_3: Solution of Cu(I), ligand and SCF_3-agent **265** in THF
Cu + L: Mixture of copper and ligand (as solid)

Entry	Order of addition[a]	Yield of 269a (%)	Yield of 268a (%)
1	**C to SCF_3**	**58**	**10**
2	SCF_3 to C	45	13
3	**C to Cu + L then 6**	**58**	10
4	Cu + L to C, then **6**	57	7
5	Cu + L to C, then **6**	33[b]	8[b]

[a]Conditions: $NiCl_2$(dme) (5 mol%), phenylhexyne (0.2 mmol, 1eq.), PhMgBr (1.2 eq.), dioxane (0.8 mL), 2 h, rt. then $CuBr.Me_2S$ (40 mol%), 4,4'-di-tert-butyl 2,2'-bipyridine (80 mol%), N-Methyl-N-[(trifluoromethyl)thio]-*p*-toluenesulfonamide **265** (2 eq.) in THF (0.6 mL), -78°C to rt, 18 h; yield determined by GC using mesitylene as an internal standard. [b]$Cu(MeCN)_4PF_6$ used as a Cu source.

The isolated yield with various best combinations of parameters were determined **(Table 3.17)**. It was found that using $Cu(MeCN)_4PF_6$ as the catalyst, with Cu and ligand added as solids to the vinyl magnesium intermediate followed by the addition of the trifluoromethylthiolating agent N-trifluoromethylthiophthalimide, gave superior results compared to other conditions (entry 3). Furthermore, isolation after 18 h provided the same yield as that obtained after 1 h.

Table 3.17 Isolated yield

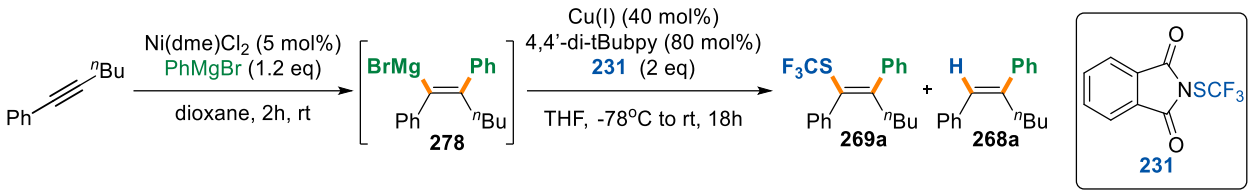

C: Vinylmagnesium species **278** prepared by Ni-catalyzed carbomagnesation of phenylhexyne
SCF_3: Solution of Cu(I), ligand and SCF_3-agent **231** in THF
Cu + L: Mixture of copper and ligand (as solid)

Entry	Order of addition	Cu(I)	Yield of 269a (%)	Yield of 268a (%)
1	C to SCF_3	$Cu(MeCN)_4PF_6$	60	6
2	C to SCF_3	$CuBr.Me_2S$	59	6
3	**Cu + L to C then 6**	$Cu(MeCN)_4PF_6$	**73**	8
4	Cu + L to C then **6**	$CuBr.Me_2S$	55	8

[a]Conditions: $NiCl_2$(dme) (5 mol%), phenylhexyne (0.2 mmol, 1eq.), PhMgBr (1.2 eq.), dioxane (0.8 mL), 2 h, rt. then $CuBr.Me_2S$ (40 mol%), 4,4'-di-tert-butyl 2,2'-bipyridine (80 mol%), N-trifluoromethylphthalimide **231** (2 eq.) in THF (0.6 mL), -78°C to rt, 18 h; isolated yields reported.

3.2.2 Scope of Carbotrifluoromethylthiolation of alkynes

With the optimized conditions established, I next evaluated the substrate scope to assess the generality of the method (**Scheme 3.4A and B**, **3.6** and **3.7**). Aryl–alkyl alkynes with diverse alkyl substituents were explored. Linear, cyclic, and moderately branched groups were well tolerated, affording products with good efficiency (58-73% yield, with 77% on 1 mmol scale). In contrast, highly branched substituents and sterically demanding *tert*-butyl and silyl groups were less reactive, nevertheless, they were still able to participate in the transformation, affording regioisomeric mixtures upon carbomagnesiation (**Scheme 3.5**). For example, *tert*-butyl phenylacetylene delivered the desired SCF_3 product, although in low yield and as a regioisomeric mixture. A benzyl substituent was also compatible, providing outcomes comparable to 1-phenylhexyne (72% vs 73%).

Variation of the aryl group revealed that substrates bearing electron-donating or moderately electron-withdrawing substituents were suitable (**Scheme 3.4B**, **269g** and **269i**), whereas strongly deactivating substituents such as CF_3 proved unreactive. Substrates bearing chloro (**269e**), tosylate (**269j**), and triflate (**269k**) groups were tolerated, highlighting the synthetic potential of the method. A protected aldehyde (**269l**) also survived the conditions, affording product in reasonable yield. Larger aromatic systems (naphthyl) and heteroaromatics such as benzodioxoles (**269m**), indoles (**269n**), and thiophenes (**269o**) also participated with modest efficiency (46-66%). In contrast, pyridine substrates gave complex mixtures, and in pyrimidines, phenylmagnesium bromide reacted with heteroaryl ring directly rather than the alkyne (as confirmed by GC–MS, **Scheme 3.5**).

Interestingly, an enyne (**269p**) substrate also underwent reaction, though with reduced yield in the trifluoromethylthiolation step. Given the utility of boronates as partners for Suzuki coupling, boronate-substituted aryl alkynes (**Scheme 3.5**) were tested; however, these gave incomplete

conversion in the first step and poor yields in the second, with the desired product inseparable from hydrolyzed byproducts and unreacted alkyne. Similarly, alkyne containing oxy-substituted tetrahydropyran and cyclohexenyl phenylacetylene underwent smooth carbomagnesiation but failed to proceed in the trifluoromethylthiolation step. Finally, dialkyl alkynes proved sluggish in the initial carbomagnesiation, precluding their evaluation in the subsequent step. Importantly, the corresponding alkenyl trifluoromethyl thioethers were obtained as single products with complete regio- and stereoselectivity.

[a]Rxn. conditions: $Ni(dme)Cl_2$ (5 mol%), **1** (0.2 mmol), R^2MgBr (1.2 eq.), dioxane (0.8 mL), 2 h, rt., then $Cu(MeCN)_4PF_6$ (0.4 eq.), *t*-Bu bpy (0.8 eq.), N-(trifluoromethylthio)phthalimide (2 eq.), 0.6 mL THF, 1 h, -78 °C to r.t.; Isolated yields reported, typically products **3** were isolated along with small amounts of olefins **4** (inseparable), [b] run at 1 mmol scale. [c]carbomagnesation run for 3h, [d]carbomagnesation at 60°C, [e]carbomagnesation at 60°C for 4h.

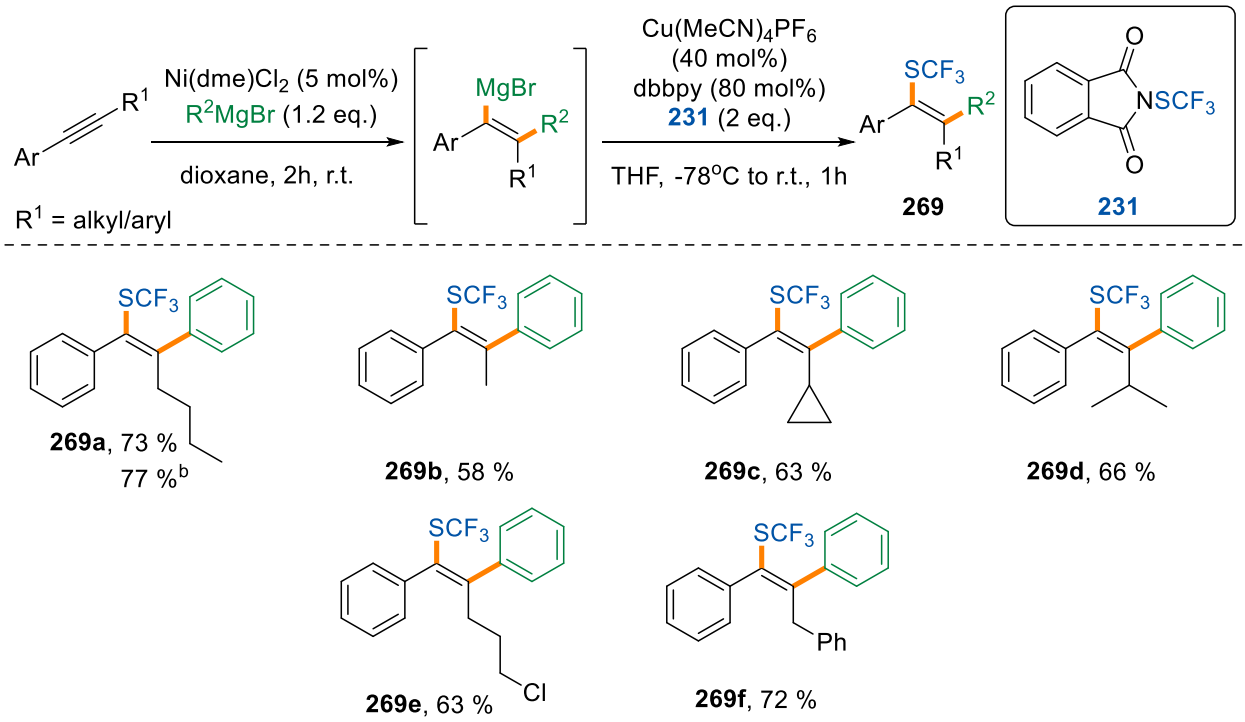

Scheme 3.4A: Scope of alkyl variants (in Aryl-alkyl alkynes)

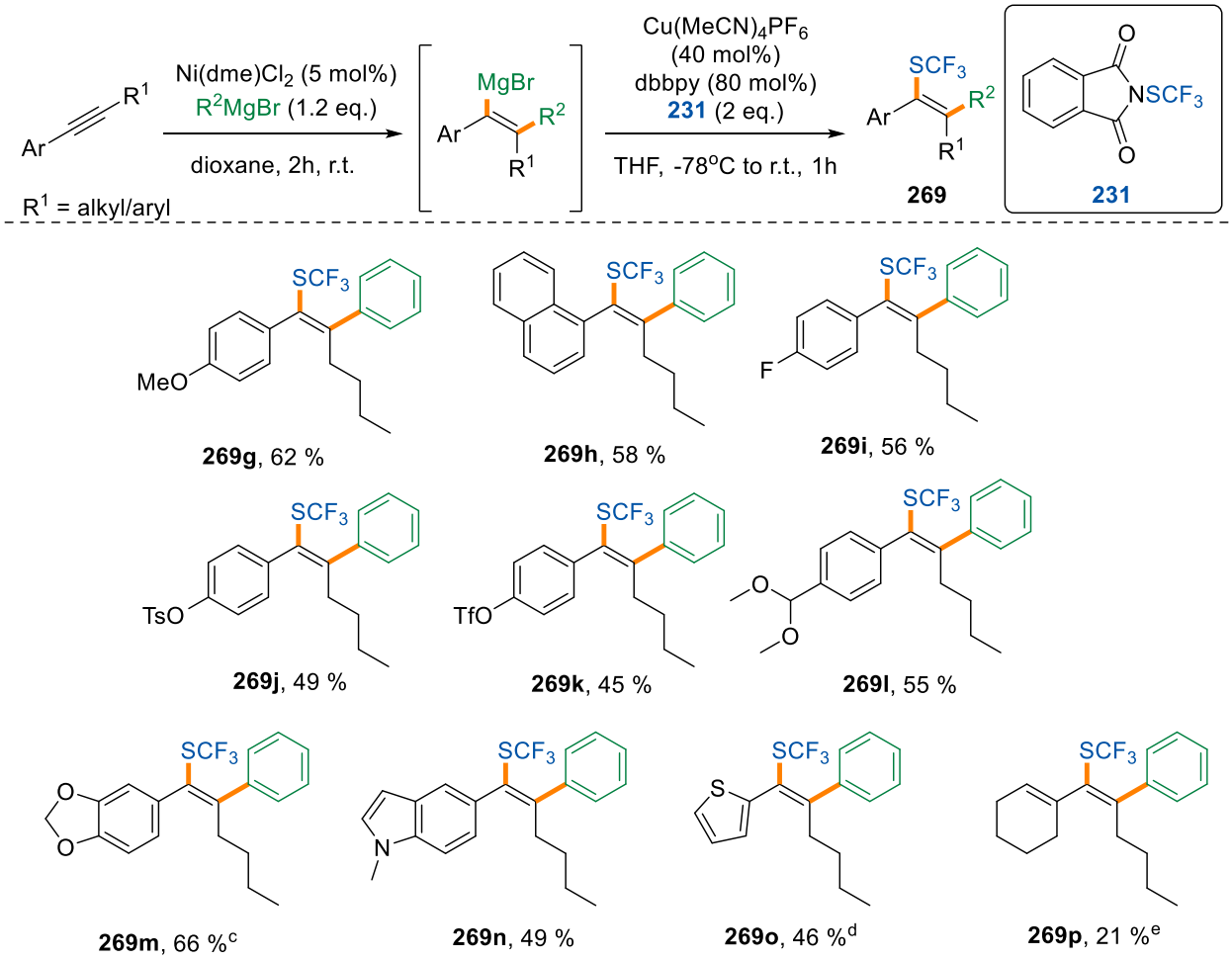

Scheme 3.4B: Scope of conjugated, (hetero)aryl variants (in Aryl-alkyl alkynes)

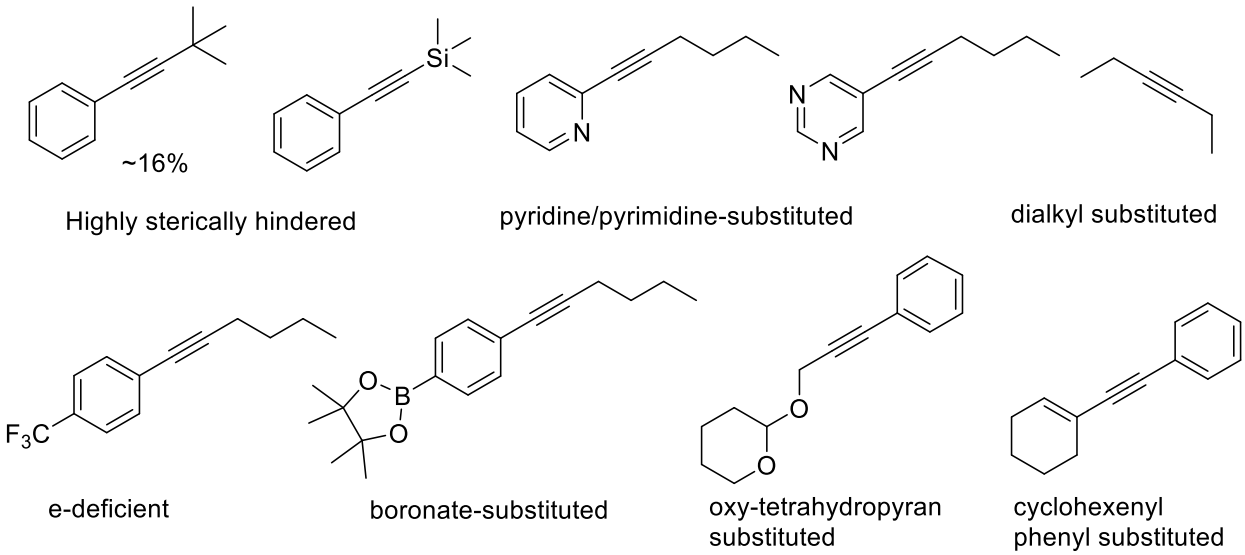

Scheme 3.5: Limitation of the method-alkynes

After exploring aryl–alkyl alkynes, attention was turned to diaryl alkynes **(Scheme 3.6)**. Symmetrical diphenylacetylene (**269q**) underwent the transformation smoothly, affording the desired product in 63% yield. For unsymmetrical substrates, the main challenge arose from the formation of regioisomers during the carbomagnesiation step, which consequently led to two regioisomeric products in the subsequent transformation. Nonetheless, substrates such as 1-/2-naphthyl (**269s**, **269t**) and *p*-methoxy-substituted (**269r**) derivatives proved effective, and in all cases the products were obtained with high stereoselectivity, even though regioselectivity was not achieved.

[f]Obtained as mixture of regiosisomers, major isomers drawn.

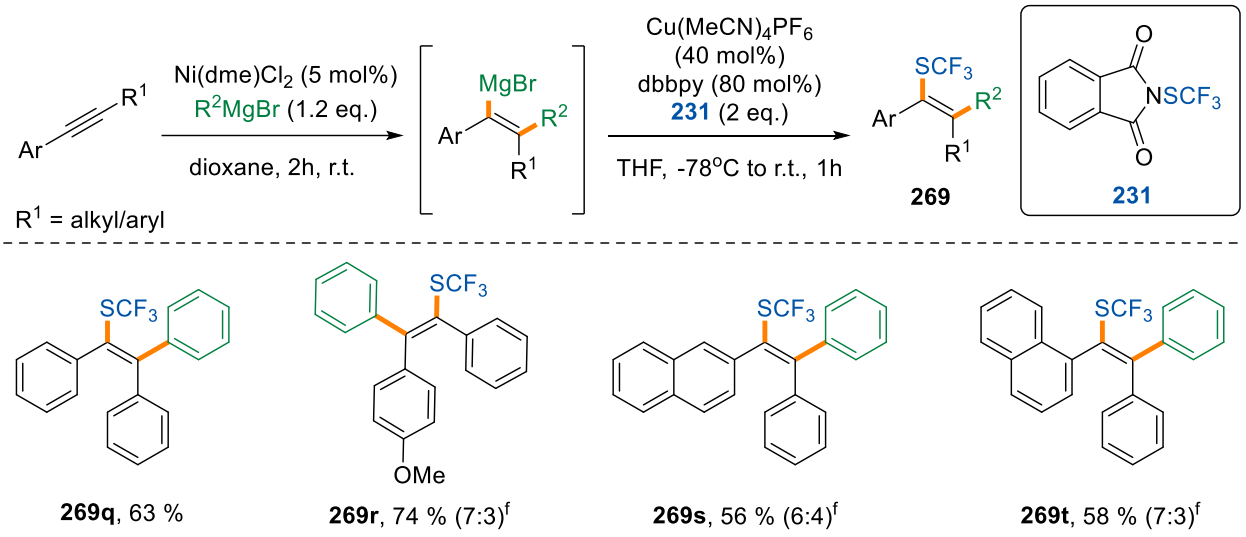

Scheme 3.6: Scope of Diaryl alkynes

Finally, the scope in respect to the Grignard reagent was examined **(Scheme 3.7)**. Both electron-rich and electron-deficient aryl Grignard's were suitable (**269u** vs **269v**), with the former generally providing higher efficiency. While the *p*-tolyl derivative producing the highest yield, the sterically hindered *o*-tolyl and mesityl were also well accommodated, affording products in 50-74% yields. The scope could also be extended to alkenyl Grignards, as demonstrated by the 1-propenyl derivative (**269z**), which afforded the product in a moderate 39% yield with complete regioselectivity. In contrast, alkynyl, alkyl, benzyl, and strongly electron-withdrawing aryl Grignard's proved unsuccessful, primarily due to failure in the carbomagnesiation step **(Scheme 3.8)**.

[g]carbomagnesiation run for 4h, [h]carbomagnesiation at 75°C.

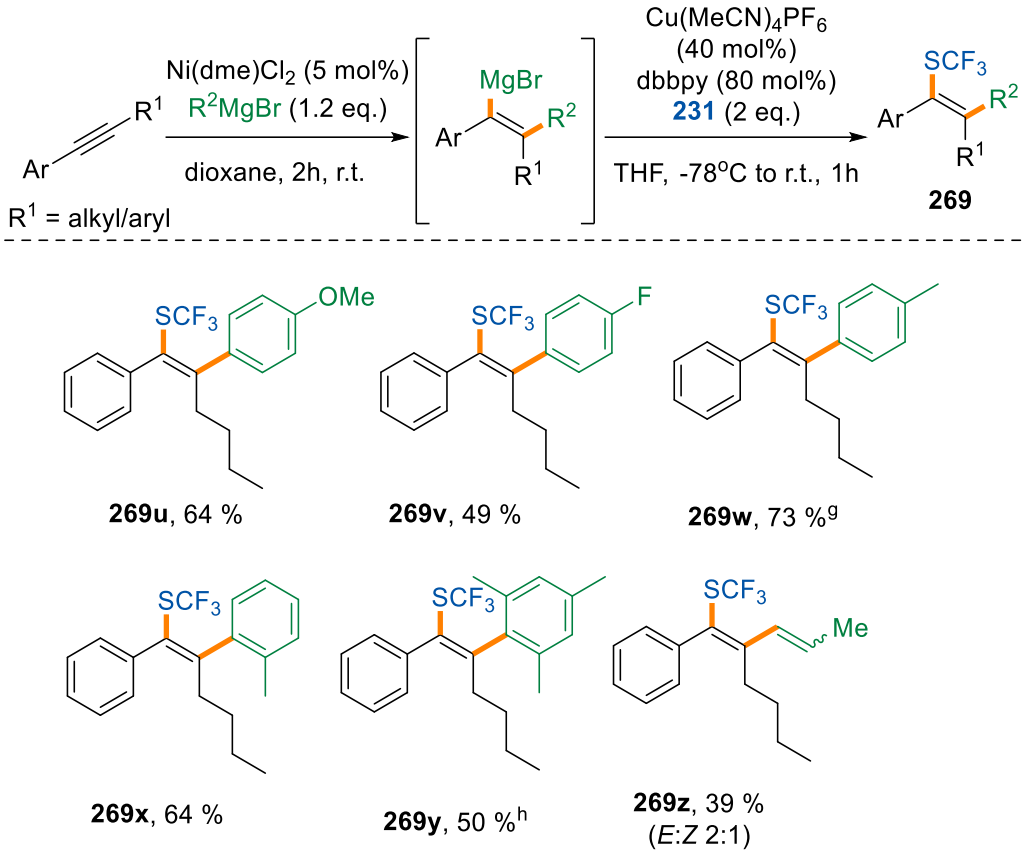

Scheme 3.7: Scope of Grignard reagents

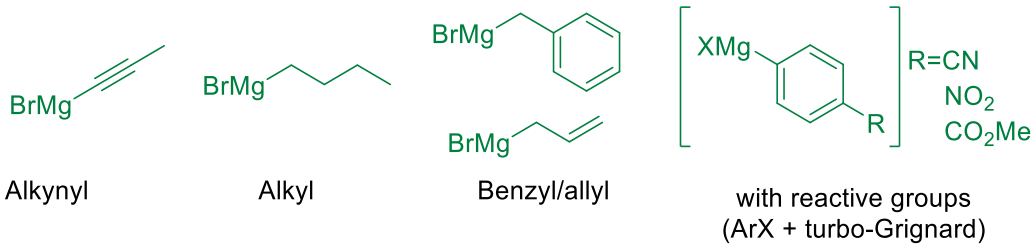

Scheme 3.8: Limitation of the method-Grignard reagents

Challenges associated with purification

In most cases, the isolated products consisted of a mixture of the desired trifluoromethylthiolated compound **269** and olefin **268** resulting from the hydrolysis of vinyl-magnesium intermediate, often displaying identical R_f values on silica gel chromatography (**Figure 3.1A**). Attempts to achieve separation using aluminum oxide (Al_2O_3) and silver nitrate ($AgNO_3$) impregnated silica were unsuccessful. Due to their highly non-polar nature, the mixture was subjected to reversed-phase C18-silica chromatography **(Figure 3.1B)**, which enabled successful separation using a MeOH–H_2O gradient (7:3 to 9:1).

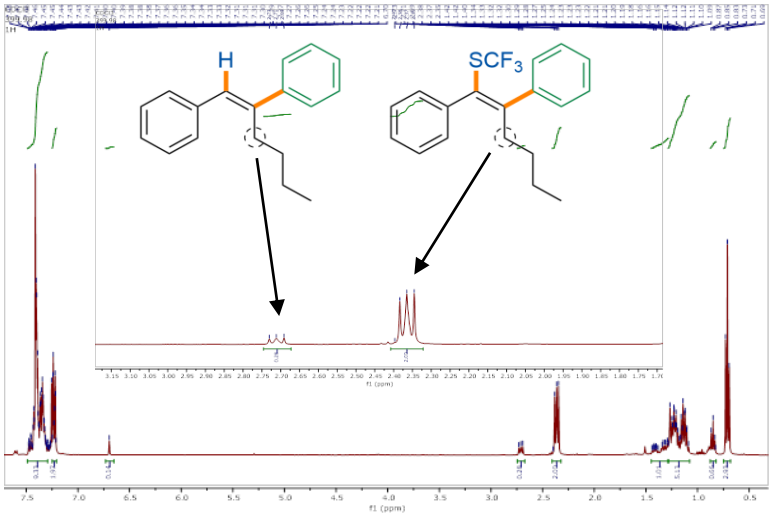

Figure 3.1A: NMR of mixture of product and byproduct
(purified on Normal Phase Chromatography

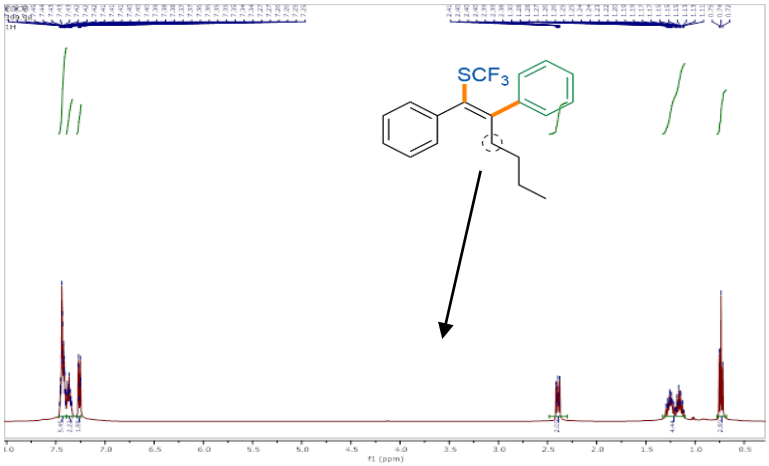

Figure 3.1B: NMR of pure product
(purified on Reverse Phase Chromatography)

3.2.3 Synthetic utility of the trifluoromethylthiolated products

Following a comprehensive evaluation of the scope, the further applicability of the method was subsequently investigated (**Scheme 3.10**). The trifluoromethylthio group in the compound **269a** was transformed into strongly electron-withdrawing functionalities like sulfoxides (**272**) and sulfones (**273**) The configuration of **273** was unambiguously confirmed by X-ray diffraction. In addition, the chloro-substituted derivative (**269e**) underwent an S_N2 reaction with alkynyl tosylamide to deliver a highly substituted skipped enyne (**274**), a valuable intermediate for further transformations. While certain functional groups could not be directly incorporated due to incompatibility with the Grignard conditions, downstream diversification was demonstrated through a successful Suzuki coupling of 4-acetylboronic acid with the aryl triflate (**269k**), affording a ketone-bearing alkenyl–SCF_3 product (**275**) in excellent 90% yield.

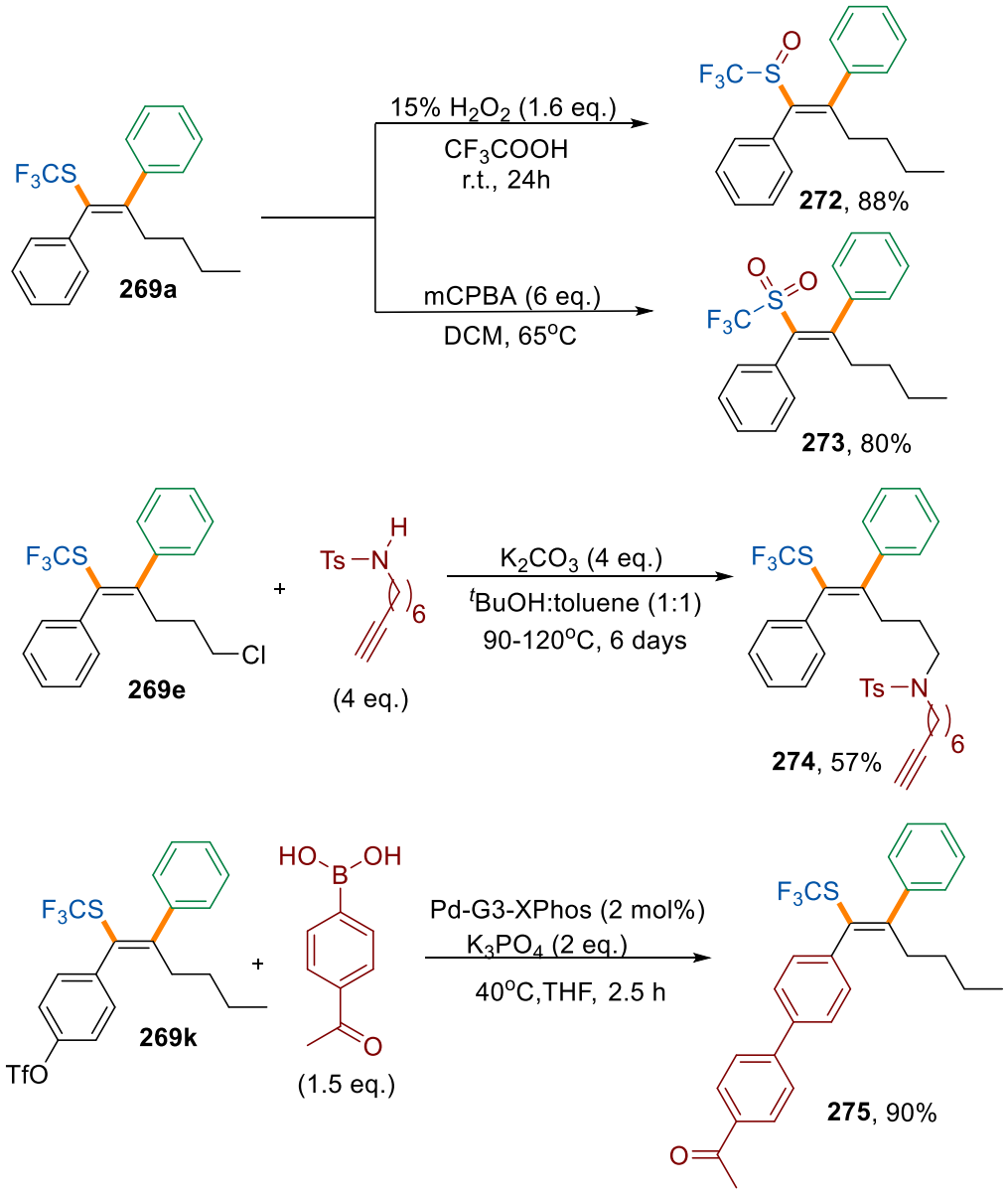

Scheme 3.10: Further transformations of vinyl trifluoromethylthio ethers

Carbotrifluoromethylthiolation using *in situ* generated vinyl magnesium halide complex

The vinyl magnesium bromide complex was prepared *in situ* using the corresponding vinyl bromide and subjected to trifluoromethylthiolation under optimized conditions **(Scheme 3.9)**. This afforded the vinyl trifluoromethylthio ether in 60%, along with 20% of hydrolysis product of vinyl magnesium, as determined by GC analysis, demonstrating that the procedure is operational in a one-pot manner starting from the generation of Grignard.

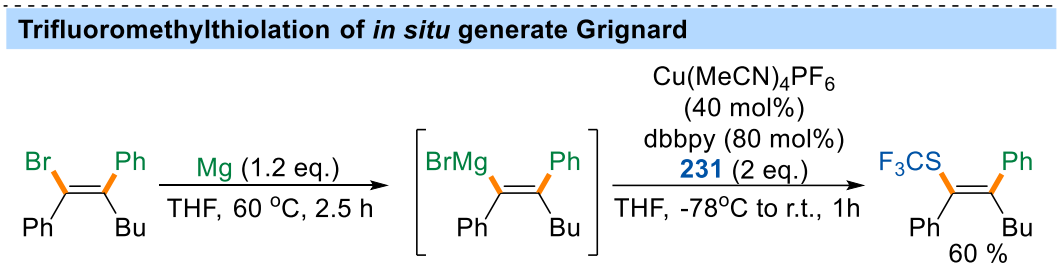

Scheme 3.9: Carbotrifluoromethylthiolation of alkynes using *in situ* generated Grignard

3.2.4 Elucidation of the configuration of compound 269g and 273

To assess the configuration of compound **269g**, a 1D-NOESY experiment was performed by selectively irradiating the aliphatic CH_2 proton at 2.37 ppm. Clear NOE correlations were observed with one pair of aromatic protons located nearest to the double bond in both the phenyl ring (7.34 ppm) and the 4-OMePh ring (7.22 ppm). These spatial interactions **(Figure 3.2)** confirm the *Z*-configuration of the vinyl trifluoromethylthioether.

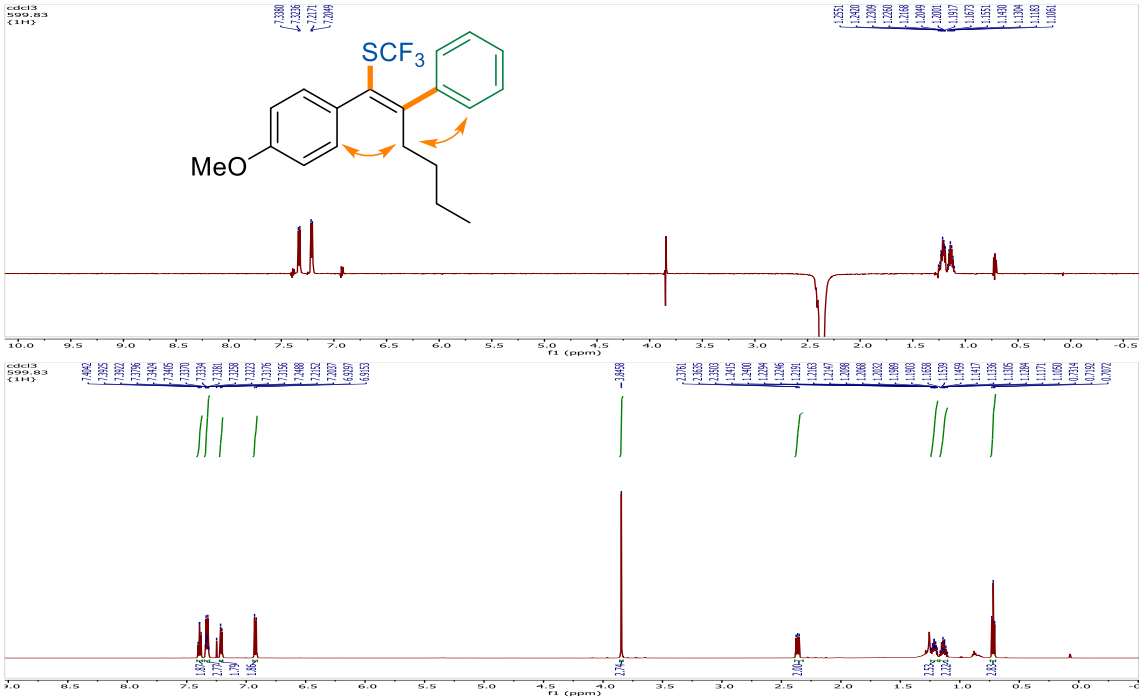

Figure 3.2: Configuration assessment of compound **269g**

Single-crystal X-ray diffraction of the sulfoxide derivative of the product (selected because oxidation does not alter the configuration of the double bond) was carried out. Colorless needle-shaped crystals of compound (**273**) were obtained by recrystallization from diethyl ether. The crystallographic data revealed a tetragonal structure and unambiguously confirmed the *Z*-configuration of the vinyl trifluoromethylthioether.

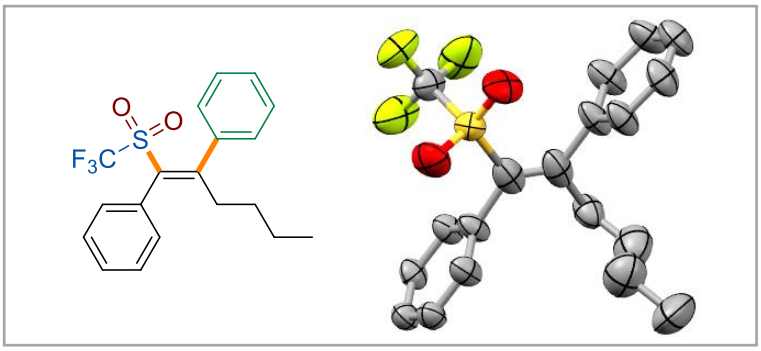

Figure 3.3: X-ray structure of sulfoxide derivative (**273**)

3.2.5 Mechanism

Based on the previous literature[367] our observations and experiments, a reasonable mechanistic pathway is proposed (**Scheme 3.11**). The reaction begins with the reduction of Ni(II) to Ni(0) by the aryl magnesium Grignard reagent. The resulting Ni(0) species coordinates with the alkyne[368–370] and undergoes reaction with the Grignard[371] reagent to form a nickelate complex (**276**). Subsequent aryl insertion into the C–Ni bond affords a *syn*-intermediate (**277**), which upon transmetallation with magnesium furnishes the carbomagnesiation product (**278**).

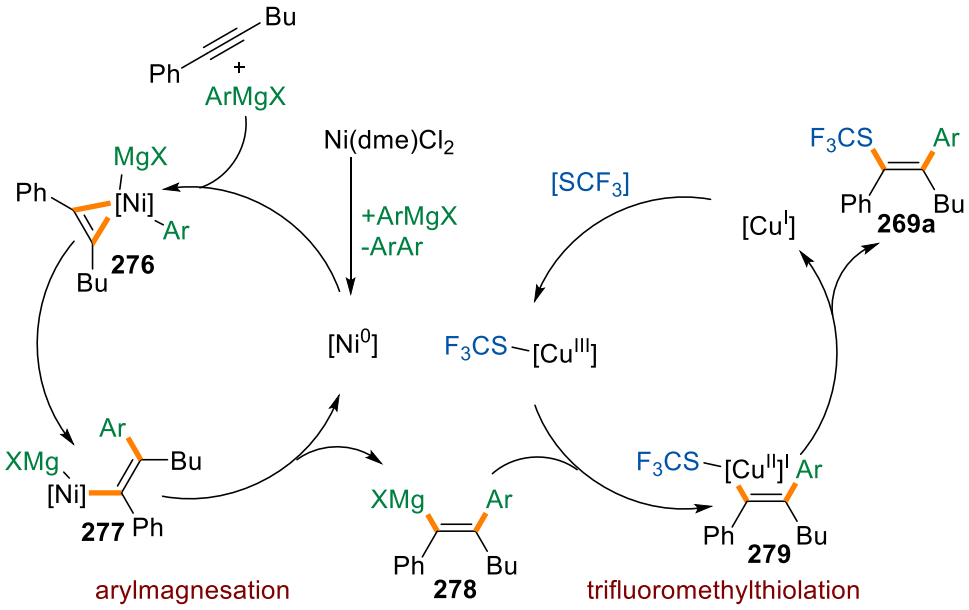

Scheme 3.11: Mechanism of carbotrifluoromethylthiolation of alkynes

In the next stage, Cu(I) activates the electrophilic SCF_3 donor to generate a Cu(III)[372,373] species, which undergoes transmetallation with the vinyl magnesium intermediate to give a vinyl copper species (**279**). Finally, reductive elimination delivers the desired SCF_3 product (**269**) while regenerating the Cu(I) catalyst.

3.2.6 Conclusion

In summary, I have developed an effective one-pot protocol for carbomagnesiation-trifluoromethylthiolation of unactivated internal alkynes. This offers exclusive *syn*-selectivity not realized by the earlier known methods, imparted from the Ni-catalyzed carbomagnesiation (step 1) with trifluoromethylthiolation proceeding with retention of configuration. The SCF_3 group is selectively installed at the α-position making it the first method of α-selective arylation-trifluoromethylthiolation, delivering favourable outcomes with high regio- and stereoselectivity.

After successfully developing the carbotrifluoromethylthiolation protocol, attention was next focused on achieving regio- and stereoselective arylboration of alkynes.

3.3 *syn*-Selective α-Boration-Arylation of Alkynes

3.3.1 Introduction

Trisubstituted alkenyl boronates serve as versatile intermediates, undergoing diverse transformations to furnish tetrasubstituted alkenes. These motifs are highly valued in medicinal chemistry, for instance, they appear in several selective estrogen receptor degraders and also find applications in macrocycles[374] for chemo- and biosensors, liquid crystals,[375] and molecular motors.[376]

This project originated from my initial attempts at carbometallation, followed by transmetallation with zinc or boron reagents and subsequent functionalization using trifluoro- or trifluoromethylthio-based electrophiles. While the former successfully afforded CF_3-containing products as stereoisomeric mixtures, attempts with trifluoromethylthio electrophiles were unsuccessful. Preliminary investigations into the carboboration of sterically hindered vinyl magnesium intermediates (derived from carbomagnesiation of internal alkynes) using alkoxy boronates yielded only trace amounts of carboborated products. In view of these limitations and considering the inherent challenges associated with achieving regio- and stereoselective synthesis of tetrasubstituted alkenes, focus subsequently shifted toward carboboration.

A wide range of mono-borations are known, employing alkenes, allenes, and alkynes as precursors. In the case of alkynes, both *syn*- and *anti*-selective vicinal difunctionalizations have been reported with borylating agents in combination with heteroatom or carbon partners (the latter, extensively discussed in the introduction), enabling access to structurally complex products. Carboboration enables the installation of diverse carbon substituents, including alkyl, fluoroalkyl, alkenyl, alkynyl, allenyl, allyl, acyl, and aryl groups predominantly yielding β-alkenyl boronates. In contrast, α-selective examples remain scarce, with only a handful reported[224,239,241–243] (five in total, including one from our group). Although arylborations[235,377–383] have been described, they

are still underexplored and mainly restricted to Cu- or Pd-catalyzed systems, or Cu/Pd co-catalysis, proceeding via borylcupration or boropalladation pathways. These reactions generally provide β-alkenyl boronates, while *syn*-selective α-boration–arylation remains unknown. Recognizing this gap, we aimed to develop a Ni-catalyzed, regioselective carbomagnesiation followed by regio- and stereo- retentive boration, thereby enabling access to α-selective alkenyl boronates. The obtained products could subsequently be cross coupled with aryl bromides, providing access to tetrasubstituted alkenes.

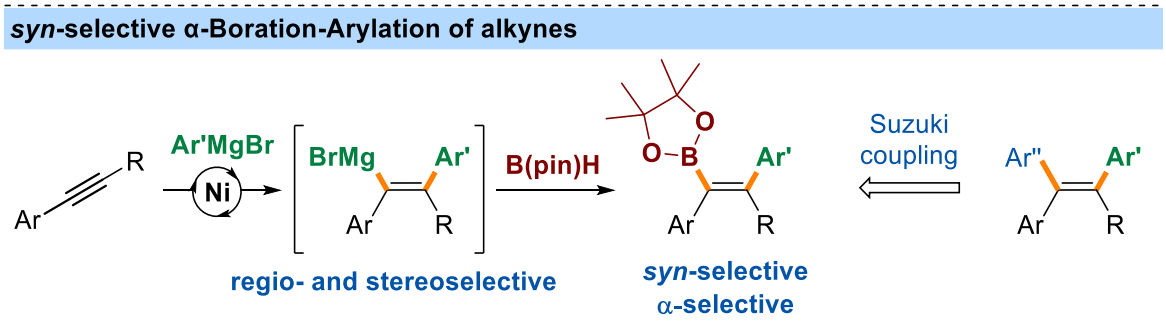

Access to substituted alkenyl boronates by carbomagnesiation strategy

3.3.2 Optimization

A preliminary optimization of the Ni-catalyzed carbomagnesiation of alkynes was carried out. Using $NiCl_2$·dme, mild conditions proved effective without requiring a ligand, affording a 78% yield (**Table 3.18**, entry 4). In contrast, LiCl additives, commonly present in turbo Grignards (used for *in situ* Grignard preparation), completely suppressed reactivity (entry 5). $Ni(acac)_2$ required higher catalyst loading (entry 9 vs 10) or the addition of a ligand and elevated temperature (55 °C) to deliver moderate efficiency (entry 11 and 12). When $NiBr_2$·diglyme was employed, a broad range of ligands, including phenanthroline, bipyridines, and amines, promoted the reaction effectively at room temperature, with PMDTA providing the highest yield (entry 18).

Table 3.18 Optimization for Ni-catalyzed carbomagnesiation of alkynes.

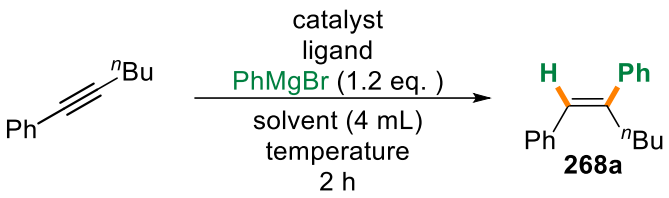

Entry	Catalyst (mol %)	Ligand (mol %)	Solvent	Temperature (°C)	Yield[a] (%)
1	$NiCl_2$·dme (5)	-	toluene	rt	(56)
2	$NiCl_2$·dme (5)	-	toluene	55	(60)
3	$NiCl_2$·dme (5)	-	hexane	rt	(50)
4	**$NiCl_2$·dme (5)**	-	**dioxane**	**rt**	**78**
5	$NiCl_2$·dme (5)	LiCl (120)	toluene	rt	traces
6	$NiCl_2$·dme (5)	TMEDA	toluene	55	(53)
7	$NiCl_2$·dme (5)	bipy (5)	toluene	55	(78)
8	$NiCl_2$·dme (5)	1,5-COD (10)	toluene	55	(60)
9	$Ni(acac)_2$ (5)	-	toluene	50	(49)
10	$Ni(acac)_2$ (10)	-	toluene	50	(66)
11	$Ni(acac)_2$ (5)	TMEDA (5)	toluene	50	(59)
12	$Ni(acac)_2$ (5)	1,5-COD (5)	toluene	50	(54)
13	$NiBr_2$·dig (5)	TMEDA (5)	toluene	rt	78
14	$NiBr_2$·dig (5)	TMEDA (5)	toluene	55	78
15	$NiBr_2$·dig (5)	TMEDA (10)	toluene	rt	76
16	$NiBr_2$·dig (5)	bipy (5)	toluene	rt	87
17	$NiBr_2$·dig (5)	bipy (10)	toluene	rt	75
18	**$NiBr_2$·dig (5)**	**PMDTA (5)**	**toluene**	**rt**	**88**
19	$NiBr_2$·dig (5)	phen (5)	toluene	rt	76
20	$NiBr_2$·dig (5)	dmbipy (5)	toluene	rt	71
21	$NiBr_2$·dig (5)	biquinoline (5)	toluene	rt	79

[a]Isolated yields, values in parentheses correspond to yields given by GC analysis.

Optimization for the one-pot protocol of carboboration

The optimization study, carried out jointly with Maciej Dajek, commenced with the evaluation of different borylating agents using the ligand free conditions of step 1 (**Table 3.19**). Pinacol borane proved to be the most effective, promoting the reaction with moderate reactivity, whereas trimethoxyborane and isopropoxy–bispinacolato borane afforded only negligible product formation (entry 3 vs 1 and 2). The diminished reactivity of the latter two reagents is likely due to unfavorable sterics around the boron center.

Table 3.19 Effect of borylating reagent[a]

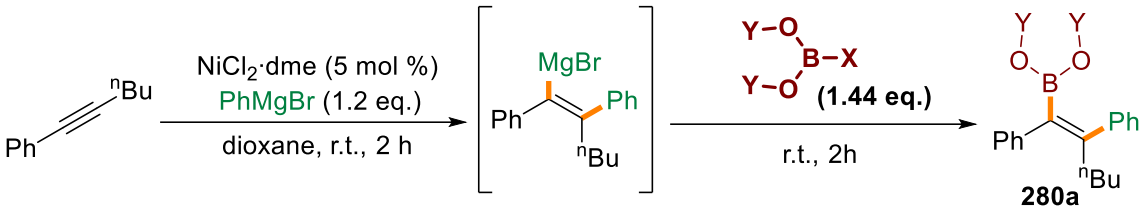

Entry	Borylating reagent (1.44 equiv.)	Yield of 280a (%)
1	$(OCH_3)_3B$	-
2	$(O^iPr)Bpin$	*traces*
3	**HBpin**	**53**

[a]Conditions: $NiCl_2$·dme (5 mol%), 1-phenyl-1-hexyne (0.5 mmol, 1 eq.), PhMgBr (1.2 eq.), dioxane (2 mL), 2 h, r.t. then borylating reagent (1.44 eq.), 2 h, r.t., isolated yields.

To improve the yield, the conditions were further evaluated using $NiBr_2$·dig as the nickel catalyst in both presence and absence of ligands **(Table 3.20)**. This system proved more effective than $NiCl_2$·dme and delivered nearly comparable performance regardless of whether a ligand was employed (entry 1 vs 5).

Table 3.20 Effect of ligand with $NiBr_2$·dig catalyst[a]

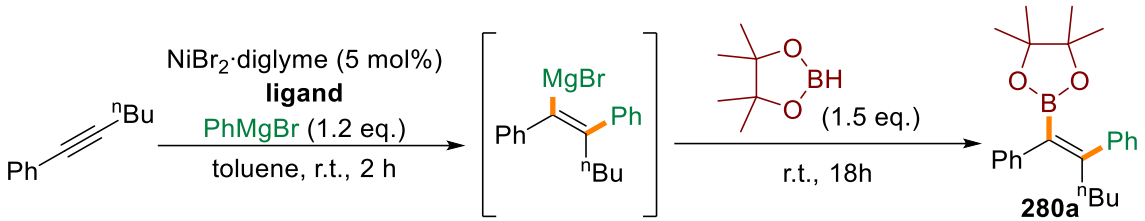

Entry	Ligand (mol%)	Yield of 280a (%)
1	-	61
2[b]	-	52
3	Bipy (5)	58
4	TMEDA (5)	56
5	**PMDTA (5)**	**63**

[a]Conditions: $NiBr_2$·diglyme (5 mol%), 1-phenyl-1-hexyne (0.5 mmol, 1 eq.), PhMgBr (1.2 eq.), toluene (2 mL), 2 h, r.t., then pinacolborane (1.5 eq.), 18 h, r.t., isolated yields, [b] $NiCl_2$·dme (5 mol%) as catalyst.

Taking forward the conditions with PMDTA ligand as they were slightly better, the equivalents of pinacol borane were assessed **(Table 3.21)**. Increase in the equivalents from 1.5 to 3 resulted in a corresponding improvement in yield (entries 1-3), however, the outcome plateaued after 3 equivalents, which proved to be the most proficient among the rest (entry 3).

Table 3.21 Effect of equivalents of pinacolborane[a]

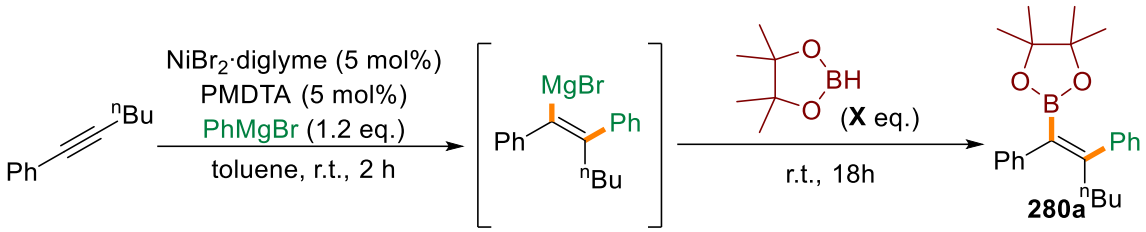

Entry	Pinacolborane (equiv.)	Yield of 280a (%)
1	1.5	63
2	2.0	67
3	**3.0**	**74**
4	3.0	72[b]
5	4.0	73

[a]Conditions: $NiBr_2$·diglyme (5 mol%), PMDTA (5 mol%), 1-phenyl-1-hexyne (0.5 mmol, 1 eq.), PhMgBr (1.2 eq.), toluene (2 mL), 2 h, r.t. then pinacolborane (1.5 eq.), 18 h, r.t., isolated yields; [b]Experiment run for 2 hours at borylating step.

Since carbomagnesiation performed better in non-polar and moderately polar solvents, solvent screening for the one-pot protocol was limited to this category **(Table 3.22)**. Dioxane led to reduced productivity when progressing from step 1 to step 2 (entry 3), whereas use of toluene improved the overall performance (entry 1). Accordingly, toluene was selected for the subsequent trials.

Table 3.22 Effect of solvent[a]

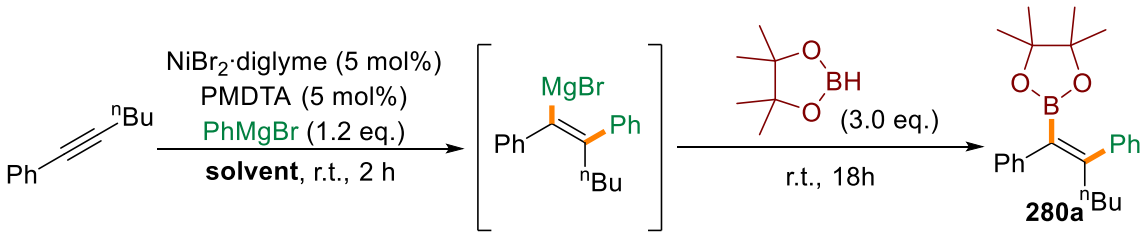

Entry	Solvent	Yield of 280a (%)
1	**toluene**	**74**
2	tetrahydrofuran	32
3	1,4-dioxane	42

[a]Conditions: $NiBr_2$·diglyme (5 mol%), PMDTA (5 mol%), 1-phenyl-1-hexyne (0.5 mmol, 1 eq.), PhMgBr (1.2 eq.), toluene (2 mL), 2 h, r.t. then pinacolborane (1.5 eq.), 18 h, r.t., isolated yields; [b]Experiments run for 2 hours at borylating step.

With the optimal catalyst, ligand, solvent, and borylating agent established, the effect of the borylating agent addition temperature was investigated **(Table 3.23)**. Raising the temperature from ambient to 60 °C decreased the reaction outcome (entry 1 vs 2), whereas lowering it to 0 °C or –20 °C marginally improved the yield, indicating a mild positive effect on the reaction efficiency (entry 3, 4 vs 1).

Table 3.23 Effect of temperature[a]

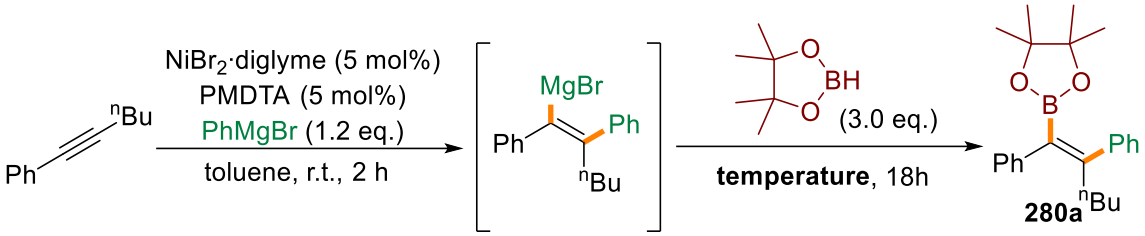

Entry	Temperature (°C)	Yield of 280a (%)
1	r.t.	74
2	60	67
3	**0**	**76**
4	-20	75

[a]Conditions: $NiBr_2$·diglyme (5 mol%), PMDTA (5 mol%), 1-phenyl-1-hexyne (0.5 mmol, 1 eq.), PhMgBr (1.2 eq.), toluene (2 mL), 2 h, r.t. then pinacolborane (1.5 eq.), 18 h, r.t., isolated yields; [b]Experiments run for 2 hours at borylating step.

Following the addition of the borylating agent, the reaction mixture became viscous and could not be stirred effectively, prompting an evaluation of the solvent volume **(Table 3.24)**. Increasing the volume from 2 to 8 mL resulted in a bell-shaped trend in the yield (entries 1-4), reaching a maximum at 4 mL. Stirring efficiency also improved noticeably at this volume.

Table 3.24 Effect of solvent volume.[a]

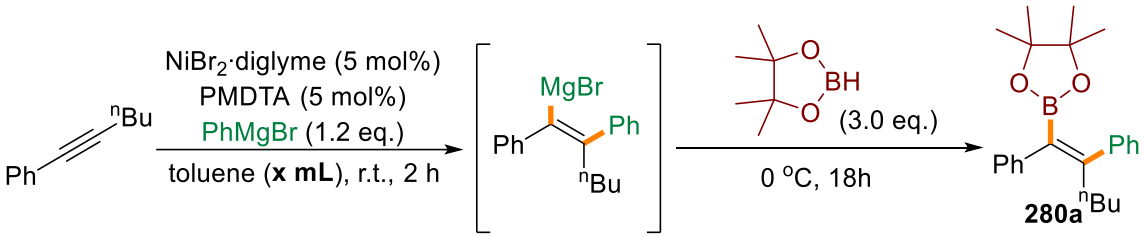

Entry	Volume of toluene (mL)	Yield of 280a (%)
1	2	76
2	**4**	**82**
3	6	77
4	8	79

[a]Conditions: $NiBr_2$.diglyme (5 mol%), PMDTA (5 mol%), 1-phenyl-1-hexyne (0.5 mmol, 1 eq.), PhMgBr (1.2 eq.), toluene, 2 h, r.t. then pinacolborane (3 eq.), 0 °C to 2-8 °C, 18 h, isolated yields.

Finally, the effect of reaction time after the addition of the borylating agent was examined **(Table 3.25)**. Stirring the reaction overnight (18h) produced slightly better yield compared to terminating it after 3 hours (entry 1 vs 2).

Table 3.25 Effect of time.[a]

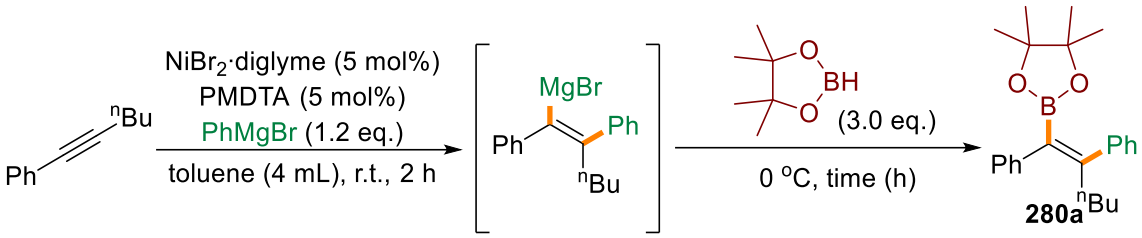

Entry	Time of boration (y h)	Yield of 280a (%)
1	3	76
2	**18**	**82**

[a]Conditions: $NiBr_2$.diglyme (5 mol%), phenyl hexyne (0.5 mmol, 1 eq.), PhMgBr (1.2 eq.), toluene (4 mL), 2 h, r.t. then pinacol borane (3 eq.), 0 °C to 2-8 °C, y h, Isolated yield.

3.3.3 Scope of Carboboration of alkynes

With all the parameters optimized, I systematically evaluated the substrate scope. The protocol displayed broad tolerance toward substitutions on both the alkyl and aryl units of the alkyne **(Scheme 3.12A and 3.12B)**. A clear trend was observed in the alkyl series: increasing chain length from methyl to butyl led to a proportional improvement in yield (68-82%), with benzyl substituents performing comparably to butyl (83% vs 82%) respectively. Cyclopropyl (**280d**) and isopropyl groups (**280e**) were also accepted, affording products in moderate 52-59% yields. Functionalized alkyl substituents bearing chloro groups (**280f**) or TMS-protected alcohols (**280g**) were successfully incorporated; in the latter case, deprotection occurred *in situ* during acidic workup to afford the corresponding free alcohol in excellent yield (92%). In contrast, sterically encumbered partners such as *tert*-butyl, trimethylsilyl, dialkyl alkynes and ester-substituted alkyne proved unreactive due to poor carbomagnesiation **(Scheme 3.14).**

On the aryl side, *para*-substituted phenyl rings bearing methoxy (**280i**) or fluoro (**280k**) groups furnished high yields, while the trifluoromethyl-substituted analogue failed to undergo carbomagnesiation. Beyond phenyl derivatives, 1-naphthyl-substituted alkynes (**280j**) provided the desired product in 73% yield. Phenyl rings bearing coupling handles such as bromo (**280l**), triflate (**280m**), and tosylate (**280n**) groups were also compatible, although the latter two provided comparatively lower yields (32-36%). In the case of the bromo derivative, minor amounts of stereoisomeric and debrominated byproducts were formed; nevertheless, these closely related compounds were successfully separated by flash chromatography and fully characterized by NMR. The additional side products, however, contributed to a reduced yield of the desired product. In the case of tosylates and triflates, increasing reaction temperature or time did not improve the outcome; notably, multiple TLC spots in the non-polar region suggested competing side processes, for triflates. Substrate bearing protected aldehyde (**280o**, as methyl acetal) were accommodated with moderate 50% yield. Heteroaryl systems such as thienyl (**280q**), indole (**280r**), and benzodioxole (**280p**) derivatives afforded modest results (54-62%), whereas quinoline substrates showed no reactivity. Conjugated enynes (e.g., hexynyl-cyclohexene) underwent carboboration, but the resulting products could not be separated cleanly from aliphatic impurities **(Scheme 3.15)**. The method could also be extended to diphenylacetylene, which afforded the desired alkenyl

boronate in appreciable 79% yield. Unsymmetrical diaryl alkynes containing electron rich and moderately deficient groups (-OMe and -F) also worked well, affording 66-73% yields. In these cases, the major regioisomer originated from aryl addition on the substituted aryl side, (confirmed by the NMR of the carbomagnesiated products i.e. the outcome of the first step) giving a regioselectivity ratio of 7:3.

[a]Reaction Conditions: $NiBr_2$·diglyme (5 mol%), PMDTA (5 mol%), alkyne (0.5 mmol, 1 eq.), Grignard reagent (1.2 eq.), toluene (4 mL), 2 h, r.t., then pinacol borane (3 eq.), 0 to 2-8 °C, 18 h, isolated yield.

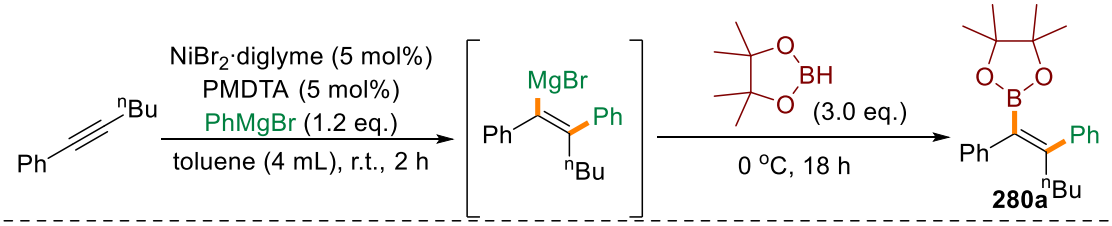

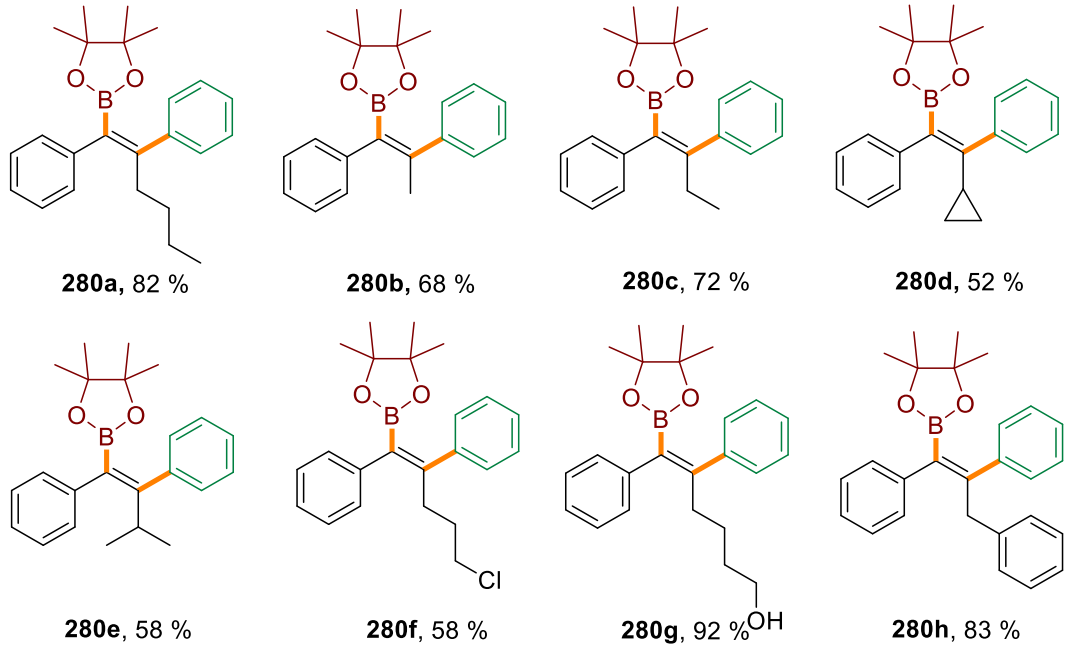

Scheme 3.12A: Scope of the alkyl counterparts (in Aryl-Alkyl alkynes)

In case of unsymmetrical diaryl regioisomers were obtained, [b]regioselectivity ratio: ~7:3, major regioisomers drawn

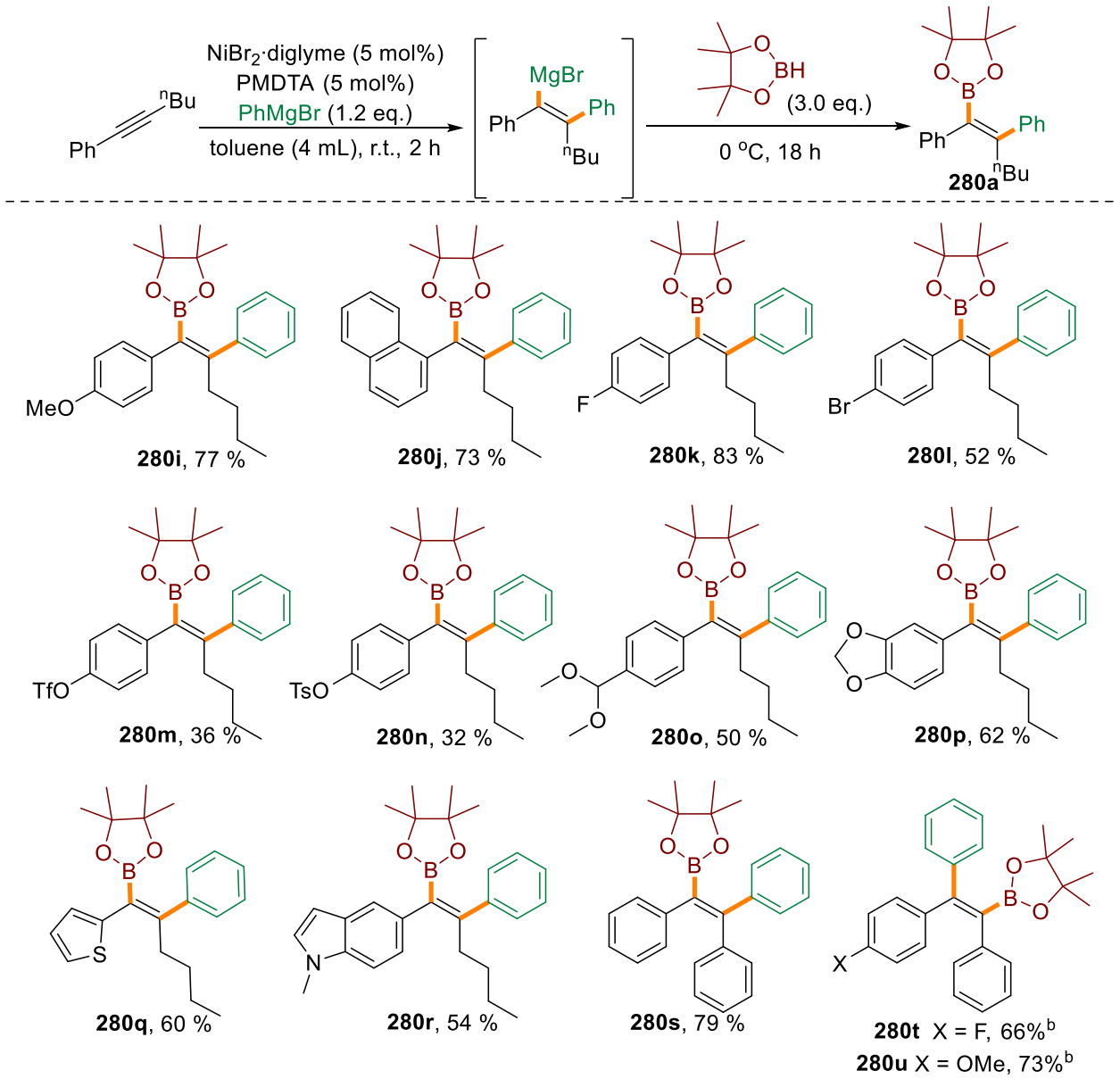

Scheme 3.12B: Scope of the aryl counterparts (in Aryl-Alkyl alkynes & Diaryl alkynes)

After testing the alkynes, the scope was expanded to various Grignard reagents **(Scheme 3.13).** Electron-rich aryl Grignard gave superior outcomes compared to moderately electron-poor analogue (**280v** vs **280w**), for which other optimization attempts did not improve yields. Both *para*- and *ortho*-tolyl Grignard's participated effectively, while the sterically congested mesityl reagent delivered the product in respectable 75% yield. Biphenyl Grignard was also well accommodated, resulting in 69% yield. Furthermore, alkenyl Grignard such as 1-propenyl underwent regioselective carboboration to provide separable *E* and *Z* isomers. However,

purification of the major *E* isomer was hampered by co-elution with aliphatic impurities **(Scheme 3.15)**.

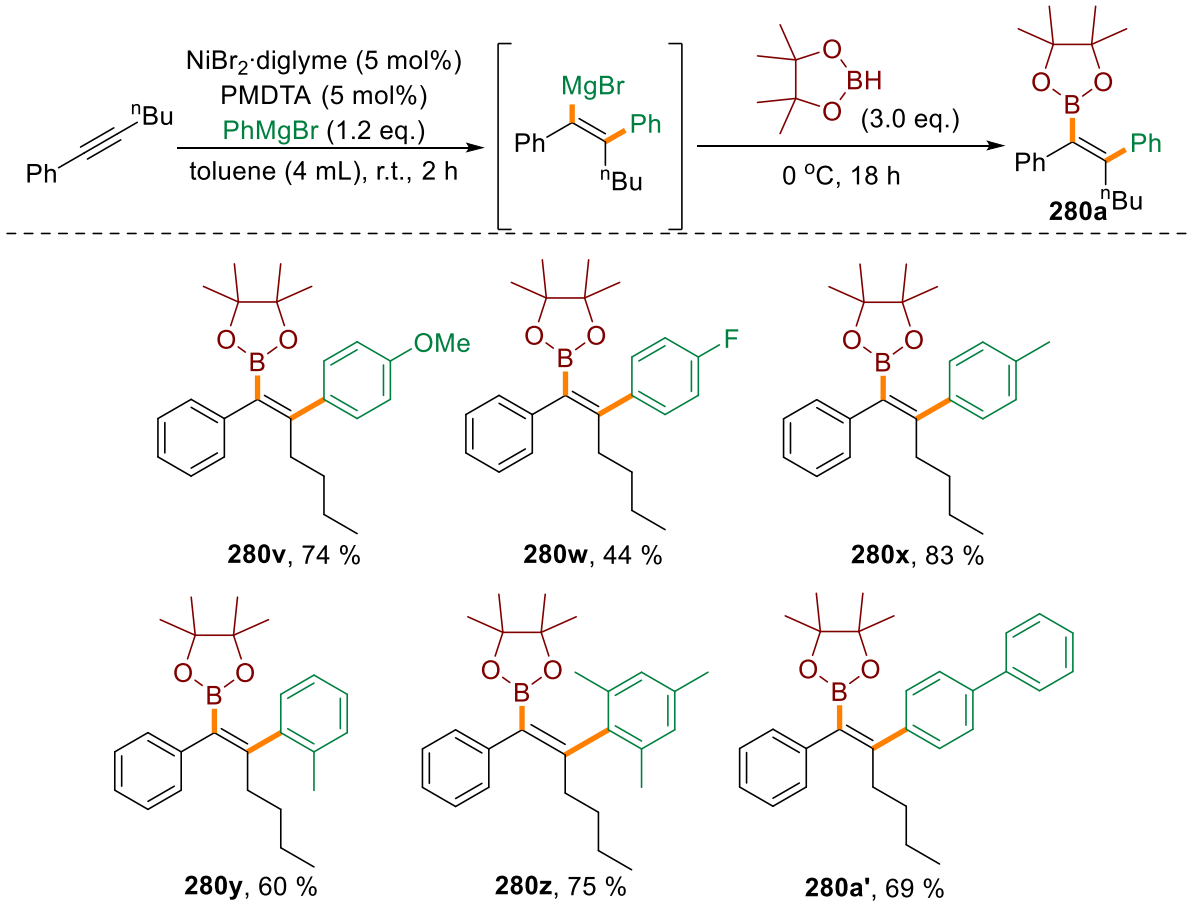

Scheme 3.13: Scope of Grignard reagent

Effects of different borylating agents like neopentyl and catechol borane were also investigated. However, neither of these reagents furnished the desired products, likely due to insufficient stability or reactivity under the reaction conditions. Additional attempts involving pinacol quenching at the end of the reaction to generate a more stable boronate also proved unsuccessful.

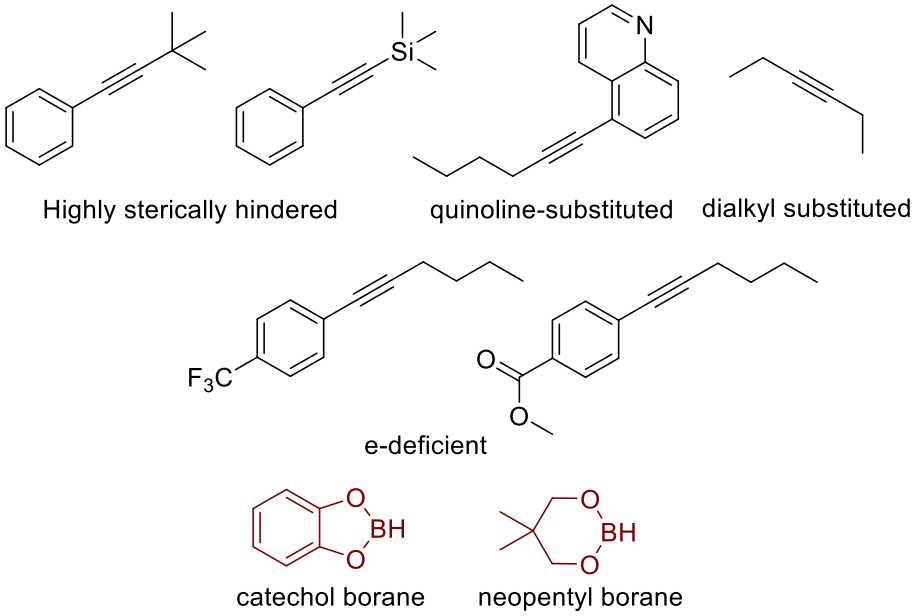

Scheme 3.14: Limitation of the method- alkynes and borylating agents

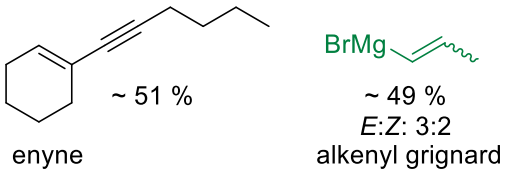

Scheme 3.15: Substrates with Isolation Difficulties

3.3.4 Access to tetratsubstituted alkenes

The trisubstituted alkenyl boronates obtained through this methodology proved to be highly functional intermediates, as they could be directly engaged in Suzuki–Miyaura cross-coupling with diverse (hetero)aryl bromides to deliver tetrasubstituted alkenes (**281a-e**) with precise stereocontrol **(Scheme 3.16)**. Pyridyl systems (**281d**), which often give complex mixtures during carbomagnesiation, successfully furnished the corresponding heteroarylated alkenes in synthetically useful yields. Likewise, acetyl-containing derivatives **281b** and **281c**, commonly incompatible with Grignard reagents were efficiently converted (40-71%). Notably, the Suzuki coupling of aryl bromide (**282**) with alkenyl boronate (**280c**) enabled a concise two-step synthesis of Tamoxifen (**281e**),[384] a clinically important breast cancer drug. This demonstrates the broad applicability and synthetic value of the developed methodology.

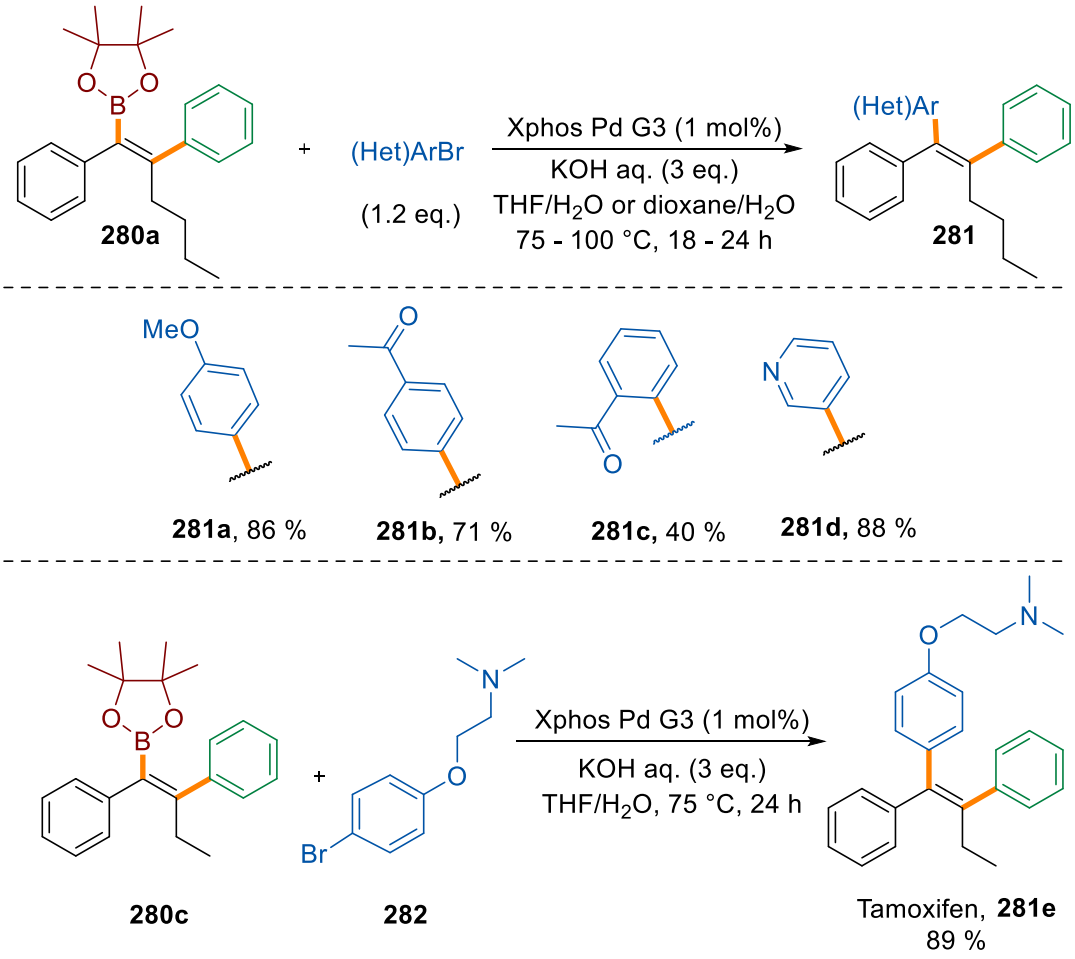

Scheme 3.16: Suzuki cross-coupling with (hetero)aryl bromides

3.3.5 Further functionalization

The versatility of vinyl boronates was further exemplified through a series of other transformations **(Scheme 3.17)**. The alkenyl boronate was readily converted into its trifluoroboronate salt (**283**), a stable compound that is particularly advantageous for reactions in aqueous media. Oxidation afforded the corresponding ketone **284** in a notable yield. A chloro substituted boronate (**280f**) underwent a clean and near quantitative conversion to an azide (**285**) which served as an intermediate for subsequent transformations. The azide was subjected to a Staudinger reduction, which proceeded quantitatively as confirmed by crude NMR. However, isolation of the free amine proved challenging, and attempts to derivatize it via Boc-protection afforded only trace amounts of the protected product. In contrast, the azide readily engaged in a Cu-catalyzed cycloaddition with phenylacetylene, delivering the corresponding triazole (**286**) in quantitative yield. Appreciably, both the formation of azides and triazoles could be achieved without chromatographic purification, highlighting the operational simplicity and practical significance of the method.

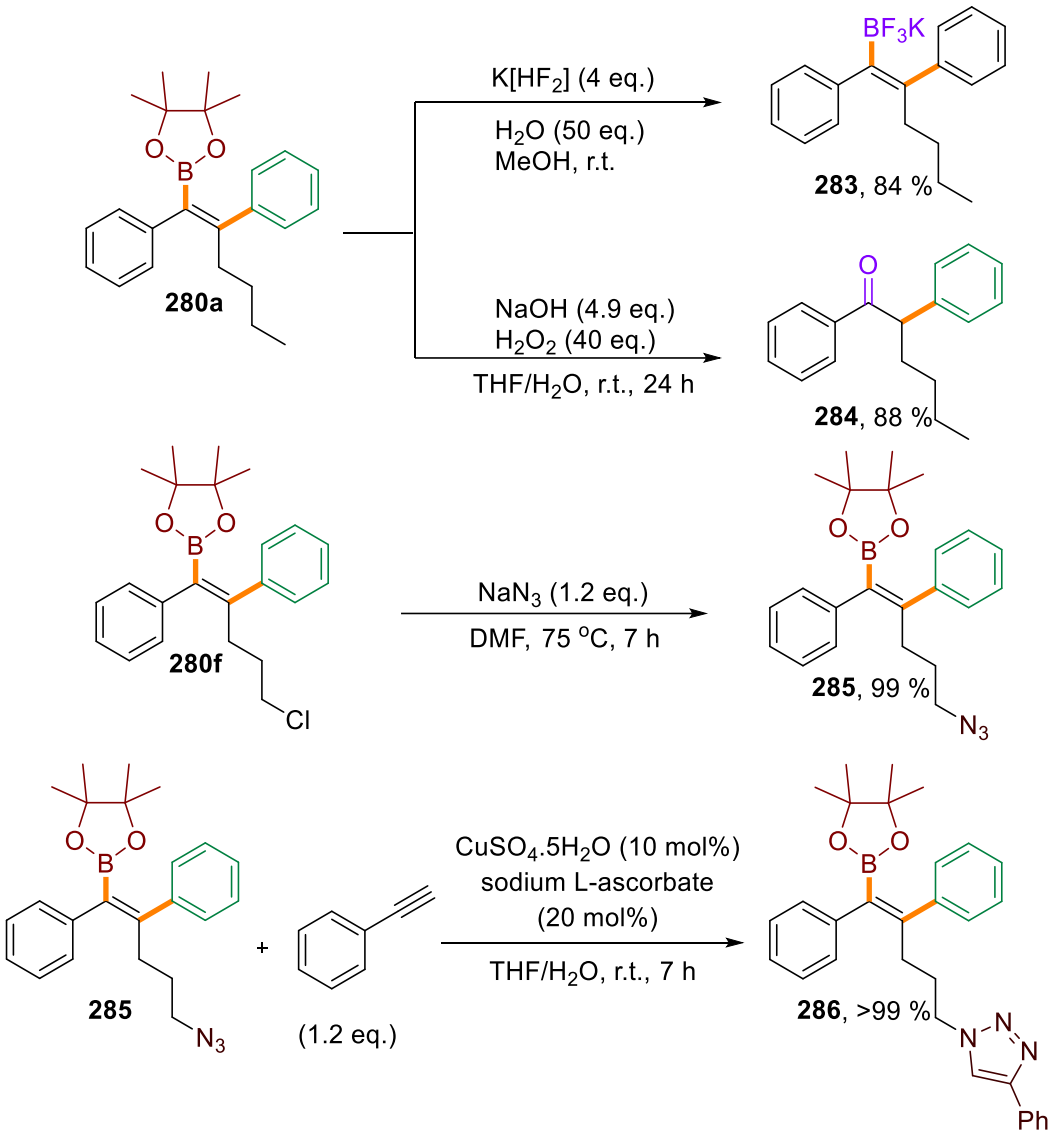

Scheme 3.17: Post-functionalizations of alkenyl boronates

3.3.6 Elucidation of the configuration of compound 280l

To confirm the configuration, 1D NOESY of compound **280l** was performed **(Figure 3.4)** by irradiating the allylic CH_2 proton at 2.34-2.37 ppm which showed space interactions with one pair of aromatic protons present near the double bond in both phenyl ring (7.31 ppm) and 4-BrPh ring (7.10 ppm), thereby confirming the *E*-configuration of the alkenyl boronate.

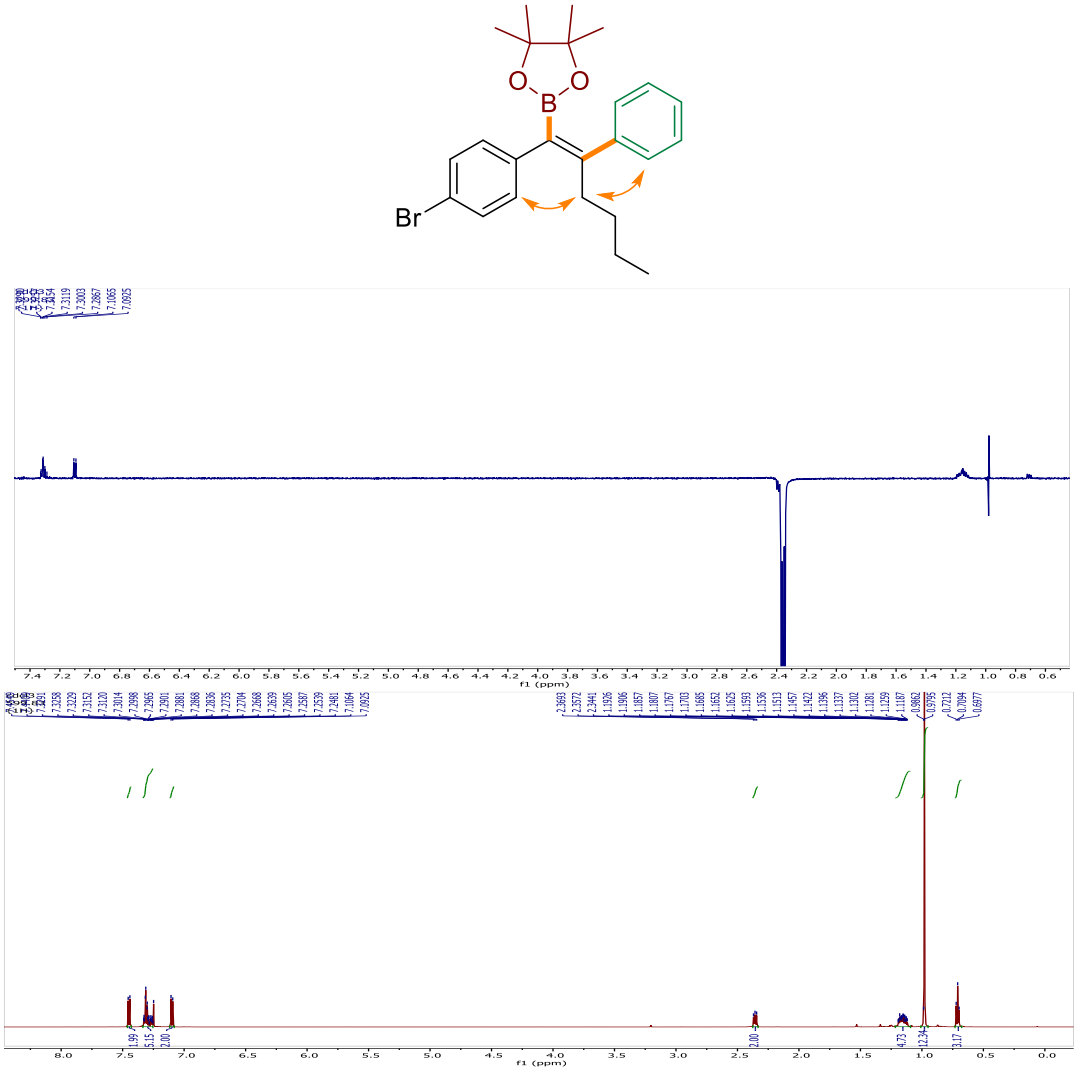

Figure 3.4: Configuration assessment of compound **280l**

I also obtained the single colourless irregular shaped crystals of the compound **280l** by recrystallizing it in MeOH. The crystallographic study revealed a monoclinic structure and unambiguously confirmed the *E*-configuration of the alkenyl boronate.

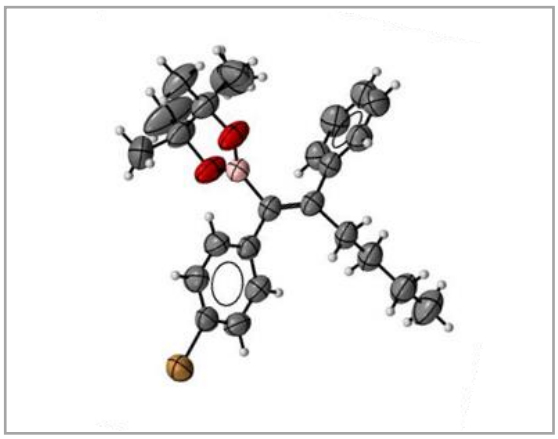

Figure 3.5: X-ray structure of the bromo derivative (**280l**)

3.3.7 Mechanism

The proposed mechanism for the carbomagnesiation step is consistent with both our earlier findings[385] and the precedents reported in the literature.[367–371] The catalytic cycle shown in **(Scheme 3.18)** is initiated by reduction of the nickel precursor, followed by the formation of a nickelate complex (**276**). Subsequent aryl insertion (**277**) and transmetallation from Ni to Mg (**278**) generates the vinyl magnesium intermediate, which represents the product of the carbomagnesiation step.

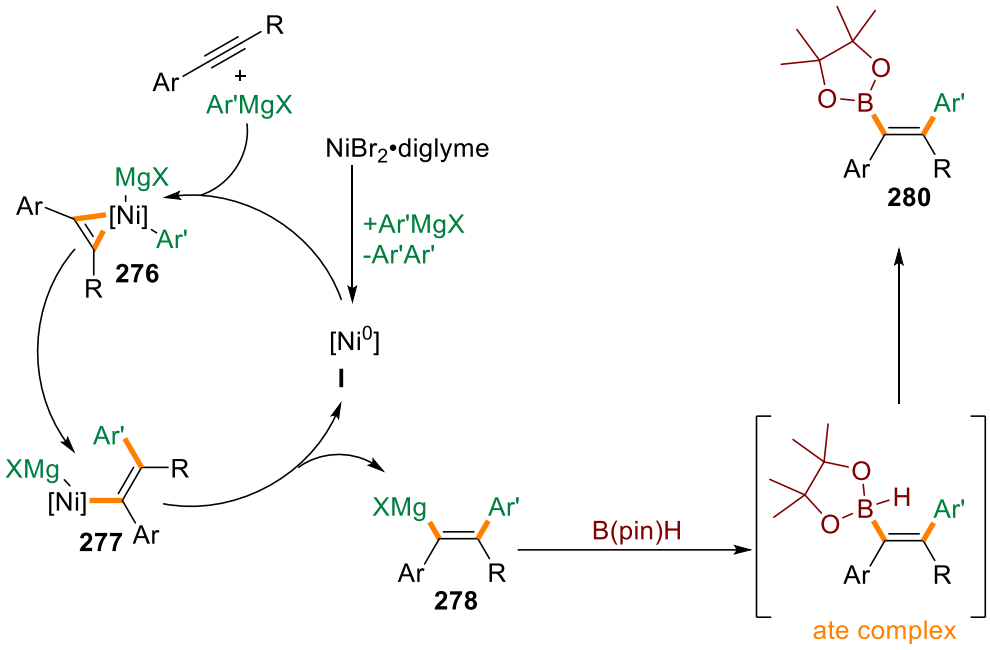

Scheme 3.18: Mechanism of carboboration of alkynes

This intermediate then reacts with the borylating agent to form an ate complex, which ultimately liberates the carboboration product (**280**). Furthermore, DFT studies provided additional support for the proposed borylation step, in particular about the lower reactivity with BpinOR.

Carboboration using *in situ* generated vinyl magnesium halide complex

The vinyl magnesium bromide complex was prepared *in situ* using the corresponding vinyl bromide and subjected to boration under optimized conditions **(Scheme 3.19)**. This afforded the vinyl boronate in 43%, along with 43% of hydrolysis product of vinyl magnesium, as determined by the isolated yields, demonstrating that the procedure is operational in a one-pot manner starting from the generation of Grignard. Additionally, the hydrolysis product of vinyl magnesium is an indication that the vinyl magnesium bromide was formed *in situ.*

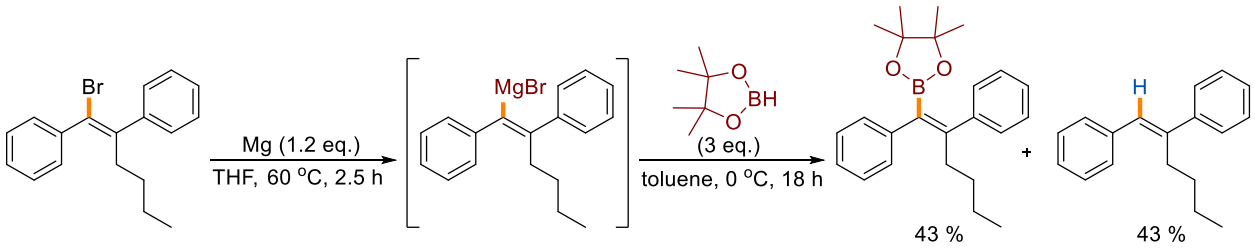

Scheme 3.19: Carboboration of alkynes using *in situ* generated Grignard

DFT studies of the Formation of ate complexes from vinylmagnesium bromides and pinacol-boron compounds

DFT calculations for the borylation step of the reaction were carried out by my supervisor, and we participated in analyzing the results. The Gibbs free energy of activation for the reaction of vinyl magnesium bromide (generated from 1-phenylpropyne as the model substrate) with B(pin)OMe was calculated to be 114.6 kJ/mol, indicating that the reaction is difficult under room temperature conditions. In contrast, the reaction with β-styryl magnesium bromide exhibited a much lower energy barrier of 67.1 kJ/mol **(Scheme 3.20)**. We hypothesized that reducing steric interactions around boron could allow the formation of an ate-complex, thereby enabling product formation. Indeed, the $\Delta G^{\ddagger}$ value for the reaction of **278** with B(pin)H was 95.4 kJ/mol, suggesting a feasible pathway. Experimental trials with different borylating agents further validated these theoretical predictions, with pinacol borane successfully yielding the desired carboborylated product.

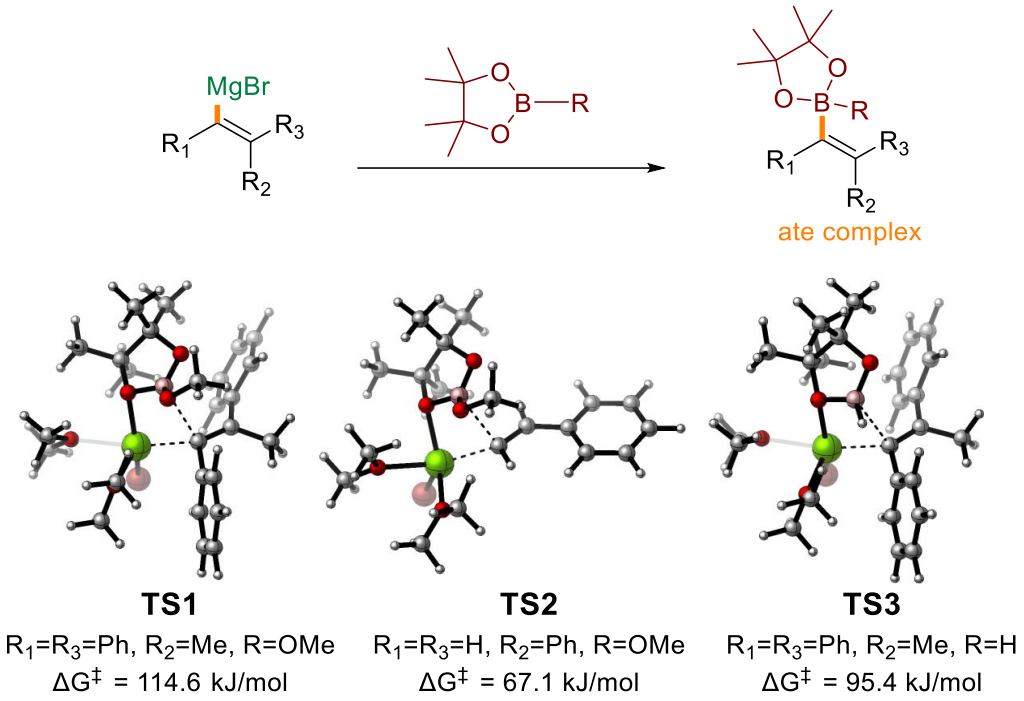

Scheme 3.20: DFT calculations supporting the formation of ate-complex

3.3.8 Competition experiments

Competition experiments were carried out to compare the relative reactivity of electron-neutral and electron-rich alkynes using PhMgBr as the limiting reagent in the carbomagnesiation step **(Scheme 3.21)**. A higher proportion of the hydrolyzed vinyl magnesium intermediate was obtained from 1-phenylhexyne compared to its methoxy-substituted derivative (**287** vs **288**), suggesting that 1-phenylhexyne undergoes carbomagnesiation more rapidly, presumably due to a more favorable interaction with the Ni catalyst. Overall, the product yields were low, which can be attributed to initial interactions between Ni(II) and PhMgBr leading to homocoupling byproducts, as confirmed by ^{1}H NMR analysis. Yields were quantified using CH_2Br_2 as an internal standard.

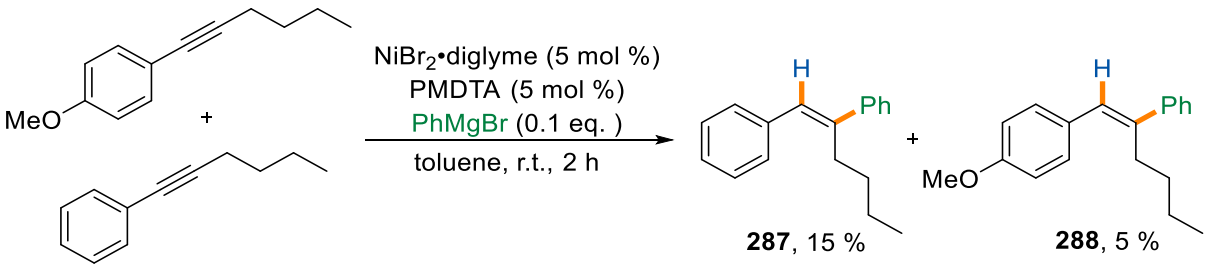

Scheme 3.21: To test relative rate of reactivity between alkynes

Next, 1-phenylhexyne was treated with excess electron-neutral and electron-rich Grignard reagents to compare their relative reactivity (**Scheme 3.22)**. The resulting carbomagnesiation products were obtained in comparable yields (**289** and **290**), indicating nearly identical reactivity of both Grignard reagents.

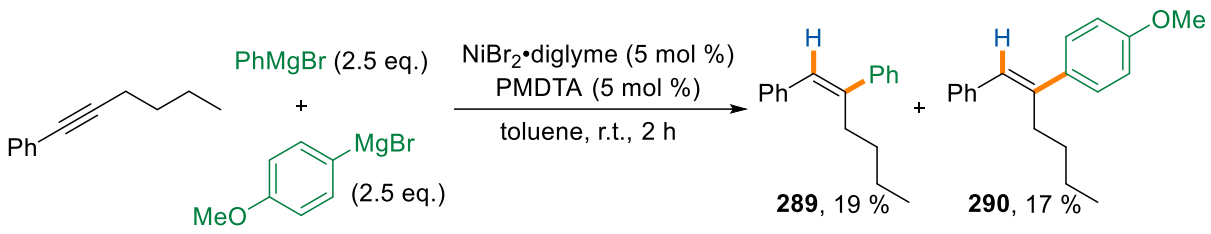

Scheme 3.22: To test relative rate of reactivity between Grignard reagents

3.3.9 Conclusion

In conclusion, we have developed an operationally simple one-pot protocol for the *syn*-selective Ni-catalyzed arylmagnesiation-α-borylation, enabling regio- and stereoselective access to highly valuable trisubstituted alkenyl boronates, with the selectivity driven by the initial carbomagnesiation step. Apart from diverse internal alkynes and Grignards being successfully incorporated, these boronates served as effective intermediates for cross-coupling (yielding geometrically defined tetrasubstituted alkenes) and other synthetically useful transformations, with their biological significance clearly demonstrated by the two-step synthesis of the anti-cancer drug Tamoxifen. Furthermore, the essential role of BpinH in facilitating ate-complex formation, primarily for steric reasons, was established through experimental observations and supported by DFT studies.

3.4 Summary of part of own research

Recognizing a significant gap in the literature, I developed a previously unrealized *syn*-selective carbotrifluoromethylthiolation method for unactivated aryl–alkyl alkynes via sequential carbomagnesiation–trifluoromethylthiolation in a one-pot process. This strategy delivered SCF_3-alkenes with unique (α) regioselectivity and complete stereoselectivity (*syn*-addition) across a broad substrate scope, yielding synthetically useful products. The versatility of the method was further demonstrated through transformations of the trifluoromethyl thioether into its more electronegative and biologically relevant sulfoxide and sulfone derivatives, along with other valuable transformations. Based on literature precedents and my observations, I proposed a plausible mechanism involving Ni(II)/Ni(0) and Cu(I)/Cu(III) catalytic cycles. Additionally, I prepared needle-shaped crystals of the sulfone derivative suitable for X-Ray crystallographic analysis, which unambiguously confirmed the configuration of the desired product.

Following the same conceptual framework, *syn*-arylation with α-borylation was explored. Initial experiments proved difficult in boration of sterically hindered trisubstituted vinyl-magnesium species. Replacement of commonly used BpinO^{i}Pr or $B(OMe)_3$ with less sterically hindered BpinH enabled efficient regio- and stereoselective access to a wide variety of trisubstituted alkenyl

boronates. The incorporation of some Grignard incompatible groups was enabled through the Suzuki cross coupling reactions, leading to configurationally defined tetrasubstituted alkenes in high yields. Additionally, I also performed other synthetic functionalizations, many of which proceeded in nearly quantitative yields and, in some cases, without the need for purification. This methodology also proved valuable for the concise synthesis of biologically significant compound, Tamoxifen with excellent efficiency. With our earlier finding, existing literature and current experimental results, I proposed a reliable mechanism, with special attention on the borylation step, which provided deeper insight into the limitations of the method. These mechanistic considerations were further supported by DFT calculations. Moreover, I obtained irregularly shaped crystals of the bromo derivative, which, despite their morphology, were suitable for X-ray crystallographic analysis and unambiguously confirmed the configuration of the target product.

I have also tried similar approaches with enones and have obtained preliminary results indicating the formation α-trifluoromethylthiolated ketones demonstrating *anti*-selectivity.

4. Experimental Section

4.1 General information

All the manipulations were performed in a nitrogen-filled glovebox or under an argon atmosphere using Schlenk techniques, unless mentioned otherwise. Flash chromatography was performed using Merck silica gel 60 (230-400 mesh). TLC analysis of reaction mixtures was performed on Merck silica gel 60 F254 TLC plates and visualized with cerium molybdate stain (Hanessian's stain) and potassium permanganate stain. ^{1}H, $^{13}C\{1H\}$, and ^{19}F NMR spectra were recorded with a Bruker AV 400 spectrometer. ^{1}H and ^{13}C chemical shifts are given in ppm relative to TMS. The solvent signals were used as references ($CDCl_3$ δ_H = 7.26 ppm, δ_C = 77.0 ppm) and the chemical shift converted to the TMS scale. Coupling constants (*J*) are reported in Hz, and the following abbreviations were used to denote multiplets: s = singlet, d = doublet, t = triplet, q = quartet, quint = quintet, m = multiplet (denotes complex pattern), dd = doublet of doublets, dt = doublet of triplets and br = broad signal. Infrared spectra were recorded with a Jasco FTIR-6200 spectometer. Electron ionization high-resolution mass spectra (EI-HR) were recorded with an Autospec Premier (Waters Inc) mass spectrometer spectrometer equipped with an electron impact (EI) ion source and the EBE double focusing geometry mass analyzer, using the narrow-range high-voltage scan technique with low-boiling perfluorokerosene (PFK) as internal standard. The instrument was controlled and recorded data were processed using MassLynx 4.1 software package (Waters Inc). Samples were introduced by using a heated direct insertion probe. Electrospray ionization high-resolution mass spectra (ESI-HR) and Atmospheric pressure chemical ionization (APCI-TOF) were carried out using Synapt G2-S mass spectrometer (*Waters Inc*) equipped with the ESI/APCI ion source and quadrupole-Time-of-flight (qTOF) mass analyzer (*Waters Inc)*. The measurements were performed with the resolving power of TOF analyzer 20000 FWHM. The instrument was controlled and recorded data were processed using MassLynx V4.1 software package (Waters Inc).

4.2 Materials

Unless otherwise noted, all commercially available compounds (ABCR, Acros, Angene, Ambeed, Fluorochem, TCI, Sigma-Aldrich, Strem) were used as received. Analytical grade dioxane was initially degassed and later dried using activated 3Å molecular sieves for 72 h. Ethyl acetate was dried over anhydrous K_2CO_3 and distilled over 4Å molecular sieves. Acetone was dried over anhydrous $CaSO_4$ and distilled. Other dry solvents were obtained using a solvent purification system (SPS). Aryl tosylate[386], Aryl halides[387–389] Alkynes,[390–406] PhMgBr,[407] Buchwald-type 3rd-generation palladacyclic precatalyst (Ligand Pd G3),[408] thiotrifluoromethylating agent[409] were prepared following literature procedure.

4.3 Synthesis of alkynes

1-(dimethoxymethyl)-4-(hex-1-yn-1-yl)benzene. A flame dried round bottom flask was evacuated and backfilled with argon (the cycle was performed twice) and then charged under a positive pressure of argon with XPhos Pd G3 (8.5 mg, 0.010 mmol, 1 mol%), XPhos (14.3 mg, 0.030 mmol, 3 mol%), Cs_2CO_3 (847.2 mg, 2.678 mmol, 2.6 eq), MeCN (2 mL), 1-bromo-4-(dimethoxymethyl) benzene (238.0 mg, 172.0 µl, 1.030 mmol). The reaction mixture was stirred for 25min at rt. Then 1-hexyne (106.8 mg, 150.5 µl, 1.339 mmol, 1.3 eq) was added and the resultant was heated to 75ºC for 5h. The resulting suspension was cooled to room temperature, diluted with water, and extracted with MTBE. The combined organic layers were dried over Na_2SO_4, concentrated providing red oil as a crude product (239.3 mg, 1.030 mmol, 100%), which was used without further purification. ^{1}H NMR (400 MHz, $CDCl_3$): 7.38 (m, 4H), 5.37 (s, 1H), 3.30 (s, 6H) 2.40 (t, J = 7.0 Hz, 2H), 1.5 (m, 4H), 0.95 (t, J = 7.3 Hz, 3H); ^{13}C NMR (400 MHz, $CDCl_3$): 137.2, 131.3, 128.5, 126.5, 124.2, 102.6, 102.3, 90.7, 80.3, 52.4, 30.8, 21.9, 19.0, 13.5; HRMS (EI-EBE) m/z: $[M]^+$ Calc'd for $C_{15}H_{20}O_2$: 232.1463, Found: 232.1467.

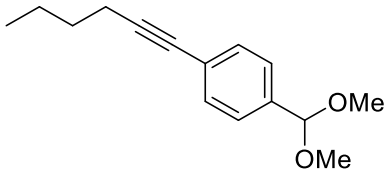

5-(hex-1-yn-1-yl)-1-methyl-1H-indole. The compound was synthesized using modified Buchwald's[400] procedure. A flame dried round bottom flask was evacuated and backfilled with argon (the cycle was performed twice) and then charged under a positive pressure of argon with XPhos Pd G3 (72.2 mg, 0.085 mmol, 1 mol%), XPhos (121.8 mg, 0.255 mmol, 3 mol%), Cs_2CO_3 (7.2 g, 22.157 mmol, 2.6 eq.), MeCN (17 mL), 5-bromo-1-methyl-*1H*-indole (1.8 g, 8.522 mmol). The reaction mixture was stirred for 25min at rt. Then 1-hexyne (910.1 mg, 1.3 mL, 11.078 mmol, 1.3 eq.) was added and the resultant was heated to 75ºC for 48h. The resulting suspension was cooled to room temperature, diluted with water, and extracted with MTBE. The combined organic layers were dried over Na_2SO_4, concentrated, and the residue was purified by flash chromatography on silica gel (60/90 petroleum ether/ethyl acetate 99.5:0.5 to 95:10) to provide the desired product as an orange oil (1.4 g, 6.625 mmol, 78%). Analytical data was in agreement with literature data.[410]

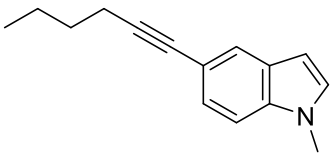

4-(hex-1-yn-1-yl)phenyl tosylate. The compound was synthesized using modified Zhang's[411] procedure. A flame dried round bottom flask was evacuated and backfilled with argon (the cycle was performed twice) and then charged under a positive pressure of argon with 4-iodophenyl 4-methylbenzenesulfonate (2.0 g, 5.344 mmol), $Pd(PPh_3)_2Cl_2$ (18.8 mg, 0.267 mmol, 5 mol%), CuI (101.8 mg, 0.534 mmol, 10 mol%), Et_3N (1.1 g, 1.5 mL, 10.689 mmol, 2 eq.), THF (22 mL), 1-hexyne (658.6 mg, 0.93 mL, 8.017 mmol, 1.5 eq.). The resultant reaction mixture was stirred for 24h at rt. The reaction mixture was diluted with water and extracted with MTBE. The combined organic layers were dried over Na_2SO_4, concentrated, and the residue was purified by flash chromatography on silica gel (60/90 petroleum ether/ethyl acetate 95:5 to 90:10) to provide the desired product as thick reddish-orange oil (1.7 g, 5.176 mmol, 97%). Analytical data was in agreement with literature data.

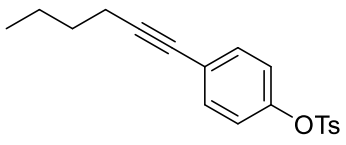

4-(hex-1-yn-1-yl)phenol. The compound was synthesized using modified Corma's[412] procedure. A flame dried round bottom flask was evacuated and backfilled with argon (the cycle was performed twice) and then charged under a positive pressure of argon with 4-iodophenol (1.9 g, 9.090 mmol), $Pd(PPh_3)_2Cl_2$ (127.7 mg, 0.181 mmol, 2 mol%), CuI (34.7 mg, 0.181 mmol, 2 mol%), dioxane (9 mL), Et_3N (6.3 mL, 4.6 g, 45.452 mmol, 5 eq.), 1-hexyne (1.27 mL, 10.908 mmol, 1.2 eq.). The resultant was subjected on a pre-heated bath (55ºC) for 30 min. The resultant was cooled to room temperature diluted with water and extracted with MTBE. The combined organic layers were dried over Na_2SO_4, concentrated, and the residue was purified by flash chromatography on silica gel (60/90 petroleum ether/ethyl acetate 90:10 to 75:25) to provide the desired product as red oil (1.5 g, 8.608 mmol, 95%). Analytical data was in agreement with literature data.[413]

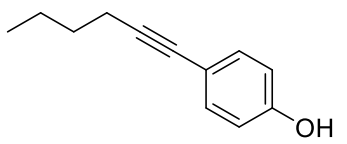

4-(hex-1-yn-1-yl)phenyl triflate. A flame dried round bottom flask was evacuated and backfilled with argon (the cycle was performed twice) and then charged under a positive pressure of argon with 4-(hex-1-yn-1-yl)phenol (1.4 g, 8.215 mmol), CH_2Cl_2 (8 mL), and pyridine (1.32 mL, 1.3 g, 16.431 mmol, 2 eq). The resultant was cooled to 0°C. Triflic anhydride (2.8 g, 1.62 mL, 9.858 mmol, 1.2 eq) was added dropwise at 0ºC and the reaction mixture was stirred at rt for 1.5h and quenched with the addition of Et_2O (15 mL) and aqueous HCl (10%, 5 mL). The reaction mixture was washed with aqueous saturated $NaHCO_3$ (10 mL) and brine (10 mL). The combined organic layers were dried over Na_2SO_4, concentrated, and the residue was purified by flash chromatography on silica gel (60/90 Petroleum ether/diethylether 100% to 98:2) to provide the desired product as light-yellow oil (2.2 g, 7.182 mmol, 88%). ^{1}H NMR (400 MHz, $CDCl_3$): 7.45 (dd, 2H), 7.18 (dd, 2H), 2.40 (t, J = 7.0 Hz, 2H), 1.53 (m, 4H), 0.95 (t, J = 7.3 Hz, 3H); ^{19}F NMR (400 MHz, $CDCl_3$): -72.89 (s , 3H); ^{13}C NMR (400 MHz, $CDCl_3$): 148.4, 133.2, 124.8, 121.2, 118.7 (q, $^1J_{CF}$ = 320.8 Hz), 92.6, 78.8, 30.6, 21.9, 19.0, 13.5; HRMS (EI-EBE) m/z: $[M]^+$ Calc'd for $C_{13}H_{13}F_3O_3S$: 306.0537, Found: 306.0536.

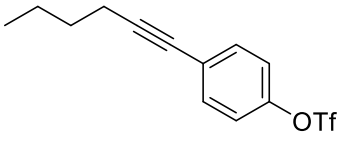

4.4 α-Selective *syn*-Carbotrifluoromethylthiolation of Alkynes

4.4.1 Procedures for evaluation of reaction conditions

Evaluation of reaction conditions for Ni-catalyzed carbomagnesiation of internal alkynes

General procedure: Under argon, in a dark vial, $NiCl_2$(dme) (10.99 mg, 1 mmol, 5 mol%) was added along with a magnetic stirring bar. To the catalyst, alkyne (1 mmol) and dioxane (4 mL) were added. The resultant solution was stirred for 5 minutes. Then phenyl magnesium bromide (0.24 mL, 0.24 mmol, 1.0 M in THF, 1.2 eq.) was added dropwise. The reaction mixture was stirred at r.t. for 2 h. The mixture was diluted with MTBE (1mL) quenched with sat. aqueous NH_4Cl (1 mL) and mesitylene (30 µl) was added as an internal standard.

Evaluation of reaction conditions for one pot procedure of carbotrifluoromethylthiolation of alkynes

General procedure: Vinylmagnesium intermediate **278** was prepared through Ni-catalyzed carbomagnesation of phenylhexyne: In the glove box, $NiCl_2$(dme) (5 mol%, 2.2 mg, 0.01 mmol) was introduced into a 4 mL vial equipped with a magnetic stir bar. To the catalyst were added phenylhexyne (31.7 mg, 0.2 mmol), mesitylene (30 µl), dioxane (0.8 mL) and then phenyl magnesium bromide solution (0.24 mL, 0.24 mmol, 1.2 eq., 1.0 M in THF) dropwise. The resulting mixture was stirred at room temperature for 2 h. To a 15-mL flame dried shlenk were added, $Cu(MeCN)_4PF_6$ (40 mol%, 29.9 mg, 0.08 mmol), 4,4' *tert*-butyl bipyridine (80 mol%, 43 mg, 0.16 mmol), N-Methyl-N-[(trifluoromethyl)thio]- *p*-toluenesulfonamide **265** (114.1 mg, 0.4 mmol, 2 eq.) and 0.6 mL of THF. The solution was cooled to -78 °C and the freshly prepared solution of vinylmagnesium intermediate **278** was added to it dropwise. The reaction mixture was removed from the cooling bath and allowed to stir at r.t. for 18 h. The mixture was quenched with sat. aq. NH_4Cl (1 mL) and diluted with MTBE (1 mL).

4.4.2 General procedures

General procedure for carbotrifluoromethylthiolation of alkynes.
In the glove box after standard cycles of evacuation and back-fill with pure N_2, $NiCl_2$(dme) (2.2 mg, 0.01 mmol, 5 mol%) was introduced into a 15-mL Schlenk tube equipped with a magnetic stir bar. To the catalyst were added alkyne (0.2 mmol), dioxane (0.8 mL) and then aryl magnesium bromide dropwise (0.24 mL, 0.24 mmol, 1.2 eq., 1.0 M in THF). The resulting mixture was stirred at rt for 2h. After that time the reaction mixture was cooled to -78°C and $Cu(MeCN)_4PF_6$ (29.9 mg, 0.08 mmol, 40 mol%), 4,4' *tert*-butyl bipyridine (43 mg, 0.16 mmol, 80 mol%) were added as a solid and N-(trifluoromethylthio) phthalimide **231** (99 mg, 0.4 mmol, 2 eq) as a solution in 0.6 mL THF. The reaction mixture was removed from the cooling bath and allowed to stir for 1h at rt. The mixture was quenched with sat. aquas NH_4Cl and diluted with MTBE. The combined organic layers were dried over Na_2SO_4, concentrated, and the residue was purified by flash chromatography on silica gel to provide the desired product **269**, typically containing small amount of inseparable trisubstituted olefin **268**.

Procedure for reaction run at 1 mmol scale for compound 269a.
A 30-mL Shlenk tube equipped with a magnetic stirring bar was charged with $NiCl_2$(dme) (10.9 mg, 0.05 mmol, 5 mol%), then evacuated and back-filled with argon (three times). To the catalyst were added 1- phenylhexyne (158.3 mg, 1.0 mmol), dioxane (4 mL) and then phenyl magnesium bromide dropwise (1.2 mL, 1.2 mmol, 1.2 eq., 1.0 M in THF). The resulting was stirred at r.t. for

2 h. After 2 h, the reaction mixture was cooled to -78 °C and $Cu(MeCN)_4PF_6$ (149.1 mg, 0.4 mmol, 40 mol%), 4,4' *tert*-butyl bipyridine (214.7 mg, 0.8 mmol, 80 mol%) were added as a solid and N-(trifluoromethylthio) phthalimide **231** (494.3 mg, 2 mmol, 2 eq.) as a solution in 3 mL THF. The reaction mixture was removed from the cooling bath and allowed to stir for 1 h at r.t.. The mixture was quenched with sat. aqueous NH_4Cl and diluted with MTBE. The combined organic layers were dried over Na_2SO_4, concentrated, and the residue was purified by column chromatography on silica gel. The title compound was isolated as a yellow oil (278.1) after chromatography on silica gel (40 g column, 40/60 petroleum ether) containing **269a** (257.4 mg, 0.765 mmol, 77%) along with small amount of **268a** (20.7 mg, 0.087 mmol, 9%). The compound can be further purified by reverse-phase chromatography (25 g C18-silica column, 7:3 to 9:1 MeOH:H_2O). First run delivered 206.0 mg (0.612 mmol, 61%) of pure **269a** and a fraction containing mixture of **269a** and **268a**. After a second separation of the mixture a total of 234.7 mg of pure **269a** (0.697 mmol, 70%) was isolated.

Procedure for carbotrifluoromethylthiolation via *in situ* formation of Grignard reagent

In a 15 mL Schlenk flask, add Mg (29.17 mg, 1.2 mmol, 1.2 eq.). Then add THF (0.2 mL) under argon. Add a small crystal of iodine. The solution turns brown. Add solution of vinyl bromide (315.25 mg, 1 mmol) in THF (0.7 mL). Heat it 60 °C for 2.5 h. Cool the reaction mixture. Add 0.2 mL to another flame dried Schlenk under argon. Then add 30 µL of mesitylene. Cool the Schlenk to -78 °C and add $Cu(MeCN)_4PF_6$ (40 mol%, 29.9 mg, 0.08 mmol), 4,4' *tert*-butyl bipyridine (80 mol%, 43 mg, 0.16 mmol) as solids and N-(trifluoromethylthio) phthalimide **231** (98.88 mg, 0.4 mmol, 2 eq.) as a solution in 0.6 mL of THF. Then remove the Schlenk from the cooling bath and stir at rt for 1 h. After 1 hour take small aliquot and quench it with sat. NH_4Cl and add MTBE. Yield calculated by GC analysis.

4.4.3 Analytical data of isolated products of carbotrifluoromethylthiolation of alkynes

Scope of alkynes

(*Z*)-(1,2-diphenylhex-1-en-1-yl)(trifluoromethyl)sulfane (269a) Prepared by reaction of 1-phenylhexyne (32.0 mg, 0.202 mmol) with phenylmagnesium bromide following general procedure. The title compound was isolated as a yellow oil (53.0 mg) after chromatography on silica gel (15 g column, 40/60 petroleum ether) containing **269a** (49.6 mg, 0.147 mmol, 73%) along with small amount of **268a** (3.4 mg, 0.014 mmol, 7%). Analytical data of **269a**: ^{1}H NMR (400 MHz, $CDCl_3$): 7.42 (m, 6H), 7.36 (m, 2H), 7.25 (m, 2H), 2.39 (t, J = 7.9 Hz, 2H), 1.21 (m, 4H), 0.73 (t, J = 7.2 Hz, 3H); ^{19}F NMR (400 MHz, $CDCl_3$): -40.0 (s, 3F); ^{13}C NMR (400 MHz, $CDCl_3$): 154.4, 141.1, 139.3, 129.3 (q, $^1J_{CF}$ = 309.9 Hz), 129.3, 128.2, 128.2, 128.1, 127.8, 127.4, 123.8, 36.4, 30.1, 22.3, 13.6; HRMS (EI-EBE) m/z: $[M]^+$ Calc'd for $C_{19}H_{19}F_3S$: 336.1160, Found: 336.1149; Indicative NMR signals of **268a**: ^{1}H NMR (400 MHz, $CDCl_3$): 7.49 (m, 2H), 6.72 (s, 1H), 2.73 (t, J = 8.1 Hz, 3H), 1.39 (m, 4H), 0.88 (t, J = 7.2 Hz, 3H); ^{13}C NMR (400 MHz, $CDCl_3$): 143.4, 143.2, 138.3, 128.7, 128.3, 128.0, 127.1, 126.6, 126.4, 30.9, 29.9, 22.7, 13.8.

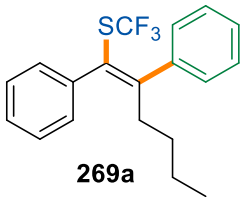

269a

(*Z*)-(1,2-diphenylprop-1-en-1-yl)trifluoromethyl)sulfane (269b) Prepared by reaction of 1-phenylpropyne (23.2 mg, 0.1997 mmol) with phenylmagnesium bromide following general procedure. The title compound was isolated as a white solid (36.1 mg) after chromatography on silica gel (15 g column, 40/60 petroleum ether), containing **269b** (34.2 mg, 0.116 mmol, 58 %) along with small amount of **268b** (1.9 mg, 0.009 mmol, 5%). Analytical data of **269b**: ^{1}H NMR (400 MHz, $CDCl_3$): 7.40 (m, 10H), 2.07 (s, 3H); ^{19}F NMR (400 MHz, $CDCl_3$): -40.2 (s, 3F); ^{13}C NMR (400 MHz,

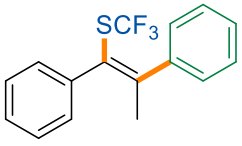

269b

$CDCl_3$): 149.9, 142.7, 139.4, 129.4, 129.2 (q, $^1J_{CF}$ = 309.9 Hz), 128.3, 128.2, 127.8, 127.6, 127.5, 123.6, 24.4; HRMS (EI-EBE) m/z: $[M]^+$ Calc'd for $C_{16}H_{13}F_3S$: 294.0690, Found: 294.0692; Indicative NMR signals of **268b**: ^{1}H NMR (400 MHz, $CDCl_3$): 7.56 (m, 2H), 6.85 (s, 1H), 2.30 (d,3H); ^{13}C NMR (400 MHz, $CDCl_3$): 144.0, 138.4, 137.4, 129.1, 128.1, 127.7, 127.2, 126.4, 126.0, 17.4.

(*Z*)-(2-cyclopropyl-1,2-diphenylvinyl)trifluoromethyl)sulfane (269c) Prepared by reaction of 2-cyclopropyl-1-phenyl ethyne (28.6 mg, 0.201 mmol) with phenylmagnesium bromide following general procedure. The title compound **269c** was isolated as a white solid (40.5 mg, 0.126 mmol, 63 %) after chromatography on silica gel (15 g column, 40/60 petroleum ether). Analytical data of **269c**: ^{1}H NMR (400 MHz, $CDCl_3$): 7.57 (d, J = 7.4 Hz, 2H), 7.37 (m, 6H), 7.08 (d, J = 6.8 Hz, 2H), 1.85 (tt, 1H), 0.61 (m, 2H), 0.39 (m, 2H); ^{19}F NMR (400 MHz, $CDCl_3$): -40.5 (s, 3F); ^{13}C NMR (400 MHz, $CDCl_3$): 155.7, 139.4, 137.1, 130.0, 129.1 (q, $^1J_{CF}$ = 310.1 Hz), 129.0, 128.2, 127.8, 127.7, 127.4, 122.5, 29.7, 16.7, 6.5; HRMS (EI-EBE) m/z: $[M]^+$ Calc'd for $C_{18}H_{15}F_3S$: 320.0842, Found: 320.0844.

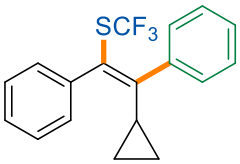

269c

(*Z*)-(3-methyl-1,2-diphenylbut-1-en-1-yl)trifluoromethyl)sulfane (269d) Prepared by reaction of 3-methyl-1-phenyl butyne (29.1 mg, 0.201 mmol) with phenylmagnesium bromide following general procedure. The title compound was isolated as a white solid (44.5 mg) after chromatography on silica gel (15 g column, 40/60 petroleum ether), containing **269d** (42.5 mg, 0.131 mmol, 66%) along with small amount of **268d** (2.0 mg, 0.008 mmol, 5%). Analytical data of **269d**: ^{1}H NMR (400 MHz, $CDCl_3$): 7.37 (m, 8H), 7.11 (m, 2H), 2.92 (hept, 1H), 0.89 (d, J = 6.9 Hz, 6H); ^{19}F NMR (400 MHz, $CDCl_3$): -39.8 (s, 3F); ^{13}C NMR (400 MHz, $CDCl_3$): 158.7, 138.9, 138.0, 129.2, 129.1 (q, $^1J_{CF}$ = 309.7 Hz), 128.9, 128.2, 127.8, 127.8, 127.2, 124.3, 32.6, 21.0; HRMS (EI-EBE) m/z: $[M]^+$ Calc'd for $C_{18}H_{17}F_3S$: 322.0998, Found: 322.1005; Indicative NMR signals of **268d**: ^{1}H NMR (400 MHz, $CDCl_3$): 6.37 (s, 1H), 3.31 (m, 1H), 1.08 (d, J = 7.0 Hz, 6H); ^{13}C NMR (400 MHz, $CDCl_3$): 128.8, 128.1, 127.5, 126.5, 126.4, 29.7, 21.9.

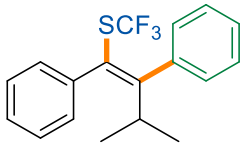

269d

(*Z*)-(5-chloro-1,2-diphenylpent-1-en-1-yl))trifluoromethyl)sulfane (269e) Prepared by reaction of 5-chloro-1-phenyl pent-1-yne (36.1 mg, 0.202 mmol) with phenylmagnesium bromide following general procedure. The title compound was isolated as a colorless oil (48.6 mg) after chromatography on silica gel (15 g column, 40/60 petroleum ether), containing **269e** (45.1 mg, 0.126 mmol, 63%) along with small amount of **268e** (3.5 mg, 0.013 mmol, 7%). Analytical data of **269e**: ^{1}H NMR (400 MHz, $CDCl_3$): 7.40 (m, 8H), 7.25 (m, 2H), 3.30 (t, J = 6.6 Hz, 2H), 2.52 (m, 2H), 1.71 (m, 2H); ^{19}F NMR (400 MHz, $CDCl_3$): -39.8 (s, 3F); ^{13}C NMR (400 MHz, $CDCl_3$): 151.9, 140.3, 138.8, 129.2 (q, $^1J_{CF}$ = 309.9 Hz), 129.2, 128.4, 128.4, 128.1, 128.1, 127.8, 125.4, 44.1, 34.1, 31.0; HRMS (EI-EBE) m/z: $[M]^+$ Calc'd for $C_{18}H_{16}ClF_3S$: 356.0613, Found: 356.0620. Indicative NMR signals of **268e**: ^{1}H NMR (400 MHz, $CDCl_3$): 7.48 (m, 2H), 7.45 (m, 4H), 7.31 (dd, 4H), 6.78 (s, 1H), 3.5 (t, J = 6.6 Hz, 2H), 2.90 (m, 2H), 1.91 (m, 2H); ^{13}C NMR (400 MHz, $CDCl_3$): 142.4, 141.4, 137.9, 129.2, 128.7, 128.5, 128.3, 127.4, 126.7, 126.5, 44.8, 31.6, 27.6.

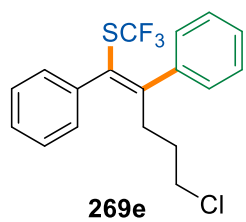

269e

(Z)-(trifluoromethyl)(1,2,3-triphenylprop-1-en-1-yl)sulfane (269f) Prepared by reaction of 1,3-diphenyl propyne (38.7 mg, 0.201 mmol) with phenylmagnesium bromide following general procedure. The title compound **269f** was isolated as a white solid (53.2 mg, 0.143 mmol, 72%) after chromatography on silica gel (15 g column, 40/60 petroleum ether). Analytical data of **269f**: ^{1}H NMR (400 MHz, $CDCl_3$): 7.55 (m, 2H), 7.46 (m, 2H), 7.39 (m, 1H), 7.31 (m, 3H), 7.16 (m, 3H), 7.09 (m, 2H), 6.88 (m, 2H), 3.77 (s, 2H); ^{19}F NMR (400 MHz, $CDCl_3$): -39.6 (s, 3F); ^{13}C NMR (400 MHz, $CDCl_3$): 151.5, 140.4, 138.9, 137.7, 129.5, 129.2 (q, $^1J_{CF}$ = 309.9 Hz), 128.9, 128.5, 128.4, 128.2, 128.1, 128.0, 127.5, 126.3, 125.8, 42.5; HRMS (EI-EBE) m/z: $[M]^+$ Calc'd for $C_{22}H_{17}F_3S$: 370.1003, Found: 370.0998.

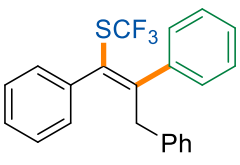

269f

(*Z*)-(1-(4-methoxyphenyl)-2-phenylhex-1-en-1-yl))trifluoromethyl)sulfane (269g) Prepared by reaction of 1-(4-methoxyphenyl)hex-1-yne (37.8 mg, 0.200 mmol) with phenylmagnesium bromide following general procedure. The title compound **269g** was isolated as a colorless oil (45.5 mg, 0.200 mmol, 62%) after chromatography on silica gel (15 g column, 40/60 petroleum ether/diethyl ether 100:0 to 97:3). Analytical data of **269g**: ^{1}H NMR (400 MHz, $CDCl_3$): 7.40 (m, 2H), 7.33 (m, 3H), 7.22 (m, 2H), 6.93 (m, 2H) 3.85 (s, 3H), 2.37 (t, J = 8.0 Hz, 2H), 1.18 (m, 4H), 0.72 (t, J = 7.2 Hz, 3H); ^{19}F NMR (400 MHz, $CDCl_3$): -40.0 (s, 3F); ^{13}C NMR (400 MHz, $CDCl_3$): 159.1, 153.7, 141.3, 131.5, 130.5, 129.3 (q, $^1J_{CF}$ = 310.1 Hz), 128.1, 128.1, 127.3, 123.7, 113.5, 55.2, 36.4, 30.1, 22.3, 13.7; HRMS (EI-EBE) m/z: $[M]^+$ Calc'd for $C_{20}H_{21}F_3OS$: 366.1265 Found: 366.1277.

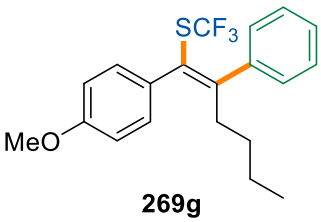

269g

(*Z*)-(1-(naphthalen-1-yl)-2-phenylhex-1-en-1-yl))trifluoromethyl)sulfane (269h) Prepared by reaction of 1-(hex-1-yn-1-yl)naphthalene (42.07 mg, 0.201 mmol) with phenylmagnesium bromide following general procedure. The title compound was isolated as a colorless oil (45.0 mg, 0.116 mmol, 58%) after chromatography on silica gel (15 g column, 40/60 petroleum ether). Analytical data of **269h**: ^{1}H NMR (400 MHz, $CDCl_3$, 8.00 (d, J = 7.4 Hz, 1H), 7.89 (ddd, 2H), 7.54 (m, 6H), 7.41 (d, 1H), 7.37(d, 2H), 2.22 (m, 2H), 1.16 (m, 2H), 0.99 (m, 2H), 0.57 (t, J = 7.3 Hz, 3H); ^{19}F NMR (400 MHz, $CDCl_3$): -39.6 (s, 3F); ^{13}C NMR (400 MHz, $CDCl_3$): 156.2, 140.6, 135.9, 133.8, 130.9, 128.7, 128.6, 128.3, 128.2, 127.6, 127.0 (q, $^1J_{CF}$ = 306.8 Hz), 126.3, 126.0, 125.2, 125.0, 121.5, 36.7, 29.7, 22.2, 13.5; HRMS (EI-EBE) m/z: $[M]^+$ Calc'd for $C_{23}H_{21}F_3S$: 386.1311 Found: 386.1326.

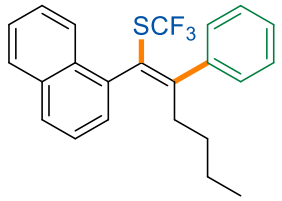

269h

(*Z*)-(1-(4-fluorophenyl)-2-phenylhex-1-en-1-yl))trifluoromethyl)sulfane (269i) Prepared by reaction of 1- (4-fluorophenyl)hex-1-yne (35.7 mg, 0.202 mmol) with phenylmagnesium bromide following general procedure. The title compound was isolated as a colorless oil (42.6 mg) after chromatography on silica gel (15 g column, 40/60 petroleum ether), containing **269i** (39.7 mg, 0.112 mmol, 56%) along with small amount of **268i** (2.9 mg, 0.011 mmol, 6%). Analytical data of **269i**: ^{1}H NMR (400 MHz, $CDCl_3$): 7.41 (m, 5H), 7.25 (d, J = 6.8 Hz 2H), 7.13 (t, J = 8.7 Hz, 2H), 2.38 (t, J = 7.9 Hz, 2H), 1.20 (m 4H), 0.75 (t, J = 7.2 Hz, 3H); ^{19}F NMR (400 MHz, $CDCl_3$): -39.9 (s, 3F), -113.6 (s, 1F); ^{13}C NMR (400 MHz, $CDCl_3$): 163.5, 161.0, 154.7, 140.9, 135.2 (d, J = 3.41 Hz), 131.1(d, J = 8.11.5hz), 129.2 (q, $^1J_{CF}$ = 309.8 Hz), 128.2, 128.0, 127.5, 122.9, 115.4 (d), 36.4, 30.0, 22.3, 13.6; HRMS (EI-EBE) m/z: $[M]^+$ Calc'd for $C_{19}H_{18}F_4S$: 354.1060 Found: 354.1071. Indicative NMR signals of **268i**: ^{1}HNMR (400 MHz, $CDCl_3$): 7.48 (d, 3H), 7.31 (dd, 4H), 7.07 (d, J = 8.7 Hz, 2H), 6.67 (s, 1H), 2.70 (t, J = 8.2 Hz, 2H), 1.40 (m, 4H) 0.88 (t, J = 7.2 Hz, 3H); ^{19}F NMR (400 MHz, $CDCl_3$): -115.7 (s, 1F); ^{13}C NMR (400 MHz, $CDCl_3$: 162.7, 160.2, 143.4, 142.9, 134.3 (d, J = 3.35 Hz), 130.3 (d, J = 7.9 Hz), 128.3, 127.1, 126.8, 126.5, 115 (d), 30.8, 29.8, 22.7, 13.8.

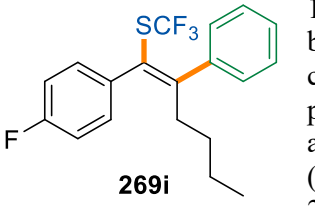

269i

(Z)-4-(2-phenyl-1-((trifluoromethyl)thio)hex-1-en-1-yl)phenyl 4-methylbenzenesulfonate (269j) Prepared by reaction of 1-(4-tosylatephenyl)hex-1-yne (65.9 mg, 0.200 mmol) with phenylmagnesium bromide following general procedure. The title compound was isolated as a yellow oil (54.9 mg) after chromatography on silica gel (15 g column, 40/60 petroleum ether/diethyl ether 10:0 to 9:1), containing **269j** (49.1 mg, 0.096 mmol, 49%) along with small amount of **268j** (5.8 mg, 0.014 mmol, 7%). Analytical data of **269j**: ^{1}H NMR (400 MHz, $CDCl_3$): 7.67 (dd, 2H), 7.39 (dd, 2H), 7.31 (dd, 3H), 7.28 (d, 2H), 7.18 (m, 2H), 7.01 (dd, 2H), 2.43 (s, 3H), 2.30 (t, J = 7.3 Hz, 2H), 1.15 (m, 4H), 0.70 (t, J = 7.2 Hz, 3H); ^{19}F NMR (400 MHz, $CDCl_3$): -39.9 (s, 3F); ^{13}C NMR (400 MHz, $CDCl_3$): δ 154.9, 149.0, 145.4, 140.6, 138.2, 130.6, 129.6, 129.1 (q), 128.6, 128.2, 127.9, 127.6, 126.5, 122.5, 122.3 36.4, 29.9, 22.3, 21.6, 13.6. HRMS (EI-EBE) m/z: $[M]^+$ Calc'd for $C_{26}H_{25}F_3O_3S_2$: 506.1197 Found: 506.1213. Indicative NMR signals of **268j**: ^{1}H NMR (400 MHz, $CDCl_3$): 7.72 (dd, 2H), 7.42 (m, 2H), 7.35 (m, 3H), 7.33 (d, 2H), 7.21 (dd, 2H), 6.97 (dd,

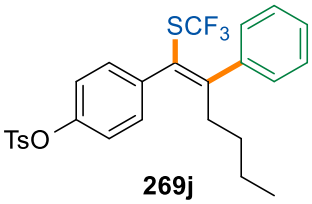

269j

2H), 6.59 (s, 1H), 2.62 (t, J = 7.4 Hz, 2H), 2.45 (s, 3H), 1.33 (m, 4H), 0.82 (t, J = 7.2 Hz, 3H); ^{13}C NMR (101 MHz, $CDCl_3$) δ 147.9, 145.2, 144.3, 142.7, 137.3, 132.4, 131.9, 129.8, 129.7, 128.5, 128.3, 127.3, 126.6, 122.1, 30.7, 29.8, 22.6, 21.7, 13.7.

(Z)-4-(2-phenyl-1-((trifluoromethyl)thio)hex-1-en-1-yl)phenyl trifluoromethanesulfonate (269k)

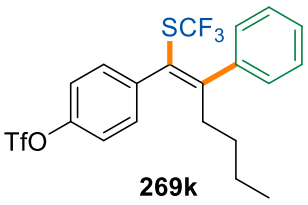

269k

Prepared by reaction of 1-(4-triflatephenyl)hex-1-yne (61.5 mg, 0.200 mmol) with phenylmagnesium bromide following general procedure. The title compound was isolated as a yellow oil (47.5 mg) after chromatography on silica gel (15 g column, 40/60 petroleum ether), containing **269k** (43.5 mg, 0.089 mmol, 45%) along with small amount of **268k** (4.0 mg, 0.010 mmol, 5%). Analytical data of **269k**: ^{1}H NMR (400 MHz, $CDCl_3$): 7.50 (m, 2H), 7.40 (m, 3H), 7.34 (m, 2H), 7.21 (m, 2H), 2.35 (t, J = 7.3 Hz, 2H), 1.19 (m, 4H), 0.71 (t, J = 7.2 Hz, 3H); ^{19}F NMR (400 MHz, $CDCl_3$): -39.9 (s, 3F), -72.7 (s, 3F); ^{13}C NMR (400 MHz, $CDCl_3$): 156.0, 148.8, 140.4, 139.8, 131.2, 129.0 (q, , $^1J_{CF}$ = 309.8 Hz), 128.3 127.9, 127.7, 121.9, 121.2, 118.7 (q, $^1J_{CF}$ = 320.8 Hz), 36.4, 29.9, 22.2, 13.5; HRMS (EI-EBE) m/z: $[M]^+$ Calc'd for $C_{20}H_{18}F_6O_3S_2$: 484.0602 Found: 484.0591. Indicative NMR signals of **268k**: ^{1}H NMR (400 MHz, $CDCl_3$): 7.46 (d, 1H), 7.27 (m, 2H), 6.64 (s, 1H), 2.67 (t, J = 7.6 Hz, 2H), 1.37 (m, 4H), 0.84 (t, J = 7.2 Hz, 3H); ^{19}F NMR (400 MHz, $CDCl_3$): -72.8 (s, 3F); ^{13}C NMR (400 MHz, $CDCl_3$): 147.9, 145.2, 142.5, 138.7, 130.4, 128.3, 127.5, 126.5, 126.0, 121.1, 30.7, 22.6, 13.7.

(Z)-(1-(4-(dimethoxymethyl)phenyl)-2-phenylhex-1-en-1-yl)(trifluoromethyl)sulfane (269l) Prepared by reaction of 1-(4-dimethoxymethylphenyl)hex-1-yne (46.4 mg, 0.199 mmol) with phenylmagnesium bromide following general procedure. The title compound was isolated as a yellow oil (49.2 mg) after chromatography on silica gel (15 g column, 40/60 petroleum ether/methyl tert-butyl ether 98.5:1.5 to 96:4), containing **269l** (45.0 mg, 0.109 mmol, 55%) along with small amount of **268l** (4.2 mg, 0.013 mmol, 7%). Analytical data of **269l**: ^{1}H NMR (400 MHz, $CDCl_3$): 7.50 (d, 2H), 7.41 (m, 4H), 7.35 (m, 1H), 7.23 (d, 2H), 5.46 (s, 1H), 3.36 (s, 6H), 2.37 (t, J = 7.4 Hz, 2H), 1.19 (m, 4H), 0.70 (t, J = 7.2 Hz, 3H); ^{19}F NMR (400 MHz, $CDCl_3$): -40.0 (s, 3F); ^{13}C NMR (400 MHz, $CDCl_3$): 154.5, 141.0, 139.5, 137.6, 129.2, 129.2 (q, $^1J_{CF}$ = 309.8 Hz), 128.1, 128.0, 127.4, 126.6, 126.5, 123.5 102.8, 52.6, 36.4, 30.0, 22.3, 13.6; HRMS (EI-EBE) m/z: $[M]^+$ Calc'd for $C_{22}H_{25}F_3O_2S$: 410.1527, Found: 410.1538. Indicative NMR signals of **268l**: ^{1}H NMR (400 MHz, $CDCl_3$: 6.69 (s, 1H), 5.42 (s, 1H), 2.71 (t, J = 7.5 Hz, 2H), 1.37 (m, 4H), 0.85 (t, J = 7.3 Hz, 3H); ^{13}C NMR (400 MHz, $CDCl_3$): 143.7, 143.1, 138.5, 136.2, 129.4, 128.6, 128.2, 127.7, 127.3, 127.1, 126.4, 103.1, 52.7, 30.8, 29.9, 22.7, 13.8.

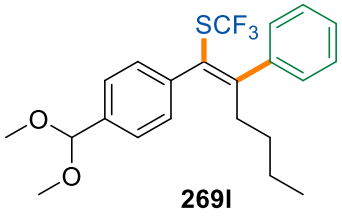

269l

(*Z*)-5-(2-phenyl-1-((trifluoromethyl)thio)hex-1-en-1-yl)benzo[d][1,3]dioxole (269m) Prepared by reaction of 5-(hex-1-yn-1-yl)benzo[*d*][1,3]dioxole (40.7 mg, 0.201 mmol) with phenylmagnesium bromide following modified general procedure (carbomagnesiation run for 3h). The title compound **269m** was isolated as a yellow oil (50.5 mg, 0.132 mmol, 66%) after chromatography on silica gel (15 g column, 40/60 petroleum ether/diethyl ether 100:0 to 97:3). Analytical data of **269m**: ^{1}H NMR (400 MHz, $CDCl_3$): 7.39 (m, 3H), 7.24 (dd, 2H), 6.89 (dd+s, 3H), 6.04 (s, 2H), 2.42 (t, J = 7.1 Hz, 2H), 1.23 (m, 4H), 0.77 (t, J = 7.1 Hz, 3H); ^{19}F NMR (400 MHz, $CDCl_3$): -40.0 (s, 3F); ^{13}C NMR (400 MHz, $CDCl_3$): 154.2, 147.5, 147.2, 141.1, 133.0, 129.3 (q, $^1J_{CF}$ = 310.1 Hz), 128.1, 128.0, 127.4, 123.6, 123.0, 109.7, 108.0, 101.2, 36.5, 30.1, 22.4, 13.6; HRMS (EI-EBE) m/z: $[M]^+$ Calc'd for $C_{20}H_{19}F_3O_2S$: 380.1058 Found: 380.1059.

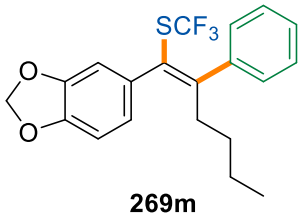

269m

(Z)-1-methyl-5-(2-phenyl-1-((trifluoromethyl)thio)hex-1-en-1-yl)-1H-indole (269n) Prepared by reaction of 5-(hex-1-yn-1-yl)-1-methyl-1*H*-indole (42.5 mg, 0.201 mmol) with phenylmagnesium bromide following general procedure. The title compound was isolated as a yellow oil (38.3 mg, 0.098 mmol, 49%) after chromatography on silica gel (15 g column, 40/60 petroleum ether/ethyl acetate 99:1 to 9:1) Analytical data of **269n**: ^{1}H NMR (400 MHz, $CDCl_3$): 7.60 (d, 1H), 7.43 (m, 2H), 7.35 (m, 2H), 7.28 (m, 3H), 7.09 (d, J = 3.1 Hz, 1H), 6.53 (d, J = 3.0, 0.8 Hz, 1H), 3.82 (s, 3H), 2.41 (t, J = 7.6 Hz, 2H), 1.25 (m, 2H), 1.13 (m, 2H), 0.72 (t, J = 7.3 Hz, 3H); ^{19}F NMR (400 MHz, $CDCl_3$): -39.9 (s, 3F); ^{13}C NMR (400 MHz, $CDCl_3$): 153.2, 141.6, 136.2, 130.3, 129.5 (q, $^{1}J_{CF}$ = 309.7 Hz), 129.3, 128.2, 128.1, 128.1, 127.2, 125.2, 123.2, 121.8, 36.5, 32.9, 30.2, 22.4, 13.7; HRMS (EI-EBE) m/z: $[M]^+$ Calc'd for $C_{22}H_{22}F_3NS$: 389.1425 Found: 389.1420.

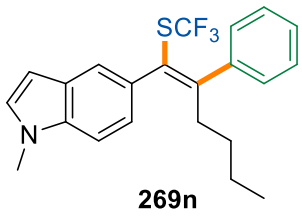

269n

(*Z*)-2-(2-phenyl-1-((trifluoromethyl)thio)hex-1-en-1-yl)thiophene (269o) Prepared by the reaction of 2-(hex-1-yn-1-yl)thiophene (33.0 mg, 0.200 mmol) with phenylmagnesium bromide following modified general procedure (carbomagnesiation at 60 °C). The title compound was isolated as a yellow oil (35.3 mg) after chromatography on silica gel (15 g column, 40/60 petroleum ether), containing **269o** (31.5 mg, 0.091 mmol, 46%) along with small amount of **268o** (3.8 mg, 0.015 mmol, 8%). Analytical data of **269o**: ^{1}H NMR (400 MHz, $CDCl_3$): 7.38 (m, 4H), 7.21 (m, 2H), 7.14 (dd, 1H), 7.03 (dd, 1H), 2.55 (t, J = 7.5 Hz, 2H), 1.31 (m, 2H), 1.21 (m, 2H), 0.78 (t, J = 7.2 Hz, 3H); ^{19}F NMR (400 MHz, $CDCl_3$): -40.8 (s, 3F); ^{13}C NMR (400 MHz, $CDCl_3$): 157.8, 141.5, 141.2, 129.2 (q, $^{1}J_{CF}$ = 310.8 Hz), 128.1, 127.9, 127.5, 126.6, 126.5, 126.3, 116.5, 37.2, 30.3, 22.4, 13.7; HRMS (EI-EBE) m/z: $[M]^+$ Calc'd for $C_{17}H_{17}F_3S_2$: 342.0724 Found: 342.0712. Indicative NMR signals of **268o**: ^{1}H NMR (400 MHz, $CDCl_3$): 7.46 (m, 2H), 7.32 (m, 2H), 7.27 (m, 2H), 7.06 (dd, 2H), 6.84 (s, 1H), 2.89 (t, J = 7.4 Hz, 2H), 1.48 (m, 4H), 0.92 (t, J = 7.2 Hz, 3H); ^{13}C NMR (400 MHz, $CDCl_3$: 143.2, 141.5, 140.9, 128.3, 128.1, 127.7, 127.1, 126.8, 124.8, 120.8, 31.3, 30.5, 22.9, 13.9.

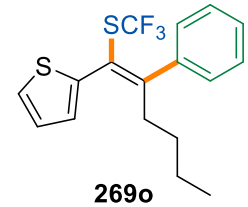

269o

((Z)-(1-(cyclohex-1-en-1-yl)-2-phenylhex-1-en-1-yl)(trifluoromethyl)sulfane (269p) Prepared by the reaction of 1-(hex-1-yn-1-yl)cyclohex-1-ene (32.4 mg, 0.199 mmol) with phenylmagnesium bromide following modified general procedure (carbomagnesation at 60 °C, 4h). The title compound was isolated as a colorless oil (14.5 mg, 0.042 mmol, 21%) after chromatography on silica gel (15 g column, 40/60 petroleum ether). Analytical data of **269p**: ^{1}H NMR (400 MHz, $CDCl_3$): 7.31 (m, 3H), 7.11 (m, 2H), 5.77 (t, 1H), 2.49 (t, 2H), 2.24 (m, 2H), 2.15 (m, 2H), 1.72 (m, 2H), 1.65 (m, 2H), 1.21 (m, 4H), 0.8 (t, J = 6.9 Hz, 3H); ^{19}F NMR (400 MHz, $CDCl_3$): -40.3 (s, 3F); ^{13}C NMR (400 MHz, $CDCl_3$): 151.4, 141.1, 135.2, 129.2 (q, $^{1}J_{CF}$ = 309.3 Hz), 128.7, 128.5, 128.2, 128.0, 127.1, 36.2, 30.4, 27.6, 25.4, 22.7, 22.4, 22.0, 13.7; HRMS (EI-EBE) m/z: $[M]^+$ Calc'd for $C_{19}H_{23}F_3S$: 340.1473 Found: 340.1466.

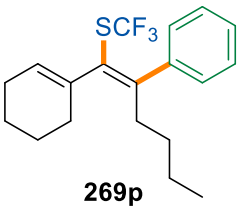

269p

(trifluoromethyl)(1,2,2-triphenylvinyl)sulfane (269q) Prepared by the reaction of diphenylacetylene (35.8 mg, 0.200 mmol) with phenylmagnesium bromide following general procedure. The title compound was isolated as a white solid (48.0 mg) after chromatography on silica gel (15 g column, 40/60 petroleum ether), containing **269q** (44.5 mg, 0.125 mmol, 63%) along with small amount of **268q** (3.4 mg, 0.013 mmol, 7%). Analytical data of **269q**: ^{1}H NMR (400 MHz, $CDCl_3$): 7.37 (m, 7H), 7.20 (m, 3H), 7.08 (m, 3H), 6.96 (dd, 2H); ^{19}F NMR (400 MHz, $CDCl_3$): -39.5 (s, 3F); ^{13}C NMR (400 MHz, $CDCl_3$): 152.4, 142.6, 141.4, 139.3, 130.5, 130.4, 129.6, 129.3 (q, $^{1}J_{CF}$ = 310.1 Hz), 128.2, 127.9, 127.8, 127.8, 127.7, 127.4, 126.1; HRMS (EI-EBE) m/z: $[M]^+$ Calc'd for $C_{21}H_{15}F_3S$: 356.0847 Found: 356.0839; Indicative NMR signals of **268q**: ^{1}H NMR (400 MHz, $CDCl_3$): 7.22 (m, 2H), 7.14 (m, 3H), 7.00 (s, 1H); ^{13}C NMR (400 MHz, $CDCl_3$): 143.4, 140.3, 137.4, 130.4, 129.5, 128.6, 128.2, 128.1, 127.6, 126.7.

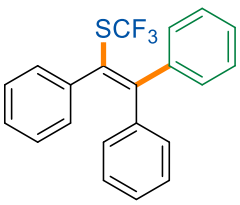

269q

(E)-(2-(4-methoxyphenyl)-1,2-diphenylvinyl)(trifluoromethyl)sulfane (269r) Prepared by the reaction of 4-methoxy diphenylacetylene (42.0 mg, 0.201 mmol) with phenyl magnesium bromide following general procedure. The title compound was isolated as a yellow oil (59.0 mg) after chromatography on silica gel (15g column, 60/90 petroleum ether/diethyl ether 99:1 to 96:4) containing **269r** and **269r'** (54.3 mg, 0.148 mmol, 74%, 7:3) along with small amount of **268r** and **268r'** (4.7 mg, 0.017 mmol, 9%). Analytical data of ***E*-269r**: ^{1}H NMR (400 MHz, $CDCl_3$): 7.37 (m, 10H), 6.87 (dd, 2H), 6.60 (dd, 2H), 3.71 (s, 3H); ^{19}F NMR (400 MHz, $CDCl_3$): -39.6 (s, 3H); ^{13}C NMR (400 MHz, $CDCl_3$): 158.8, 152.1, 142.9, 139.8, 133.7, 131.9, 130.4, 129.6, 129.3 (q, $^{1}J_{CF}$ = 310.8 Hz), 128.1 (d), 127.8, 127.1, 124.6, 113.2, 55.0; Analytical data of **269r'**: ^{1}H NMR (400 MHz, $CDCl_3$): 7.29 (dd, 2H), 7.22 (m, 5H), 7.09 (dd, 3H), 6.95 (dd, 2H), 6.72 (dd, 2H), 3.77 (s, 3H); ^{19}F NMR (400 MHz, $CDCl_3$): -39.5 (s, 3H); ^{13}C NMR (400 MHz, $CDCl_3$): 159.1, 151.2, 142.8, 141.7, 131.8, 131.6, 130.3, 129.6, 129.5, 129.4 (q), 128.2, 127.6 (d), 127.6, 113.4, 55.1; HRMS (EI-EBE) m/z: $[M]^+$ Calc'd for $C_{22}H_{17}F_3OS$: 386.0952 Found: 386.0950. Indicative NMR signals of **268r** and **268r'**:^{1}H NMR (400 MHz, $CDCl_3$): 7.15 (m, 8H), 6.92 (s, 1H), 6.66 (dd, 2H), 3.84 (s, 3H), *Z*- isomer 3.75 (s, 3H); ^{13}C NMR (400 MHz, $CDCl_3$): 132.5, 131.5, 130.8, 130.4, 128.7, 128.1, 127.9, 127.4, 126.6, 114.0, 113.4, 55.1.

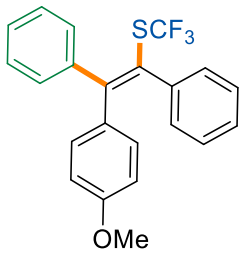

269r

(1-(naphthalen-2-yl)-2,2-diphenylvinyl)(trifluoromethyl)sulfane (269s) Prepared by the reaction of 2-(phenylethynyl)naphthalene (45.8 mg, 0.200 mmol) with phenyl magnesium bromide following general procedure. The title compound was isolated as a white solid (50.5 mg) after chromatography on silica gel (15g column, 60/90 petroleum ether) containing **269s** and **269s'** (45.6 mg, 0.112 mmol, 56%, 6:4) along with small amount of **268s** and **268s'** (4.9 mg, 0.016 mmol, 8%). Analytical data of **269s**: ^{1}H NMR (400 MHz, $CDCl_3$): 7.92 (s, 1H), 7.74 (dd, 2H), 7.65 (d, *J* = 8.6 Hz, 1H), 7.41 (m, 8H), 7.36 (m, 2H), 7.16 (m, 1H), 7.04 (m, 2H); ^{19}F NMR (400 MHz, $CDCl_3$): -39.4; ^{13}C NMR (400 MHz, $CDCl_3$): 152.9, 142.7, 141.4, 139.0, 130.5, 130.4, 129.8, 129.6, 129.3 (q, $^{1}J_{CF}$ = 310.8 Hz), 128.3 (d), 128.1, 127.9, 127.9, 127.9, 127.8, 127.6, 127.5, 126.4, 126.0; Analytical data of ***E*-269s'**: ^{1}H NMR (400 MHz, $CDCl_3$): 7.68 (s, 1H), 7.54 (d, *J* = 8.7 Hz, 2H), 7.08 (m, 1H), 6.99 (m, 2H); ^{19}F NMR (400 MHz, $CDCl_3$): -39.4; ^{13}C NMR (400 MHz, $CDCl_3$): 152.2, 139.3, 136.9, 133.0, 132.8, 132.6, 132.3, 130.2, 130.1, 128.2, 128.1(d), 128.0 (q), 127.2; HRMS (EI-EBE) m/z: $[M]^+$ Calc'd for $C_{25}H_{17}F_3S$: 406.1003 Found: 406.0995. Indicative NMR signals of **268s** and **268s'**: ^{13}C NMR (400 MHz, $CDCl_3$): 143.4, 143.0, 142.4, 140.4, 135.1, 129.6, 129.1, 128.7, 128.2, 128.0, 127.7, 127.1, 125.8 (d).

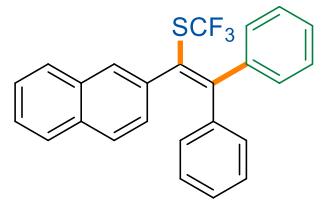

269s

(1-(naphthalen-1-yl)-2,2-diphenylvinyl)(trifluoromethyl)sulfane (269t) Prepared by the reaction of 1-(phenylethynyl)naphthalene (46.2 mg, 0.202 mmol) with phenyl magnesium bromide following general procedure. The title compound was isolated as a white solid (51 mg) after chromatography on silica gel (15g column, 60/90 petroleum ether) containing **269t** and **269t'** (47.3 mg, 0.116 mmol, 58%, 7:3) along with a small amount of **268t** and **268t'** (3.6 mg, 0.0118 mmol, 6%). Analytical data of **269t**: ^{1}H NMR (400 MHz, $CDCl_3$): 8.19 (d, *J* = 8.3 Hz, 1H), 7.77 (d, *J* = 8.2 Hz, 1H), 7.75 (d, *J* = 1.9 Hz, 1H), 7.43 (m, 10H), 7.02 (d, *J* = 2.6 Hz, 1H), 6.93 (d, *J* = 2.1 Hz, 3H); ^{19}F NMR (400 MHz, $CDCl_3$): -39.2 (s, 3F); ^{13}C NMR (400 MHz, $CDCl_3$): δ 153.7, 141.9, 141.1, 136.1, 133.5, 131.0, 129.7, 129.3 (q, $^{1}J_{CF}$ = 310.8 Hz), 129.2, 129.0, 128.3, 128.1, 127.9, 127.6, 126.2, 125.7, 125.3,125.1, 124.3; Analytical data of ***E*-269t'**: ^{1}H NMR (400 MHz, CDCl3) 8.00 (d, *J* = 9.0 Hz, 1H), 7.83 (d, *J* = 7.8 Hz, 1H), 7.67 (d, *J* = 8.1 Hz, 1H), 7.04 (d, *J* = 1.9 Hz, 1H), 7.01 (m, 1H), 6.95 (m, 1H), 6.91 (m, 1H); ^{19}F NMR (400 MHz, $CDCl_3$): -39.3 (s, 3F) ^{13}C NMR (400 MHz, $CDCl_3$): 151.4, 141.4, 139.6, 139.2, 133.5, 129.1, 129.1 (q, $^{1}J_{CF}$ = 311.8 Hz), 128.8, 128.5, 128.3, 128.1, 127.9, 127.7, 127.4, 126.6, 126.3, 125.7, 125.6, 125.0; HRMS (EI-EBE) m/z: $[M]^+$ Calc'd for $C_{25}H_{17}F_3S$: 406.1003 Found: 406.0997. Indicative NMR signals of **268t** and **268t'**: ^{1}H NMR (400 MHz, $CDCl_3$): 7.93 (dd, 2H), 7.04 (dd, 3H); ^{13}C NMR (400 MHz, $CDCl_3$): 142. 9, 140.4, 137.8, 137.0, 132.0, 129.8, 129.1, 127.8, 126.9, 126.3, 126.0, 125.9, 125.9.

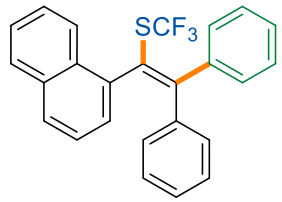

269t

Scope of Grignard reagent:

(*Z*)-(2-(4-methoxyphenyl)-1-phenylhex-1-en-1-yl) (trifluoromethyl)sulfane (269u) Prepared by the reaction of 1-phenyl-hexyne (31.8 mg, 0.200 mmol) with 4-methoxy phenyl magnesium bromide following general procedure. The title compound was isolated as a yellow oil (48.8 mg) after chromatography on silica gel (15g column, 60/90 petroleum ether/diethyl ether- 100 to 97:3) containing **269u** (47 mg, 0.128 mmol, 64%) along with a small amount of **268u** (1.8 mg, 0.006 mmol, 3%). Analytical data of **269u**: ^{1}H NMR (400 MHz, $CDCl_3$): 7.40 (m, 4H), 7.34 (m, 1H), 7.18 (dd, 2H), 6.96 (dd, 2H), 3.86 (s, 3H), 2.35 (t, J = 7.4 Hz, 2H), 1.18 (m, 4H), 0.72 (t, J = 7.2 Hz, 3H); ^{19}F NMR (400 MHz, $CDCl_3$): -39.9 (s, 3F); ^{13}C NMR (400 MHz, $CDCl_3$): 158.9, 153.9, 139.5, 133.2, 129.4, 129.3, 129.3 (q, $^{1}J_{CF}$ = 309.8 Hz), 128.1, 127.7, 123.5, 113.5, 55.1, 36.4, 30.2, 22.3, 13.7; HRMS (EI-EBE) m/z: $[M]^+$ Calc'd for $C_{20}H_{21}F_3OS$: 366.1265 Found 366.1261. Indicative NMR signals of **268u**: ^{1}H NMR (400 MHz, $CDCl_3$: 7.37 (m, 7H), 6.66 (s, 1H), 3.84 (s, 3H), 2.70 (t, J = 7.6 Hz, 2H), 1.40 (m, 4H), 0.87 (t, J = 7.2 Hz, 3H); ^{13}C NMR (400 MHz, $CDCl_3$): 142.7, 138.5, 135.4, 128.7, 127.6, 126.7, 126.3, 113.7, 55.2, 31.0, 29.9, 22.8, 13.8.

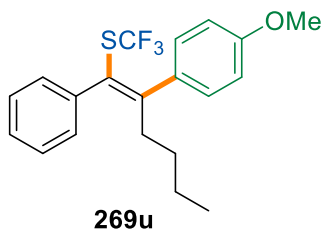

269u

(*Z*)-(2-(4-fluorophenyl)-1-phenylhex-1-en-1-yl)(trifluoromethyl)sulfane (269v) Prepared by the reaction of 1-phenyl-hexyne (32.2 mg, 0.203 mmol) with 4-fluoro phenyl magnesium bromide following general procedure. The title compound was isolated as a colorless oil (38.9 mg) after chromatography on silica gel (15g column, 40/60 petroleum ether) containing **269v** (35.0 mg, 0.203 mmol, 49%) along with a small amount of **268v** (3.9 mg, 0.015 mmol, 8%). Analytical data of **269v**: ^{1}H NMR (400 MHz, $CDCl_3$): 7.40 (m, 4H), 7.35 (m, 1H), 7.20 (m, 2H), 7.10 (m, 2H), 2.35 (t, J = 7.3 Hz, 2H), 1.18 (m, 4H), 0.72 (t, J = 7.2 Hz, 3H); ^{19}F NMR (400 MHz, $CDCl_3$): -40.0 (s, 3F), -114.4 (s, 1F); ^{13}C NMR (400 MHz, $CDCl_3$): 162.1 (d), 153.4, 139.1, 136.9 (d, J = 3.5 Hz), 129.3 (q, $^{1}J_{CF}$ = 309.9 Hz), 129.8 (d, J = 8.02 Hz), 129.2, 128.7, 128.2, 127.9, 126.5, 124.4, 115.2 (d), 36.4, 30.1, 22.3, 13.6 (d); HRMS (EI-EBE) m/z: $[M]^+$ Calc'd for $C_{19}H_{18}F_4S$: 354.1065 Found: 354.1053. Indicative NMR signals of **268v**: ^{1}H NMR (400 MHz, $CDCl_3$: 7.43 (m, 4H), 7.32 (d, 2H), 7.29 (d, 1H), 7.05 (m, 2H), 6.65 (s, 1H), 2.68 (t, J = 7.3 Hz, 2H), 1.35 (m, 4H), 0.85 (t, J = 7.2 Hz, 3H); ^{19}F NMR (400 MHz, $CDCl_3$): -115.7 (s, 1F); ^{13}C NMR (400 MHz, $CDCl_3$): 162.1 (d), 142.3, 139.1, 138.1, 128.1, 128.0, 115.1 (d), 30.8, 30.0, 22.7, 13.8.

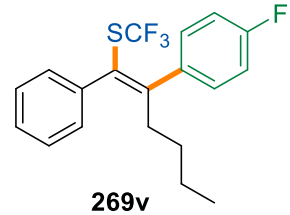

269v

(*Z*)-(1-phenyl-2-(p-tolyl)hex-1-en-1-yl)(trifluoromethyl)sulfane (269w) Prepared by the reaction of 1-phenyl-hexyne (31.9 mg, 0.201 mmol) with *p*-tolyl magnesium bromide following modified general procedure (carbomagnesiation done at rt, 4h). The title compound was isolated as a colorless oil (51 mg, 0.201 mmol, 73%) after chromatography on silica gel (15g column, 40/60 petroleum ether). Analytical data of **269w**: ^{1}H NMR (400 MHz, $CDCl_3$): 7.43 (m, 4H), 7.37 (m, 1H), 7.27 (d, J = 7.9 Hz, 2H), 7.16 (d, J = 8.0 Hz, 2H), 2.44 (s, 3H), 2.39 (t, J = 7.4 Hz, 2H), 1.22 (m, 4H), 0.75 (t, J = 7.2 Hz, 3H); ^{19}F NMR (400 MHz, $CDCl_3$): -39.9 (s, 3F) (s); ^{13}C NMR (400 MHz, $CDCl_3$): 154.3, 139.5, 138.1, 137.1, 129.3 (q, $^{1}J_{CF}$ = 309.9 Hz), 129.3, 128.9, 128.1, 128.0, 127.7, 123.5, 36.4, 30.1, 22.3, 21.2, 13.6; HRMS (EI-EBE) m/z: $[M]^+$ Calc'd for $C_{20}H_{21}F_3S$: 350.1316 Found: 350.1322.

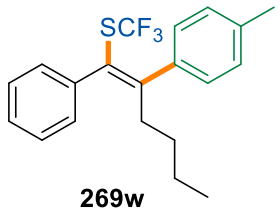

269w

(*Z*)-(1-phenyl-2-(o-tolyl)hex-1-en-1-yl)(trifluoromethyl)sulfane (269x) Prepared by the reaction of 1-phenyl-hexyne (31.9 mg, 0.201 mmol) with *o*-tolyl magnesium bromide following general procedure. The title compound was isolated as a light-yellow oil (50.0 mg) after chromatography on silica gel (15g column, 40/60 petroleum ether) containing **269x** (45.0 mg, 0.201 mmol, 64%) along with a small amount of **268x** (5.0 mg, 0.201 mmol, 10%). Analytical data of **269x**: ^{1}H NMR (400 MHz, $CDCl_3$): 7.43 (m, 4H), 7.37 (m, 1H), 7.28 (d, 2H), 7.24 (m, 1H), 7.06 (d, J = 6.9 Hz, 1H), 2.42 (ddd, 1H), 2.35 (s, 3H), 2.21 (ddd 1H), 1.24 (m, 4H), 0.73 (t, J = 7.3 Hz, 3H); ^{19}F NMR (400 MHz, $CDCl_3$): -39.2 (s, 3F) (s); ^{13}C NMR (400 MHz, $CDCl_3$): 152.3, 140.3, 138.7, 134.5, 130.2, 129.4 (q, $^{1}J_{CF}$ = 309.8), 129.4, 128.4, 128.2, 127.9, 127.5, 125.5, 125.1, 35.8, 29.8, 22.5, 19.1, 13.6; HRMS (EI-EBE) m/z: $[M]^+$ Calc'd for $C_{20}H_{21}F_3S$: 350.1316 Found: 350.1306. Indicative NMR signals of **268x**: ^{1}H NMR (400 MHz, $CDCl_3$: 7.35 (dd, 3H), 7.20 (dd, 4H), 6.36 (s, 1H), 2.60 (t, J = 7.1 Hz, 2H), 2.38 (s, 3H), 0.85 (t, J = 7.2 Hz, 3H); ^{13}C NMR (400 MHz, $CDCl_3$): 144.1, 143.9, 138.0, 135.2, 130.1, 129.1, 128.7, 128.6, 126.6, 126.4, 125.3, 125.1, 32.4, 30.3, 22.9, 19.9, 13.8.

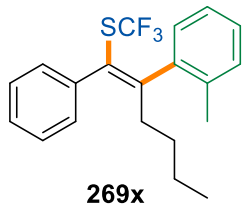

269x

(*Z*)-(2-mesityl-1-phenylhex-1-en-1-yl)(trifluoromethyl)sulfane (269y) Prepared by the reaction of 1-phenyl-hexyne (31.9 mg, 0.201 mmol) with mesityl magnesium bromide following general procedure (carbomagnesiation done at 75°C). The title compound was isolated as a colorless oil (38 mg, 0.200 mmol, 50%) after chromatography on silica gel (15g column, 40/60 petroleum ether). Analytical data of **269y**: ^{1}H NMR (400 MHz, $CDCl_3$): 7.42 (m, 4H), 7.35 (m, 1H), 6.93 (s, 2H), 2.33 (s, 3H) 2,26 ((s + t), 8H), 1.24 (m, 2H), 1.09 (m, 2H), 0.70 (t, J = 7.3 Hz, 3H); ^{19}F NMR (400 MHz, $CDCl_3$): -38.5 (s, 3F); ^{13}C NMR (400 MHz, $CDCl_3$): 149.8, 138.4, 136.8, 136.7, 134.7, 129.3 (q, $^{1}J_{CF}$ = 309.9 Hz), 129.3, 128.4, 128.2, 127.9, 125.6, 35.9, 29.9, 22.9, 21.0, 19.7, 13.6; HRMS (EI-EBE) m/z: $[M]^+$ Calc'd for $C_{22}H_{25}F_3S$: 378.1629 Found: 378.1625.

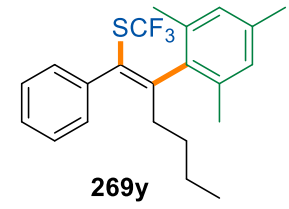

269y

((Z)-1-phenyl-2-((E)-prop-1-en-1-yl)hex-1-en-1-yl)(trifluoromethyl)sulfane (269z) Prepared by the reaction of 1-phenyl-hexyne (31.75 mg, 0.200 mmol) with prop-1-en-1-yl magnesium bromide following general procedure. The title compound was isolated as a colorless oil (23.5 mg, 0.200 mmol, 39%, *E:Z* 2:1) after chromatography on silica gel (15g column, 40/60 petroleum ether). Analytical data of ***Z*-269z**: ^{1}H NMR (400 MHz, $CDCl_3$: 7.32 (m, 5H), 7.04 (d, J = 13.9 Hz, 1H), 6.08 (dq, 1H), 2.26 (t, J = 8.0 Hz, 2H), 1.95 (dd, J = 5.0 Hz, 3H), 1.39 (m, 4H), 0.79 (t, 3H); ^{19}F NMR (400 MHz, $CDCl_3$): -40.4 (s, 3F); ^{13}C NMR (400 MHz, $CDCl_3$): 150.7, 140.8, 130.9, 129.7 (q, $^{1}J_{CF}$ = 302.8 Hz), 129.4, 129.1, 128.9, 128.0, 127.6, 127.4, 31.8, 30.6, 22.7, 18.8, 13.6; Analytical data of ***E*-269z':** ^{1}H NMR (400 MHz, $CDCl_3$: 5.76 (dq, 1H), 2.16 (t, J = 7.7 Hz, 2H), 1.73 (dd, J = 5.3 Hz, 3H), 1.19 (m, 4H), 0.79 (t, 3H); ^{19}F NMR (400 MHz, $CDCl_3$): -39.4 (s, 3F); ^{13}C NMR (400 MHz, $CDCl_3$): 149.3, 139.1, 131.1, 129.3 (q, $^{1}J_{CF}$ = 310.5 Hz), 128.7, 128.4, 127.9, 127.8, 125.9, 121.2, 34.4, 30.2, 22.4, 14.7, 13.7; HRMS (APCI-TOF) m/z: $[M - H]^+$ Calc'd for $C_{16}H_{18}F_3S$: 299.1086 Found: 299.1080.

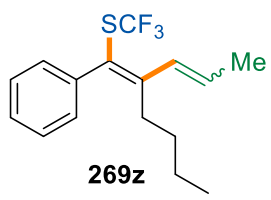

269z

4.4.4 Further transformations of the selected SCF_3-substituted olefins.

(Z)-(1-((trifluoromethyl)sulfinyl)hex-1-ene-1,2-diyl)dibenzene (272) In a 4mL dark vial add compound **269a** (23.6 mg, 0.070 mmol), 15% H_2O_2 (11.5 µl, 0.112 mmol, 1.6 eq), and CF_3COOH (0.7 mL) under argon. Stir the reaction for 24h at rt. The resultant was poured into DI water, neutralized with aq.$NaHCO_3$ and extracted with MTBE. The combined organic layers were dried over Na_2SO_4, concentrated, and the residue was purified by flash chromatography on silica gel (60/90 petroleum ether/ethyl acetate 97:3 to 94:6) to provide the desired product as a white solid (21.8 mg, 0.061 mmol, 88%). ^{1}H NMR (400 MHz, $CDCl_3$): δ 7.44 (m, 6H), 7.36 (dd, 2H), 7.23 (m, 2H), 2.39 (m, 2H), 1.18 (m, 4H), 0.71 (t, J = 7.2 Hz, 3H); ^{19}F NMR (376 MHz, $CDCl_3$) δ -67.89

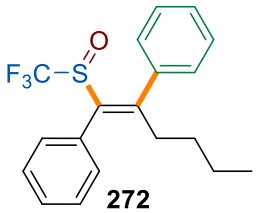

272

(s, 3F); ^{13}C NMR (400 MHz, $CDCl_3$): δ 160.7, 137.2, 136.7, 130.7, 130.3, 128.9, 128.8, 128.5, 128.2, 128.1, 125.2 (q, $^{1}J_{CF}$ = 337.9 Hz), 36.9, 29.5, 22.3, 13.5; HRMS (APCI-TOF) m/z: $[M + H]^+$ Calc'd for $C_{19}H_{20}F_3OS$: 353.1182 Found: 353.1189.

(Z)-(1-((trifluoromethyl)sulfonyl)hex-1-ene-1,2-diyl)dibenzene (273) In a 4mL dark vial add compound **269a** (18.5 mg, 0.055 mmol), mCPBA (57 mg, 0.330 mmol, 6 eq) and dry DCM (0.7 mL) under argon.

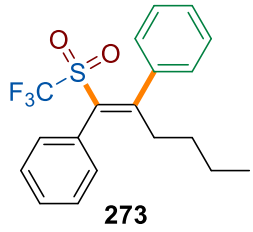

273

Close the vial with a cup. Heat the reaction at 65°C for 17h. The resultant was quenched with $NaHSO_3$ at 0°C. Workup with aq.$NaHCO_3$ and MTBE. The combined organic layers were dried over Na_2SO_4, concentrated, and the residue was purified by flash chromatography on silica gel (60/90 petroleum ether/diethyl ether 99.5: 0.5 to 94:6) to provide the desired product as a yellow solid (16.2 mg, 0.043 mmol, 80%). ^{1}H NMR (400 MHz, $CDCl_3$): 7.44 (m, 8H), 7.24 (dd, 2H), 2.29 (t, J = 7.5 Hz, 2H), 1.14 (m, 4H), 0.66 (t, J = 7.3 Hz, 3H); ^{19}F NMR (400 MHz, $CDCl_3$): -74.60 (s, 3F); ^{13}C NMR (400 MHz, $CDCl_3$): δ 166.4, 137.4, 132.1, 131.4, 131.3, 129.5, 128.6, 128.3, 127.7, 126.9, 119.9 (q, $^{1}J_{CF}$ = 329.2 Hz), 39.8, 29.1, 22.3, 13.4; HRMS (APCI-TOF) m/z: $[M - H]^+$ Calc'd for $C_{19}H_{18}F_3O_2S$: 367.0975 Found: 367.0982.

(Z)-N-(4,5-diphenyl-5-((trifluoromethyl)thio)pent-4-en-1-yl)-4-methyl-N-(oct-7-yn-1-yl)benzenesulfonamide (274) In a vial add compound **269e** (27.0 mg, 0.075 mmol) , 4-methyl-N-(oct-7-yn-1-yl)benzenesulfonamide (83.8 mg, 0.300 mmol, 4 eq), dry K_2CO_3 (41.5 mg, 0.300 mmol, 4 eq), NaI (2.5 mg, 0.015 mmol, 0.2 eq), ^{t}BuOH: toluene (1:1) 0.16 mL each.

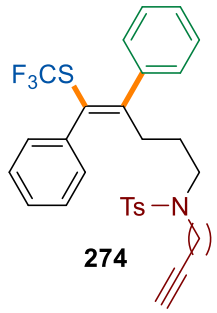

274

Close the vial with a cup. Heat it at 90°C for 72h. The temperature was further increased to 120°C and the resultant was heated for another 72h. After 6 days the reaction was cooled to rt. The reaction mixture was diluted with MTBE and extracted with HCl (1.0 M). The aqueous phase was neutralized with NaOH 1.0 M, extracted with MTBE, washed with brine and dried over Na_2SO_4. The residue was purified by flash chromatography on silica gel (60/90 petroleum ether/Ethyl acetate 90:10 to 85:15) to provide the desired product as a colorless oil (25.7 mg, 0.042 mmol, 57%). ^{1}H NMR (400 MHz, $CDCl_3$): 7.54 (d, 2H), 7.39 (m, 8H), 7.22 (m, 4H), 2.85 (m, 4H), 2.40 (s, 3H), 2.35 (t, J = 7.8 Hz, 2H), 2.15 (td, 2H), 1.95 (t, J = 2.7 Hz, 1H), 1.45 (m, 4H), 1.25 (m, 4H), 1.11 (m, 2H); ^{19}F NMR (400 MHz, $CDCl_3$): -39.8 (s, 3F); ^{13}C NMR (400 MHz, $CDCl_3$): δ 152.5, 143.0, 140.4, 138.9, 136.7, 129.5, 129.2, 129.1 (q, $^{1}J_{CF}$ = 310.1 Hz), 128.3 (d), 128.1 (d), 127.7, 127.0, 124.8, 84.4, 68.3, 47.9, 47.7, 33.8, 28.2, 28.2, 28.1, 26.8, 26.0, 21.4, 18.2; HRMS (APCI-TOF) m/z: $[M + H]^+$ Calc'd for $C_{33}H_{37}F_3NO_2S_2$: 600.2213 Found: 600.2221.

(Z)-1-(4'-(2-phenyl-1-((trifluoromethyl)thio)hex-1-en-1-yl)-[1,1'-biphenyl]-4-yl)ethan-1-one (275) In a vial add Pd-G3-Xphos (2.0 mg 0.001 mmol, 3.5 mol%). Then add compound **269k** (33.9 mg, 0.0700 mmol), 4-acetyl phenyl boronic acid (17.5 mg, 0.106 mmol, 1.5 eq), THF (0.14 mL), followed by 0.5M K_3PO_4 solution (30.7 mg, 0.140 mmol, 2 eq) in degassed water (0.28 mL). Heat it at 40°C for 2.5h. Cool it to rt. Pour the reaction mixture in DI water and extract the organic layer with MTBE and dry over Na_2SO_4. Purify the residue with flash chromatography on silica gel (60/90 petroleum ether/ethyl acetate 97:3 to 92:8) to provide the desired product as a light-yellow oil (29.0 mg, 0.063 mmol, 90%). ^{1}H NMR (400 MHz, $CDCl_3$): 8.05 (d, J = 8.3 Hz, 2H), 7.75 (d, J = 8.1 Hz, 2H), 7.68 (d, J = 8.1 Hz, 2H), 7.52 (d, J = 8.0 Hz, 2H), 7.42 (m, 2H), 7.36 (m, 1H), 7.25 (d, J = 6.9 Hz, 2H), 2.65 (s, 3H), 2.42 (t, J = 7.3 Hz, 2H), 1.26 (m, 2H), 1.16 (m, 2H), 0.73 (t, J = 7.2 Hz, 3H); ^{19}F NMR (400 MHz, $CDCl_3$): -39.9; ^{13}C NMR (400 MHz, $CDCl_3$): δ 197.6, 155.1, 145.0, 140.9, 139.4, 139.1, 136.0, 129.9, 129.2 (q, $^{1}J_{CF}$ = 310.1 Hz), 128.9, 128.2, 128.0, 127.5, 127.1, 127.0, 123.2, 36.6, 30.1, 26.6, 22.3, 13.6; HRMS (EI-EBE) m/z: $[M]^+$ Calc'd for $C_{27}H_{25}F_3OS$: 454.1578 Found: 454.1566.

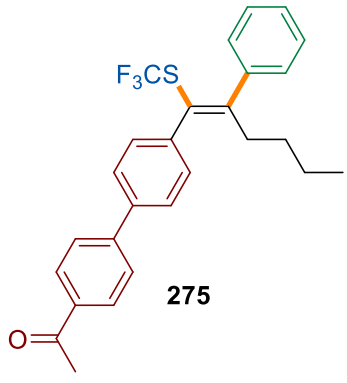

275

4.4.5 X-ray Crystallographic Data for compound 273

Crystal Data and Experimental[414]

R_1=9.41%

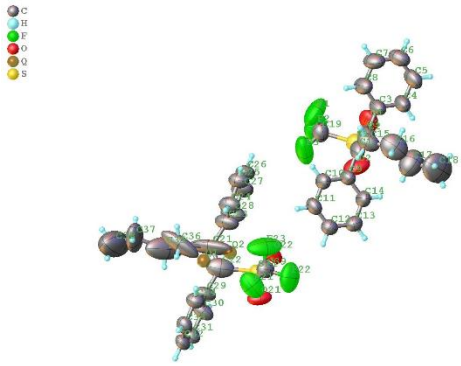

Experimental. Single colourless needle-shaped crystals of **273** were obtained by recrystallisation from diethyl ether. A suitable crystal 0.41×0.16×0.04 mm^3 was selected and loop on an XtaLAB Synergy, Dualflex, HyPix-Arc 150 diffractometer. The crystal was kept at a steady T = 298 K during data collection. The structure was solved with the ShelXT (Sheldrick, 2015) structure solution program using the Intrinsic Phasing solution methods solution method and by using **Olex2** (Dolomanov et al., 2009) as the graphical interface. The model was refined with version 2018/3 of ShelXL 2018/3 (Sheldrick, 2015) using Least Squares minimisation.

Crystal Data. $C_{19}H_{19}F_3O_2S$, M_r = 368.40, tetragonal, $I4_1/a$ (No. 88), a = 50.5323(14) Å, b = 50.5323(14) Å, c = 5.9145(2) Å, $\alpha = \beta = \gamma = 90^\circ$, V = 15102.8(10) Å^3, T = 298 K, Z = 32, Z' = 2, μ(Cu K$_\alpha$) = 1.863, 44861 reflections measured, 7369 unique (R_{int} = 0.0838) which were used in all calculations. The final wR_2 was 0.2999 (all data) and R_1 was 0.0941 (I > 2(I)).

Compound	**273**
Formula	$C_{19}H_{19}F_3O_2S$
$D_{calc.}$/ g cm^{-3}	1.296
μ/mm^{-1}	1.863
Formula Weight	368.40
Colour	colourless
Shape	needle
Size/mm^3	0.41×0.16×0.04
T/K	298
Crystal System	tetragonal
Space Group	$I4_1/a$
a/Å	50.5323(14)
b/Å	50.5323(14)
c/Å	5.9145(2)
α/°	90
β/°	90
γ/°	90
V/Å^3	15102.8(10)
Z	32
Z'	2
Wavelength/Å	1.54184
Radiation type	Cu K$_\alpha$
Θ_{min}/°	2.473
Θ_{max}/°	76.725
Measured Refl.	44861
Independent Refl.	7369
Reflections with I > 2(I)	3552
R_{int}	0.0838
Parameters	454
Restraints	9
Largest Peak	0.680
Deepest Hole	-0.613
GooF	1.059
wR_2 (all data)	0.2999
wR_2	0.2486
R_1 (all data)	0.1657
R_1	0.0941

Structure Quality Indicators

Reflections:	d min (CuKα) 2Θ=153.4° 0.79	I/σ(I) 12.3	Rint m=6.38 8.38%	Full 135.4° 92% to 153.4° 99.4
Refinement:	Shift 1.819	Max Peak 0.7	Min Peak -0.6	GooF 1.059

Experimental Extended. A colourless needle-shaped crystal with dimensions 0.41×0.16×0.04 mm^3 was loop. Data were collected using an XtaLAB Synergy, Dualflex, HyPix-Arc 150 diffractometer operating at $T = 298$ K.

Data were measured using ω scans of 0.5° per frame for 0.3 s using Cu K_α radiation. The diffraction pattern was indexed and the total number of runs and images was based on the strategy calculation from the program CrysAlisPro (Rigaku, V1.171.44.85a, 2024) The maximum resolution that was achieved was $\Theta = 76.725^\circ$ (0.79 Å).

The diffraction pattern was indexed and the unit cell was refined on 3552 reflections, 92.3% of the observed reflections.

Data reduction, scaling and absorption corrections were performed using CrysAlisPro (Rigaku, V1.171.44.85a, 2024). The final completeness is 99.40 % out to 76.725° in Θ. A gaussian absorption correction was performed using CrysAlisPro 1.171.44.85a (Rigaku Oxford Diffraction, 2024). Numerical absorption correction based on gaussian integration over a multifaceted crystal model. Empirical absorption correction using spherical harmonics, implemented in SCALE3 ABSPACK scaling algorithm. The absorption coefficient μ of this material is 1.863 mm^{-1} at this wavelength (λ = 1.542 Å) and the minimum and maximum transmissions are 0 and 0.

The structure was solved and the space group $I4_1/a$ (# 88) determined by the ShelXT (Sheldrick, 2015) structure solution program using Intrinsic Phasing methods and refined by Least Squares using version 2018/3 of ShelXL 2018/3 (Sheldrick, 2015). All non-hydrogen atoms were refined anisotropically. Hydrogen atom positions were calculated geometrically and refined using the riding model. Hydrogen atom positions were calculated geometrically and refined using the riding model.

Table 4.4.5.1: Fractional Atomic Coordinates (×10^4) and Equivalent Isotropic Displacement Parameters (Å²×10^3) for **273**. U_{eq} is defined as 1/3 of the trace of the orthogonalised U_{ij}.

Atom	x	y	z	U_{eq}
S1	3403.0(3)	2291.0(3)	7920(2)	79.8(5)
S21	2791.7(2)	3827.1(2)	3211(2)	63.2(4)
F1	3173.5(11)	2088.2(13)	4433(9)	180(2)
F2	2938.0(9)	2098.5(11)	7313(9)	156.4(19)
F3	3006.4(11)	2439.9(11)	5412(13)	199(3)
F21	3030.3(8)	4126.6(9)	239(8)	140.9(17)
F22	3272.5(8)	3968.4(12)	2688(9)	166(2)
F23	3141.2(11)	3730.4(10)	96(10)	186(3)
O1	3490.9(11)	2039.4(9)	8576(9)	136.2(19)
O2	3319.0(12)	2471.5(11)	9572(9)	144(2)
O21	2747.9(9)	4050.3(8)	4554(7)	108.1(15)
O22	2867.1(9)	3587.9(8)	4209(9)	120.9(17)

Atom	x	y	z	U_{eq}
C1	3625.2(16)	2481.5(15)	6070(12)	109(2)
C2	3809.4(16)	2380.8(16)	5089(13)	116(3)
C3	3892.1(14)	2086.2(13)	5227(11)	105(2)
C4	4046.8(14)	1991.7(13)	6940(12)	108(2)
C5	4153.3(15)	1740.5(14)	6825(13)	116(2)
C6	4110.6(17)	1585.6(15)	5001(14)	118(2)
C7	3950.8(17)	1673.5(14)	3306(13)	121(3)
C8	3842.3(16)	1926.3(14)	3408(11)	118(3)
C9	3556.1(13)	2778.9(11)	5948(10)	87.5(17)
C10	3410.3(12)	2877.8(11)	4170(9)	83.9(16)
C11	3334.2(11)	3139.7(11)	4179(10)	83.7(16)
C12	3404.0(12)	3301.0(11)	5922(10)	84.1(16)
C13	3552.0(12)	3206.3(12)	7665(11)	87.1(17)
C14	3628.3(12)	2945.6(12)	7683(10)	90.8(18)
C15	3992.0(17)	2551.4(14)	3465(12)	109(2)
C16	4262(3)	2606(2)	4160(20)	181(4)
C17	4314(2)	2698(3)	6240(20)	187(5)
C18	4608(2)	2765(2)	6770(30)	251(7)
C19	3114.6(15)	2226.6(16)	6170(14)	101(2)
C21	2410(3)	3627.0(14)	621(18)	262(9)
C22	2498.3(17)	3831.9(15)	1298(15)	137(3)
C23	2550.3(17)	3362.8(12)	844(12)	113(2)
C24	2712.9(15)	3265.6(12)	-806(11)	104(2)
C25	2787.0(14)	3005.9(13)	-774(12)	100(2)
C26	2703.0(15)	2840.5(12)	895(14)	103(2)
C27	2541.5(16)	2932.4(12)	2528(13)	110(2)
C28	2464.4(16)	3191.7(14)	2498(12)	118(3)
C29	2373.2(13)	4112.7(10)	995(12)	92.5(18)
C30	2219.5(12)	4210.0(12)	2668(12)	97(2)
C31	2123.9(11)	4463.7(11)	2594(10)	79.9(15)
C32	2180.6(10)	4621.5(11)	822(10)	76.3(15)
C33	2335.2(11)	4528.6(11)	-891(10)	81.4(16)
C34	2429.0(12)	4271.7(11)	-858(10)	82.9(16)
C35	1986(3)	3665(3)	-1150(30)	274(11)
C36	2224(2)	3672.9(19)	-1747(19)	237(8)
C37	1784(2)	3620(3)	-3370(30)	214(7)
C38	1556(4)	3672(3)	-3620(50)	393(17)
C39	3071.4(12)	3915.4(13)	1379(12)	86.3(16)

Table 4.4.5.2: Anisotropic Displacement Parameters ($\times 10^4$) **273** The anisotropic displacement factor exponent takes the form: $-2\pi^2[h^2a^{*2} \times U_{11} + ... + 2hka^* \times b^* \times U_{12}]$

Atom	U_{11}	U_{22}	U_{33}	U_{23}	U_{13}	U_{12}
S1	95.1(11)	78.8(10)	65.3(8)	2.5(7)	-3.8(7)	-3.4(8)
S21	66.7(8)	58.4(7)	64.3(7)	0.4(6)	-4.8(6)	5.5(6)
F1	148(4)	264(7)	127(4)	-71(4)	-23(3)	-42(4)
F2	116(3)	187(5)	166(4)	26(4)	2(3)	-57(3)
F3	144(4)	149(4)	302(8)	78(5)	-104(5)	-17(3)
F21	119(3)	145(4)	158(4)	68(3)	46(3)	7(3)
F22	80(3)	242(6)	175(4)	24(4)	-11(3)	-40(3)

Atom	U_{11}	U_{22}	U_{33}	U_{23}	U_{13}	U_{12}
F23	177(5)	136(4)	245(6)	-79(4)	136(4)	-32(3)
O1	156(5)	94(3)	158(4)	41(3)	-50(4)	9(3)
O2	178(5)	134(4)	120(4)	-58(3)	31(4)	-11(4)
O21	136(4)	78(3)	110(3)	-36(2)	41(3)	-10(2)
O22	110(3)	91(3)	162(4)	60(3)	2(3)	31(2)
C1	118(6)	117(6)	93(4)	-24(4)	-45(4)	33(5)
C2	117(6)	128(6)	103(5)	-34(5)	-40(5)	44(5)
C3	134(6)	91(4)	90(4)	-17(4)	-31(4)	46(4)
C4	128(6)	96(5)	98(4)	-14(4)	-39(4)	43(4)
C5	136(6)	106(5)	106(5)	14(5)	-19(5)	48(5)
C6	154(7)	88(5)	113(5)	-2(4)	-1(5)	42(5)
C7	173(8)	89(5)	101(5)	-26(4)	-9(5)	24(5)
C8	172(7)	94(5)	87(4)	-14(4)	-40(5)	37(5)
C9	112(5)	65(3)	86(4)	-5(3)	-29(3)	20(3)
C10	104(4)	74(4)	73(3)	-2(3)	-25(3)	14(3)
C11	90(4)	77(4)	84(4)	11(3)	-12(3)	22(3)
C12	87(4)	71(4)	94(4)	-5(3)	-8(3)	9(3)
C13	92(4)	76(4)	94(4)	-15(3)	-11(3)	3(3)
C14	109(5)	80(4)	84(4)	-8(3)	-34(3)	13(3)
C15	129(6)	91(5)	109(5)	20(4)	29(5)	21(4)
C16	159(11)	181(11)	203(13)	31(10)	47(10)	-1(8)
C17	170(11)	229(13)	162(10)	-26(10)	-5(9)	-13(9)
C18	136(9)	213(13)	400(20)	8(14)	12(12)	-54(9)
C19	99(5)	99(5)	107(5)	13(4)	-20(4)	-1(4)
C21	550(30)	54(5)	179(11)	22(6)	129(14)	53(9)
C22	161(8)	101(6)	148(7)	8(5)	70(6)	-7(5)
C23	183(8)	61(4)	96(5)	10(4)	18(5)	25(4)
C24	150(6)	71(4)	91(4)	12(3)	8(4)	7(4)
C25	122(6)	70(4)	108(5)	-9(4)	7(4)	13(4)
C26	120(6)	55(3)	134(6)	-7(4)	-18(5)	7(3)
C27	157(7)	59(4)	115(5)	7(4)	1(5)	-3(4)
C28	169(7)	82(5)	104(5)	-4(4)	35(5)	24(5)
C29	105(5)	51(3)	121(5)	2(3)	28(4)	9(3)
C30	94(4)	78(4)	117(5)	31(4)	32(4)	24(3)
C31	73(4)	80(4)	87(4)	-1(3)	5(3)	23(3)
C32	63(3)	66(3)	100(4)	0(3)	-11(3)	16(3)
C33	84(4)	75(4)	85(4)	18(3)	-10(3)	5(3)
C34	94(4)	70(4)	85(4)	-5(3)	6(3)	14(3)
C35	163(11)	174(11)	480(30)	-102(15)	144(17)	-52(9)
C36	293(16)	153(9)	264(14)	131(10)	162(13)	135(10)
C37	130(9)	190(11)	321(17)	38(11)	-121(11)	-46(8)
C38	243(19)	247(19)	690(50)	-170(20)	-130(30)	28(15)
C39	75(4)	81(4)	103(4)	-3(4)	7(4)	-3(3)

Table 4.4.5.3: Bond Lengths in Å for **273**.

Atom	Atom	Length/Å	Atom	Atom	Length/Å
S1	O1	1.401(4)	S1	C19	1.817(7)
S1	O2	1.403(5)	S21	O21	1.397(4)
S1	C1	1.839(9)	S21	O22	1.398(4)

Atom	Atom	Length/Å
S21	C22	1.865(10)
S21	C39	1.836(6)
F1	C19	1.278(8)
F2	C19	1.293(8)
F3	C19	1.289(8)
F21	C39	1.279(7)
F22	C39	1.305(7)
F23	C39	1.255(7)
C1	C2	1.209(9)
C1	C9	1.544(9)
C2	C3	1.548(9)
C2	C15	1.586(11)
C3	C4	1.366(8)
C3	C8	1.369(8)
C4	C5	1.380(8)
C5	C6	1.350(10)
C6	C7	1.361(10)
C7	C8	1.392(9)
C9	C10	1.378(7)
C9	C14	1.376(8)
C10	C11	1.378(7)
C11	C12	1.360(7)
C12	C13	1.360(8)
C13	C14	1.373(8)
C15	C16	1.452(13)
C16	C17	1.338(13)
C17	C18	1.553(14)
C21	C22	1.196(9)
C21	C23	1.517(9)
C21	C36	1.702(13)
C22	C29	1.563(9)
C23	C24	1.367(9)
C23	C28	1.376(9)
C24	C25	1.365(8)
C25	C26	1.362(9)
C26	C27	1.347(9)
C27	C28	1.367(9)
C29	C30	1.351(8)
C29	C34	1.388(8)
C30	C31	1.371(7)
C31	C32	1.348(7)
C32	C33	1.363(7)
C33	C34	1.383(7)
C35	C36	1.257(13)
C35	C37	1.68(2)
C37	C38	1.194(16)

Table 4.4.5.4: Bond Angles in ° for **273**

Atom	Atom	Atom	Angle/°
O1	S1	O2	119.5(4)
O1	S1	C1	116.5(3)
O1	S1	C19	104.4(3)
O2	S1	C1	105.0(3)
O2	S1	C19	105.7(4)
C19	S1	C1	104.1(3)
O21	S21	O22	120.1(3)
O21	S21	C22	102.0(3)
O21	S21	C39	105.1(3)
O22	S21	C22	118.9(3)
O22	S21	C39	104.5(3)
C39	S21	C22	104.5(3)
C2	C1	S1	122.3(7)
C2	C1	C9	124.1(8)
C9	C1	S1	113.5(5)
C1	C2	C3	125.9(9)
C1	C2	C15	120.6(8)
C3	C2	C15	113.4(6)
C4	C3	C2	122.0(6)
C4	C3	C8	118.8(6)
C8	C3	C2	118.4(6)
C3	C4	C5	120.6(6)
C6	C5	C4	120.7(6)
C5	C6	C7	119.6(6)
C6	C7	C8	120.1(7)
C3	C8	C7	120.2(6)
C10	C9	C1	120.6(5)
C14	C9	C1	120.1(5)
C14	C9	C10	119.2(5)
C9	C10	C11	119.6(5)
C12	C11	C10	120.4(5)
C11	C12	C13	120.4(5)
C12	C13	C14	119.8(6)
C13	C14	C9	120.5(5)
C16	C15	C2	118.5(7)
C17	C16	C15	120.8(11)
C16	C17	C18	116.7(13)
F1	C19	S1	111.7(6)
F1	C19	F2	107.9(7)
F1	C19	F3	106.1(7)
F2	C19	S1	110.2(5)
F3	C19	S1	112.8(6)
F3	C19	F2	107.9(7)
C22	C21	C23	124.0(11)

Atom	Atom	Atom	Angle/°
C22	C21	C36	111.2(8)
C23	C21	C36	116.7(7)
C21	C22	S21	119.2(8)
C21	C22	C29	126.7(9)
C29	C22	S21	113.8(5)
C24	C23	C21	122.3(7)
C24	C23	C28	118.1(6)
C28	C23	C21	117.9(8)
C25	C24	C23	120.1(6)
C26	C25	C24	121.0(7)
C27	C26	C25	119.8(6)
C26	C27	C28	119.6(7)
C27	C28	C23	121.4(7)
C30	C29	C22	118.6(6)
C30	C29	C34	119.0(5)
C34	C29	C22	122.3(6)
C29	C30	C31	121.3(6)
C32	C31	C30	120.2(5)
C31	C32	C33	119.8(5)
C32	C33	C34	120.6(5)
C33	C34	C29	119.0(5)
C36	C35	C37	111.6(15)
C35	C36	C21	107.1(12)
C38	C37	C35	131(2)
F21	C39	S21	112.9(4)
F21	C39	F22	105.6(6)
F22	C39	S21	107.4(5)
F23	C39	S21	113.1(5)
F23	C39	F21	110.4(6)
F23	C39	F22	107.0(6)

Table 4.4.5.5: Torsion Angles in ° for **273**.

Atom	Atom	Atom	Atom	Angle/°
S1	C1	C2	C3	-1.0(10)
S1	C1	C2	C15	178.6(5)
S1	C1	C9	C10	-98.3(6)
S1	C1	C9	C14	78.3(7)
S21	C22	C29	C30	-77.4(7)
S21	C22	C29	C34	98.2(7)
O1	S1	C1	C2	14.7(7)
O1	S1	C1	C9	-164.1(4)
O1	S1	C19	F1	-60.8(7)
O1	S1	C19	F2	59.1(7)
O1	S1	C19	F3	179.8(7)
O2	S1	C1	C2	149.4(6)
O2	S1	C1	C9	-29.3(5)
O2	S1	C19	F1	172.3(6)
O2	S1	C19	F2	-67.8(6)
O2	S1	C19	F3	52.9(8)
O21	S21	C22	C21	-148.6(9)
O21	S21	C22	C29	24.4(5)
O21	S21	C39	F21	-55.7(6)
O21	S21	C39	F22	60.2(5)
O21	S21	C39	F23	178.1(6)
O22	S21	C22	C21	-13.9(10)
O22	S21	C22	C29	159.1(5)
O22	S21	C39	F21	177.0(5)
O22	S21	C39	F22	-67.1(6)
O22	S21	C39	F23	50.8(7)
C1	S1	C19	F1	61.9(7)
C1	S1	C19	F2	-178.2(6)
C1	S1	C19	F3	-57.5(7)
C1	C2	C3	C4	-83.4(10)

Atom	Atom	Atom	Atom	Angle/°
C1	C2	C3	C8	106.7(9)
C1	C2	C15	C16	110.4(10)
C1	C9	C10	C11	175.2(6)
C1	C9	C14	C13	-175.5(6)
C2	C1	C9	C10	82.9(9)
C2	C1	C9	C14	-100.5(9)
C2	C3	C4	C5	-169.2(7)
C2	C3	C8	C7	169.5(8)
C2	C15	C16	C17	-49.1(15)
C3	C2	C15	C16	-70.0(9)
C3	C4	C5	C6	1.2(12)
C4	C3	C8	C7	-0.7(13)
C4	C5	C6	C7	-3.1(13)
C5	C6	C7	C8	3.0(13)
C6	C7	C8	C3	-1.1(13)
C8	C3	C4	C5	0.7(12)
C9	C1	C2	C3	177.7(5)
C9	C1	C2	C15	-2.8(11)
C9	C10	C11	C12	0.5(9)
C10	C9	C14	C13	1.2(10)
C10	C11	C12	C13	0.7(9)
C11	C12	C13	C14	-0.9(9)
C12	C13	C14	C9	0.0(10)
C14	C9	C10	C11	-1.4(10)
C15	C2	C3	C4	97.0(9)
C15	C2	C3	C8	-72.9(9)
C15	C16	C17	C18	-176.7(9)
C19	S1	C1	C2	-99.7(7)
C19	S1	C1	C9	81.5(5)
C21	C22	C29	C30	94.9(12)
C21	C22	C29	C34	-89.5(11)
C21	C23	C24	C25	-165.4(8)
C21	C23	C28	C27	166.7(8)
C22	S21	C39	F21	51.3(6)
C22	S21	C39	F22	167.3(5)
C22	S21	C39	F23	-74.9(6)
C22	C21	C23	C24	-92.2(13)
C22	C21	C23	C28	102.8(13)
C22	C21	C36	C35	-101.8(13)
C22	C29	C30	C31	174.1(6)
C22	C29	C34	C33	-172.8(6)
C23	C21	C22	S21	-12.1(15)
C23	C21	C22	C29	176.0(7)
C23	C21	C36	C35	108.1(12)
C23	C24	C25	C26	-0.5(11)
C24	C23	C28	C27	1.0(13)
C24	C25	C26	C27	0.9(11)
C25	C26	C27	C28	-0.3(11)
C26	C27	C28	C23	-0.7(12)
C28	C23	C24	C25	-0.4(12)
C29	C30	C31	C32	0.5(10)

Atom	Atom	Atom	Atom	Angle/°
C30	C29	C34	C33	2.8(10)
C30	C31	C32	C33	-0.5(9)
C31	C32	C33	C34	1.7(9)
C32	C33	C34	C29	-2.8(9)
C34	C29	C30	C31	-1.7(10)
C36	C21	C22	S21	-159.6(6)
C36	C21	C22	C29	28.5(14)
C36	C21	C23	C24	53.7(13)
C36	C21	C23	C28	-111.3(10)
C36	C35	C37	C38	-157(2)
C37	C35	C36	C21	-163.5(9)
C39	S21	C22	C21	102.1(9)
C39	S21	C22	C29	-84.9(5)

Table 4.4.5.6: Hydrogen Fractional Atomic Coordinates (×10⁴) and Equivalent Isotropic Displacement Parameters (Å²×10³) for **273**. U_{eq} is defined as 1/3 of the trace of the orthogonalised U_{ij}.

Atom	x	y	z	U_{eq}
H4	4080.71	2097.44	8193.52	129
H5	4255.47	1677.34	8016.05	139
H6	4189.89	1419.9	4902.25	142
H7	3914.07	1564.38	2079.42	145
H8	3735.7	1986.9	2235.42	141
H10	3363.43	2768.44	2970.67	101
H11	3234.52	3206.63	2986.99	100
H12	3350.23	3476.96	5921.57	101
H13	3601.32	3318	8841.28	105
H14	3729.53	2881.15	8874.89	109
H15A	3999.34	2461.93	2015.66	131
H15B	3904.67	2719.93	3218.35	131
H16A	4361.3	2443.01	3983.35	217
H16B	4334.6	2731.83	3092.68	217
H17A	4254.18	2568.22	7327.23	225
H17B	4210.25	2857.29	6467.57	225
H18A	4615.6	2912.58	7784.5	376
H18B	4698.62	2808.14	5391.55	376
H18C	4691.11	2614.1	7458.64	376
H24	2773.15	3376.49	-1950.07	124
H25	2896.55	2941.01	-1910.03	120
H26	2756.88	2664.49	907.73	123
H27	2482.8	2820.22	3669.5	132
H28	2351.34	3253.84	3619.89	142
H30	2177.65	4102.68	3894.48	116
H31	2019.56	4527.18	3770.96	96
H32	2114.41	4793.09	768.71	92
H33	2377.93	4639.2	-2093.86	98
H34	2528.07	4206.3	-2059.84	99
H35A	1940.04	3829.91	-402.72	329
H35B	1960.73	3522.41	-79.98	329
H36A	2265.17	3842.62	-2431.12	284
H36B	2260.83	3534.73	-2842.25	284
H37A	1872.73	3707.81	-4615.91	257

Atom	x	y	z	U_{eq}
H37B	1795.73	3432.16	-3692.28	257
H38A	1478.99	3553.48	-4701.71	589
H38B	1539.04	3851	-4153.54	589
H38C	1464.93	3654.9	-2199.7	589

4.5 *syn*-Selective α-Boration-Arylation of Alkynes

4.5.1 Synthesis of alkynes

Trimethyl((6-phenylhex-5-yn-1-yl)oxy)silane A flame dried 100 mL round bottom flask was evacuated and backfilled with argon (the cycle was performed twice) and then charged under positive pressure of argon with 6-phenylhex-5-yn-1-ol (2.2 g, 12.7 mmol) followed by dichloromethane (38 mL). The resultant was cooled to 0 °C. Then triethyl amine (2.8 g, 27.896 mmol, 2.2 eq., 3.8 mL) was added dropwise. The reaction mixture was stirred for 5 min at 0 °C. Then TMSCl (2.20 g, 20.288 mmol, 1.6 eq., 2.6 mL) was added dropwise. The reaction was removed from the cooling bath and allowed to stir for 3 h at r.t. Then it was diluted with water and extracted with MTBE. The combined organic layers were dried over Na_2SO_4, concentrated, and the residue was purified by chromatography on silica gel (60/90 petroleum ether/ethyl acetate 98:2 to 90:10) to provide the desired product as yellow oil. ^{1}H NMR (400 MHz $CDCl_3$): δ 7.39 (m, 2H), 7.27 (m, 3H), 3.64 (t, J = 6.1 Hz, 2H), 2.44 (t, J = 6.6 Hz, 2H), 1.68 (m, 4H), 0.12 (s, 9H); ^{13}C NMR (101 MHz, $CDCl_3$): δ 131.5, 128.1, 127.5, 124.0, 90.0, 80.8, 62.1, 31.8, 25.2, 19.2, -0.4; HRMS (APCI-TOF) m/z: $[M + H]^+$ Calc'd for $C_{15}H_{23}OSi$: 247.1518 Found: 247.1519.

4.5.2 Procedures for evaluation of reaction conditions

Evaluation of reaction conditions for Ni-catalysed carbomagnesiation of alkynes

General Procedure: In a glove box after standard cycles of evacuation and back-fill with pure N_2, catalyst was introduced into a 10-ml round bottom flask with a magnetic stirring bar. To the catalyst were added alkyne (1.0 mmol), ligand and solvent (4 mL). The resultant was allowed to stir for 5 min at r.t. Then aryl magnesium bromide was added dropwise (1.2 mL, 1.2 mmol, 1.0 M in THF) and it was stirred at r.t. for 2 h. After that time, the reaction mixture was quenched with 2 mL of saturated NH_4Cl water solution and stirred vigorously for 15 minutes. Layers were separated and the water phase was extracted with MTBE (3 x 2 mL). The combined organic layers were dried over Na_2SO_4, concentrated, and the residue was subjected to GC analysis with internal standard (mesitylene) or purified by flash chromatography on silica gel to provide the quenched product of carbomagnesiation step.

Evaluation of reaction conditions for one pot procedure of Ni-catalysed carboboration of alkynes

General Procedure: In a glove box after standard cycles of evacuation and back-fill with pure N_2, catalyst (0.025 mmol, 5 mol%) was introduced into a 10-ml round bottom flask with a magnetic stirring bar. Next, 1-phenyl-1-hexyne (79.5 mg, 0.5 mmol, 1.0 eq.), ligand (0.025 mmol, 5 mol%) and solvent were added. The resultant was allowed to stir for 5 min at r.t. Then, phenylmagnesium bromide was added dropwise (0.6 mL, 0.6 mmol, 1.0 M in THF) and stirred at r.t. for 2 h. After that time, the reaction mixture was either cooled or left at room temperature and borylating reagent was added dropwise. Mixture was stirred at given temperature for given time. The reaction was cooled to 0 °C, quenched by the slow dropwise addition of 3M HCl (1.2 mL) and remained in the cooling bath until the effervescence diminished. Then it was removed from the cooling bath and stirred for another 30 min at r.t. Extraction was performed using water and MTBE (3 x 2.5 mL). The combined organic layers were dried over Na_2SO_4, concentrated, and the residue was purified by flash chromatography on silica gel to provide the desired product **280**.

4.5.3 General procedures

General procedure for carboborylation of alkynes:

In a glove box after standard cycles of evacuation and back-fill with pure N_2, $NiBr_2$·diglyme (8.8 mg, 0.025 mmol, 5 mol%) was introduced into a 10-ml round bottom flask with a magnetic stirring bar. Next, alkyne (0.5 mmol, 1.0 eq.), PMDTA (4.4 mg, 0.025 mmol, 5 mol%, 5.3 µL) and toluene (4 mL) were added. The resultant was allowed to stir for 5 min at r.t. Then, aryl magnesium bromide was added dropwise (0.6 mL, 0.6 mmol, 1.0 M in THF) and stirred at r.t. for 2 h. After that time, the reaction mixture was cooled to 0 ºC and pinacolborane (198.5 mg, 1.5 mmol, 3.0 eq., 225 µL) was added dropwise and it was further stirred overnight at 2-8 ºC. After 18 h, mixture was quenched by the slow dropwise addition of 3M HCl (1.2 mL) and remained in the cooling bath until the effervescence diminished. Then it was removed from the cooling bath and stirred for another 30 min at r.t. Extraction was performed using water and MTBE (3 x 2.5 mL). The combined organic layers were dried over Na_2SO_4, concentrated, and the residue was purified by flash chromatography on silica gel to provide the desired product **280**.

Procedure for reaction run at 5 mmol scale for compound 280a.

A 100-mL Shlenk tube equipped with a magnetic bar was charged with $NiBr_2$.diglyme (88.3 mg, 0.25 mmol, 5 mol%), then evacuated and back-filled with argon (three times). To the catalyst were added 1- phenylhex-1-yne (790.0 mg, 5.00 mmol), PMDTA (43.2 mg, 0.25 mmol, 5 mol%), toluene (40 mL) and the phenylmagnesium bromide dropwise (6.0 mL, 6.00 mmol, 1.2 equiv., 1.0 M in THF). The resulting mixture was stirred at r.t. for 2 h. After 2 h, the reaction mixture was cooled to 0 ºC and pinacolborane (1.912 g, 15.0 mmol, 3.0 equiv.) was added dropwise and it was further allowed to stir overnight at 2-8 ºC. After 18 h the reaction was cooled to 0 ºC and quenched with the dropwise addition of 3 M HCl (12 mL). After the effervescence ceased, it was removed from the cooling bath and stirred for another 30 min at r.t. The organic layer was separated and water phase was extracted using MTBE (3 x 25 mL). The combined layers were dried over Na_2SO_4. The title compound was isolated as a white solid (1.328 g, 73 %) after chromatography on silica.

Procedure for reaction run at 3 mmol scale for compound 280f.

A 100-mL Shlenk tube equipped with a magnetic bar was charged with $NiBr_2$.diglyme (53.0 mg, 0.15 mmol, 5 mol%), then evacuated and back-filled with argon (three times). To the catalyst were added 5-chloro-1-phenylpent-1-yne (539.4 mg, 3.00 mmol), PMDTA (26.0 mg, 0.15 mmol, 5 mol%), toluene (24 mL) and the phenylmagnesium bromide dropwise (3.6 mL, 3.60 mmol, 1.2 equiv., 1.0 M in THF). The resulting mixture was stirred at r.t. for 2 h. After 2 h, the reaction mixture was cooled to 0 ºC and pinacolborane (1.160 g, 9.00 mmol, 3.0 equiv.) was added dropwise and it was further allowed to stir overnight at 2-8 ºC. After 18 h the reaction was cooled to 0 ºC and quenched with the dropwise addition of 3 M HCl (7.2 mL). After the effervescence ceased, it was removed from the cooling bath and stirred for another 30 min at r.t. The organic layer was separated and water phase was extracted using MTBE (3 x 15 mL). The combined layers were dried over Na_2SO_4. The title compound was isolated as a white solid (644.7 mg, 56 %) after chromatography on silica.

Procedure for carboboration via *in situ* formation of Grignard reagent

In a 15 mL Schlenk flask, add Mg (29.17 mg, 1.2 mmol, 1.2 eq.). Then add THF (0.2 mL) under argon. Add a small crystal of iodine. The solution turns brown. Add solution of vinyl bromide (315.25 mg, 1 mmol) in THF (0.7 mL). Heat it 60 ºC for 2.5 h. Cool the reaction mixture. Add 0.2

mL to another round bottom flask then cool the flask to 0 °C and add pinacol borane (76.78 mg, 1.5 mmol, 3 eq., 87.06 µL) dropwise followed by toluene (1.6 mL). Stir at 2-8 °C for 18 h. Quench the reaction with 3N HCl (0.5 mL). Stir at rt for 30 min. Workup with sat. NH_4Cl and MTBE. Dry the organic layer over Na_2SO_4. Concentrate the crude and purify it over silica gel chromatography. The title compound was obtained as a white solid (30.93 mg, 0.085 mmol, 43 %).

Procedure for Competition Experiments

Experiment to test the relative reactivity of alkynes: In a 10 mL round bottom flask, add $NiBr_2$.dig (1.81 mg, 0.005 mmol, 5 mol%), 1-phenyl hexyne (157.99 mg, 0.998 mmol, 10 eq., 175.54 µL) and 4-methoxy phenyl hexyne (188.63 mg, 1.001 mmol, 10 eq.), PMDTA (0.84 mg, 0.005 mmol, 5 mol%, 1.01 µL), toluene (0.8 mL) under Ar atmosphere. Then add PhMgBr (0.1 mmol) dropwise. Stir the reaction at rt for 2 h. Workup with sat. NH_4Cl and MTBE. Dry the organic layer over Na_2SO_4. Concentrate the crude and prepare a solution of it in $CDCl_3$ in the standard measuring flask (1 mL). Take 0.5 mL to the NMR tube and add CH_2Br_2 (0.1 mmol). Calculate the NMR yield using internal standard.

Experiment to test the relative reactivity of Grignard reagents: In a 10 mL round bottom flask, add $NiBr_2$.dig (8.82 mg, 0.025 mmol, 5 mol%), 1-phenyl hexyne (79.31 mg, 0.501 mmol, 88.12 µL), PMDTA (4.33 mg, 0.025 mmol, 5 mol%), toluene (4 mL). Then add PhMgBr (1.57 mL, 1.25 mmol, 2.5 eq.) and *p*-OMePhMgBr (1.29 mL, 1.25 mmol, 2.5 eq.) dropwise. Stir the reaction mixture for 2 h. Workup with sat. NH_4Cl and MTBE. Dry the organic layer over Na_2SO_4. Concentrate the crude and prepare a solution of it in $CDCl_3$ in the standard measuring flask (1 mL). Take 0.5 mL to the NMR tube and add CH_2Br_2 (0.1 mmol). Calculate the NMR yield using internal standard.

4.5.4 Analytical data of isolated products of carboborylation of alkynes

(*E*)-2-(1,2-diphenylhex-1-en-1-yl)-4,4,5,5-tetramethyl-1,3,2-dioxaborolane (280a)

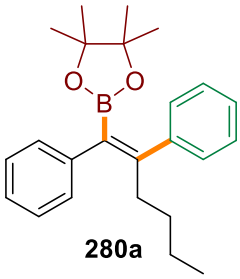

280a

Prepared by reaction of 1-phenylhex-1-yne (79.5 mg, 0.502 mmol) with phenylmagnesium bromide following general procedure. The title compound was isolated as a white solid (148.4 mg, 0.410 mmol, 82 %) after flash chromatography on silica gel (petroleum ether/ethyl acetate 99:1). Analytical data of **280a**: ^{1}H NMR (400 MHz $CDCl_3$): δ 7.31 (m, 10H), 2.42 (t, J = 7.6 Hz, 2H), 1.20 (m, 4H), 1.01 (s, 12H), 0.73 (t, J = 7.0 Hz, 3H); ^{13}C NMR (101 MHz, $CDCl_3$): δ 152.4, 144.0, 141.5, 128.5, 128.3, 128.0, 127.8, 126.9, 125.8, 83.2, 33.6, 30.6, 24.3, 22.5, 13.8; HRMS (ESI-TOF) m/z: $[M + Na]^+$ Calc'd for $C_{24}H_{31}BO_2Na$: 385.2315 Found: 385.2318.

(*E*)-2-(1,2-diphenylprop-1-en-1-yl)-4,4,5,5-tetramethyl-1,3,2-dioxaborolane (280b)

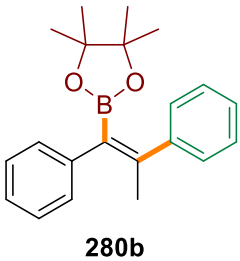

280b

Prepared by reaction of 1-phenylprop-1-yne (58.3 mg, 0.502 mmol) with phenylmagnesium bromide following general procedure. The title compound was isolated as a white solid (109.0 mg, 0.340 mmol, 68 %) after flash chromatography on silica gel (petroleum ether/ethyl acetate 99:1). Analytical data of **280b**: ^{1}H NMR (400 MHz $CDCl_3$): δ 7.45 (m, 2H), 7.32 (m, 8H), 2.09 (s, 3H), 1.07 (s, 12H); ^{13}C NMR (101 MHz, $CDCl_3$): δ 147.7, 145.5, 141.7, 128.7, 128.1, 128.0, 127.8, 127.1, 125.9, 83.3, 24.4, 21.5; HRMS (ESI-TOF) m/z: $[M + Na]^+$ Calc'd for $C_{21}H_{25}BO_2Na$: 343.1845 Found: 343.1849.

(*E*)-2-(1,2-diphenylbut-1-en-1-yl)-4,4,5,5-tetramethyl-1,3,2-dioxaborolane (280c)

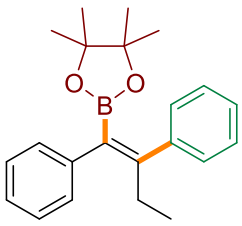

280c

Prepared by reaction of 1-phenylbut-1-yne (130.2 mg, 1.000 mmol) with phenylmagnesium bromide following general procedure. The title compound was isolated as a colourless oil (240.6 mg, 0.720 mmol, 72 %) after flash chromatography on silica gel (petroleum ether/ethyl acetate 99:1). Analytical data of **280c**: ^{1}H NMR (400 MHz $CDCl_3$): δ 7.36 (m, 6H), 7.27 (m, 4H), 2.44 (q, J = 7.5 Hz, 2H), 1.02 (s, 12H), 0.88 (t, J = 7.5 Hz, 3H); ^{13}C NMR (101 MHz, $CDCl_3$): δ 153.7, 143.6, 141.5, 128.4, 128.4, 128.1, 127.9, 127.0, 125.9, 83.2, 27.1, 24.4, 13.2; HRMS (APCI-TOF) m/z: $[M]^{+\cdot}$ Calc'd for $C_{22}H_{27}BO_2$: 334.2104 Found: 334.2113.

(*E*)-2-(2-cyclopropyl-1,2-diphenylvinyl)-4,4,5,5-tetramethyl-1,3,2-dioxaborolane (280d)

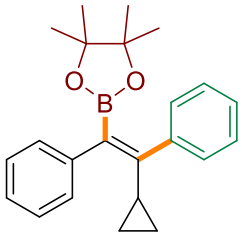

280d

Prepared by reaction of 2-cyclopropyl-1-phenyleth-1-yne (71.1 mg, 0.500 mmol) with phenylmagnesium bromide following general procedure. The title compound was isolated as a white solid (90.5 mg, 0.261 mmol, 52 %) after flash chromatography on silica gel (petroleum ether/ethyl acetate 99:1). Analytical data of **280d**: ^{1}H NMR (400 MHz $CDCl_3$): δ 7.44 (m, 2H), 7.37 (m, 2H), 7.25 (m, 6H), 1.91 (m, 1H), 0.93 (s, 12H), 0.57 (m, 2H), 0.36 (m, 2H); ^{13}C NMR (101 MHz, $CDCl_3$): δ 152.6, 140.9, 139.8, 130.0, 129.2, 128.0, 127.2, 126.7, 125.8, 83.0, 24.2, 14.9, 5.8; HRMS (ESI-TOF) m/z: $[M + Na]^+$ Calc'd for $C_{23}H_{27}BO_2Na$: 369.2002 Found: 369.2004.

(*E*)-4,4,5,5-tetramethyl-2-(3-methyl-1,2-diphenylbut-1-en-1-yl)-1,3,2-dioxaborolane (280e)

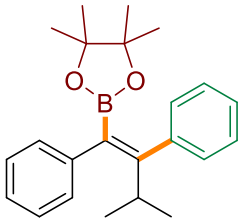

280e

Prepared by reaction of 3-methyl-1-phenylbut-1-yne (72.5 mg, 0.502 mmol) with phenylmagnesium bromide following general procedure. The title compound was isolated as a white solid (102.4 mg, 0.294 mmol, 58 %) after flash chromatography on silica gel (petroleum ether/ethyl acetate 99:1). Analytical data of **280e**: ^{1}H NMR (400 MHz $CDCl_3$): δ 7.29 (m, 10H), 3.03 (m, 1H), 0.91 (d, J = 8.0 Hz, 6H), 0.89 (s, 12H); ^{13}C NMR (101 MHz, $CDCl_3$): δ 156.3, 140.7, 140.6, 130.2, 128.4, 128.1, 127.1, 126.5, 125.8, 83.1, 30.4. 24.2, 21.3; HRMS (ESI-TOF) m/z: $[M + Na]^+$ Calc'd for $C_{23}H_{29}BO_2Na$: 371.2158 Found: 371.2160.

(*E*)-2-(5-chloro-1,2-diphenylpent-1-en-1-yl)-4,4,5,5-tetramethyl-1,3,2-dioxaborolane (280f)

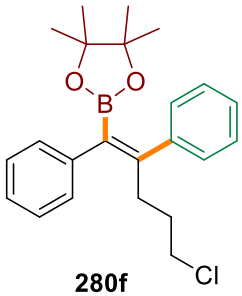

280f

Prepared by reaction of 5-chloro-1-phenylpent-1-yne (89.8 mg, 0.502 mmol) with phenylmagnesium bromide following general procedure. The title compound was isolated as a white solid (110.5 mg, 0.289 mmol, 58 %) after flash chromatography on silica gel (petroleum ether/ethyl acetate 99:1). Analytical data of **280f**: ^{1}H NMR (400 MHz $CDCl_3$): δ 7.35 (m, 7H), 7.24 (m, 3H), 3.33 (t, J = 6.9 Hz, 2H), 2.56 (m, 2H), 1.72 (m, 2H), 1.01 (s, 12H); ^{13}C NMR (101 MHz, $CDCl_3$): δ 150.2, 143.1, 141.0, 128.3, 128.3, 128.2, 128.1, 127.3, 126.1, 83.4, 44.6, 31.5, 31.3, 24.3; HRMS (APCI-TOF) m/z: $[M + H]^+$ Calc'd for $C_{23}H_{29}ClBO_2$: 383.1949 Found: 383.1948.

(*E*)-5,6-diphenyl-6-(4,4,5,5-tetramethyl-1,3,2-dioxaborolan-2-yl)hex-5-en-1-ol (280g)

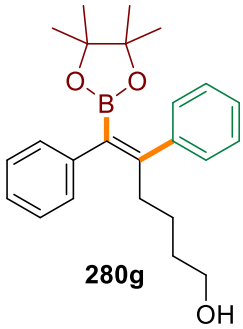

280g

Prepared by reaction of trimethyl((6-phenylhex-5-yn-1-yl)oxy)silane (123.3 mg, 0.500 mmol) with phenylmagnesium bromide following general procedure. The title compound was isolated as a colourless oil (174.6 mg, 0.461 mmol, 92 %) after flash chromatography on silica gel (petroleum ether/ethyl acetate 90:10 to 85:15). Analytical data of **280g**: ^{1}H NMR (400 MHz $CDCl_3$): δ 7.32 (m, 10H), 3.42 (t, J = 8.0 Hz, 2H), 2.43 (t, J = 8.0 Hz, 2H), 1.40 (m, 2H), 1.28 (m, 2H), 0.99 (s, 12H); ^{13}C NMR (101 MHz, $CDCl_3$): δ 151.8, 143.6, 141.3, 128.4, 128.3, 128.1, 127.9, 127.1, 125.9, 83.3, 62.5, 33.3, 32.3, 24.4, 24.3; IR (CH_2Cl_2): 3438 (O-H) cm^{-1}; HRMS (APCI-TOF) m/z: $[M - H]^+$ Calc'd for $C_{24}H_{30}BO_3$: 377.2288 Found: 377.2292

(*E*)-4,4,5,5-tetramethyl-2-(1,2,3-triphenylprop-1-en-1-yl)-1,3,2-dioxaborolane (280h)

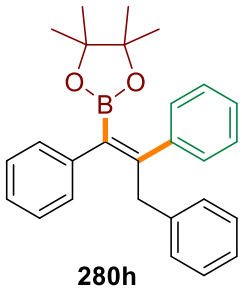

280h

Prepared by reaction of 1,3-diphenylprop-1-yne (96.2 mg, 0.500 mmol) with phenylmagnesium bromide following general procedure. The title compound was isolated as a white solid (163.9 mg, 0.413 mmol, 83 %) after flash chromatography on silica gel (petroleum ether/ethyl acetate 99:1). Analytical data of **280h**: ^{1}H NMR (400 MHz $CDCl_3$): δ 7.37 (m, 6H), 7.25 (m, 4H), 7.14 (d, J = 7.0 Hz, 2H), 7.09 (d, J = 6.7 Hz, 1H), 7.03 (d, J = 7.4 Hz, 2H), 3.85 (s, 2H), 1.05 (s, 12H); ^{13}C NMR (101 MHz, $CDCl_3$): δ 149.2, 143.4, 141.1, 139.4, 128.9, 128.7, 128.4, 128.3, 128.0, 127.8, 127.0, 126.2, 125.6, 83.4, 39.7, 24.4; HRMS (APCI-TOF) m/z: $[M - H]^+$ Calc'd for $C_{27}H_{28}BO_2$: 395.2182 Found: 395.2189.

(*E*)-2-(1-(4-methoxyphenyl)-2-phenylhex-1-en-1-yl)-4,4,5,5-tetramethyl-1,3,2-dioxaborolane (280i)

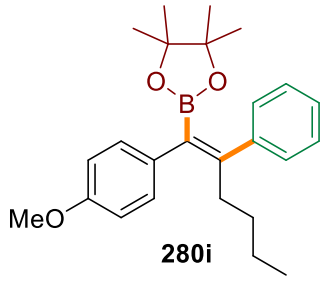

280i

Prepared by reaction of 1-(4-methoxyphenyl)hex-1-yne (94.6 mg, 0.502 mmol) with phenylmagnesium bromide following general procedure. The title compound was isolated as colourless oil (150.8 mg, 0.385 mmol, 77 %) after flash chromatography on silica gel (petroleum ether/ethyl acetate 99:1). Analytical data of **280i**: ^{1}H NMR (400 MHz $CDCl_3$): δ 7.31 (m, 5H), 7.17 (d, J = 8.2 Hz, 2H), 6.89 (d, J = 8.8 Hz, 2H), 3.82 (s, 3H), 2.42 (t, J = 7.5 Hz, 2H), 1.2 (m, 4H), 1.0 (s, 12H), 0.74 (t, J = 7.0 Hz, 3H); ^{13}C NMR (101 MHz, $CDCl_3$): δ 157.8, 152.1, 144.1, 133.8, 129.5, 128.3, 127.8, 126.9, 113.5, 83.2, 55.1, 33.5, 30.6, 24.4, 22.5, 13.8; HRMS (APCI-TOF) m/z: $[M + H]^+$ Calc'd for $C_{25}H_{34}BO_3$: 393.2601 Found: 393.2602.

(*E*)-4,4,5,5-tetramethyl-2-(1-(naphthalen-1-yl)-2-phenylhex-1-en-1-yl)-1,3,2-dioxaborolane (280j)

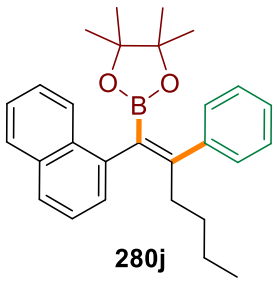

280j

Prepared by reaction of 1-(hex-1-yn-1-yl)naphthalene (104.4 mg, 0.501 mmol) with phenylmagnesium bromide following general procedure. The title compound was isolated as red oil (150.3 mg, 0.365 mmol, 73 %) after flash chromatography on silica gel (petroleum ether/ethyl acetate 99.5:0.5). Analytical data of **280j**: ^{1}H NMR (400 MHz $CDCl_3$): δ 8.14 (m, 1H), 7.87 (m, 1H), 7.77 (d, J = 8.20 Hz, 1H), 7.50 (m, 5H), 7.39 (m, 3H), 7.34 (m, 1H), 2.20 (td, J = 7.4 Hz, 5.6 Hz, 2H), 1.11 (m, 4H), 1.01 (s, 6H), 0.90 (s, 6H), 0.60 (t, J = 7.3 Hz, 3H); ^{13}C NMR (101 MHz, $CDCl_3$): δ 154.5, 143.8, 139.6, 133.6, 132.2, 128.4, 128.0, 127.9, 127.1, 126.4, 126.3, 125.6, 125.6, 125.5, 125.4, 83.2, 34.3, 30.3, 24.4, 24.2, 22.4, 13.7; HRMS (APCI-TOF) m/z: $[M + H]^+$ Calc'd for $C_{28}H_{34}BO_2$: 413.2652 Found: 413.2654.

(*E*)-2-(1-(4-fluorophenyl)-2-phenylhex-1-en-1-yl)-4,4,5,5-tetramethyl-1,3,2-dioxaborolane (280k)

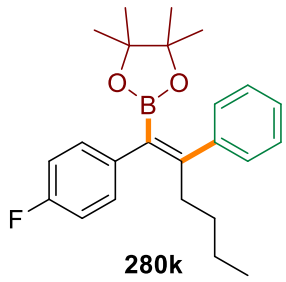

280k

Prepared by reaction of 1-(4-fluorophenyl)hex-1-yne (88.1 mg, 0.499 mmol) with phenylmagnesium bromide following general procedure. The title compound was isolated as a white solid (159.4 mg, 0.419 mmol, 83 %) after flash chromatography on silica gel (petroleum ether/ethyl acetate 99.5:0.5). Analytical data of **3k**: ^{1}H NMR (400 MHz $CDCl_3$): δ 7.32 (m, 5H), 7.20 (m 2H), 7.03 (m, 2H), 2.38 (t, J = 7.4 Hz, 2H), 1.17 (m, 4H), 1.00 (s, 12H), 0.72 (t, J = 6.9 Hz, 3H); ^{19}F NMR (376 MHz $CDCl_3$): δ -117.3 (s, 1F); ^{13}C NMR (101 MHz, $CDCl_3$): δ 162.5, 160.1, 153.0, 143.7, 137.3 (d, J = 3.34 Hz), 129.9 (d, J = 7.73 Hz), 128.1 (d, J = 36.0 Hz), 127.0, 114.9 (d, J = 21.1 Hz), 83.3, 33.6, 30.5, 24.3, 22.5, 13.7; HRMS (APCI-TOF) m/z: $[M + H]^+$ Calc'd for $C_{24}H_{31}FBO_2$: 381.2401 Found: 381.2400.

(*E*)-2-(1-(4-bromophenyl)-2-phenylhex-1-en-1-yl)-4,4,5,5-tetramethyl-1,3,2-dioxaborolane (280l)

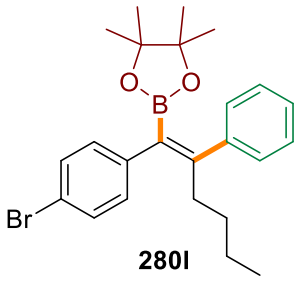

280l

Prepared by reaction of 1-(4-bromophenyl)hex-1-yne (118.9 mg, 0.501 mmol) with phenylmagnesium bromide following general procedure. The title compound was isolated as a white solid (115.7 mg, 0.262 mmol, 52 %) after flash chromatography on silica gel (25 g column, 60/90 petroleum ether/ethyl acetate 99.5:0.5). Analytical data of **3l**: ^{1}H NMR (400 MHz $CDCl_3$): δ 7.47 (m, 2H), 7.31 (m, 5H), 7.12 (m, 2H), 2.38 (t, J = 7.4 Hz, 2H), 1.17 (m, 4H), 1.00 (s, 12H), 0.72 (t, J = 6.9 Hz, 3H); ^{13}C NMR (101 MHz, $CDCl_3$): δ 153.3, 143.6, 140.4, 131.2, 130.3, 128.2, 127.9, 127.1, 119.8, 83.3, 33.7, 30.4, 24.3, 22.5, 13.8; HRMS (APCI-TOF) m/z: $[M]^{+\cdot}$ Calc'd for $C_{24}H_{30}BBrO_2$: 440.1522 Found: 440.1530.

(*E*)-4-(2-phenyl-1-(4,4,5,5-tetramethyl-1,3,2-dioxaborolan-2-yl)hex-1-en-1-yl)phenyl trifluoromethanesulfonate (280m)

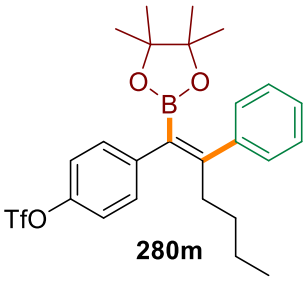

280m

Prepared by reaction of 4-(hex-1-yn-1-yl)phenyl trifluoromethanesulfonate (153.3 mg, 0.500 mmol) with phenylmagnesium bromide following general procedure. The title compound was isolated as a white solid (91.6 mg, 0.180 mmol, 36 %) after flash chromatography on silica gel (25 g column, 60/90 petroleum ether/ethyl acetate 100 to 99.5:0.5). Analytical data of **280m**: ^{1}H NMR (400 MHz $CDCl_3$): δ 7.32 (m, 6H), 7.22 – 7.26 (m, 2H), 7.24 (d, J = 2.3 Hz, 1H), 2.35 (t, J = 7.4 Hz, 2H), 1.16 (m, 4H), 0.99 (s, 12H), 0.70 (t, J = 6.9 Hz, 3H); ^{19}F NMR (376 MHz $CDCl_3$): δ -72.9 (s, 3H); ^{13}C NMR (101 MHz, $CDCl_3$): δ 154.2, 147.8, 143.3, 142.0, 130.3, 128.1, 127.9, 127.2, 120.9, 118.7 (q, J = 320.6 Hz), 83.5, 33.7, 30.3, 24.3, 22.4, 13.6; HRMS (APCI-TOF) m/z: $[M]^{+\cdot}$ Calc'd for $C_{25}H_{30}F_3SBO_5$: 510.1859 Found: 510.1866.

(*E*)-4-(2-phenyl-1-(4,4,5,5-tetramethyl-1,3,2-dioxaborolan-2-yl)hex-1-en-1-yl)phenyl 4-methylbenzenesulfonate (280n)

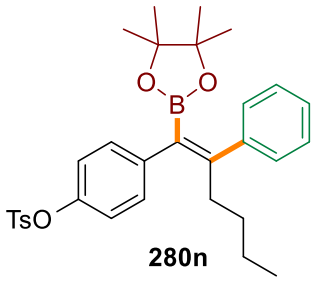

280n

Prepared by reaction of 4-(hex-1-yn-1-yl)phenyl 4-methylbenzenesulfonate (164.3 mg, 0.500 mmol) with phenylmagnesium bromide following general procedure. The title compound was isolated as a white solid (85.3 mg, 0.160 mmol, 32 %) after chromatography on silica gel (petroleum ether/ethyl acetate 95:5 to 80:20). Analytical data of **280n**: ^{1}H NMR (400 MHz $CDCl_3$): δ 7.69 (d, J = 8.30 Hz, 2H), 7.31 (m, 5H), 7.27 (d, J = 8.0 Hz, 2H), 7.13 (d, J = 8.2 Hz, 2H), 6.94 (d, J = 8.6 Hz, 2H), 2.43 (s, 3H), 2.32 (t, J = 8.0 Hz, 2H), 1.15 (m, 4H), 0.97 (s, 12H), 0.69 (t, J = 6.9 Hz, 3H); ^{13}C NMR (101 MHz, $CDCl_3$): δ 153.3, 147.8, 145.2, 143.5, 140.5, 132.3, 129.6, 129.6, 128.6, 128.1, 127.9, 127.1, 122.0, 83.3, 33.5, 30.3, 24.3, 22.4, 21.6, 13.7; HRMS (APCI-TOF) m/z: $[M + H]^+$ Calc'd for $C_{31}H_{38}SBO_5$: 533.2533 Found: 533.2524.

(*E*)-2-(1-(4,4-(dimethoxymethyl)phenyl)-2-phenylhex-1-en-1-yl)-4,4,5,5-tetramethyl-1,3,2-dioxaborolane (280o)

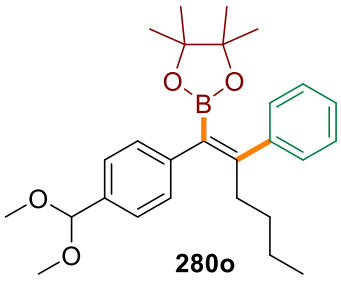

Prepared by reaction of 1-(dimethoxymethyl)-4-(hex-1-yn-1-yl)benzene (116.7 mg, 0.502 mmol) with phenylmagnesium bromide following modified general procedure (quenched the reaction with water). The title compound was isolated as yellow oil (108.7 mg, 0.250 mmol, 50 %) after chromatography on silica gel (petroleum ether/ethyl acetate 96:4). Analytical data of **280o**: ^{1}H NMR (400 MHz $CDCl_3$): δ 7.42 (d, J = 8.1 Hz, 2H), 7.33 (m, 5H), 7.25 (d, J = 8.4 Hz, 2H), 5.40 (s, 1H), 3.36 (s, 6H), 2.39 (t, J = 8.0 Hz, 2H), 1.17 (m, 4H), 0.99 (s, 12H) 0.70 (t, J = 7.0 Hz, 3H); ^{13}C NMR (101 MHz, $CDCl_3$): δ 152.7, 143.9, 141.7, 135.5, 128.3, 128.3, 127.8, 127.0, 126.4, 103.4, 83.2, 52.8, 33.6, 30.5, 24.3, 22.4, 13.7; HRMS (APCI-TOF) m/z: $[M]^{+\bullet}$ Calc'd for $C_{27}H_{37}BO_4$: 436.2785 Found: 436.2787.

(*E*)-2-(1-(benzo[d][1,3]dioxol-5-yl)-2-phenylhex-1-en-1-yl)-4,4,5,5-tetramethyl-1,3,2-dioxaborolane (280p)

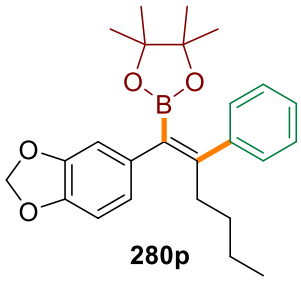

Prepared by reaction of 5-(hex-1-yn-1-yl)benzo[*d*][1,3]dioxole (101.4 mg, 0.501 mmol) with phenylmagnesium bromide following general procedure. The title compound was isolated as a colourless oil (125.2 mg, 0.308 mmol, 62 %) after flash chromatography on silica gel (petroleum ether/ethyl acetate 99:1). Analytical data of **280p**: ^{1}H NMR (400 MHz $CDCl_3$): δ 7.31 (m, 5H), 6.80 (d, J = 7.9 Hz, 1H), 6.74 (d, J = 1.7 Hz, 1H), 6.69 (dd, J = 7.9 Hz, 1.7 Hz, 1H), 5.95 (s, 2H), 2.42 (t, J = 7.3 Hz, 2H), 1.18 (m, 4H), 1.0 (s, 12H), 0.74 (t, J = 8.0 Hz, 3H); ^{13}C NMR (101 MHz, $CDCl_3$): δ 152.5, 147.3, 145.7, 143.8, 135.3, 128.3, 127.8, 126.9, 121.5, 109.1, 108.1, 100.7, 83.2, 33.6, 30.5, 24.3, 22.5, 13.8; HRMS (APCI-TOF) m/z: $[M + H]^+$ Calc'd for $C_{25}H_{32}BO_4$: 407.2394 Found: 407.2395.

(*E*)-4,4,5,5-tetramethyl-2-(2-phenyl-1-(thiophen-2-yl)hex-1-en-1-yl)-1,3,2-dioxaborolane (280q)

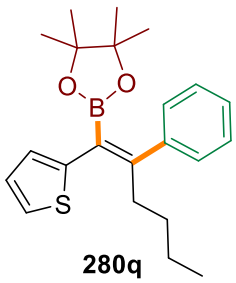

Prepared by reaction of 2-(hex-1-yn-1-yl)thiophene (82.5 mg, 0.502 mmol) with phenylmagnesium bromide following general procedure. The title compound was isolated as yellow oil (109.7 mg, 0.299 mmol, 60 %) after flash chromatography on silica gel (petroleum ether/ethyl acetate 99.5:0.5). Analytical data of **280q**: ^{1}H NMR (400 MHz $CDCl_3$): δ 7.31 (m, 5H), 7.25 (dd, J = 5.2 Hz, 1.2 Hz, 1H), 7.02 (dd, J = 5.2 Hz, 3.5 Hz, 1H), 6.93 (dd, J = 3.5 Hz, 1.2 Hz, 1H), 2.65 (t, J = 7.6 Hz, 2H), 1.29 (m, 4H), 1.03 (s, 12H), 0.80 (t, J = 7.0 Hz, 3H); ^{13}C NMR (101 MHz, $CDCl_3$): δ 154.1, 143.9, 142.6, 128.3, 127.9, 127.1, 126.8, 125.7, 124.4, 83.5, 34.7, 30.5, 24.4, 22.6, 13.8; HRMS (APCI-TOF) m/z: $[M + H]^+$ Calc'd for $C_{22}H_{30}SBO_2$: 369.2060 Found 369.2062.

(*E*)-1-methyl-5-(2-phenyl-1-(4,4,5,5-tetramethyl-1,3,2-dioxaborolan-2-yl)hex-1-en-1-yl)-1*H*-indole (280r)

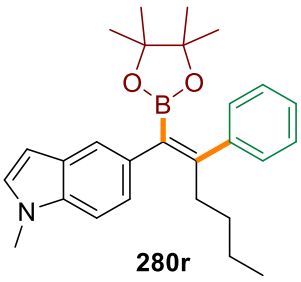

Prepared by reaction of 5-(hex-1-yn-1-yl)-1-methyl-1*H*-indole (105.8 mg, 0.500 mmol) with phenylmagnesium bromide following modified general procedure (quenched the reaction with water). The title compound was isolated as a yellow solid (112.2 mg, 0.270 mmol, 54 %) after flash chromatography on silica gel (petroleum ether/ethyl acetate 98:2). Analytical data of **280r**: ^{1}H NMR (400 MHz $CDCl_3$): δ 7.51 (s, 1H), 7.43 (d, J = 7.4 Hz, 2H), 7.32 (m, 3H), 7.27 (d, J = 8.6 Hz, 1H), 7.16 (d, J = 8.4 Hz, 1H), 7.04 (d, J = 3.1 Hz, 1H), 6.49 (d, J = 3.0 Hz, 1H), 3.80 (s, 3H), 2.48 (t, J = 7.7 Hz, 2H), 1.22 (m, 4H), 1.02 (s, 12H), 0.74 (t, J = 7.2 Hz, 3H); ^{13}C NMR (101 MHz, $CDCl_3$): δ 151.3, 144.4,

135.4, 132.5, 128.6, 128.5, 128.4, 127.8, 126.7, 122.8, 120.3, 108.7, 100.9, 83.1, 33.5, 32.8, 30.7, 24.4, 22.6, 13.9; HRMS (APCI-TOF) m/z: $[M + H]^+$ Calc'd for $C_{27}H_{35}BNO_2$: 416.2761 Found: 416.2763.

4,4,5,5-tetramethyl-2-(1,2,2-triphenylvinyl)-1,3,2-dioxaborolane (280s)

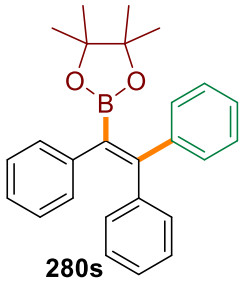

280s

Prepared by reaction of diphenylacetylene (89.5 mg, 0.502 mmol) with phenylmagnesium bromide following general procedure. The title compound was isolated as a white solid (151.9 mg, 0.397 mmol, 79 %) after flash chromatography on silica gel (petroleum ether/ethyl acetate 99:1). Analytical data of **280s**: ^{1}H NMR (400 MHz $CDCl_3$): δ 7.42 (dd, *J* = 6.5 Hz, 3.1 Hz, 2H), 7.35 (dd, *J* = 5.2 Hz, 2.1 Hz, 3H), 7.17 (d, *J* = 6.8 Hz, 2H), 7.12 (m, 6H), 7.03 (dd, *J* = 6.7 Hz, 3.0 Hz, 2H), 1.19 (s, 12H); ^{13}C NMR (101 MHz, $CDCl_3$): δ 151.4, 144.7, 141.9, 141.7, 130.9, 129.8, 129.4, 128.0, 128.0, 127.6, 127.6, 126.8, 125.9, 83.7, 24.6; HRMS (ESI-TOF) m/z: $[M + Na]^+$ Calc'd for $C_{26}H_{27}BO_2Na$: 405.2002 Found: 405.2005.

2-(1-(4-fluorophenyl)-2,2-diphenylvinyl)-4,4,5,5-tetramethyl-1,3,2-dioxaborolane (280t)

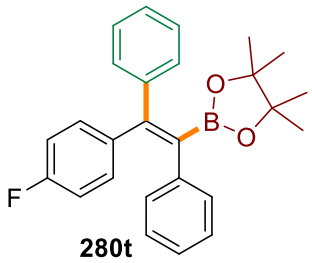

280t

Prepared by reaction of 4-fluoro diphenylacetylene (98.11 mg, 0.500 mmol) with phenylmagnesium bromide following general procedure. The title compound was isolated as a white solid (131.5 mg, 0.328 mmol, 66 %, 7:3) after flash chromatography on silica gel (petroleum ether/ethyl acetate 99.5:0.5). Analytical data of **280u**: ^{1}H NMR (400 MHz $CDCl_3$): 7.32 (m, 5H), 7.12 (m, 5H), 6.94 (m, 2H), 6.78 (t, *J* = 8.6 Hz, 2H), 1.14 (s, 12H); ^{19}F NMR (400 MHz, $CDCl_3$): -115.0 (s, 1F); ^{13}C NMR (101 MHz, $CDCl_3$): 162.8, 160.4, 150.2, 144.4, 141.4, 141.5, 137.7 (d, *J* = 3.3 Hz), 132.6 (d, *J* = 7.9 Hz), 129.7, 129.3, 128.1 (d, *J* = 10.6 Hz), 126.0, 114.5 (d, *J* = 21.3 Hz), 83.7, 24.5 Analytical data of **280u':** ^{1}H NMR (400 MHz $CDCl_3$): 7.32 (m, 5H), 7.12 (m, 5H), 7.01 (m, 2H), 6.85 (t, *J* = 8.6 Hz, 2H); ^{19}F NMR (400 MHz, $CDCl_3$): -116.65 (s, 1F); ^{13}C NMR (101 MHz, $CDCl_3$): 162.4, 159.9, 151.8, 141.6, 137.6 (d, *J* = 3.4 Hz), 130.9 (d, *J* = 7.8 Hz), 129.6, 127.9, 127.7, 126.9, 114.9 (d, *J* = 21.2 Hz), 83.7; HRMS (ESI-TOF) m/z: $[M + Na]^+$ Calc'd for $C_{26}H_{26}BFNaO_2$: 423.1908 Found: 423.1915.

2-(1-(4-methoxyphenyl)-2,2-diphenylvinyl)-4,4,5,5-tetramethyl-1,3,2-dioxaborolane (280u)

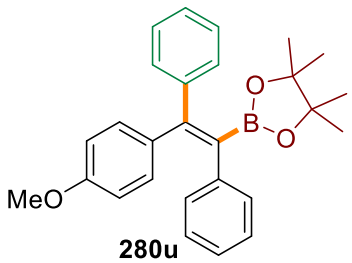

280u

Prepared by reaction of 4-methoxy diphenylacetylene (104.30 mg, 0.500 mmol) with phenylmagnesium bromide following general procedure. The title compound was isolated as a white solid (150.0 mg, 0.363 mmol, 73 %, 7:3) after flash chromatography on silica gel (petroleum ether/ethyl acetate 99.5:0.5 to 99:1). Analytical data of **280t**: ^{1}H NMR (400 MHz $CDCl_3$): 7.34 (m, 5H), 7.17 (m, 2H), 7.09 (m, 3H), 6.89 (d, *J* = 8.4 Hz, 2H), 6.63 (d, *J* = 8.5 Hz, 2H), 3.72 (s, 3H), 1.13 (s, 12H); ^{13}C NMR (101 MHz, $CDCl_3$): 158.4, 151.1, 145.0, 142.1, 134.2, 132.3, 129.8, 129.4, 128.0, 127.9, 127.5, 125.7, 112.9, 83.5, 55.0, 24.5, Analytical data of **280t':** 7.34 (m, 5H), 7.17 (m, 2H), 7.09 (m, 3H), 6.98 (d, *J* = 8.5 Hz, 2H), 6.70 (d, *J* = 8.3 Hz, 2H), 3.74 (s, 3H), 1.14 (s, 12H). ^{13}C NMR (101 MHz, $CDCl_3$): 157.7, 150.5, 144.8, 142.1, 134.1, 130.9,130.6, 129.7, 127.6, 127.4, 126.6, 113.5, 83.6, 55.0, 24.6; HRMS (ESI-TOF) m/z: $[M + Na]^+$ Calc'd for $C_{27}H_{29}BNaO_3$: 435.2107 Found: 435.2117.

(*E*)-2-(2-(4-methoxyphenyl)-1-phenylhex-1-en-1-yl)-4,4,5,5-tetramethyl-1,3,2-dioxaborolane (280v)

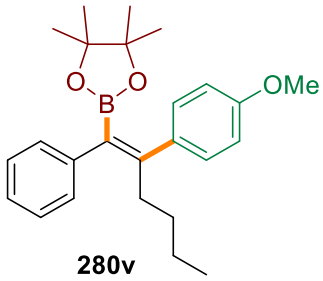

280v

Prepared by reaction of 1-phenylhex-1-yne (79.5 mg, 0.502 mmol) with 4-methoxy phenylmagnesium bromide following general procedure. The title compound was isolated as a white solid (145.9 mg, 0.371 mmol, 74 %) after flash chromatography on silica gel (petroleum ether/ethyl acetate 99:1). Analytical data of **280v**: ^{1}H NMR (400 MHz $CDCl_3$): δ 7.32 (m, 4H), 7.23 (m, 3H), 6.87 (m, 2H), 3.82 (s, 3H), 2.38 (t, J = 8.0 Hz, 2H), 1.19 (m, 4H), 1.04 (s, 12H), 0.73 (t, J = 7.0 Hz, 3H); ^{13}C NMR (101 MHz, $CDCl_3$): δ 158.8, 152.0, 141.7, 136.4, 129.4, 128.5, 128.0, 125.7, 113.2, 83.2, 55.3, 33.6, 30.7, 24.4, 22.5, 13.8; HRMS (APCI-TOF) m/z: $[M]^{+\bullet}$ Calc'd for $C_{25}H_{33}BO_3$: 392.2523 Found: 392.2533.

(*E*)-2-(2-(4-fluorophenyl)-1-phenylhex-1-en-1-yl)-4,4,5,5-tetramethyl-1,3,2-dioxaborolane (280w)

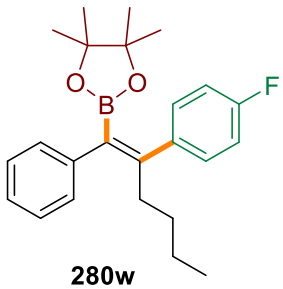

280w

Prepared by reaction of 1-phenylhex-1-yne (79.5 mg, 0.502 mmol) with h 4-fluoro phenylmagnesium bromide following general procedure. The title compound was isolated as a colourless oil (84.1 mg, 0.221 mmol, 44 %) after flash chromatography on silica gel (petroleum ether/ethyl acetate 99:1). Analytical data of **280w**: ^{1}H NMR (400 MHz $CDCl_3$): δ 7.35 (m, 4H), 7.23 (m, 3H), 7.02 (m, 2H), 2.38 (t, J = 8.0 Hz, 2H), 1.18 (m, 4H), 1.02 (s, 12H), 0.73 (t, J = 8.0 Hz, 3H); ^{19}F NMR (376 MHz $CDCl_3$): δ -115.8 (s, 1F); ^{13}C NMR (101 MHz, $CDCl_3$): δ 163.3, 160.9, 151.4, 141.3, 139.9 (d, J = 3.29 Hz), 129.9 (d, J = 7.9 Hz), 128.2 (d, J = 31.5 Hz), 125.9, 114.6 (d, J = 21.0 Hz), 83.3, 33.7, 30.5, 24.3, 22.4, 13.8; HRMS (APCI-TOF) m/z: $[M + H]^+$ Calc'd for $C_{24}H_{31}FBO_2$: 381.2401 Found: 381.2406.

(*E*)-4,4,5,5-tetramethyl-2-(1-phenyl-2-(*p*-tolyl)hex-1-en-1-yl)-1,3,2-dioxaborolane (280x)

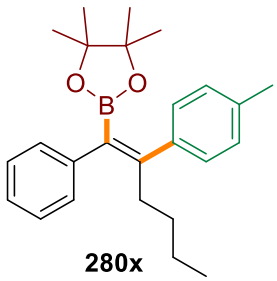

280x

Prepared by reaction of 1-phenylhex-1-yne (79.4 mg, 0.501 mmol) with *p*-tolyl magnesium bromide following general procedure. The title compound was isolated as a colourless oil (155.4 mg, 0.413 mmol, 83 %) after flash chromatography on silica gel (petroleum ether/ethyl acetate 99:1). Analytical data of **280x**: ^{1}H NMR (400 MHz $CDCl_3$): δ 7.34 (m, 2H), 7.25 (m, 5H), 7.14 (m, 2H), 2.40 (t, J = 8.0 Hz, 2H), 2.37 (s, 3H), 1.20 (m, 4H), 1.03 (s, 12H), 0.73 (t, J = 7.04 Hz, 3H); ^{13}C NMR (101 MHz, $CDCl_3$): δ 152.4, 141.6, 141.0, 136.5, 128.5, 128.5, 128.2, 128.0, 125.7, 83.2, 33.5, 30.6, 24.4, 22.5, 21.2, 13.8; HRMS (APCI-TOF) m/z: $[M + H]^+$ Calc'd for $C_{25}H_{34}BO_2$: 377.2652 Found: 377.2656.

(*E*)-4,4,5,5-tetramethyl-2-(1-phenyl-2-(*o*-tolyl)hex-1-en-1-yl)-1,3,2-dioxaborolane (280y)

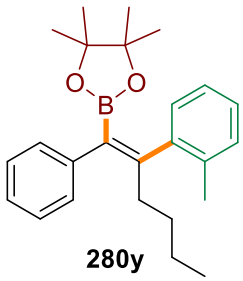

280y

Prepared by reaction of 1-phenylhex-1-yne (79.4 mg, 0.501 mmol) with *o*-tolyl magnesium bromide following general procedure. The title compound was isolated as a white solid (112.9 mg, 0.300 mmol, 60 %) after flash chromatography on silica gel (25 g column, 60/90 petroleum ether/ethyl acetate 99.5:0.5). Analytical data of **280y**: ^{1}H NMR (400 MHz $CDCl_3$): δ 7.36 (m, 2H), 7.30 (m, 2H), 7.24 (m, 1H), 7.16 (m, 4H), 2.45 (m, 1H), 2.38 (s, 3H), 2.18 (m, 1H), 1.25 (m, 4H), 0.92 (s, 6H), 0.88 (s, 6H), 0.76 (t, J = 7.2 Hz, 3H); ^{13}C NMR (101 MHz, $CDCl_3$): δ 151.3, 143.0, 140.9, 136.0, 129.6, 129.6, 128.5, 128.0, 126.6, 125.8, 124.7, 82.9, 34.0, 30.2, 24.2, 24.1, 22.8, 19.6, 13.8; HRMS (APCI-TOF) m/z: $[M + H]^+$ Calc'd for $C_{25}H_{34}BO_2$: 377.2652 Found: 377.2657.

(*E*)-2-(2-(1,3,5-trimethylphen-2-yl)-1-phenylhex-1-en-1-yl)-4,4,5,5-tetramethyl-1,3,2-dioxaborolane (280z)

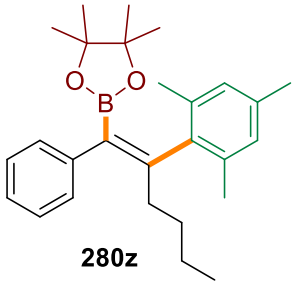

280z

Prepared by reaction of 1-phenylhex-1-yne (79.3 mg, 0.501 mmol) with 2-mesityl magnesium bromide following general procedure. The title compound was isolated as a white solid (151.2 mg, 0.373 mmol, 75 %) after flash chromatography on silica gel (petroleum ether/ethyl acetate 99:1). Analytical data of **280z**: ^{1}H NMR (400 MHz $CDCl_3$): δ 7.34 (m, 4H), 7.24 (m, 1H), 6.85 (s, 2H), 2.33 (m, 11H), 1.34 (m, 2H), 1.17 (m, 2H), 0.89 (s, 12H), 0.78 (t, *J* = 7.1 Hz, 3H); ^{13}C NMR (101 MHz, $CDCl_3$): δ 149.6, 141.1, 139.5, 136.3, 135.6, 128.4, 128.0, 127.7, 125.7, 82.7, 34.5, 30.5, 24.1, 23.3, 20.9, 20.2, 13.8; HRMS (APCI-TOF) m/z: $[M + H]^+$ Calc'd for $C_{27}H_{38}BO_2$: 405.2965 Found: 405.2969.

(*E*)-2-(2-([1,1'-biphenyl]-4-yl)-1-phenylhex-1-en-1-yl)-4,4,5,5-tetramethyl-1,3,2-dioxaborolane (280a')

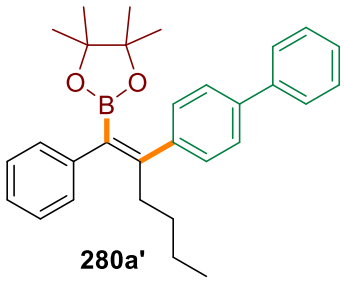

280a'

Prepared by reaction of 1-phenylhex-1-yne (79.5 mg, 0.502 mmol) with 4-biphenylmagnesium bromide following general procedure. The title compound was isolated as a colourless oil (151.1 mg, 0.345 mmol, 69 %) after flash chromatography on silica gel (petroleum ether/ethyl acetate 99:1). Analytical data of **280a'**: ^{1}H NMR (400 MHz $CDCl_3$): δ 7.63 (d, *J* = 8.0 Hz, 2H), 7.58 (d, *J* = 8.0 Hz, 2H), 7.45 (m, 4H), 7.36 (m, 3H), 7.26 (m, 2H), 7.23 (m, 1H), 2.45 (t, *J* = 7.7 Hz, 2H), 1.25 (m, 4H), 1.03 (s, 12H), 0.75 (t, *J* = 7.1 Hz, 3H); ^{13}C NMR (101 MHz, $CDCl_3$): δ 152.1, 143.0, 141.5, 141.1, 139.8, 128.7, 128.7, 128.5, 128.1, 127.1, 127.0, 126.6, 125.9, 83.3, 33.5, 30.6, 24.4, 22.5, 13.8; HRMS (APCI-TOF) m/z: $[M + H]^+$ Calc'd for $C_{30}H_{36}BO_2$: 439.2808 Found: 439.2816.

4.5.5 Further transformations of the selected vinyl boronates

Potassium (*E*)-(1,2-diphenylhex-1-en-1-yl)trifluoroborate (283)

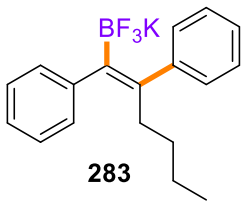

283

Compound was synthesized following slightly modified literature procedure.[415] In a 20 mL polypropylene container equipped with a stirring bar, **280a** (181.2 mg, 0.500 mmol) and methanol (5 mL) were placed. KHF_2 (156.2 mg, 2.00 mmol, 4.0 eq.) was added followed by dropwise addition of water (0.45 mL, 25.0 mmol, 50 eq.). Reaction was carried out at room temperature for 18 h. Solvents were evaporated in vacuum and the resulting solid was triturated in hot acetone. Mixture was filtered and remaining solids were washed with hot acetone. The filtrate was evaporated, and the resulting solid was triturated in diethyl ether. Mixture was filtered and precipitate was washed with diethyl ether followed by drying in vacuo. Product was obtained as a white powder (143.4 mg, 0.419 mmol, 84 %). Analytical data of **283**: ^{1}H NMR (400 MHz, DMSO-d_6): δ 7.25 (m, 2H), 7.16 (m, 4H), 7.06 (m, 1H), 6.99 (m, 3H), 2.00 (m, 2H), 0.93 (m, 4H), 0.56 (t, *J* = 6.7 Hz, 3H); ^{19}F NMR (376 MHz, DMSO-d_6): δ -130.78 (br. s, FWHM = 85 Hz, 3F); ^{13}C NMR (101 MHz, DMSO-d_6): δ 149.7, 146.6, 140.1, 129.3, 128.6, 127.0, 126.8, 124.8, 123.5, 35.4, 30.9, 22.3, 14.2, 1C missing; *HRMS not measured due to high fragmentation in both positive and negative polarization*.

1,2-diphenylhexan-1-one (284)

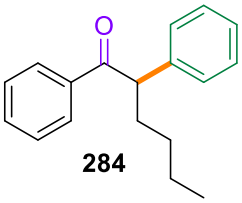

In a 4ml dark vial equipped with a stirring bar, **280a** (72.6 mg, 0.200 mmol) was placed followed by addition of THF (0.8 mL). The solution was cooled to 0 ºC and 30% H_2O_2 (916.0 mg, 8.080 mmol, 40 eq., 0.83 mL) was added. Then 3 M NaOH (0.33 mL) was added dropwise. The reaction was stirred at 0 ºC for 3 h, then it was allowed to warm to r.t. and stirred overnight. After 24 h, the reaction was diluted with water. The organic layer was separated and water phase was extracted with MTBE. The combined organic layers were dried over Na_2SO_4, solvent was evaporated, and the residue was purified by flash chromatography on silica gel (petroleum ether/methyl *tert*-butyl ether in gradient from 100 to 98:2) to provide the desired product as a white solid (44.4 mg, 0.175 mmol, 88 %). Analytical data of **284**: ^{1}H NMR (400 MHz $CDCl_3$): δ 7.98 (d, *J* = 7.6 Hz, 2H), 7.48 (m, 1H), 7.39 (m, 2H), 7.31 (m, 4H), 7.21 (m, 1H), 4.56 (t, *J* = 7.3 Hz, 1H), 2.21 (m, 1H), 1.85 (m, 1H), 1.31 (m, 4H), 0.88 (t, *J* = 7.0 Hz, 3H); ^{13}C NMR (101 MHz, $CDCl_3$): δ 200.1, 139.8, 137.0, 132.7, 128.8, 128.6, 128.5, 128.2, 126.9, 53.6, 33.8, 29.9, 22.7, 13.9. IR (CH_2Cl_2): 1681 (C=O), 1233 (C-O) cm^{-1}; HRMS (APCI-TOF) m/z: $[M + H]^+$ Calc'd for $C_{18}H_{21}O$: 253.1592 Found: 253.1594.

(*E*)-2-(5-azido-1,2-diphenylpent-1-en-1-yl)-4,4,5,5-tetramethyl-1,3,2-dioxaborolane (285)

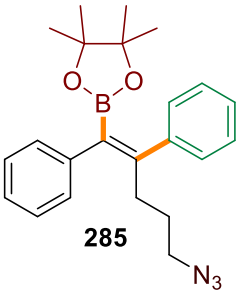

In a 4ml dark vial equipped with a stirring bar, **280f** (38.3 mg, 0.100 mmol) and NaN_3 (7.9 mg, 0.120 mmol, 1.2 eq.) were placed followed by addition of DMF (0.7 mL). The mixture was stirred at 75 ºC for 7 h, then it was cooled to 0 °C. and diluted with water. Mixture was extracted with MTBE. The combined organic layers were dried over Na_2SO_4, solvent was evaporated, and the crude product (yellow solid (38.4 mg, 0.099 mmol, 99 %) was employed in next reaction without further purification. Analytical data of **285**: ^{1}H NMR (400 MHz $CDCl_3$): δ 7.35 (m, 6H), 7.30 (m, 1H), 7.24 (m, 3H), 3.08 (t, *J* = 7.1 Hz, 2H), 2.49 (t, *J* = 8.0 Hz, 2H), 1.52 (m, 2H), 1.01 (s, 12H); ^{13}C NMR (101 MHz, $CDCl_3$): δ 150.3, 143.1, 141.0, 128.2, 128.1, 127.3, 126.1, 83.4, 51.0, 30.8, 27.5, 24.3; IR (CH_2Cl_2): 2096 (N=N=N) 1144 (C-N) cm^{-1}; HRMS (APCI-TOF) m/z: $[M]^{+\cdot}$ Calc'd for $C_{23}H_{28}BN_3O_2$: 389.2275 Found: 389.2267.

(*E*)-1-(4,5-diphenyl-5-(4,4,5,5-tetramethyl-1,3,2-dioxaborolan-2-yl)pent-4-en-1-yl)-4-phenyl-1*H*-1,2,3-triazole (286)

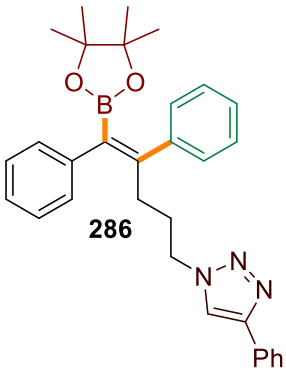

In a 10 ml round bottom flask equipped with a stirring bar, **285** (38.4 mg, 0.100 mmol) copper (II) sulfate pentahydrate (2.5 mg, 0.01 mmol, 10 mol%), sodium ascorbate (3.9 mg, 0.02 mmol, 20 mol%) and phenyl acetylene (12.3 mg, 0.120 mmol, 1.2 eq., 13.2 µL) were placed followed by addition of THF (2 mL) and degassed water (2 mL). The reaction was stirred at room temperature for 7 h. Mixture was passed through a pad of celite, then diluted with saturated solution of NH_4Cl in water. Filtrate was extracted with MTBE. The combined organic layers were dried over Na_2SO_4, solvent was evaporated and analyzed by NMR without further purification to provide the desired product as a white solid (49.1 mg, 0.100 mmol, quant.). Analytical data of **286**: ^{1}H NMR (400 MHz $CDCl_3$): δ 7.73 (d, *J* = 7.5 Hz, 2H), 7.33 (m, 10H), 7.21 (d, *J* = 7.5 Hz, 2H), 7.16 (d, *J* = 7.4 Hz, 1H), 4.17 (t, *J* = 7.0 Hz, 2H), 2.51 (t, *J* = 7.5 Hz, 2H), 1.85 (quint., *J* = 7.2 Hz, 2H), 0.99 (s, 12H); ^{13}C NMR (101 MHz, $CDCl_3$): δ 149.5, 147.5, 142.8, 140.7, 130.7, 128.7, 128.4, 128.3, 128.2, 127.9, 127.5, 126.3, 125.7, 119.3, 83.5, 49.6, 30.3, 28.8, 24.3; IR (CH_2Cl_2): 1144 (C-N) cm^{-1}; HRMS (APCI-TOF) m/z: $[M + H]^+$ Calc'd for $C_{31}H_{35}BN_3O_2$: 492.2822 Found: 492.2831.

Suzuki-Coupling reactions of selected vinyl boronates.

(*Z*)-(1-(4-methoxyphenyl)hex-1-ene-1,2-diyl)dibenzene (281a)

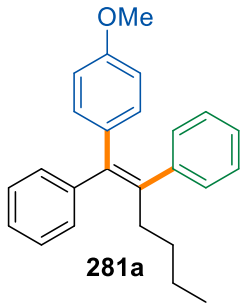

Compound was synthesized following Suzuki coupling procedure with 36.2 mg, (0.100 mmol, 1.0 eq.) of **280a**, 0.9 mg (0.001 mmol, 1 mol%) of XPhos Pd G3 and 22.4 mg (0.120 mmol, 1.2 eq., 15.0 µL) of 4-bromoanisole in aq. KOH (0.08 mL, 0.3 mmol, 3 eq., 4M) and 0.3 mL of THF at 75 °C, 18 h reaction. The desired product was obtained as a white solid (29.3 mg, 0.086 mmol, 86 %) using silica gel chromatography (petroleum ether). Analytical data of **281a**: ^{1}H NMR (400 MHz $CDCl_3$): δ 7.38 (m, 2H), 7.29 (m, 3H), 7.18 (m, 5H), 6.83 (m, 2H), 6.58 (m, 2H), 3.69 (s, 3H), 2.46 (t, *J* = 8.0 Hz, 2H), 1.30 (m, 4H), 0.81 (t, *J* = 7.2 Hz, 3H); ^{13}C NMR (101 MHz, $CDCl_3$): δ 157.4, 143.8, 142.8, 140.2, 138.4, 135.5, 131.9, 129.6, 129.5, 128.1, 127.9, 126.5, 126.0, 112.7, 55.0, 35.7, 31.1, 22.8, 13.9; HRMS (APCI-TOF) m/z: $[M + H]^+$ Calc'd for $C_{25}H_{27}O$: 343.2062 Found: 343.2067.

(*Z*)-1-(4-(1,2-diphenylhex-1-en-1-yl)phenyl)ethan-1-one (281b)

Compound was synthesized following Suzuki coupling procedure with 36.2 mg, (0.100 mmol, 1.0 eq.) of

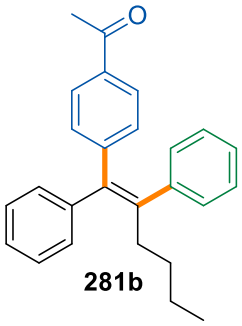

280a, 0.9 mg (0.001 mmol, 1 mol%) of XPhos Pd G3 and 23.9 mg (0.120 mmol, 1.2 eq., 15.0 µL) of 4'-bromoacetophenone in aq. KOH (0.08 mL, 0.3 mmol, 3 eq., 4M) and 0.3 mL of 1,4-dioxane at 100 °C, 18 h reaction. The desired product was obtained as a white solid (25.1 mg, 0.071 mmol, 71 %) using silica gel chromatography (petroleum ether/ethyl acetate 98.5:1.5). Analytical data of **281b**: ^{1}H NMR (400 MHz $CDCl_3$): δ 7. 60 (d, *J* = 8.6 Hz, 2H), 7.36 (m, 2H), 7.30 (m, 1H), 7.23 (m, 2H), 7.16 (m, 3H), 7.11 (m, 2H), 6.97 (d, *J* = 8.4 Hz, 2H), 2.47 (m, 5H), 1.27 (m, 4H), 0.78 (t, *J* = 8.0 Hz, 3H); ^{13}C NMR (101 MHz, $CDCl_3$): δ 197.7, 148.3, 143.0, 142.7, 141.9, 138.1, 134.3, 130.8, 129.5, 129.4, 128.3, 128.0, 127.5, 126.9, 126.5, 35.7, 31.0, 26.4, 22.7, 13.8; IR (CH_2Cl_2): 1683 (C=O), 1266 (C-O), cm^{-1}; HRMS (APCI-TOF) m/z: $[M + H]^+$ Calc'd for $C_{26}H_{27}O$: 355.2062 Found: 355.2065.

(*Z*)-1-(2-(1,2-diphenylhex-1-en-1-yl)phenyl)ethan-1-one (281c)

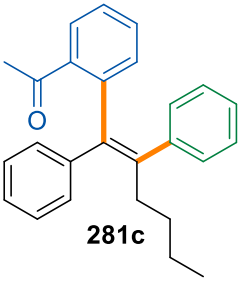

Compound was synthesized following Suzuki coupling procedure with 36.2 mg, (0.100 mmol, 1.0 eq.) of **280a**, 0.9 mg (0.001 mmol, 1 mol%) of XPhos Pd G3 and 23.9 mg (0.120 mmol, 1.2 eq., 15.0 µL) of 2'-bromoacetophenone in aq. KOH (0.08 mL, 0.3 mmol, 3 eq., 4M) and 0.3 mL of 1,4-dioxane at 100 °C, 18 h reaction. The desired product was obtained as a white solid (14.1 mg, 0.040 mmol, 40 %) using silica gel chromatography (petroleum ether/ethyl acetate 99:1). Analytical data of **281c**: ^{1}H NMR (400 MHz $CDCl_3$): δ 7.30 (m, 5H), 7.22 (m, 1H), 7.16 (m, 1H), 7.10 (m, 7H), 2.49 (t, *J* = 8.0 Hz, 2H), 2.00 (s, 3H), 1.27 (m, 4H), 0.80 (t, *J* = 7.2 Hz, 3H); ^{13}C NMR (101 MHz, $CDCl_3$): δ 201.7, 142.9, 142.5, 142.2, 140.6, 139.9, 137.5, 132.9, 130.1, 130.0, 129.4, 127.7, 127.6, 127.4, 126.5, 126.1, 125.9, 34.8, 31.0, 28.6, 22.8, 13.8; IR (CH_2Cl_2): 1692 (C=O), 1246 (C-O) cm^{-1}; HRMS (APCI-TOF) m/z: $[M + H]^+$ Calc'd for $C_{26}H_{27}O$: 355.2062 Found: 355.2068.

(*Z*)-3-(1,2-diphenylhex-1-en-1-yl)pyridine (281d)

Compound was synthesized following Suzuki coupling procedure with 36.2 mg, (0.100 mmol, 1.0 eq.) of **280a**, 0.9 mg (0.001 mmol, 1 mol%) of XPhos Pd G3 and 19.0 mg (0.120 mmol, 1.2 eq., 11.6 µL) of 3-bromopyridine in aq. KOH (0.08 mL, 0.3 mmol, 3 eq., 4M) and 0.3 mL of THF at 75 °C, 18 h reaction. The desired product was obtained as a white solid (27.5 mg, 0.088 mmol, 88 %) using silica gel chromatography (petroleum ether/ethyl acetate 93:7). Analytical data of **281d**: ^{1}H NMR (400 MHz $CDCl_3$): δ 8.21 (br. s, 1H), 8.13 (br. s, 1H), 7.37 (m, 2H), 7.27 (m, 3H), 7.13 (m, 6H), 6.94 (dd, J = 7.1 Hz, 4.7 Hz, 1H), 2.46 (t, J = 8.0 Hz, 2H), 1.27 (m, 4H), 0.78 (t, J = 7.2 Hz, 3H); ^{13}C NMR (101 MHz, $CDCl_3$): δ 151.4, 146.6, 143.5, 142.3, 141.6, 138.7, 137.6, 135.5, 129.5, 129.5, 128.3, 128.1, 127.0, 126.6, 122.4, 35.7, 30.9, 22.7, 13.8; HRMS (APCI-TOF) m/z: $[M + H]^+$ Calc'd for $C_{23}H_{24}N$: 314.1909 Found: 314.1908.

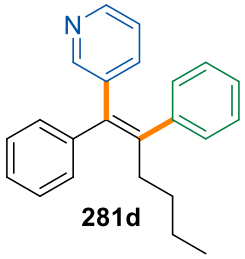

281d

(*Z*)-2-(4-(1,2-diphenylbut-1-en-1-yl)phenoxy)-*N*,*N*-dimethylethan-1-amine, Tamoxifen (281e)

Compound was synthesized following Suzuki coupling procedure with 36.8 mg, (0.110 mmol, 1.1 eq.) of **280c**, 0.9 mg (0.001 mmol, 1 mol%) of XPhos Pd G3 and 24.4 mg (0.100 mmol, 1.0 eq.) of (2-(4-bromophenoxy)ethyl)dimethylamine **5** in aq. KOH (0.08 mL, 0.3 mmol, 3 eq., 4M) and 0.3 mL of THF at 75 °C, 24 h reaction. The desired product was obtained as a white solid (33.0 mg, 0.089 mmol, 89 %) using silica gel chromatography (dichloromethane/methanol from 100:0 to 90:10). Analytical data of **281e**: ^{1}H NMR (400 MHz $CDCl_3$): 7.35 (m, 2H), 7.26 (m, 3H), 7.14 (m, 5H), 6.78 (m, 2H), 6.57 (m, 2H), 3.95 (t, J = 5.7 Hz, 2H), 2.68 (t, J = 5.8 Hz, 2H), 2.47 (q, J = 7.4 Hz, 2H), 2.31 (s, 6H), 0.93 (t, J = 7.4 Hz, 3H); ^{13}C NMR (101 MHz, $CDCl_3$): 156.7, 143.8, 142.4, 141.3, 138.2, 135.5, 131.8, 129.7, 129.4, 128.1, 127.8, 126.5, 126.0, 113.4, 65.5, 58.2, 45.8, 29.0, 13.6; HRMS (APCI-TOF) m/z: $[M + H]^+$ Calc'd for $C_{26}H_{30}NO$: 372.2327 Found: 372.2329. Analytical data were in accordance with the literature data.[389]

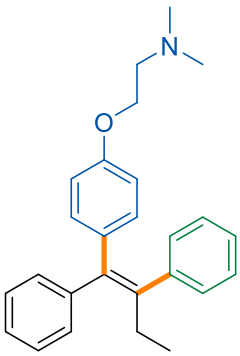

281e

4.5.6 Computational studies

General.

All calculations were performed by my supervisor Wojciech Chaładaj with Gaussian 16 package.[416] Structures of minima and transition states were optimized employing M06 functional[417] and def2-SVP basis set.[418] Frequency analysis was performed at the same level of theory to provide correction to thermodynamic functions and confirm the nature of optimized structures (minima and transition states featured zero and one imaginary frequency, respectively). Single point energies were calculated with M06 functional[419] employing def2-TZVPP[418] basis set and solvation (toluene) with the SMD model.[419] Molecular structures were visualized in CYLview.[420]

Optimized geometries, energies and corrections to thermodynamic functions.

BpinH

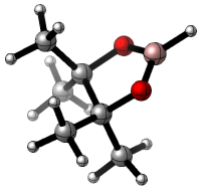

E (M06/Def2-SVP) = -411.297740956
E (M06/Def2-TZVPP/SMD(toluene)//M06/Def2-SVP) = -411.766453317

Zero-point correction= 0.189060 (Hartree/Particle)
Thermal correction to Energy= 0.198373
Thermal correction to Enthalpy= 0.199317
Thermal correction to Gibbs Free Energy= 0.156319

Charge = 0 Multiplicity = 1

B	-0.00010300	1.93159200	0.00001100
O	-1.06019700	1.18425800	-0.41244700
O	1.06006400	1.18434700	0.41244400
H	-0.00017200	3.12894000	0.00003500
C	-0.77953100	-0.18347000	-0.05591400
C	0.77953900	-0.18338600	0.05595000
C	1.47129400	-0.44193600	-1.27263000
H	2.54232500	-0.21015500	-1.16560600
H	1.37489400	-1.49323600	-1.58713400
H	1.06610500	0.20089400	-2.07034100
C	-1.34122700	-1.10006100	-1.11989400
H	-1.05908000	-2.14769800	-0.92089400
H	-2.44071100	-1.03897500	-1.11998400
H	-0.99103400	-0.82592200	-2.12490700
C	-1.47133200	-0.44210600	1.27262800
H	-2.54226300	-0.20976200	1.16585100
H	-1.37540800	-1.49353500	1.58681700
H	-1.06570800	0.20029100	2.07047500
C	1.34143000	-1.09993900	1.11986700
H	1.05922200	-2.14757600	0.92095400
H	2.44091900	-1.03893200	1.11973100
H	0.99146000	-0.82575100	2.12493600

BpinOMe

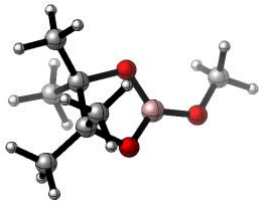

E (M06/Def2-SVP) = -525.736475383
E (M06/Def2-TZVPP/SMD(toluene)//M06/Def2-SVP) = -526.335530913

Zero-point correction= 0.223081 (Hartree/Particle)
Thermal correction to Energy= 0.235208
Thermal correction to Enthalpy= 0.236152
Thermal correction to Gibbs Free Energy= 0.186203

Charge = 0 Multiplicity = 1

B	1.17107800	-0.39956800	-0.12742500
O	0.17493500	-1.26895500	-0.48050000
O	0.70285100	0.81246900	0.31819900
C	-1.05348000	-0.69134000	-0.01610500
C	-0.70630800	0.83376200	0.03775800
O	2.47957500	-0.71414700	-0.21020400
C	3.45002200	0.23464200	0.13830000
H	3.40420800	0.49051000	1.21143700
H	4.44515700	-0.18222400	-0.07564600
H	3.33291400	1.17236400	-0.43224600

C	-1.33610100	-1.27796700	1.35822400
H	-2.30930500	-0.94813200	1.75536600
H	-1.34961900	-2.37594900	1.27725800
H	-0.55188400	-1.00394500	2.08220900
C	-1.42097800	1.60899400	1.12202600
H	-1.12926600	2.67006100	1.07641600
H	-2.51415200	1.55102200	0.98686300
H	-1.16978300	1.23498800	2.12456200
C	-0.88650400	1.52544300	-1.30409100
H	-1.95002600	1.65496800	-1.56025200
H	-0.42002300	2.52180500	-1.25537900
H	-0.39823600	0.96203700	-2.11542600
C	-2.16839000	-1.05275600	-0.97246600
H	-2.35507600	-2.13730400	-0.93234300
H	-3.10315900	-0.53603200	-0.69675300
H	-1.91558900	-0.79593100	-2.0107960

2-methyl-1,2-diphenylvinylmagnesium bromide x 2Me$_2$O

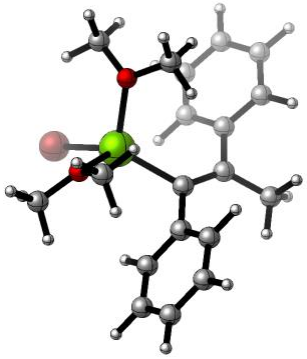

E (M06/Def2-SVP) = -3662.05165728
E (M06/Def2-TZVPP/SMD(toluene)//M06/Def2-SVP) = -3663.44085406

Zero-point correction=	0.393765 (Hartree/Particle)
Thermal correction to Energy=	0.420872
Thermal correction to Enthalpy=	0.421816
Thermal correction to Gibbs Free Energy=	0.334577

Charge = 0 Multiplicity = 1

C	0.23082500	-2.14245300	-0.59730300
C	-0.59874900	-1.09284400	-0.36262100
C	-0.20580600	-3.54788400	-0.92660800
H	-0.10243900	-4.23334200	-0.06484800
H	-1.26042700	-3.58426200	-1.23731300
H	0.40956100	-3.97602500	-1.73660100
C	-2.06218300	-1.24572700	-0.37836300
C	-2.74375800	-2.11728700	0.49206900
C	-2.84956100	-0.42583900	-1.21051500
C	-4.13553100	-2.17024000	0.52577800
H	-2.15789400	-2.75375500	1.16601300
C	-4.24007200	-0.48855500	-1.18983100
H	-2.34271300	0.27042100	-1.89235600
C	-4.89444200	-1.35775900	-0.31564600
H	-4.63452500	-2.85781600	1.21653900
H	-4.82094000	0.15074800	-1.86268500
H	-5.98711400	-1.40253400	-0.29267300
C	1.70117700	-1.93637300	-0.53191900
C	2.54593800	-2.87754200	0.07995800

C	2.29792500	-0.77832000	-1.05679400
C	3.91059900	-2.63739100	0.22289700
H	2.12055500	-3.80580800	0.47578400
C	3.66100400	-0.53101000	-0.91168800
H	1.68942400	-0.07338400	-1.63623700
C	4.47514000	-1.45574000	-0.25850200
H	4.54188000	-3.38195700	0.71818100
H	4.08619600	0.38568000	-1.33372100
H	5.54791100	-1.27118500	-0.14922000
Mg	0.05961300	0.89090700	0.09533300
C	-2.22045800	0.94862300	2.14872800
H	-3.11155700	0.43872300	1.73915800
H	-1.51953300	0.18527700	2.51699900
H	-2.51687000	1.60200500	2.98859500
C	-2.38937800	2.73469500	0.61914900
H	-3.28909600	2.29874200	0.14783200
H	-2.69496900	3.42447000	1.42541300
H	-1.79644100	3.27936900	-0.12945800
C	2.41501900	1.78323400	1.87424700
H	3.37821200	1.35997000	1.53576100
H	2.16741500	2.65697900	1.25415600
H	2.49501900	2.07650100	2.93576100
C	1.61031100	-0.36574000	2.43982000
H	2.56831600	-0.82694400	2.13840800
H	1.62742700	-0.15133600	3.52352300
H	0.79556100	-1.06787300	2.20604400
Br	0.75865900	2.81552100	-1.24693100
O	-1.56993600	1.70498100	1.14794500
O	1.38126200	0.82603600	1.71060700

β-Styrylmagnesium bromide x 2Me$_2$O

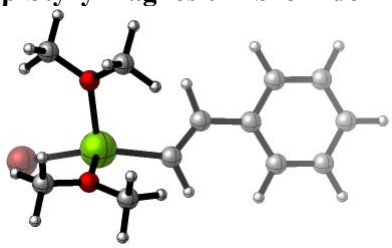

E (M06/Def2-SVP) = -3392.07420503
E (M06/Def2-TZVPP/SMD(toluene)//M06/Def2-SVP) = -3393.17399167

Zero-point correction=	0.285841 (Hartree/Particle)
Thermal correction to Energy=	0.306738
Thermal correction to Enthalpy=	0.307682
Thermal correction to Gibbs Free Energy=	0.232987

Charge = 0 Multiplicity = 1

C	1.86182700	-0.29257600	-0.18178700
C	0.88498500	-0.02735600	0.71306100
C	3.32402000	-0.26855700	0.00778000
C	3.93190900	0.03356000	1.23687700
C	4.16337500	-0.55579300	-1.07920000
C	5.31488000	0.05039400	1.36888400
H	3.30258300	0.25460100	2.10502200
C	5.54950500	-0.54020800	-0.95192500
H	3.70742300	-0.79959200	-2.04590300

C	6.13368100	-0.23540000	0.27502500
H	5.76340100	0.28686100	2.33887700
H	6.17879100	-0.76972800	-1.81739500
H	7.22233400	-0.22281200	0.38183000
Mg	-1.17471100	-0.16448100	0.29664700
C	-1.07244500	2.84484100	1.09147500
H	-1.38420700	3.29633500	2.04992500
H	-0.04380100	2.46534600	1.17732900
H	-1.11431800	3.61859600	0.30230700
C	-3.26400700	2.10972400	0.57824000
H	-3.65410100	2.62063900	1.47597900
H	-3.37160400	2.78319000	-0.29295500
H	-3.83265500	1.18109900	0.41737800
Br	-3.11084200	-1.58359600	0.72165900
O	-1.90765300	1.75477500	0.76283900
C	-2.40380100	-0.30062800	-2.60886800
H	-2.95976600	-1.06338900	-2.04501700
H	-3.08890600	0.51896200	-2.89474100
H	-1.97106800	-0.74191800	-3.52381800
C	-0.61597500	1.22754700	-2.35051900
H	-0.17896800	0.89714100	-3.30956600
H	-1.24833300	2.11725800	-2.53428800
H	0.19986400	1.48031100	-1.65592000
O	-1.37502900	0.18910900	-1.76827400
H	1.58792900	-0.57934400	-1.21514800
H	1.27514900	0.23173000	1.71748800

TS1

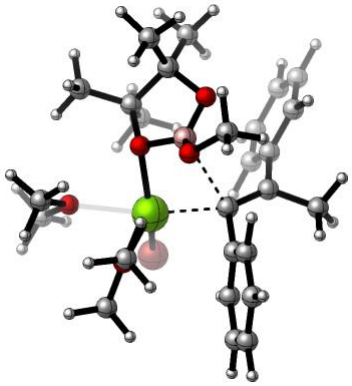

E (M06/Def2-SVP) = -4187.78625985
E (M06/Def2-TZVPP/SMD(toluene)//M06/Def2-SVP) = -4189.76048499

Zero-point correction=	0.617921 (Hartree/Particle)
Thermal correction to Energy=	0.657128
Thermal correction to Enthalpy=	0.658072
Thermal correction to Gibbs Free Energy=	0.548545

Charge = 0 Multiplicity = 1

C	-0.47440200	-2.29667600	0.59178700
C	0.40260400	-1.39664800	0.07013500
C	-0.19223400	-3.76910300	0.78198200
H	-0.99505500	-4.38553900	0.33931600
H	0.76708600	-4.09254600	0.35399000
H	-0.18846900	-4.01825400	1.85904500
C	1.76545300	-1.93321300	-0.21119900

C	2.14451400	-2.58427500	-1.39718900
C	2.75228900	-1.80725200	0.78745200
C	3.43646300	-3.07552600	-1.58047600
H	1.40288100	-2.73596800	-2.18332300
C	4.04435000	-2.29291300	0.60477800
H	2.48325500	-1.31824700	1.73291700
C	4.40111000	-2.92643300	-0.58619400
H	3.68823700	-3.59123400	-2.51328300
H	4.77838400	-2.18580800	1.41066400
H	5.41349100	-3.31582100	-0.72923500
C	-1.80346200	-1.94554300	1.17008500
C	-2.99049700	-2.49681300	0.66510100
C	-1.87611000	-1.16769300	2.33182700
C	-4.21193900	-2.25933600	1.28501500
H	-2.94918100	-3.10362700	-0.24666600
C	-3.10128200	-0.92909200	2.95763900
H	-0.95225600	-0.74912200	2.74972000
C	-4.27293100	-1.47164100	2.43667900
H	-5.12783600	-2.68949600	0.86690800
H	-3.13314300	-0.32081600	3.86704300
H	-5.23258000	-1.29267700	2.93138900
Mg	0.79790900	0.83711400	0.31086300
C	2.98029100	0.55752800	-1.96627500
H	3.68446100	-0.29236700	-1.93274900
H	2.05035100	0.22820200	-2.45390400
H	3.43466300	1.38984900	-2.53712900
C	3.80306100	1.40592300	0.07725100
H	4.52422300	0.57298100	0.16182900
H	4.29084800	2.26226100	-0.42703400
H	3.47163500	1.69732800	1.08602200
Br	1.19612700	1.20112100	2.74195200
O	2.66699100	0.99054500	-0.65552200
C	-1.92136400	1.73212800	-0.95125000
C	-2.90268500	0.70979300	-1.61973800
B	-0.85335100	-0.22769900	-1.64494200
O	-0.62132000	1.11961400	-1.21295300
O	-2.19399300	-0.52789000	-1.53432800
C	-4.23663700	0.58067100	-0.91834500
H	-4.85320200	-0.16555200	-1.44459000
H	-4.12880900	0.24295700	0.12215400
H	-4.77896900	1.54131800	-0.93225200
C	-2.11263800	1.83973100	0.54892500
H	-2.11917000	0.85246400	1.03441500
H	-1.30839100	2.44879100	0.99563600
H	-3.06205300	2.34116400	0.79202500
C	-1.95786500	3.11385200	-1.56940400
H	-2.98546100	3.51294000	-1.53638800
H	-1.31624000	3.80082400	-0.99605300
H	-1.61741300	3.11168700	-2.61503600
C	-3.12417300	0.99361900	-3.10165900
H	-3.66185500	0.13860800	-3.54123100
H	-3.72906700	1.89823400	-3.27099700
H	-2.16939600	1.10427400	-3.64275900
C	1.10376600	4.14931600	0.92250800
H	0.83262300	3.72493500	1.89896000
H	2.14652200	4.51730200	0.97344000

H	0.44067900	4.99967400	0.67039900
C	1.40277300	3.55661400	-1.31750500
H	0.87479800	4.48277900	-1.61507000
H	2.49152400	3.76143500	-1.32737700
H	1.16841300	2.77006100	-2.04780100
O	0.98189500	3.12983000	-0.04592300
O	-0.06529200	-0.73655500	-2.64371300
C	-0.54642300	-1.85360100	-3.34102900
H	0.20897300	-2.16667100	-4.07802500
H	-0.74961300	-2.70293100	-2.66054100
H	-1.48593200	-1.62436600	-3.87430100

TS2

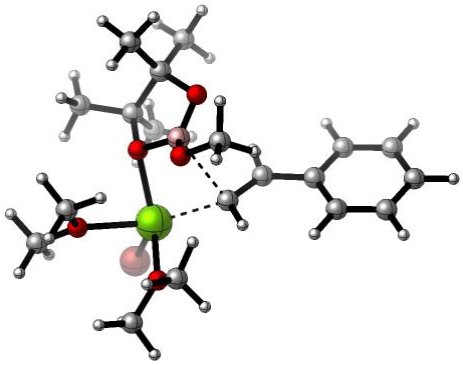

E (M06/Def2-SVP) = -3917.82295928
E (M06/Def2-TZVPP/SMD(toluene)//M06/Def2-SVP) = -3919.50990969

Zero-point correction=	0.510152 (Hartree/Particle)
Thermal correction to Energy=	0.543389
Thermal correction to Enthalpy=	0.544333
Thermal correction to Gibbs Free Energy=	0.445116

Charge = 0 Multiplicity = 1

C	2.16241000	-0.27813500	-0.59142800
C	1.08085500	-0.72940500	0.07965700
C	3.56928500	-0.70267400	-0.47672300
C	3.99585800	-1.73539200	0.37425800
C	4.54446300	-0.05124400	-1.24704100
C	5.33534400	-2.09629900	0.45072100
H	3.25636300	-2.26677500	0.98282300
C	5.88736800	-0.40975700	-1.17477700
H	4.22994700	0.75679000	-1.91720700
C	6.29074100	-1.43545000	-0.32337500
H	5.64129400	-2.90630700	1.12031500
H	6.62528400	0.11607900	-1.78838500
H	7.34476800	-1.72201600	-0.26266300
Mg	-1.11356100	-0.81038500	-0.14204200
C	-0.63769500	-2.52872300	2.50948100
H	-0.07195800	-3.47496300	2.58740100
H	0.04686300	-1.67532900	2.61067700
H	-1.38248900	-2.49187900	3.32751600
C	-2.28786000	-3.40207200	1.07346100
H	-1.87767100	-4.41581800	1.22782100
H	-3.11809600	-3.23850500	1.78791500
H	-2.65853300	-3.31379300	0.04096600

Br	-2.11065100	-1.69085900	-2.22602100
O	-1.27737300	-2.43252200	1.25732500
C	-0.97292200	2.37011900	-0.63487300
C	0.14571200	3.28454400	-0.03228800
B	0.25288100	1.27481900	1.00010200
O	-0.99140100	1.27660600	0.31746800
O	1.02141400	2.34691400	0.60516300
C	0.93178300	4.07293600	-1.05634600
H	1.68256000	4.69412200	-0.54360500
H	1.46466900	3.41155800	-1.75418800
H	0.27176300	4.74246900	-1.63309100
C	-0.61976000	1.83200200	-2.00975400
H	0.37812700	1.36849900	-2.02974000
H	-1.35109700	1.06741700	-2.32262800
H	-0.64494800	2.63551000	-2.76217800
C	-2.35963900	2.97555600	-0.66588500
H	-2.37808900	3.88198300	-1.29396900
H	-3.06389100	2.24937900	-1.10590100
H	-2.71852000	3.23636400	0.34048000
C	-0.38311300	4.21587600	1.04993300
H	0.47249000	4.68517900	1.56021700
H	-1.01698600	5.01586700	0.63484000
H	-0.96408600	3.66449800	1.80811300
C	-4.42567000	-0.55397400	0.21409900
H	-4.30654500	-0.92991000	-0.81238200
H	-5.04126900	-1.26150800	0.80299300
H	-4.93833000	0.42645700	0.19725500
C	-3.15528000	0.07214800	2.08715400
H	-3.59809300	1.08649700	2.11531800
H	-3.74423500	-0.58786200	2.75457500
H	-2.12034900	0.14137200	2.45576500
O	-3.13978000	-0.43172400	0.77550500
O	0.28562700	0.72678700	2.26145400
C	1.48405600	0.80757300	2.98775600
H	1.34350900	0.31461800	3.96230200
H	2.31274700	0.30707300	2.45302500
H	1.78109800	1.85609600	3.16417400
H	2.04454600	0.54272100	-1.32111200
H	1.36676200	-1.51954400	0.80779800

R_1=5.28%

Crystal Data and Experimental

Experimental. Single colourless irregular-shaped crystals of **280l** were obtained by recrystalization from MeOH. A suitable crystal 0.23×0.22×0.07 mm^3 was selected and mounted on a loop on an XtaLAB Synergy, Dualflex, HyPix-Arc 150 diffractometer. The crystal was kept at a steady T = 293.15(10) K during data collection. The structure was solved with the ShelXS (Sheldrick, 2008) structure solution program using the Direct Methods solution method and by using **Olex2** (Dolomanov et al., 2009) as the graphical interface. The model was refined with version 2018/3 of ShelXL 2018/3 (Sheldrick, 2015) using Least Squares minimisation.

Crystal Data. $C_{24}H_{30}BBrO_2$, M_r = 441.20, monoclinic, $P2_1/n$ (No. 14), a = 13.5811(3) Å, b = 11.3061(3) Å, c = 15.2587(3) Å, β = 90.089(2)°, α = γ = 90°, V = 2342.97(9) Å^3, T = 293.15(10) K, Z = 4, Z' = 1, μ(Cu K$_\alpha$) = 2.497, 10414 reflections measured, 4002 unique (R_{int} = 0.0265) which were used in all calculations. The final wR_2 was 0.1574 (all data) and R_1 was 0.0528 (I > 2(I)).

Compound	**280l**
Formula	$C_{24}H_{30}BBrO_2$
$D_{calc.}$/ g cm^{-3}	1.251
μ/mm^{-1}	2.497
Formula Weight	441.20
Colour	colourless
Shape	irregular
Size/mm^3	0.23×0.22×0.07
T/K	293.15(10)
Crystal System	monoclinic
Space Group	$P2_1/n$
a/Å	13.5811(3)
b/Å	11.3061(3)
c/Å	15.2587(3)
α/°	90
β/°	90.089(2)
γ/°	90
V/Å^3	2342.97(9)
Z	4
Z'	1
Wavelength/Å	1.54184
Radiation type	Cu K$_\alpha$
Θ_{min}/°	4.355
Θ_{max}/°	74.729
Measured Refl.	10414
Independent Refl.	4002
Reflections with I > 2(I)	2894
R_{int}	0.0265
Parameters	269
Restraints	0
Largest Peak	0.705
Deepest Hole	-0.650
GooF	1.071
wR_2 (all data)	0.1574
wR_2	0.1435
R_1 (all data)	0.0711
R_1	0.0528

Structure Quality Indicators

Reflections:	d min (CuKα) 2Θ=149.5° 0.80	I/σ(I) 30.1	Rint m=2.69 2.65%	Full 135.4° 83% to 149.5° 88.9
Refinement:	Shift 0.000	Max Peak 0.7	Min Peak -0.7	GooF 1.071

Experimental Extended. A colourless irregular-shaped crystal with dimensions 0.23×0.22×0.07 mm^3 was mounted on a loop. Data were collected using an XtaLAB Synergy, Dualflex, HyPix-Arc 150 diffractometer operating at $T = 293.15(10)$ K.

Data were measured using ω scans of 0.5° per frame for 0.4 s using Cu Kα radiation. The diffraction pattern was indexed and the total number of runs and images was based on the strategy calculation from the program CrysAlisPro (Rigaku, V1.171.44.115a, 2025) The maximum resolution that was achieved was $\theta = 74.729°$ (0.80 Å).

The diffraction pattern was indexed and the total number of runs and images was based on the strategy calculation from the program CrysAlisPro (Rigaku, V1.171.44.115a, 2025) and the unit cell was refined using CrysAlisPro (Rigaku, V1.171.44.115a, 2025) on 4409 reflections, 42% of the observed reflections.

Data reduction, scaling and absorption corrections were performed using CrysAlisPro (Rigaku, V1.171.44.115a, 2025). The final completeness is 88.90 % out to 74.729° in θ. A gaussian absorption correction was performed using CrysAlisPro 1.171.44.115a (Rigaku Oxford Diffraction, 2025). Numerical absorption correction based on gaussian integration over a multifaceted crystal model. Empirical absorption correction using spherical harmonics, implemented in SCALE3 ABSPACK scaling algorithm. The absorption coefficient μ of this material is 2.497 mm^{-1} at this wavelength (λ = 1.542Å) and the minimum and maximum transmissions are 0.437 and 1.000.

The structure was solved and the space group $P2_1/n$ (# 14) determined by the ShelXS (Sheldrick, 2008) structure solution program using Direct Methods and refined by Least Squares using version 2018/3 of ShelXL 2018/3 (Sheldrick, 2015). All non-hydrogen atoms were refined anisotropically. Hydrogen atom positions were calculated geometrically and refined using the riding model. Hydrogen atom positions were calculated geometrically and refined using the riding model.

Table 4.5.7.1: Fractional Atomic Coordinates (×10⁴) and Equivalent Isotropic Displacement Parameters (Å²×10³) for **280l**. U_{eq} is defined as 1/3 of the trace of the orthogonalised U_{ij}.

Atom	x	y	z	U_{eq}
Br1	8245.3(4)	4515.9(5)	1418.9(3)	100.4(2)
O1	7717(2)	956(2)	5664(2)	93.4(10)
O2	7491(2)	2854(2)	5971(2)	94.1(10)
C1	8870(2)	2893(3)	4190(2)	60.8(8)
C2	8140(3)	2452(3)	3639(3)	74.9(10)
C3	7946(3)	2924(4)	2830(3)	79.2(10)
C4	8479(3)	3882(3)	2554(2)	69.6(9)
C5	9190(3)	4367(3)	3078(3)	75.5(11)
C6	9383(3)	3877(3)	3889(3)	71.9(10)
C7	9044(2)	2352(3)	5063(2)	61.1(8)
C8	9934(2)	2060(3)	5388(2)	62.0(8)
C9	10897(2)	2149(3)	4887(3)	70.6(9)
C10	11587(3)	3103(4)	5263(3)	81.6(11)
C11	12546(3)	3222(4)	4786(3)	96.6(14)
C12	13217(4)	4126(5)	5192(5)	128(2)

Atom	x	y	z	U_{eq}
C13	10039(2)	1635(3)	6303(2)	63.2(8)
C14	10466(3)	559(3)	6499(3)	77.7(11)
C15	10582(3)	206(4)	7363(3)	90.6(13)
C16	10289(3)	916(4)	8038(3)	90.0(12)
C17	9856(3)	1980(4)	7856(3)	88.3(12)
C18	9736(3)	2345(3)	7004(3)	75.4(10)
C19	6881(3)	989(4)	6265(3)	83.2(12)
C20A	7283(11)	569(19)	7123(18)	115(6)
C20B	7290(30)	1150(90)	7405(19)	180(20)
C21	6153(4)	73(5)	5992(4)	114(2)
C22	6580(3)	2252(4)	6230(4)	92.2(15)
C23	6203(5)	2815(5)	7038(5)	174(4)
C24	5845(4)	2417(8)	5443(6)	196(5)
B1	8074(3)	2052(4)	5599(3)	60.4(9)

Table 4.5.7.2: Anisotropic Displacement Parameters (×10^4) **280l**. The anisotropic displacement factor exponent takes the form: $-2\pi^2[h^2a^{*2} \times U_{11} + ... + 2hka^* \times b^* \times U_{12}]$

Atom	U_{11}	U_{22}	U_{33}	U_{23}	U_{13}	U_{12}
Br1	83.9(3)	127.0(5)	90.4(4)	36.1(3)	9.5(3)	19.7(3)
O1	74.2(16)	67.4(15)	139(3)	-17.0(16)	44.3(19)	-6.8(13)
O2	79.2(17)	62.9(15)	140(3)	-3.2(15)	50(2)	-1.7(13)
C1	52.5(17)	64.9(19)	65.1(19)	-3.9(15)	10.5(16)	3.4(15)
C2	68(2)	79(2)	78(2)	10.1(19)	-1(2)	-13.0(18)
C3	68(2)	92(3)	78(2)	9(2)	-8(2)	-10(2)
C4	59.7(19)	83(2)	66(2)	9.1(19)	10.6(18)	14.5(18)
C5	71(2)	69(2)	86(3)	9.8(19)	18(2)	-2.5(18)
C6	63(2)	73(2)	79(2)	-8.0(19)	7(2)	-8.4(17)
C7	53.0(17)	66.4(19)	63.8(19)	-4.8(16)	4.2(16)	-0.9(15)
C8	52.8(17)	64.5(19)	69(2)	-8.1(16)	8.9(16)	-1.5(15)
C9	51.3(18)	88(2)	73(2)	-4.8(19)	6.9(17)	3.1(17)
C10	61(2)	108(3)	76(2)	-4(2)	4(2)	-2(2)
C11	67(2)	127(4)	96(3)	5(3)	8(3)	-6(2)
C12	80(3)	138(4)	165(6)	-3(4)	6(4)	-32(3)
C13	49.3(16)	72(2)	68(2)	-3.2(17)	3.8(16)	-1.9(15)
C14	68(2)	79(2)	86(3)	-2(2)	11(2)	4.3(19)
C15	81(3)	89(3)	102(3)	19(3)	12(3)	12(2)
C16	81(3)	116(3)	73(3)	9(2)	-1(2)	4(3)
C17	88(3)	106(3)	71(2)	-18(2)	0(2)	3(2)
C18	74(2)	78(2)	75(2)	-6.8(19)	-2(2)	5.5(19)
C19	70(2)	78(2)	102(3)	-3(2)	25(2)	-9.3(19)
C20A	101(7)	144(10)	99(12)	55(8)	-19(7)	-24(6)
C20B	180(30)	300(60)	50(12)	31(19)	-26(14)	-70(40)
C21	91(3)	102(3)	149(5)	-39(3)	41(3)	-35(3)
C22	68(2)	78(3)	131(4)	1(2)	40(3)	1(2)
C23	175(6)	119(4)	228(8)	-74(5)	138(6)	-40(4)
C24	65(3)	275(9)	248(10)	148(8)	-3(5)	10(4)
B1	54(2)	66(2)	61(2)	4.0(18)	2.9(18)	2.3(18)

Table 4.5.7.3: Bond Lengths in Å for **280l**.

Atom	Atom	Length/Å
Br1	C4	1.901(4)
O1	C19	1.462(4)
O1	B1	1.334(5)
O2	C22	1.465(4)
O2	B1	1.331(4)
C1	C2	1.391(5)
C1	C6	1.391(5)
C1	C7	1.485(5)
C2	C3	1.371(6)
C3	C4	1.369(5)

Atom	Atom	Length/Å
C4	C5	1.367(6)
C5	C6	1.380(6)
C7	C8	1.346(5)
C7	B1	1.589(5)
C8	C9	1.519(4)
C8	C13	1.483(5)
C9	C10	1.540(5)
C10	C11	1.499(5)
C11	C12	1.502(7)
C13	C14	1.380(5)
C13	C18	1.400(5)
C14	C15	1.387(6)
C15	C16	1.366(6)
C16	C17	1.367(6)
C17	C18	1.374(6)
C19	C20A	1.49(2)
C19	C20B	1.84(3)
C19	C21	1.491(6)
C19	C22	1.487(6)
C22	C23	1.480(7)
C22	C24	1.571(9)

Table 4.5.7.4: Bond Angles in ° for **280l**

Atom	Atom	Atom	Angle/°
B1	O1	C19	107.8(3)
B1	O2	C22	107.6(3)
C2	C1	C7	120.4(3)
C6	C1	C2	116.3(4)
C6	C1	C7	123.2(3)
C3	C2	C1	122.7(4)
C4	C3	C2	118.9(4)
C3	C4	Br1	119.4(3)
C5	C4	Br1	119.9(3)
C5	C4	C3	120.7(4)
C4	C5	C6	119.7(4)
C5	C6	C1	121.5(4)
C1	C7	B1	114.7(3)
C8	C7	C1	124.9(3)
C8	C7	B1	120.2(3)
C7	C8	C9	124.9(3)
C7	C8	C13	120.7(3)
C13	C8	C9	114.4(3)
C8	C9	C10	112.5(3)
C11	C10	C9	114.3(3)
C10	C11	C12	112.8(4)
C14	C13	C8	122.0(3)
C14	C13	C18	117.6(4)
C18	C13	C8	120.4(3)
C13	C14	C15	120.5(4)
C16	C15	C14	121.0(4)
C15	C16	C17	119.3(4)
C16	C17	C18	120.5(4)
C17	C18	C13	121.1(4)
O1	C19	C20A	105.0(8)
O1	C19	C20B	111.2(15)
O1	C19	C21	108.8(3)
O1	C19	C22	102.4(3)
C21	C19	C20A	105.4(8)
C21	C19	C20B	122(2)
C22	C19	C20A	115.9(12)
C22	C19	C20B	91(3)
C22	C19	C21	118.4(5)
O2	C22	C19	103.0(3)
O2	C22	C23	108.6(4)
O2	C22	C24	105.9(4)
C19	C22	C24	108.4(5)
C23	C22	C19	118.6(5)
C23	C22	C24	111.4(6)
O1	B1	C7	122.6(3)
O2	B1	O1	112.6(3)
O2	B1	C7	124.7(3)

Table 4.5.7.5: Hydrogen Fractional Atomic Coordinates (×10⁴) and Equivalent Isotropic Displacement Parameters (Å²×10³) for **280l**. U_{eq} is defined as 1/3 of the trace of the orthogonalised U_{ij}.

Atom	x	y	z	U_{eq}
H2	7768.18	1810.96	3828.44	90
H3	7460.16	2599.11	2473.61	95
H5	9542.3	5023.95	2888.39	91
H6	9866.48	4213.06	4242	86
H9A	10756.63	2329.99	4278.62	85
H9B	11229	1389.21	4906.27	85
H10A	11249.38	3858.91	5247.2	98
H10B	11723.01	2918.72	5872.18	98
H11A	12415.65	3442.74	4182.84	116
H11B	12876.6	2461.48	4782.07	116
H12A	13818.59	4166.68	4863.26	192
H12B	13360.87	3904.6	5785.59	192
H12C	12900.89	4885.65	5185.36	192
H14	10677.29	67.96	6048.31	93
H15	10862.72	-526.46	7484.8	109
H16	10383.71	678.79	8615.88	108
H17	9641.81	2459.34	8312.77	106
H18	9448.53	3076.42	6891.12	90
H20A	7597.23	-183.56	7043.49	172
H20B	6754.81	490.24	7536.37	172
H20C	7753.79	1131.09	7339.07	172
H20D	7934.92	804.36	7469.97	263
H20E	6838.18	755.46	7786.82	263
H20F	7322.44	1974.04	7554.05	263
H21A	5929.38	238.44	5407.07	171
H21B	5602.27	83.18	6385.16	171
H21C	6458.42	-692.48	6006.15	171
H23A	6698.05	2778.51	7486.97	261
H23B	5623.78	2404.99	7231.1	261
H23C	6042.75	3626.59	6919.95	261
H24A	5756.59	3245.3	5329.07	294
H24B	5222.23	2067.73	5589.15	294
H24C	6106.93	2038.72	4930.79	294

Table 4.5.7.6 Atomic Occupancies for all atoms that are not fully occupied in **280l**.

Atom	Occupancy
C20A	0.68(6)
H20A	0.68(6)
H20B	0.68(6)
H20C	0.68(6)
C20B	0.32(6)
H20D	0.32(6)
H20E	0.32(6)
H20F	0.32(6)

5. Bibliography

(1) Liu, Y.; Woerpel, K. A. Uncatalyzed Carbometallation Involving Group 13 Elements: Carboboration and Carboalumination of Alkenes and Alkynes. *Synthesis* **2022**, *55*, 2261–2272. https://doi.org/10.1055/s-0042-1751362.

(2) Carbometallation of Alkenes and Alkynes. In *Comprehensive Organic Synthesis*; Elsevier, 1991; pp 865–911. https://doi.org/10.1016/b978-0-08-052349-1.00111-6.

(3) S. Müller, D.; Marek, I. Copper Mediated Carbometalation Reactions. *Chem. Soc. Rev.* **2016**, *45* (16), 4552–4566. https://doi.org/10.1039/C5CS00897B.

(4) Carbometallation Reactions. In *Metal-Catalyzed Cross-Coupling Reactions*; Wiley, 2004; pp 395–478. https://doi.org/10.1002/9783527619535.ch7.

(5) Marsico, G.; Scafato, P.; Belviso, S.; Superchi, S. Regio- and Stereoselective Intermolecular Carbolithiation Reactions. *RSC Adv.* **2020**, *10* (54), 32581–32601. https://doi.org/10.1039/D0RA06101H.

(6) Igawa, K.; Tomooka, K. γ-Silyl Group Effect in Hydroalumination and Carbolithiation of Propargylic Alcohols. *Angew. Chem. Int. Ed.* **2006**, *45* (2), 232–234. https://doi.org/10.1002/anie.200503176.

(7) McKinley, N. F.; O'Shea, D. F. Carbolithiation of Diphenylacetylene as a Stereoselective Route to (*Z*)-Tamoxifen and Related Tetrasubstituted Olefins. *J. Org. Chem.* **2006**, *71* (25), 9552–9555. https://doi.org/10.1021/jo061949s.

(8) Heijnen, D.; Van Zuijlen, M.; Tosi, F.; Feringa, B. L. An Atom Efficient Synthesis of Tamoxifen. *Org. Biomol. Chem.* **2019**, *17* (9), 2315–2320. https://doi.org/10.1039/C8OB02977F.

(9) Hojo, M.; Murakami, Y.; Aihara, H.; Sakuragi, R.; Baba, Y.; Hosomi, A. Iron-Catalyzed Regio- and Stereoselective Carbolithiation of Alkynes. *Angew. Chem.* **2001**, *113* (3), 641–643. https://doi.org/10.1002/1521-3757(20010202)113:3%253C641::AID-ANGE641%253E3.0.CO;2-V.

(10) Shirakawa, E.; Ikeda, D.; Ozawa, T.; Watanabe, S.; Hayashi, T. Iron-Catalyzed Carbolithiation of Alkynes Having No Heteroatoms. *Chem. Commun.* **2009**, *0* (14), 1885–1887. https://doi.org/10.1039/B900345B.

(11) Shirakawa, E.; Yamagami, T.; Kimura, T.; Yamaguchi, S.; Hayashi, T. Arylmagnesiation of Alkynes Catalyzed Cooperatively by Iron and Copper Complexes. *J. Am. Chem. Soc.* **2005**, *127* (49), 17164–17165. https://doi.org/10.1021/ja0542136.

(12) Scott, B. L.; McCleskey, T. M.; Chaudhary, A.; Hong-Geller, E.; Gnanakaran, S. The Bioinorganic Chemistry and Associated Immunology of Chronic Beryllium Disease. *Chem. Commun.* **2008**, No. 25, 2837. https://doi.org/10.1039/b718746g.

(13) E. Field-Theodore, T.; A. Couchman, S.; D. Wilson, D. J.; L. Dutton, J. Carboberyllation: Addition of Organoberyllium Species to Alkenes and Alkynes. A Comparison with Carboboration. *Dalton Trans.* **2017**, *46* (24), 7686–7692. https://doi.org/10.1039/C7DT01370A.

(14) Nishimoto, Y.; Yasuda, M. Carbometalation and Heterometalation of Carbon-Carbon Multiple-Bonds Using Group-13 Heavy Metals: Carbogallation, Carboindation, Heterogallation, and Heteroindation. *Chem. – Asian J.* **2020**, *15* (6), 636–650. https://doi.org/10.1002/asia.201901730.

(15) Yamaguchi, M.; Hayashi, A.; Hirama, M. Alkynyldichlorogalliums Are Unstable in Hydrocarbon Solvents Dimerization of Alkynyldichlorogalliums via Carbogallation. *Chem. Lett.* **1995**, *24* (12), 1093–1094. https://doi.org/10.1246/cl.1995.1093.

(16) Yamaguchi, M.; Sotokawa, T.; Hirama, M. Allylgallation Reaction of Carbon–Carbon Triple Bonds with Allylsilanes and GaCl3. *Chem. Commun.* **1997**, No. 8, 743–744. https://doi.org/10.1039/a700552k.

(17) Hayashi, S.; Hirano, K.; Yorimitsu, H.; Oshima, K. Gallium-Mediated Allyl Transfer from Bulky Homoallyl Alcohol to Aldehydes or Alkynes: Control of Dynamic σ-Allylgalliums Based on Retro-Allylation Reaction. *J. Organomet. Chem.* **2007**, *692* (1–3), 505–513. https://doi.org/10.1016/j.jorganchem.2006.08.047.

(18) Lee, P. H.; Heo, Y.; Seomoon, D.; Kim, S.; Lee, K. Regioselective Allylgallation of Terminal Alkynes. *Chem. Commun.* **2005**, No. 14, 1874–1876. https://doi.org/10.1039/B417975G.

(19) Takai, K.; Ikawa, Y.; Ishii, K.; Kumanda, M. Tertiary Amine-Accelerated Allylgallation of Terminal Alkynes. *Chem. Lett.* **2002**, *31* (2), 172–173. https://doi.org/10.1246/cl.2002.172.

(20) Yamaguchi, M.; Tsukagoshi, T.; Arisawa, M. Ethenylation of Silyl Enol Ether with Silylethyne. *J. Am. Chem. Soc.* **1999**, *121* (16), 4074–4075. https://doi.org/10.1021/ja984022l.

(21) Arisawa, M.; Miyagawa, C.; Yamaguchi, M. Equatorial Preference in the $GaCl_3$ -Promoted Ethenylation of Cyclic Ketones. *Synthesis* **2004**, *2002* (01), s-2002-19298. https://doi.org/10.1055/s-2002-19298.

(22) Arisawa, M.; Miyagawa, C.; Yoshimura, S.; Kido, Y.; Yamaguchi, M. GaCl3-Promoted Ethenylation of Thioester Silyl Enolate and Dienolate with Silylethyne. *Chem. Lett.* **2001**, *30* (11), 1080–1081. https://doi.org/10.1246/cl.2001.1080.

(23) Arisawa, M.; Akamatsu, K.; Yamaguchi, M. GaCl3-Promoted Ethenylation of Silylated β-Dicarbonyl Compound with Silylethyne. Synthesis of Ethenylmalonate. *Org. Lett.* **2001**, *3* (5), 789–790. https://doi.org/10.1021/ol015583b.

(24) Amemiya, R.; Nishimura, Y.; Yamaguchi, M. GaCl3-Catalyzed α-Ethenylation Reaction of Ketone. *Synthesis* **2004**, *2004*, 1307–1314. https://doi.org/10.1055/s-2004-822363.

(25) Kobayashi, K.; Arisawa, M.; Yamaguchi, M. B-Silylethenylation of Phenol with Silylethyne Using Gallium Trichloride.

(26) Yamaguchi, M.; Kido, Y.; Hayashi, A.; Hirama, M. Friedel–Crafts β-Silylvinylations. *Angew. Chem. Int. Ed. Engl.* **1997**, *36* (12), 1313–1315. https://doi.org/10.1002/anie.199713131.

(27) Kido, Y.; Yamaguchi, M. Linear Trimerization Reaction of Silylacetylene Promoted by GaCl3. *J. Org. Chem.* **1998**, *63* (23), 8086–8087. https://doi.org/10.1021/jo9813639.

(28) Tsuchimoto, T.; Maeda, T.; Shirakawa, E.; Kawakami, Y. Friedel–Crafts Alkenylation of Arenes Using Alkynes Catalysed by Metal Trifluoromethanesulfonates. *Chem. Commun.* **2000**, *0* (17), 1573–1574. https://doi.org/10.1039/B003702H.

(29) Araki, S.; Imai, A.; Shimizu, K.; Yamada, M.; Mori, A.; Butsugan, Y. Carboindation of Alkynes. Regio- and Stereoselective Allylation of Carbon-Carbon Triple Bonds of Alkynols by Allylic Indium Reagents. *J. Org. Chem.* **1995**, *60* (6), 1841–1847. https://doi.org/10.1021/jo00111a049.

(30) Araki, S.; Imai, A.; Shimizu, K.; Butsugan, Y. Carboindation of Alkynols. A Facile Synthesis of Yomogi Alcohol. *Tetrahedron Lett.* **1992**, *33* (18), 2581–2582. https://doi.org/10.1016/S0040-4039(00)92248-2.

(31) Klaps, E.; Schmid, W. Carboindation of Carbon−Carbon Triple Bonds: Regioselective Indium-Mediated Allylation of Functionalized Alkynes and Transformation into Halogen-Substituted 1,4-Dienes. *J. Org. Chem.* **1999**, *64* (20), 7537–7546. https://doi.org/10.1021/jo9908593.

(32) Ranu, B. C.; Majee, A. Indium-Mediated Regioselective Markovnikov Allylation Ofunactivated Terminal Alkynes. *Chem. Commun.* **1997**, No. 13, 1225–1226. https://doi.org/10.1039/A702241G.

(33) Fujiwara, N.; Yamamoto, Y. Allylation of Unactivated and/or Functionalized Alkynes with Allylindiums. *J. Org. Chem.* **1997**, *62* (8), 2318–2319. https://doi.org/10.1021/jo9701041.

(34) Fujiwara, N.; Yamamoto, Y. Allyl- and Benzylindium Reagents. Carboindation of Carbon−Carbon and Carbon−Nitrogen Triple Bonds. *J. Org. Chem.* **1999**, *64* (11), 4095–4101. https://doi.org/10.1021/jo990160x.

(35) Nishimoto, Y.; Yi, J.; Takata, T.; Baba, A.; Yasuda, M. Regio- and Stereoselective Allylindation of Alkynes Using InBr3 and Allylic Silanes: Synthesis, Characterization, and Application of 1,4-Dienylindiums toward Skipped Dienes. *Molecules* **2018**, *23* (8), 1884. https://doi.org/10.3390/molecules23081884.

(36) Nishimoto, Y.; Hirase, R.; Yasuda, M. Anti-Carboalumination of Alkynes Using Aluminum Trihalide and Silyl Ketene Imines: Stereo- and Regioselective Synthesis of Alkenylaluminum Compounds Bearing a Cyano Group. *Org. Lett.* **2018**, *20* (12), 3651–3655. https://doi.org/10.1021/acs.orglett.8b01371.

(37) Nishimoto, Y.; Ueda, H.; Yasuda, M.; Baba, A. Carbogallation of Alkynes Using Gallium Tribromide and Silyl Ketene Acetals and Synthetic Application to Cross-Coupling with Aryl Iodides. *Chem. – Eur. J.* **2011**, *17* (40), 11135–11138. https://doi.org/10.1002/chem.201102255.

(38) Nishimoto, Y.; Kang, K.; Yasuda, M. Regio- and Stereoselective Anti-Carbozincation of Alkynyl Ethers Using ZnBr2 toward (Z)-β-Zincated Enol Ether Synthesis. *Org. Lett.* **2017**, *19* (14), 3927–3930. https://doi.org/10.1021/acs.orglett.7b01847.

(39) Nishimoto, Y.; Moritoh, R.; Yasuda, M.; Baba, A. Regio- and Stereoselective Generation of Alkenylindium Compounds from Indium Tribromide, Alkynes, and Ketene Silyl Acetals. *Angew. Chem. Int. Ed.* **2009**, *48* (25), 4577–4580. https://doi.org/10.1002/anie.200901417.

(40) Kang, K.; Nishimoto, Y.; Yasuda, M. Regio- and Stereoselective Carboindation of Internal Alkynyl Ethers with Organosilicon or -Stannane Nucleophiles. *J. Org. Chem.* **2019**, *84* (21), 13345–13363. https://doi.org/10.1021/acs.joc.9b01505.

(41) Nishimoto, Y.; Takeuchi, M.; Yasuda, M.; Baba, A. Regio- and Stereoselective Carbobismuthination of Alkynes. *Angew. Chem. Int. Ed.* **2012**, *51* (4), 1051–1054. https://doi.org/10.1002/anie.201107127.

(42) Negishi, E.; Van Horn, D. E.; Yoshida, T. Controlled Carbometalation. 20. Carbometalation Reaction of Alkynes with Organoalene-Zirconocene Derivatives as a Route to Stereo-and Regiodefined Trisubstituted Alkenes. *J. Am. Chem. Soc.* **1985**, *107* (23), 6639–6647. https://doi.org/10.1021/ja00309a036.

(43) Huo, S. Carboalumination Reactions. In *Patai's Chemistry of Functional Groups*; Wiley, 2016; pp 1–64. https://doi.org/10.1002/9780470682531.pat0834.

(44) Van Horn, D. E.; Valente, L. F.; Idacavage, M. J.; Negishi, E.-I. Controlled Carbometallation. *J. Organomet. Chem.* **1978**, *156* (1), C20–C24. https://doi.org/10.1016/S0022-328X(00)84891-3.

(45) Van Horn, D. E.; Negishi, E. Selective Carbon-Carbon Bond Formation via Transition Metal Catalysts. 8. Controlled Carbometalation. Reaction of Acetylenes with Organoalane-Zirconocene Dichloride Complexes as a Route to Stereo- and Regio-Defined Trisubstituted Olefins. *J. Am. Chem. Soc.* **1978**, *100* (7), 2252–2254. https://doi.org/10.1021/ja00475a058.

(46) Wipf, P.; Lim, S. Rapid Carboalumination of Alkynes in the Presence of Water. *Angew. Chem. Int. Ed. Engl.* **1993**, *32* (7), 1068–1071. https://doi.org/10.1002/anie.199310681.

(47) Takimoto, M.; Usami, S.; Hou, Z. Scandium-Catalyzed Regio- and Stereospecific Methylalumination of Silyloxy/Alkoxy-Substituted Alkynes and Alkenes. *J. Am. Chem. Soc.* **2009**, *131* (51), 18266–18268. https://doi.org/10.1021/ja909126k.

(48) Hayami, H.; Oshima, K.; Nozaki, H. Dihexylmagnesium Promoted Carboalumination of Silylacetylenes. *Tetrahedron Lett.* **1984**, *25* (39), 4433–4436. https://doi.org/10.1016/S0040-4039(01)81458-1.

(49) Miller, R. B.; Al-Hassan, M. I. Stereospecific Synthesis of (Z)-Tamoxifen via Carbometallation of Alkynylsilanes. *J. Org. Chem.* **1985**, *50* (12), 2121–2123. https://doi.org/10.1021/jo00212a023.

(50) Miller, J. A.; Negishi, E. Zirconium-Catalyzed Allylalumination and Benzylalumination of Alkynes. *Tetrahedron Lett.* **1984**, *25* (51), 5863–5866. https://doi.org/10.1016/S0040-4039(01)81705-6.

(51) Eisch, J. J.; Kaska, W. C. The Synthesis of Aluminoles via the Addition and Cyclization Reactions of Arylaluminum Compounds[1]. *J. Am. Chem. Soc.* **1966**, *88* (13), 2976–2983. https://doi.org/10.1021/ja00965a018.

(52) Ma, S.; Negishi, E. Anti-Carbometalation of Homopropargyl Alcohols and Their Higher Homologues via Non-Chelation-Controlled Syn-Carbometalation and Chelation-Controlled Isomerization. *J. Org. Chem.* **1997**, *62* (4), 784–785. https://doi.org/10.1021/jo9622688.

(53) Ilan Marek. *Titanium and Zirconium in Organic Synthesis*; Vch Verlagsgesellschaft Mbh, 2002.

(54) Yatnanoi, S.; Takahiro Imai; Matsumoto, T.; Keisuke, S. MAO-CatalyzedAllylzirconationofl-AIkynes. *Tetrahedron Lett.* **1997**, *38* (17), 3031–3034.

(55) Yamanoi, S.; Matsumoto, T.; Suzuki, K. Reaction of 1-Iodoalkynes with Allylzirconiums: Generation of Alkylidene Carbenoid via Allylzirconation. *Tetrahedron Lett.* **1999**, *40* (14), 2793–2796. https://doi.org/10.1016/S0040-4039(99)00296-8.

(56) Suzuki, N.; Kondakov, D. Y.; Kageyama, M.; Kotora, M.; Hara, R.; Takahashi, T. Novel Type of Carbozirconation Reaction of Alkynes. *Tetrahedron* **1995**, *51* (15), 4519–4540. https://doi.org/10.1016/0040-4020(94)01138-P.

(57) Nishihara, Y.; Miyasaka, M.; Okamoto, M.; Takahashi, H.; Inoue, E.; Tanemura, K.; Takagi, K. Zirconocene-Mediated Highly Regio- and Stereoselective Synthesis of Multisubstituted Olefins Starting from 1-Alkynylboronates. *J. Am. Chem. Soc.* **2007**, *129* (42), 12634–12635. https://doi.org/10.1021/ja075234y.

(58) Takahashi, T.; Xi, Z.; Fischer, R.; Huo, S.; Xi, C.; Nakajima, K. Intermolecular Coupling Reaction of Alkynes with Vinyl Bromide with Selective Skeletal Rearrangement. *J. Am. Chem. Soc.* **1997**, *119* (19), 4561–4562. https://doi.org/10.1021/ja970055+.

(59) Takahashi, T.; Kondakov, D. Y.; Xi, Z.; Suzuki, N. A Vinylzirconation Reaction of Alkynes. *J. Am. Chem. Soc.* **1995**, *117* (21), 5871–5872. https://doi.org/10.1021/ja00126a035.

(60) Liu, Y.; Zhong, Z.; Nakajima, K.; Takahashi, T. Alkynylzirconation of Alkynes and Application to One-Pot Bisalkynylation of Alkynes. *J. Org. Chem.* **2002**, *67* (21), 7451–7456. https://doi.org/10.1021/jo026037e.

(61) Takahashi, T.; Xi, C.; Xi, Z.; Kageyama, M.; Fischer, R.; Nakajima, K.; Negishi, E. Selective Intermolecular Coupling of Alkynes with Nitriles and Ketones via β,β‘ Carbon−Carbon Bond Cleavage of Zirconacyclopentenes. *J. Org. Chem.* **1998**, *63* (20), 6802–6806. https://doi.org/10.1021/jo980022s.

(62) Takahashi, T.; Xi, C.; Ura, Y.; Nakajima, K. Metallo-Esterification of Alkynes: Reaction of Alkynes with Cp_2 $ZrEt_2$ and Chloroformate. *J. Am. Chem. Soc.* **2000**, *122* (13), 3228–3229. https://doi.org/10.1021/ja994234y.

(63) Nishihara, Y.; Saito, D.; Tanemura, K.; Noyori, S.; Takagi, K. Regio- and Stereoselective Synthesis of Multisubstituted Vinylsilanes via Zirconacycles†. *Org. Lett.* **2009**, *11* (16), 3546–3549. https://doi.org/10.1021/ol901236s.

(64) Titanium And Zirconium In Organic Chemistry - Ilan Marek.

(65) Flynn, A. B.; Ogilvie, W. W. Stereocontrolled Synthesis of Tetrasubstituted Olefins. *Chem. Rev.* **2007**, *107* (11), 4698–4745. https://doi.org/10.1021/cr050051k.

(66) Miura, K. Allylstannylation of Aikynes v/a a Radical Process: Stereoselective Synthesis of Di- and Tri-Substituted Vinylstannanes.

(67) Konno, T.; Takehana, T.; Chae, J.; Ishihara, T.; Yamanaka, H. Highly Regio- and Stereoselective Carbostannylation Reaction of Fluorine-Containing Internal Acetylenes with Allylstannanes. *J. Org. Chem.* **2004**, *69* (6), 2188–2190. https://doi.org/10.1021/jo030272v.

(68) Yamaguchi, M.; Hayashi, A.; Hirama, M. Carbometalation of Ketone Enolates with 1-Alkynes: An Alkylidenation Reaction of Silyl Enol Ethers Promoted by Stannic Chloride-Tri-n-Butylamine (SnCl4-Bu3N) Reagent. *J. Am. Chem. Soc.* **1993**, *115* (8), 3362–3363. https://doi.org/10.1021/ja00061a058.

(69) Yamaguchi, M.; Hayashi, A.; Hirama, M. Ortho-Vinylation and Ortho-Alkenylation of Phenols. *J. Am. Chem. Soc.* **1995**, *117* (3), 1151–1152. https://doi.org/10.1021/ja00108a041.

(70) Matsukawa, Y.; Asao, N.; Kitahara, H. Lewis Acid Catalyzed Allylstannylation of Unactivated Alkynes t.

(71) Shirakawa, E.; Yoshida, H.; Kurahashi, T.; Nakao, Y.; Hiyama, T. Carbostannylation of Alkynes Catalyzed by an Iminophosphine−Palladium Complex. *J. Am. Chem. Soc.* **1998**, *120* (12), 2975–2976. https://doi.org/10.1021/ja974206k.

(72) Yoshida, H.; Shirakawa, E.; Kurahashi, T.; Nakao, Y.; Hiyama, T. Palladium−Iminophosphine-Catalyzed Alkynylstannylation of Alkynes. *Organometallics* **2000**, *19* (26), 5671–5678. https://doi.org/10.1021/om000828u.

(73) Shirakawa, E.; Yamasaki, K.; Yoshida, H.; Hiyama, T. Nickel-Catalyzed Carbostannylation of Alkynes with Allyl-, Acyl-, and Alkynylstannanes: Stereoselective Synthesis of Trisubstituted Vinylstannanes. *J. Am. Chem. Soc.* **1999**, *121* (43), 10221–10222. https://doi.org/10.1021/ja992597s.

(74) Shirakawa, E.; Hiyama, T. Transition Metal-Catalyzed Carbostannylation of Alkynes and Dienes.

(75) Shirakawa, E.; Yoshida, H.; Nakao, Y.; Hiyama, T. Mechanistic Aspects of Palladium-Catalyzed Allylstannylation of Alkynes. *Org. Lett.* **2000**, *2* (15), 2209–2211. https://doi.org/10.1021/ol0000861.

(76) Nakao, Y.; Satoh, J.; Shirakawa, E.; Hiyama, T. Regio- and Stereoselective Decarbonylative Carbostannylation of Alkynes Catalyzed by Pd/C. *Angew. Chem. Int. Ed.* **2006**, *45* (14), 2271–2274. https://doi.org/10.1002/anie.200504283.

(77) Wobser, S. D.; Stephenson, C. J.; Delferro, M.; Marks, T. J. Carbostannolysis Mediated by Bis(Pentamethylcyclopentadienyl)Lanthanide Catalysts. Utility in Accessing Organotin Synthons. *Organometallics* **2013**, *32* (5), 1317–1327. https://doi.org/10.1021/om301031e.

(78) Chemla, F.; Ferreira, F. Carbocupration of Alkynes. In *Patai's Chemistry of Functional Groups*; Wiley, 2011. https://doi.org/10.1002/9780470682531.pat0444.

(79) Basheer, A.; Marek, I. Recent Advances in Carbocupration of α-Heterosubstituted Alkynes. *Beilstein J. Org. Chem.* **2010**, *6*. https://doi.org/10.3762/bjoc.6.77.

(80) Kato, N.; Miyaura, N. A Stereoselective Synthesis of 1,2-Diarylethenyl Ethyl Ethers *via* the Carbocupration-Cross Coupling Sequence. *Tetrahedron* **1996**, *52* (42), 13347–13354. https://doi.org/10.1016/0040-4020(96)00794-6.

(81) Levin, A.; Basheer, A.; Marek, I. Regiodivergent Carbometalation Reactions of Ynol Ether Derivatives. *Synlett* **2010**, *2010* (02), 329–332. https://doi.org/10.1055/s-0029-1219221.

(82) Alexakis, A.; Normant, J.; Villieras, J. Organocuivreux Vinyliques: IV. Etude de La Regioselectivite de l'addition d'un Alkylcuivre Sur Des Alcynes β et γ Fonctionnels. *J. Organomet. Chem.* **1975**, *96* (3), 471–485. https://doi.org/10.1016/S0022-328X(00)91950-8.

(83) Chechik-Lankin, H.; Marek, I. Regio- and Stereoselective Synthesis of Novel (*E*)-1-Alkenyl Carbamate via Carbocupration Reaction. *Org. Lett.* **2003**, *5* (26), 5087–5089. https://doi.org/10.1021/ol036154b.

(84) Chechik-Lankin, H.; Livshin, S.; Marek, I. Regiocontrolled Carbometallation Reactions of Ynamides. *Synlett* **2005**, No. 13, 2098–2100. https://doi.org/10.1055/s-2005-871962.

(85) Meijer, J.; Westmijze, H.; Vermeer, P. Stereospecific Addition of Organocopper(I) Reagents to 1-alkynylphosphines. A New Example of A-hetero-substituted Vinylcopper(I) Compounds. *Recl. Trav. Chim. Pays-Bas* **1976**, *95* (5), 102–104. https://doi.org/10.1002/recl.19760950504.

(86) Kanemura, S.; Kondoh, A.; Yorimitsu, H.; Oshima, K. Carbocupration of 1-Alkynylphosphines Followed by Trapping with Electrophiles. *Org. Lett.* **2007**, *9* (10), 2031–2033. https://doi.org/10.1021/ol0706657.

(87) Wu, Z. Cis-Carbocupration of Acetylenic Phosphine Oxides and Its Application in the Stereoselective Synthesis of Polysubstituted Vinyl Phosphine Oxides. *N. Y.* **2004**, No. 15.

(88) Konno, T.; Morigaki, A.; Ninomiya, K.; Miyabe, T.; Ishihara, T. Convenient and Efficient Access to Fluoroalkylated Vinylphosphonates via Highly Regio- and Stereoselective Hydrometalation or Carbometalation Reactions of Fluorine-Containing Alkynylphosphonates. *Synthesis* **2008**, *2008* (4), 564–572. https://doi.org/10.1055/s-2008-1032143.

(89) Gil, J. M.; Oh, D. Y. Carbocupration of Diethyl 1-Alkynyl Phosphonates: Stereo- and Regioselective Synthesis of 1,2,2-Trisubstituted Vinyl Phosphonates. *J. Org. Chem.* **1999**, *64* (8), 2950–2953. https://doi.org/10.1021/jo982123w.

(90) Fiandanese, V.; Marchese, G.; Naso, F.; Ronzinit, L.; Rotunno, D. AN EASY ROUTE TO INSECT PHEROMONES WITH A F-Z or Z-f CONJUGATED DIENE STRUCTURE.

(91) Creton, I.; Marek, I.; Brasseur, D.; Jestin, J.-L.; Normant, J.-F. Phenylthioacetylene as a Source of Stereodefined Trisubstituted Alkenes. *Tetrahedron Lett.* **1994**, *35* (37), 6873–6876. https://doi.org/10.1016/0040-4039(94)85028-3.

(92) Rao, S. A.; Knochel, P. Stereospecific Preparation of Polyfunctional Olefins by the Carbometalation of Alkynes with Polyfunctional Zinc-Copper Organometallics. Stereospecific Preparation of Five-Membered Carbocycles by Intramolecular Carbocupration. *J. Am. Chem. Soc.* **1991**, *113* (15), 5735–5741. https://doi.org/10.1021/ja00015a030.

(93) Xu, Q.; Huang, X. Cis -Carbocuperation of Acetylenic Sulfoxides and Corresponding Applications in the Regio- and Stereoselective Synthesis of Polysubstituted Vinyl Sulfoxides. *Tetrahedron Lett.* **2004**, *45* (29), 5657–5660. https://doi.org/10.1016/j.tetlet.2004.05.141.

(94) Kosugi, H.; Kitaoka, M.; Tagami, K.; Takahashi, A.; Uda, H. Simple and Stereocontrolled Preparation of Optically Pure (E)- and (Z)-1-Alkenyl p-Tolyl Sulfoxides via 1-Alkynyl p-Tolyl Sulfoxides. *J. Org. Chem.* **1987**, *52* (6), 1078–1082. https://doi.org/10.1021/jo00382a019.

(95) Meijer, J.; Vermeer, P. Chemistry of Acetylenic Ethers 108 Stereospecific Addition of Organocopper(I) Reagents to 1-alkynyl Sulfones. *Recl. Trav. Chim. Pays-Bas* **1975**, *94* (1), 14–15. https://doi.org/10.1002/recl.19750940107.

(96) Shengming Ma; Zhan Lu. Copper(I)-Mediated Highly Stereoselective Syn-Carbometalation of Secondary or Tertiary Propargylic Alcohols with Primary Grignard Reagents in Toluene with a High Linear Regioselectivity. *Adv. Synth. Catal.* **2006**, *348* (14), 1894–1898. https://doi.org/10.1002/adsc.200606004.

(97) Alexakis, A.; Villieras, J. ORGANOCUIVREUX VINYLIQUES.

(98) Alexakis, A.; Commercon, A.; Coulentianos, C.; Normant, J. F. Carbocupration of Acetylenic Acetals and Ketals: Synthesis of α-β Ethylenic Acetals, and of Dienals and Dienones. *Pure Appl. Chem.* **1983**, *55* (11), 1759–1766. https://doi.org/10.1351/pac198355111759.

(99) MacNeil, K. J.; Burton, D. J. Regiospecific Syn Addition of (Polyfluoroaryl)Copper Reagents to Fluorinated Acetylenes: Preparation and Subsequent Functionalization of Internal Vinylcopper Reagents. *J. Org. Chem.* **1993**, *58* (16), 4411–4417. https://doi.org/10.1021/jo00068a041.

(100) Marshall, J. A.; Pinney, K. G. Stereoselective Synthesis of 2,5-Dihydrofurans by Sequential SN2' Cleavage of Alkynyloxiranes and Silver(I)-Catalyzed Cyclization of the Allenylcarbinol Products. *J. Org. Chem.* **1993**, *58* (25), 7180–7184. https://doi.org/10.1021/jo00077a048.

(101) Alesxkis, A.; Cahiez, G. ORGANOCUIVREUX VINYLIQUES. *J. Organomet. Chem.* **1979**, *177*, 293–298.

(102) *Organocopper Reagents: Substitution, Conjugate Addition, Carbo/Metallocupration, and Other Reactions - Lipshutz - Major Reference Works - Wiley Online Library*. https://onlinelibrary.wiley.com/doi/abs/10.1002/0471264180.or041.02 (accessed 2025-05-27).

(103) Rao, S. A.; Knochel, P. Stereospecific Preparation of Polyfunctional Olefins by the Carbometalation of Alkynes with Polyfunctional Zinc-Copper Organometallics. Stereospecific Preparation of Five-

Membered Carbocycles by Intramolecular Carbocupration. *J. Am. Chem. Soc.* **1991**, *113* (15), 5735–5741. https://doi.org/10.1021/ja00015a030.

(104) Normant, J. F.; Bourgain, M. Synthese Stereospecifique and Reactivite d' Organocuivreux Vinyliques. *Tetrahedron Lett.* **1971**, *12* (27), 2583–2586. https://doi.org/10.1016/S0040-4039(01)96925-4.

(105) Bourgain-Commerçon, M.; Foulon, J. P.; Normant, J. F. Organocuivreux vinyliques (23): Accès à des organocuivreux vinyliques portant un groupe silicié en position allylique. *Tetrahedron Lett.* **1983**, *24* (46), 5077–5080. https://doi.org/10.1016/S0040-4039(00)94045-0.

(106) Foulon, J. P.; Bourgain-Commerçon, M.; Normant, J. F. Vinyl Copper Derivatives N° 291. *Tetrahedron* **1986**, *42* (5), 1389–1397. https://doi.org/10.1016/S0040-4020(01)87358-0.

(107) Obayashi, M.; Utimoto, K.; Nozaki, H. A Stereoselective Synthesis of (E)-1,2-Disubstituted Vinylsilanes from Ethynyltrimethylsilane and Alkylcopper via 1-Trimethylsilyl-1(Z)-Alkenylcopper. *Tetrahedron Lett.* **1977**, *18* (21), 1805–1806. https://doi.org/10.1016/s0040-4039(01)83609-1.

(108) WESTMIJZE, H.; J, M.; P, V. THE STEREOSPECIFIC SYNTHESIS OF VINYLSILANES AND 1-HALOGENO-VINYL-SILANES FROM TRIPHENYLSILYLACETYLENE. *Ster. Synth. VINYLSILANES 1-HALOGENO-VINYL-SILANES TRIPHENYLSILYLACETYLENE* **1977**.

(109) Adam, W.; Sahin, C.; Schneider, M. Mechanism of the Diastereoselective, Boron Trifluoride-Catalyzed Cyclization of Olefinic Tosylhydrazones to Stereolabeled, Bridgehead-Substituted Azoalkanes. *J. Am. Chem. Soc.* **1995**, *117* (6), 1695–1702. https://doi.org/10.1021/ja00111a005.

(110) Nakamura, E.; Miyachi, Y.; Koga, N.; Morokuma, K. Theoretical Studies of Heteroatom-Directed Carbometalation. Addition of Methylcopper, Dimethylcopper Anion, and Methyllithium to Substituted Acetylenes. *J. Am. Chem. Soc.* **1992**, *114* (17), 6686–6692. https://doi.org/10.1021/ja00043a011.

(111) Nakamura, E.; Mori, S.; Nakamura, M.; Morokuma, K. Theoretical Studies on the Addition of Polymetallic Lithium Organocuprate Clusters to Acetylene. Cooperative Effects of Metals in a Trap-and-Bite Reaction Pathway. *J. Am. Chem. Soc.* **1997**, *119* (21), 4887–4899. https://doi.org/10.1021/ja964208p.

(112) Nakamura, E.; Mori, S. Wherefore Art Thou Copper? Structures and Reaction Mechanisms of Organocuprate Clusters in Organic Chemistry. *Angew. Chem.* **2000**, *39* (21), 3750–3771. https://doi.org/10.1002/1521-3773(20001103)39:21%253C3750::AID-ANIE3750%253E3.0.CO;2-L.

(113) Cahiez, G.; Alexakis, A.; Normant, J. F. Simple Stereospecific Synthesis of the Insect Sex Pheromones of Cossus Cossus, Eupoecilia Ambiguella and Orgyia Pseudotsugata. *Tetrahedron Lett.* **1980**, *21* (15), 1433–1436. https://doi.org/10.1016/S0040-4039(00)92738-2.

(114) Sviridov, A. F.; Ermolenko, M. S.; Yashunsky, D. V.; Kochetkov, N. K.; Zelinsky, N. D. SELENOESTERS IN ORGANIC SYNTHESIS. 2. SYNTHESIS OF&P- UNSATURATED KETONES.

(115) Ousset, J. B.; Mioskowski, C.; Yang, Y.-L.; Falck, J. R. Enol Ethers: Preparation and Synthetic Applications. *Tetrahedron Lett.* **1984**, *25* (51), 5903–5906. https://doi.org/10.1016/S0040-4039(01)81716-0.

(116) Chemla, F.; Ferreira, F. Carbocupration of Alkynes. In *Patai's Chemistry of Functional Groups*; Wiley, 2011. https://doi.org/10.1002/9780470682531.pat0444.

(117) Carbozincation of Alkenes and Alkynes. In *Patai's Chemistry of Functional Groups*; Wiley, 2009. https://doi.org/10.1002/9780470682531.pat0382.

(118) Courtois, G.; Masson, A.; Miginiac, L. *C R Acad Sci Paris Ser* **1977**, *C 285*, 207.

(119) Knochel, P.; Normant, J. F. Addition of Functionalized Allylic Bromides to Terminal Alkynes. *Tetrahedron Lett.* **1984**, *25* (14), 1475–1478. https://doi.org/10.1016/S0040-4039(01)80190-8.

(120) Negishi, E.; Miller, J. A. Selective Carbon-Carbon Bond Formation via Transition Metal Catalysis. 37. Controlled Carbometalation. 16. Novel Syntheses of .Alpha.,.Beta.-Unsaturated Cyclopentenones via Allylzincation of Alkynes. *J. Am. Chem. Soc.* **1983**, *105* (22), 6761–6763. https://doi.org/10.1021/ja00360a060.

(121) Maezaki, N.; Sawamoto, H.; Yoshigami, R.; Suzuki, T.; Tanaka, T. Geometrically Selective Synthesis of Functionalized β,β-Disubstituted Vinylic Sulfoxides by Cu-Catalyzed Conjugate Addition of Organozinc Reagents to 1-Alkynyl Sulfoxides. *Org. Lett.* **2003**, *5* (8), 1345–1347. https://doi.org/10.1021/ol034289b.

(122) Sklute, G.; Bolm, C.; Marek, I. Regio- and Stereoselective Copper-Catalyzed Carbozincation Reactions of Alkynyl Sulfoximines and Sulfones. *Org. Lett.* **2007**, *9* (7), 1259–1261. https://doi.org/10.1021/ol070070b.

(123) Xie, M.; Gu, X.; Wang, J.; Zhang, J.; Lin, G.; Wang, S. Regio- and Stereospecific Synthesis of Polysubstituted Alkenes by Carbozincation of Acetylenic Sulfones. *Appl. Organomet. Chem.* **2009**, *23* (7), 258–266. https://doi.org/10.1002/aoc.1508.

(124) Xie, M.; Lin, G.; Zhang, J.; Li, M.; Feng, C. Regio- and Stereoselective Synthesis of Tetrasubstituted Allylic Alcohols by Three-Component Reaction of Acetylenic Sulfone, Dialkylzinc, and Aldehyde. *J. Organomet. Chem.* **2010**, *695* (6), 882–886. https://doi.org/10.1016/j.jorganchem.2010.01.003.

(125) Zhang, Y.; Cao, Q.; Xi, Y.; Wu, X.; Qu, J.; Chen, Y. Nickel-Catalyzed Carbonylative Negishi Cross-Coupling of Unactivated Secondary Alkyl Electrophiles with 1 Atm CO Gas. *J. Am. Chem. Soc.* **2024**, *146* (12), 7971–7978. https://doi.org/10.1021/jacs.4c02023.

(126) Gourdet, B.; Rudkin, M. E.; Watts, C. A.; Lam, H. W. Preparation of Multisubstituted Enamides via Rhodium-Catalyzed Carbozincation and Hydrozincation of Ynamides. *J. Org. Chem.* **2009**, *74* (20), 7849–7858. https://doi.org/10.1021/jo901658v.

(127) Gourdet, B.; Lam, H. W. Stereoselective Synthesis of Multisubstituted Enamides via Rhodium-Catalyzed Carbozincation of Ynamides. *J. Am. Chem. Soc.* **2009**, *131* (11), 3802–3803. https://doi.org/10.1021/ja900946h.

(128) Lingua, H.; Vibert, F.; Mouysset, D.; Siri, D.; Bertrand, M. P.; Feray, L. Iron(II)/Copper(I)-Mediated Stereoselective Carbozincation of Ynamides. One-Pot Synthesis of α-Allyl-Tetrasubstituted-Enamides. *Tetrahedron* **2017**, *73* (25), 3415–3422. https://doi.org/10.1016/j.tet.2017.04.065.

(129) Sallio, R.; Corpet, M.; Habert, L.; Durandetti, M.; Gosmini, C.; Gillaizeau, I. Cobalt-Catalyzed Carbozincation of Ynamides. *J. Org. Chem.* **2017**, *82* (2), 1254–1259. https://doi.org/10.1021/acs.joc.6b02612.

(130) Takimoto, M.; Gholap, S. S.; Hou, Z. Alkylative Carboxylation of Ynamides and Allenamides with Functionalized Alkylzinc Halides and Carbon Dioxide by a Copper Catalyst. *Chem. – Eur. J.* **2019**, *25* (35), 8363–8370. https://doi.org/10.1002/chem.201901153.

(131) Xue, S.; He, L.; Liu, Y.-K.; Han, K.-Z.; Qing-Xiang Guo. An Efficient CuI-Promoted Synthesis of Tri- and Tetrasubstituted Alkenes Using Organozinc Species. *Synthesis* **2006**, No. 4, 666–674. https://doi.org/10.1055/s-2006-926299.

(132) Negishi, E.; Van Horn, D. E.; Yoshida, T.; Rand, C. L. Selective Carbon-Carbon Bond Formation via Transition Metal Catalysis. 31. Controlled Carbometalation. 15. Zirconium-Promoted Carbozincation of Alkynes. *Organometallics* **1983**, *2* (4), 563–565. https://doi.org/10.1021/om00076a021.

(133) Ramazanov, I. R.; Kadikova, R. N.; Gabdullin, A. M.; Dzhemilev, U. M. Catalytic Carbozincation of Acetylenic Compounds Catalyzed by Transition Metal Complexes. *Russ. Chem. Rev.* **2025**, *94* (3), RCR5158. https://doi.org/10.59761/RCR5158.

(134) Kadikova, R. N.; Ramazanov, I. R.; Gabdullin, A. M.; Mozgovoj, O. S.; Dzhemilev, U. M. Niobium- and Zirconium-Catalyzed Reactions of Substituted 2 Alkynylamines with Et_2 Zn. *RSC Adv.* **2021**, *11* (8), 4631–4638. https://doi.org/10.1039/D0RA10132J.

(135) Gabdullin, A. M.; Kadikova, R. N.; Ramazanov, I. R. Cp2ZrCl2/EtMgBr-Catalyzed Addition of Diethylzinc to Alk-2-Yn-1-Amines. *Russ. J. Org. Chem.* **2023**, *59* (12), 2132–2137. https://doi.org/10.1134/S1070428023120102.

(136) Gabdullin, A. M.; Kadikova, R. N.; Mozgovoj, O. S.; Ramazanov, I. R. Reactions of Substituted 1-Alkynylphosphines with Et2Zn Catalyzed by the Cp2ZrCl2—EtMgBr System. *Russ. Chem. Bull.* **2024**, *73* (7), 1900–1906. https://doi.org/10.1007/s11172-024-4307-6.

(137) Kadikova, R. N.; Ramazanov, I. R.; Gabdullin, A. M.; Mozgovoi, O. S.; Dzhemilev, U. M. Carbozincation of Substituted 2-Alkynylamines, 1-Alkynylphosphines, 1-Alkynylphosphine Sulfides with Et2Zn in the Presence of Catalytic System of Ti(O-iPr)4 and EtMgBr. *Catalysts* **2019**, *9* (12), 1022. https://doi.org/10.3390/catal9121022.

(138) Huang, Q.; Su, Y.-X.; Sun, W.; Hu, M.-Y.; Wang, W.-N.; Zhu, S.-F. Iron-Catalyzed Vinylzincation of Terminal Alkynes. *J. Am. Chem. Soc.* **2022**, *144* (1), 515–526. https://doi.org/10.1021/jacs.1c11072.

(139) Wang, W.-N.; Huang, Q.; Jin, Y.; Zhou, Q.-L.; Zhu, S.-F. Iron-Catalyzed Alkenylzincation of Internal Alkynes. *Chin. J. Chem.* **2023**, *41* (24), 3547–3552. https://doi.org/10.1002/cjoc.202300356.

(140) Cheung, C. W.; Zhurkin, F. E.; Hu, X. *Z* -Selective Olefin Synthesis via Iron-Catalyzed Reductive Coupling of Alkyl Halides with Terminal Arylalkynes. *J. Am. Chem. Soc.* **2015**, *137* (15), 4932–4935. https://doi.org/10.1021/jacs.5b01784.

(141) Zhurkin, F. E.; Hu, X. γ-Selective Allylation of (*E*)-Alkenylzinc Iodides Prepared by Reductive Coupling of Arylacetylenes with Alkyl Iodides. *J. Org. Chem.* **2016**, *81* (13), 5795–5802. https://doi.org/10.1021/acs.joc.6b01306.

(142) Cheung, C. W.; Hu, X. Stereoselective Synthesis of Trisubstituted Alkenes through Sequential Iron-Catalyzed Reductive Anti-Carbozincation of Terminal Alkynes and Base-Metal-Catalyzed Negishi Cross-Coupling. *Chem. – Eur. J.* **2015**, *21* (50), 18439–18444. https://doi.org/10.1002/chem.201504049.

(143) Barzanò, G.; Cheseaux, A.; Hu, X. Z-Selective Synthesis of Vinyl Boronates through Fe-Catalyzed Alkyl Radical Addition. *Org. Lett.* **2019**, *21* (2), 490–493. https://doi.org/10.1021/acs.orglett.8b03772.

(144) Nishikawa, T.; Yorimitsu, H.; Oshima, K. Cobalt-Catalyzed Regio- and Stereoselective Allylzincation of 1-Phenyl-1-Alkynes. *Synlett* **2004**, No. 9, 1573–1574. https://doi.org/10.1055/s-2004-829086.

(145) Murakami, K.; Yorimitsu, H.; Oshima, K. Cobalt-Catalyzed Arylzincation of Alkynes. *Org. Lett.* **2009**, *11* (11), 2373–2375. https://doi.org/10.1021/ol900883j.

(146) Corpet, M.; Gosmini, C. Cobalt-Catalysed Synthesis of Highly Substituted Styrene Derivatives via Arylzincation of Alkynes. *Chem. Commun.* **2012**, *48* (94), 11561. https://doi.org/10.1039/c2cc36676b.

(147) Cobalt-Catalyzed Benzylzincation of Alkynes. *Synfacts* **2010**, *2010*, 1037–1037. https://doi.org/10.1055/s-0030-1257959.

(148) Nogi, K.; Fujihara, T.; Terao, J.; Tsuji, Y. Carboxyzincation Employing Carbon Dioxide and Zinc Powder: Cobalt-Catalyzed Multicomponent Coupling Reactions with Alkynes. *J. Am. Chem. Soc.* **2016**, *138* (17), 5547–5550. https://doi.org/10.1021/jacs.6b02961.

(149) Stüdemann, T.; Ibrahim-Ouali, M.; Knochel, P. A Nickel-Catalyzed Carbozincation of Aryl-Substituted Alkynes. *Tetrahedron* **1998**, *54* (7), 1299–1316. https://doi.org/10.1016/S0040-4020(97)10226-5.

(150) Stüdemann, T.; Knochel, P. New Nickel-Catalyzed Carbozincation of Alkynes: A Short Synthesis of (*Z*)-Tamoxifen. *Angew. Chem. Int. Ed. Engl.* **1997**, *36* (1–2), 93–95. https://doi.org/10.1002/anie.199700931.

(151) Ming, J.; Hayashi, T. Rhodium-Catalyzed Arylzincation of Alkynes: Ligand Control of 1,4-Migration Selectivity. *Org. Lett.* **2018**, *20* (19), 6188–6192. https://doi.org/10.1021/acs.orglett.8b02668.

(152) Itami, K.; Yoshida, J. Carbomagnesiation Reactions. In *PATAI'S Chemistry of Functional Groups*; Rappoport, Z., Marek, I., Eds.; Wiley, 2008; pp 631–679. https://doi.org/10.1002/9780470751879.ch14.

(153) Murakami, K. Studies on Carbometalation of Alkynes and Nucleophilic Substitution of Chlorosilanes with Organomagnesium and Organozinc Reagents.

(154) Murakami, K.; Yorimitsu, H. Recent Advances in Transition-Metal-Catalyzed Intermolecular Carbomagnesiation and Carbozincation. *Beilstein J. Org. Chem.* **2013**, *9*, 278–302. https://doi.org/10.3762/bjoc.9.34.

(155) Normant, J. F.; Alexakis, A. Carbometallation (C-Metallation) of Alkynes: Stereospecific Synthesis of Alkenyl Derivatives. *Synthesis* **2002**, *1981*, 841–870. https://doi.org/10.1055/s-1981-29622.

(156) Ghosh, S.; Chakrabortty, R.; Ganesh, V. Dual Functionalization of Alkynes Utilizing the Redox Characteristics of Transition Metal Catalysts. *ChemCatChem* **2021**, *13* (20), 4262–4298. https://doi.org/10.1002/cctc.202100838.

(157) Kandil, S. A.; Dessy, R. E. Intramolecular Organometal-Acetylene and Acetylene-Acetylene Interactions. Routes to Benzylidenefluorene and C_4 Ring Systems. *J. Am. Chem. Soc.* **1966**, *88* (13), 3027–3034. https://doi.org/10.1021/ja00965a025.

(158) Richey, H. G.; Rothman, A. M. Intramolecular Cyclizations of Acetylenic Grignard Reagents. *Tetrahedron Lett.* **1968**, *9* (12), 1457–1460. https://doi.org/10.1016/S0040-4039(01)98978-6.

(159) Fujikura, S.; Inoue, M.; Utimoto, K.; Nozaki, H. Intramolecular Carbometallation of Grignard Reagents Having the Terminal Trimethylsilylacetylene Group. *Tetrahedron Lett.* **1984**, *25* (19), 1999–2002. https://doi.org/10.1016/S0040-4039(01)90096-6.

(160) J. K. Crandall; P. Battioni; J. T. Wehlacz; R. Bindra. *J Am Chem Soc* **1975**, *97* (7171).

(161) Kambe, N.; Moriwaki, Y.; Fujii, Y.; Iwasaki, T.; Terao, J. Silver-Catalyzed Regioselective Carbomagnesiation of Alkynes with Alkyl Halides and Grignard Reagents. *Org. Lett.* **2011**, *13* (17), 4656–4659. https://doi.org/10.1021/ol2018664.

(162) Kunz, T.; Knochel, P. Synthesis of Functionalized Benzo[b]Thiophenes by the Intramolecular Copper-Catalyzed Carbomagnesiation of Alkynyl(Aryl)Thioethers. *Angew. Chem. Int. Ed.* **2012**, *51* (8), 1958–1961. https://doi.org/10.1002/anie.201106734.

(163) Frischmuth, A.; Knochel, P. Preparation of Functionalized Indoles and Azaindoles by the Intramolecular Copper-Mediated Carbomagnesiation of Ynamides. *Angew. Chem. Int. Ed.* **2013**, *52* (38), 10084–10088. https://doi.org/10.1002/anie.201304380.

(164) Agbaria, M.; Egbaria, N.; Nairoukh, Z. Dearomative Spirocyclization of Ynamides. *Chem. Sci.* **2024**, *15* (45), 19136–19141. https://doi.org/10.1039/D4SC05541A.

(165) Eisch, J. J.; Merkley, J. H. Intramolecular Coordinative Assistance in the Addition of Grignard Reagents to Unconjugated Carbon-Carbon Unsaturation. *J. Organomet. Chem.* **1969**, *20* (1), P27–P31. https://doi.org/10.1016/S0022-328X(00)80077-7.

(166) Richey, H. G.; Von Rein, F. W. Promotion by Hydroxyl Functions of Additions of Grignard Reagents to Alkynes. *J. Organomet. Chem.* **1969**, *20* (1), P32–P35. https://doi.org/10.1016/S0022-328X(00)80078-9.

(167) Desilva, A.; Francis, C.; Ward, A. Grignard Addition Reactions to 1,4-Difunctionalized But-2-Ynes. *Aust. J. Chem.* **1993**, *46* (11), 1657. https://doi.org/10.1071/CH9931657.

(168) Bury, P.; Hareau, G.; Kocieski, P. Two Syntheses of Manoalide Da Heteroatom-Assisted Aikyne Carbometallation.

(169) Tessier, P. E.; Penwell, A. J.; Souza, F. E. S.; Fallis, A. G. (Z)-Tamoxifen and Tetrasubstituted Alkenes and Dienes via a Regio- and Stereospecific Three-Component Magnesium Carbometalation Palladium(0) Cross-Coupling Strategy. *Org. Lett.* **2003**, *5* (17), 2989–2992. https://doi.org/10.1021/ol0347794.

(170) Forgione, P.; Fallis, A. G. Magnesium Mediated Carbometallation of Propargyl Alcohols: Direct Routes to Dihydroxydienes and Enediyne Alcohols. *Tetrahedron Lett.* **2000**, *41* (1), 11–15. https://doi.org/10.1016/S0040-4039(99)01994-2.

(171) Wong, T.; Tjepkema, M. W.; Audrain, H.; Wilson, P. D.; Fallis, A. G. A Versatile Synthesis of (E)- and (Z)-l-Halo-2-(Alkoxymethyl)- 1,3-Butadienes and Their Condensation with Aldehydes.

(172) Tessier, P. E.; Nguyen, N.; Clay, M. D.; Fallis, A. G. Aryl Annulation of Cyclic Ketones via a Magnesium Carbometalation−6-π- Electrocyclization Protocol. *Org. Lett.* **2005**, *7* (5), 767–770. https://doi.org/10.1021/ol047602y.

(173) Engelhardt, F. C.; Shi, Y.-J.; Cowden, C. J.; Conlon, D. A.; Pipik, B.; Zhou, G.; McNamara, J. M.; Dolling, U.-H. Synthesis of a NO-Releasing Prodrug of Rofecoxib. *J. Org. Chem.* **2006**, *71* (2), 480–491. https://doi.org/10.1021/jo051712g.

(174) Vermeer, P.; De Graaf, C.; Meijer, J. Chemistry of Acetylenic Ethers 103 Stereospecific Addition of Grignard Compounds to 1-alkynyl Sulfides in the Presence of Copper(I) Halide. *Recl. Trav. Chim. Pays-Bas* **1974**, *93* (1), 24–25. https://doi.org/10.1002/recl.19740930111.

(175) B. Jousseaume. *Thesis,*; University of Bordeaux I, 1977.

(176) Xie, C.; Huang, X. Carbomagnesiation of Acetylenic Sulfones Catalyzed by CuCN and Its Application in the Stereoselective Synthesis of Polysubstituted Vinyl Sulfones. *N. Y.* **2003**, No. 4.

(177) Xie, M.; Liu, L.; Wang, J.; Wang, S. Stereoselective Synthesis of Vinyl Sulfones by Carbomagnesiation of Acetylenic Sulfone in the Presence of CuCN. *J. Organomet. Chem.* **2005**, *690* (17), 4058–4062. https://doi.org/10.1016/j.jorganchem.2005.06.006.

(178) Liu, C.; Zha, C.; Jia, J.; Fan, J.; Liang, Z.; Yin, Z.; Sun, Y.; Xie, M. Three-Component Coupling of Acetylenic Sulfones, Grignard Reagents and α, β-Unsaturated Carbonyls: A Convenient Synthesis of Diallylic Alcohols. *J. Organomet. Chem.* **2016**, *825–826*, 75–82. https://doi.org/10.1016/j.jorganchem.2016.10.026.

(179) Xie, M.; Feng, C.; Zhang, J.; Liu, C.; Fang, K.; Shu, G.; Zuo, W. CuI-Catalyzed Tandem Carbomagnesiation/Carbonyl Addition of Grignard Reagents with Acetylenic Ketones: Convenient Access to Tetrasubstituted Allylic Alcohols. *J. Organomet. Chem.* **2011**, *696* (21), 3397–3401. https://doi.org/10.1016/j.jorganchem.2011.07.031.

(180) Yasui, H.; Yorimitsu, H.; Oshima, K. Transformations of N-Allyl-N-(Phenylethynyl)Arenesulfonamides into 2,2-Disubstituted 4-Pentenenitriles through Aza-Claisen Rearrangement That Follows Carbomagnesiation.

(181) Jousseaume, B.; Duboudin, J.-G. Reactions d'addition d'organomagnesiens Aux Alcools α-Acetyleniques. *J. Organomet. Chem.* **1975**, *91* (1), C1–C3. https://doi.org/10.1016/S0022-328X(00)91880-1.

(182) Negishi, E.; Zhang, Y.; Cederbaum, F. E.; Webb, M. B. A Selective Method for the Synthesis of Stereodefined Exocyclic Alkenes via Allylmetalation of Propargyl Alcohols. *J. Org. Chem.* **1986**, *51* (21), 4080–4082. https://doi.org/10.1021/jo00371a036.

(183) Duboudin, J.-G.; Jousseaume, B. Synthesis and Intramolecular Cyclisation of Gem Vinylic Di-Grignard Reagents. *Synth. Commun.* **1979**, *9* (1), 53–56. https://doi.org/10.1080/00397917908065642.

(184) Fang, G.-H.; Yan, Z.-J.; Yang, J.; Deng, M.-Z. The First Preparation of 4-Substituted 1,2-Oxaborol-2(5H)-Ols and Their Palladium--Catalyzed Cross-Coupling with Aryl Halides to Prepare Stereodefined- 2,3-Disubstituted Allyl Alcohols. *Synthesis* **2006**, *2006*, 1148–1154. https://doi.org/10.1055/s-2006-926388.

(185) Zhang, D.; Ready, J. M. Iron-Catalyzed Carbometalation of Propargylic and Homopropargylic Alcohols. *J. Am. Chem. Soc.* **2006**, *128* (47), 15050–15051. https://doi.org/10.1021/ja0647708.

(186) Okada, K.; Oshima, K.; Utimoto, K. Allylmagnesation and Diallylation of Acetylenic Compounds Catalyzed by Manganese Salts. *J. Am. Chem. Soc.* **1996**, *118* (25), 6076–6077. https://doi.org/10.1021/ja960791y.

(187) Shinokubo, H.; Oshima, K. Manganese-Catalyzed Carbomagnesation of Alkynes. *Catal. Surv. Asia* **2003**, *7* (1), 39–46. https://doi.org/10.1023/A:1023432624548.

(188) Murakami, K.; Ohmiya, H.; Yorimitsu, H.; Oshima, K. Nickel-Catalyzed Carbometalation Reactions of [2-(1-Propynyl)Phenyl]Methanol with 1-Alkenylmagnesium Reagents. *Chem. Lett.* **2007**, *36* (8), 1066–1067. https://doi.org/10.1246/cl.2007.1066.

(189) Snider, B. B.; Karras, M.; Conn, R. S. E. Nickel-Catalyzed Addition of Grignard Reagents to Silylacetylenes. Synthesis of Tetrasubstituted Alkenes.

(190) Conn, R. S. E.; Karras, M.; Snider, B. B. Nickel-Catalyzed Addition of Methylmagnesium Bromide to Alkynylsilanes. Stereospecific Synthesis of Tetrasubstituted Alkenes. *Isr. J. Chem.* **1984**, *24* (2), 108–112. https://doi.org/10.1002/ijch.198400019.

(191) Itami, K.; Kamei, T.; Yoshida, J. Diversity-Oriented Synthesis of Tamoxifen-Type Tetrasubstituted Olefins. *J. Am. Chem. Soc.* **2003**, *125* (48), 14670–14671. https://doi.org/10.1021/ja037566i.

(192) Duboudin, J. G.; Jousseaume, B. Reactivite Des Organomagnesiens Vis-a-Vis de Composes Acetyleniques En Presence Du Complexe de Nickel (PPh3)2NiCl2. *J. Organomet. Chem.* **1978**, *162* (2), 209–222. https://doi.org/10.1016/S0022-328X(00)82039-2.

(193) Xue, F.; Zhao, J.; Andy Hor, T. S. Ambient Arylmagnesiation of Alkynes Catalysed by Ligandless Nickel(Ii). *Chem. Commun.* **2013**, *49* (86), 10121–10123. https://doi.org/10.1039/C3CC45202F.

(194) Xue, F.; Zhao, J.; Hor, T. S. A.; Hayashi, T. Nickel-Catalyzed Three-Component Domino Reactions of Aryl Grignard Reagents, Alkynes, and Aryl Halides Producing Tetrasubstituted Alkenes. *J. Am. Chem. Soc.* **2015**, *137* (9), 3189–3192. https://doi.org/10.1021/ja513166w.

(195) Wu, B.; Chopra, R.; Yoshikai, N. One-Pot Benzo[b]Phosphole Synthesis through Sequential Alkyne Arylmagnesiation, Electrophilic Trapping, and Intramolecular Phospha-Friedel–Crafts Cyclization. *Org. Lett.* **2015**, *17* (22), 5666–5669. https://doi.org/10.1021/acs.orglett.5b02950.

(196) Sheng Wang; Chanjuan Xi. Nickel-Catalyzed Arylative Carboxylation of Alkynes with Arylmagnesium Reagents and Carbon Dioxide Leading to Trisubstituted Acrylic Acids. *Org. Lett.* **2018**, *20* (13), 4131–4134. https://doi.org/10.1021/acs.orglett.8b01693.

(197) Hung, C.-H.; Santhoshkumar, R.; Chang, Y.-C.; Cheng, C.-H. Synthesis of Trisubstituted Acrylic Acids through Nickel-Catalyzed Carbomagnesiation of Alkynes and Carbon Dioxide Fixation. *Eur. J. Org. Chem.* **2018**, *2018* (48), 6924–6928. https://doi.org/10.1002/ejoc.201801364.

(198) Alexakis, A.; Cahiez, G. ORGANOCUIVREUX VINYLIQUES.

(199) Takahashi, T.; Aoyagi, K.; Denisov, V.; Suzuki, N.; Choueiry, D.; Negishi, E. Zirconium Catalyzed C□C Bond Formation Reaction of Conjugated Diynes with EtMgBr. *Tetrahedron Lett.* **1993**, *34* (51), 8301–8304. https://doi.org/10.1016/S0040-4039(00)61416-8.

(200) Yamagami, T.; Shintani, R.; Shirakawa, E.; Hayashi, T. Iron-Catalyzed Arylmagnesiation of Aryl(Alkyl)Acetylenes in the Presence of an N-Heterocyclic Carbene Ligand. *Org. Lett.* **2007**, *9* (6), 1045–1048. https://doi.org/10.1021/ol063132r.

(201) Shirakawa, E.; Ikeda, D.; Masui, S.; Yoshida, M.; Hayashi, T. Iron–Copper Cooperative Catalysis in the Reactions of Alkyl Grignard Reagents: Exchange Reaction with Alkenes and Carbometalation of Alkynes. *J. Am. Chem. Soc.* **2012**, *134* (1), 272–279. https://doi.org/10.1021/ja206745w.

(202) Liu, Y.; Wang, L.; Deng, L. Selective Double Carbomagnesiation of Internal Alkynes Catalyzed by Iron-N-Heterocyclic Carbene Complexes: A Convenient Method to Highly Substituted 1,3-Dienyl Magnesium Reagents. *J. Am. Chem. Soc.* **2016**, *138* (1), 112–115. https://doi.org/10.1021/jacs.5b12522.

(203) Ilies, L.; Yoshida, T.; Nakamura, E. Synthesis of Polysubstituted Enynes through Iron-Catalyzed Carbomagnesiation of Conjugated Diynes. *Synlett* **2014**, *25* (04), 527–530. https://doi.org/10.1055/s-0033-1340476.

(204) Murakami, K.; Ohmiya, H.; Yorimitsu, H.; Oshima, K. Chromium-Catalyzed Arylmagnesiation of Alkynes. *Org. Lett.* **2007**, *9* (8), 1569–1571. https://doi.org/10.1021/ol0703938.

(205) Fujii, Y.; Terao, J.; Kambe, N. Silver-Catalyzed Carbomagnesiation of Terminal Aryl and Silyl Alkynes and Enynes in the Presence of 1,2-Dibromoethane. *Chem. Commun.* **2009**, *0* (9), 1115–1117. https://doi.org/10.1039/B820521C.

(206) Kambe, N.; Moriwaki, Y.; Fujii, Y.; Iwasaki, T.; Terao, J. Silver-Catalyzed Regioselective Carbomagnesiation of Alkynes with Alkyl Halides and Grignard Reagents. *Org. Lett.* **2011**, *13* (17), 4656–4659. https://doi.org/10.1021/ol2018664.

(207) Tamura, Y.; Minami, Y.; Nishiyama, Y.; Sakata, Y.; Karaki, F.; Hosoya, T.; Yoshida, S. Synthesis of Multisubstituted Cycloalkenes through Carbomagnesiation of Strained Cycloalkynes. *Chem. Commun.* **2020**, *56* (52), 7147–7150. https://doi.org/10.1039/D0CC02788J.

(208) Altarejos, J.; Valero, A.; Manzano, R.; Carreras, J. Synthesis of Tri- and Tetrasubstituted Alkenyl Boronates from Alkynes. *Eur. J. Org. Chem.* **2022**, *2022* (30), e202200521. https://doi.org/10.1002/ejoc.202200521.

(209) Daini, M.; Yamamoto, A.; Suginome, M. Palladium-Catalyzed Trans- and Cis-Carboboration of Alkynes Tethered to Chloroborane with Organozirconium Reagents: Ligand-Dependent Complementary Stereoselectivity. *J. Am. Chem. Soc.* **2008**, *130* (10), 2918–2919. https://doi.org/10.1021/ja711160h.

(210) Yamamoto, A.; Suginome, M. Nickel-Catalyzed Trans-Alkynylboration of Alkynes via Activation of a Boron−Chlorine Bond. *J. Am. Chem. Soc.* **2005**, *127* (45), 15706–15707. https://doi.org/10.1021/ja055396z.

(211) Liu, P.; Fukui, Y.; Tian, P.; He, Z.-T.; Sun, C.-Y.; Wu, N.-Y.; Lin, G.-Q. Cu-Catalyzed Asymmetric Borylative Cyclization of Cyclohexadienone-Containing 1,6-Enynes. *J. Am. Chem. Soc.* **2013**, *135* (32), 11700–11703. https://doi.org/10.1021/ja404593c.

(212) Kubota, K.; Iwamoto, H.; Yamamoto, E.; Ito, H. Silicon-Tethered Strategy for Copper(I)-Catalyzed Stereo- and Regioselective Alkylboration of Alkynes. *Org. Lett.* **2015**, *17* (3), 620–623. https://doi.org/10.1021/ol503620n.

(213) Kim-Lee, S.-H.; Alonso, I.; Mauleón, P.; Arrayás, R. G.; Carretero, J. C. Rationalizing the Role of NaOtBu in Copper-Catalyzed Carboboration of Alkynes: Assembly of Allylic All-Carbon Quaternary Stereocenters. *ACS Catal.* **2018**, *8* (10), 8993–9005. https://doi.org/10.1021/acscatal.8b02123.

(214) Mikhailov, B. M.; Bubnov, Yu. N. *Izv Akad Nauk SSSR Ser Khim* **1965**, 1310.

(215) Mikhailov, B. M.; Bubnov, Yu. N. A Method for Preparation of 1,4-Dienes via Allylboration of Vinyl Ethers. *Tetrahedron Lett.* **1971**, *12* (24), 2127–2130. https://doi.org/10.1016/S0040-4039(01)96799-1.

(216) Suginome, M.; Shirakura, M.; Yamamoto, A. Nickel-Catalyzed Addition of Alkynylboranes to Alkynes. *J. Am. Chem. Soc.* **2006**, *128* (45), 14438–14439. https://doi.org/10.1021/ja064970j.

(217) Han, J. T.; Yun, J. Copper-Catalyzed Synthesis of Tetrasubstituted Enynylboronates via Chemo-, Regio-, and Stereoselective Borylalkynylation. *Org. Lett.* **2018**, *20* (7), 2104–2107. https://doi.org/10.1021/acs.orglett.8b00665.

(218) Li, K.; Yu, S.-H.; Zhuo, K.-F.; Lu, X.; Xiao, B.; Gong, T.-J.; Fu, Y. Synthesis of Conjugated Boron-Enynes via Cis-Alkynylboration of Terminal Alkynes. *Adv. Synth. Catal.* **2019**, *361* (17), 3937–3942. https://doi.org/10.1002/adsc.201900294.

(219) Mannathan, S.; Jeganmohan, M.; Cheng, C.-H. Nickel-Catalyzed Borylative Coupling of Alkynes, Enones, and Bis(Pinacolato)Diboron as a Route to Substituted Alkenyl Boronates. *Angew. Chem. Int. Ed.* **2009**, *48* (12), 2192–2195. https://doi.org/10.1002/anie.200805293.

(220) Cheng, T.; Liu, B.; Wu, R.; Zhu, S. Cu-Catalyzed Carboboration of Acetylene with Michael Acceptors. *Chem. Sci.* **2022**, *13* (25), 7604–7609. https://doi.org/10.1039/D2SC02306G.

(221) Alfaro, R.; Parra, A.; Alemán, J.; García Ruano, J. L.; Tortosa, M. Copper(I)-Catalyzed Formal Carboboration of Alkynes: Synthesis of Tri- and Tetrasubstituted Vinylboronates. *J. Am. Chem. Soc.* **2012**, *134* (37), 15165–15168. https://doi.org/10.1021/ja307670k.

(222) Yoshida, H.; Kageyuki, I.; Takaki, K. Copper-Catalyzed Three-Component Carboboration of Alkynes and Alkenes. *Org. Lett.* **2013**, *15* (4), 952–955. https://doi.org/10.1021/ol4001526.

(223) Bidal, Y. D.; Lazreg, F.; Cazin, C. S. J. Copper-Catalyzed Regioselective Formation of Tri- and Tetrasubstituted Vinylboronates in Air. *ACS Catal.* **2014**, *4* (5), 1564–1569. https://doi.org/10.1021/cs500130y.

(224) Su, W.; Gong, T.-J.; Zhang, Q.; Zhang, Q.; Xiao, B.; Fu, Y. Ligand-Controlled Regiodivergent Copper-Catalyzed Alkylboration of Unactivated Terminal Alkynes. *ACS Catal.* **2016**, *6* (10), 6417–6421. https://doi.org/10.1021/acscatal.6b02039.

(225) Itoh, T.; Shimizu, Y.; Kanai, M. Ligand-Enabled, Copper-Catalyzed Regio- and Stereoselective Synthesis of Trialkylsubstituted Alkenylboronates from Unactivated Internal Alkynes. *J. Am. Chem. Soc.* **2016**, *138* (24), 7528–7531. https://doi.org/10.1021/jacs.6b04646.

(226) Mun, B.; Kim, S.; Yoon, H.; Kim, K. H.; Lee, Y. Total Synthesis of Isohericerin, Isohericenone, and Erinacerin A: Development of a Copper-Catalyzed Methylboronation of Terminal Alkynes. *J. Org. Chem.* **2017**, *82* (12), 6349–6357. https://doi.org/10.1021/acs.joc.7b00920.

(227) Kim-Lee, S.-H.; Mauleón, P.; Arrayás, R. G.; Carretero, J. C. Dynamic Multiligand Catalysis: A Polar to Radical Crossover Strategy Expands Alkyne Carboboration to Unactivated Secondary Alkyl Halides. *Chem* **2021**, *7* (8), 2212–2226. https://doi.org/10.1016/j.chempr.2021.06.002.

(228) Jia, J.-S.; Luo, J.-R.; Li, W.-H.; Cui, F.-H.; Pan, Y.-M.; Tang, H.-T. Copper-Metallized Porous N-Heterocyclic Carbene Ligand Polymer-Catalyzed Regio- and Stereoselective 1,2-Carboboration of Alkynes. *Adv. Sci.* **2024**, *11* (7), 2308238. https://doi.org/10.1002/advs.202308238.

(229) Prakash, A.; Basappa, S.; Urkude, R. R.; Jangir, R.; Dhayal, R. S.; Kumar Bose, S. Zero-Valent Copper Catalysis Enables Regio- and Stereoselective Difunctionalization of Alkynes. *Angew. Chem.* **2025**, *137* (8), e202418901. https://doi.org/10.1002/ange.202418901.

(230) Nakagawa, N.; Hatakeyama, T.; Nakamura, M. Iron-Catalyzed Diboration and Carboboration of Alkynes. *Chem. – Eur. J.* **2015**, *21* (11), 4257–4261. https://doi.org/10.1002/chem.201406595.

(231) Daini, M.; Suginome, M. Palladium-Catalyzed Carboboration of Alkynes Using Chloroborane and Organozirconium Reagents. *Chem. Commun.* **2008**, *0* (41), 5224–5226. https://doi.org/10.1039/B809433K.

(232) Zhou, Y.; You, W.; Smith, K. B.; Brown, M. K. Copper-Catalyzed Cross-Coupling of Boronic Esters with Aryl Iodides and Application to the Carboboration of Alkynes and Allenes. *Angew. Chem.* **2014**, *126* (13), 3543–3547. https://doi.org/10.1002/ange.201310275.

(233) Lesieur, M.; Bidal, Y. D.; Lazreg, F.; Nahra, F.; Cazin, C. S. J. Versatile Relay and Cooperative Palladium(0) N-Heterocyclic Carbene/Copper(I) N-Heterocyclic Carbene Catalysis for the Synthesis of Tri- and Tetrasubstituted Alkenes. *ChemCatChem* **2015**, *7* (14), 2108–2112. https://doi.org/10.1002/cctc.201500268.

(234) Semba, K.; Yoshizawa, M.; Ohtagaki, Y.; Nakao, Y. Arylboration of Internal Alkynes by Cooperative Palladium/Copper Catalysis. *Bull. Chem. Soc. Jpn.* **2017**, *90* (12), 1340–1343. https://doi.org/10.1246/bcsj.20170226.

(235) Huang, Y.; M. Bergmann, A.; Kevin Brown, M. (Hetero)Arylboration of Alkynes: A Strategy for the Synthesis of α,α-Bis(Hetero)Arylketones. *Org. Biomol. Chem.* **2019**, *17* (24), 5913–5915. https://doi.org/10.1039/C9OB00961B.

(236) Bin, H.-Y.; Wei, X.; Zi, J.; Zuo, Y.-J.; Wang, T.-C.; Zhong, C.-M. Substrate-Controlled Regio- and Stereoselective Synthesis of Boron-Substituted 1,4-Dienes via Copper-Catalyzed Boryl–Allylation of Alkynes with Allyl Phosphates and Bis(Pinacolato)Diboron. *ACS Catal.* **2015**, *5* (11), 6670–6679. https://doi.org/10.1021/acscatal.5b01441.

(237) Mateos, J.; Rivera-Chao, E.; Fañanás-Mastral, M. Synergistic Copper/Palladium Catalysis for the Regio- and Stereoselective Synthesis of Borylated Skipped Dienes. *ACS Catal.* **2017**, *7* (8), 5340–5344. https://doi.org/10.1021/acscatal.7b01833.

(238) Rivera-Chao, E.; Fañanás-Mastral, M. Synthesis of Stereodefined Borylated Dendralenes through Copper-Catalyzed Allylboration of Alkynes. *Angew. Chem.* **2018**, *130* (31), 10093–10097. https://doi.org/10.1002/ange.201806334.

(239) Gao, Y.; Kim, N.; Mendoza, S. D.; Yazdani, S.; Faria Vieira, A.; Liu, M.; Kendrick, A. I.; Grotjahn, D. B.; Bertrand, G.; Jazzar, R.; Engle, K. M. (CAAC)Copper Catalysis Enables Regioselective Three-Component Carboboration of Terminal Alkynes. *ACS Catal.* **2022**, *12* (12), 7243–7247. https://doi.org/10.1021/acscatal.2c00614.

(240) Yu, S.-H.; Gong, T.-J.; Fu, Y. Three-Component Borylallenylation of Alkynes: Access to Densely Boryl-Substituted Ene-Allenes. *Org. Lett.* **2020**, *22* (8), 2941–2945. https://doi.org/10.1021/acs.orglett.0c00643.

(241) Wang, S.; Zhang, J.; Kong, L.; Tan, Z.; Bai, Y.; Zhu, G. Palladium-Catalyzed Anti-Selective Fluoroalkylboration of Internal and Terminal Alkynes. *Org. Lett.* **2018**, *20* (18), 5631–5635. https://doi.org/10.1021/acs.orglett.8b02336.

(242) Domański, S.; Gatlik, B.; Chaładaj, W. Pd-Catalyzed Boroperfluoroalkylation of Alkynes Opens a Route to One-Pot Reductive Carboperfluoroalkylation of Alkynes with Perfluoroalkyl and Aryl Iodides. *Org. Lett.* **2019**, *21* (13), 5021–5025. https://doi.org/10.1021/acs.orglett.9b01618.

(243) Guo, W.-H.; Zhao, H.-Y.; Luo, Z.-J.; Zhang, S.; Zhang, X. Fluoroalkylation–Borylation of Alkynes: An Efficient Method To Obtain (Z)-Tri- and Tetrasubstituted Fluoroalkylated Alkenylboronates. *ACS Catal.* **2019**, *9* (1), 38–43. https://doi.org/10.1021/acscatal.8b02842.

(244) Zhang, L.; Cheng, J.; Carry, B.; Hou, Z. Catalytic Boracarboxylation of Alkynes with Diborane and Carbon Dioxide by an N-Heterocyclic Carbene Copper Catalyst. *J. Am. Chem. Soc.* **2012**, *134* (35), 14314–14317. https://doi.org/10.1021/ja3063474.

(245) Cheng, L.-J.; Mankad, N. P. Copper-Catalyzed Borocarbonylative Coupling of Internal Alkynes with Unactivated Alkyl Halides: Modular Synthesis of Tetrasubstituted β-Borylenones. *Angew. Chem.* **2018**, *130* (32), 10485–10489. https://doi.org/10.1002/ange.201804883.

(246) Kirsch, P. *Modern Fluoroorganic Chemistry: Synthesis, Reactivity, Applications*, 2nd ed.; Wiley-VCH: Weinheim, Germany, 2013.

(247) Chachignon, H.; Cahard, D. State-of-the-Art in Electrophilic Trifluoromethylthiolation Reagents. *Chin. J. Chem.* **2016**, *34* (5), 445–454. https://doi.org/10.1002/cjoc.201500890.

(248) Abubakar, S. S.; Benaglia, M.; Rossi, S.; Annunziata, R. Organocatalytic α-Trifluoromethylthiolation of Silylenol Ethers: Batch vs Continuous Flow Reactions. *Catal. Today* **2018**, *308*, 94–101. https://doi.org/10.1016/j.cattod.2017.09.013.

(249) Shao, X.; Wang, X.; Yang, T.; Lu, L.; Shen, Q. An Electrophilic Hypervalent Iodine Reagent for Trifluoromethylthiolation. *Angew. Chem. Int. Ed.* **2013**, *52* (12), 3457–3460. https://doi.org/10.1002/anie.201209817.

(250) Xu, X.-H.; Matsuzaki, K.; Shibata, N. Synthetic Methods for Compounds Having CF3–S Units on Carbon by Trifluoromethylation, Trifluoromethylthiolation, Triflylation, and Related Reactions. *Chem. Rev.* **2015**, *115* (2), 731–764. https://doi.org/10.1021/cr500193b.

(251) Rueping, M.; Tolstoluzhsky, N.; Nikolaienko, P. Copper-Catalyzed Trifluoromethyl Thiolation—Mild and Efficient Synthesis of Trifluoromethyl Thioethers. *Chem. – Eur. J.* **2013**, *19* (42), 14043–14046. https://doi.org/10.1002/chem.201302692.

(252) Barata-Vallejo, S.; Bonesi, S.; Postigo, A. Late Stage Trifluoromethylthiolation Strategies for Organic Compounds. *Org. Biomol. Chem.* **2016**, *14* (30), 7150–7182. https://doi.org/10.1039/C6OB00763E.

(253) Ren, Y.; Yan, Q.; Li, Y.; Gao, Y.; Zhao, J.; Li, L.; Liu, Z.-Q.; Li, Z. Free Radical Promoted Trifluoromethylthiolation of Alkynes to Access SCF3-Containing Dibenzazepines or Dioxodibenzothiazepines. *J. Org. Chem.* **2022**, *87* (13), 8773–8781. https://doi.org/10.1021/acs.joc.2c00623.

(254) Barthelemy, A.-L.; Magnier, E.; Dagousset, G. Direct Trifluoromethylthiolation Reactions Involving Radical Processes. *Synthesis* **2018**, *50*, 4765–4776. https://doi.org/10.1055/s-0037-1611278.

(255) Liu, H.; Ge, H.; Shen, Q. Reagents for Direct Trifluoromethylthiolation. In *Emerging Fluorinated Motifs*; Ma, J., Cahard, D., Eds.; Wiley, 2020; pp 309–341. https://doi.org/10.1002/9783527824342.ch12.

(256) Shen, Q. A Toolbox of Reagents for Trifluoromethylthiolation: From Serendipitous Findings to Rational Design. *J. Org. Chem.* **2023**, *88* (6), 3359–3371. https://doi.org/10.1021/acs.joc.2c02777.

(257) Zhang, J.; Yang, J.-D.; Zheng, H.; Xue, X.-S.; Mayr, H.; Cheng, J.-P. Exploration of the Synthetic Potential of Electrophilic Trifluoromethylthiolating and Difluoromethylthiolating Reagents. *Angew. Chem. Int. Ed.* **2018**, *57* (39), 12690–12695. https://doi.org/10.1002/anie.201805859.

(258) Zheng, H.; Huang, Y.; Weng, Z. Recent Advances in Trifluoromethylthiolation Using Nucleophilic Trifluoromethylthiolating Reagents. *Tetrahedron Lett.* **2016**, *57* (13), 1397–1409. https://doi.org/10.1016/j.tetlet.2016.02.073.

(259) Emeléus, H. J.; Nabi, S. N. 227. Reaction of Trifluoromethanesulphenyl Chloride with Ammonia, Amines, and Phosphine. *J. Chem. Soc. Resumed* **1960**, 1103–1108.

(260) Harris, J. F. **The Free-Radical Addition of Trifluoromethanesulfenyl Chloride to Haloölefins**. *J. Am. Chem. Soc.* **1962**, *84* (16), 3148–3153. https://doi.org/10.1021/ja00875a022.

(261) Harris, J. F.; Stacey, F. W. The Free Radical Addition of Trifluoromethanethiol to Fluoroölefins. *J. Am. Chem. Soc.* **1961**, *83* (4), 840–845. https://doi.org/10.1021/ja01465a026.

(262) Haas, A.; Lieb, M.; Zhang, Y. Reaction of Trihalogenmethanesulfenyl Chlorides, Acetates and Trifluoroacetates with Norbornene. *J. Fluor. Chem.* **1985**, *29* (3), 311–322. https://doi.org/10.1016/S0022-1139(00)82330-1.

(263) Haas, A.; Lieb, M.; Zhang, Y. Catalytic Addition of Trihalogenomethanesulfenyl Chlorides to Olefinic Compounds. *J. Fluor. Chem.* **1985**, *30* (2), 203–210. https://doi.org/10.1016/S0022-1139(00)80889-1.

(264) Haas, A.; Möller, G. Preparation and Reactivity of Tris(Trifluoromethylselanyl)Carbenium [(CF3Se)3C+] and Trifluoromethylsulfanylacetic Acid Derivatives [(CF3S)3–nCXn(O)R]. *Chem. Ber.* **1996**, *129* (11), 1383–1388. https://doi.org/10.1002/cber.19961291112.

(265) Kang, K.; Xu, C.; Shen, Q. Copper-Catalyzed Trifluoromethylthiolation of Aryl and Vinyl Boronic Acids with a Shelf-Stable Electrophilic Trifluoromethylthiolating Reagent. *Org. Chem. Front.* **2014**, *1* (3), 294–297. https://doi.org/10.1039/C3QO00068K.

(266) Zhu, S.-Q.; Xu, X.-H.; Qing, F.-L. Oxidative Trifluoromethylthiolation of Terminal Alkynes with AgSCF3: A Convenient Approach to Alkynyl Trifluoromethyl Sulfides. *Eur. J. Org. Chem.* **2014**, *2014* (21), 4453–4456. https://doi.org/10.1002/ejoc.201402533.

(267) Munavalli, S.; Rohrbaugh, D. K.; Rossman, D. I.; Berg, F. J.; Wagner, G. W.; Durst, H. D. Trifluoromethylsulfenylation of Masked Carbonyl Compounds. *Synth. Commun.* **2000**, *30* (16), 2847–2854. https://doi.org/10.1080/00397910008087435.

(268) Pluta, R.; Nikolaienko, P.; Rueping, M. Direct Catalytic Trifluoromethylthiolation of Boronic Acids and Alkynes Employing Electrophilic Shelf-Stable N-(Trifluoromethylthio)Phthalimide. *Angew. Chem. Int. Ed.* **2014**, *53* (6), 1650–1653. https://doi.org/10.1002/anie.201307484.

(269) Küthle, E.; Klauke, E.; Grewe, F. Fluordichlormethylthio-Verbindungen Und Ihre Verwendung Im Pflanzenschutz. *Angew. Chem.* **1964**, *76* (19), 807–816. https://doi.org/10.1002/ange.19640761903.

(270) Xiao, Q.; He, Q.; Li, J.; Wang, J. 1,4-Diazabicyclo[2.2.2]Octane-Promoted Aminotrifluoromethylthiolation of α,β-Unsaturated Carbonyl Compounds: N-Trifluoromethylthio-4-Nitrophthalimide Acts as Both the Nitrogen and SCF3 Sources. *Org. Lett.* **2015**, *17* (24), 6090–6093. https://doi.org/10.1021/acs.orglett.5b03116.

(271) Xu, C.; Ma, B.; Shen, Q. N-Trifluoromethylthiosaccharin: An Easily Accessible, Shelf-Stable, Broadly Applicable Trifluoromethylthiolating Reagent. *Angew. Chem.* **2014**, *126* (35), 9470–9474. https://doi.org/10.1002/ange.201403983.

(272) Zhang, P.; Li, M.; Xue, X.-S.; Xu, C.; Zhao, Q.; Liu, Y.; Wang, H.; Guo, Y.; Lu, L.; Shen, Q. N-Trifluoromethylthio-Dibenzenesulfonimide: A Shelf-Stable, Broadly Applicable Electrophilic Trifluoromethylthiolating Reagent. *J. Org. Chem.* **2016**, *81* (17), 7486–7509. https://doi.org/10.1021/acs.joc.6b01178.

(273) Glenadel, Q.; Alazet, S.; Baert, F.; Billard, T. Multigram Scale Syntheses of First and Second Generation of Trifluoromethanesulfenamide Reagents. *Org. Process Res. Dev.* **2016**, *20* (5), 960–964. https://doi.org/10.1021/acs.oprd.6b00062.

(274) Liu, T.; Qiu, G.; Ding, Q.; Wu, J. Assembly of 3-(Trifluoromethyl)Thiochromenes via a Regioselective Trifluoromethylthioarylation of (3-Arylprop-2-Ynyl)Oxybenzenes with Trifluoromethanesulfanylamide. *Tetrahedron* **2016**, *72* (11), 1472–1476. https://doi.org/10.1016/j.tet.2016.01.053.

(275) Xiao, Q.; Zhu, H.; Li, G.; Chen, Z. Synthesis of Trifluoromethanesulfanylbenzofulvenes via a Cascade Electrophilic Cyclization under Mild Conditions. *Adv. Synth. Catal.* **2014**, *356* (18), 3809–3815. https://doi.org/10.1002/adsc.201400561.

(276) Ferry, A.; Billard, T.; Langlois, B. R.; Bacqué, E. Trifluoromethanesulfanylamides as Easy-to-Handle Equivalents of the Trifluoromethanesulfanyl Cation (CF3S+): Reaction with Alkenes and Alkynes. *Angew. Chem. Int. Ed.* **2009**, *48* (45), 8551–8555. https://doi.org/10.1002/anie.200903387.

(277) Haas, A.; Lieb, M.; Zhang, Y. Electrophilic Reactions of Trihalogenomethanesulfenyl Acetates and Trifluoroacetates. *J. Fluor. Chem.* **1985**, *29* (3), 297–310. https://doi.org/10.1016/S0022-1139(00)82329-5.

(278) Haas, A.; Oh, D. Y. Zur Chemie derVerbindungen, 2. Perhalogenierte Sulfenylcarboxylate. *Chem. Ber.* **1969**, *102* (1), 77–82. https://doi.org/10.1002/cber.19691020111.

(279) Xinxin Shao; Wang, X.; ao Yang; Long Lu*; Qilong Shen*. An Electrophilic Hypervalent Iodine Reagent for Trifluoromethylthiolation. *Angew. Chem. Int. Ed.* **2013**, *52* (12), 3457–3460.

(280) Vinogradova, E. V.; Müller, P.; Buchwald, S. L. Structural Reevaluation of the Electrophilic Hypervalent Iodine Reagent for Trifluoromethylthiolation Supported by the Crystalline Sponge Method for X-Ray Analysis. *Angew. Chem. Int. Ed.* **2014**, *53* (12), 3125–3128. https://doi.org/10.1002/anie.201310897.

(281) Shao, X.; Xu, C.; Lu, L.; Shen, Q. Structure–Reactivity Relationship of Trifluoromethanesulfenates: Discovery of an Electrophilic Trifluoromethylthiolating Reagent. *J. Org. Chem.* **2015**, *80* (6), 3012–3021. https://doi.org/10.1021/jo502645m.

(282) Shao, X.; Xu, C.; Lu, L.; Shen, Q. Shelf-Stable Electrophilic Reagents for Trifluoromethylthiolation. *Acc. Chem. Res.* **2015**, *48* (5), 1227–1236. https://doi.org/10.1021/acs.accounts.5b00047.

(283) Ji, Y.; Brueckl, T.; Baxter, R. D.; Fujiwara, Y.; Seiple, I. B.; Su, S.; Blackmond, D. G.; Baran, P. S. Innate C-H Trifluoromethylation of Heterocycles. *Proc. Natl. Acad. Sci.* **2011**, *108* (35), 14411–14415. https://doi.org/10.1073/pnas.1109059108.

(284) Huang, H.-L.; Yan, H.; Gao, G.-L.; Yang, C.; Xia, W. Metal-Free Direct Aryltrifluoromethylation of Allylic Alcohols with Langlois' Reagent through Concomitant 1,2-Aryl Migration. *Asian J. Org. Chem.* **2015**, *4* (7), 674–677. https://doi.org/10.1002/ajoc.201500096.

(285) Zhang, K.; Xu, X.-H.; Qing, F.-L. Copper-Promoted Trifluoromethanesulfonylation and Trifluoromethylation of Arenediazonium Tetrafluoroborates with NaSO2CF3. *J. Org. Chem.* **2015**, *80* (15), 7658–7665. https://doi.org/10.1021/acs.joc.5b01295.

(286) Chu, X.-Q.; Meng, H.; Xu, X.-P.; Ji, S.-J. One-Pot Synthesis of Allylic Sulfones, Ketosulfones, and Triflyl Allylic Alcohols from Domino Reactions of Allylic Alcohols with Sulfinic Acid under Metal-Free Conditions. *Chem. – Eur. J.* **2015**, *21* (32), 11359–11368. https://doi.org/10.1002/chem.201500469.

(287) Jiang, L.; Qian, J.; Yi, W.; Lu, G.; Cai, C.; Zhang, W. Direct Trifluoromethylthiolation and Perfluoroalkylthiolation of C(Sp2)□H Bonds with CF3SO2Na and RfSO2Na. *Angew. Chem. Int. Ed.* **2015**, *54* (49), 14965–14969. https://doi.org/10.1002/anie.201508495.

(288) Chachignon, H.; Maeno, M.; Kondo, H.; Shibata, N.; Cahard, D. Novel Use of CF_3 SO_2 Cl for the Metal-Free Electrophilic Trifluoromethylthiolation. *Org. Lett.* **2016**, *18* (10), 2467–2470. https://doi.org/10.1021/acs.orglett.6b01026.

(289) Jiang, L.; Yan, Q.; Wang, R.; Ding, T.; Yi, W.; Zhang, W. Trifluoromethanesulfinyl Chloride for Electrophilic Trifluoromethythiolation and Bifunctional Chlorotrifluoromethythiolation. *Chem. – Eur. J.* **2018**, *24* (70), 18749–18756. https://doi.org/10.1002/chem.201804027.

(290) Sun, D.-W.; Jiang, M.; Liu, J.-T. Novel Bifunctionalization of Activated Methylene: Base-Promoted Trifluoromethylthiolation of β-Diketones with Trifluoromethanesulfinyl Chloride. *Chem. – Eur. J.* **2019**, *25* (46), 10797–10802. https://doi.org/10.1002/chem.201901781.

(291) Huang, Z.; Okuyama, K.; Wang, C.; Tokunaga, E.; Li, X.; Shibata, N. 2-Diazo-1-Phenyl-2-((Trifluoromethyl)Sulfonyl)Ethan-1-One: Another Utility for Electrophilic Trifluoromethylthiolation Reactions. *ChemistryOpen* **2016**, *5* (3), 188–191. https://doi.org/10.1002/open.201500225.

(292) Yang, Y.-D.; Azuma, A.; Tokunaga, E.; Yamasaki, M.; Shiro, M.; Shibata, N. Trifluoromethanesulfonyl Hypervalent Iodonium Ylide for Copper-Catalyzed Trifluoromethylthiolation of Enamines, Indoles, and β-Keto Esters. *J. Am. Chem. Soc.* **2013**, *135* (24), 8782–8785. https://doi.org/10.1021/ja402455f.

(293) Arimori, S.; Takada, M.; Shibata, N. Reactions of Allyl Alcohols and Boronic Acids with Trifluoromethanesulfonyl Hypervalent Iodonium Ylide under Copper-Catalysis. *Dalton Trans.* **2015**, *44* (45), 19456–19459. https://doi.org/10.1039/C5DT02214B.

(294) Huang, Z.; Okuyama, K.; Wang, C.; Tokunaga, E.; Li, X.; Shibata, N. 2-Diazo-1-Phenyl-2-((Trifluoromethyl)Sulfonyl)Ethan-1-One: Another Utility for Electrophilic Trifluoromethylthiolation Reactions. *ChemistryOpen* **2016**, *5* (3), 188–191. https://doi.org/10.1002/open.201500225.

(295) Wang, D.; Carlton, C. G.; Tayu, M.; McDouall, J. J. W.; Perry, G. J. P.; Procter, D. J. Trifluoromethyl Sulfoxides: Reagents for Metal-Free C−H Trifluoromethylthiolation. *Angew. Chem.* **2020**, *132* (37), 16052–16056. https://doi.org/10.1002/ange.202005531.

(296) Li, X.; Li, Y.; Yang, J.; Shi, H.; Ai, Z.; Han, C.; He, J.; Du, Y. Synthesis of 3-SCF2H-/3-SCF3-Chromones via Interrupted Pummerer Reaction/Intramolecular Cyclization Mediated by Difluoromethyl or Trifluoromethyl Sulfoxide and Tf2O. *Org. Lett.* **2022**, *24* (39), 7216–7221. https://doi.org/10.1021/acs.orglett.2c03017.

(297) Man, E. H.; Coffman, D. D.; Muetterties, E. L. Synthesis and Properties of Bis-(Trifluoromethylthio)-Mercury. *J. Am. Chem. Soc.* **1959**, *81* (14), 3575–3577. https://doi.org/10.1021/ja01523a023.

(298) Harris, J. F. Free-Radical Reactions of Fluoroalkanesulfenyl Halides. II.[1] Free-Radical Reactions of Trifluoromethanesulfenyl Chloride with Alkanes. *J. Org. Chem.* **1966**, *31* (3), 931–935. https://doi.org/10.1021/jo01341a070.

(299) HJ Emeleus; DE MacDuffie. Preparation and Properties of Trifluoromethylthiosilver. *J Chem Soc* **1961**, 2597–2599.

(300) Adams, D. J.; Clark, J. H. Preparation of Trifluoromethyl Aryl Sulfides Using Silver(I) Trifluoromethanethiolate and an Inorganic Iodide. *J. Org. Chem.* **2000**, *65* (5), 1456–1460. https://doi.org/10.1021/jo9915933.

(301) Wang, K.-P.; Young Yun, S.; Mamidipalli, P.; Lee, D. Silver-Mediated Fluorination, Trifluoromethylation , and Trifluoromethylthiolation of Arynes. *Chem. Sci.* **2013**, *4* (8), 3205–3211. https://doi.org/10.1039/C3SC50992C.

(302) Karmakar, R.; Mamidipalli, P.; Salzman, R. M.; Hong, S.; Yun, S. Y.; Guo, W.; Xia, Y.; Lee, D. Benzannulation of Triynes Initiated by an Alder-Ene Reaction and Subsequent Trifluoromethylthiolate Addition. *Org. Lett.* **2016**, *18* (15), 3530–3533. https://doi.org/10.1021/acs.orglett.6b01443.

(303) Zheng, C.; Ma, M.; Huang, S.; Jiang, C.; Liu, Y.; Fu, Y.; Zhao, K.; Feng, R.; Hong, J. Stereoretentive Trifluoromethylthiolation of (*E*)-styrylboronic Acid with AgSCF3 or *N*-Trifluoromethylthiosuccinimide. *Tetrahedron Lett.* **2022**, *103*, 153982. https://doi.org/10.1016/j.tetlet.2022.153982.

(304) Pan, S.; Li, H.; Huang, Y.; Xu, X.-H.; Qing, F.-L. Copper-Catalyzed, Stereoselective Bis-Trifluoromethylthiolation of Propiolic Acid Derivatives with AgSCF3. *Org. Lett.* **2017**, *19* (12), 3247–3250. https://doi.org/10.1021/acs.orglett.7b01366.

(305) Wu, W.; Dai, W.; Ji, X.; Cao, S. Silver-Mediated Anti-Markovnikov and Markovnikov-Selective Hydrotrifluoromethylthiolation of Terminal Alkynes. *Org. Lett.* **2016**, *18* (12), 2918–2921. https://doi.org/10.1021/acs.orglett.6b01286.

(306) Hu, J.; Huang, Y.; Xu, X.; Qing, F. Copper-Catalyzed Hydroxytrifluoromethylthiolation of Arylpropynones. *Chin. J. Org. Chem.* **2019**, *39* (1), 177. https://doi.org/10.6023/cjoc201808041.

(307) Song, Y.-K.; Qian, P.-C.; Chen, F.; Deng, C.-L.; Zhang, X.-G. Synthesis of 2-(Trifluoromethylthio)-Indenones by Silver-Mediated Cascade Trifluoromethylthiolation/Cyclization of Arylpropynones. *Tetrahedron* **2016**, *72* (47), 7589–7593. https://doi.org/10.1016/j.tet.2016.10.013.

(308) Bi, M.-X.; Liu, S.; Huang, Y.; Xu, X.-H.; Qing, F.-L. Cascade Trifluoromethylthiolation and Cyclization of N-[(3-Aryl)Propioloyl]Indoles. *Beilstein J. Org. Chem.* **2020**, *16* (1), 657–662. https://doi.org/10.3762/bjoc.16.62.

(309) Guo, C.-H.; Chen, D.-Q.; Chen, S.; Liu, X.-Y. Synthesis of Tetrasubstituted α,β-Unsaturated Aldehydes via Radical 1,4-Aryl Migration/Trifluoromethylthiolation Cascade Reaction of Aryl Propynyl Ethers. *Adv. Synth. Catal.* **2017**, *359* (17), 2901–2906. https://doi.org/10.1002/adsc.201700534.

(310) Yagupolskii, L. M.; Kondratenko, N. V.; Sambur, V. P. A New Method for the Syntheses of Aryl and Heteroaryl Trifluoromethyl Sulfides. *Synthesis* **2002**, *1975*, 721–723. https://doi.org/10.1055/s-1975-23905.

(311) Kondratenko, N. V.; Kolomeytsev, A. A.; Popov, V. I.; Yagupolskii, L. M. Synthesis and Reactions of Trifluoromethylthio(Seleno)- and Pentafluorophenylthio(Seleno)-Copper. *Synthesis* **2002**, *1985*, 667–669. https://doi.org/10.1055/s-1985-31301.

(312) Yang, Y.; Xu, L.; Yu, S.; Liu, X.; Zhang, Y.; Vicic, D. A. Triphenylphosphine-Mediated Deoxygenative Reduction of CF3SO2Na and Its Application for Trifluoromethylthiolation of Aryl Iodides. *Chem. – Eur. J.* **2016**, *22* (3), 858–863. https://doi.org/10.1002/chem.201504790.

(313) Weng, Z.; He, W.; Chen, C.; Lee, R.; Tan, D.; Lai, Z.; Kong, D.; Yuan, Y.; Huang, K. An Air-Stable Copper Reagent for Nucleophilic Trifluoromethylthiolation of Aryl Halides. *Angew. Chem. Int. Ed.* **2013**, *52* (5), 1548–1552. https://doi.org/10.1002/anie.201208432.

(314) Nikolaienko, P.; Pluta, R.; Rueping, M. Direct Trifluoromethylthiolation of Alcohols under Mild Reaction Conditions: Conversion of R□OH into R□SCF3. *Chem. – Eur. J.* **2014**, *20* (32), 9867–9870. https://doi.org/10.1002/chem.201402679.

(315) Lefebvre, Q.; Fava, E.; Nikolaienko, P.; Rueping, M. Hydrotrifluoromethylthiolation of α-Diazo Esters – Synthesis of α-SCF 3 Substituted Esters. *Chem. Commun.* **2014**, *50* (50), 6617–6619. https://doi.org/10.1039/C4CC02060J.

(316) Yagupolskii, L. M.; Kondratenko, N. V.; Sambur, V. P. A New Method for the Syntheses of Aryl and Heteroaryl Trifluoromethyl Sulfides. *Synthesis* **2002**, *1975*, 721–723. https://doi.org/10.1055/s-1975-23905.

(317) Rueping, M.; Tolstoluzhsky, N.; Nikolaienko, P. Copper-Catalyzed Trifluoromethyl Thiolation—Mild and Efficient Synthesis of Trifluoromethyl Thioethers. *Chem. – Eur. J.* **2013**, *19* (42), 14043–14046. https://doi.org/10.1002/chem.201302692.

(318) Nikolaienko, P.; Yildiz, T.; Rueping, M. Trifluoromethylthiolation of Unsymmetrical Λ3-Iodane Derivatives: Additive-Free, Selective and Scalable Introduction of the SCF3 Group. *Eur. J. Org. Chem.* **2016**, *2016* (6), 1091–1094. https://doi.org/10.1002/ejoc.201501623.

(319) Tlili, A.; Alazet, S.; Glenadel, Q.; Billard, T. Copper-Catalyzed Perfluoroalkylthiolation of Alkynes with Perfluoroalkanesulfenamides. *Chem. – Eur. J.* **2016**, *22* (29), 10230–10234. https://doi.org/10.1002/chem.201601338.

(320) Tyrra, W.; Naumann, D.; Hoge, B.; Yagupolskii, Y. L. A New Synthesis of Trifluoromethanethiolates—Characterization and Properties of Tetramethylammonium, Cesium and Di(Benzo-15-Crown-5)Cesium Trifluoromethanethiolates. *J. Fluor. Chem.* **2003**, *119* (1), 101–107. https://doi.org/10.1016/S0022-1139(02)00276-2.

(321) Kremlev, M. M.; Tyrra, W.; Naumann, D.; Yagupolskii, Y. L. *S*-Trifluoromethyl Esters of Thiocarboxylic Acids, RC(O)SCF3. *Tetrahedron Lett.* **2004**, *45* (32), 6101–6104. https://doi.org/10.1016/j.tetlet.2004.06.073.

(322) Zhang, C.-P.; Vicic, D. A. Nickel-Catalyzed Synthesis of Aryl Trifluoromethyl Sulfides at Room Temperature. *J. Am. Chem. Soc.* **2012**, *134* (1), 183–185. https://doi.org/10.1021/ja210364r.

(323) Yin, G.; Kalvet, I.; Englert, U.; Schoenebeck, F. Fundamental Studies and Development of Nickel-Catalyzed Trifluoromethylthiolation of Aryl Chlorides: Active Catalytic Species and Key Roles of Ligand and Traceless MeCN Additive Revealed. *J. Am. Chem. Soc.* **2015**, *137* (12), 4164–4172. https://doi.org/10.1021/jacs.5b00538.

(324) Fang, W.-Y.; Dong, T.; Han, J.-B.; Zha, G.-F.; Zhang, C.-P. Expeditious Trifluoromethylthiolation and Trifluoromethylselenolation of Alkynyl(Phenyl)Iodoniums by [XCF 3] − (X = S, Se) Anions. *Org. Biomol. Chem.* **2016**, *14* (48), 11502–11509. https://doi.org/10.1039/C6OB02107G.

(325) Yang, X.-G.; Zheng, K.; Zhang, C. Electrophilic Hypervalent Trifluoromethylthio-Iodine(III) Reagent. *Org. Lett.* **2020**, *22* (5), 2026–2031. https://doi.org/10.1021/acs.orglett.0c00405.

(326) Glenadel, Q.; Alazet, S.; Tlili, A.; Billard, T. Mild and Soft Catalyzed Trifluoromethylthiolation of Boronic Acids: The Crucial Role of Water. *Chem. – Eur. J.* **2015**, *21* (42), 14694–14698. https://doi.org/10.1002/chem.201502338.

(327) Arimori, S.; Takada, M.; Shibata, N. Reactions of Allyl Alcohols and Boronic Acids with Trifluoromethanesulfonyl Hypervalent Iodonium Ylide under Copper-Catalysis. *Dalton Trans.* **2015**, *44* (45), 19456–19459. https://doi.org/10.1039/C5DT02214B.

(328) Xiao-Guang Yang; Ke Zheng; Chi Zhang. Electrophilic Hypervalent Trifluoromethylthio-Iodine(III) Reagent. *Org. Lett.* **2020**, *22* (5), 2026–2031.

(329) Pluta, R.; Nikolaienko, P.; Rueping, M. Direct Catalytic Trifluoromethylthiolation of Boronic Acids and Alkynes Employing Electrophilic Shelf-Stable N-(Trifluoromethylthio)Phthalimide. *Angew. Chem. Int. Ed.* **2014**, *53* (6), 1650–1653. https://doi.org/10.1002/anie.201307484.

(330) Kojima, Y.; Hirano, K. Copper-Mediated Trifluoromethylthiolation of Alkenyl Iodides with AgSCF3. *Chem. Lett.* **2023**, *52* (10), 791–793. https://doi.org/10.1246/cl.230335.

(331) B. Dürr, A.; Yin, G.; Kalvet, I.; Napoly, F.; Schoenebeck, F. Nickel-Catalyzed Trifluoromethylthiolation of Csp 2 –O Bonds. *Chem. Sci.* **2016**, *7* (2), 1076–1081. https://doi.org/10.1039/C5SC03359D.

(332) King, E. R.; Tarrago, M.; Ghosh, A. Metallaphotoredox Catalysis Enables Facile (Trifluoromethyl)Thiolation of Alkenyl Iodides. *Catal. Sci. Technol.* **2023**, *13* (24), 7059–7067. https://doi.org/10.1039/D3CY01394D.

(333) Mudshinge, S. R.; Yang, Y.; Xu, B.; Hammond, G. B.; Lu, Z. Gold (I/III)-Catalyzed Trifluoromethylthiolation and Trifluoromethylselenolation of Organohalides. *Angew. Chem.* **2022**, *134* (12), e202115687. https://doi.org/10.1002/ange.202115687.

(334) Huang, Y.; Ding, J.; Wu, C.; Zheng, H.; Weng, Z. Synthesis of Vinyl Trifluoromethyl Thioethers via Copper-Mediated Trifluoromethylthiolation of Vinyl Bromides. *J. Org. Chem.* **2015**, *80* (5), 2912–2917. https://doi.org/10.1021/acs.joc.5b00144.

(335) Tao, Z.-K.; Li, C.-K.; Li, J.-A.; Shoberu, A.; Zhang, W.; Zou, J.-P. Copper-Catalyzed Vicinal Cyano-, Thiocyano-, and Chlorophosphorylation of Alkynes: A Phosphinoyl Radical-Initiated Approach for Difunctionalized Alkenes. *Org. Lett.* **2021**, *23* (11), 4342–4347. https://doi.org/10.1021/acs.orglett.1c01286.

(336) Zhang, M.; Zeng, X. Metal–Free Radical Thiocyanatosulfonation of Terminal Alkynes in Aqueous Medium. *Org. Lett.* **2021**, *23* (9), 3326–3330. https://doi.org/10.1021/acs.orglett.1c00820.

(337) Zheng, C.; Huang, S.; Liu, Y.; Jiang, C.; Zhang, W.; Fang, G.; Hong, J. Geometrically Selective Denitrative Trifluoromethylthiolation of β-Nitrostyrenes with AgSCF3 for (E)-Vinyl Trifluoromethyl Thioethers. *Org. Lett.* **2020**, *22* (12), 4868–4872. https://doi.org/10.1021/acs.orglett.0c01714.

(338) Pan, S.; Huang, Y.; Qing, F.-L. Synthesis of Trifluoromethylthiolated Alkenes and Ketones by Decarboxylative Functionalization of Cinnamic Acids. *Chem. – Asian J.* **2016**, *11* (20), 2854–2858. https://doi.org/10.1002/asia.201601098.

(339) Cheng, Z.-F.; Tao, T.-T.; Feng, Y.-S.; Tang, W.-K.; Xu, J.; Dai, J.-J.; Xu, H.-J. Cu(II)-Mediated Decarboxylative Trifluoromethylthiolation of α,β-Unsaturated Carboxylic Acids. *J. Org. Chem.* **2018**, *83* (1), 499–504. https://doi.org/10.1021/acs.joc.7b02232.

(340) Honeker, R.; Garza-Sanchez, R. A.; Hopkinson, M. N.; Glorius, F. Visible-Light-Promoted Trifluoromethylthiolation of Styrenes by Dual Photoredox/Halide Catalysis. *Chem. – Eur. J.* **2016**, *22* (13), 4395–4399. https://doi.org/10.1002/chem.201600190.

(341) Zhang, P.; Li, M.; Xue, X.-S.; Xu, C.; Zhao, Q.; Liu, Y.; Wang, H.; Guo, Y.; Lu, L.; Shen, Q. N-Trifluoromethylthio-Dibenzenesulfonimide: A Shelf-Stable, Broadly Applicable Electrophilic Trifluoromethylthiolating Reagent. *J. Org. Chem.* **2016**, *81* (17), 7486–7509. https://doi.org/10.1021/acs.joc.6b01178.

(342) Wu, J.-J.; Xu, J.; Zhao, X. Selenide-Catalyzed Stereoselective Construction of Tetrasubstituted Trifluoromethylthiolated Alkenes with Alkynes. *Chem. – Eur. J.* **2016**, *22* (43), 15265–15269. https://doi.org/10.1002/chem.201603975.

(343) Jiang, L.; Ding, T.; Yi, W.; Zeng, X.; Zhang, W. Fluoroalkylsulfonyl Chlorides Promoted Vicinal Chloro-Fluoroalkylthiolation of Alkenes and Alkynes. *Org. Lett.* **2018**, *20* (8), 2236–2240. https://doi.org/10.1021/acs.orglett.8b00581.

(344) Jiang, L.; Yan, Q.; Wang, R.; Ding, T.; Yi, W.; Zhang, W. Trifluoromethanesulfinyl Chloride for Electrophilic Trifluoromethythiolation and Bifunctional Chlorotrifluoromethythiolation. *Chem. – Eur. J.* **2018**, *24* (70), 18749–18756. https://doi.org/10.1002/chem.201804027.

(345) Li, J.; Yang, Z.; Guo, R.; Jin, M. Y.; Wang, J. (Joelle). Atom-Economical and Stereoselective Difunctionalization of Electron-Withdrawing Alkynes with N-Trifluoromethylthiophthalimide. *Asian J. Org. Chem.* **2018**, *7* (9), 1784–1787. https://doi.org/10.1002/ajoc.201800351.

(346) Chu, D.; Ellman, J. A. Three-Component Friedel–Crafts Transformations: Synthesis of Alkyl and Alkenyl Trifluoromethyl Sulfides and Alkenyl Iodides. *Org. Lett.* **2022**, *24* (15), 2921–2925. https://doi.org/10.1021/acs.orglett.2c00924.

(347) Ouyang, Y.; Xu, X.-H.; Qing, F.-L. Hydrotrifluoromethylthiolation of Unactivated Alkenes and Alkynes with Trifluoromethanesulfonic Anhydride through Deoxygenative Reduction and Photoredox Radical Processes. *Angew. Chem.* **2019**, *131* (51), 18679–18683. https://doi.org/10.1002/ange.201911323.

(348) Zhang, B.-S.; Gao, L.-Y.; Zhang, Z.; Wen, Y.-H.; Liang, Y.-M. Three-Component Difluoroalkylation and Trifluoromethylthiolation/Trifluoromethylselenolation of π-Bonds. *Chem. Commun.* **2018**, *54* (10), 1185–1188. https://doi.org/10.1039/C7CC09083H.

(349) Li, H.; Cheng, Z.; Tung, C.-H.; Xu, Z. Atom Transfer Radical Addition to Alkynes and Enynes: A Versatile Gold/Photoredox Approach to Thio-Functionalized Vinylsulfones. *ACS Catal.* **2018**, *8* (9), 8237–8243. https://doi.org/10.1021/acscatal.8b02194.

(350) Ji, M.; Yu, J.; Zhu, C. Cyanotrifluoromethylthiolation of Unactivated Dialkyl-Substituted Alkynes via Cyano Migration: Synthesis of Trifluoromethylthiolated Acrylonitriles. *Chem. Commun.* **2018**, *54* (50), 6812–6815. https://doi.org/10.1039/C8CC01189C.

(351) Zhang, Q.; Li, X.; Zhang, W.; Wang, Y.; Pan, Y. Photocatalyzed Radical Relayed Regio- and Stereoselective Trifluoromethylthiolation–Boration. *Org. Lett.* **2021**, *23* (14), 5410–5414. https://doi.org/10.1021/acs.orglett.1c01737.

(352) Wang, S.-Y.; Liu, C.; Yang, W.; Tian, Z.-Y.; Yuan, L.; Xie, L.-Y. Efficient Synthesis of SCF 3 - Containing 3-Alkenylquinoxalinones via Three-Component Radical Cascade Reaction. *Org. Biomol. Chem.* **2024**, *22* (18), 3740–3745. https://doi.org/10.1039/D4OB00363B.

(353) Xu, L.; Sun, F.; Zhao, H.; Shi, H.; Wu, Y.; Li, X.; Du, Y. Synthesis of Trifluoromethylthiolated Quinolinones via Trifluoromethanesulfanamide-Induced Electrophilic Intramolecular Cyclization of N-Arylpropynamides. *Adv. Synth. Catal.* **2023**, *365* (22), 3837–3842. https://doi.org/10.1002/adsc.202300719.

(354) Liang, Y.; Ji, J.; Zhang, X.; Jiang, Q.; Luo, J.; Zhao, X. Enantioselective Construction of Axially Chiral Amino Sulfide Vinyl Arenes by Chiral Sulfide-Catalyzed Electrophilic Carbothiolation of Alkynes. *Angew. Chem. Int. Ed.* **2020**, *59* (12), 4959–4964. https://doi.org/10.1002/anie.201915470.

(355) Zeng, Y.-F.; Tan, D.-H.; Chen, Y.; Lv, W.-X.; Liu, X.-G.; Li, Q.; Wang, H. Direct Radical Trifluoromethylthiolation and Thiocyanation of Aryl Alkynoate Esters: Mild and Facile Synthesis

of 3-Trifluoromethylthiolated and 3-Thiocyanated Coumarins. *Org. Chem. Front.* **2015**, *2* (11), 1511–1515. https://doi.org/10.1039/C5QO00271K.

(356) Ren, Y.; Yan, Q.; Li, Y.; Gao, Y.; Zhao, J.; Li, L.; Liu, Z.-Q.; Li, Z. Free Radical Promoted Trifluoromethylthiolation of Alkynes to Access SCF3-Containing Dibenzazepines or Dioxodibenzothiazepines. *J. Org. Chem.* **2022**, *87* (13), 8773–8781. https://doi.org/10.1021/acs.joc.2c00623.

(357) Chen, X.; Pei, C.; Liu, B.; Li, J.; Zou, D.; Wu, Y.; Wu, Y. Copper-Assisted Trifluoromethylthiolation/Radical Cascade Cyclization of Alkynes to Construct SCF 3 -Containing Dioxodibenzothiazepines. *Chem. Commun.* **2022**, *58* (62), 8674–8677. https://doi.org/10.1039/D2CC02171D.

(358) Qiu, Y.-F.; Zhu, X.-Y.; Li, Y.-X.; He, Y.-T.; Yang, F.; Wang, J.; Hua, H.-L.; Zheng, L.; Wang, L.-C.; Liu, X.-Y.; Liang, Y.-M. AgSCF3-Mediated Trifluoromethylthiolation/Radical Cascade Cyclization of 1,6-Enynes. *Org. Lett.* **2015**, *17* (15), 3694–3697. https://doi.org/10.1021/acs.orglett.5b01657.

(359) Uppalabat, T.; Hassa, N.; Sawektreeratana, N.; Leowanawat, P.; Janthakit, P.; Nalaoh, P.; Promarak, V.; Soorukram, D.; Reutrakul, V.; Kuhakarn, C. Cascade Oxidative Trifluoromethylthiolation and Cyclization of 3-Alkyl-1-(2-(Alkynyl)Phenyl)Indoles. *J. Org. Chem.* **2023**, *88* (9), 5403–5419. https://doi.org/10.1021/acs.joc.2c03045.

(360) Fan, J.; Yan, Q.; Liu, H.; Li, L.; Liu, Z.-Q.; Li, Z. Photo-Promoted Cascade Cyclization of Aryl Alkynes: Access to Thiocyanate/Trifluoromethylthio-Containing Quinolino[2,1- b]Quinazolinones. *New J. Chem.* **2023**, *47* (45), 20713–20717. https://doi.org/10.1039/D3NJ04433E.

(361) Ye, Z.; Zhang, Y.; Guo, G.; Shao, X.; Wu, J.-R. Silver-Catalyzed 1,2-Thiosulfonylation of Alkenes: Development of a Nucleophilic D3-Methylthiolating Reagent. *J. Org. Chem.* **2024**, *89* (19), 14369–14383. https://doi.org/10.1021/acs.joc.4c01787.

(362) Li, H.; Liu, S.; Huang, Y.; Xu, X.-H.; Qing, F.-L. Tandem Trifluoromethylthiolation/Aryl Migration of Aryl Alkynoates to Trifluoromethylthiolated Alkenes. *Chem. Commun.* **2017**, *53* (73), 10136–10139. https://doi.org/10.1039/C7CC06232J.

(363) Jin, D.-P.; Gao, P.; Chen, D.-Q.; Chen, S.; Wang, J.; Liu, X.-Y.; Liang, Y.-M. AgSCF3-Mediated Oxidative Trifluoromethythiolation of Alkynes with Dearomatization to Synthesize SCF3-Substituted Spiro[4,5]Trienones. *Org. Lett.* **2016**, *18* (14), 3486–3489. https://doi.org/10.1021/acs.orglett.6b01702.

(364) Reddy, C. R.; Srinivasu, E.; Subbarao, M. Seleno/Thio-Functionalized Ipso-Annulation of N-Propiolyl-2-Arylbenzimidazole to Construct Azaspiro[5,5]Undecatrienones. *J. Org. Chem.* **2023**, *88* (23), 16485–16496. https://doi.org/10.1021/acs.joc.3c01991.

(365) Raji Reddy, C.; Ajaykumar, U.; D. Patil, A.; Ramesh, R. Ipso -Cyclization of Unactivated Biaryl Ynones Leading to Thio-Functionalized Spirocyclic Enones. *Org. Biomol. Chem.* **2023**, *21* (31), 6379–6388. https://doi.org/10.1039/D3OB00974B.

(366) Yang, W.-C.; Zhang, M.-M.; Sun, Y.; Chen, C.-Y.; Wang, L. Electrochemical Trifluoromethylthiolation and Spirocyclization of Alkynes with AgSCF3: Access to SCF3-Containing Spiro[5,5]Trienones. *Org. Lett.* **2021**, *23* (17), 6691–6696. https://doi.org/10.1021/acs.orglett.1c02260.

(367) Duboudin, J. G.; Jousseaume, B. Reactivite Des Organomagnesiens Vis-a-Vis de Composes Acetyleniques En Presence Du Complexe de Nickel (PPh3)2NiCl2. *J. Organomet. Chem.* **1978**, *162* (2), 209–222. https://doi.org/10.1016/S0022-328X(00)82039-2.

(368) Walther, D.; Klettke, T.; Schmidt, A.; Görls, H.; Imhof, W. Synthesis, Properties, and Solid-State Structures of Bis(Alkyne)Metal(0) Complexes (Metal = Ni, Pt) with Substituted Alkynediols and Alkynols. *Organometallics* **1996**, *15* (9), 2314–2319. https://doi.org/10.1021/om950896u.

(369) Rosenthal, U.; Nauck, C.; Arndt, P.; Pulst, S.; Baumann, W.; Burlakov, V. V.; Görls, H. Preparation and Properties of the Complex (Dipy)Ni(η 2 -PhC 2 SiMe 3). On the Correlation of Structural Bonding Parameters with IR and NMR Spectroscopic Data in Transition Metal Alkyne Complexes. *J. Organomet. Chem.* **1994**, *484* (1), 81–87. https://doi.org/10.1016/0022-328X(94)87189-2.

(370) Walther, D.; Schmidt, A.; Klettke, T.; Imhof, W.; Görls, H. Bis(Tetramethylbutynediol)Nickel(0), the First Pure Monoalkyne Complex of Nickel and Its Chemistry. *Angew. Chem. Int. Ed. Engl.* **1994**, *33* (13), 1373–1376. https://doi.org/10.1002/anie.199413731.

(371) Kaschube, W.; Pörschke, K.-R.; Angermund, K.; Krüger, C.; Wilke, G. Zur Lewis-Acidität von Nickel(0), X. Diorganylmagnesium-Komplexe von Nickel(0): (TMEDA)MgCH3(μ-CH3)Ni(C2H4)2. *Chem. Ber.* **1988**, *121* (11), 1921–1929. https://doi.org/10.1002/cber.19881211108.

(372) Saravanan, P.; Anbarasan, P. Copper-Catalyzed Trifluoromethylthiolation of Di(Hetero)Aryl-Λ3-Iodanes: Mechanistic Insight and Application to Synthesis of (Hetero)Aryl Trifluoromethyl Sulfides. *Adv. Synth. Catal.* **2015**, *357* (16–17), 3521–3528. https://doi.org/10.1002/adsc.201500606.

(373) Tlili, A.; Alazet, S.; Glenadel, Q.; Billard, T. Copper-Catalyzed Perfluoroalkylthiolation of Alkynes with Perfluoroalkanesulfenamides. *Chem. – Eur. J.* **2016**, *22* (29), 10230–10234. https://doi.org/10.1002/chem.201601338.

(374) Feng, H.-T.; Yuan, Y.-X.; Xiong, J.-B.; Zheng, Y.-S.; Zhong Tang, B. Macrocycles and Cages Based on Tetraphenylethylene with Aggregation-Induced Emission Effect. *Chem. Soc. Rev.* **2018**, *47* (19), 7452–7476. https://doi.org/10.1039/C8CS00444G.

(375) Schultz, A.; Laschat, S.; Diele, S.; Nimtz, M. Tetraphenylethene-Derived Columnar Liquid Crystals and Their Oxidative Photocyclization. *Eur. J. Org. Chem.* **2003**, *2003* (15), 2829–2839. https://doi.org/10.1002/ejoc.200300118.

(376) Buttard, F.; Sharma, J.; Alexandre Champagne, P. Recent Advances in the Stereoselective Synthesis of Acyclic All-Carbon Tetrasubstituted Alkenes. *Chem. Commun.* **2021**, *57* (34), 4071–4088. https://doi.org/10.1039/D1CC00596K.

(377) You, C.; Sakai, M.; Daniliuc, C. G.; Bergander, K.; Yamaguchi, S.; Studer, A. Regio- and Stereoselective 1,2-Carboboration of Ynamides with Aryldichloroboranes. *Angew. Chem. Int. Ed.* **2021**, *60* (40), 21697–21701. https://doi.org/10.1002/anie.202107647.

(378) *Versatile Relay and Cooperative Palladium(0) N-Heterocyclic Carbene/Copper(I) N-Heterocyclic Carbene Catalysis for the Synthesis of Tri- and Tetrasubstituted Alkenes - Lesieur - 2015 - ChemCatChem - Wiley Online Library*. https://chemistry-europe.onlinelibrary.wiley.com/doi/full/10.1002/cctc.201500268 (accessed 2025-05-15).

(379) Daini, M.; Yamamoto, A.; Suginome, M. Palladium-Catalyzed Trans- and Cis-Carboboration of Alkynes Tethered to Chloroborane with Organozirconium Reagents: Ligand-Dependent Complementary Stereoselectivity. *J. Am. Chem. Soc.* **2008**, *130* (10), 2918–2919. https://doi.org/10.1021/ja711160h.

(380) Daini, M.; Suginome, M. Palladium-Catalyzed Carboboration of Alkynes Using Chloroborane and Organozirconium Reagents. *Chem. Commun.* **2008**, *0* (41), 5224–5226. https://doi.org/10.1039/B809433K.

(381) Liu, S.; Zeng, X.; Xu, B. Ligandless Copper-Catalyzed Carboborylation of Heteroatom-Substituted Alkynes. *Adv. Synth. Catal.* **2018**, *360* (17), 3249–3253. https://doi.org/10.1002/adsc.201800656.

(382) Zhou, Y.; You, W.; Smith, K. B.; Brown, M. K. Copper-Catalyzed Cross-Coupling of Boronic Esters with Aryl Iodides and Application to the Carboboration of Alkynes and Allenes. *Angew. Chem.* **2014**, *126* (13), 3543–3547. https://doi.org/10.1002/ange.201310275.

(383) Semba, K.; Yoshizawa, M.; Ohtagaki, Y.; Nakao, Y. Arylboration of Internal Alkynes by Cooperative Palladium/Copper Catalysis. *Bull. Chem. Soc. Jpn.* **2017**, *90* (12), 1340–1343. https://doi.org/10.1246/bcsj.20170226.

(384) Howell, A.; Howell, S. J. Tamoxifen Evolution. *Br. J. Cancer* **2023**, *128* (3), 421–425. https://doi.org/10.1038/s41416-023-02158-5.

(385) Shah, P.; Chaładaj, W. α-Selective Syn-Carbotrifluoromethylthiolation of Alkynes. *Org. Lett.* **2025**, *27* (10), 2498–2503. https://doi.org/10.1021/acs.orglett.5c00570.

(386) Abas, H.; Linsdall, S. M.; Mamboury, M.; Rzepa, H. S.; Spivey, A. C. Total Synthesis of (+)-Lophirone H and Its Pentamethyl Ether Utilizing an Oxonium–Prins Cyclization. *Org. Lett.* **2017**, *19* (10), 2486–2489. https://doi.org/10.1021/acs.orglett.7b00642.

(387) Houston, S. D.; Fahrenhorst-Jones, T.; Xing, H.; Chalmers, B. A.; Sykes, M. L.; Stok, J. E.; Soto, C. F.; Burns, J. M.; Bernhardt, P. V.; Voss, J. J. D.; Boyle, G. M.; Smith, M. T.; Tsanaktsidis, J.; Savage, G. P.; Avery, V. M.; Williams, C. M. The Cubane Paradigm in Bioactive Molecule Discovery: Further Scope, Limitations and the Cyclooctatetraene Complement. *Org. Biomol. Chem.* **2019**, *17* (28), 6790–6798. https://doi.org/10.1039/C9OB01238A.

(388) Stýskala, J.; Cankař, P.; Soural, M.; Bednář, P.; Lemr, K. Synthesis of Some Deuterated Dialkylaminoethyls as Possible Standards for the Mass Spectrometric Monitoring of Chemical Warfare Agents. *J. Label. Compd. Radiopharm.* **2008**, *51* (1), 19–22. https://doi.org/10.1002/jlcr.1464.

(389) Chang, M.-Y.; Cheng, Y.-C.; Sun, P.-P. Pd(OAc)2-Catalyzed Desulfinative Cross-Coupling of Sodium Sulfinates with β-Bromostyrenes: Synthesis of Tamoxifen. *Synthesis* **2017**, *49*, 2411–2422. https://doi.org/10.1055/s-0036-1588705.

(390) Ngassa, F. N.; Lindsey, E. A.; Haines, B. E. The First Cu- and Amine-Free Sonogashira-Type Cross-Coupling in the C-6-Alkynylation of Protected 2′-Deoxyadenosine. *Tetrahedron* **2009**, *65* (21), 4085–4091. https://doi.org/10.1016/j.tet.2009.03.064.

(391) Roesch, K. R.; Larock, R. C. Synthesis of Isoindolo[2,1-a]Indoles by the Palladium-Catalyzed Annulation of Internal Acetylenes. *J. Org. Chem.* **2001**, *66* (2), 412–420. https://doi.org/10.1021/jo000997o.

(392) Dixon, L. I.; Carroll, M. A.; Gregson, T. J.; Ellames, G. J.; Harrington, R. W.; Clegg, W. Synthesis and Reactivity of Aryl(Alkynyl)Iodonium Salts. *Eur. J. Org. Chem.* **2013**, *2013* (12), 2334–2345. https://doi.org/10.1002/ejoc.201300092.

(393) Wang, B.; Yiren Ong, D.; Li, Y.; Hao Pang, J.; Watanabe, K.; Takita, R.; Chiba, S. Stereo-Controlled Anti -Hydromagnesiation of Aryl Alkynes by Magnesium Hydrides. *Chem. Sci.* **2020**, *11* (20), 5267–5272. https://doi.org/10.1039/D0SC01773F.

(394) Choi, G.; Kim, H. E.; Hwang, S.; Jang, H.; Chung, W. Phosphorus(III)-Mediated, Tandem Deoxygenative Geminal Chlorofluorination of 1,2-Diketones. *Org. Lett.* **2020**, *22* (11), 4190–4195. https://doi.org/10.1021/acs.orglett.0c01258.

(395) Yoshida, M.; Hayashi, M.; Shishido, K. Palladium-Catalyzed Diastereoselective Coupling of Propargylic Oxiranes with Terminal Alkynes. *Org. Lett.* **2007**, *9* (9), 1643–1646. https://doi.org/10.1021/ol070224n.

(396) Zhang, W.-W.; Zhang, X.-G.; Li, J.-H. Palladium-Catalyzed Decarboxylative Coupling of Alkynyl Carboxylic Acids with Benzyl Halides or Aryl Halides. *J. Org. Chem.* **2010**, *75* (15), 5259–5264. https://doi.org/10.1021/jo1010284.

(397) Zhao, J.; Yu, Y.; Ma, S. Ligand Effects on the Pd-Catalyzed Cross-Coupling Reaction of 3-Iodoalk-2-Enoates with Propargyl/1,2-Allenylic Metallic Species: An Efficient Regiodivergent Synthesis of 2,4,5-Trienoates. *Chem. – Eur. J.* **2010**, *16* (1), 74–80. https://doi.org/10.1002/chem.200901287.

(398) Lu, B.; Li, C.; Zhang, L. Gold-Catalyzed Highly Regioselective Oxidation of C−C Triple Bonds without Acid Additives: Propargyl Moieties as Masked α,β-Unsaturated Carbonyls. *J. Am. Chem. Soc.* **2010**, *132* (40), 14070–14072. https://doi.org/10.1021/ja1072614.

(399) Teske, J.; Plietker, B. Fe-Catalyzed Cycloisomerization of Aryl Allenyl Ketones: Access to 3-Arylidene-Indan-1-Ones. *Org. Lett.* **2018**, *20* (8), 2257–2260. https://doi.org/10.1021/acs.orglett.8b00612.

(400) Gelman, D.; Buchwald, S. L. Efficient Palladium-Catalyzed Coupling of Aryl Chlorides and Tosylates with Terminal Alkynes: Use of a Copper Cocatalyst Inhibits the Reaction. *Angew. Chem. Int. Ed.* **2003**, *42* (48), 5993–5996. https://doi.org/10.1002/anie.200353015.

(401) Saga, Y.; Motoki, R.; Makino, S.; Shimizu, Y.; Kanai, M.; Shibasaki, M. Catalytic Asymmetric Synthesis of R207910. *J. Am. Chem. Soc.* **2010**, *132* (23), 7905–7907. https://doi.org/10.1021/ja103183r.

(402) Zeng, Q.; Cai, P.; Li, Z.; Qin, J.; Tang, B. Z. An Imidazole-Functionalized Polyacetylene: Convenient Synthesis and Selective Chemosensor for Metal Ions and Cyanide. *Chem. Commun.* **2008**, No. 9, 1094–1096. https://doi.org/10.1039/B717764J.

(403) Mori, A.; Shimada, T.; Kondo, T.; Sekiguchi, A. A Highly Effective Pd/Cu-Catalyzed Coupling Reaction of Terminal Alkynes with Organic Halides Promoted by Tetrabutylammonium Fluoride or Hydroxide. *Synlett* **2001**, *2001*, 649–651. https://doi.org/10.1055/s-2001-13390.

(404) Lautens, M.; Yoshida, M. Rhodium-Catalyzed Addition of Arylboronic Acids to Alkynyl Aza-Heteroaromatic Compounds in Water. *J. Org. Chem.* **2003**, *68* (3), 762–769. https://doi.org/10.1021/jo0205255.

(405) Okuro, K.; Furuune, M.; Enna, M.; Miura, M.; Nomura, M. Synthesis of Aryl- and Vinylacetylene Derivatives by Copper-Catalyzed Reaction of Aryl and Vinyl Iodides with Terminal Alkynes. *J. Org. Chem.* **1993**, *58* (17), 4716–4721. https://doi.org/10.1021/jo00069a040.

(406) Gauthier, R.; Mamone, M.; Paquin, J.-F. Gold-Catalyzed Hydrofluorination of Internal Alkynes Using Aqueous HF. *Org. Lett.* **2019**, *21* (22), 9024–9027. https://doi.org/10.1021/acs.orglett.9b03425.

(407) Yu, F.; Li, P.; Wang, B.; Han, K. Reversible Near-Infrared Fluorescent Probe Introducing Tellurium to Mimetic Glutathione Peroxidase for Monitoring the Redox Cycles between Peroxynitrite and Glutathione in Vivo. *J. Am. Chem. Soc.* **2013**, *135* (20), 7674–7680. https://doi.org/10.1021/ja401360a.

(408) Bruno, N. C.; Tudge, M. T.; Buchwald, S. L. Design and Preparation of New Palladium Precatalysts for C–C and C–N Cross-Coupling Reactions. *Chem. Sci.* **2013**, *4* (3), 916–920. https://doi.org/10.1039/C2SC20903A.

(409) Glenadel, Q.; Alazet, S.; Baert, F.; Billard, T. Multigram Scale Syntheses of First and Second Generation of Trifluoromethanesulfenamide Reagents. *Org. Process Res. Dev.* **2016**, *20* (5), 960–964. https://doi.org/10.1021/acs.oprd.6b00062.

(410) Dalgleish, S.; Robertson, N. A Stable near IR Switchable Electrochromic Polymer Based on an Indole -Substituted Nickel Dithiolene. *Chem. Commun.* **2009**, *0* (39), 5826–5828. https://doi.org/10.1039/B913174D.

(411) Zheng, G.; Zhao, J.; Li, Z.; Zhang, Q.; Sun, J.; Sun, H.; Zhang, Q. Highly Regio- and Stereoselective Intermolecular Seleno- and Thioamination of Alkynes. *Chem. – Eur. J.* **2016**, *22* (10), 3513–3518. https://doi.org/10.1002/chem.201504534.

(412) Leyva-Pérez, A.; Cabrero-Antonino, J. R.; Rubio-Marqués, P.; Al-Resayes, S. I.; Corma, A. Synthesis of the Ortho/Meta/Para Isomers of Relevant Pharmaceutical Compounds by Coupling a Sonogashira Reaction with a Regioselective Hydration. *ACS Catal.* **2014**, *4* (3), 722–731. https://doi.org/10.1021/cs401075z.

(413) Ackermann, L.; Lygin, A. V. Cationic Ruthenium(II) Catalysts for Oxidative C–H/N–H Bond Functionalizations of Anilines with Removable Directing Group: Synthesis of Indoles in Water. *Org. Lett.* **2012**, *14* (3), 764–767. https://doi.org/10.1021/ol203309y.

(414) Dolomanov, O. V.; Bourhis, L. J.; Gildea, R. J.; Howard, J. a. K.; Puschmann, H. OLEX2: A Complete Structure Solution, Refinement and Analysis Program. *J. Appl. Crystallogr.* **2009**, *42* (2), 339–341. https://doi.org/10.1107/S0021889808042726.

(415) Brals, J.; McGuire, T. M.; Watson, A. J. B. A Chemoselective Polarity-Mismatched Photocatalytic $C(Sp^3)-C(Sp^2)$ Cross-Coupling Enabled by Synergistic Boron Activation. *Angew. Chem. Int. Ed.* **2023**, *62* (42), e202310462. https://doi.org/10.1002/anie.202310462.

(416) 19) Gaussian 16, Revision C.01, M. J. Frisch, G. W. Trucks, H. B. Schlegel, G. E. Scuseria, M. A. Robb, J. R. Cheeseman, G. Scalmani, V. Barone, G. A. Petersson, H. Nakatsuji, X. Li, M. Caricato, A. V. Marenich, J. Bloino, B. G. Janesko, R. Gomperts, B. Mennucci, H. P. Hratchian, J. V. Ortiz, A. F. Izmaylov, J. L. Sonnenberg, D. Williams-Young, F. Ding, F. Lipparini, F. Egidi, J. Goings, B. Peng, A. Petrone, T. Henderson, D. Ranasinghe, V. G. Zakrzewski, J. Gao, N. Rega, G. Zheng, W. Liang, M. Hada, M. Ehara, K. Toyota, R. Fukuda, J. Hasegawa, M. Ishida, T. Nakajima, Y. Honda, O. Kitao, H. Nakai, T. Vreven, K. Throssell, J. A. Montgomery, Jr., J. E. Peralta, F. Ogliaro, M. J. Bearpark, J. J. Heyd, E. N. Brothers, K. N. Kudin, V. N. Staroverov, T. A. Keith, R. Kobayashi, J. Normand, K. Raghavachari, A. P. Rendell, J. C. Burant, S. S. Iyengar, J. Tomasi, M. Cossi, J. M. Millam, M. Klene, C. Adamo, R. Cammi, J. W. Ochterski, R. L. Martin, K. Morokuma, O. Farkas, J. B. Foresman, and D. J. Fox, Gaussian, Inc., Wallingford CT, 2019.

(417) Zhao, Y.; Truhlar, D. G. The M06 Suite of Density Functionals for Main Group Thermochemistry, Thermochemical Kinetics, Noncovalent Interactions, Excited States, and Transition Elements: Two New Functionals and Systematic Testing of Four M06-Class Functionals and 12 Other Functionals. *Theor. Chem. Acc.* **2008**, *120* (1), 215–241. https://doi.org/10.1007/s00214-007-0310-x.

(418) Weigend, F.; Ahlrichs, R. Balanced Basis Sets of Split Valence, Triple Zeta Valence and Quadruple Zeta Valence Quality for H to Rn: Design and Assessment of Accuracy. *Phys. Chem. Chem. Phys.* **2005**, *7* (18), 3297–3305. https://doi.org/10.1039/B508541A.

(419) Marenich, A. V.; Cramer, C. J.; Truhlar, D. G. Universal Solvation Model Based on Solute Electron Density and on a Continuum Model of the Solvent Defined by the Bulk Dielectric Constant and Atomic Surface Tensions. *J. Phys. Chem. B* **2009**, *113* (18), 6378–6396. https://doi.org/10.1021/jp810292n.

(420) CYLview20; Legault, C. Y., Université de Sherbrooke, 2020 (Http://Www.Cylview.Org).